

Aus dem Adolf-Butenandt-Institut
Lehrstuhl für Stoffwechselbiochemie
Ludwig-Maximilians-Universität München
Vorstand: Prof. Dr. rer. nat. Dr. h. c. Christian Haass

Signal peptide peptidase-like 3 (SPPL3) is a type II
membrane protein-selective sheddase that
regulates cellular N-glycosylation

Dissertation
zum Erwerb des Doktorgrades der Naturwissenschaften
an der Medizinischen Fakultät
der Ludwig-Maximilians-Universität München

vorgelegt von
MATTHIAS VOSS
aus Kiel

2014

Gedruckt mit Genehmigung der Medizinischen Fakultät
der Ludwig-Maximilians-Universität München

Betreuer: Prof. Dr. rer. nat. Dr. h. c. Christian Haass
Zweitgutachter: Prof. Dr. rer. nat. Michael Mederos y Schnitzler
Dekan: Prof. Dr. med. Dr. h. c. Maximilian Reiser, FACR, FRCR

Tag der mündlichen Prüfung: 18. Dezember 2014

Eidesstattliche Versicherung

Ich erkläre hiermit an Eides statt, dass ich die vorliegende Dissertation mit dem Titel
Signal peptide peptidase-like 3 (SPPL3) is a type II membrane protein-selective sheddase that regulates cellular N-glycosylation

selbstständig verfasst, mich außer der angegebenen keiner weiteren Hilfsmittel bedient und alle Erkenntnisse, die aus dem Schrifttum ganz oder annähernd übernommen sind, als solche kenntlich gemacht und nach ihrer Herkunft unter Bezeichnung der Fundstelle einzeln nachgewiesen habe.

Ich erkläre des Weiteren, dass die hier vorgelegte Dissertation nicht in gleicher oder in ähnlicher Form bei einer anderen Stelle zur Erlangung eines akademischen Grades eingereicht wurde.

München, den 22. Juli 2014

(Matthias Voss)

Teile der Ergebnisse dieser Dissertation (Abschnitt 4.1. und 4.2) sind bereits veröffentlicht worden in:

Voss, M., Fukumori, A., Kuhn, P.-H., Künzel, U., Klier, B., Grammer, G., Haug-Kröper, M., Kremmer E., Lichtenhaller, S.F., Steiner, H., Schröder, B., Haass, C., Fluhrer, R. (2012). Foamy virus envelope protein is a substrate for signal peptide peptidase-like 3 (SPPL3). *J. Biol. Chem.* **287**, 43401-43409.

(Die Publikation befindet sich im Anhang)

Des Weiteren wird die *revised version* des folgenden Manuskripts, welches Daten aus dieser Dissertation enthält (Abschnitt 4.3), derzeit bei *The EMBO Journal* begutachtet:

Voss, M., Künzel, U., Higel, F., Kuhn, P.-H., Colombo, A., Fukumori, A., Haug-Kröper, M., Klier, B., Grammer, G., Seidl, A., Schröder, B., Obst, R., Steiner, H., Lichtenhaller, S.F., Haass, C., Fluhrer, R. Shedding of glycan-modifying enzymes by signal peptide peptidase-like 3 (SPPL) affects cellular N-glycosylation.

(Das Manuskript befindet sich im Anhang)

Darüber hinaus ist im Rahmen dieser Arbeit ein Übersichtsartikel entstanden, der im Dezember 2013 publiziert worden ist:

Voss, M., Schröder, B., Fluhrer R. (2013). Mechanism, specificity, and physiology of signal peptide peptidase (SPP) and SPP-like proteases. *Biochim. Biophys. Acta* **1828**, 282-2839.

(Die Publikation befindet sich im Anhang)

Ein weiteres Manuskript mit Daten dieser Dissertation (Abschnitt 4.4) befindet sich derzeit in Vorbereitung.

Meinen Großeltern

Contents

Summary	1
Zusammenfassung	3
1. Introduction	5
1.1. Regulated Intramembrane Proteolysis	5
1.1.1. Primary Cleavage: Ectodomain Shedding	5
1.1.2. Secondary Cleavage: Intramembrane Proteolysis	6
1.2. Intramembrane-cleaving metalloproteases	7
1.3. Intramembrane-cleaving serine proteases	8
1.3.1 Catalytic mechanism, topology and structure of rhomboids	9
1.3.2 Substrate requirements and regulation of rhomboid activity	9
1.3.3 Proteolytically inactive rhomboid-like proteins	10
1.4. Intramembrane-cleaving aspartyl proteases	10
1.4.1 Presenilins and the γ -secretase complex	11
1.4.1.1 Presenilin topology and γ -secretase complex architecture	11
1.4.1.2 Physiological function of γ -secretase-mediated intramembrane proteolysis	13
1.4.1.2.1 Notch regulated intramembrane proteolysis and cell fate determination	14
1.4.1.2.2 APP intramembrane proteolysis and Alzheimer's Disease	14
1.4.2 SPP and SPPLs	16
1.4.2.1 Key features of SPP/SPPL-type GxGD proteases	16
1.4.2.2 Physiological functions of mammalian SPP/SPPL family members	18
1.4.2.2.1 SPP	18
1.4.2.2.2 The SPPL2 subfamily	20
1.4.2.2.3 SPPL3	21
1.4.3 Archaeal presenilin homologues	23
1.4.4 Common features of presenilin- and SPP/SPPL-type GxGD proteases	23
1.4.4.1 GxGD protease structure	23
1.4.4.2 Substrate requirements of GxGD proteases	24
1.4.4.3 Mechanism of GxGD protease-mediated intramembrane proteolysis	25
1.4.4.4 GxGD protease inhibitors	26
1.5. Foamy Viruses	28
1.5.1 Foamy Virus envelope glycoprotein	29

1.6. Protein glycosylation	30
1.6.1 Glycosyltransferase & glycosidases	31
1.6.2 Cellular N-glycosylation	31
1.6.3 Cellular O-glycosylation	34
2. Aims of the study	35
3. Materials & Methods	37
3.1 Materials	37
3.1.1 Laboratory equipment & reagents	37
3.1.2. Animals	37
3.1.4 Cell lines	37
3.1.4 Plasmids	38
3.2 Experimental procedures	39
3.2.1 Molecular cloning	39
3.2.1.1 Overview of expression constructs generated	39
3.2.1.2 Polymerase chain reaction.....	41
3.2.1.3 Submerged agarose gel electrophoresis	41
3.2.1.4 Restriction endonuclease digestion of DNA.....	41
3.2.1.5 Ligation	42
3.2.1.6 Site-directed mutagenesis	42
3.2.1.7 Transformation of <i>E. coli</i>	42
3.2.1.8 Preparation of plasmid DNA	43
3.2.1.9 Sequencing	43
3.2.2 Animal work	43
3.2.2.1 Animal housing and breeding.....	43
3.2.2.3 Tissue homogenisation	44
3.2.2.4 Generation of murine embryonic fibroblasts	45
3.2.2.5 Flow cytometric analysis of NK cell counts	45
3.2.2.5 In vitro differentiation of bone marrow-derived dendritic cells	46
3.2.3 Cell biology	46
3.2.3.1 General techniques	46
3.2.3.2 Transfection with plasmid DNA	47
3.2.3.3 RNAi.....	47
3.2.3.4 Inhibitor treatment	47
3.2.3.5 Immunocytochemistry and confocal microscopy	48

3.2.4 Biochemical methods	49
3.2.4.1 Preparation of cellular membranes	49
3.2.4.2 Preparation of whole cell lysates	49
3.2.4.3. Immunoprecipitations	50
3.2.4.4 Co-immunoprecipitations	50
3.2.4.5 Enzymatic deglycosylation	51
3.2.4.6 Trichloroacetic acid precipitation	51
3.2.4.7 SDS-polyacrylamide gel electrophoresis	51
3.2.4.7.1 Sample preparation	51
3.2.4.7.2 Gel casting and running equipment	52
3.2.4.7.3 Tris-glycine SDS-PAGE	52
3.2.4.7.4 Tris-tricine SDS-PAGE	53
3.2.4.7.5 Urea tris-bicin gels after Wiltfang	53
3.2.4.8 Electroblotting	54
3.2.4.9 Protein detection by Western blotting	54
3.2.4.10 Lectin blotting	57
3.2.4.11 MALDI-TOF mass spectrometric analysis of C-peptide cleavage products	57
3.2.4.12 RNA isolation and quantitative RT-PCR	58
3.2.4.13 Secretome analysis	58
4. Results	59
4.1 FVen is substrate for intramembrane proteolysis by SPPL3 and SPPL2a/2b	59
4.1.1 Cloning and expression of epitope-tagged FVen	59
4.1.2 FVen leader peptide is endoproteolysed by over-expressed SPPL3 in HEK293 cells	62
4.1.3 FVen leader peptide is endoproteolysed by over-expressed SPPL2a and SPPL2b	62
4.2 FVen proteolysis reveals unique properties of SPPL3	64
4.2.1 SPPL3-mediated cleavage of FVen is independent of shedding	64
4.2.2 SPPL3-mediated cleavage of FVen is insensitive to GxGD protease inhibitors	66
4.2.3 SPPL2a/SPPL2b endoproteolys the SPPL3 cleavage product ICD(L3)	68
4.2.4 Determination of SPPL cleavage sites in FVen	72
4.2.5 SPPL3 isoform 1 exhibits no proteolytic activity towards FVen	74
4.3 SPPL3 affects cellular N-glycosylation under physiological conditions	76
4.3.1 Characterisation of <i>Sppl3</i> -deficient mice	76
4.3.2 SPPL3 affects the electrophoretic mobility of cellular glycoproteins	78
4.3.3 SPPL3 alters cellular glycosylation of post-ER-localised glycoproteins	82

4.3.4 SPPL3 facilitates secretion of GnT-V	85
4.3.5 SPPL3-mediated GnT-V endoproteolysis occurs close to the lipid bilayer boundary	89
4.3.6 GnT-V is not a γ -secretase substrate	91
4.3.7 SPPL3 modulates cellular GnT-V activity	92
4.3.8 Impact of SPPL3 on cellular N-glycosylation is not solely due to effects on GnT-V	93
4.3.9 SPPL3 facilitates β 3GnT1 and β 4GalT1 secretion	95
4.4 SPPL3 facilitates secretion of type II membrane protein ectodomains	97
4.4.1 SPECS analysis identifies new potential SPPL3 substrates	97
4.4.2 Validation of selected newly identified candidate SPPL3 substrates	102
5. Discussion	105
5.1 Identification of FVenv as the first SPPL3 substrate	105
5.1.1 FVenv LP: signal peptide or type III membrane protein signal anchor?	105
5.1.2 FVenv is endoproteolysed by SPPL3 and SPPL2a/SPPL2b	106
5.1.3 Implications of FVenv intramembrane proteolysis for the virus life cycle	107
5.1.4 Signal/leader peptides of other retroviral env proteins	109
5.1.5 Analysis of SPPL3-mediated intramembrane proteolysis of FVenv	110
5.1.5.1 SPPL3 is hardly sensitive to transition state analogue GxGD protease inhibitors	110
5.1.5.2 SPPL3 cleaves a full-length membrane protein substrate	112
5.1.5.3 SPPL2a/SPPL2b cleave the SPPL3 cleavage product	113
5.1.5.4 Comparison of SPPL3 and other intramembrane proteases	114
5.2 SPPL3 facilitates secretion of selected type II membrane proteins	115
5.2.1 SPPL3 acts as a type II membrane-selective protein convertase or sheddase	115
5.2.2 SPPL3 substrates identified by a candidate-based approach	116
5.2.3 SPPL3 substrates identified by a proteome-wide approach	118
5.2.4 Two distinct classes of SPPL3 substrates	119
5.3 Physiological function(s) of SPPL3	120
5.3.1 SPPL3 is a global cellular regulator of complex N-glycosylation	120
5.3.1.1 Glycosyltransferase proteolysis	122
5.3.1.2 SPPL3 facilitates GnT-V secretion	124
5.3.1.3 SPPL3 facilitates secretion of β 3GnT1 and β 4GalT1	125
5.3.1.4 Other glycan-modifying SPPL3 substrates and candidate substrates	126
5.3.1.5 SPPL3 may serve as global cellular Golgi enzyme sheddase	127
5.3.2 Potential physiological implications of other newly identified SPPL3 substrates	127
5.3.2.1 SPPL3 may control integrity of the glycoprotein-galectin lattice	128

5.3.2.2 SPPL3 may affect glycosaminoglycan biosynthesis	129
5.3.2.3 SPPL3 may affect O-mannosylation	132
5.3.2.4 Effects on the biological activity of cellular glycoproteins	133
5.3.3 Sppl3 deficiency in mice	133
5.3.3.1 General considerations	133
5.3.3.2 NK cell deficiency	134
5.3.3.3 Male infertility	135
5.3.3.4 Strain-dependency of the Sppl3 knockout phenotype	137
5.3.3.5 Other SPPL3 in vivo models	137
5.4 How is SPPL3 activity regulated?	138
5.5 Does SPPL3 have a role in Golgi proteostasis?	140
References	143
Abbreviations	165
Acknowledgements	169
Curriculum vitae	171
Appendix	175

Summary

Intramembrane proteolysis - hydrolysis of membrane proteins within or close to their membrane-spanning regions - is a crucial cellular process that is conserved throughout all kingdoms of life. It is executed by distinct classes of polytopic membrane proteins, the intramembrane-cleaving proteases, that provide a hydrophilic, proteinaceous environment accommodating membrane protein substrates as well as water molecules within the hydrophobic membrane interior and catalyse peptide bond hydrolysis. In particular, intramembrane-cleaving aspartyl proteases have received attention as the presenilins, the catalytic subunits of the γ -secretase complex, were identified as key players in Alzheimer's disease pathophysiology. In addition to presenilins, mammalian genomes harbour presenilin homologues which include signal peptide peptidase (SPP) and SPP-like (SPPL) proteases.

Among these, the Golgi-resident protease SPPL3 stands out as it is highly conserved among metazoa and SPPL3 orthologues are also found in plants. However, due to the lack of known substrates, SPPL3 has thus far hardly been characterised. Hence, the purpose of this study was to identify its substrates and elucidate its physiological function(s).

In the first part of this study, the foamy virus envelope glycoprotein (FVenv) was identified as the first substrate of SPPL3. This allowed to study SPPL3's proteolytic activity in detail, with a focus on its substrate selectivity and sensitivity towards previously characterised inhibitors of intramembrane-cleaving aspartyl proteases. Importantly, this study revealed in addition that two other intramembrane-cleaving proteases, SPPL2a and SPPL2b, also endoproteolysed FVenv. SPPL2b in particular had been studied in detail before and therefore SPPL3- and SPPL2b-mediated endoproteolysis of FVenv were examined in parallel to directly compare these phylogenetically related intramembrane-cleaving proteases. This uncovered an unexpected idiosyncrasy of SPPL3 that clearly sets SPPL3 apart from other intramembrane-cleaving aspartyl proteases: SPPL3 endoproteolysed full-length FVenv and did not require the substrate's prior tailoring by another proteolytic activity - an otherwise common phenomenon among intramembrane-cleaving aspartyl proteases.

In the second part, the physiological function of SPPL3 was investigated. Alterations in the cellular levels of proteolytically active SPPL3 turned out to impact the composition of N-glycans attached to endogenous cellular glycoproteins. SPPL3 over-expression was accompanied by a decrease in glycoprotein molecular weight, i.e. a hypoglycosylation phenotype, while loss of SPPL3 expression in cell culture models but also *in vivo* resulted in a hyperglycosylation phenotype. This led to the identification of Golgi glycan-modifying enzymes such as GnT-V and β 3GnT1 as novel physiological substrates of SPPL3. Loss or reduction of SPPL3 expression, for instance, led to a marked intracellular accumulation of these enzymes, explaining the more extensive N-glycan elaboration and the hyperglycosylation phenotype observed under these conditions. At the same time secretion of these enzymes was reduced under these conditions. Together with additional observations such as the mapping of the SPPL3 cleavage site to the membrane-spanning region of GnT-V, this study demonstrates that SPPL3-mediated

intramembrane proteolysis of such glycan-modifying enzymes liberates their active site-harbouring ectodomains. Acting in this manner, SPPL3 controls the intracellular pool of active glycan-modifying enzymes.

Importantly, the finding that SPPL3 proteolytically cleaves full-length glycan-modifying enzymes and sheds their ectodomains is well in line with the observations made for FVen and suggested that SPPL3 acts functionally equivalent to classical sheddases or rhomboid proteases but much unlike all other characterised mammalian intramembrane-cleaving aspartyl proteases. To examine whether these observations hold also true on a global cellular scale, a proteomic approach was undertaken in the third part of the study to define the SPPL3 degradome of HEK293 cells in conditions of SPPL3 over-expression. On the one hand, this led to the identification of numerous novel, mostly Golgi-resident candidate SPPL3 substrates and, considering the physiological implications, suggests that SPPL3 is very intricately linked to Golgi function. On the other hand, this approach supports the initial hypothesis that SPPL3 acts as a cellular type II membrane protein-selective sheddase.

Taken together, this study provides the first in-depth characterisation of the intramembrane protease SPPL3 and reveals the cellular function of SPPL3. SPPL3 displays considerable and marked differences to other intramembrane-cleaving aspartyl proteases and emerges as a fundamental cellular sheddase that exhibits strong selectivity for type II-oriented, Golgi-resident membrane proteins. Products of SPPL3-mediated endoproteolysis of these Golgi factors are secreted and/or may be subject to intracellular degradation which compromises their catalytic activity. Thus, SPPL3 indirectly controls protein glycosylation in the Golgi apparatus.

Zusammenfassung

Intramembranproteolyse, die hydrolytische Spaltung von Membranproteinen innerhalb ihrer Transmembrandomänen, ist ein wichtiger zellulärer Prozess, der in allen Reichen der Lebewesen konserviert ist. Die Intramembranproteolyse wird von unterschiedlichen Klassen von polytopen Membranproteinen, den Intramembranproteasen, ausgeführt, die eine hydrophile Proteinumgebung innerhalb des hydrophoben Bereichs der Membran bilden. In dieser Umgebung finden sowohl Membranproteinsubstrate als auch Wassermoleküle Platz und Hydrolyse der Peptidbindung wird durch die Intramembranproteasen katalysiert. Vor allem die Aspartylintramembranproteasen haben sehr viel Aufmerksamkeit auf sich gezogen, da die Preseniline, die katalytischen Untereinheiten des γ -Sekretasekomplexes, als Schlüsselenzyme in der Pathophysiologie der Alzheimer-Erkrankung identifiziert wurden. Neben den Presenilinen finden sich in Säugetiergenomen auch Presenilinhomologe, welche sowohl die Signalpeptidpeptidase (SPP) als auch SPP-ähnliche (*SPP-like*, SPPL) Proteasen umfassen.

Aus diesen sticht die im Golgi lokalisierte Protease SPPL3 heraus, da sie in vielzelligen Tieren hochkonserviert ist und sich SPPL3-Orthologe auch in Pflanzen finden. Gleichzeitig ist SPPL3 jedoch, vor allem aufgrund der Tatsache, dass keine Substrate beschrieben wurden, bisher kaum charakterisiert. Daher war es das Ziel dieser Arbeit Substrate von SPPL3 zu identifizieren und seine physiologische Funktion(-en) aufzuklären.

Im ersten Teil dieser Arbeit wurde ein erstes SPPL3-Substrat, das foamy-virale Hüllglykoprotein (FVenv), identifiziert. Dies erlaubte die proteolytische Aktivität von SPPL3 und insbesondere seine Substratselektivität sowie seine Sensitivität gegenüber Inhibitoren von Aspartylintramembranproteasen im Detail zu untersuchen. Es konnte ebenfalls festgestellt werden, dass zwei weitere Intramembranproteasen, SPPL2a und SPPL2b, FVenv ebenfalls endoproteolytisch spalten. Vor allem SPPL2b war bereits zuvor im Detail untersucht worden und daher konnte die SPPL3- beziehungsweise SPPL2b-vermittelte Endoproteolyse von FVenv verglichen werden. Dies offenbarte eine unerwartete Eigenheit von SPPL3, welche SPPL3 deutlich von anderen Intramembranproteasen, vor allem den anderen Aspartylintramembranproteasen, unterscheidet: SPPL3 spaltete das FVenv-Holoprotein und bedarf keinem vorherigen Zuschneiden des Substrates durch eine andere proteolytische Aktivität - ein sonst sehr verbreitetes Phänomen bei Intramembranproteasen.

Im zweiten Teil sollte die physiologischen Funktion von SPPL3 untersucht werden. Dabei zeigte sich, dass Änderungen in der zellulären SPPL3-Aktivität große Auswirkungen auf die Zusammensetzung der N-Glykane auf endogenen zellulären Glykoproteinen haben. SPPL3-Überexpression ging mit einer Reduktion des Molekulargewichts untersuchter Glykoproteine, einem so genannten Hypoglykosylierungsphänotyp, einher, während der Verlust der SPPL3-Expression im Zellkulturmödell aber auch *in vivo* in einem Hyperglykosylierungsphänotyp resultierte. Dies führte zur Identifizierung von glykanmodifizierenden Enzymen im Golgi wie beispielsweise GnT-V und β 3GnT1 als physiologische SPPL3-Substrate. Verlust oder Reduktion der SPPL3-Expression führte zu einer starken intrazellulären Akkumulation dieser

Substrate, was die unter diesen Bedingungen beobachtete umfassendere N-Glykanausarbeitung sowie den Hyperglykosylierungsphänotyp erklärte. Gleichzeitig wurde die Sekretion dieser Enzyme unter diesen Bedingungen stark beeinträchtigt. Zusammen mit weiteren Beobachtungen wie der Bestimmung der SPPL3-Schnittstelle im Bereich der Transmembrandomäne von GnT-V zeigte diese Studie, dass die von SPPL3 vermittelte Intramembranproteolyse solcher glykan-modifizierenden Enzyme deren Ektodomainen freisetzt und SPPL3 folglich auf diese Weise das intrazelluläre Reservoir aktiver glykan-modifizierender Enzyme kontrolliert.

Hervorzuheben ist dabei, dass diese Erkenntnis in guter Übereinstimmung mit den für FVen gemachten Beobachtungen steht. Dies legt wiederum nahe, dass SPPL3 in funktioneller Hinsicht mit einer klassischen *Sheddase* oder einer Rhomboidprotease gleichgestellt ist, sich jedoch von allen anderen charakterisierten Aspartylintramembranproteasen in Säugetieren unterscheidet. Um herauszufinden, ob diese Beobachtungen auch auf globaler zellulärer Ebene Bestätigung finden, wurde eine Proteomanalyse im dritten Teil dieser Arbeit durchgeführt, um das SPPL3-Degradom in HEK293-Zellen unter Überexpressionsbedingungen zu definieren. Dies führte einerseits zur Identifizierung vieler weiterer neuer, zumeist im Golgi lokalizierter SPPL3-Substratkandidaten und legte andererseits unter physiologischen Gesichtspunkten nahe, dass SPPL3 sehr mit der Funktion des Golgi-Apparats verwoben ist. Andererseits unterstützten diese Ergebnisse sehr deutlich die formulierte Hypothese, dass SPPL3 als zelluläre Typ-II-Membranprotein-selektive *Sheddase* agiert.

Zusammengefasst liefert diese Arbeit die erste ausführliche Charakterisierung der Intramembranprotease SPPL3. SPPL3 zeigt erhebliche Unterschiede zu anderen Aspartylintramembranproteasen und erweist sich damit als bedeutende zelluläre *Sheddase* mit einer auffälligen Selektivität für Typ-II-orientierte, im Golgi lokalisierte Membranproteine. Produkte der Endoproteolyse dieser Golgi-Proteine werden sekretiert und/oder werden möglicherweise intrazellulär degradiert, was wiederum ihre eigentliche intrazelluläre Funktion beeinträchtigt. Folglich kontrolliert SPPL3 indirekt die Proteinglykosylierung im Golgi-Apparat.

1. Introduction

Physiological processes require tightly regulated and concerted activity of proteins. This is ensured by a number of mechanisms, including the regulation of gene expression, but on the post-translational level by regulation of protein secretion or its sub-cellular localisation and trafficking as well as by post-translational modifications. Among the latter, hydrolytic cleavage of peptide bonds or proteolysis is special as it is a non-reversible process. Proteolytic processing of protein substrates allows for instance for the activation of catalytically inactive zymogens, the release of bioactive factors from cells or scaffolds and the regulated degradation or inactivation of proteins (Turk *et al.*, 2012).

Like extracellular and intracellular protein factors, membrane-anchored proteins are also subject to proteolytic processing, yet they harbour hydrophobic transmembrane domains (TMDs) which span the hydrophobic core of cellular membranes (Rath & Deber, 2012) and thus are hardly accessible to conventional proteases. It is meanwhile, however, established that proteolytic cleavage can in fact occur within membrane-spanning protein domains of numerous membrane proteins and that this process, also termed regulated intramembrane proteolysis (RIP) (Brown *et al.*, 2000), is mediated by non-conventional proteases, the intramembrane-cleaving proteases (I-CLIPs) (Wolfe & Kopan, 2004).

1.1. Regulated Intramembrane Proteolysis

The term RIP was coined by Brown *et al.* in 2000 and describes a two-step proteolytic processing of transmembrane proteins (Brown *et al.*, 2000) which is schematically depicted for a single-pass membrane protein in Fig. 1.1. In an initiating step, transmembrane protein substrates are proteolytically cleaved within the juxtamembrane region. In case of single-pass membrane proteins this liberates the bulk of their respective ectodomain into the luminal and/or extracellular space, leaving behind a membrane-embedded fragment with a significantly shortened ectodomain. The subsequent secondary cleavage occurs within the substrate's TMD and liberates an additional luminal/extracellular protein fragment as well as a cytosolic peptide, the intracellular domain (ICD). In most cases the secondary cleavage depends on the preceding primary one as full-length membrane protein substrates cannot be processed by most intramembrane proteases catalysing the secondary cleavage. RIP is conserved from prokaryotes to mammals and proteolytic processing of numerous membrane protein substrates follows this basic principle (Brown *et al.*, 2000). Importantly, RIP of a particular membrane protein substrate will generate distinct cleavage products which may be biologically active and have important (patho-)physiological functions (Brown *et al.*, 2000; Lichtenthaler *et al.*, 2011).

1.1.1. Primary Cleavage: Ectodomain Shedding

When considering type I or type II single-pass membrane protein RIP substrates, the primary cleavage event is termed *shedding* as it liberates the bulk of the protein's ectodomain from its membrane anchor. Enzymes catalysing this proteolytic cleavage are referred to as *sheddases*.

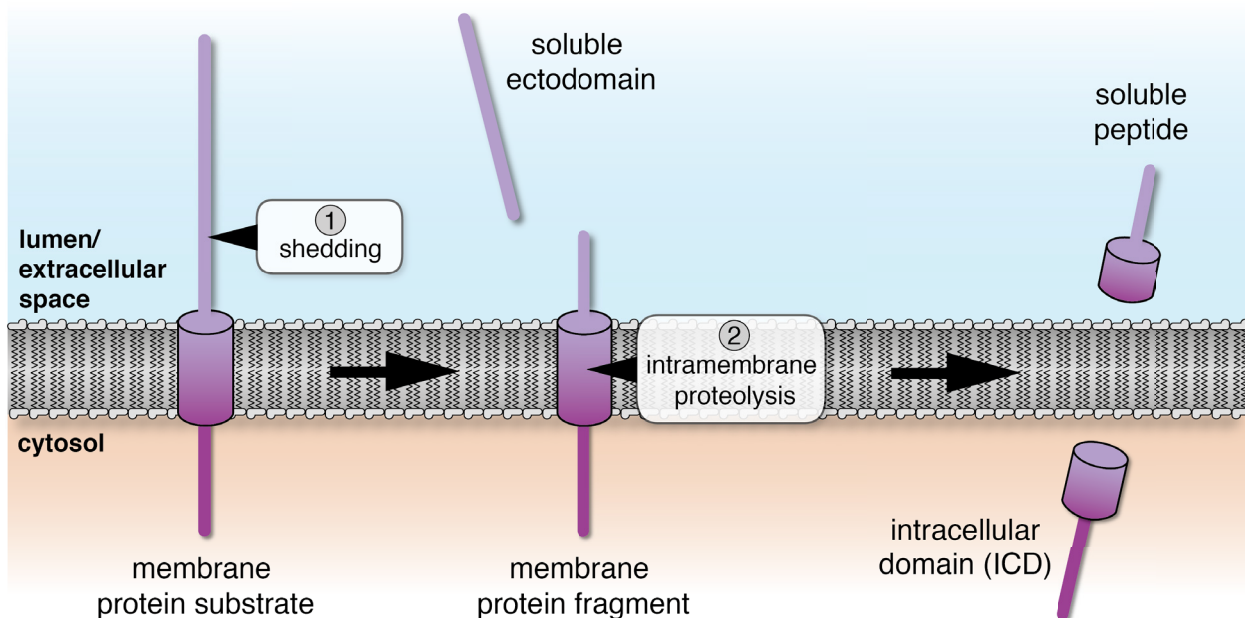


Fig. 1.1: Regulated intramembrane proteolysis (RIP). Membrane-spanning substrates are first endoproteolysed within their juxtamembrane region (*shedding*, (1)) generating a soluble ectodomain and a membrane-embedded protein fragment. The latter may then be subject to intramembrane proteolysis within its TMD (2), liberating a soluble fragment into the luminal or extracellular space and an ICD into the cytosol.

Often, they belong to the *a disintegrin and metalloprotease* (ADAM) family of metzincin metalloproteases. These are type I membrane proteins which mediate ectodomain shedding of numerous membrane protein substrate proteins via their Zn^{2+} -harbouring metalloprotease domain (reviewed in (Edwards *et al*, 2008)). Depending on the substrate's topology, ADAM-mediated ectodomain shedding generates membrane-embedded N- or C-terminal fragments (NTFs or CTFs) that often are subject to subsequent intramembrane proteolysis. Alternatively, membrane-proximal ectodomain cleavage may also be catalysed by other proteases, for instance by aspartyl proteases (e.g. β -site of amyloid precursor protein cleaving enzyme 1 (BACE), see 1.4.1.2.2), type II transmembrane serine proteases (Hooper *et al*, 2001), and others.

Moreover, type III membrane proteins that comprise more than one TMD may similarly be subject to RIP (Brown *et al*, 2000). Unlike during RIP of single-pass membrane proteins, cleavage products of type III proteins generated by the primary cleavage event are not released from membranes or secreted. In this case the primary membrane-proximal cleavage that initiates RIP occurs within a luminal loop between two TMDs and, accordingly, both cleavage products remain tethered to the membrane via these TMDs.

1.1.2. Secondary Cleavage: Intramembrane Proteolysis

Following ectodomain removal, truncated membrane-embedded protein fragments may subsequently be endoproteolysed within their membrane-spanning domains by I-CLiPs. All I-CLiPs are multi-pass membrane proteins and can, like conventional proteases (Hartley, 1960), be subcategorised according to the respective mechanism of catalysis (Wolfe, 2009). So far, intramembrane-cleaving metalloproteases (section 1.2) as well as serine (section 1.3) and aspartyl proteases (section 1.4) have been described. Currently, no intramembrane-cleaving

cysteine proteases are known but very recently a novel glutamate I-CLiP was identified (Manolaridis *et al*, 2013).

Intramembrane proteolysis, however, is clearly distinct from proteolysis catalysed by conventional proteases on soluble substrates. First, access to polar water molecules which are critically required for hydrolytic cleavage of peptide bonds is limited within the membrane's hydrophobic interior. However, structural studies on selected I-CLiPs have meanwhile established that these enzymes overcome this by providing a proteinaceous environment which enables water molecules to reach the scissile peptide bond allowing for proteolysis within the hydrophobic membrane plane (reviewed in (Urban & Shi, 2008)). Second, due to the hydrophobic nature of the membrane core, polar or charged amino acid residues are usually excluded from substrate TMDs (Heijne, 2006; Rath & Deber, 2012) and TMD peptides often adopt an α -helical conformation (Popot & Engelman, 2000; Rath & Deber, 2012) which would hinder proteases from accessing the peptide backbone and thus prevent proteolysis. It was therefore hypothesised that intramembrane proteolysis may only occur when substrate TMDs harbour an intrinsic structural flexibility or instability to support a local unfolding upon binding to an I-CLiP which then allows for proteolytic attack on scissile bonds (Lemberg & Martoglio, 2004).

1.2. Intramembrane-cleaving metalloproteases

Intramembrane-cleaving metalloproteases were the first I-CLiPs identified. The human family member, S2P (Fig. 1.2a), was identified 1997 by complementation cloning as a factor facilitating liberation of membrane-tethered transcription factors into the cytosol and the nucleus (Rawson *et al*, 1997). Human S2P and S2P-like I-CLiPs found in other species are multi-pass membrane proteins and harbour a **HExxH** motif¹ characteristic of zinc-dependent metalloprotease in one of their TMDs and an additional **LDG** motif in another one (Fig. 1.2a) (Brown *et al*, 2000; Wolfe, 2009). These motifs are critically required for proteolytic activity and, therefore, were anticipated to co-ordinate the active site Zn^{2+} ion (Rawson *et al*, 1997; Zelenski *et al*, 1999). This notion

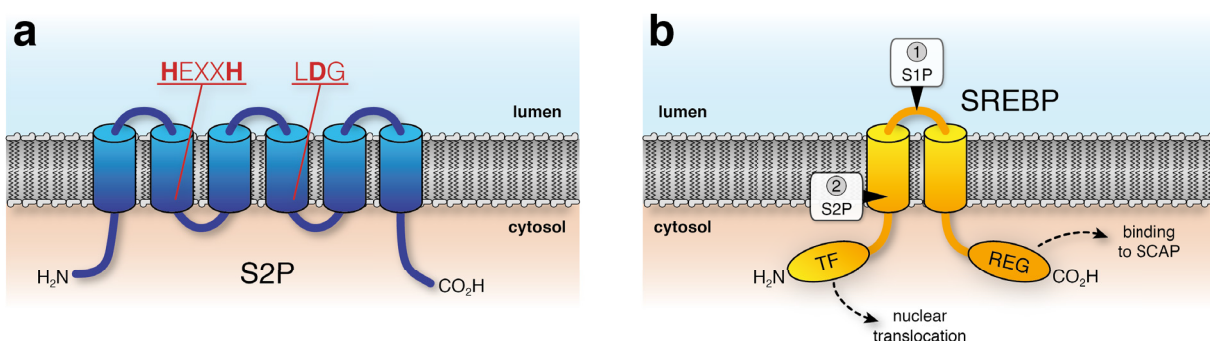


Fig. 1.2: Intramembrane-cleaving metalloproteases. (a) Schematic depiction of the S2P which harbours six TMDs and has cytosolic N- and C-termini. Catalytic consensus motifs in TMD2 and TMD4 are highlighted in red, residues co-ordinating the active site Zn^{2+} in bold. (b) Processing of SREBPs by S1P and S2P proteases. SREBPs have a hair-pin topology and are successively cleaved by S1P within the luminal loop and by S2P in their first TMD. The latter cleavage liberates the *trans*-activating domain (TF) that translocates to the nucleus. The regulatory domain (REG) binds to the cholesterol sensor SCAP. S1P and S2P process other substrates in a similar fashion. Adapted from (Wolfe, 2009).

¹ Here and in the following catalytically required active site residues are highlighted in bold.

received strong support from a crystal structure that was recently reported for *Methanocaldococcus jannaschii* S2P (Feng *et al*, 2007).

S2P and S2P-like proteases facilitate proteolytic release of biologically active protein fragments from their membrane anchors (reviewed in (Brown *et al*, 2000; Wolfe, 2009; Chen & Zhang, 2010)). In humans their substrates include membrane-bound transcription factors such as the human sterol regulatory element binding protein (SREBP) (Hua *et al*, 1995) and others that have a hairpin topology with two membrane-spanning segments (Fig. 1.2b). Importantly, S2P strictly follows the RIP scheme and requires its substrates to be cleaved within their luminal loop prior to intramembrane cleavage. This is mediated by another protease, the site-1 protease (S1P), a subtilisin-like serine protease (Shen & Prywes, 2004). In bacteria, S2P substrates are transcription factors that are tethered to the membrane by a single TMD but they likewise have to be tailored before being endoproteolysed by S2P. Unlike S2P, however, S1P is not conserved throughout species and in other organisms unrelated proteases possess a S1P activity (Chen & Zhang, 2010).

In mammals, the S1P-S2P proteolytic cascade was found to be crucially involved in the regulation of cholesterol metabolism (Fig. 1.2b) (Brown *et al*, 2000; Wolfe, 2009; Chen & Zhang, 2010). SREBPs are membrane-tethered transcription factors that, when translocated to the nucleus, regulate expression of genes involved in the biosynthesis of cholesterol (Brown & Goldstein, 1997). Under normal conditions, SREBPs are retained in the ER by interaction with the membrane protein SCAP which at the same time functions as a cholesterol sensor. As S1P and S2P localise to post-ER compartments they cannot access their substrates. Consequently, SREBP signalling is prevented. Upon depletion of cellular cholesterol, however, SCAP facilitates anterograde transport of SREBPs to the Golgi compartment. There, S1P and S2P endoproteolysse SREBPs and their *trans*-activating domain is released from its membrane anchor, translocates to the nucleus, and up-regulates cholesterol biosynthesis (Brown *et al*, 2000; Wolfe, 2009; Chen & Zhang, 2010). In a very similar manner the transcription factor ATF6 is liberated from post-ER membranes as part of the unfolded protein response in eukaryotes (Kaufman *et al*, 2002) and bacterial S2P-like proteases liberate specific bacterial transcription initiation factors, the σ -factors, from membranes (Chen & Zhang, 2010).

1.3. Intramembrane-cleaving serine proteases

Intramembrane-cleaving serine proteases or *rhomboids* (Fig. 1.3) are present in all kingdoms of life and have evolved fundamental but at the same time highly diverse physiological functions. In bacteria rhomboids are implicated in quorum sensing, while in intracellular protozoan parasites rhomboids cleave adhesins and are required for host cell invasion (Urban, 2006; Freeman, 2008; Urban & Dickey, 2011). Being clearly crucial to epidermal growth factor (EGF) signalling in *Drosophila*, the rhomboids' role in other invertebrates and vertebrates is less well understood (Urban, 2006; Urban & Dickey, 2011). The mammalian rhomboid RHBDF4 was recently found to be up-regulated by ER stress and to function as an ubiquitin-dependent intramembrane proteases that cleaves unstable membrane proteins and initiates their degradation by the ER-associated degradation (ERAD) machinery (Fleig *et al*, 2012). The mitochondrial rhomboid protease PARL has been intricately linked to mitochondrial function,

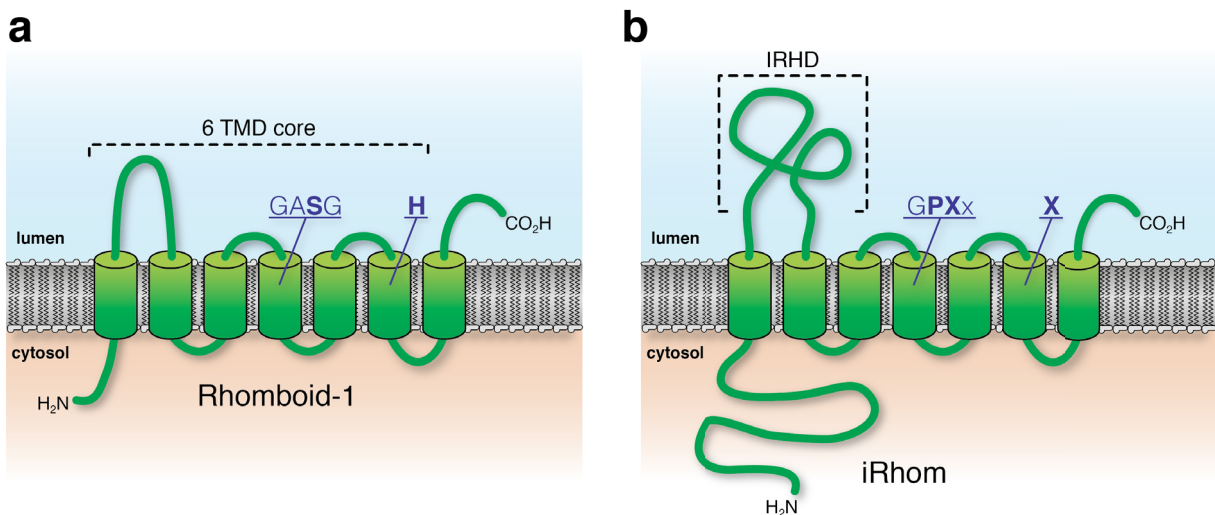


Fig. 1.3: Rhomboid I-CLiPs. (a) Schematic depiction of *Drosophila* Rhomboid-1. Rhomboid-1 is a rhomboid with a 6+1 topology, containing a TMD C-terminal to the six TMD rhomboid core (dotted line). Catalytic residues in TMD4 and TMD6 are highlighted in bold. The catalytic serine is found in a conserved GxSx motif. (b) Schematic depiction of an iRhom, which - unlike active rhomboids - has an extended N-terminus, a large iRhom homology domain (IRHD) between TMD1 and TMD2 and a proline residue directly upstream of the catalytic serine position. Active site serine and histidine residues may be missing in iRhoms (X). Adapted from (Freeman, 2008).

mitophagy and apoptosis and may be involved in Parkinson's disease pathophysiology (reviewed in (Urban & Dickey, 2011)). Presently, however, the physiological role of other mammalian rhomboid proteases remains largely unknown.

1.3.1 Catalytic mechanism, topology and structure of rhomboids

Rhomboids employ a catalytic serine-histidine dyad to catalyse peptide bond hydrolysis (Fig. 1.3a) (Lemberg *et al*, 2005). They are polytopic membrane proteins, but *in silico* topology analyses predict some degree of variation in rhomboid topology (Lemberg & Freeman, 2007a). All rhomboids comprise a six TMD core domain that harbours the residues of the serine-histidine dyad in TMD4 and TMD6, respectively. Some rhomboids, for example *Drosophila* Rhomboid-1 (Fig. 1.3a), contain an additional C-terminal TMD, while others like mitochondrial rhomboids have an additional TMD N-terminal of the six TMD core.

In recent years, a number of crystal structures have been obtained for bacterial rhomboids (reviewed in (Lemberg & Freeman, 2007b; Freeman, 2008; Urban, 2010)). In sum, they revealed that the six TMD helices of the rhomboid core form a tight bundle in the membrane plane and prove that proteolysis catalysed by rhomboids in fact occurs inside the membrane plane as the active site is buried within this core bundle.

1.3.2 Substrate requirements and regulation of rhomboid activity

Rhomboids endoproteolyse type I membrane protein substrates (i.e. in N_{out}/C_{in} topology), such as EGF ligands like *Drosophila* Spitz (Urban, 2006; Lemberg & Freeman, 2007b; Freeman, 2008). The topology of mitochondrial rhomboids, however, is inverted and, accordingly, they cleave N_{in}/C_{out} substrates (Lemberg & Freeman, 2007a; 2007b). Cleavage within rhomboid substrates occurs in a region close to the membrane boundary and rhomboids in fact appear to exhibit some degree of specificity towards particular substrate regions (Urban & Freeman, 2003;

Strisovsky *et al*, 2009). Importantly, a recent study established that rhomboids recognise a rather specific sequence motif within their substrates that harbours a small amino acid residue in the P1 position as well as hydrophobic and large ones in P4 and P2' positions making rhomboids sequence-specific I-CLiPs (Strisovsky *et al*, 2009).

Intriguingly, rhomboid I-CLiPs directly endoproteolyse full-length substrates and do not rely on prior substrate processing by another protease (Urban, 2006; Lemberg & Freeman, 2007b; Freeman, 2008). Hence, they do formally not follow the RIP concept (see 1.1) as they are not regulated by a preceding proteolytic shedding event. In fact, rhomboids themselves act functionally equivalent to sheddases as they liberate membrane-bound precursors. Their activity seems to be controlled by regulation of gene expression (Urban, 2006) and by sub-cellular segregation of substrate and protease (reviewed in (Urban, 2006; Freeman, 2008)).

1.3.3 Proteolytically inactive rhomboid-like proteins

In addition to active rhomboid I-CLiPs, proteolytically inactive homologues, the so-called inactive rhomboids (iRhoms, Fig. 1.3b) and the derlins, have been identified (Lemberg & Freeman, 2007a; Adrain & Freeman, 2012). Sequence analysis of iRhoms revealed that they form a distinctive sub-clade of the rhomboid family (Lemberg & Freeman, 2007a) but also that some iRhoms lack either or both catalytic residues required for rhomboid proteolytic activity suggesting they are not proteolytically active (Lemberg & Freeman, 2007a; Adrain & Freeman, 2012). iRhoms share with most mammalian rhomboids the characteristic topology. Unlike active rhomboids, they harbour, however, a conserved proline residue immediately upstream of the expected position of the catalytic serine and a characteristic insertion of a conserved, cysteine-rich and likely globular iRhom homology domain (IRHD) between TMD1 and TMD2 (Lemberg & Freeman, 2007a; Freeman, 2008). iRhoms are highly conserved in animals (Lemberg & Freeman, 2007a) and only recently have been characterised functionally (Zettl *et al*, 2011; Adrain *et al*, 2012; McIlwain *et al*, 2012). iRhoms apparently lack proteolytic activity towards transmembrane proteins yet retain their capacity to associate with such factors and appear to control ER-to-Golgi trafficking of transmembrane proteins (Adrain & Freeman, 2012). In *Drosophila*, for instance, iRhom blocks ER-to-Golgi transport of growth factors (Zettl *et al*, 2011), whereas in mice iRhom2 promotes ER export of certain membrane protein clients (Adrain *et al*, 2012; McIlwain *et al*, 2012). The existence of inactive protease pseudo-enzymes is, however, a unique feature of rhomboid I-CLiPs and presently no proteolytically inactive homologues of other I-CLiPs have been described.

1.4. Intramembrane-cleaving aspartyl proteases

Intramembrane-cleaving aspartyl proteases constitute the third family of I-CLiPs². In aspartyl I-CLiPs, one of the catalytic aspartate residues is found within a conserved GxGD motif and these proteases are therefore collectively referred to as GxGD proteases (Steiner *et al*, 2000). They include the presenilins (Steiner *et al*, 2000) (see 1.4.1), signal peptide peptidase (SPP)

² Note that, herein, the terms "family" and "subfamily" are not used in accordance with the MEROPS peptidase database (merops.sanger.ac.uk). MEROPS lists GxGD proteases as two independent protease families with presenilins (A22A) and SPP/SPPs (A22B) each forming a subfamily of the protease family A22 and TFPPs (A24A) and PFPs (A24B) of the family A24.

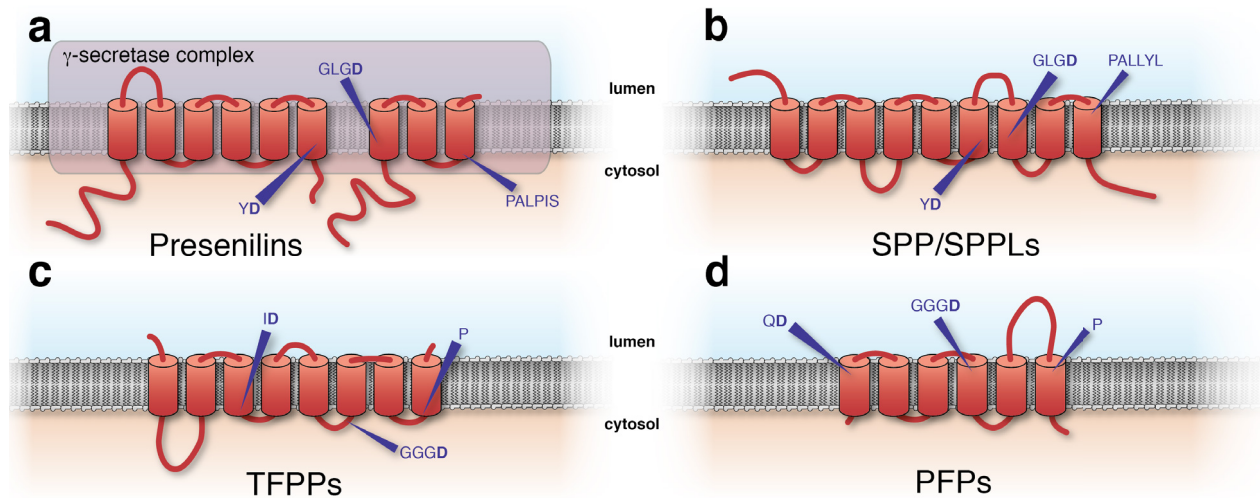


Fig. 1.4: GxGD-type aspartyl ICLIPs. The family of GxGD-type intramembrane-cleaving aspartyl proteases comprises the presenilins (a), SPP/SPPLs (b), TFPPs (c), and PFPs (d). All these proteases are multi-pass membrane proteins harbouring an active site GxGD motif in one of their TMDs and a second catalytic aspartate residue in another TMD (purple arrowheads). Human GxGD proteases have a conserved PAL motif within their last TMD and in TFPPs and PFPs a conserved proline residue can be found at the very same site. Note that presenilins (a) and SPP/SPPLs (b) share a highly homologous structural organisation but their overall topology is inverted. Presenilins are not catalytically active *in vivo* unless found with additional co-factors within the γ -secretase complex (purple box). Structures depicted here resemble human PS1 (a), human SPP (b), *Vibrio cholerae* TcpJ (c), and *Methanococcus maripaludis* FlaK (d). Taken from (Voss *et al*, 2013).

and SPP-like (SPPL) proteases (Weihofen *et al*, 2002; Ponting *et al*, 2002; Grigorenko *et al*, 2002) (see 1.4.2) as well as the bacterial type IV pre-pilin peptidases (TFPPs) (Steiner *et al*, 2000; LaPointe & Taylor, 2000) and the Archaeal pre-flagellin peptidases (PFPs) (Bardy & Jarrell, 2003) (Fig. 1.4).

1.4.1 Presenilins and the γ -secretase complex

As early as 1995 it became apparent that mutations in *PSEN1* and *PSEN2*, the genes encoding the two human presenilins, presenilin 1 (PS1) and presenilin 2 (PS2), respectively, are associated with early-onset, familial forms of Alzheimer's disease (AD) (Rogaev *et al*, 1995; Sherrington *et al*, 1995; Levy-Lahad *et al*, 1995b; 1995a). Presenilins have since been subject to extensive examination and, hence, are without doubt the best-studied GxGD proteases.

1.4.1.1 Presenilin topology and γ -secretase complex architecture

Presenilins are the catalytic subunits of the heterotetrameric γ -secretase complex (Fig. 1.5). In addition to presenilin (either PS1 or PS2 in mammals), the γ -secretase complex contains the single-span membrane protein Nicastrin as well as presenilin enhancer-2 (PEN-2) and an isoform of the polytopic membrane protein anterior pharynx defective-1 (APH-1) (Haass, 2004). Most likely these subunits are found in the γ -secretase complex in a 1:1:1:1 stoichiometry (Sato *et al*, 2007). All four subunits are required but at the same time sufficient for assembly of an active γ -secretase complex (Edbauer *et al*, 2003; Kimberly *et al*, 2003). In addition, studies observed co-isolation of additional protein factors with the γ -secretase complex, e.g. of CD147 (Zhou *et al*, 2005). However, in a subsequent study such factors failed to co-isolate with

catalytically active γ -secretase (Winkler *et al*, 2009), questioning their suspected roles as crucial complex components.

Presenilin itself is a multi-pass membrane protein and adopts a nine TMD topology (Fig. 1.4a & Fig. 1.5a) (Henricson *et al*, 2005; Laudon *et al*, 2005; Spasic *et al*, 2006). Its proteolytic activity depends on two aspartate residues located in the adjacent TMD6 and TMD7, the first one within a conserved YD motif (D257 in human PS1), the second within the GxGD motif (D385 in human PS1) (Wolfe *et al*, 1999; Steiner *et al*, 1999; Laudon *et al*, 2004). In the native γ -secretase complex, these two residues were found to be facing each other in close proximity and to be accessible to water, supporting their role in catalysis (Tolia *et al*, 2006; Sato *et al*, 2006a). Also, the PAL motif in the N-terminal region of TMD9 was shown to be accessible to water and to be located close to the catalytic aspartate residue D257 in TMD6 (Tolia *et al*, 2008; Sato *et al*, 2008). Taken together, these biochemical data suggest that TMD6, TMD7, and TMD9 of presenilin tightly associate to form the hydrophilic active site of γ -secretase. Interestingly, a similar spatial arrangement of TMD6, TMD7, and TMD9 is apparent in the crystal structures of Archaeal GxGD proteases (Hu *et al*, 2011; Li *et al*, 2013).

Presenilin is endoproteolysed within the extended cytosolic loop that connects TMD6 and TMD7 by an at that time elusive "presenilinase" activity that generates presenilin NTF and CTF (Thinakaran *et al*, 1996). Presenilinase activity, however, is impaired when the catalytic aspartate residues are mutagenised (Wolfe *et al*, 1999) and presenilinase precision is affected by FAD mutations in presenilin (Fukumori *et al*, 2010), suggesting that endoproteolysis is in fact autocatalytic. Presenilin NTF and CTF remain tightly associated as heterodimer (Capell *et al*,

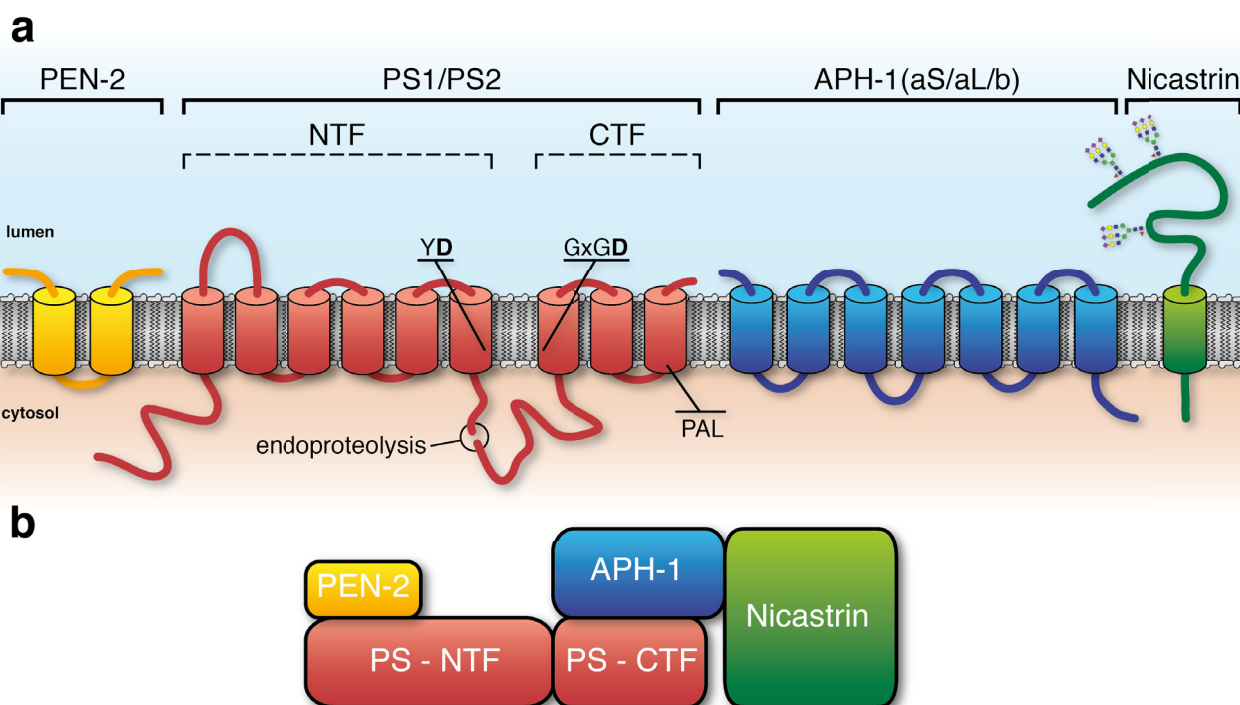


Fig. 1.5: Architecture of the human γ -secretase complex. (a) Active, mature γ -secretase is a heterotrimeric complex consisting of PEN-2 (yellow), either PS1 or PS2 (red), an APH-1 isoform (blue), and the glycoprotein Nicastrin (green). Active site motifs in presenilin are highlighted. Note that presenilin NTF and CTF are generated by endoproteolysis between TMD6 and TMD7. (b) Spatial subunit arrangement of native γ -secretase as determined by chemical cross-linking. Adapted from (Steiner *et al*, 2008b).

1998) and are bound by transition state analogue inhibitors of γ -secretase suggesting that the NTF/CTF heterodimer is the actual active subunit of γ -secretase (Esler *et al*, 2000).

Nicastrin was identified by co-immunoprecipitation with PS1 and PS2 in human cells (Yu *et al*, 2000). It is a type I membrane protein with a large ectodomain and, in its mature form, harbours a number of asparagine-linked complex glycans (Edbauer *et al*, 2002; Yang *et al*, 2002; Leem *et al*, 2002). Its ectodomain was proposed to serve as substrate receptor of the γ -secretase complex (Shah *et al*, 2005), but this finding is currently debated (Chávez-Gutiérrez *et al*, 2008). PEN-2 is a small hairpin protein that stabilises the presenilin NTC/CTF heterodimer (Prokop *et al*, 2004). The fourth complex component is APH-1 which adopts a seven TMD topology (Fortna *et al*, 2004). Elaborate biochemical analysis using chemical cross-linking of endogenous γ -secretase complexes purified from cultured cells revealed an overall model of intra-complex interactions (Fig. 1.5b). According to this, PEN-2 associates with the respective presenilin NTF, which in turn is associated with the presenilin CTF. APH-1 was cross-linked to both the presenilin CTF and to Nicastrin suggesting a tight spatial interaction of these subunits (Steiner *et al*, 2008b).

As an oligomeric complex, γ -secretase has to be assembled in a concerted and stepwise manner and progress of assembly can be examined experimentally by monitoring Nicastrin maturation and presenilin endoproteolysis. Experimental evidence (LaVoie *et al*, 2003; Takasugi *et al*, 2003; Capell *et al*, 2005) suggests that γ -secretase assembly proceeds as follows: In the ER, it is initiated by the formation of a Nicastrin and APH-1 heterodimer which subsequently binds the presenilin holoprotein. Association of PEN-2 with the Nicastrin-APH-1-presenilin heterotrimereric sub-complex then triggers presenilin endoproteolysis and the fully assembled heterotetrameric γ -secretase complex reaches the Golgi compartment where Nicastrin becomes complexly N-glycosylated. ER-localised γ -secretase appears to be catalytically inactive (Cupers *et al*, 2001) and proteolytically active γ -secretase complexes likely reside at the plasma membrane as well as within the endosomal/lysosomal compartment (Kaether *et al*, 2006).

1.4.1.2 Physiological function of γ -secretase-mediated intramembrane proteolysis

Numerous (> 90) membrane proteins have been described to be hydrolysed by the γ -secretase complex (Kopan & Ilagan, 2004; Haapasalo & Kovacs, 2011) and more are being identified. γ -secretase-mediated cleavage of such substrates liberates protein fragments from the membrane with potential biological activity. In some cases, it is well established that ICDs generated can potentially translocate to the nucleus and regulate transcription of target genes. In such cases, RIP in fact constitutes a pathway of signal transduction (Fortini, 2002). However, in light of the large number of substrates identified and the apparent absence of primary sequence-based substrate recognition motifs (Beel & Sanders, 2008), it was postulated that γ -secretase acts as an intramembrane equivalent of the cytosolic proteasome and facilitates non-selective degradative turn-over of type I membrane protein fragments (Kopan & Ilagan, 2004). However, proteomic datasets challenge this view as only a minor fraction of proteins in HeLa cells were found to be subject to γ -secretase cleavage (Hemming *et al*, 2008) suggesting that not all type I membrane proteins are turned over by γ -secretase and γ -secretase displays a certain degree of substrate selectivity. Intramembrane cleavage of γ -secretase substrates has

been linked to various fundamental (patho-)physiological processes (reviewed in (Haapasalo & Kovacs, 2011), including Notch-dependent cell fate determination and differentiation (see 1.4.1.2.1) and AD aetiology (see 1.4.1.2.2).

1.4.1.2.1 Notch regulated intramembrane proteolysis and cell fate determination

Notch signalling is a juxtacrine signalling pathway which determines cell fate specification in early ontogenetic events as well as in adult organisms (reviewed in (Artavanis-Tsakonas *et al*, 1999)). Notch receptors are type I transmembrane proteins that undergo extensive post-translational modifications, including proteolytic processing (Fortini, 2002). Nascent Notch is subject to processing by furin in the Golgi network (S1 cleavage), is subsequently trafficked to the cell surface where, upon interaction with its membrane-anchored ligands on neighbouring cells, it is cleaved by ADAM proteases (S2 cleavage). Subsequent intramembrane cleavage of the membrane-embedded shedding product is mediated by the γ -secretase complex (S3 and S4 cleavages) (Fortini, 2002). This leads to the liberation of the Notch ICD (NICD) (Schroeter *et al*, 1998; De Strooper *et al*, 1999) as well as to secretion of a Notch β -peptide (Okochi *et al*, 2006). NICD translocates to the nucleus of the signal-receiving cell and interacts with the DNA-binding protein CSL (C promoter binding factor/suppressor of hairless/Lag-1) and the co-activator Mastermind to promote transcription of target genes (Fortini, 2002). The fundamental importance of Notch signalling in metazoan development is highlighted in animal models deficient in pathway components. In particular, mice that lack functional PS1 and PS2, PEN-2, Nicastrin, or the APH-1 isoform APH-1A die *in utero* and are characterised by severe developmental defects that resemble those observed for animals deficient in Notch (Wong *et al*, 1997; Li *et al*, 2003; Serneels *et al*, 2005; Bammens *et al*, 2011).

1.4.1.2.2 APP intramembrane proteolysis and Alzheimer's Disease

The amyloid precursor protein (APP) is another type I membrane protein that is a γ -secretase substrate (reviewed in (Haass, 2004; Haapasalo & Kovacs, 2011; Lichtenthaler *et al*, 2011; Zhang *et al*, 2012)). The proteolytic processing of APP may either be amyloidogenic producing hydrophobic amyloid β (A β) peptides or non-amyloidogenic (Fig. 1.6) (Lichtenthaler *et al*, 2011; Zhang *et al*, 2012). Ectodomain shedding that initiates the amyloidogenic processing of APP is executed by the β -site of APP cleaving enzyme 1 (BACE1). BACE1 cleavage generates a soluble APP ectodomain (sAPP β) and a membrane-embedded 99 amino acid CTF (CTF β). The latter, in turn, is substrate to γ -secretase-mediated intramembrane proteolysis, which generates an APP ICD (AICD) as well as A β peptides (see below), the latter being key players in AD pathophysiology (Selkoe, 1991; Hardy & Higgins, 1992; Haass & Selkoe, 2007). The physiological function of the AICD, however, is controversial (see discussion in (Lichtenthaler *et al*, 2011; Zhang *et al*, 2012)). Alternatively, APP is endoproteolysed by α -secretase activity (Esch *et al*, 1990), which is predominantly executed by ADAM10 (Kuhn *et al*, 2010). α -secretase shedding occurs within the A β domain of APP and, thus, precludes A β peptide generation and is non-amyloidogenic (Lichtenthaler *et al*, 2011; Zhang *et al*, 2012). In addition to sAPP α , a 83 amino acid CTF α is generated by α -secretase cleavage of APP and, like CTF β , CTF α is subject to γ -secretase-catalysed intramembrane proteolysis leading to the generation of the cytosolic

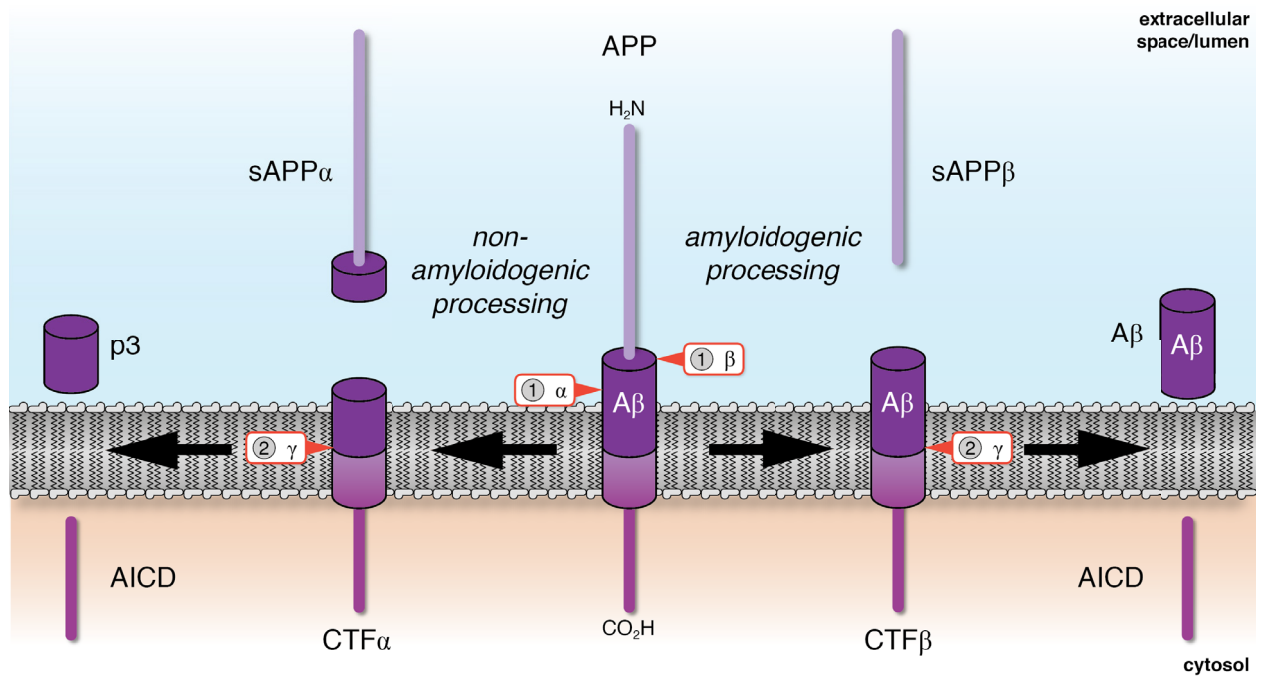


Fig. 1.6: RIP of APP. Schematic overview of non-amyloidogenic (left) and amyloidogenic (right) proteolytic processing of APP. Non-amyloidogenic processing is initiated (1) by an α -secretase (α) and the resulting CTF α is cleaved subsequently (2) by γ -secretase (γ). Amyloidogenic processing is initiated (1) by β -secretase (β) and the resulting CTF β is also subsequently (2) cleaved by γ -secretase (γ). Note that γ -secretase-mediated cleavage of CTF β results in heterogenous A β peptides that are variable in length (not depicted). Adapted from (Lichtenthaler *et al*, 2011).

AICD and an additional secreted protein fragment, p3 (Lichtenthaler *et al*, 2011; Zhang *et al*, 2012). p3 is significantly truncated compared to A β peptides, is less hydrophobic and less prone to form soluble oligomers (Dulin *et al*, 2008), which are considered the key synaptotoxic A β species (Haass & Selkoe, 2007).

AD is a devastating and - presently - inevitably progressive neurodegenerative disease that affects millions of ageing people worldwide (Jakob-Roetne & Jacobsen, 2009; Holtzman *et al*, 2011; Ballard *et al*, 2011). It is accompanied by macroscopic brain atrophy and, histopathologically, by synapse loss and the presence of two distinct types of proteinaceous aggregates, extracellular amyloid plaques and intracellular neurofibrillary tangles (reviewed in (Jakob-Roetne & Jacobsen, 2009; Holtzman *et al*, 2011)). Amyloid plaques are primarily found in cortical regions and their main constituents are A β peptides. It was hypothesised that A β peptides in fact constitute the pathogenic driver that initiates a cascade of pathophysiological events leading ultimately to AD pathology (*amyloid cascade hypothesis*) (Selkoe, 1991; Hardy & Higgins, 1992). Today, this notion is still regarded the key mechanism underlying AD pathology (discussed in (Karran *et al*, 2011)).

However, amyloidogenic processing of APP *per se* is not considered a pathological process. In fact, A β peptides can be found in bodily fluids (like cerebrospinal fluid) of healthy individuals demonstrating that A β generation is a normal physiological process (Seubert *et al*, 1992; Shoji *et al*, 1992). Importantly, γ -secretase cleavage of CTF β generates A β peptides of variable length ranging from 37 to 43 amino acids (Lichtenthaler *et al*, 2011; Holtzman *et al*, 2011). The most abundant product species under normal physiological conditions is A β 40 that comprises residues 1 to 40 of the A β domain of APP. Slightly longer species, in particular A β 42, are likewise generated but only in minor amounts (roughly 10% of total A β) (Holtzman *et al*, 2011).

yet the more hydrophobic A β 42 is regarded as the major neurotoxic species and pathogenic factor initiating AD pathophysiology (reviewed in (Haass & Selkoe, 2007)). Recently, A β 43 also (re-)emerged as highly neurotoxic A β species *in vivo* (Saito *et al*, 2011). Intriguingly, in a minority of AD cases (< 5%), referred to as familial AD (FAD), onset may occur rather early (age < 60 years) and these patients often harbour autosomal-dominant mutations in *PSEN1* (Rogaev *et al*, 1995; Sherrington *et al*, 1995) or, less frequently, in *PSEN2* (Levy-Lahad *et al*, 1995b; 1995a) and *APP* (Goate *et al*, 1991). A seminal study established that FAD mutations in *PSEN1* or *PSEN2* lead to increased secretion of longer, neurotoxic A β species (i.e. A β 42/A β 43) (Scheuner *et al*, 1996) and elevated levels of A β 42/A β 43 have since then been considered the underlying etiologic cause of FAD. FAD mutations can for instance cause an elevated overall A β production (including an absolute increase in A β 42/A β 43 abundance), e.g. in patients harbouring the "Swedish" M596L *APP* mutation at the BACE1 cleavage site (Citron *et al*, 1992). FAD mutations may also increase the A β 42/A β 43 to A β 40 ratio, i.e. lead to an elevated A β 42/A β 43 production at the expense of A β 40 without a significant effect on total A β production (Suzuki *et al*, 1994). Taken together, long A β species such as A β 42 and A β 43 are considered key drivers of AD pathology (Selkoe, 1991; Hardy & Higgins, 1992; Haass & Selkoe, 2007) and, hence, interference with *APP* intramembrane proteolysis has been considered a promising therapeutic strategy (see 1.4.4.4) (Karran *et al*, 2011). Importantly, however, FAD mutations in *APP* do not necessarily always affect *APP* processing and A β generation but can also change A β 's biophysical properties, e.g. its propensity for aggregation or oligomerisation (Nilsberth *et al*, 2001).

1.4.2 SPP and SPPLs

SPP and the SPPLs (Fig. 1.7) were identified in 2002 in three independent studies (Weihofen *et al*, 2002; Grigorenko *et al*, 2002; Ponting *et al*, 2002). In two of these studies bioinformatic database searches using PSI-BLAST and BLAST algorithms, respectively, were performed to find genes homologous to the presenilins and five such putative protein-coding genes were uncovered in humans (Ponting *et al*, 2002; Grigorenko *et al*, 2002). At the same time Weihofen *et al*. used a photocrosslinkable derivative of 1,3-di-(N-carboxybenzoyl-L-leucyl-L-leucyl)-amino acetone ((Z-LL)₂ ketone), a compound that had been found to inhibit signal peptide endoproteolysis *in vitro* before (Weihofen *et al*, 2000), to identify SPP as enzyme responsible for this activity and subsequently identified the related SPPL proteases (Weihofen *et al*, 2002). In humans and in rodents, the SPP/SPPL subfamily of GxGD proteases comprises SPP and SPPL3 as well as SPPL2a, SPPL2b, and SPPL2c.

1.4.2.1 Key features of SPP/SPPL-type GxGD proteases

Sequence analyses of all SPP/SPPLs predict a characteristic nine TMD topology resembling that of presenilin (Fig. 1.7, see 1.4.1.1) (Weihofen *et al*, 2002; Ponting *et al*, 2002; Grigorenko *et al*, 2002; Friedmann *et al*, 2004). Strikingly, the predicted topology of SPP/SPPLs is inverted compared to that of presenilins and experimental evidence supports the luminal and cytosolic localisation of SPP/SPPL N- and C-termini as well as the luminal accessibility of the loop connecting TMD6 and TMD7 (Friedmann *et al*, 2004; Nyborg *et al*, 2004). All SPP/SPPL family

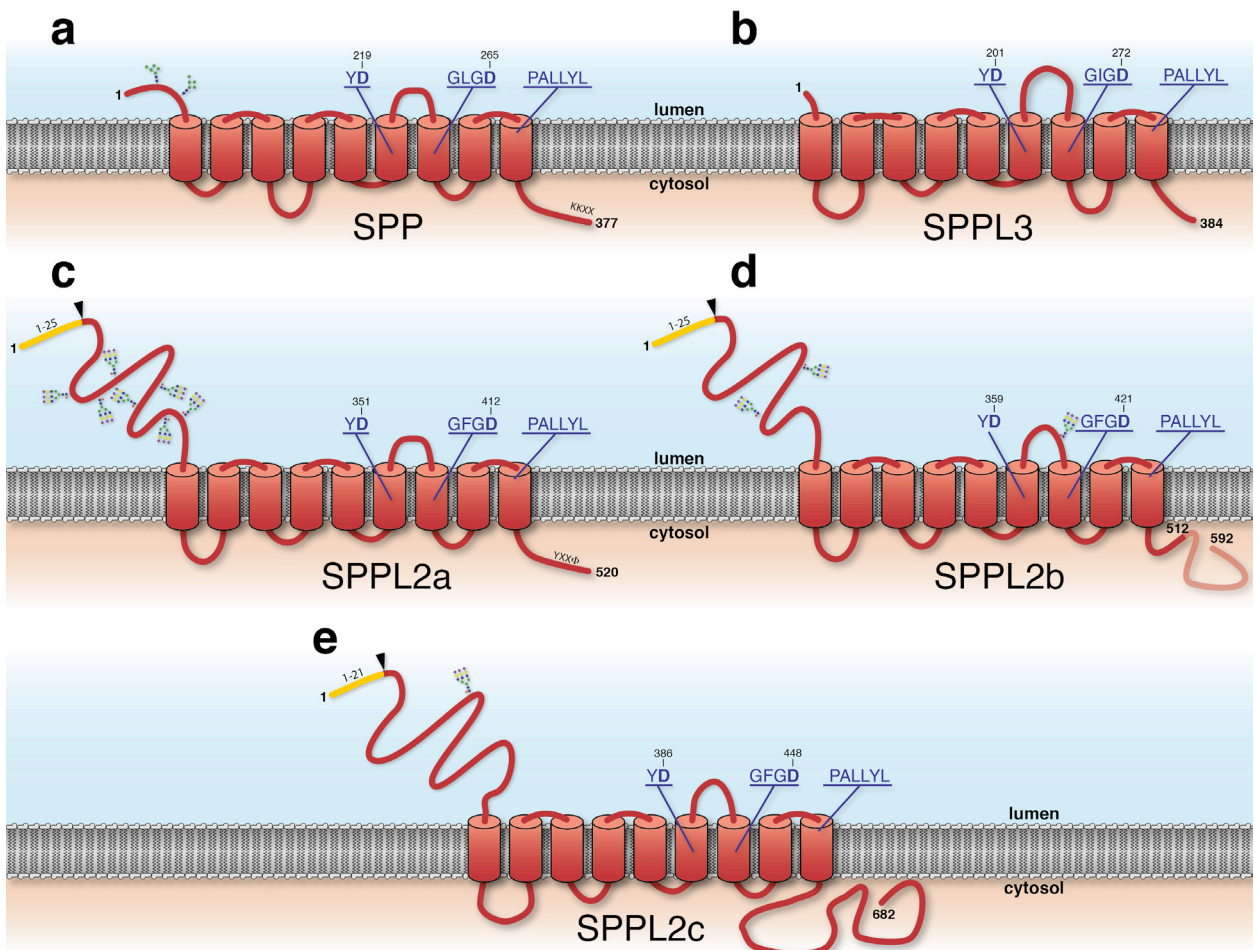


Fig. 1.7: Human SPP/SPPL family members. In humans, the SPP/SPPL family comprises SPP (a), SPPL3 (b), SPPL2a (c), SPPL2b (d), and SPPL2c (e). All members share a nine TMD topology. They harbour catalytic YD and GxGD motifs as well as a PALLYL motif (all shown in purple, catalytic aspartates are given in bold and with their respective amino acid position). SPP (a) contains two putative consensus N-glycosylation sites as well as a C-terminal KKXX ER retention signal. SPPL3 (b) is not glycosylated, while SPPL2a (c), SPPL2b (d), and SPPL2c (e) harbour several consensus N-glycosylation sites. SPP and SPPL3 lack N-terminal signal sequences. SPPL2 subfamily members contain N-terminal signal sequences that are post-translationally removed (Friedmann *et al.*, 2004). These are highlighted in yellow according to the respective Uniprot entries and cleavage sites indicated by the black arrowheads. The SPPL2a C-terminus harbours a YKKΦ lysosomal sorting signal. Two SPPL2b isoforms are conserved in humans and mice and they differ in the length of their cytoplasmic C-termini (shaded). Taken from (Voss *et al.*, 2013).

members harbour catalytic (Y/F)D and GxGD motifs in their predicted TMD6 and TMD7, respectively. In addition, they contain a QPALLY motif in the tip region of TMD9 that is similar to that found in presenilins (Weihofen *et al.*, 2002; Grigorenko *et al.*, 2002; Ponting *et al.*, 2002). Amino acid substitutions in the proline, alanine or leucine residues of this motif affect the proteolytic activity of SPP (Wang *et al.*, 2006) which was also observed for the corresponding mutations in presenilin (Tomita *et al.*, 2001; Wang *et al.*, 2004; 2006). Taken together, these observations suggest that key features of the active site architecture are conserved among presenilin- and SPP/SPPL-type GxGD proteases (Voss *et al.*, 2013).

In spite of these similarities, some differences between presenilins and SPP/SPPLs stand out: Exogenous expression of SPP/SPPLs in cell culture leads to increased turnover of the respective substrates suggesting that SPP/SPPLs are proteolytically active as monomers or homomeric oligomers and do not require accessory cellular co-factors. Enzymatic activity of

SPP can be reconstituted by exogenous expression of solely human SPP in yeast (Weihofen *et al*, 2002), whereas reconstitution of γ -secretase in the same setting requires exogenous expression of all four complex components (Edbauer *et al*, 2003), indicating that SPP (and likely the SPPLs) do not require the formation of a γ -secretase-like complex to be active. Moreover, unlike presenilins (see 1.4.1.1), there is currently no conclusive evidence that SPP/SPPLs do undergo autocatalytic endoproteolysis.

1.4.2.2 Physiological functions of mammalian SPP/SPPL family members

There is unambiguous evidence that mammalian SPP/SPPL family members³ are active aspartyl I-CLiPs as their proteolytic activity is impaired by mutagenesis of the catalytically active aspartate residues or following treatment with transition state analogue inhibitors (Weihofen *et al*, 2002; Friedmann *et al*, 2006; Fluhrer *et al*, 2006; Martin *et al*, 2008), but additional non-proteolytic functions of these protein cannot be excluded. In addition, several studies have contributed greatly to the present understanding their physiological function (Grigorenko *et al*, 2004; Krawitz *et al*, 2005; Casso *et al*, 2005; Tang *et al*, 2010; Casso *et al*, 2012; Schneppenheim *et al*, 2013; Beisner *et al*, 2013; Bergmann *et al*, 2013; Bronckers *et al*, 2013; Schneppenheim *et al*, 2014) which will be discussed in the following sections.

1.4.2.2.1 SPP

SPP is a glycosylated polytopic membrane protein (Weihofen *et al*, 2002), contains a C-terminal KKXX ER retention signal and, in line with this, was found to localise to the ER in human and murine cells (Urny *et al*, 2003; Krawitz *et al*, 2005; Friedmann *et al*, 2006). SPP appears to be of fundamental importance *in vivo*, in particular during metazoan development. For instance, *Drosophila melanogaster* larvae that lack *spp*, the *Drosophila* orthologue of human SPP, display a severe developmental phenotype, die early, and have abnormal tracheae (Casso *et al*, 2005). This phenotype was rescued by exogenous expression of active SPP, but not of the catalytically inactive mutant pointing to a fundamental role of its aspartyl protease activity in development (Casso *et al*, 2005). SPP was initially identified due to its proteolytic activity towards signal peptides (Weihofen *et al*, 2000; 2002), but has meanwhile also been linked to the proteolytic processing of other substrates.

N-terminal signal peptides ensure proper co-translational targeting of nascent secretory and membrane pre-proteins (Paetzl *et al*, 2002). Subsequently, they are cleaved off the nascent pre-protein by the signal peptidase complex but remain embedded in the ER membrane due to their considerably high degree of hydrophobicity (Paetzl *et al*, 2002). By endoproteolysis within their hydrophobic membrane-spanning domain, signal peptides can be liberated from the ER membrane and may subsequently be subject to proteasomal degradation (Fig. 1.8a). For the prolactin signal peptide this proteolytic activity was initially found to be (Z-LL)₂ ketone-sensitive (Weihofen *et al*, 2000) and was later attributed to SPP (Weihofen *et al*, 2002). Meanwhile, SPP has been described to endoproteolyse signal peptides of several other proteins after their liberation from nascent proteins by signal peptidase (reviewed in (Voss *et al*, 2013)).

³ Note that proteolytic activity of SPPL2c has not yet been observed, see section 1.4.2.2.2.

Importantly, together with signal peptidase activity, SPP can generate immunogenic peptide fragments of MHC class I signal peptides (Lemberg *et al*, 2001; Bland *et al*, 2003) and of non-MHC signal peptides (Hage *et al*, 2008), thus contributing to immune surveillance and an alternative pathway of generation of antigenic peptides for presentation via polymorphic MHC molecules.

In addition to the intramembrane cleavage of signal peptides, SPP may - following pre-cleavage by the signal peptidase complex - also endoproteolysis internal membrane-spanning sequences (Fig. 1.8b). IgSF1, for instance, was found to be cleaved at an internal stop-transfer sequence in the ER membrane by signal peptidase and a (Z-LL)₂ ketone-sensitive protease, most likely by SPP (Robakis *et al*, 2008). Signal peptidase and SPP also participate in proteolytic processing

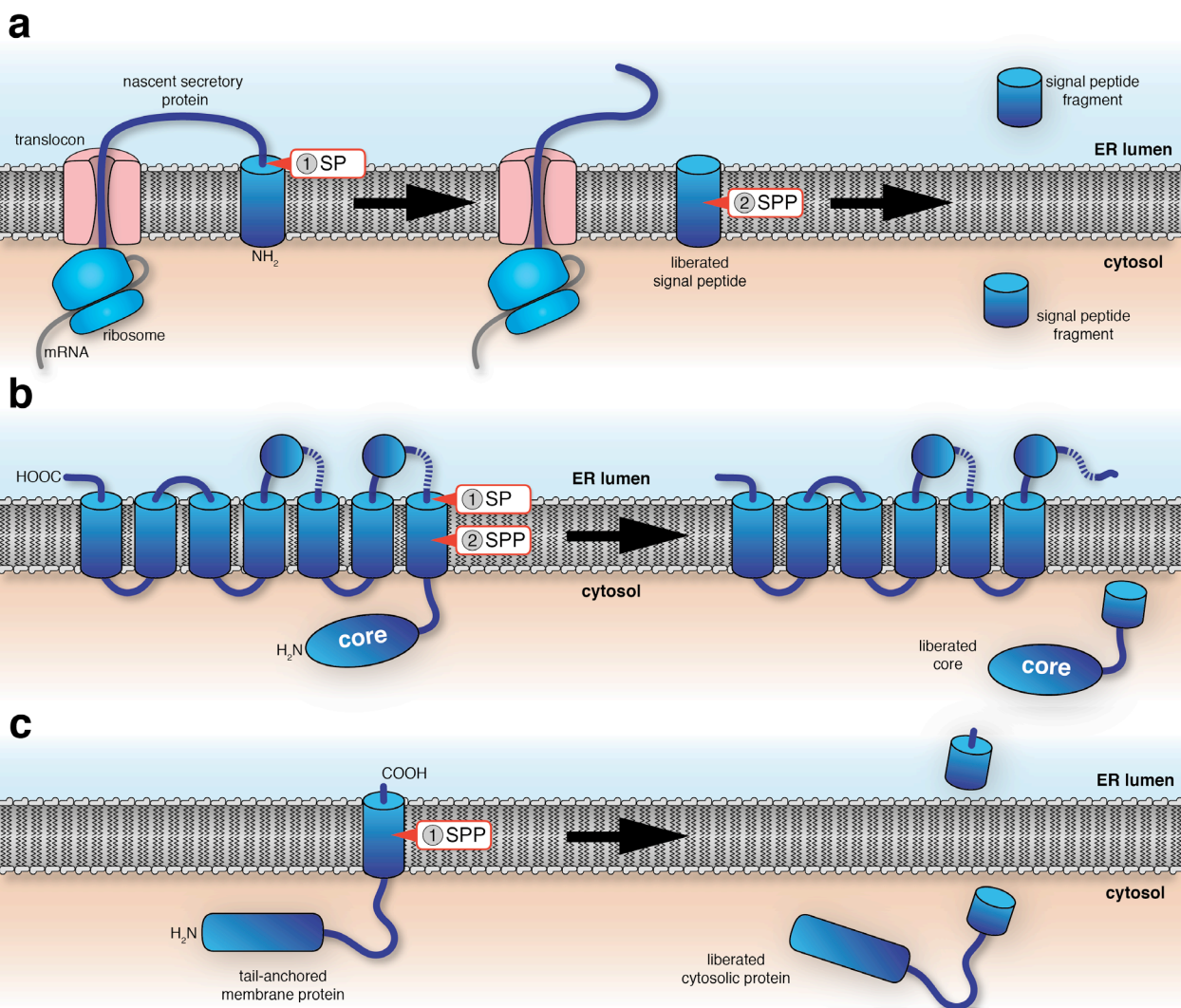


Fig. 1.8: SPP-mediated intramembrane proteolysis. Schematic overview of processes proteolytic SPP activity was implicated in. (a) SPP-mediated signal peptide cleavage. Signal peptides of nascent secretory proteins synthesised at the ER translocon are first cleaved off by signal peptidase (SP) and are subsequently endoproteolysed within their membrane-spanning hydrophobic core by SPP. Note that in rare exceptions signal peptide removal and cleavage may occur post-translationally (not depicted). (b) SPP cleaves within internal protein sequences. The hepatitis C virus core protein is liberated by stepwise proteolytic processing of the viral polyprotein precursor by SP and SPP. (c) SPP liberates cytosolic protein domains from tail-anchored ER membrane proteins. In contrast to processes depicted in a and b, liberation of tail-anchored proteins such as HO-1 from their membrane anchors does not require SP pre-cleavage. Note that, depending on the individual substrate, liberated protein fragments may face very diverse fates including degradation (e.g. of signal peptide fragments), loading onto MHC complexes and recruitment to specific cellular sub-compartments (not depicted).

of the polyprotein precursor of flaviviruses such as hepatitis C virus (Fig. 1.8b) (McLauchlan *et al*, 2002; Targett-Adams *et al*, 2006; Heimann *et al*, 2006). Importantly, this SPP-dependent cleavage is indispensable for proper virus propagation (Randall *et al*, 2007; Targett-Adams *et al*, 2008; Okamoto *et al*, 2008).

Only recently, tail-anchored ER-resident membrane proteins were described as novel SPP substrate class (Hsu *et al*, 2014; Boname *et al*, 2014). The N-terminal cytosolic domains of such proteins are tethered to the ER membrane via C-terminal TMDs that are post-translationally inserted into the lipid bilayer (Shao & Hegde, 2011). SPP cleaves within such C-terminal TMDs, for instance of heme oxygenase-1 (HO-1) but also of other tail-anchored proteins, liberating cytosolic domains from their ER membrane anchor and allowing for nuclear translocation or proteasomal degradation (Fig. 1.8c) (Hsu *et al*, 2014; Boname *et al*, 2014).

Finally, SPP has also been implicated in ER retrotranslocation and ERAD (Loureiro *et al*, 2006; Christianson *et al*, 2012; Harbut *et al*, 2012). Loureiro *et al*., for instance, reported that human cytomegalovirus US2 physically interacts with SPP and that this complex facilitates retrotranslocation of MHC class I molecules from the ER leading to down regulation of MHC class I surface expression and immune evasion (Loureiro *et al*, 2006) (though this was recently questioned (Boname *et al*, 2014)). Also, SPP was recently found to be part of the human ER retrotranslocation machinery (Christianson *et al*, 2012). In protozoan parasites this machinery is less complex than in mammals as they lack several orthologues of human pathway components (Harbut *et al*, 2012). Nonetheless, Harbut *et al*. found that *Plasmodium falciparum* SPP is involved in retrotranslocation and that treatment with small molecule inhibitors targeting SPP interferes with this activity and is toxic to *Plasmodium* (Nyborg *et al*, 2006; Harbut *et al*, 2012).

1.4.2.2.2 The SPPL2 subfamily

In humans and rodents, the SPPL2 subfamily comprises SPPL2a, SPPL2b, and SPPL2c (Weihofen *et al*, 2002; Grigorenko *et al*, 2002; Ponting *et al*, 2002). These have an N-terminal signal peptide (Friedmann *et al*, 2004) and comprise an extended and highly glycosylated N-terminal exoplasmic region upstream of the conserved nine TMD core (Fig. 1.7) (Friedmann *et al*, 2004; Krawitz *et al*, 2005).

SPPL2 subfamily members appear to be differentially localised in the cell: SPPL2a was found to harbour a lysosomal sorting signal within its luminal C-terminus (Behnke *et al*, 2011) and, accordingly, both over-expressed (Friedmann *et al*, 2006; Behnke *et al*, 2011) as well as endogenous SPPL2a (Behnke *et al*, 2011) were primarily observed to localise to the lysosomal or late endosomal compartment. Conflicting results, however, have so far been obtained for over-expressed SPPL2b which was observed primarily at the cell surface (Friedmann *et al*, 2004; Behnke *et al*, 2011), the Golgi (Martin *et al*, 2008), or in the lysosomal compartment (Krawitz *et al*, 2005).

In cell culture-based assays, SPPL2a and SPPL2b appear to have - to certain degree - an overlapping substrate repertoire as over-expressed tumour necrosis factor α (TNF α) (Fluhrer *et al*, 2006; Friedmann *et al*, 2006), Bri2 (Martin *et al*, 2008), CD74 NTFs (Schneppenheim *et al*, 2014) and transmembrane protein 106B (TMEM106B) (Brady *et al*, 2014) are endoproteolysed both by over-expressed SPPL2a and SPPL2b. FasL and transferrin receptor 1 (TfR1) NTFs,

however, appear to be primarily processed by over-expressed SPPL2a (Kirkin *et al*, 2007) and SPPL2b (Zahn *et al*, 2013), respectively. Observations in such experimental settings, however, need to be considered with caution as *in vivo* SPPL2b appears not to contribute to CD74 NTF endoproteolysis and CD74 NTF cleavage is exclusively mediated by SPPL2a (Schneppenheim *et al*, 2014). Moreover, endogenous SPPL2a and SPPL2b are differentially expressed and localised suggesting that *in vivo* they likely do not assume redundant functions (Schneppenheim *et al*, 2014).

In a physiological context, SPPL2a/2b-mediated substrate intramembrane proteolysis serve either as a mechanism of signal transduction or membrane protein degradation. For TNF α and FasL NTFs, for instance, it has been discussed that SPPL2a/2b-mediated cleavage generates ICDs that translocate to the nucleus and act as transcription factors that up-regulate target gene expression (Friedmann *et al*, 2006; Kirkin *et al*, 2007; Lückerath *et al*, 2011). In contrast, impaired turnover of the CD74 NTF causes a severe deficiency in mature B lymphocytes and CD8 $^{+}$ dendritic cells in mice deficient in *Sppl2a* (Schneppenheim *et al*, 2013; Bergmann *et al*, 2013; Beisner *et al*, 2013). In fact, accumulation of the CD74 NTF leads to massive intracellular ultrastructural changes and disturbed endocytic trafficking in *Sppl2a*-deficient cells (Schneppenheim *et al*, 2013) and to an early developmental arrest in splenic B cell maturation (Schneppenheim *et al*, 2013; Bergmann *et al*, 2013; Beisner *et al*, 2013). In animals deficient in both *Sppl2a* and *Cd74*, however, B lymphocyte and dendritic cell populations were found to be normal (Schneppenheim *et al*, 2013; Bergmann *et al*, 2013; Beisner *et al*, 2013).

For SPPL2c, no substrates have been identified and the SPPL2a/SPPL2b substrate TNF α is not processed by over-expressed SPPL2c (Friedmann *et al*, 2006). Hence, for the lack of an identified substrate, it is currently unclear whether SPPL2c is actually an active protease. While, in theory, the *SPPL2C* ORF is functional and encodes a putative protein, it is intron-less and highly polymorphic in nature and could therefore constitute a recently evolved pseudogene (Golde *et al*, 2009).

1.4.2.2.3 *SPPL3*

With no known (physiological) substrate, SPPL3 is presently an orphan protease. It is the smallest member of the SPP/SPPL family, is devoid of an N-terminal signal peptide and is not glycosylated (Friedmann *et al*, 2004). Its sub-cellular localisation is controversial since over-expressed SPPL3 was observed to co-localise with ER markers (Krawitz *et al*, 2005), Golgi markers (Friedmann *et al*, 2006), or both (Casso *et al*, 2012). To complicate matters, early studies also attributed proteolytic activity observed towards artificial SPP model substrates *in vitro* to SPPL3 (Nyborg *et al*, 2006; Narayanan *et al*, 2007). Together with the ER localisation observed and the closer degree of homology of SPPL3 to SPP than to the SPPL2 subfamily members, this led to the hypothesis that SPP and SPPL3 might in fact be functionally redundant (Krawitz *et al*, 2005; Nyborg *et al*, 2006). A more elaborate analysis, however, challenged this notion as catalytically inactive SPPL3 did not bind to a signal peptide-based substrate, while the respective SPP mutant did (Schrul *et al*, 2010). Similarly, there is no *in vivo* support for this notion as a *D. melanogaster* model that lacks functional *spp* and *sppL* genes (*sppL* is the



Fig. 1.9: Alignment of orthologues of human SPPL3. Protein sequences were aligned using the ClustalW algorithm implemented in the CLC Main Workbench 6 software platform. Non-conserved residues are highlighted by a red background. *Gallus gallus* SPPL3 depicted here is a predicted gene product. Some species harbour an additional SPPL3 isoform that contains a roughly 30 amino acid insertion in the conserved SPPL3 backbone. This applies also to *Xenopus laevis*. Here, only the short isoform that does not contain this insertion is included. Sequence accession numbers are (in the order depicted) NP_620584, NP_083288, NP_001233544, XP_415261, CAJ83465, NP_001015068, NP_567918 and NP_001064518.

Drosophila orthologue of mammalian SPPL3) does not exacerbate the phenotype observed in *spp* deficient animals before (Casso *et al.*, 2012).

Importantly, however, SPPL3's high degree of evolutionary conservation in metazoa (Fig. 1.9) but its absence in single-celled organisms like *Plasmodium* point to an important physiological function that might have only evolved in multicellular organisms. Presently, however, such a function of SPPL3 remains completely enigmatic and SPPL3 deficient flies lack an overt phenotype (Casso *et al.*, 2012). A *Spp3* genetrap mouse line generated by Tang *et al.* was also subject to an initial phenotypic analysis (Tang *et al.*, 2010). Notably, on a B6;129S5 hybrid background homozygous *Spp3* knockout mice presented with reduced body size and weight, mild neurological abnormalities and sterility in males as well reduced numbers of natural killer (NK) cells (Tang *et al.*, 2010).

1.4.3 Archaeal presenilin homologues

In Archaea, a number of putative genes were described that encode multi-pass membrane proteins which display homology to both eukaryotic presenilins and SPP/SPPLs (Ponting *et al*, 2002; Grigorenko *et al*, 2002; Torres-Arancibia *et al*, 2010) and these are collectively referred to as presenilin/SPP homologues (PSHs). They likely share the nine TMD structure of mammalian GxGD proteases and harbour catalytic residues within **YD** and **GxGD** motifs in the predicted TMD6 and TMD7, respectively. Presently, Archaeal PSHs cannot be unambiguously classified into either the presenilin or the SPP/SPPL subfamily of GxGD proteases. They may also constitute a common ancestors, making a clear distinction between the presenilin- and SPP/SPPL-type GxGD protease only possible in higher organisms (Voss *et al*, 2013).

1.4.4 Common features of presenilin- and SPP/SPPL-type GxGD proteases

In light of the apparent homology of presenilins and SPP/SPPLs (as well as of PSHs) in sequence and in predicted membrane topology, it can be anticipated that key functional aspects of these proteases are in fact conserved. Therefore, protease structure (section 1.4.4.1), substrate requirements (section 1.4.4.2), mechanism of catalysis (section 1.4.4.3), and the development of small molecule inhibitors (section 1.4.4.4) will be comparatively summarised for this protease family.

1.4.4.1 GxGD protease structure

Due to its nature, structural analyses of the fully assembled, proteolytically active γ -secretase complex have so far been restricted to electron microscopy (EM) and cryo-EM. The most recent study reported the cryo-EM structure of detergent-solubilised γ -secretase produced recombinantly in HEK293 cells at a resolution of 4.5 Å (Lu *et al*, 2014). The structure nicely resolves 19 membrane-spanning peptide backbones (likely corresponding to the 19 TMD expected within the γ -secretase complex, Fig. 1.5) within a planar, membrane-embedded domain that adopts a horse shoe-like shape. This domain is capped by a large luminal structure, likely the Nicastrin ectodomain.

This restriction similarly applies to the SPP/SPPL subfamily of I-CLIPs and the only structural data available for SPP is an EM study of purified active human SPP tetramers (Miyashita *et al*, 2011). However, Li *et al*. recently reported the first crystal structure of a more distantly related Archaeal PSH (Li *et al*, 2013). They found that the PSH MCMJR1 adopts a previously unobserved fold and anticipate that presenilin- and SPP/SPPL-type GxGD protease will adopt a similar spatial structure. As predicted (Torres-Arancibia *et al*, 2010), MCMJR1 contains nine α -helical TMDs connected by flexible loops. Of note and in line with prior biochemical analyses (see 1.4.1.1), TMD6 and TMD7, which harbour the catalytic residues, as well as TMD9 appear to be densely packed together forming the active site. This, in turn, is embedded in the membrane and is accessible to water. However, the crystal structure was obtained in an obviously inactive conformation as the catalytic aspartate residues are too far apart from each other to support catalysis. Therefore, structural changes might occur when the enzyme folds into an active conformation.

1.4.4.2 Substrate requirements of GxGD proteases

A striking distinction between presenilins and SPP/SPPLs is their apparent selectivity for a specific membrane protein topology: Presently, γ -secretase substrates identified are membrane proteins adopting a type I topology (i.e. N_{out}/C_{in}) ((Haapasalo & Kovacs, 2011) provide an overview of γ -secretase substrates reported). In contrast, all SPP/SPPL substrates identified are type II membrane proteins or signal peptides that adopt a type II orientation in the membrane (i.e. N_{in}/C_{out}) (Voss *et al*, 2013).

Presently, however, specific motifs in primary sequence that define whether and where intramembrane proteolysis of a given membrane protein occurs have neither been identified for the presenilins nor for the SPP/SPPL subfamily (Beel & Sanders, 2008; Lemberg & Martoglio, 2004). When discussing SPP substrate requirements, Lemberg and Martoglio proposed that two key features are required for a substrate to be cleaved (Lemberg & Martoglio, 2004): (i) Putative substrates have to be tailored for subsequent intramembrane proteolysis by a preceding proteolytic cleavage that removes the substrates ectodomain (i.e. shedding or a shedding-like event). (ii) SPP substrates have to exhibit structural flexibility within the scissile membrane-spanning region in order to be proteolytically accessible.

In fact, shedding is considered the regulatory step of γ -secretase-mediated intramembrane proteolysis (section 1.1) (Brown *et al*, 2000). Both APP and Notch - but also numerous other γ -secretase substrates identified - are subject to ectodomain shedding prior to intramembrane cleavage and the length of a substrate's ectodomain was found to negatively correlate with processing by the γ -secretase *in vivo* (Struhal & Adachi, 2000). Furthermore, APP CTFs but not full-length APP could be co-isolated with mature γ -secretase complexes (Xia *et al*, 2000). Similar requirements also seem to apply to the SPP homologue SPPL2b, which also requires its substrate Bri2 to be shed prior to cleavage and also in this case the substrate's ectodomain length negatively correlated with intramembrane cleavage (Martin *et al*, 2009). SPP substrates on the other hand do not undergo conventional ectodomain shedding, yet they are removed from nascent proteins by signal peptidase (Fig. 1.8a) (Paetzel *et al*, 2002) and Lemberg *et al*. demonstrated that SPP-mediated processing of a signal peptide requires its prior liberation from the pre-protein by signal peptidase (Lemberg & Martoglio, 2002). The selectivity for substrates with a short luminal ectodomain of SPP was also corroborated in a recent study for tail-anchored ER membrane proteins, another class of SPP substrates (Fig. 1.8c) (Boname *et al*, 2014). Taken together, shortening of the luminal portion of a putative substrate is strictly required for γ -secretase- as well as for SPP- and SPPL2b-mediated intramembrane proteolysis. Helix-destabilising residues (e.g. proline or glycine) within TMDs were likewise found to be critically required for SPP-mediated signal peptide cleavage (Lemberg & Martoglio, 2002) and for SPPL2b-mediated endoproteolysis of the Bri2 NTF (Fluhrer *et al*, 2012). In line with this, it was also postulated that factors like structural flexibility and not the mere primary structure determine whether a particular protein is a γ -secretase substrate (Beel & Sanders, 2008). Finally, for both γ -secretase and SPPL2b substrates it has recently been shown that substrate juxtapamembrane regions also affect intramembrane cleavage (Ren *et al*, 2007; Hemming *et al*, 2008; Martin *et al*, 2009).

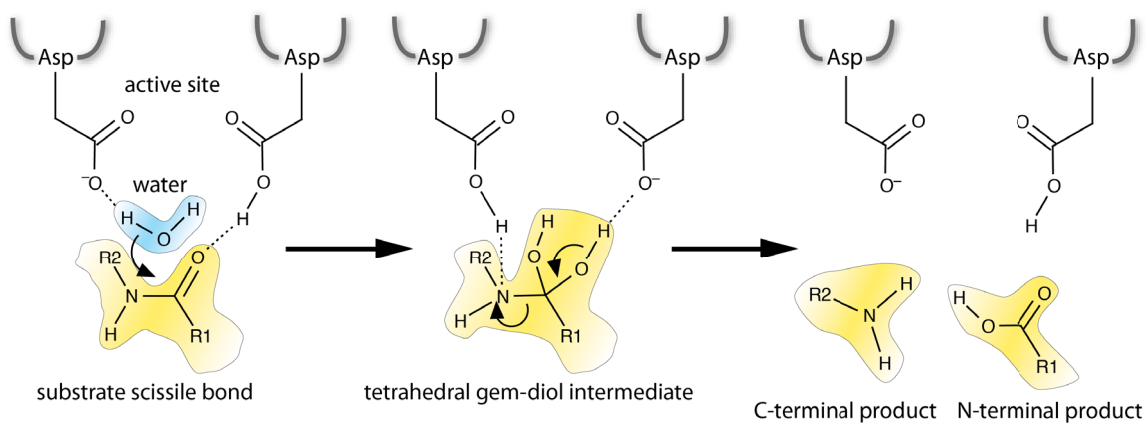


Fig. 1.10: Mechanism of aspartyl protease-mediated endoproteolysis. A protonated aspartate residue polarises the carbonyl carbon of the scissile bond to become more susceptible to nucleophilic attack while the second de-protonated residue increases nucleophilicity of a water molecule close-by. This facilitates nucleophilic attack of the polarised water molecule to the carbonyl carbon leading to formation of a tetrahedral intermediate and, upon reformation of the carbonyl carbon, to generation of a carboxylic acid (the newly formed C-terminus) and a primary amine (the newly formed N-terminus). Substrate peptide backbone is given in yellow, an active site water molecule in blue. Adapted from (Wolfe, 2009).

1.4.4.3 Mechanism of GxGD protease-mediated intramembrane proteolysis

Conventional aspartyl proteases utilise two proximal aspartate residues in their active site to hydrolyse peptide bonds (Fig. 1.10) (Suguna *et al*, 1987). GxGD proteases likewise harbour two conserved aspartate residues in adjacent TMDs (e.g. D257 and D385 in human PS1) that are required for catalysis (Wolfe *et al*, 1999; Steiner *et al*, 1999; Laudon *et al*, 2004). In the native γ -secretase complex these two residues were found to be facing each other in close proximity (Tolia *et al*, 2006; Sato *et al*, 2006a) suggesting that catalysis proceeds in a manner similar to that of conventional aspartyl proteases.

In light of its link to AD, γ -secretase-mediated intramembrane processing of APP CTFs in particular has been studied extensively. Intriguingly, cleavage within APP CTFs is executed by γ -secretase at multiple positions (Fig. 1.11) (reviewed in (Takami & Funamoto, 2012)) and generates distinct product species that have only minor differences in length but profound differences in their biological activity (compare e.g. A β 40 vs. A β 42/A β 43, see 1.4.1.2.2). In an

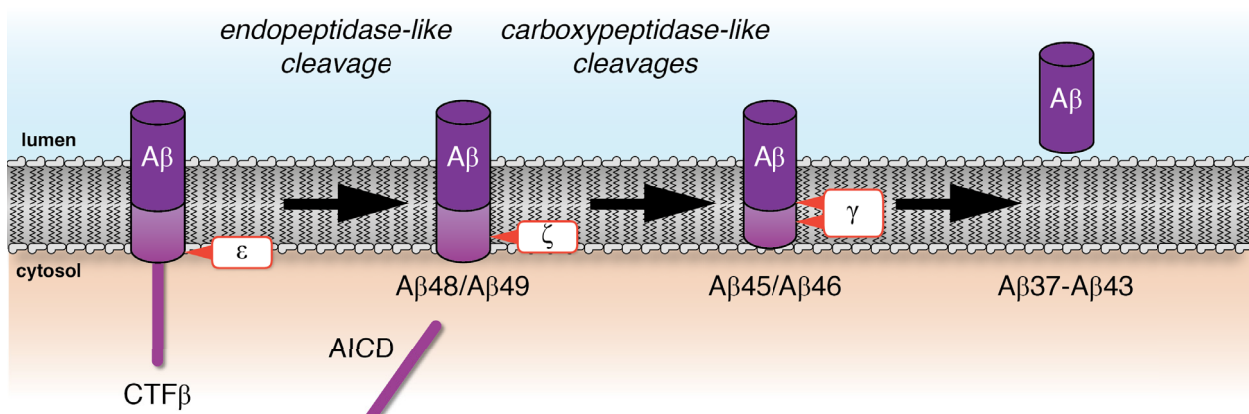


Fig. 1.11: Mechanism of γ -secretase-mediated intramembrane proteolysis of the APP CTF β . Initial cleavage of γ -secretase at the ϵ -site liberates the AICD and generates either A β 48 or A β 49. Cleavage at ζ - and γ -sites trims the C-terminus of the long A β species and liberates tri- and tetrapeptides (not shown). Eventually, soluble A β peptides are released which may vary in length.

initial step, γ -secretase liberates the AICD in an endopeptidase-like fashion (ϵ -cleavage). ϵ -cleavage may occur at two positions generating either AICD(49) or AICD(50) and corresponding A β 48 and A β 49 counterparts, respectively. The latter are substrate to downstream trimming by a carboxypeptidase-like activity of γ -secretase (referred to as ζ - and γ -cleavages) to eventually give rise to shorter peptides (A β 37 to A β 43) (Qi-Takahara *et al*, 2005). Detection of tri- and tetra-peptides that are released during A β processing strongly speaks in favour of this successive cleavage model (Takami *et al*, 2009; Takami & Funamoto, 2012). It was suggested that two independent A β product lines are initiated by ϵ -cleavage: The most abundant species A β 40, for instance, is generated by successive cleavage of A β 49 via A β 46 and pathogenic A β 43. A β 48, on the other hand, is processed to A β 45 which then gives rise to the pathogenic A β 42 and eventually, by tetra-peptide release, to A β 38 (Takami *et al*, 2009; Takami & Funamoto, 2012). Recent work, however, suggests that there is no strict separation of the two product lines and that both product lines cross each other (Okochi *et al*, 2013; Matsumura *et al*, 2013).

Given the homology of SPP/SPPLs and presenilins, the former may in fact utilise a similar successive proteolytic strategy. In support of this, SPPL2b-mediated TNF α intramembrane proteolysis produces multiple ICD and C-peptide cleavage products (Fluhrer *et al*, 2006). In contrast, SPP-mediated cleavage of the prolactin signal peptide was shown to occur primarily at one single position and only minor amounts of additional cleavage products were observed (Sato *et al*, 2006b). Therefore, the exact mechanism of SPP/SPPL-mediated intramembrane proteolysis is currently not understood.

1.4.4.4 GxGD protease inhibitors

Given the strong link of A β generation and AD pathophysiology, major efforts have been undertaken to pharmacologically interfere with its biogenesis. To this end numerous potent γ -secretase inhibitors (GSIs) have been developed (Fig. 1.12) (reviewed in (Wolfe, 2012)). Such compounds are structurally diverse and include transition-state analogue inhibitors like the hydroxyethylamine L-685,458 (Shearman *et al*, 2000), the dipeptide-base N-[N-(3,5-Difluorophenacetyl)-L-alanyl]-S-phenylglycine t-butyl ester (DAPT) (Dovey *et al*, 2001), or helical peptides (Bihel *et al*, 2004). Importantly, all these compounds as well as various derivatives thereof have allowed to functionally analyse the γ -secretase complex. As a transition state analogue inhibitor, L-685,458 is expected to bind to the enzyme's active site and indeed a photo-reactive derivative was found to target both presenilin NTF and CTF (Li *et al*, 2000b). Helical peptides similarly bound the presenilin NTF/CTF interface but competition experiments revealed that they interact with the so-called docking site which is clearly distinct from the active site (Kornilova *et al*, 2005). DAPT on the other hand was found to target yet another site and covalently labelled the PS1 CTF acting likely as an allosteric inhibitor of γ -secretase activity (Morohashi *et al*, 2006).

In light of initially promising results, one GSI, semagacestat, entered clinical trials to treat AD but a phase III study recently had to be terminated before completion due serious adverse effects (Doody *et al*, 2013). These observations point to a major issue of γ -secretase inhibition: Most GSIs affect γ -secretase activity in general and inhibit processing of all γ -secretase substrates. Hence, they also impair Notch signalling which could potentially account for the adverse effects

observed (Doody *et al*, 2013). In a distinct disease setting, however, interference with Notch signalling may in fact be desirable: Notch may have oncogenic properties and activating mutations within *NOTCH1* can be found in 50 % of T cell acute lymphoblastic leukemias (Weng *et al*, 2004). Treatment of such patients with GSIs has been very promising (Real *et al*, 2009). (Z-LL)₂ ketone was the first inhibitor described to restrain SPP activity (Weihofen *et al*, 2000). Peptide aldehydes such as (Z-LL)₂ ketone are typical serine/cysteine protease inhibitors (Wolfe, 2012) and, accordingly, Weihofen *et al*. initially expected signal peptide endoproteolysis to be mediated by a cysteine protease (Weihofen *et al*, 2000). Yet in their ketal form, such compounds mimic the transition state of aspartyl protease catalysis (Wolfe, 2012). When derivatised to a photo-reactive diazirine, (Z-LL)₂ ketone was shown to cross-link to SPP (Weihofen *et al*, 2002) and this was reduced in a concentration-dependent manner when treated with the parental compound (Weihofen *et al*, 2003), suggesting that (Z-LL)₂ ketone targets SPP's active site. Meanwhile, (Z-LL)₂ ketone has been shown to inhibit activity of SPP of various organisms (Casso *et al*, 2005; Nyborg *et al*, 2006; Narayanan *et al*, 2007; Harbut *et al*, 2012) and of human SPPL2a and SPPL2b (Fluhrer *et al*, 2006; Friedmann *et al*, 2006; Kirkin *et al*, 2007; Martin *et al*, 2008) *in vitro* as well as in cell culture, in most cases with IC₅₀ values in

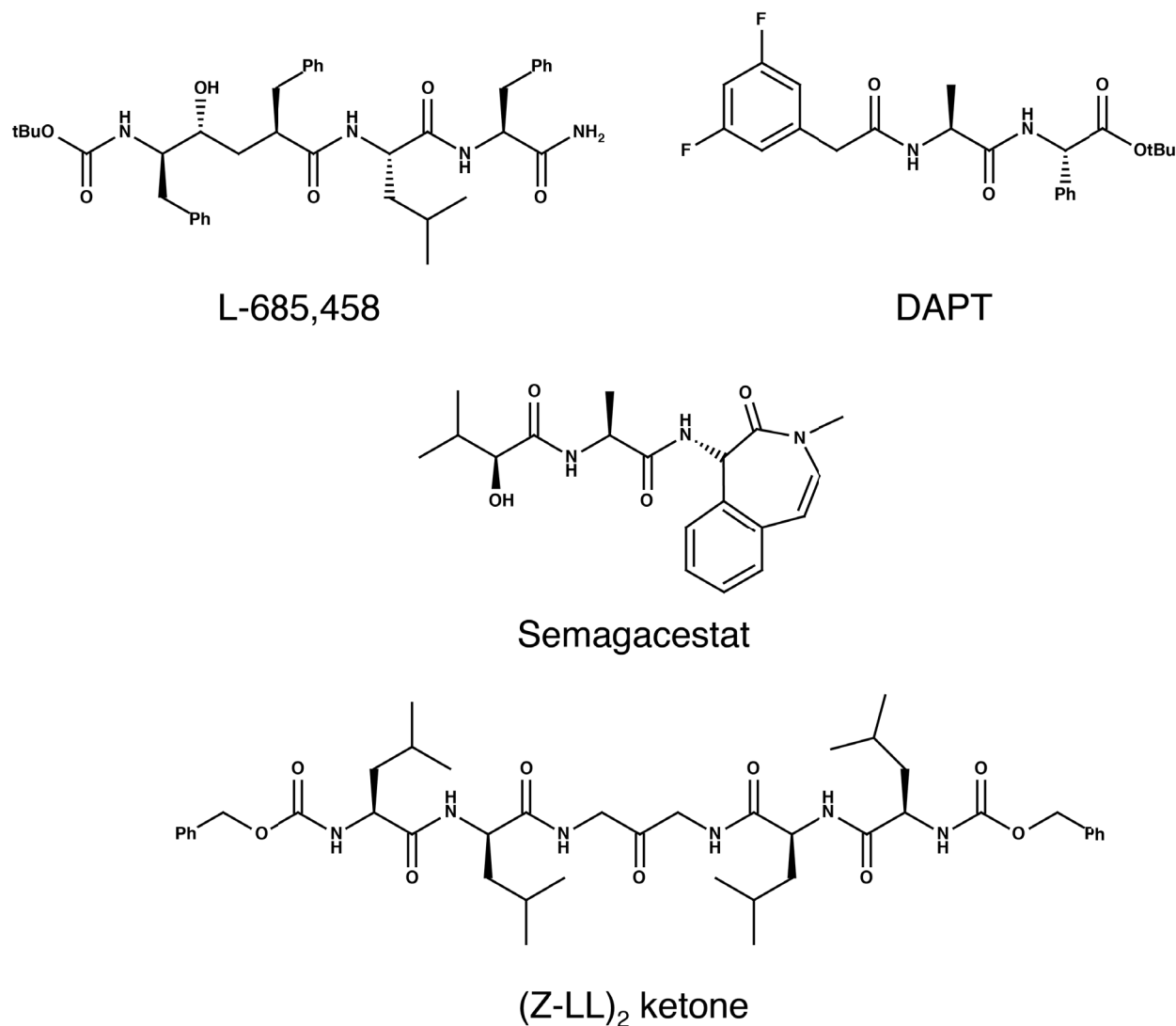


Fig. 1.12: Small molecule GSIs and GxGD protease inhibitors. N-[N-(3,5-Difluorophenacetyl)-L-alanyl]-S-phenylglycine t-butyl ester (DAPT), 1,3-di-(N-carboxybenzoyl-L-leucyl-L-leucyl)-amino acetone ((Z-LL)₂ ketone). For details see section 1.4.4.4.

the micro-molar range. Only recently, more potent SPP inhibitors have been developed but details regarding their nature have not been disclosed (Harbut *et al*, 2012).

Interestingly, there is abundant experimental evidence that most active site-targeting GSIs impair the proteolytic activity of both presenilin- as well as SPP/SPPL-type GxGD proteases and, hence, can in principle be considered general GxGD protease inhibitors. Labelling of SPP with the photo-reactive (Z-LL)₂ ketone derivative, for instance, was reduced by L-685,458 (Weihofen *et al*, 2003). L-685,458 also inhibits proteolytic activity of SPP (Weihofen *et al*, 2003; Iben *et al*, 2007) as well as of SPPL2a and SPPL2b (Fluhrer *et al*, 2006; Friedmann *et al*, 2006; Martin *et al*, 2008) suggesting that the active site architecture is conserved among presenilin- and SPP/SPPL-type GxGD proteases. In contrast, the allosteric GSI DAPT does neither impair SPP nor SPPL2b activity (Weihofen *et al*, 2003; Martin *et al*, 2008) and does not compete with active site labelling of SPP (Weihofen *et al*, 2003) suggesting that the binding site of DAPT is not conserved among the two GxGD protease sub-families.

1.5. Foamy Viruses

In the course of this study, the foamy virus (FV) envelope glycoprotein (FVen) was identified as first SPPL3 substrate. Foamy viruses (FVs) are complex retroviruses but several key features of their life cycles, clearly distinguish FVs from orthoretroviruses and, accordingly, they are grouped as separate *Spumavirinae* subfamily within the *Retroviridae* (Lecellier & Saïb, 2000; Rethwilm, 2010; Lindemann & Rethwilm, 2011). *In vitro*, FV exhibits an astonishingly broad tropism and can infect cell lines derived from various tissues and species (Hill *et al*, 1999). In line with this, the FV envelope glycoprotein (FVen) mediates virus attachment to a highly ubiquitous receptor, the glycosaminoglycan (GAG) heparan sulphate (HS) (Plochmann *et al*, 2012; Nasimuzzaman & Persons, 2012).

FVs are endemic in various animal species, including non-human primates, cats, and others (Meiering & Linial, 2001). Prevalence in these host species is generally very high but may vary (Meiering & Linial, 2001). In infected animals, FVs establish a life-long persistent infection but there is no solid evidence for FV-associated disease (Meiering & Linial, 2001). FV transmission likely occurs by biting or licking (reviewed in (Meiering & Linial, 2001)) and in non-human primates virus replication is mostly restricted to superficial oropharyngeal epithelial cells (Murray *et al*, 2008).

Cases of FV infections in humans have also been documented (Achong *et al*, 1971; Schweizer *et al*, 1997; Meiering & Linial, 2001; Betsem *et al*, 2011). These findings triggered extensive investigations to unravel potential link(s) of FV infections in humans to disease but, in sum, there is presently no solid evidence supporting FV-associated aetiology of human disease and, like in animal hosts, FVs are considered to be apathogenic (reviewed in (Meiering & Linial, 2001)). Furthermore, humans appear to be dead-end hosts as no human-to-human FV transmission has been documented (Betsem *et al*, 2011). In line with this, the original "human" FV isolate (Achong *et al*, 1971) was found to be in fact highly homologous to a chimpanzee isolate of a simian FV (Herchenröder *et al*, 1994). Other human FV infection were exclusively observed in persons with (mostly occupational) contact to non-human primates (Heneine *et al*, 1998; Schweizer *et al*, 1997), but there is no evidence for a wide-spread prevalence of simian

FV in the general human population (Ali *et al*, 1996; Schweizer *et al*, 1995). However, a recent study showed that non-human primate-to-human FV transmission is frequently occurring locally among hunters in Central Africa (Betsem *et al*, 2011).

Due to their broad tissue tropism and their apathogenic nature FVs have become increasingly attractive as gene therapy vectors and FV particle-based systems were already successfully used to correct primary immunodeficiencies in animal models (Bauer *et al*, 2008; Uchiyama *et al*, 2012). Importantly, even after a > 4 year follow-up, no signs of malignant transformation of transplanted FV-transduced cells were observed, a problem commonly associated with gene therapeutic approaches (Bauer *et al*, 2013). Hence, FVs emerge as a safe alternative to γ -retroviral vectors for gene therapy.

1.5.1 Foamy Virus envelope glycoprotein

Surface proteins of enveloped viruses are required to mediate attachment to host cells and to facilitate entry via fusion of viral and host cell membranes. This also applies to retroviruses where the envelope (env) glycoprotein fulfils these two crucial functions (reviewed in (Blumenthal *et al*, 2012)). FVs likewise encode an env glycoprotein, FVenv (Lindemann & Rethwilm, 2011; Berka *et al*, 2013) (Fig. 1.13). It is synthesised as a pro-protein that requires proteolytic processing to generate the N-terminal leader peptide (LP, gp18^{LP}) as well as the surface (SU, gp80^{SU}) and the C-terminal transmembrane (TM, gp48TM) subunits (Lindemann & Goepfert, 2003; Berka *et al*, 2013). SU and TM subunits are highly conserved among retroviruses and mediate receptor binding and membrane fusion, respectively (Blumenthal *et al*, 2012). Similar observations have been made for FVenv: FVenv SU was shown to be indispensable for receptor binding (Duda *et al*, 2006) and FVenv TM contains a hydrophobic

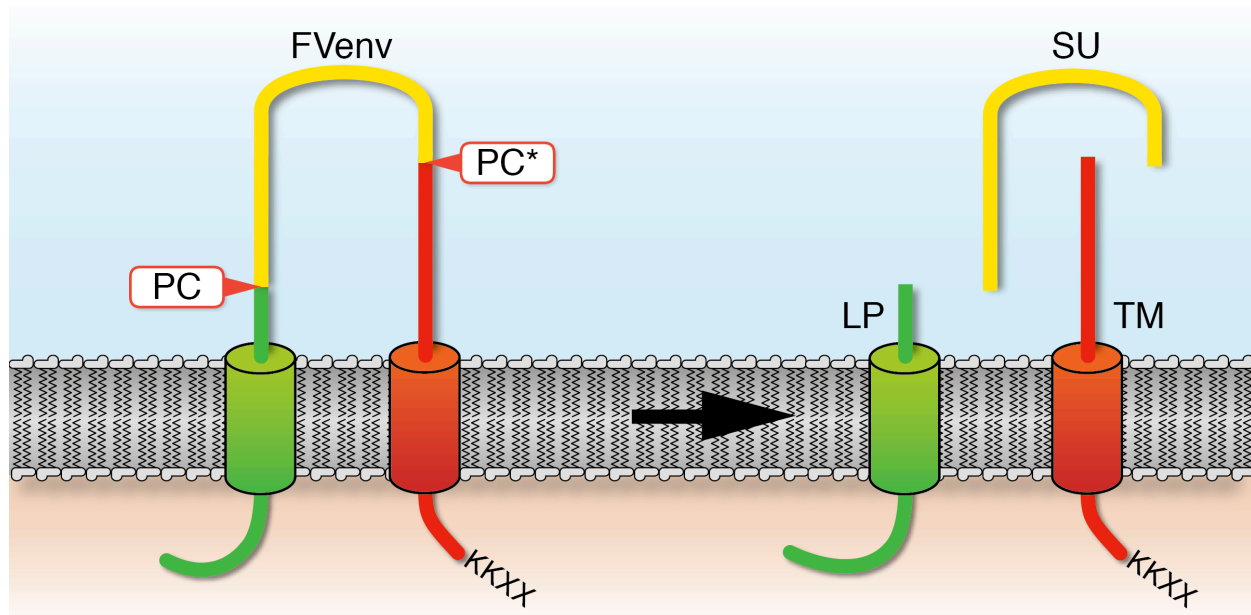


Fig. 1.13: Proteolytic processing of FVenv. FVenv is synthesised as a type III precursor and is subsequently endoproteolysed by furin or furin-like pro-protein convertases (PC) to generate its three subunits, LP (green), SU (yellow), and TM (red). As experimental evidence suggests that endoproteolysis at the indicated sites is mediated by distinct proteolytic activities (Bansal *et al*, 2000), these have been designated PC and PC*.

stretch that is expected to function as fusion peptide (Wang & Mulligan, 1999; Berka *et al*, 2013). Unlike other retroviral env proteins, however, the N-terminal LP is a unique features of FVenv (Lindemann & Goepfert, 2003; Berka *et al*, 2013). An N-terminal cytosolic stretch within LP of FVs mediates interaction with the viral capsid (Lindemann *et al*, 2001; Wilk *et al*, 2001) pointing to a pivotal role of the foamy viral LP subunit in particle assembly and budding (Lindemann & Rethwilm, 2011).

The FVenv precursor initially adopts a type III topology, assembles into a tri-partite trimeric complex, and is subject to post-translational proteolytic processing (Berka *et al*, 2013). Furin or a furin-like pro-protein convertase (PC) separate LP and SU (Duda *et al*, 2004; Geiselhart *et al*, 2004) as well as SU and TM (Bansal *et al*, 2000). Importantly, the latter cleavage is strictly required for viral infectivity (Bansal *et al*, 2000), whereas cleavage between LP and SU is not (Duda *et al*, 2004). Interestingly, the LP is incorporated into viral particles and is essential for egress of progeny virions from host cells while being dispensable for attachment and entry (Lindemann *et al*, 2001). Importantly, while both cleavages occur at primary sequence motifs that clearly correspond to consensus substrate motifs of furin/PC, the exact identity of the cellular protease(s) executing both cleavages, is presently elusive. Yet both cleavages have to be catalysed by distinct proteases as these cleavage events are differentially affected by mutations that alter the sub-cellular localisation of FVenv (Bansal *et al*, 2000).

Another striking difference of orthoretroviral envs and FVenv is a C-terminal ER retention signal found in the latter which ensures ER localisation of FVenv when expressed in the absence of other viral structural proteins (Goepfert *et al*, 1995; 1997). The exact role of this motif is presently unclear as it is not conserved among all FVs and is dispensable for virus propagation (Goepfert *et al*, 1999). Interestingly, initial observations pointed to assembly at and budding of FV particles from intracellular (possibly ER) membranes (Goepfert *et al*, 1999), but a more detailed study reported an interaction of gag and FVenv at the *trans*-Golgi network (TGN) (Yu *et al*, 2006). Accordingly, the exact identity of the site of intracellular particle assembly and egress remains elusive (Lindemann & Rethwilm, 2011).

1.6. Protein glycosylation

Numerous cellular proteins are subject to covalent post-translational modifications, including modifications by carbohydrate moieties termed glycosylation. Experimental work described in this study revealed that SPPL3 affected cellular glycosylation *in vivo* and *in vitro*. Glycosylation is common to transmembrane proteins and secreted proteins but also affects cytosolic and/or nuclear proteins (Moremen *et al*, 2012). Glycoproteins can be found in all kingdoms of life, but, while simpler structures prevail in prokaryotes, eukaryotes and multicellular organisms in particular are characterised by a highly diversified glycome which may be subject to developmental and environmental changes. Glycan moieties may be covalently linked to proteins in multiple ways (Sears & Wong, 1998; Moremen *et al*, 2012). Mostly, however, glycans are attached to proteins in an N-glycosidic amide linkage via the side chains of luminal asparagine residues (N-glycosylation) or in an O-glycosidic fashion to serine or threonine residues (O-glycosylation).

Several glycan structures are strictly required for multicellular life as animal models defective in normal glycosylation pathways often exhibit striking phenotypic abnormalities and inborn deficiencies in saccharide or glycosylation metabolism result in congenital disorders of glycosylation (CDGs) in man (reviewed in (Hennet, 2012)). Accordingly, protein glycosylation is crucial to cellular ER quality control, cell-cell interactions, intercellular signalling, tumour metastasis, and various other processes (Lowe & Marth, 2003; Moremen *et al*, 2012).

1.6.1 Glycosyltransferase & glycosidases

Given their polyvalent nature and the unique chemistry of their anomeric centres, carbohydrates may be subject to diverse modifications and substitutions. In a cellular setting, such modifications are catalysed by the enzymatic activities of glycosyltransferases (GTs) and glycosidases as well as other glycan-modifying enzymes (GMEs). GTs employ mono-saccharides conjugated to nucleoside or lipid phosphates as substrates to catalyse formation of glycosidic bonds (Paulson & Colley, 1989; Freeze & Elbein, 2009). Such activated sugar donors are synthesised from monosaccharide precursors within the cytosol and the nucleus and are subsequently transported to the ER and Golgi lumen (Freeze & Elbein, 2009).

Mammalian genomes contain numerous putative GMEs including roughly 200 GTs that each possess a certain specificity towards their donor and acceptor substrates (Stanley, 2011; Moremen *et al*, 2012). In fact, the presence of certain glycan structures in a cell reflects the expression levels of GTs involved in biosynthesis of these structures (Paulson & Colley, 1989). With only few exceptions, most Golgi-localised GTs and other GMEs are type II transmembrane glycoproteins that comprise a short cytosolic N-terminal stretch followed by a TMD that at the same time functions as signal anchor and a luminal stem region as well as the C-terminal catalytic domain (Paulson & Colley, 1989; Sears & Wong, 1998; Varki *et al*, 2009).

1.6.2 Cellular N-glycosylation

In vertebrates, a distinction is made between three types of N-linked glycans: (i) high mannose-type glycans, (ii) complex glycans, and (iii) hybrid-type glycans (Fig. 1.14). Whereas they clearly differ in their degree of branching and, more importantly, in the extent and variety of terminal modifications, all three types share a $\text{Man}_3\text{GlcNAc}_2$ core as they all derive from a common precursor. Hybrid-type and complex glycans differ in their degree of branching and the former contain no GlcNAc modifications on their $\alpha 1,6$ -linked core mannose residue. Basic N-glycan structures (i.e. of the high mannose-type) are highly conserved among eukaryotes and are essential to eukaryotic cellular viability as mediators of fundamental cellular ER quality control (Moremen *et al*, 2012). Accordingly, inhibition of early steps of their biosynthesis, i.e. by treatment with the GlcNAc analogue tunicamycin, leads to cellular dysfunction and cell death (Lowe & Marth, 2003).

The biosynthesis of N-glycans has been extensively reviewed (Schachter, 1991; Sears & Wong, 1998; Lowe & Marth, 2003; Stanley *et al*, 2009; Moremen *et al*, 2012). N-glycosylation commences at the rough ER membrane by attachment of a pre-assembled $\text{Glc}_3\text{Man}_9\text{GlcNAc}_2$ glycan to the side-chain amino group of an asparagine residue within the sequon Asn-X-Ser/Thr (X being any amino acid, but not proline; rarely, the sequon Asn-X-Cys is also glycosylated).

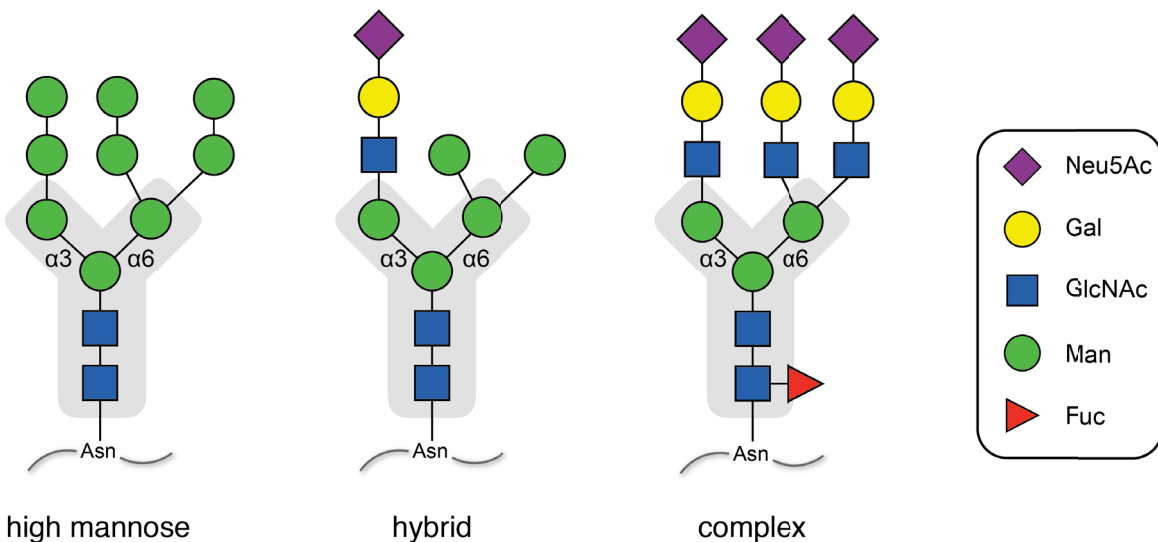


Fig. 1.14: Types of eukaryotic N-glycans. The $\text{Man}_3\text{GlcNAc}_2$ core structure that is common to all N-glycans is shaded in grey. High-mannose glycans have not been subject to trimming in the ER. Hybrid glycans harbour an GlcNAc-initiated branch on the $\alpha 1,3$ -initiated arm that is terminally modified. Complex glycans harbour GlcNAc branches also on the $\alpha 1,6$ -initiated arm and may be highly and very diversely branched and core-fucosylated. Terminal modifications of the hybrid and the complex glycan depicted and GlcNAc branching of the complex glycan are exemplary. For clarity stereochemical details are largely omitted. Neu5Ac, sialic acid, Gal, galactose, GlcNAc, N-acetylglucosamine, Man, mannose, Fuc, fucose.

This reaction occurs co-translationally and is catalysed by the oligosaccharyltransferase complex that transfers $\text{Glc}_3\text{Man}_9\text{GlcNAc}_2$ from its membrane-tethered dolichol pyrophosphate-conjugated precursor to the nascent glycoprotein. Terminal glucose and mannose residues of $\text{Glc}_3\text{Man}_9\text{GlcNAc}_2$ glycans are trimmed by ER-resident α -glucosidases as well as by Golgi α -mannosidase I (Golgi Man I). This process is tightly linked to chaperone-assisted folding of nascent secretory and membrane proteins and, in case this fails, to ER quality control and ER retrotranslocation of un- or mal-folded proteins (Moremen *et al.*, 2012). Glycoproteins carrying trimmed N-glycans (i.e. $\text{Man}_5\text{GlcNAc}_2$) are then transported to the Golgi network for subsequent modifications. Importantly, glycoproteins that are ER-resident are not subject to these modifications and retain high mannose-type N-glycans. An example is the immature ER-resident variant of the γ -secretase complex component Nicastrin (Yang *et al.*, 2002; Leem *et al.*, 2002).

In the Golgi, a GlcNAc residue is attached in β -linkage to the C2 of the $\alpha 1,3$ -linked mannose residue of the glycan core by N-acetylglucosaminyltransferase I (GnT-I), initiating synthesis of both hybrid and complex glycans (Fig. 1.15). $\text{GlcNAcMan}_5\text{GlcNAc}_2$ glycans generated by GnT-I may then be modified by Golgi α -mannosidase II which removes mannose residues bound to the core $\alpha 1,6$ -linked mannose residue. The resulting structure, $\text{GlcNAcMan}_3\text{GlcNAc}_2$, acts as precursor for the generation of multi-antennary, complex N-glycans: GnT-II, for instance, attaches GlcNAc to the $\alpha 1,6$ -linked core mannose residue generating bi-antennary glycans. These, in turn, may then be subject to further elaboration through attachment of additional GlcNAc residues to the two core mannose residues by GnT-IV, GnT-V and others. This process is collectively referred to as GlcNAc branching (Schachter, 2000). Hybrid-type glycans are generated when $\text{GlcNAcMan}_5\text{GlcNAc}_2$ glycans are not trimmed by α -mannosidase II.

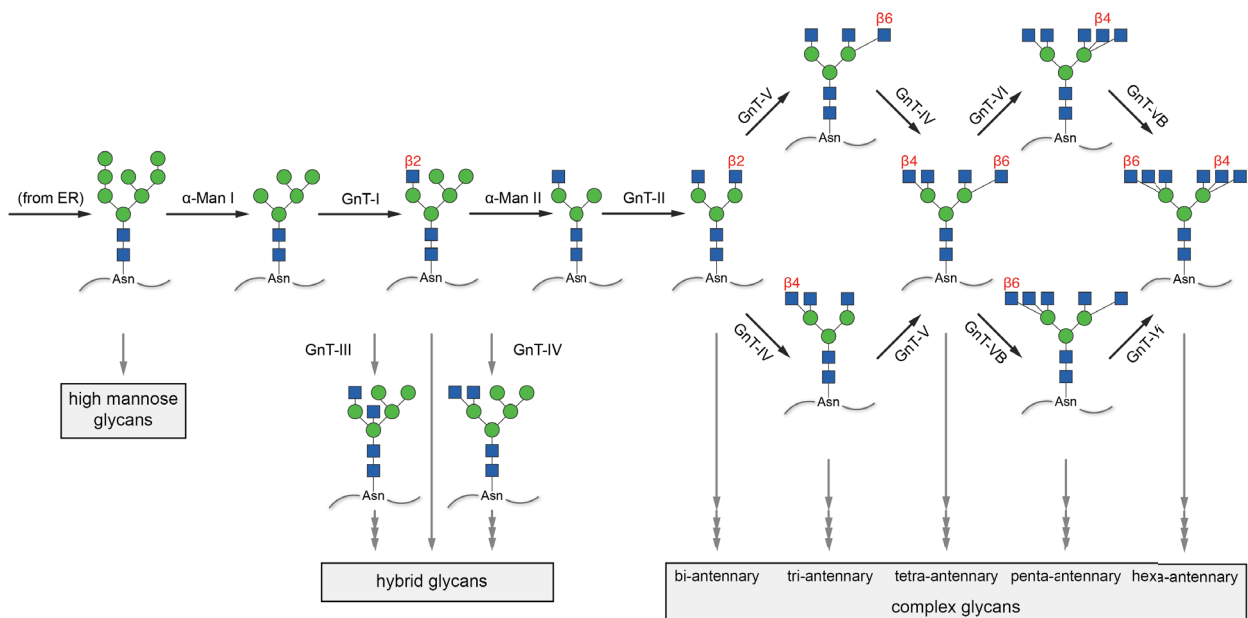


Fig. 1.15: Golgi GlcNAc branching. High-mannose precursor N-glycan on glycoproteins delivered from the ER to the Golgi are subject to GlcNAc branching that generates hybrid and complex glycans. For detailed description refer to main text. GlcNAc residues are added by numerous N-acetylglucosaminyltransferases (GnTs) in distinct stereochemical manner (red). N-glycans are subsequently modified in the *trans* Golgi and the TGN (indicated by grey arrows) to obtain mature N-glycans. Adapted from (Stanley *et al*, 2009).

Following the branching of glycan cores mediated by the activity of GnTs, terminal GlcNAc residues in complex, yet also in hybrid-type glycans are subject to diverse additional modifications in the *trans* Golgi. These terminal modifications include the enzymatic addition of (poly-)N-acetyllactosamines in the *medial/trans* Golgi as well as fucosylation and terminal sialylation in the *trans* Golgi network (TGN) and these terminal glycan patterns often are alike on N-glycans, O-glycans, and glycolipids (Stanley & Cummings, 2009).

Importantly, the outlined biosynthetic route towards complex N-glycans is not strictly followed in a linear manner. The order of action of GMEs on glycan substrates is particularly important in determining the product structure as individual modifications may actually preclude or promote successive processing steps. Such modifications have been referred to as *no-go* and *go* signals (Schachter, 1991). Examples for the latter include α -mannosidase II that can only trim glycans that were acted on by GnT-I before and GnT-IV and GnT-V that require prior modification of their substrates by GnT-II. An important *no-go* signal is generated by GnT-III: GnT-III adds a so called bisecting GlcNAc residue in β 1,4 linkage to the core mannose residue and this addition prevents further branching as bisected glycans cannot be processed by GnT-II, GnT-IV, and GnT-V. In addition, GMEs often compete for substrates. This results in a high diversity of glycan structures - even on the same protein - which is referred to as micro-heterogeneity (Schachter, 1991; Moremen *et al*, 2012). Also, expression and activity of enzymatic factors involved in glycan biosynthesis may be subject to regulation and, in light of the vast number of distinct enzymatic activities involved in glycan biosynthesis, glycan structures are specific for species, cell type as well as developmental stage (Ohtsubo & Marth, 2006).

1.6.3 Cellular O-glycosylation

Many cellular and secreted glycoproteins are extensively modified by O-glycosylation. These may be subject to modification by α -linked GalNAc as in mucin-type O-glycans, by β -linked xylose in GAG-carrying proteoglycans, by α -linked mannose found on α -dystroglycan and by other saccharides (Sears & Wong, 1998; Moremen *et al*, 2012; Brockhausen *et al*, 2009; Dobson *et al*, 2013). Depending on the exact type of O-glycosylation, the initial glycan attachment occurs in the ER or the Golgi and is catalysed by specific GTs that do not participate in N-glycosylation. The individual types of O-glycans are subsequently often elongated by stepwise action of numerous additional pathway-specific, Golgi-resident GTs. However, terminal glycan structures of N-glycans and mucin-type O-glycans - but not other types of O-glycans - are often generated by the same set of *trans* Golgi and TGN GTs (Stanley & Cummings, 2009). While primary amino acid sequence motifs that define N-glycan attachment are well-described, similar motifs for O-glycosylation are not particularly well-defined (Sears & Wong, 1998; Brockhausen *et al*, 2009; Moremen *et al*, 2012).

2. Aims of the study

This study is focussed on SPPL3, an on the one hand highly conserved representative but on the other hand the least characterised one of the SPP/SPPL proteases. With SPPL3 being an orphan protease, the primary aim of the present study is to identify a SPPL3 substrate that allows to examine the protease's proteolytic activity in detail. As initial reports suggest a certain degree of functional redundancy between SPPL3 and SPP (Krawitz *et al*, 2005; Nyborg *et al*, 2006), atypical signal peptides such as of FVenv have become promising candidate substrates for SPPL3. Therefore, it is to be tested here whether SPPL3 is capable of endoproteolysing FVenv. If this does in fact apply, SPPL3-mediated endoproteolysis of FVenv should reveal the substrate requirements of SPPL3 and assess its sensitivity towards GSIs.

In addition to that, the physiological function of SPPL3 will be investigated. To this end previously established cell culture models as well as a recently generated *Spp3*-deficient gene-trap mouse line (Tang *et al*, 2010) will be surveyed for phenotypic abnormalities. Assuming that SPPL3 exerts its biological function(s) first and foremost via its activity as a protease, in-depth analysis of phenotypic abnormalities in those models at hand should allow to infer candidate SPPL3 substrates. Impaired proteolytic processing of such, e.g. in *Spp3*-deficient mice, should then cause or contribute to the phenotypic abnormalities observed.

Finally, based on the insights obtained concerning SPPL3's substrate selectivity, a proteomic screen will be undertaken to completely define the SPPL3 degradome, i.e. its global substrate repertoire, which would then, in turn, help to understand the physiological role of SPPL3 in its entirety.

3. Materials & Methods

3.1 Materials

3.1.1 Laboratory equipment & reagents

Unless indicated otherwise in the respective detailed description of experimental procedures, standard laboratory equipment was used. Plastic consumables were from Sarstedt (Nümbrecht, Germany), greiner bio-one (Kremsmünster, Austria) and Thermo Fisher Scientific (Waltham, USA). Liquid and powder chemicals of analytical grade were purchased from Merck (Darmstadt, Germany), Sigma-Aldrich (St. Louis, USA), Carl Roth (Karlsruhe, Germany), biomol (Hamburg, Germany), Serva (Heidelberg, Germany) or AppliChem (Darmstadt, Germany). Centrifuges, incubators and safety cabinets were from Eppendorf (Hamburg, Germany) and Thermo Fisher Scientific. Unless indicated otherwise, all buffers and reagents were prepared in or dissolved in double-distilled water.

3.1.2. Animals

B6;129S5-Spl3Gt(OST279815)Lex/Mmucl mice had been generated by Lexicon Pharmaceuticals (The Woodlands, USA) and Genentech (San Francisco, USA) and kindly made available to the research community. They were obtained through the Mutant Mouse Regional Resource Center (MMRRC) at the University of California at Davis (USA).

3.1.4 Cell lines

Tab. 3.1 lists all clonal cell lines used throughout or generated in the course of this study as well as their respective sources.

Tab. 3.1: Cell lines used and generated during the course of this study. Bold number in brackets refer to expression constructs cloned in this study and listed in Tab. 3.2. Continued on the following page.

Cell line	stably transfected plasmid(s)	antibiotic resistance	source
HeLa	none	none	ATCC
HEK293 TetR/T-REx™	pcDNA6/TR	blasticidin	life technologies
HEK293 TetR SPPL2a-HA wt	pcDNA6/TR pcDNA4/TO/SPPL2a-HA wt	blasticidin zeocin	Dr Regina Fluhrer, LMU Munich (Martin <i>et al.</i> , 2008)
HEK293 TetR SPPL2a-HA D412A	pcDNA6/TR pcDNA4/TO/SPPL2a-HA D412A	blasticidin zeocin	Dr Regina Fluhrer, LMU Munich (Martin <i>et al.</i> , 2008)
HEK293 TetR SPPL2b-HA wt	pcDNA6/TR pcDNA4/TO/SPPL2b-HA wt	blasticidin zeocin	Dr Regina Fluhrer, LMU Munich (Martin <i>et al.</i> , 2008)
HEK293 TetR SPPL2b-HA D421A	pcDNA6/TR pcDNA4/TO/SPPL2b-HA D421A	blasticidin zeocin	Dr Regina Fluhrer, LMU Munich (Martin <i>et al.</i> , 2008)
HEK293 TetR SPPL3-HA wt (isoform 2)	pcDNA6/TR pcDNA4/TO/SPPL3-HA wt (isoform 2)	blasticidin zeocin	Dr. Regina Fluhrer, LMU Munich (Martin <i>et al.</i> , 2008)
HEK293 TetR SPPL3-HA wt (isoform 1)	pcDNA6/TR pcDNA4/TO/SPPL3-HA wt (isoform 1), (7)	blasticidin zeocin	this study

Cell line	stably transfected plasmid(s)	antibiotic resistance	source
HEK293 TetR SPPL3-HA D271A (isoform 2)	pcDNA6/TR pcDNA4/TO/SPPL3-HA D471A (isoform 2)	blasticidin zeocin	Dr. Regina Fluhrer, LMU Munich (Martin <i>et al</i> , 2008)
HEK293 TetR SPPL3-HA D200N/D271N (isoform 2)	pcDNA6/TR pcDNA4/TO/SPPL3-HA D200N/D271N (isoform 2)	blasticidin zeocin	this study
HEK293 TetR SPPL2a-HA wt FVenv	pcDNA6/TR pcDNA4/TO/SPPL2a-HA wt pcDNA3.1hygro/FVenv (2)	blasticidin zeocin hygromycin	this study
HEK293 TetR SPPL2a-HA D412A FVenv	pcDNA6/TR pcDNA4/TO/SPPL2a-HA D412A pcDNA3.1hygro/FVenv (2)	blasticidin zeocin hygromycin	this study
HEK293 TetR SPPL2b-HA wt FVenv	pcDNA6/TR pcDNA4/TO/SPPL2b-HA wt pcDNA3.1hygro/FVenv (2)	blasticidin zeocin hygromycin	this study
HEK293 TetR SPPL2b-HA D421A FVenv	pcDNA6/TR pcDNA4/TO/SPPL2b-HA D421A pcDNA3.1hygro/FVenv (2)	blasticidin zeocin hygromycin	this study
HEK293 TetR SPPL3-HA wt (isoform 2) FVenv	pcDNA6/TR pcDNA4/TO/SPPL3-HA wt (isoform 2) pcDNA3.1hygro/FVenv (2)	blasticidin zeocin hygromycin	this study
HEK293 TetR SPPL3-HA D271A (isoform 2) FVenv	pcDNA6/TR pcDNA4/TO/SPPL3-HA D471A (isoform 2) pcDNA3.1hygro/FVenv (2)	blasticidin zeocin hygromycin	this study
HEK293 TetR FVenv ΔE	pcDNA6/TR pcDNA3.1hygro/FVenv ΔE (5)	blasticidin hygromycin	this study
HEK293 TetR FVenv ΔE(AP)	pcDNA6/TR pcDNA3.1hygro/FVenv ΔE(AP) (6)	blasticidin hygromycin	this study
HEK293 TetR Flag-GnT-V-V5	pcDNA6/TR pcDNA3.1hygro/Flag-GnT-V-V5 (10)	blasticidin hygromycin	this study
HEK293 TetR SPPL3-HA wt (isoform 2) Flag-GnT-V-V5	pcDNA6/TR pcDNA4/TO/SPPL3-HA wt (isoform 2) pcDNA3.1hygro/Flag-GnT-V-V5 (10)	blasticidin zeocin hygromycin	this study
HEK293 TetR SPPL3-HA D200N/D271N (isoform 2) Flag-GnT-V-V5	pcDNA6/TR pcDNA4/TO/SPPL3-HA D200N/D271N (isoform 2) pcDNA3.1hygro/Flag-GnT-V-V5 (10)	blasticidin zeocin hygromycin	this study
HEK293 TetR TRC2-pLKO.5-puroP	pcDNA6/TR TRC2-pLKO.5-puroP	blasticidin puromycin	Dr. Regina Fluhrer, LMU Munich, unpublished
HEK293 TetR TRC2-SPPL3-puroP	pcDNA6/TR TRC2-pLKO.5-puroP	blasticidin puromycin	Dr. Regina Fluhrer, LMU Munich, unpublished
MEF Spp3 ^{+/+} E5	none	none	this study
MEF Spp3 ^{-/-} E2	none	none	this study
MEF PS1/PS2 ^{+/+}	pMSSVLT	none	Dr. Bart De Strooper, Leuven (Herreman <i>et al</i> , 2003)
MEF PS1/PS2 ^{-/-}	pMSSVLT	none	Dr. Bart De Strooper, Leuven (Herreman <i>et al</i> , 2003)

3.1.4 Plasmids

pcDNA3.1hygro+ and pcDNA4/TO/myc-his A were purchased from life technologies (Carlsbad, USA). pCiES which includes the full-length coding sequence of FVenv of simian origin (SFVcpz(hu)) was kindly provided by David W. Russell (University of Washington, USA). The ORF shuttle clone OCABo5050G0617D/100061790 containing the human GnT-V coding sequence was obtained from Source BioScience, Nottingham, UK. C-terminally HA-tagged human SPPL3 (isoform 2) cloned into pcDNA4/TO had previously been generated in the laboratory of Dr. Regina Fluhrer (Ludwig-Maximilians University Munich) and the original

plasmid containing the coding sequence of human *SPPL3* (isoform 2) had kindly been provided by Dr. Bruno Martoglio (ETH Zurich, Switzerland). Plasmids encoding *SPPL3*-specific and non-targeting control shRNAs were purchased from Sigma. Expression constructs cloned in this study are listed in Tab. 3.2.

3.2 Experimental procedures

3.2.1 Molecular cloning

3.2.1.1 Overview of expression constructs generated

Tab. 3.2 lists all constructs generated in this study that were subsequently used for expression in eukaryotic cells and give a brief description of the cloning strategy employed, including sequences of primers used for amplification by polymerase chain reaction (PCR) and restriction enzymes used. Epitope tags as well as restriction enzyme cleavage sites were introduced via primers. All oligonucleotide primers were ordered from either Sigma or Thermo Fisher Scientific, obtained as lyophilisate and dissolve in sterile water (final molarity: 100 µM).

Tab. 3.2: Expression constructs generated. Primer sequences are listed in Tab. 3.3 under the primer number given here as reference. Primers used for site-directed mutagenesis (SDM) are listed in Tab. 3.4. *, These GnT-V expression constructs were cloned by Ulrike Künzel. Continued on the following page.

construct #	construct name	description	vector backbone	enzyme strategy	primer number
1	ORF Flag V5 HindIII/Xhol	Generation of vector that enables HindIII/Xhol insertion of full-length FVenV cds; includes N-terminal initiator ATG, Flag tag, HindIII site, spacing region, Xhol site, in-frame KKKNNQ ER retention signal, stop codon; generated via pre-annealing of primers and cloning into NheI/PspOMI-opened pcDNA3.1hygro+	pcDNA3.1 hygro+	NheI PspOMI	P0 P-1
2	FVenV wt	Flag- and V5-tagged full-length FVenV, including C-terminal ER retention signal; FVenV coding sequence (aa 2 to 983) cloned into ORF Flag V5 HindIII/Xhol via HindIII and Xhol; PCR template: pCiES	pcDNA3.1 hygro+	HindIII Xhol	P65 P66
3	FVenV mut	Full-length Flag- and V5-tagged full-length FVenV, harbouring R123A/R126A mutations; generated by SDM; PCR template: FVenV wt	pcDNA3.1 hygro+	HindIII Xhol	Tab. 3.4
4	FVenV mut/ΔKKXX	Full-length Flag- and V5-tagged full-length FVenV, harbouring R123A/R126A mutations, stop codon inserted upstream of C-terminal KKKNNQ; generated by SDM; PCR template: FVenV mut	pcDNA3.1 hygro+	HindIII Xhol	Tab. 3.4
5	FVenV ΔE	comprises FVenV amino acids 32 to 106, N-terminally Flag-tagged, C-terminally V5-tagged; PCR template: pCiES	pcDNA3.1 hygro+	HindIII Xhol	P42 P43
6	FVenV ΔE AP	comprises FVenV amino acids 32 to 106, N-terminally V5-tagged, C-terminally Flag-tagged, ends with alanine-proline motif; tags introduced by PCR, AP motif by SDM; PCR template: FVenV ΔE	pcDNA3.1 hygro+	HindIII Xhol	P57 P59 Tab. 3.4

construct #	construct name	description	vector backbone	enzyme strategy	primer number
7	hsSPPL3 isoform 1	cloned overlap extension PCR with internal primers introducing the sequence differences to SPPL3 isoform 2; first PCR: P-1 & P122; P-2 & P122; second PCR: P-1 & P-2; PCR template: SPPL3 isoform 2 in pcDNA4/TO	pcDNA4/TO	EcoRI Xhol	P-2 P-3 P121 P122
8	hsSPPL3 isoform 2 D200N/D271N	mutant of human SPPL3 isoform 2, generated by two successive site-directed mutagenesis reactions; PCR template: SPPL3 isoform 2 in pcDNA4/TO	pcDNA4/TO	EcoRI Xhol	Tab. 3.4
9	GnT-V*	untagged, full-length human GnT-V; PCR template: ORF shuttle clone OCABo5050G0617D/100061790	pcDNA3.1 hygro+	KpnI Xhol	P166 P167
10	Flag-GnT-V-V5*	N-terminally Flag- and C-terminally V5-tagged full-length human GnT-V; PCR template: GnT-V	pcDNA3.1 hygro+	KpnI Xhol	P168 P169
11	GnT-V NTF*	comprises amino acids 2 to 61 of human GnT-V; N-terminally V5-, C-terminally Flag-tagged, ends with alanine-proline motif; ; PCR template: GnT-V	pcDNA3.1 hygro+	KpnI Xhol	P176 P180

Tab. 3.3: Oligonucleotides used for molecular cloning. Continued on the following page.

primer names	primer sequence (5' → 3')
P0/Flag-V5-KKxx-Nhel/PspOMI_fw	CTAGCACCAGTGGACTACAAGGACGACGACAAGAAGCTTCGCTCGAGGGTAAGCCTATCCCTAACCTCTCCTCGGTCTCGATTCTACGACGAAAAAGAAGAATCAGTAGT
P-1/Flag-V5-KKxx-Nhel/PspOMI_rev	GGCCACTACTGATTCTTCTTTCGTCGTAGAATCGAGACCGAGGAGAGGGTTAGGGATAGGCTTACCCCTCGAGGCAGCTCTTGTAGTCCATGGTG
P65/pfoa2-Hind-for	TCCAAGCTTGCACCACCAATGACACTGCAAC
P66/pfoa983-Xho-rev	CGCTCGAGAGGAATCCATGATACAATCTTAA
P42/Flag-HindIII_for	CTCCAAGCTTATGACTACAAGGACGACGACG
P43/V5-Stopp_rev	CGCTCGAGGTACGTAGAATCGAGACCGAGGGAGAGG
P57/pfoa32-Hind-V5-for	CTCCAAGCTTGACCATGGTAAGCCTATCCCTAACCTCTCCTCGGTCTCGATTCTACGCAGCAGAAGGAACAAAT TATACTGGAC
P59/pfoa106-Flag-Xho-rev	CGCTCGAGCGGCTACTTGTGTCGTCGTCTGTAGTCTATTACAGGTCTTAACCTGAATATC
P-2/Fluhrer - SPPL3 fw EcoRI	CGGAATTCATGGCGGAGCAGACC
P-3/Fluhrer - SPPL3 HA rw Xho neu	CCGCTCGAGTCAGGCGTAGTCGGCACGTCGTAGGGTAAGCTACTTCCAGGAATCGGGAGCTGCT
P121/hsSPPL3 iso 1_fw	TTCAATGGGAACAGGAACCAATAATTGGCTTCCAACCAATGGACTCTACCCGGGCTCGGTCCTCCAATGGGAG CATGTGTCTCT
P122/hsSPPL3 iso 1_rev	AGAGACACATGCTCCCATTGGAAGGAACCGAGCCCCGGGTAGAGTCCATTGGTGGAAAGCCAATTATTGGTCTGT TCCCCATTGAA
P166/hsMGAT5_fw	GCTTGGTACCGACCATGGCTCTCTTCACTCCG
P167/hsMGAT5_rev	CTCTAGACTCGAGCTATAGGCAGTCTTGCAG
P168/hsMGAT5_Flag_fw	CTTGGTACCGACCATGGACTACAAGGACGACGACAAGGCTCTTCACTCCGTGGAAG
P169/hsMGAT5_V5_rev	GGCCCTCTAGACTCGAGCTACGTAGAATCGAGACCGAGGGTTAGGGATAGGCTACCTAGGCAGTCTTGC AGAGAGCCAC

primer names	primer sequence (5' → 3')
P176/hsMGAT5-V5_fw	GCTTGGTACCGACCATGGGTAAGCCTATCCCTAACCCCTCCTCGGTCTCGATTCTACGGCTCTTCACCTCCGTGGAAG
P180/hsMGAT5-trunc-Flag_rev	CTCTAGACTCGAGCTAGGGGGCCTTGTCGTCGTCGTCCTGTAGTCCAGTGCCTTGATGTACCTTTG

3.2.1.2 Polymerase chain reaction

DNA was amplified by PCR with primers and templates indicated in Tab. 3.2 and 3.3 using the Pwo polymerase (PEQLAB, Erlangen, Germany). A 50 µl reaction mixture included 5 ng DNA template, 0.5 µM of each oligonucleotide primer, dNTPs at 400 µM (Roche, Rotkreuz, Switzerland), reaction buffer and 1 U Pwo Polymerase. Reactions were performed in an Eppendorf Mastercycler personal with an initial denaturation for 5 min at 94°C followed by 30 cycles of 1 min at 95°C, 1 min at 55°C and 4 min/1 kb at 68°C and a final incubation for 10 min at 68°C.

SPPL3 isoform 1 was cloned by overlap extension PCR using SPPL3 isoform 2 as a template and sequence alterations were included in the oligonucleotide primers. Two individual PCRs were performed using one terminally and one internally annealing primer. The individual two PCR products were then fused in another PCR using only flanking PCR primers.

3.2.1.3 Submerged agarose gel electrophoresis

TAE buffer (50x): 40 mM Tris pH 8.0, 20 mM Na(CH₃COO)₂, 2 mM EDTA
DNA sample buffer (10x): 100 mM Tris pH 9.0, 10 mM EDTA, 50% (v/v) glycerol, 0.5% (w/v) Orange G

DNA fragments were analysed by submerged agarose gel electrophoresis (SAGE). To this end, samples were mixed with sample buffer and separated 1x TAE-buffered gels containing 0.5 to 2 % (w/v) agarose (Invitrogen, Carlsbad, USA) containing 0.2 µg/ml ethidium bromide. Samples were compared to commercial DNA markers (Invitrogen, Carlsbad, USA) and analysed by UV illumination. For subsequent processing, DNA fragments of the expected size were excised from the gel and extracted using the NucleoSpin Gel and PCR clean-up kit (Macherey-Nagel, Düren, Germany) according to the manufacturer's instructions.

3.2.1.4 Restriction endonuclease digestion of DNA

Restriction endonucleases from commercial sources (Thermo Fisher Scientific or New England Biolabs, Ipswich, USA) were used to digest DNA. To this end, DNA was diluted in water, supplemented with the respective reaction buffer, mixed with the respective enzymes (5 to 20 U) according to the manufacturer's recommendations and incubated at 37°C for 2 to 16 h. Reaction products were purified as described in 3.2.1.3. Individual restriction enzymes used for cloning are listed in Tab. 3.2.

3.2.1.5 Ligation

Ligations were performed using T4 DNA Ligase (Thermo Fisher Scientific) and the supplied reaction buffer. Reactions with a total volume of 20 μ l containing roughly 50 to 100 ng restriction enzyme-digested target vector and 1 to 2 μ g digested DNA fragments were incubated at room temperature for 2 h or alternatively at 14°C overnight.

3.2.1.6 Site-directed mutagenesis

Tab. 3.4 lists oligonucleotides used for site-directed mutagenesis. They were designed in strict accordance with guidelines from the QuikChange II Site-Directed Mutagenesis Kit (Agilent Technologies, Santa Clara, USA). A 50 μ l reaction mixture included 10 ng DNA template, 125 ng of each oligonucleotide primer, dNTPs at 400 μ M (Roche), 2,5 U Pfu turbo DNA polymerase (Agilent) and the reaction buffer supplied. Reactions were performed with an initial denaturation for 1 min at 95°C followed by 16 cycles of 30 s at 95°C, 30 s at 55°C and 2 min/1 kb at 68°C and a final incubation for 10 min at 68°C. Afterwards, 1 μ l of DpnI (New England Biolabs) was added and the reaction mix was incubated at 37°C for 1.5 h to digest template DNA.

Tab. 3.4: Oligonucleotide primers used for site-directed mutagenesis.

primer name	sequence (5' → 3', mismatches bold)	mutation	target
P69/TAG_fw	CGGTCTCGATTCTACGTAGACGAAAAAGAAGAAC	stop codon insertion	FVenv
P70/TAG_rev	GATTCTTCTTTCTCGTACGTAGAACATCGAGACCG		
P93/AP-mut-fw	GACGACGACGACAAG GGCCCC TAGCCGCTCGAGTC	alanine-proline insertion	FVenv
P94/AP-mut-rev	GACTCGAGCGGC TAGGGGGC CTTGTCTCGTCGTC		
P73/RR123/126AAfw	CCCTTACAGACTAGA GCCATTG CAG CC TCCCTAGAACATGCAGC	R123A/R126A	FVenv
P74/ RR123/126AArev	GCTGCATTCTAAGGG GGC TGCAAT GGC TCTAGTCTGTAAGGG		
P132_hSPPL3D-->N_fw	CTCCATGTTGGGCATCGGA AA CATCGTTATGCCTGGCTCC	D271N	SPPL3
P133_hSPPL3D-->N_rev	GGAGACCAGGCATAACGAT GTT CCGATGCCAACATGGAG		
P138-hSPPL3D-->N2_fw	CTCTCAGGGCTTCTCATCTAT AA CGTCTTTGGGTATTTCTC	D200N	SPPL3
P139-hSPPL3D-->N3_rev	GAGAAAAATACCCAAAAGAC GTT TATAGATGAGAAGCCCTGAGAG		

3.2.1.7 Transformation of *E. coli*

LB medium: 1% (w/v) bactotrypton, 0.5% (w/v) yeast extract, 1% (w/v) NaCl
autoclaved at 120°C and 1.2 bar for 20 min

CaCl₂ buffer: 50 mM CaCl₂, 10 mM Tris pH 8.0

LB agar plates: LB medium supplemented with 15 g/l agar, autoclaved at 120°C at 1.2 bar for 20 min, supplemented with 100 μ g/ml ampicillin or spectinomycin following cooling, poured into plastic Petri dishes

To obtain heat shock-competent cells, an overnight culture of *E. coli* DH5 α was diluted in fresh LB medium and incubated at 37°C and 250 rpm until an OD₆₀₀ of 0.5 was reached. Cells were pelleted by centrifugation at 1,500g and 4°C for 5 min. They were then resuspended in ice-cold

CaCl₂ buffer and chilled on ice for 30 min. Cells were pelleted again, resuspended in 1 ml of CaCl₂ and aliquots were stored at -80°C.

For transformation, 100 µl of cells were thawed on ice and mixed with 10 µl of a ligation reaction, 1 µl of a site-directed mutagenesis reaction or 50 ng intact plasmid DNA. Following incubation on ice for 10 min, the mixture was incubated at 42°C for 2 min and instantly chilled on ice for an additional 2 min. 1 ml of sterile LB medium was added and samples were agitated for 1 h at 37°C. The mixture was then either plated on LB agar plates or used to inoculate sterile LB medium. In either case, media were supplemented with ampicillin or spectinomycin (100 µg/µl, Carl Roth) to select for transformed cells.

3.2.1.8 Preparation of plasmid DNA

Plasmid DNA was isolated from bacterial cultures agitated overnight at 37°C using commercial kits according to the manufacturer's instructions (Macherey-Nagel). DNA concentration was determined photometrically using a UV-Vis NanoPhotometer (Implen, Munich, Germany) and plasmid identity was verified by restriction endonuclease digestion and SAGE.

3.2.1.9 Sequencing

Plasmid sequence identity was verified prior to use. To this end, plasmid samples were sent to GATC Biotech (Konstanz, Germany) and sequence information was obtained by Sanger sequencing using standard sequencing primers or, alternatively, internal sequencing primers (Tab. 3.5). Sequence analysis was performed using the CLC Main Workbench, v6.6 (CLC bio, Aarhus, Denmark).

Tab. 3.5: Oligonucleotide primers used for sequencing. Classical sequencing primers provided by GATC Biotech such as T7_for, CMV_for, BGH_rev etc. are not listed.

primer name	sequence (5' → 3')	target
P61/foa-env-2080_rev	GTAGCTGTGGGAGAACTATG	FVenv
P62/Foa-env-1400_for	GGAACCCATAGTGGTGAAGG	FVenv
P164/MmMGAT5_int	TGGGTTCATTACCAGTG	MGAT5
P174/mmMGAT5_int_rev	CACTGGTAATGAACCCAG	MGAT5
P175/mmMGAT5_int_fw	GATCCGGCGAATGGCTGACG	MGAT5

3.2.2 Animal work

3.2.2.1 Animal housing and breeding

Mice were kept at specific pathogen-free conditions at the Institute of Immunology, Ludwig-Maximilians University Munich, Munich, Germany. To maintain the mixed B6;129S5 background, heterozygous B6;129S5-Sppl3^{Gt(OST279815)Lex}/Mmucl mice were inter-crossed. At the same time, B6;129S5-Sppl3^{Gt(OST279815)Lex}/Mmucl were crossed back to the Institute of Immunology's C57BL/6 strain for 5 generations.

3.2.2.2 Mouse genotyping

Tail lysis buffer: 100 mM Tris, pH 8.5, 5 mM EDTA, 0.2% (w/v) SDS, 200 mM NaCl, freshly added proteinase K (100 µg/ml, Roche)

Mouse genotyping was conducted on genomic DNA isolated from tail clips or cultured cells. Samples were agitated in 500 µl tail lysis buffer overnight and debris was sedimented by centrifugation at 13 krpm for 5 min. DNA was precipitated from the supernatant by addition of 0.8 volumes of isopropanol, mixing, and centrifugation at 13 krpm and 4°C for 20 min. The pellet was washed once with 70% (v/v) ethanol. Next, the dried pellet was resuspended in 200 µl sterile water and incubated at 55°C for 1 h. The solution was refrigerated until use.

Primers used for genotyping PCRs are listed in Tab. 3.6. Reactions were set-up as described in 3.2.1.2 but the GoTaqGreen polymerase and the supplied reaction buffer (Promega, Madison, USA) were used instead of Pwo polymerase. Correct insertion of the genetrap into the SPPL3 locus was tested by a touchdown PCR. An initial denaturation for 10 min at 94°C was followed by 10 PCR cycles (each 15 s at 95°C, 30 s at 65°C (decreased by 1°C every cycle) and 30 s at 72°C). 30 additional cycles followed (each 15 s at 95°C, 30 s at 55°C and 30 s at 72°C) and the reaction was terminated after a final elongation of 5 min at 72°C. Presence of the intact wild-type allele was checked by two additional PCR reactions (2 min at 95°C, 30 to 35 cycles (each 1 min at 94°C, 30 s at 64°C, 1 min at 72°C, 10 min at 72°C). PCR products were separated by SAGE (3.2.1.3).

Tab. 3.6: Oligonucleotide primers used for genotyping.

primer name	sequence (5' → 3')	amplicon
P95/L3-KO-pair1_for	GCAGGCATCTGCAGAACTCATG	ca. 440 bp, wt allele
P96/L3-KO-pair1_rev	GCCGTGACACAGCAAGTGCA	
P158/L3-KO-rev2	TTTACTAGGGAGAGGCGTCAT	ca. 340 bp, wt allele
P159/L3-KO-fw2	AAGTGCTGGATTAAAGGCAGA	
P97/LTR2	AAATGGCGTTACTTAAGCTAGCTTGC	ca. 220 bp, inserted genetrap
P98/PRT340T2 3'	AAACCTTACTAGGGAGAGGCGTCA	

3.2.2.3 Tissue homogenisation

Homogenisation buffer: 5 mM Tris x HCl, pH 7.4, 250 mM sucrose, 5 mM EGTA, supplemented with protease inhibitor mix (1:500, Sigma)

Organs were removed at necropsy of sacrificed animals and frozen instantly on dry ice. Thawed organs were cut into pieces and homogenised in homogenisation buffer using a Wheaton tissue grinder (Thermo Fisher Scientific) and 23G needles afterwards. Homogenates were centrifuged for 5 min at 5 krpm and 4°C. Supernatants were transferred into an ultracentrifugation tube (Beckman-Coulter, Brea, USA) and subjected to centrifugation at 100,000g and 4°C for 1 h. Pellets were resuspended in homogenisation buffer containing 2% (v/v) Triton X-100 and incubated on ice for 30 min. Lysates were cleared by centrifugation (13 krpm, 4°C, 30 min).

Protein content was determined as detailed elsewhere (3.2.4.2) and samples were subjected to SDS-PAGE and Western blotting (3.2.4.7 to 3.2.4.9).

3.2.2.4 Generation of murine embryonic fibroblasts

basic medium: DMEM GlutaMax® (life technologies) supplemented with 10% (v/v) FCS, 2 mM L-glutamine, 50 U/ml penicillin and 50 µg/ml streptomycin

Murine embryonic fibroblasts (MEFs) were obtained from B6.129S5-SplI3^{Gt(OST279815)Lex}/Mmucd (N5) mice. Following mating with a heterozygous male, a heterozygous pregnant female was sacrificed and P13.5 embryos were taken from the corpse. Head and limbs as well as inner organs were removed from the embryo and the remaining material was cut in piece and resuspended in 1 ml sterile HBSS (life technologies, Carlsbad, USA). 2 ml sterile trypsin (0.05% (w/v))-EDTA (life technologies) was added and the tissue was digested for 20 min at 37°C. 7 ml DMEM medium (GlutaMax®, life technologies) supplemented with 15% (v/v) fetal calf serum (Sigma), 2 mM L-glutamine (life technologies) and 50 U/ml penicillin/50 µg/ml streptomycin (life technologies) were added and cells were sedimented by centrifugation. Cell pellets were then resuspended in basic medium and cultivated as described elsewhere (3.2.3.1). Embryos were genotyped as described in 3.2.2.2 using the head to isolate genomic DNA. Primary MEFs were expanded and used for experiments. In addition, MEFs were immortalised as described earlier (Xu, 2005).

3.2.2.5 Flow cytometric analysis of NK cell counts

FACS medium: DMEM (life technologies) supplemented with 10 mM Hepes and 1% (w/v) BSA

Inguinal, axillary and brachial lymph nodes were removed from sacrificed mice and taken up in 5 ml FACS medium. They were homogenised between the rough edges of microscope slides and pipetted through a nylon mesh. Following centrifugation at 1,500 rpm for 5 min, the supernatant was removed, cells were resuspended in 1 ml FACS medium and counted using a Neubauer chamber. The removed spleen was treated similarly, but the cell suspension was underlaid with 3 ml Lympholyte M (Cedarlane Labs, Burlington, Canada) and centrifuged at 2,000 rpm (i.e. 671 rcf) for 15 min without brake. Cells were collected from the interphase, mixed with 5 ml FACS medium and centrifuged again at 1,500 rpm for 5 min. The supernatant was discarded and cells were resuspended in 2 ml FACS medium and counted. For each staining, 1 to 5 million cells were used and staining was conducted in a 96-well plate. Fc receptors were blocked with an anti-mouse CD16/32 antibody (1:400 in FACS medium, 50 µl/well; BioLegend, San Diego, USA) on ice for 10 min. Cells were sedimented and taken up in 50 µl of the respective antibody solution. FITC-conjugated anti-mouse NKp46 (clone 29A1.4) and PE-conjugated anti-mouse CD49b (clone DX5) as well as the respective isotype control antibodies were obtained from eBioscience (San Diego, USA). They were pre-diluted 1:400 in FACS medium and centrifuged at 13 krpm for 5 min to remove aggregates. Antibody binding was done at 4°C in darkness for 20 to 30 min. Cells were washed once with 200 µl FACS medium and then taken up in 200 µl FACS buffer supplemented with DAPI. Measurements were

done using a FACSCanto™ (Becton Dickinson, Franklin Lanes, USA) and were analysed with the FlowJo software suite. These experiments were performed together with Anne Behrendt, Institute of Immunology, Ludwig-Maximilians University Munich.

3.2.2.5 In vitro differentiation of bone marrow-derived dendritic cells

PBS: 140 mM NaCl, 10 mM Na₂HPO₄, 1.75 mM KH₂PO₄, pH 7.4,
autoclaved at 120°C and 1.2 bar for 20 min

DC medium: RPMI 1640 (life technologies) supplemented with 10% (v/v) FCS,
2 mM L-glutamine, 50 U/ml penicillin and 50 µg/ml streptomycin

Bone marrow-derived dendritic cells (BMDCs) were generated by *ex vivo* generation of haematopoietic stem cells in the presence of GM-CSF and IL-4. Femur and tibia were surgically removed from sacrificed mice, cleaned and briefly dipped into ethanol. Under sterile conditions, epiphyses were cut off and bones diaphyses were rinsed with PBS to liberate bone marrow cells. The cell solution was collected and cells were pelleted by centrifugation (350g, 4°C, 8 min). The cell pellet was resuspended in 5 ml 1x Pharm lyse (Becton-Dickinson) and incubated at room temperature for 3 min to lyse erythrocyte contaminants. 35 ml PBS were added and cells were pelleted again. Cells were resuspended in DC medium and plated in a T-75 tissue culture flask. Dendritic cell (DC) differentiation was started by addition of 0.1 µg/ml GM-CSF and 0.1 µg/ml IL-4 (both from PeproTech, Rocky Hill, USA). After 2 to 3 days, 10 ml of DC medium supplemented with GM-CSF and IL-4 were added. One week after plating, cells were counted and 5 x 10⁶ cells were plated on fresh 10 cm dishes in 5 ml DC medium. Where indicated, cells were stimulated with CpG (Enzo) at 0.3 µM.

3.2.3 Cell biology

3.2.3.1 General techniques

basic medium: DMEM GlutaMax® (life technologies) supplemented with 10% (v/v) FCS,
2 mM L-glutamine, 50 U/ml penicillin and 50 µg/ml streptomycin

PBS: 140 mM NaCl, 10 mM Na₂HPO₄, 1.75 mM KH₂PO₄, pH 7.4
autoclaved at 120°C and 1.2 bar for 20 min

All cells were cultivated in water-jacket incubators in a humidified atmosphere containing 5% (v/v) CO₂. All cells were cultivated in basic medium supplemented with 5 µg/ml blasticidin, 100 µg/ml hygromycin, 1 µg/ml puromycin or 200 µg/ml zeocin (all from life technologies) according to Tab. 3.1 and passaged every 3 to 4 days. To this end, cells were washed once with phosphate-buffered saline (PBS) and detached by incubation in trypsin(0.05%)-EDTA (life technologies). Following centrifugation at 1,000 rpm for 5 min, the cell pellet was resuspended in fresh medium and, when required, the cells were counted in a Neubauer chamber and plated.

All experiments were conducted on poly-L-lysine coated plates. To obtain these, culture dishes were covered with poly-L-lysine (Sigma) dissolved in PBS at 100 µg/ml. Following incubation for

1 h, the poly-L-lysine solution was removed and plates were washed three times with sterile PBS. Experiments were performed in DMEM medium supplemented solely with 10% (v/v) FCS. Over-expression of tet operator-controlled wild-type or mutant SPPL2a, SPPL2b and SPPL3 was induced by supplementing the culture medium with 1 µg/ml doxycycline (Carl Roth). For subsequent analysis by biochemical methods, conditioned supernatants were collected, subjected to centrifugation at 13 krpm and 4°C for 20 min to remove detached cells and the supernatant was transferred into a new reaction tube. It was either directly subjected to gel electrophoresis (see 3.2.4.7) or proteins were enriched by trichloroacetic acid precipitation (see 3.2.4.6). Cells were washed once with ice-cold PBS, detached in 1 ml PBS using a cell scraper and sedimented by centrifugation. Material was either used directly or stored at -20°C or -80°C until further use.

3.2.3.2 Transfection with plasmid DNA

Cells were transfected with plasmid DNA using Lipofectamine 2000 (Life Technologies). For a single 6 or 10 cm dish, 8 µl Lipofectamine 2000 were pre-incubated in 500 µl Optimem (Life Technologies) at room temperature for 5 min. At the same time 4 to 8 µg plasmid DNA were mixed with 500 µl Optimem. Both solutions were mixed and incubated at room temperature for 20 min before being added to the culture dish at roughly 75% confluence. Cells and conditioned supernatants were used for experimentation 48 h after transfection. To obtain stably transfected cells, cells were serially diluted into basic medium supplemented with the respective antibiotic to select for plasmid-encoded resistance genes. Resistant pooled cells or single cell-derived clones were expanded and analysed for exogenous protein expression as described.

3.2.3.3 RNAi

To reduce endogenous gene expression, cells were transiently transfected with siGENOME SMART pool siRNAs targeting *SPPL2a* (#M-006040-01), *SPPL3* (#M-006042-02), *B3GNT1* (#M-012307-01), *B4GALT1* (#M-012965-00), *EXTL3* (#M-012578-00), *XYLT2* (#M-013040-01), *B3GALT6* (#M-021340-01), *HS6ST1* (#M-011944-01), *HS6ST2* (#M-015558-01), *SGK196* (#M-005321-00) or *MGAT5* (#M-011334-01) obtained from Thermo Fisher Scientific. As control, cells were transfected with siGENOME non-targeting siRNA pool #2 (#D001206-14). *SPPL2b*-targeting siRNA (#SI04256070) and a respective control siRNA were from Qiagen (Hilden, Germany). All siRNAs were dissolved in sterile, RNA-free water (Qiagen) at 20 µM. In a 6 cm dish, 1.2 ml Optimem, 3 µl siRNA (pool) and 12 µl Lipofectamine RNAiMax (Life Technologies) were incubated for 20 min. 1.6 to 2.0 x 10⁶ cells (freshly trypsinised and diluted in 1.8 ml DMEM supplemented with 10% (v/v) FCS) were added. After 16 to 24 h the culture medium was changed and cells were analysed 3 to 5 days later.

3.2.3.4 Inhibitor treatment

In the course of this study, cells were treated with various small molecules. Compounds were diluted in culture medium, treatment was generally performed for 16 to 24 h and cells were directly harvested afterwards. Inhibitors used were: kifunensine (Santa Cruz Biotechnology, Dallas, USA), (Z-LL)₂ ketone (Merck, Darmstadt, Germany), DAPT (Enzo) and L-685,458

(Merck). The compounds were used at concentrations indicated in the respective figure legend. Kifunensine was dissolved in sterile double-distilled water and all other inhibitors were dissolved in DMSO.

3.2.3.5 Immunocytochemistry and confocal microscopy

PBS:	140 mM NaCl, 10 mM Na ₂ HPO ₄ , 1.75 mM KH ₂ PO ₄ , pH 7.4
Mowiol:	6.0 g glycerol, 2.4 g Mowiol 4-88 (Carl Roth), 12.0 ml 0.2 M Tris x HCl pH 8.5 6.0 ml double-distilled water, 25 mg/ml DABCO (Carl Roth) Glycerol and Mowiol were stirred for 1 h at room temperature, water was added and the mixture was stirred for another hour, following addition of Tris buffer, the mixture was incubated at 50°C for 2 h and stirred for 2 min every 20 min. After centrifugation for 15 min at 5,000 g, the supernatant was frozen until use.
4% (w/v) PFA:	4 g PFA (Sigma) were added to approximately 80 ml of heated (ca. 60°C) PBS; while being stirred 1 M NaOH was added dropwise until the solution cleared; following filtering and cooling the solution was adjusted to a pH of approximately 6.9 using dilute HCl and a total volume of 100 ml with PBS

Sub-cellular localisation of individual proteins was analysed by immunofluorescence staining and confocal laser-scanning microscopy. Cells were grown on poly-L-lysine-coated glass coverslips in 6-well or 24-well cell culture dishes and transfected as described in 3.2.2.2. Medium was aspirated and cells were washed twice with PBS. Cells were fixed by incubation in 4% (w/v) paraformaldehyde (PFA) dissolved in PBS for 20 min. The solution was discarded and fixed cells were washed three times with PBS. Cells were permeabilised in PBS supplemented with 0.2% (v/v) Triton X-100 and 50 mM NH₄Cl for 20 min. Coverslips were washed again three times with PBS and incubated in PBS supplemented with 5% (w/v) BSA at room temperature for 1 h. Coverslips were incubated in primary antibodies at ambient temperature for 1 h and afterwards washed six times with PBS. The procedure was repeated for fluorophore-conjugated secondary antibodies (anti-rabbit and anti-mouse, each conjugated to Alexa488 or Alexa555, 1:500; life technologies). Finally, coverslips were washed once in water and embedded in Mowiol on microscope slides. Primary antibodies used are listed in Tab. 3.7. All antibodies were diluted in PBS containing 1% (w/v) BSA. For detection using the anti-Flag M2 mAb, cells were briefly (5 min) fixed in PFA and subsequently incubated for 1 min in methanol (-20°C). Following drying, cells were rehydrated in PBS for 10 min at room temperature and blocking as well as immunodetection proceeded as described earlier. All samples were analysed using the 510Meta confocal laser-scanning microscope (Carl Zeiss, Jena, Germany). Images were acquired in multi-channel scanning mode and processed using the LSM Image Browser (Carl Zeiss).

Tab. 3.7: Primary antibodies used for immunocytochemical staining.

* For pAbs, the respective catalogue number is given.

antigen	species & type	clone #*	dilution	source
KDEL	mouse, mAb	10C3	1:100	Enzo
V5 tag	rabbit, pAb	AB3792	1:400	Millipore
Flag tag	mouse, mAb	M2	1:800	Sigma

3.2.4 Biochemical methods

3.2.4.1 Preparation of cellular membranes

hypotonic buffer: 10 mM Tris pH 7.6, 1 mM EDTA, 1 mM EGTA, adjust pH to 7.6
supplemented with protease inhibitor mix (1:500)

basic buffer: 40 mM Tris pH 7.8, 40 mM KCH₃COO, 1.6 mM Mg(CH₃COO)₂,
100 mM sucrose, 0.8 mM DTT

sample buffer (2x): 20% (v/v) glycerol, 3% (w/v) SDS, 3% (w/v) DTT, bromophenol blue (traces)
dissolved in 4x upper Tris buffer (see 3.2.4.7.3)

To obtain cellular membranes, cell pellets were resuspended in hypotonic buffer (800 µl/6 cm dish), vortexed and chilled on ice for 10 min. Following passing through a syringe with a 23G needle for 15 times, samples were subjected to centrifugation at 5 krpm and 4°C for 5 min to remove cellular debris and intact organelles such as nuclei and mitochondria. The post-nuclear supernatant was transferred into a new reaction tube and centrifuged at 13 krpm and 4°C for 45 min to sediment membranes. The supernatant was discarded and the membrane pellet was either lysed (see 3.2.4.2) or contained proteins were precipitated. In the latter case, pellets were resuspended in 40 µl basic buffer, mixed with 120 µl chloroform/methanol (1:2) and incubated on ice for 1 h. Following centrifugation (13 krpm, 4°C, 30 min), the supernatant was discarded. Protein precipitates were allowed to dry and were subsequently resuspended in 2x sample buffer.

3.2.4.2 Preparation of whole cell lysates

lysis buffer: 50 mM Tris pH 7.6, 150 mM NaCl, 2 mM EDTA, 1.2% (v/v) NP-40,
1% (v/v) Triton X-100, supplemented with protease inhibitor mix (1:500)

sample buffer (5x): 50% (v/v) glycerol, 7.5% (w/v) SDS, 7.5% (w/v) DTT,
bromophenol blue (traces), dissolved in 4x upper Tris buffer (see 3.2.4.7.3)

Cell pellets were resuspended in lysis buffer (100 to 300 µl/pellet of a 6 cm dish), vortexed extensively and incubated on ice for 30 to 60 min. Cell debris etc. was removed by centrifugation (13 krpm, 4°C, 30 min) and the supernatant was transferred into a new reaction tube. Membrane pellets obtained as described (see 3.2.4.1) were treated similarly to extract proteins.

Protein concentrations in lysates were determined by means of a bicinchoninic acid (BCA)-based commercial kit (Interchim, Montluçon, France) according to the manufacturer's

instructions. In brief, lysates were diluted and mixed with 200 µl reagent in a 96-well plate. Following incubation at 37°C for 15 to 30 min, the absorbance at 562 nm was measured photometrically in a plate reader (Power Wave XS, BioTek, Winooski, USA). A serial dilution of BSA was always measured in parallel as reference. Cell and membrane extracts were stored at -20°C for subsequent use, often supplemented with 5x sample buffer for SDS-PAGE (see 3.2.4.7).

3.2.4.3. Immunoprecipitations

STEN buffer: 50 mM Tris pH 7.6, 150 mM NaCl, 2 mM EDTA, 0.2% (v/v) NP-40

sample buffer (2x): 20% (v/v) glycerol, 3% (w/v) SDS, 3% (w/v) DTT, bromophenol blue (traces) dissolved in 4x upper Tris buffer (see 3.2.4.7.3)

Cell or membrane lysates were either directly subjected to immunoprecipitation or were first adjusted to the same total protein content. All samples were brought to a final volume of 1 ml with STEN buffer. 25 to 50 µl protein A- or protein G-conjugated sepharose beads (GE Healthcare, Chalfont St Giles, UK) and the respective antibody (usually 1 µg, Tab. 3.8) were added. Alternatively, anti-Flag M2-conjugated agarose beads (Sigma) were used. Immunoprecipitations were agitated at 4°C overnight. Beads were sedimented by centrifugation (7 krpm, 4°C, 5 min) and washed five times with 1 ml STEN buffer. Finally, beads were dried by removing excess buffer with a 27G needle, resuspended in 2x sample buffer and subjected to SDS-PAGE (see 3.2.4.7).

Tab. 3.8: Antibodies used for immunoprecipitations.

antigen	antibody type	antibody species	clone/cat. #	quantity	source
HA tag	mAb	rabbit	6908	1 µl	Sigma
Nicastrin	pAb	rabbit	N1660	6 µg	Sigma
V5 tag	pAb	rabbit	R960-25	1 µl	Millipore

3.2.4.4 Co-immunoprecipitations

basic buffer: 40 mM Tris pH 7.8, 40 mM KCH₃COO, 1.6 mM Mg(CH₃COO)₂, 100 mM sucrose, 0.8 mM DTT

sample buffer (5x): 50% (v/v) glycerol, 7.5% (w/v) SDS, 7.5% (w/v) DTT, bromophenol blue (traces), dissolved in 4x upper Tris buffer (see 3.2.4.7.3)

sample buffer (2x): 20% (v/v) glycerol, 3% (w/v) SDS, 3% (w/v) DTT, bromophenol blue (traces) dissolved in 4x upper Tris buffer (see 3.2.4.7.3)

For co-immunoprecipitation, cellular membranes (see 3.2.4.1) were lysed in basic buffer supplemented with 1% (w/v) CHAPSO (for FVenv co-immunoprecipitations) on ice for 1 h. Following centrifugation at 13 krpm and 4°C for 45 min, 5% of the lysate's volume were mixed with 5x sample buffer. The remaining lysate was subjected to anti-Flag immunoprecipitation as described in 3.2.4.3. Beads were washed six times in the respective lysis buffer, dried,

resuspended in 2x sample buffer and subjected to SDS-PAGE and Western blot (see 3.2.4.7 to 3.2.4.9) detection of co-precipitated proteins.

3.2.4.5 Enzymatic deglycosylation

deglycosylation buffer: 50 mM Na₂PO₄, pH 7.2, 12 mM EDTA, 0.4% (v/v) NP-40
sample buffer (5x): 50% (v/v) glycerol, 7.5% (w/v) SDS, 7.5% (w/v) DTT,
bromophenol blue (traces), dissolved in 4x upper Tris buffer

For enzymatic deglycosylation, lysates were supplemented with 1x glycoprotein denaturation buffer (New England Biolabs) as well as additional 0.5% (w/v) SDS (1% (w/v) total) and incubated at 95°C for 10 min. They were subsequently diluted with deglycosylation buffer to adjust the total SDS concentrations to 0.1 to 0.2% (w/v). Diluted samples were divided and 1 to 3 µl PNGase F (Roche) or Endo H were added. The reactions were incubated at 37°C overnight and stopped by addition of 5x sample buffer. As control, samples were incubated overnight without the addition of glycosidase.

3.2.4.6 Trichloroacetic acid precipitation

sample buffer (2x): 20% (v/v) glycerol, 3% (w/v) SDS, 3% (w/v) DTT, bromophenol blue (traces)
dissolved in 4x upper Tris buffer (see 3.2.4.7.3)

To enrich secreted proteins in conditioned supernatants devoid of FCS for analysis by Western blotting, trichloroacetic acid (TCA) precipitations were performed. To this end, cells were washed twice with pre-warmed Optimem medium and cultivated in Optimem for 6 to 48 h. Media were collected as described (see 3.2.3.1). 800 µl conditioned supernatant were mixed with 200 µl freshly prepared aqueous 100% (w/v) TCA and incubated on ice for 1 h. Following centrifugation (13 krpm, 4°C, 30 min), pellets were washed twice with acetone (-20°C). After drying, precipitated proteins were resuspended in 2x sample buffer and the pH was adjusted by addition of 1 to 3 µl 1 M Tris x HCl, pH 7.8. Samples were incubated at 95°C for 10 to 15 min and stored at -20°C.

3.2.4.7 SDS-polyacrylamide gel electrophoresis

Depending on the protein size and the individual application protein samples were either separated on Tris-glycine- (see 3.2.4.7.3) or Tris-tricine-buffered (see 3.2.4.7.4) SDS-polyacrylamide (SDS-PAGE) gels. In addition, to separate hydrophobic small molecular protein fragments urea tris-tricine gels were used (see 3.2.4.7.5).

3.2.4.7.1 Sample preparation

sample buffer (5x): 50% (v/v) glycerol, 7.5% (w/v) SDS, 7.5% (w/v) DTT,
bromophenol blue (traces), dissolved in 4x upper Tris buffer
(see 3.2.4.7.3)
sample buffer (2x): 20% (v/v) glycerol, 3% (w/v) SDS, 3% (w/v) DTT, bromophenol blue
(traces)
dissolved in 4x upper Tris buffer (see 3.2.4.7.3)

2x sample buffer (Wiltfang): 0.72 M Bis-Tris, 0.32 M Bicin, 2% (w/v) SDS, 5% β -mercaptoethanol, 30% (w/v) sucrose, bromophenol blue (traces)

All samples that were subjected to electrophoretic separation were mixed with sample buffers as indicated. For Western blot applications that required non-reducing conditions sample buffers lacking DTT were used. All samples were heat-denatured by incubation at 95°C or 65°C for 10 min prior to loading into gels.

For separation on urea tris-bicine gels (3.2.4.7.5), samples were mixed with the respective sample buffer and always denatured by incubation at 95°C for 5 min.

3.2.4.7.2 Gel casting and running equipment

Electrophoresis was performed using MINI-PROTEAN system (Bio-Rad, Hercules, USA) and gels with a thickness of 1.5 mm were cast between system-compatible glass plates. Tris-glycine separating gels were cast and overlaid with isopropanol for polymerisation. Tris-tricine separating and spacer gels (see were polymerised together, again overlaid with isopropanol. The respective stacking gels were polymerised in a second step and plastic combs were used to generate pockets. Electrophoresis was conducted in the indicated running buffer(s) at a constant voltage (70V during the stacking phase and 120V during separation) using PowerPack HC power supplies (Bio-Rad). Sea Blue pre-stained protein marker (life technologies) was used as molecular weight reference on every gel. Mighty small II chambers and the respective casting equipment (Hoefer, Holliston, USA) were used for *Wiltfang* (3.2.4.7.5) gels.

3.2.4.7.3 Tris-glycine SDS-PAGE

Lower Tris (4x): 1.5 M Tris, 0.4% (w/v) SDS, pH 8.8

Upper Tris (4x): 0.5 M Tris, 0.8% (w/v) SDS, pH 6.8

Running buffer: 25 mM Tris, 200 mM Glycine, 0.1 (w/v) SDS

Tab. 3.9 summarises the recipes for gels with 8%, 10%, 12% and 15% acrylamide content. Acrylamide (40% (w/v), acrylamid/bisacrylamid ratio 37.5:1) was purchased from Serva. Mixtures were prepared as indicated and the polymerisation was initiated by addition of the indicated amount of 10% (w/v) ammonium persulphate and N, N, N', N'-tetramethylethylenediamine (Carl Roth).

Tab. 3.9: Tris-glycine composition. For 8 ml separating gel, sufficient for one 1.5 mm MINI-PROTEAN gel, and 5 ml stacking gel.

	separating gel (8%)	separating gel (10%)	separating gel (12%)	separating gel (15%)	stacking gel
H₂O	4.4 ml	4 ml	3.6 ml	3 ml	3.25 ml
acrylamide	1.6 ml	2 ml	2.4 ml	3 ml	0.5 ml
lower Tris	2 ml	2 ml	2 ml	2 ml	-
upper Tris	-	-	-	-	1.25 ml
TEMED	15 µl	15 µl	15 µl	15 µl	15 µl
10% (w/v) APS	15 µl	15 µl	15 µl	15 µl	15 µl

3.2.4.7.4 Tris-tricine SDS-PAGE

Tris-tricine gel buffer:	3 M Tris x HCl, pH 8.45, 0.3% (w/v) SDS
acrylamide solution:	48 % (w/v) acrylamide, 1.5% (w/v) bisacrylamide
anode buffer:	200 mM Tris, pH 8.9
kathode buffer:	100 mM Tris, 100 mM tricine, 0.1% (w/v) SDS

For electrophoretic separation of small proteins and protein fragments below 16 kDa Tris-tricine gels were used which were prepared as summarised in Tab. 3.10. The spacing gel solution was carefully laid over the not yet polymerised separating gel solution to avoid mixing of the phases. The spacing gel solution was covered with isopropanol for polymerisation. The stacking gel was prepared as described earlier (see 3.2.4.7.2) using the mixture described in Tab. 3.10. Electrophoresis was performed in MINI-PROTEAN chambers (Bio-Rad) but distinct anode and kathode buffers were used.

Tab. 3.10: Tris-tricine gel composition. For two gels, 1.5 mm thickness.

	separating gel (16.5%)	spacing gel (10%)	stacking gel (4%)
H₂O	-	3.5 ml	4.2 ml
acrylamide solution	3.5 ml	1.5 ml	0.5 ml
Tris-tricine gel buffer	3.5 ml	2.5 ml	1.55 ml
32% (v/v) glycerol	3.5 ml	-	-
TEMED	6.5 µl	8 µl	10 µl
10% (w/v) APS	65 µl	70 µl	50 µl

3.2.4.7.5 Urea tris-bicin gels after Wiltfang

separating gel buffer:	1.6 M Tris, 0.4 M H ₂ SO ₄
spacing gel buffer:	0.8 Bis-Tris, 0.2 M H ₂ SO ₄
stacking gel buffer:	0.72 M Bis-Tris, 0.32 M Bicin
anode buffer:	0.2 M Tris, 0.05 M H ₂ SO ₄
kathode buffer:	0.2 M Bicin, 0.25% (w/v) SDS, 0.1 M NaOH

Tab. 3.11: Urea tris-bicin or *Wiltfang* gel composition. For two gels, 1.5 mm thickness. * Urea, water and separating gel buffer were mixed and heated in the microwave until the urea was dissolved.

	separating gel (11%)	spacing gel	stacking gel
urea	9.6 g*	-	-
H₂O	2 ml*	1.36 ml	0.74 ml
separating gel buffer	5 ml*	-	-
spacing gel buffer	-	2 ml	-
stacking gel buffer	-	-	1.5 ml
acrylamide/bisacrylamide	5.5 ml	0.6 ml	0.675 ml
10% (w/v) APS	80 µl	16 µl	18 µl
TEMED	10 µl	4 µl	6 µl

Urea tris-bicin or *Wiltfang* gels were cast according to a modified version (Tab. 3.11) of a previously published protocol (Wiltfang *et al*, 1997). The separating gel was cast first and was overlaid with isopropanol until it was polymerised. The spacing gel was prepared on top of the separating gel in a similar manner. Finally, a comb was polymerised in the stacking gel to obtain pockets for loading. Gels were wrapped into damp tissues and stored for one night at room temperature prior to use.

3.2.4.8 Electroblotting

transfer buffer: 25 mM Tris, 200 mM glycine

Proteins separated by gel electrophoresis were transferred to polyvinylidenefluoride (PVDF; immobilon P transfer membrane, 0.45 µm pore width; Millipore, Billerica, USA) or nitrocellulose membranes (NC; Protran B 79, pore width 0.1 µm; GE Healthcare) by tank electroblotting using the MINI-PROTEAN system (Bio-Rad). To this end, gels were disassembled following electrophoreses, the stacking gel was discarded and the separating gel (in case of Tris-tricine gels together with the spacing gel) were soaked in transfer buffer. Filter paper (GE Healthcare) and sponges were also soaked in transfer buffer. NC membranes were pre-incubated in the same buffer for 20 min, while PVDF membranes were first activated for 2 min in isopropanol, washed for 2 min in distilled water and then incubated in transfer buffer until use. Following assembly of the blotting apparatus, electroblotting was performed at a constant current of 400 mA per chamber for 1 h generated by PowerPack HC power supplies (Bio-Rad). Gels were discarded and PVDF membranes were directly processed as described in 3.2.4.9. NC membranes, however, were boiled in PBS (see 3.2.3.1) for 5 min before Western blotting.

3.2.4.9 Protein detection by Western blotting

TBS-T: 50 mM Tris, 150 mM NaCl, 0.05% (v/v) Tween 20, pH 7.6

blocking solution: 2% (w/v) Tropix I-BLOCK™ (life technologies), 0.1% (v/v) Tween 20, dissolved in PBS (see 3.2.3.1)

stripping buffer: 62.5 mM Tris x HCl pH 6.7, 2% (w/v) SDS, 0.7% (v/v) β-mercaptoethanol

Following electroblotting, membranes incubated in blocking solution either at room temperature for 1 h or at 4°C overnight. Next, membranes were incubated with the respective primary antibody (Tab. 3.12) at room temperature for 1 h or at 4°C overnight (up to 48 h). Membranes were washed three times for 15 min with TBS-T and then incubated with horseradish peroxidase (HRP)-conjugated secondary antibodies (Tab. 3.12) at room temperature for up to 1 h. Subsequently, membranes were washed again three times for 15 min with TBS-T. All incubation and washing steps were conducted with light agitation and all antibodies were diluted in blocking solution as detailed in (Tab. 3.12). HRP-conjugated secondary anti-mouse (1:10⁴) and anti-rabbit (1:10⁴) antibodies were from Promega, anti-goat (1:4,000) from Santa Cruz Biotechnologies and anti-rat (1:5,000) antibodies were either from Promega or from Dianova (Hamburg, Germany).

Antibody binding was visualised by means of enhanced chemical luminescence (ECL™) technology. Blots were incubated in either ECL™ (GE Healthcare), ECL Plus (Thermo Fisher Scientific) or ECL Prime (GE Healthcare) Western blot detection reagent according to the manufacturer's instructions. Signals were documented on medical X-ray films (Fujifilm, Tokio, Japan or Kodak, Rochester, USA) which were developed using an automated film developer (CAWOMAT 2000 IR; CAWO, Schrobenhausen, Germany). Developed films were digitalised with an Epson Perfection V700 PHOTO scanner (Epson, Suwa, Japan) and the supplied software. Images were cropped and edited in strict accordance with guidelines described in (Rossner & Yamada, 2004) using Adobe Photoshop CS5 (Adobe Systems, San Jose, USA).

For densitometric quantification of Western blot intensities, ECL signals were acquired digitally using the Luminescent Image Analyzer LAS-4000 (Fujifilm) and intensities values were obtained using the supplied software package Multi Gauge v3.0. ICD ratios were calculated from signal intensities obtained from analysis of the very same Western blot. Statistical analyses were conducted with GraphPad Prism (Graphpad, La Jolla, USA) as indicated in the respective figure legends. The statistical significance is indicated in the results section with * (p < 0.5) and ** (p < 0.05).

To remove bound primary and secondary antibodies from membranes for redecoration, membranes were incubated in stripping buffer at 50°C for 30 to 40 min. Subsequently, they were washed multiple times with TBS-T. The immunodetection procedure was repeated as detailed above.

Tab. 3.12: Antibodies used for Western blotting. #, non-reducing conditions required, ¹, HRP-conjugated antibody, ^{II}, Developmental Studies Hybridoma Bank, Iowa City, USA, ^{III}, Santa Cruz Biotechnologies.

antigen	antibody type	antibody species	clone/cat. #	dilution/quantity	source
APP	mAb	mouse	2D8	0.1 to 0.2 µg/ml	Elisabeth Kremmer, Munich
APP	pAb	rabbit	6687	1:1,000	Eurogentec
β4GalT1	pAb	goat	AF3609	1:2,000	R&D
β3GalT6	pAb	rabbit	ab103375	1:1,000	Abcam
β3GnT1	mAb	mouse	724057	1:1,000 [#]	R&D
Calnexin	pAb	rabbit	-	1:3,000	Enzo
CD68	mAb	rat	FA-11	1:500 [#]	AbD serotec
ER α-mannosidase I	mAb	mouse	30-Y	1:500 to 1:1,000	SCBT ^{III}
EXTL3	mAb	mouse	G-5	1:1,000	SCBT ^{III}
Flag tag	mAb	mouse	M2	1:1,000	Sigma
Flag tag	pAb	rabbit	F7425	1:3,000	Sigma
GnT-V	mAb	mouse	706824	1:1,000	R&D
HA tag ¹	mAb	rat	3F10	1:1,000	Roche
HS6ST1	pAb	sheep	AF5057	1:500	R&D
HS6ST2	pAb	rabbit	HPA034625	1:500 [#]	Sigma
human Lamp2	mAb	mouse	H4B4	1:5,000	DSHB ^{II}
human Lamp2	pAb	rabbit	ab37024	1:1,000	Abcam
mouse Lamp2	mAb	rat	ABL-93c	1:2,000	DSHB ^{II}
N-cadherin	mAb	mouse	10C32	1:1,000	BD
Nicastrin	mAb	mouse	35	1:2,000	BD
Nicastrin	pAb	rabbit	N1660	1:5,000	Sigma
Presenilin 1	pAb	rabbit	2953	1:1,000	Eurogentec
Sgk196	mAb	mouse	S-23	1:500 [#]	SCBT ^{III}
human SPPL2a	mAb	mouse	6E9	undiluted	Elisabeth Kremmer, Munich
mouse SPPL2a	pAb	rabbit	-	1:1,000	Bernd Schröder, Kiel
SPPL2b	mAb	mouse	3F9	undiluted	Elisabeth Kremmer, Munich
SPPL3	mAb	mouse	7F9	1:10	Elisabeth Kremmer, Munich
SPPL3	mAb	mouse	6A2	1:10	Elisabeth Kremmer, Munich
V5 tag	mAb	mouse	2F11F7	1:1,000	life technologies
V5 tag	pAb	rabbit	R960-25	1:1,000	Millipore
XylT2	mAb	mouse	G-1	1:1,000	SCBT ^{III}

3.2.4.10 Lectin blotting

lectin buffer:	10 mM HEPES pH 7.5, 150 mM NaCl, 0.1 mM CaCl ₂ , 0.08% (w/v) NaN ₃
PBS-T:	0.05% (v/v) Tween 20 dissolved in PBS (see 3.2.3.1)
blocking solution:	5% (w/v) BSA in PBS-T

In order to visualise protein-conjugated glycans, biotinylated lectins were employed that had been purchased from Vector Laboratories (Burlingame, USA). anti-Nicastrin immunoprecipitates were separated by SDS-PAGE and electroblotted as described (see 3.2.4.7. and 3.2.4.8). Membranes were first incubated in blocking solution at 4°C overnight. They were then washed once with PBS-T and successively treated with streptavidin and biotin blocking solutions provided as a commercial kit (Vector Laboratories) according to the manufacturer's instructions. Following biotin blocking, membranes were incubated with the respective biotinylated lectins (2 to 10 µg/ml, diluted in lectin buffer) at room temperature for 1 h. Membranes were washed three times for 10 min with PBS-T. Following incubation in 2 µg/µl streptavidin-HRP conjugated (diluted in PBS-T; Vector Laboratories) at room temperature for 30 min, membranes were washed again three times with PBS-T and lectin binding was visualised using ECL chemistry and X-ray film detection procedures as detailed earlier (see 3.2.4.9).

3.2.4.11 MALDI-TOF mass spectrometric analysis of C-peptide cleavage products

IP-MS buffer:	10 mM Tris pH 8.0, 140 mM NaCl, 5 mM EDTA, sterile filtered supplemented with 0.1% (w/v) octyl-β-D-glucopyranoside (Sigma)
Matrix:	0.3% (w/v) trifluoroacetic acid, 40% (v/v) acetonitrile, saturated with 4-hydroxycinnamic acid

To capture and purify Flag-tagged C-peptide species, conditioned supernatants from 6 to 10 cm dishes transfected with the respective substrate expression constructs were collected and subjected to anti-Flag M2 immunoprecipitation (10 µl beads, overnight, 4°C). Beads were washed six times with 1 ml IP-MS buffer and once with 1 ml fresh, sterile-filtered and double-distilled water. Residual liquid was removed and dry beads were stored at -20°C until further analysis.

15 to 20 µl of the matrix solution were added to the sedimented beads, mixed gently and incubated at room temperature for 5 min to eluted captured peptides. Beads were then sedimented by centrifugation (1 min, 13 krpm) and 1 to 2 µl of the supernatant were spotted on the target plate (Assay sample plate, 96 spots, coat, Applied Biosystems). After drying, captured peptides were analysed by MALDI-TOF mass spectrometry using a Voyager DE STR (Applied Biosystems) mass spectrometer at the Center for Protein Analysis, Ludwig-Maximilians University Munich. For measurements, the mass spectrometer was set to linear mode but small peptides (1 to 5 kDa) were also analysed in reflector mode. Preset mass spectrometer parameters were used and grid voltage and delay time were set to 90-95% and 100-300 ns for the linear mode and 60-65% and 150-250 ns for the reflector mode, respectively. Data were analyzed using Data Explorer 4.3 (Applied Biosystems) and GPM/W 5.02 (Lighthouse data) software. Molecular masses were calibrated using the calibration mixture 2 of the Sequazyme

Peptide Mass Standards Kit (Applied Biosystems) and relative peak intensities were determined in relation to peptide in the standard. Mass spectrometric measurements were performed by Dr Akio Fukumori, German Center for Neurodegenerative Diseases (DZNE) - Munich.

3.2.4.12 RNA isolation and quantitative RT-PCR

Total cellular RNA was isolated from cells using QIAshredder homogeniser columns and the RNeasy RNA isolation kit (Qiagen) following the manufacturer's instructions. RNA concentrations were determined by UV-Vis spectroscopy. Up to 2 µg total RNA was reverse-transcribed with the high capacity reverse transcription kit (Applied Biosystems) according to the manufacturer's instructions and cDNA reaction products were stored at -20°C. Quantitative real-time PCR was performed using 2x TaqMan master mix (Applied Biosystems) and pre-designed FAM-labelled 20x TaqMan probes targeting *SPPL2a* (Cat. # Hs01002698_g1) and *SPPL2b* (Cat. # Hs00292699_m1) mRNAs (Applied Biosystems). Reactions were performed with preset cycle settings in a 7500 Fast Real-Time PCR System (Applied Biosystems). Signals were normalised to levels of *ACTB* mRNA obtained using VIC-labelled probes (Cat. # 4326315E) and relative mRNA levels were calculated with the $\Delta\Delta C_T$ method.

3.2.4.13 Secretome analysis

To identify novel *SPPL3* substrates, a recently developed protocol was applied which combines a novel technique to selectively isolate *de novo* synthesised secreted glycoproteins with quantitative mass spectrometry (Kuhn *et al*, 2012). *SPPL3* over-expression was induced by supplementing the cell culture medium with 1 µg/ml doxycycline for 48 h prior to metabolic labelling. Cells were trypsinised and counted. For each sample, cells were plated in two T-75 cell culture flasks (15×10^6 cells in 10 ml basic medium per flask) and media were supplemented with 50 µM tetraacetyl-N-azidoacetyl-mannosamine and 0.1 µg/ml doxycycline. As a control, uninduced cells were plated in parallel in an identical manner, yet omitting the supplementation with doxycycline. Cells were incubated for 48 h, the conditioned supernatants from the respective two flasks were collected and pooled. Following sterile filtration (filter pore width 0.2 µm), samples were frozen at -20°C for further processing. Samples were then subjected to the previously established protocol (Kuhn *et al*, 2012). In brief, non-metabolised tetraacetyl-N-azidoacetyl-mannosamine was washed out with PBS by ultrafiltration in VivaSpin 20 columns with a molecular weight cut-off of 30 kDa (GE Healthcare) that retained labelled proteins. Concentrated proteins were subjected to biotinylation with DBCO-PEG12-biotin (Click Chemistry Tools, Scottsdale, USA). Unreacted DBCO-PEG12-biotin was washed as detailed earlier. Biotinylated proteins in the concentrated retentate were then affinity-purified via streptavidin beads. Beads were washed with PBS and eluted for electrophoretic separation by SDS-PAGE. Proteins in cut out gel slices were trypsinised and samples were subjected to analyses by nanoLC coupled with high-resolution mass spectrometry and label-free quantification as detailed in (Kuhn *et al*, 2012). Click chemistry reactions, protein purification and analysis were performed by Dr. Peer-Hendrik Kuhn, PhD, from the German Center for Neurodegenerative Diseases (DZNE) - Munich.

4. Results

4.1 FVenv is substrate for intramembrane proteolysis by SPPL3 and SPPL2a/2b

4.1.1 Cloning and expression of epitope-tagged FVenv

In light of earlier studies that suggested a certain degree of functional redundancy between SPP and SPPL3 regarding signal peptide endoproteolysis (Krawitz *et al*, 2005; Nyborg *et al*, 2006), atypical signal peptides were considered potential candidate SPPL3 substrates. As FVenv harbours such an atypical signal or leader peptide (see 1.5.1), it was tested whether it is proteolytically processed by SPPL3. In order to examine whether FVenv is subject to intramembrane proteolysis in a cellular model system, FVenv was cloned into an eukaryotic expression vector and terminal epitope tags were added to allow for detection of FVenv and proteolytic products thereof with tag-specific antibodies. Similar strategies have been employed before to detect cleavage products of SPPL2a- and/or SPPL2b-mediated intramembrane proteolysis (e.g. in (Martin *et al*, 2008)). At the FVenv N-terminus, immediately following the translation-initiating methionine residue, a Flag tag was introduced (Fig. 4.1a) allowing for detection of unprocessed full-length FVenv, the LP and LP-derived fragments generated by intramembrane proteolysis using anti-Flag antibodies. The C-terminal portion of FVenv was likewise tagged with a V5 tag which was introduced right in front of the C-terminal KKKNQ ER retention signal in order not to interfere with proper sub-cellular targeting of epitope-tagged FVenv (Fig. 4.1a). While in FV-infected cells FVenv is endoproteolysed at two sites (designated *PC* and *PC** in Fig. 4.1a) leading to the generation of the three individual subunits LP, SU and TM (Fig. 1.12), in cells solely expressing FVenv and no additional viral co-factors FVenv proteolysis proceeds in a distinct manner and no proteolytic cleavage between the SU and TM subunits (i.e. *PC**) is observed (Bansal *et al*, 2000). To reduce generation of LP two point mutations (R123A and R126A, Fig. 4.1b) were simultaneously introduced into the PC cleavage site as these had previously efficiently reduced LP generation (Duda *et al*, 2004). This FVenv mutant will subsequently be referred to as FVenv mut.

To ensure that the introduction of these epitope tags did not interfere with proper expression, proteolytic processing or sub-cellular targeting of FVenv, these constructs were transiently transfected into HeLa cells and analysed by immunocytochemistry and confocal microscopy as well as Western blotting. FVenv wild-type localisation was assessed by staining with an anti-V5 mAb (Fig. 4.1c, top row). Immunoreactivity was mainly observed in the perinuclear region and, to a lesser extent, in vesicular cytosolic structures. Anti-V5 immunoreactivity in cells transfected with tagged FVenv was found to be largely overlapping with an ER-specific staining of an anti-KDEL directed pAb, suggesting that tagged FVenv wild-type mostly localises to the ER as observed earlier for over-expressed FVenv (Goepfert *et al*, 1997) and that introduction of the epitope tags did not alter sub-cellular targeting. Staining with an anti-Flag antibody was similarly overlapping with anti-V5 immunoreactivity (Fig. 4.1c, second row), i.e. most likely also LP generated from the pre-protein by endoproteolysis remained localised to the ER. FVenv mut did

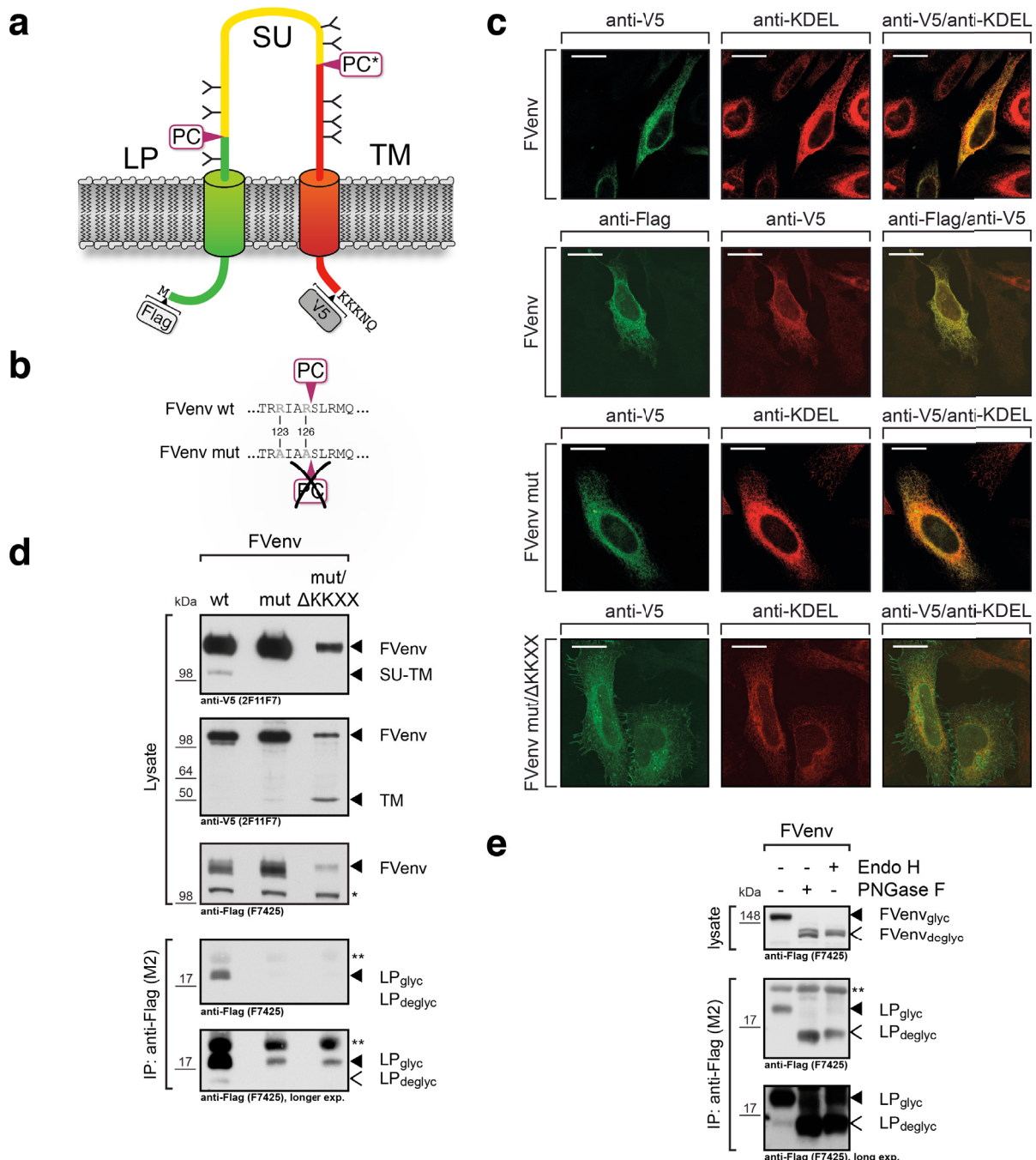


Fig. 4.1: Cloning and expression of epitope-tagged FVenv. (a) Schematic overview of FVenv. FVenv is proteolytically processed by furin and/or furin-like pro-protein convertases at two sites (PC and PC*) which generates its three subunits LP (green), SU (yellow), and TM (red). Putative N-glycosylation sites are indicated by "Y" (several additional ones in SU have been omitted for clarity). Epitope tags were introduced as indicated by the grey boxes. Not drawn to scale. (b) Sequence clip of the N-terminal PC cleavage site of FVenv and the R123A/R126A mutant (FVenv mut) used. FVenv mut is expected to be less efficiently processed at PC. (c) Sub-cellular localisation of FVenv constructs used. HeLa cells were transiently transfected as indicated, were subjected to immunocytochemical staining and analysed by confocal laser-scanning microscopy. Note that untransfected cells were deliberately imaged next to transfected cells to show that anti-V5 and anti-Flag stainings are in fact specific. Scale bar = 20 μ M. (d) Proteolytic processing of FVenv constructs in HEK293 cells. HEK293 cells were transiently transfected as indicated and total cell lysates were analysed for FVenv and fragments thereof by SDS-PAGE and Western blot (upper panel). For detection of LP, lysates had to be subjected to anti-Flag immunoprecipitation for enrichment. (e) Deglycosylation of FVenv and LP. Cell lysates and anti-Flag immunoprecipitates were enzymatically deglycosylated by endoglycosidase H (Endo H) or peptide-N-glycosidase F (PNGase F) and analysed by SDS-PAGE and Western Blot. *, unspecific band, **, IgG light chain, glyc, glycosylated species, deglyc, deglycosylated species.

not display an altered sub-cellular localisation (Fig. 4.1c, third row). As expected (Goepfert *et al*, 1997), however, when the C-terminal ER retention motif was removed by site-directed mutagenesis, anti-V5 immunoreactivity markedly changed and FVen mut/ΔKKXX was observed on the cell surface as well as in cell surface protrusions, yet a perinuclear ER staining was still apparent (Fig. 4.1c, bottom row).

Proteolytic processing of FVen was examined by SDS-PAGE and Western blot detection of cell lysates from HEK293 cells transiently transfected with the expression constructs indicated (Fig. 4.1d). Importantly, FVen wild-type was found to be proteolytically processed at the PC site as expected (Bansal *et al*, 2000), since in addition to an anti-V5 and anti-Flag immunoreactive high molecular weight band corresponding to full-length, unprocessed FVen, an anti-V5 reactive, yet not anti-Flag reactive fragment of slightly lower molecular weight was observed in these cells. This additional fragment likely corresponds to the C-terminal SU-TM product generated by cleavage at PC. The corresponding N-terminal cleavage product, LP, was observed with a molecular weight of roughly 18 kDa in anti-Flag immunoprecipitates of transfected cells. Levels of both SU-TM and LP were drastically reduced in cell lysates transfected with FVen mut and residual LP levels could only be detected following longer exposure. The reduction of SU-TM and LP levels in these mutants further corroborates their biogenesis by endoproteolysis at this position. An anti-V5-reactive fragment of roughly 50 kDa that likely corresponds to the 48 kDa TM subunit was only observed in cells expressing the FVen mut/ΔKKXX mutant. Hence, in line with previous observations (Bansal *et al*, 2000), cleavage at PC* only occurred when FVen was not retained in the ER.

Following anti-Flag immunoprecipitation, an additional N-terminal protein fragment was detected that had a slightly lower molecular weight than LP (Fig. 4.1d, open arrowhead). FVen is extensively modified post-translationally by N-glycosylation and the LP subunit contains two putative consensus N-glycosylation sites and one (N109) appears to be occupied in cultured cells (Lüftnegger *et al*, 2005). To examine whether this smaller anti-Flag-reactive fragments derives from subsequent endoproteolysis of LP or is merely due to non-quantitative cellular glycosylation at N109, lysates from HEK cells transfected with FVen were subjected to treatment with peptide:N-glycosidase F (PNGase F) and endo-β-N-acetylglucosaminidase H (Endo H) (Fig. 4.1e). Glycosidase treatment led to reduction in molecular weight of both full-length FVen as well as immunoprecipitated LP, clearly showing that both species are modified by N-glycans. Of note, longer exposures of blots of immunoprecipitated LP revealed that the previously observed LP fragment (Fig. 4.1d, open arrowhead) co-migrated with glycosidase-digested LP and, therefore, likely corresponds to non-glycosylated LP and not to a proteolytic cleavage product. In addition, both FVen as well as its N-terminal cleavage product LP were sensitive to treatment with Endo H which underpins their ER localisation.

Taken together, these experiments demonstrate that introduction of the terminal epitope tags does neither interfere with intracellular localisation and trafficking nor with proteolytic processing of FVen as the tagged wild-type protein and tagged FVen mutants behaved like untagged FVen. Therefore, the tagged FVen constructs used throughout subsequent experiments represent a valid model to assess intramembrane proteolysis of FVen.

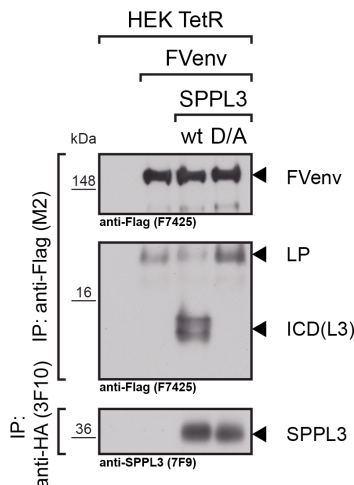


Fig. 4.2: SPPL3 endoproteolyses FVenv. HEK293 TetR cells that stably over-express HA-tagged active SPPL3 wild-type (wt) or inactive SPPL3 D271A (D/A) upon induction with doxycycline were stably transfected with FVenv. HEK293 TetR cells were used as controls. Cell lysates were subjected to anti-Flag (upper panels) or anti-HA immunoprecipitation (*IP*) (lower panel) to detect FVenv as well as smaller anti-Flag-reactive proteolytic fragments thereof and the expressed protease species, respectively. SPPL3 wild-type co-expression led to generation of an ICD, ICD(L3). Note that, depending on the gel resolution, ICD(L3) sometimes can be observed as a doublet.

4.1.2 FVenv leader peptide is endoproteolysed by over-expressed SPPL3 in HEK293 cells

To examine whether FVenv LP can be endoproteolysed by SPPL3, tagged FVenv was co-expressed with HA-tagged catalytically active SPPL3 or a putatively inactive D271A mutant (Fig. 4.2). To this end, HEK293 T-Rex® (HEK293 TetR) cells that stably express active or mutant SPPL3 upon doxycycline induction were used. Upon stable co-expression of FVenv with proteolytically active SPPL3 a small anti-Flag-immunoreactive fragment, ICD(L3), was detected in immunoprecipitates. This fragment could neither be observed in immunoprecipitates of cells expressing only FVenv nor of cells co-expressing FVenv and SPPL3 D271A. Instead a slight accumulation of LP became apparent under the latter conditions. These observations suggest that proteolytically active SPPL3 endoproteolyses FVenv in LP leading to the generation of an ICD, ICD(L3).

4.1.3 FVenv leader peptide is endoproteolysed by over-expressed SPPL2a and SPPL2b

To assess whether other SPPL intramembrane protease can also cleave FVenv, FVenv was similarly co-expressed with catalytically active SPPL2a (Fig. 4.3a) and SPPL2b (Fig. 4.3b) and the respective catalytically inactive mutants (SPPL2a D412A and SPPL2b D421A, respectively). Surprisingly, also in cells expressing FVenv and active SPPL2a an anti-Flag-reactive LP fragment was detected in immunoprecipitates which was termed ICD(L2) (Fig. 4.3a). In immunoprecipitates of cells co-expressing inactive SPPL2a D412A and FVenv, however, no ICD(L2) was detected, but a drastic accumulation of LP was apparent. Such an accumulation of substrates upon co-expression of inactive mutants had previously been observed, for instance for Bri2 (Martin *et al*, 2008). In addition to LP, other fragments likewise accumulated upon over-expression of SPPL2a D412A. These fragments displayed a higher molecular weight than that of ICD(L2) but were smaller than LP. Processing of FVenv in cells expressing SPPL2b

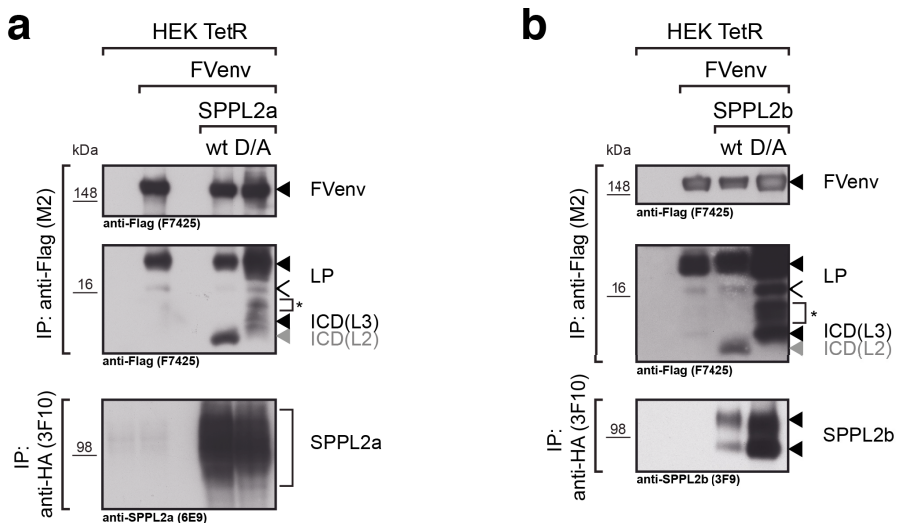


Fig. 4.3: SPPL2a and SPPL2b endoproteolysis FVenv. HEK293 TetR cells that stably over-express HA-tagged active SPPL2a wild-type (wt) or inactive SPPL2a D412A (D/A) (a) or HA-tagged active SPPL2b wt or inactive SPPL2b D421A (D/A) (b) upon induction with doxycycline were stably transfected with FVenv. Cell lysates were subjected to anti-Flag (upper panels) or anti-HA (lower panel) immunoprecipitation (IP) to detect FVenv as well as smaller anti-Flag-reactive proteolytic fragments thereof and the expressed protease species, respectively. Expression of active SPPL2a and SPPL2b led to detection of an ICD, *ICD(L2)* (grey). Upon co-expression of the respective D/A mutants, however, a marked accumulation of glycosylated and unglycosylated LP (closed and open arrowheads) as well as of other fragments (*) and ICD(L3) was observed.

(Fig. 4.3b) was similar to that observed for SPPL2a co-expression: In cells expressing FVenv and active SPPL2b an ICD was observed and in those expressing SPPL2b D421A this ICD was absent but instead LP and the previously observed additional fragments accumulated.

In order to check whether LP-derived fragments accumulating following SPPL2a D412A or SPPL2b D421A over-expression are generated by endogenous activity of SPPL3 or other endogenous proteases that turn over the accumulating LP, cells stably co-expressing SPPL2a D412A and FVenv were transfected with SPPL3-specific siRNA pools or a non-targeting control siRNA pool to reduce endogenous SPPL3 levels (Fig. 4.4a). This led to a marked reduction of one band accumulating in conditions of SPPL2a D412A expression showing that this band reflects in fact ICD(L3). Additional bands were unaffected by SPPL3 siRNA transfection and, accordingly, most likely are due to another, presently elusive endogenous protease acting upon LP.

These observations also suggested that ICD(L3) observed upon co-expression of FVenv and SPPL3 wild-type and the ICD species generated by SPPL2a and SPPL2b are in fact distinct. To underpin this, immunoprecipitates obtained from cells co-expressing FVenv with either biologically active SPPL3, SPPL2a, or SPPL2b were co-migrated (Fig. 4.4b). Interestingly, judged by their electrophoretic mobility, ICD species generated by SPPL2a and SPPL2b appear to be identical and are therefore collectively referred to as ICD(L2). ICD(L3) generated by SPPL3, however, displayed a slightly higher molecular weight than ICD(L2), showing that it represents a distinct ICD species.

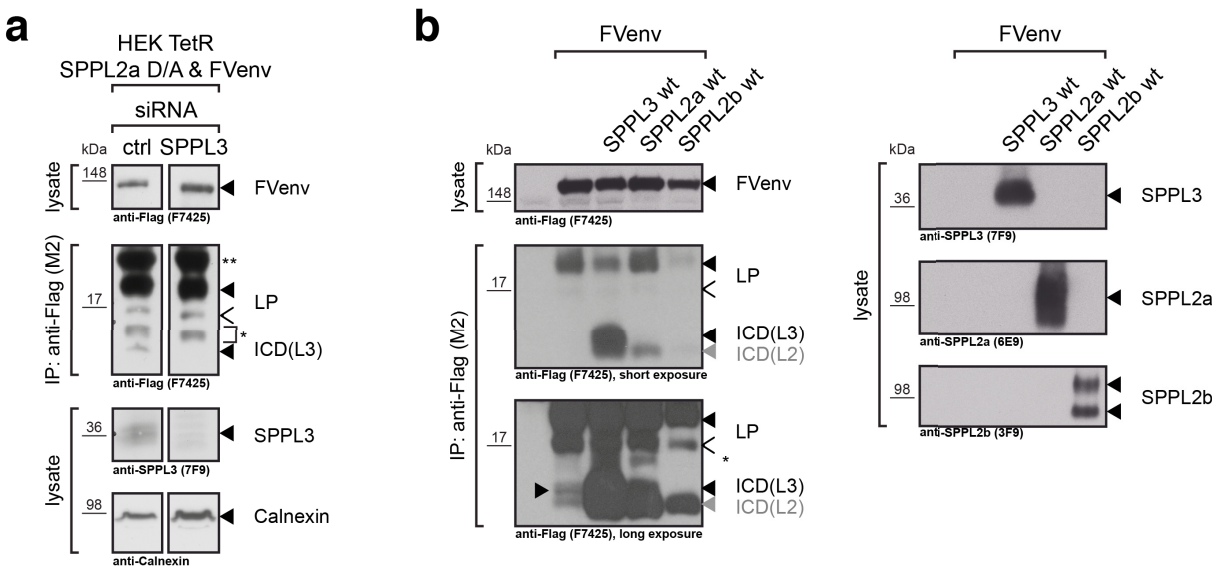


Fig. 4.4: ICD(L3) and ICD(L2) are distinct ICD species. (a) ICD(L3) accumulates upon over-expression of inactive SPPL2a. Endogenous SPPL3 levels were reduced in HEK293 TetR cells that stably over-express inactive SPPL2a (D412A) (*D/A*) by transfection with a SPPL3-specific siRNA pool (20 nM) and a non-targeting siRNA pool (ctrl, 20 nM). Reduction of SPPL3 was monitored by Western blot of cell lysates with an anti-SPPL3 mAb. Calnexin signals were used as loading control. FVenv-derived LP fragments were analysed following anti-Flag immunoprecipitation of cell lysates. *, LP-derived fragment of elusive nature, **, IgG light chain. (b) Co-migration of ICD(L3) and ICD(L2). ICD species were anti-Flag immunoprecipitated from lysates of cells stably co-expressing FVenv and active SPPL3, SPPL2a, and SPPL2b, respectively. Note that upon longer exposure of anti-Flag immunoprecipitates ICD(L3) may also be detected in cells only expressing FVenv (black arrowhead in image).

4.2 FVenv proteolysis reveals unique properties of SPPL3

Taken together, these observations collectively show that FVenv is subject to endoproteolysis mediated by both SPPL3 and SPPL2a/SPPL2b when co-expressed in cultured cells. Importantly, FVenv represents the first transmembrane protein substrate of SPPL3 and, hence, allows for more detailed mechanistic analyses of this so far hardly characterised protease. At the same time FVenv is also a substrate of SPPL2a/SPPL2b, but endoproteolysis by SPPL3 and SPPL2a/SPPL2b leads to the generation of distinct product species. Therefore, analyses of the proteolytic processing of FVenv allowed for direct comparison of these distinct proteases.

4.2.1 SPPL3-mediated cleavage of FVenv is independent of shedding

Furin/PC-mediated endoproteolysis of the FVenv separates the N-terminal LP moiety from SU-TM and this cleavage occurs C-terminally of amino acid residue R126 (Duda *et al.*, 2004; Geiselhart *et al.*, 2004), i.e. in a distance of < 40 amino acids (aa) from the predicted first TMD⁴. Hence, this cleavage event is reminiscent of a classical membrane-proximal shedding event of a single-pass transmembrane protein that is crucially required for subsequent intramembrane proteolysis by SPP, SPPL2b and the presenilins (see 1.1). To experimentally address whether FVenv intramembrane proteolysis by SPPL2b and by SPPL3 is likewise dependent on the shedding-like furin/PC-mediated pre-cleavage of full-length FVenv, the R123A/R126A mutant of FVenv (FVenv mut) was employed. When expressed in HEK293 cells, generation of LP and SU-

⁴ According to Uniprot annotations (entry ID: P14351) the type II-oriented TMD1 comprises amino acids 66 to 88 in SFVcpz(hu) FVenv. TMHMM 2.0 (<http://www.cbs.dtu.dk/services/TMHMM/>), however, predicts amino acids 69 to 91 as membrane-spanning region.

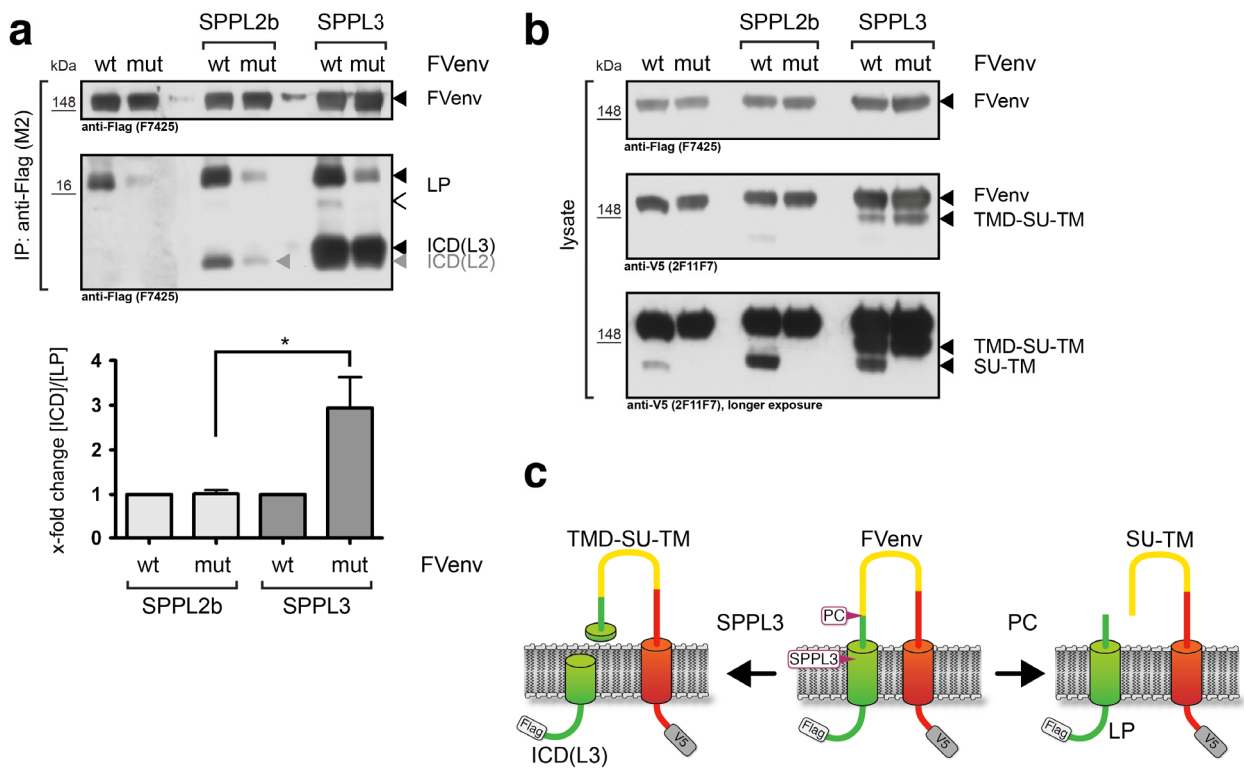


Fig. 4.5: SPPL3-mediated cleavage of FVenv is independent of shedding. SPPL2b or SPPL3 expression was induced by doxycycline treatment in the respective stably transfected HEK293 TetR cells. FVenv wild-type or FVenv R123A/R126A (*FVenv mut*) were transiently co-transfected and cells were lysed 48 h after transfection to monitor generation of ICD species in anti-Flag immunoprecipitates (a) or of high molecular weight FVenv species in straight lysates (b). Western blots signals of immunoprecipitates were quantified and the ICD-to-LP ratio ($[ICD]/[LP]$) was determined in three independent experiments. Data represent means \pm SEM. *, $p < 0.049$ (Student's unpaired t test). (c) Schematic model of proteolytic processing of full-length FVenv by either furin/PC (PC, to right side) or SPPL3 (to left side). Putative cleavage products detected in a & b are also depicted.

TM from FVenv mut was markedly reduced compared to cells transfected with FVenv wild-type (Fig. 4.1d & Fig. 4.5). Thus, FVenv mut represents a valid model for a substrate that does not undergo membrane-proximal shedding.

Protease activity on FVenv mut and the FVenv wild-type control substrate was assessed by quantification of ICD(L2) and ICD(L3) levels in immunoprecipitates from cells co-expressing these substrates with active SPPL2b and SPPL3, respectively (Fig. 4.5a). In line with previous observations (Martin *et al*, 2009), SPPL2b-mediated generation of ICD(L2) was reduced in cells expressing FVenv mut and only faint amounts of ICD(L2) could be detected. These, however, correlated with the level of residual LP generated from FVenv mut and quantification of three independent experiments revealed that the ICD-to-LP ratio was unchanged in cells co-expressing SPPL2b with either FVenv wild-type or FVenv mut, suggesting that SPPL2b can only produce ICD(L2) from LP, i.e. relies on FVenv cleavage by furin/PC. Strikingly, however, in cells co-expressing SPPL3 and FVenv mut substantial amounts of ICD(L3) were still detectable yet LP generation was reduced as expected. In fact, amounts of ICD(L3) generated from FVenv and FVenv mut were very similar. Also, significant changes in the ICD-to-LP ratio could be observed suggesting that SPPL3 is capable of processing full-length FVenv independent of a membrane-proximal pre-cleavage. This was corroborated by the detection of an anti-V5 reactive, yet not anti-Flag reactive high molecular weight FVenv fragment in lysates of cells co-

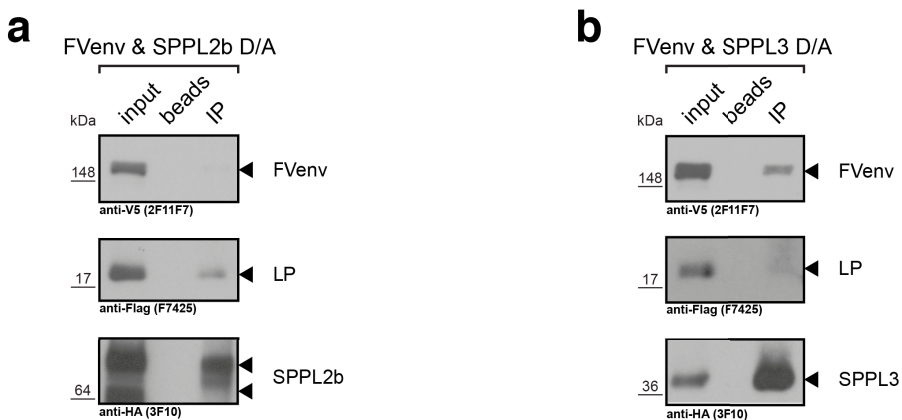


Fig. 4.6: Co-immunoprecipitation of FVenv by catalytically inactive SPPL2b and SPPL3 mutants. CHAPSO lysates of membranes isolated from HEK293 TetR cells stably expressing HA-tagged SPPL2b D421A (**a**) or SPPL3 D271A (**b**) were subjected to anti-HA 6908 immunoprecipitation (*IP*). Alternatively, to check for unspecific binding, anti-HA serum was omitted and lysates were only incubated with protein A-conjugated sepharose beads (*beads*). To determine the amount of protein immunoprecipitated 5% of the IP input (*input*) were co-migrated.

transfected with SPPL3 and FVenv mut but not of cells transfected with FVenv mut alone or with SPPL2b and FVenv mut (Fig. 4.5b). This SPPL3-specific fragment was devoid of its original N-terminus and had a molecular weight lower than full-length FVenv but slightly higher than SU-TM generated by furin/PC cleavage (Fig. 4.5c). Therefore, this fragment, termed TMD-SU-TM, presumably is generated by intramembrane cleavage of full-length FVenv together with ICD(L3). Importantly, this fragment was also observed upon co-expression of SPPL3 with FVenv wild-type. Hence, even when truncated LP is available, full-length FVenv is endoproteolysed by SPPL3.

These observations point to strikingly distinct substrate preferences of SPPL2b and SPPL3. To support this, catalytically inactive protease mutants were over-expressed in HEK293 cells and used to co-immunoprecipitate co-expressed FVenv species from cell lysates obtained (Fig. 4.6). SPPL2b D421A co-precipitated LP but failed to co-precipitate detectable amounts of full-length FVenv (Fig. 4.6a). SPPL3 D271A on the other hand preferentially co-isolated full-length FVenv and only faint amounts of LP (Fig. 4.6b). Therefore, it was conclusively shown that SPPL2b can only accept pre-cleaved FVenv LP that has a sufficiently shortened ectodomain as a substrate. LP can similarly be endoproteolysed by SPPL3 but SPPL3 appears to preferentially accept full-length FVenv as a substrate. Moreover, the co-immunoprecipitation experiments revealed a physical interaction of SPPL2b and SPPL3 with their respective substrates suggesting that these protease directly endoproteolysse FVenv and arguing against FVenv endoproteolysis being an indirect consequence of SPPL2b or SPPL3 expression.

4.2.2 SPPL3-mediated cleavage of FVenv is insensitive to GxGD protease inhibitors

Several compounds are known to inhibit proteolytic processing of transmembrane protein substrates by GxGD I-CLIPs (see 1.4.4.1). (Z-LL)₂ ketone and the GSI L-685,458, for instance, inhibit proteolytic activity of SPP as well as SPPL2a/SPPL2b (Weihofen *et al*, 2000; 2003; Fluhrer *et al*, 2006; Friedmann *et al*, 2006; Kirkin *et al*, 2007; Martin *et al*, 2008), while DAPT does not block SPP or SPPL2b activity (Martin *et al*, 2008; Weihofen *et al*, 2003). For lack of a

known transmembrane protein substrate the effect of these compounds on SPPL3 activity has so far not been studied. Therefore, these inhibitors were assessed for their potency to inhibit SPPL2b- and SPPL3-mediated proteolytic processing of FVenv.

To this end, HEK293 cells stably co-expressing FVenv and catalytically active SPPL2b (Fig. 4.7a) or SPPL3 (Fig. 4.7b) were treated with increasing concentrations of (Z-LL)₂ ketone, L-685,458 or DAPT and ICD(L2) and ICD(L3) levels, respectively, were analysed. As expected, SPPL2b-mediated generation of ICD(L2) from FVenv LP was blocked in a concentration-dependent manner by both (Z-LL)₂ ketone and L-685,458 (Fig. 4.7a). Treatment with both compounds also led to an accumulation of LP and of ICD(L3) as well as another LP degradation product, mimicking the effect previously observed upon over-expression of catalytically inactive SPPL2b D421A (Fig. 4.3b). DAPT, however, did not affect SPPL2b-mediated processing as neither an accumulation of LP nor a reduction in ICD(L2) levels were observed. DAPT also did not affect SPPL3-mediated processing of FVenv (Fig. 4.7b). Similarly, neither (Z-LL)₂ ketone nor L-685,458 affected LP levels in cells co-expressing FVenv and SPPL3 and both compounds also failed to block production of ICD(L3) at concentrations of up to 50 μ M. This is in stark contrast to the observations made for SPPL2b (Fig. 4.7a) and clearly shows that, unlike SPP as well as SPPL2a/SPPL2b, SPPL3 - in an over-expression setting - appears to be insensitive to treatment with the GxGD protease inhibitors at the concentrations tested. Strikingly, however, treatment of FVenv- and SPPL3-expressing cells with (Z-LL)₂ ketone and L-685,458 was accompanied by inhibitor dose-dependent accumulation of ICD(L3) (Fig. 4.7b).

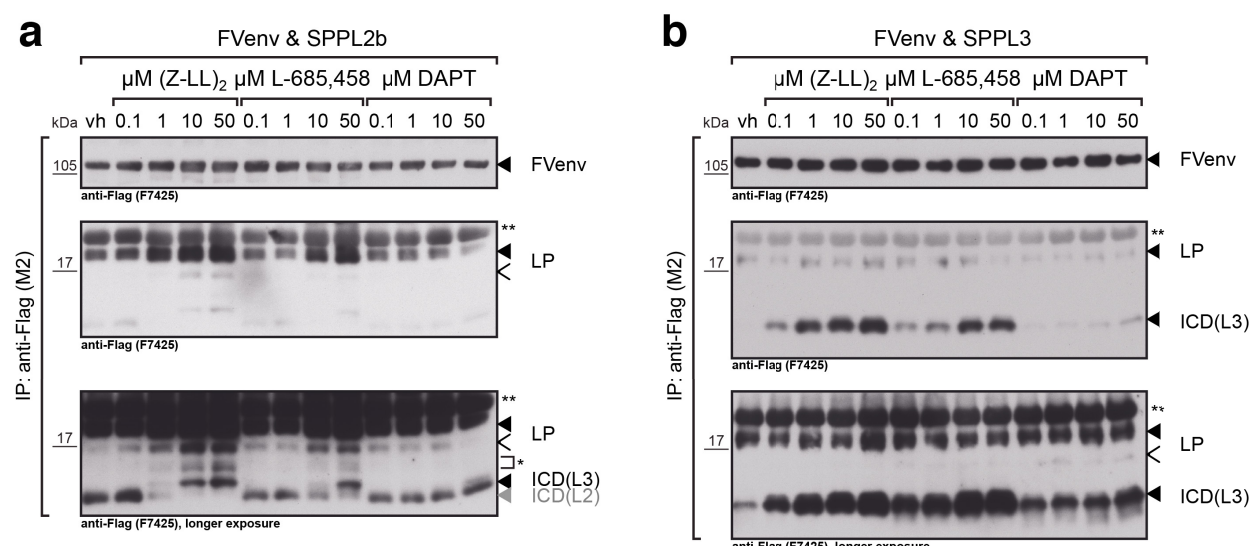


Fig. 4.7: Effects of GxGD protease inhibitor treatment on SPPL2b- and SPPL3-mediated processing of FVenv. HEK293 cells stably co-expressing FVenv and either active SPPL2b (a) or active SPPL3 (b) were treated with increasing concentrations of (Z-LL)₂ ketone ((Z-LL)₂), L-685,458, or DAPT as well as DMSO (vh, vehicle) for 16 h before lysis. anti-Flag immunoprecipitates of cell lysates were analysed by SDS-PAGE and Western blot for ICD generation. Note that, similar to SPPL2b(D421A) co-expression in Fig. 4.3b, ICD(L3) and a LP-derived fragment of unclear origin (*) accumulated with increasing concentrations of (Z-LL)₂ ketone ((Z-LL)₂) or L-685,458. **, IgG light chain.

4.2.3 SPPL2a/SPPL2b endoproteolyse the SPPL3 cleavage product ICD(L3)

A possible explanation for the striking accumulation of ICD(L3) upon (Z-LL)₂ ketone or L-685,458 treatment (Fig. 4.7b) is that these compounds not only fail to inhibit SPPL3's activity but instead promote or activate it. Alternatively, these inhibitors block the activity of (an) endogenous protease(s) that is capable of further processing and/or degrading ICD(L3) generated by SPPL3.

In the experiments described previously Tris-Tricine gels were used to analyse anti-Flag immunoprecipitates by Western blot. These failed, however, to resolve ICD(L3) generated in cells co-expressing SPPL3 and FVenv into a sharp band. The ICD(L3) signal observed appeared rather smoky. ICD(L2) on the other hand was clearly detectable as a distinct protein band (compare for instance ICD(L3) and ICD(L2) bands in (Fig. 4.5a)). These observations suggested that the previously described ICD(L3) band could contain in fact additional smaller protein fragments that represent degradation products. To clarify this, immunoprecipitates obtained from cells co-expressing FVenv with either SPPL2b or SPPL3 were separated in parallel in Tris-Tricine gels (Fig. 4.8a) as previously and in Tris-Glycine gels (Fig. 4.8b). Strikingly, Tris-Glycine gels achieved a much higher resolution of the ICD species and revealed that lysates obtained from cells expressing SPPL3 and FVenv contain two distinct anti-Flag reactive ICD species, genuine ICD(L3) as well as a smaller ICD. Notably, the latter ICD co-migrated with ICD(L2) generated in cells stably expressing SPPL2b and FVenv. Next, stably SPPL3- and FVenv-transfected cells were treated with GxGD protease inhibitors (Fig. 4.9a) to determine whether ICD(L2) generation observed in these cells is dependent on endogenous SPPL2a and/or SPPL2b activity. Of note, generation of ICD(L3) and ICD(L2) upon SPPL3 over-expression appeared to be very efficient and detection in cell lysates was possible even without prior enrichment by immunoprecipitation. Indeed, (Z-LL)₂ ketone as well as L-685,458 treatment resulted in a reduction of ICD(L2) and a concomitant accumulation of ICD(L3), yet levels of the corresponding TMD-SU-TM cleavage product did not change (Fig. 4.9a). In contrast, neither

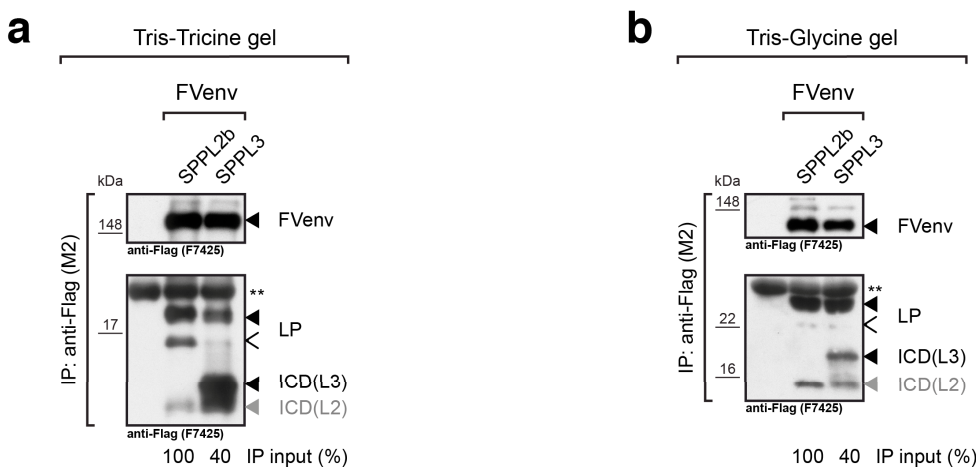


Fig. 4.8: SPPL3 expression leads to generation of both ICD(L3) as well as ICD(L2). Tris-Tricine (a), which had been used to separate FVenv ICD species in all preceding experiments shown, and Tris-Glycine (b) gels were tested for their capacity to separate ICD species from immunoprecipitates (IP) of HEK293 cells stably co-expressing FVenv and active SPPL2b or active SPPL3. Tris-Glycine gels clearly separated the previously observed ICD(L3) into ICD(L3) and ICD(L2). Note that ICD(L2) generation in SPPL3-expressing cells was highly efficient as less lysate input (40% IP input) was sufficient to detect amounts of ICD(L2) similar to those in SPPL2b-expressing cells. **, IgG light chain.

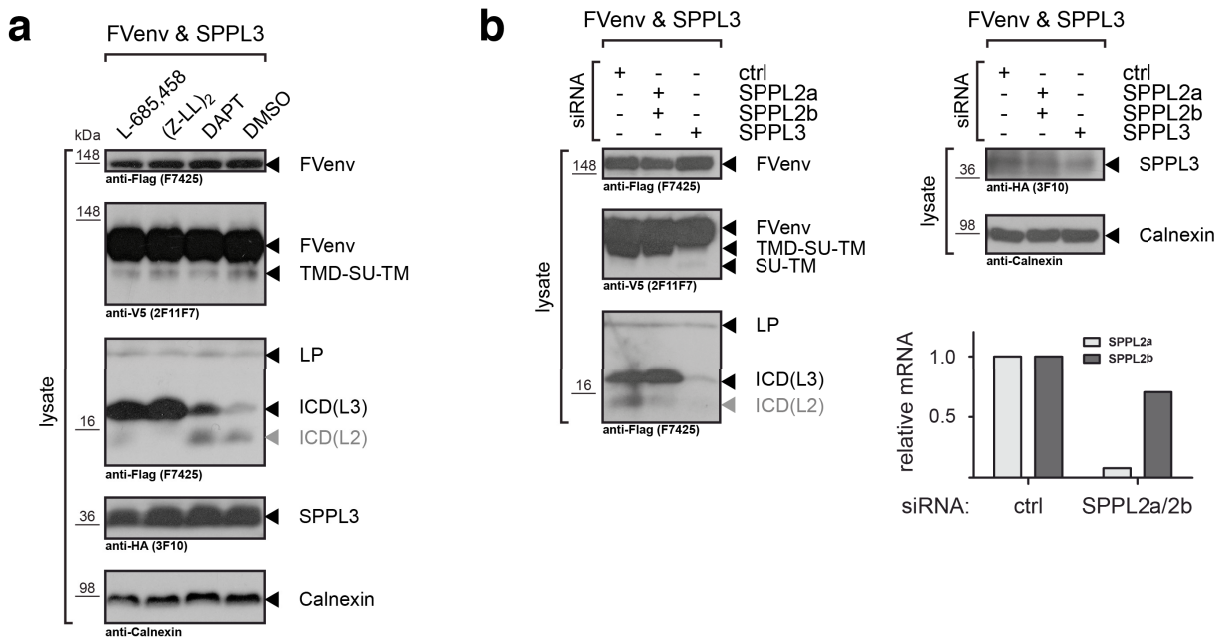


Fig. 4.9: ICD(L2) is produced from ICD(L3) by endogenous SPPL2a/SPPL2b. HEK293 cells stably co-expressing FVen and active SPPL3 were treated with GxGD protease inhibitors (a) or transfected with siRNAs (b) to examine generation of ICD(L3) and ICD(L2). For inhibitor treatment, media were supplemented with the inhibitors as indicated at a concentration of 10 μ M for 16 h. For SPPL2a/SPPL2b and SPPL3 knock-downs, cells were reversely transfected with either SPPL2a- and SPPL2b- or SPPL3-specific siRNA pool as well as a non-targeting control siRNA pool (ctrl) and analysed after four days in culture. Cells were lysed and 80 μ g total protein were subjected to Tris-Glycine SDS-PAGE and Western Blot. Knock-down of SPPL3 was monitored by Western blot and of SPPL2a/SPPL2b by quantitative TaqMan RT-PCR using specific probes. mRNA levels were normalised to β -actin levels and relative mRNA changes were calculated using the $\Delta\Delta C_T$ method. (Experimental work presented herein was performed by Ulrike Künzel.)

DAPT nor DMSO treatment led to changes in ICD(L2) levels. In support of prior observations (Fig. 4.7b), this unambiguously shows that inhibitor treatment does not directly affect SPPL3 activity but instead targets ICD(L3) downstream processing by a protease activity that has an inhibitor sensitivity profile reminiscent of other GxGD proteases. Moreover, reduction of endogenous SPPL2a and SPPL2b levels by siRNA transfection likewise slightly reduced ICD(L2) and concomitantly ICD(L3) accumulated (Fig. 4.9b). Treatment with SPPL3-specific siRNA reduced the levels of the products generated by SPPL3-mediated FVen cleavage, TMD-SU-TM and ICD(L3). Interestingly, however, this was accompanied by a reduction in ICD(L2) levels.

In all experiments performed proteolytic processing of FVen was examined under conditions of SPPL3 or SPPL2a/SPPL2b over-expression conditions. Hence, it remained to be examined whether FVen is similarly endoproteolysed by endogenous SPPL proteases and whether under these conditions ICD(L3) generated by SPPL3 is likewise turned over into ICD(L2). Therefore, FVen ICD generation was analysed in HEK293 cells that stably express FVen but do not over-express SPPL proteases (Fig. 4.10). By means of a two-step immunoprecipitation strategy low levels of ICD(L3) and ICD(L2) generated by endogenous cellular protease activities could be observed. siRNA-mediated reduction of endogenous SPPL2a and SPPL2b resulted in loss of ICD(L2) signals while ICD(L3) was still produced.

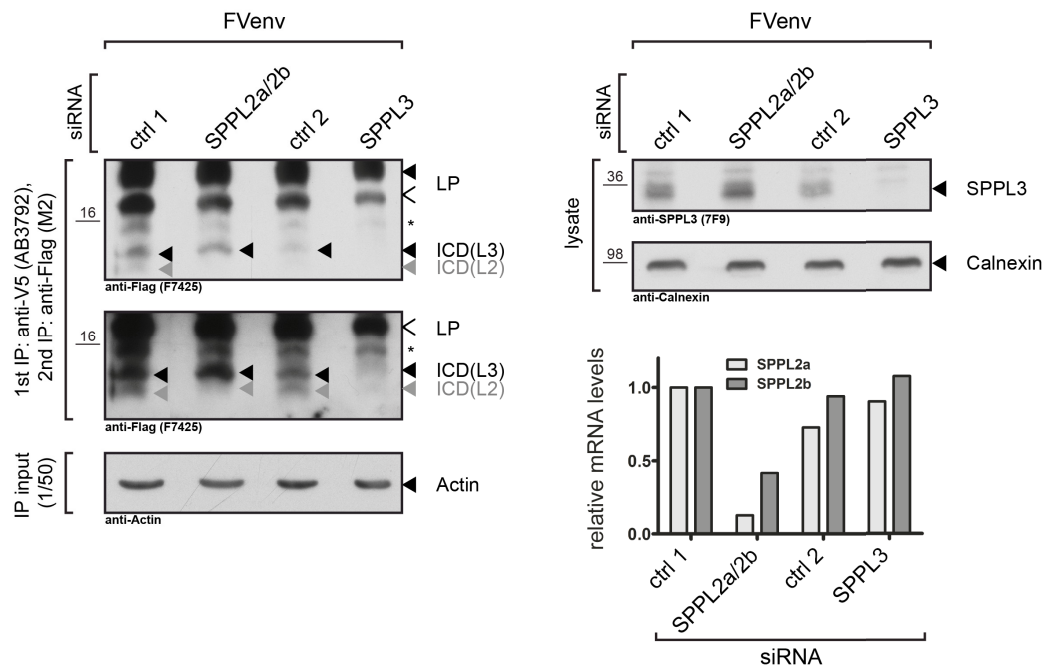


Fig. 4.10: Proteolytic processing of FVenv by endogenous SPPL3 and SPPL2a/SPPL2b. HEK293 cells stably expressing FVenv were reversely transfected with SPPL2a/SPPL2b- and SPPL3-specific siRNA as well as respective non-targeting controls (*ctrl*) as indicated (10 nM each) and analysed five days later. Knock-down efficiency was assessed by Western blot for SPPL3 (Calnexin was used as a loading control) and by quantitative TaqMan RT-PCR for SPPL2a and SPPL2b using specific probes (right panels). mRNA levels were normalised to β -actin levels and relative mRNA changes were calculated using the $\Delta\Delta C_T$ method. To detect endogenously produced ICD species in cell lysates (left panels) a two-step immunoprecipitation (*IP*) strategy was employed: First, lysates with equal amounts of total protein (see actin levels in input) were cleared from full-length FVenv by anti-V5 immunoprecipitation and subsequently lysates were subjected to anti-Flag immunoprecipitation. The latter were analysed by Tris-Glycine SDS-PAGE and Western blot. *, degradation product of LP, see Fig. 4.3.

Reduction of endogenous SPPL3, however, resulted in decreased detection of both ICD(L3) and ICD(L2).

Taken together, this suggests that ICD(L3) is efficiently turned over by endogenous SPPL2a/SPPL2b to produce ICD(L2). In order to unambiguously show that ICD(L2) is in fact generated by a direct turnover of ICD(L3), SPPL3-over-expressing cells were transfected with FVenv mut or the FVenv wild-type control and ICD(L2) generation was monitored (Fig. 4.11). Due to impaired furin/PC cleavage, LP is hardly available as a substrate for SPPL2a/SPPL2b-mediated intramembrane proteolysis in cells expressing FVenv mut (Fig. 4.5 & Fig. 4.11a). However, cell lysates of FVenv mut-transfected and SPPL3-co-expressing cells still contained substantial amounts of both ICD(L3) and ICD(L2) and the ICD(L2)/ICD(L3) ratio was not changed compared to cells expressing SPPL3 and FVenv wild-type (Fig. 4.11b & c). This demonstrates that ICD(L2) observed in FVenv mut-expressing cells was not generated by SPPL2a/SPPL2b-mediated turnover of LP but of ICD(L3). Consequently, FVenv-derived substrates accepted for intramembrane proteolysis by SPPL2a/SPPL2b can either be generated by membrane-proximal furin/PC cleavage or, alternatively, by prior cleavage mediated by SPPL3. Moreover, it has to be highlighted that processing of ICD(L3) by endogenous SPPL2a/SPPL2b activity appears to be highly efficient. In fact, ICD(L2) generation from ICD(L3) appears to be more efficient than from LP: ICD(L2) levels were readily detectable when 80 μ g total protein from cell lysates of cells co-expressing FVenv and SPPL3 wild-type were analysed (Fig. 4.9), while in cells co-expressing

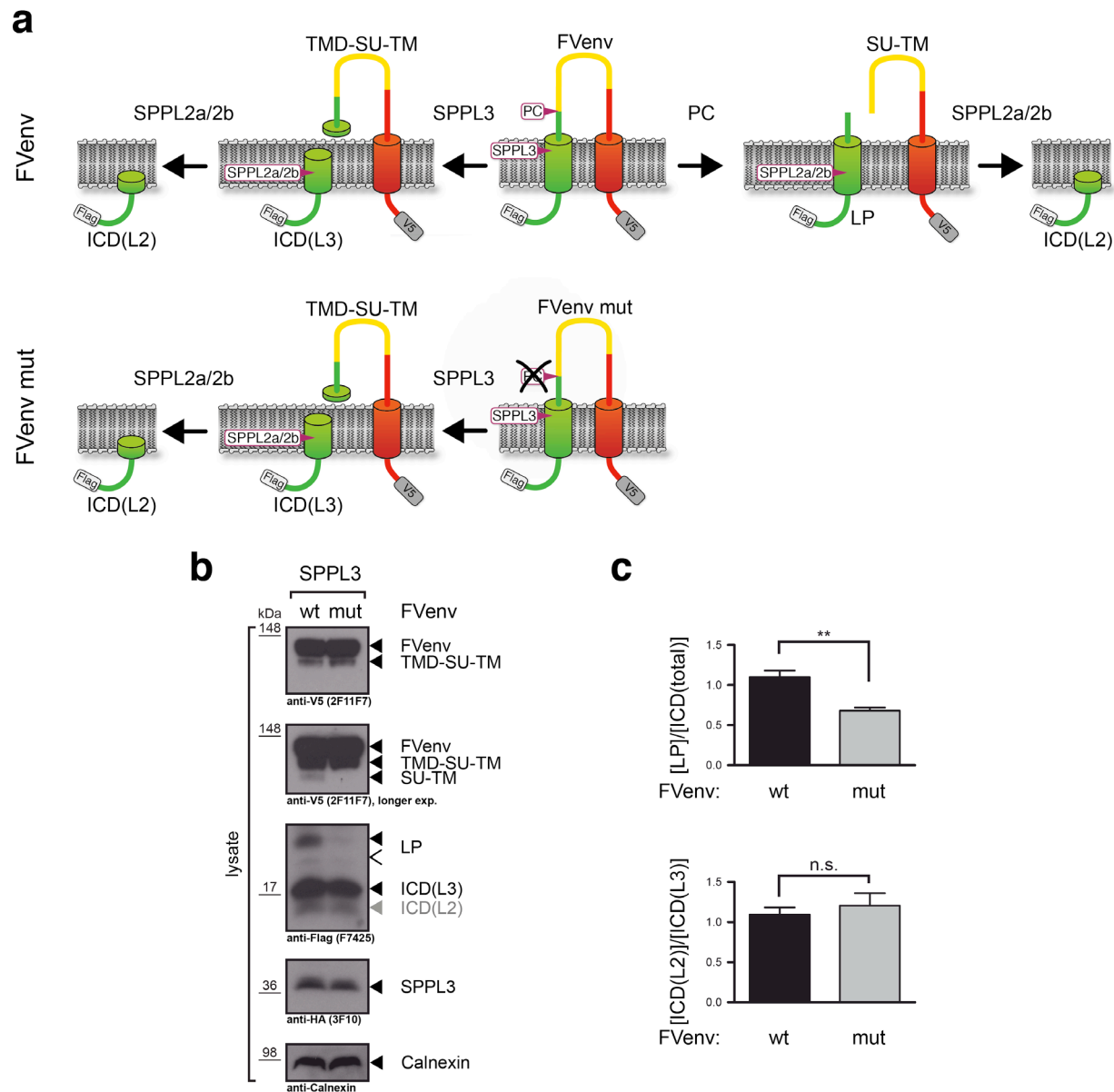


Fig. 4.11: ICD(L2) is produced by endogenous SPPL2a/SPPL2b from ICD(L3) when SPPL3 is over-expressed. (a) Overview of possible mechanisms how ICD(L2) can be generated in cells over-expressing SPPL3. Full-length FVen wild-type (centre of top row) is either directly endoproteolysed by SPPL3 (arrow to the left) which leads to the generation of ICD(L3) which is then turned over by SPPL2a or SPPL2b to obtain ICD(L2) or it is cleaved by PC (arrow to the right) generating LP18 which may then be converted to ICD(L2) by SPPL2a or SPPL2b. Full-length FVen mut is not substantially turned over by PC, i.e. the majority of ICD(L2) will be generated by conversion of the SPPL3 cleavage product, ICD(L3). (b) Analysis of ICD(L2) generation from FVen wild-type and FVen mut in SPPL3 over-expressing cells. HEK293 cells stably expressing active SPPL3 were transfected with either FVen wild-type or FVen mut bearing the R123A/R126A substitutions and proteolytic processing was monitored by Western blot. To this end 80 µg protein from total cell lysates were subjected to Tris-Glycine SDS-PAGE. (c) Quantification of FVen cleavage products. Western blot signals were quantified in three independent experiments and the ratios of FVen species abundance were calculated as depicted (right panels). While the ICD(L2)-to-ICD(L3) ratio was not significantly different in cells expressing either FVen wild-type or FVen mut, the LP-to-ICD(total) ratio was (**, $p < 0.004$ (Student's unpaired t test)). Data represent means \pm SEM.

SPPL2a or SPPL2b and FVenv ICD(L2) was only detected following enrichment by immunoprecipitation (Fig. 4.3).

4.2.4 Determination of SPPL cleavage sites in FVenv

In sum, these observations point to a consecutive proteolytic processing of FVenv by the intramembrane proteases SPPL3 and SPPL2a/SPPL2b. Since collaborative processing of a substrate by different GxGD protease has not been observed previously, this raises additional mechanistic questions, in particular, how consecutive intramembrane proteolysis proceeds and where cleavage by the two apparently very distinct proteolytic activities occurs. To address this, the exact amino acid residue(s) at which cleavage of FVenv by either SPPL3 or SPPL2a/SPPL2b occurs were determined by MALDI-TOF mass spectrometry. To this end a truncated FVenv model substrate, FVenv Δ E, was cloned (Fig. 4.12a). FVenv Δ E includes an N-terminal Flag tag as well as a C-terminal V5 tag to allow for detection of ICDs in cell lysates and C-peptides in conditioned cell culture supernatant, respectively. Such cleavage products were expected to be produced by intramembrane proteolysis of this construct. Similar substrate

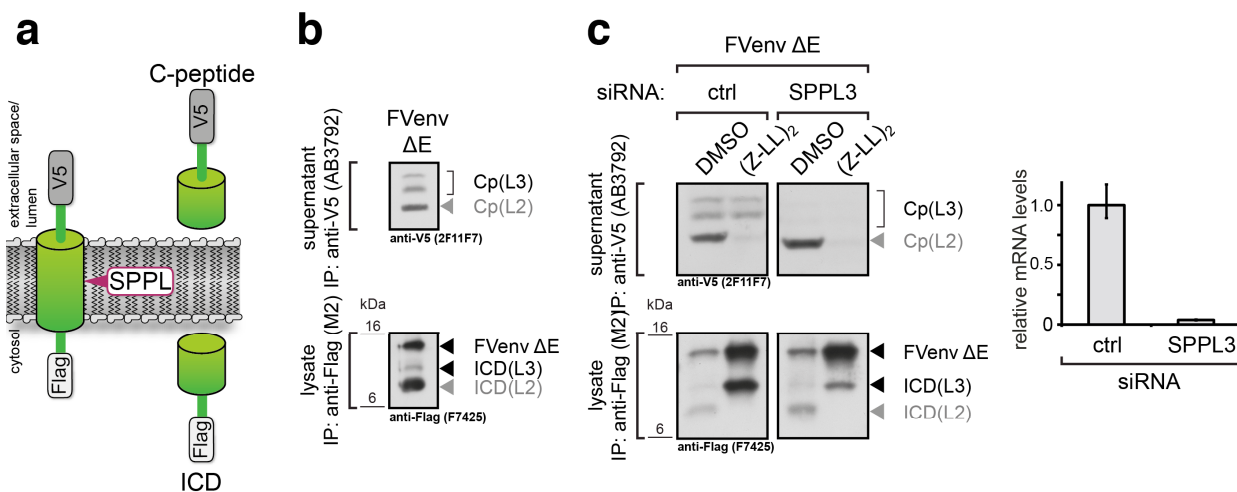


Fig. 4.12: Proteolytic processing of FVenv Δ E by SPPL intramembrane proteases. (a) Schematic overview of FVenv Δ E. This construct is derived from the FVenv coding sequence and comprises amino acids 32 to 106 and, hence, harbours the first, type II-oriented TMD1 (amino acids 66 to 88, green cylinder, the construct is not drawn to scale). Terminal tags were introduced (grey boxes). It was anticipated that this construct is directly endoproteolysed by SPPL3 or SPPL2a/SPPL2b to generate secreted, V5-tagged C-peptides (Cp) and intracellular Flag-tagged ICDs. (b) Transient expression of FVenv Δ E in HEK293 cells. Conditioned supernatants were harvested and subjected to anti-V5 immunoprecipitation (IP) (top panel) while cells were lysed and lysates subjected to anti-Flag immunoprecipitation (bottom panel). Precipitates were loaded on Wiltfang (top panel) or Tris-Tricine gels (bottom panel) and analysed by Western blot. FVenv Δ E represents the uncleaved substrate; cleavage products are labelled according to results from (c). Note that Wiltfang gels do not separate proteins according to their molecular weight, i.e. the faster migrating C-peptide species must not necessarily be the smallest. (c) SPPL2a/SPPL2b and SPPL3 generate distinct cleavage products from FVenv Δ E. HEK293 cells stably expressing FVenv Δ E were reversely transfected with non-targeting (ctrl) or SPPL3-specific (SPPL3) siRNA pools (10 nM). 72 h post transfection cells were treated with either DMSO or (Z-LL)₂ ketone (10 μ M) for 16 h. Conditioned media and cells were analysed as described for (b). Cp(L3) and ICD(L3) represent SPPL3-specific cleavage products, Cp(L2) and ICD(L2) are specific for SPPL2a/SPPL2b. SPPL3 knock-down efficiency was analysed by quantitative TaqMan RT-PCR (right panel). SPPL3 mRNA levels were normalised to β -actin levels and relative mRNA changes were calculated using the $\Delta\Delta C_T$ method. Transfection with SPPL3-specific siRNAs resulted in loss of > 95% of endogenous SPPL3 mRNA. Bars represent mean values from three technical replicates, error bars the SD.

constructs have already been used in previous studies in particular since they allow for direct analysis of γ -secretase- or SPPL-mediated intramembrane proteolysis due to their substantially shortened ectodomains (Kopan *et al*, 1996; Fluhrer *et al*, 2006; Martin *et al*, 2008; Zahn *et al*, 2013). Indeed, following FVenv ΔE expression in HEK293 cells three putative C-peptide bands were detected in conditioned media as well as two distinct putative ICD species in cell lysates (Fig. 4.12b), the latter being reminiscent of ICD(L3) and ICD(L2) generated by intramembrane proteolysis of full-length FVenv. To attribute these cleavage products to the proteolytic activity of either SPPL3 or SPPL2a/SPPL2b, stably FVenv ΔE -expressing HEK293 cells were transfected with SPPL3-specific siRNAs and at the same time subjected to (Z-LL)₂ ketone treatment to inhibit SPPL2a/SPPL2b activity (Fig. 4.12c). (Z-LL)₂ ketone treatment markedly reduced the amounts of one C-peptide in cell culture supernatants and of the smaller ICD species in cell lysates. As these bands were unaffected by SPPL3-specific siRNA transfection, they likely derive from endogenous SPPL2a/SPPL2b activity in HEK293 cells and, hence, are referred to as Cp(L2) and ICD(L2), respectively. Reduction of endogenous SPPL3 by RNAi similarly resulted in reduction of two C-peptide bands collectively named Cp(L3). Interestingly, even in cells transfected with non-targeting siRNAs, (Z-LL)₂ ketone also led to accumulation of both the larger ICD as well as of the educt band, FVenv ΔE . Accumulation of the ICD was markedly decreased following SPPL3 knock-down, showing that this ICD, ICD(L3), is an SPPL3-specific cleavage product. FVenv ΔE has a shortened ectodomain and also lacks the furin/PC cleavage, suggesting that it can be directly accepted as a substrate of SPPL2a/SPPL2b and SPPL3. Indeed, the observed accumulation of the FVenv ΔE educt as well as of ICD(L3) in cell lysates following inhibitor treatment demonstrate that both species can in fact be turned over by SPPL2a/SPPL2b. Taken together, FVenv ΔE is endoproteolysed by SPPL2a/SPPL2b and SPPL3 similar to full-length FVenv. Unlike full-length FVenv, however, FVenv ΔE can also be directly cleaved by SPPL2a/SPPL2b independent of prior proteolysis by either furin/PC or SPPL3.

To identify the exact site(s) at which SPPL-mediated endoproteolysis of FVenv occurs, C-peptide species were analysed by MALDI-TOF mass spectrometry. To this end, another truncated FVenv substrate was constructed, FVenv ΔE_{inv} . Unlike FVenv ΔE , however, this construct was C-terminally Flag-tagged to achieve secretion of Flag-tagged FVenv-derived C-peptides generated by SPPL activity in transfected cells. These peptides were affinity-purified via their epitope tag and subsequently analysed by MALDI-TOF MS analysis. In initial experiments detection of such peptides, however, was hampered by C-terminal degradation which was attributed to the activity of secreted cellular or serum exopeptidase(s) (data not shown). To circumvent this technical problem, an alanine and a proline residue were added to the construct's C-terminus to prevent carboxypeptidase attack. This construct, FVenv ΔE_{inv} (AP), was stably transfected into HEK293 cells. These were treated with either DMSO or (Z-LL)₂ ketone to inhibit SPPL2a/SPPL2b activity and conditioned media were subjected to anti-Flag immunoprecipitation to purify Flag-tagged C-peptides generated by endogenous protease activities. Four distinct peaks, a very prominent one and three less intense ones, were observed in immunoprecipitates analysed by mass spectrometry (Fig. 4.13a). Their observed mass was well in line with the calculated mass of four peptides originating in the annotated TMD and

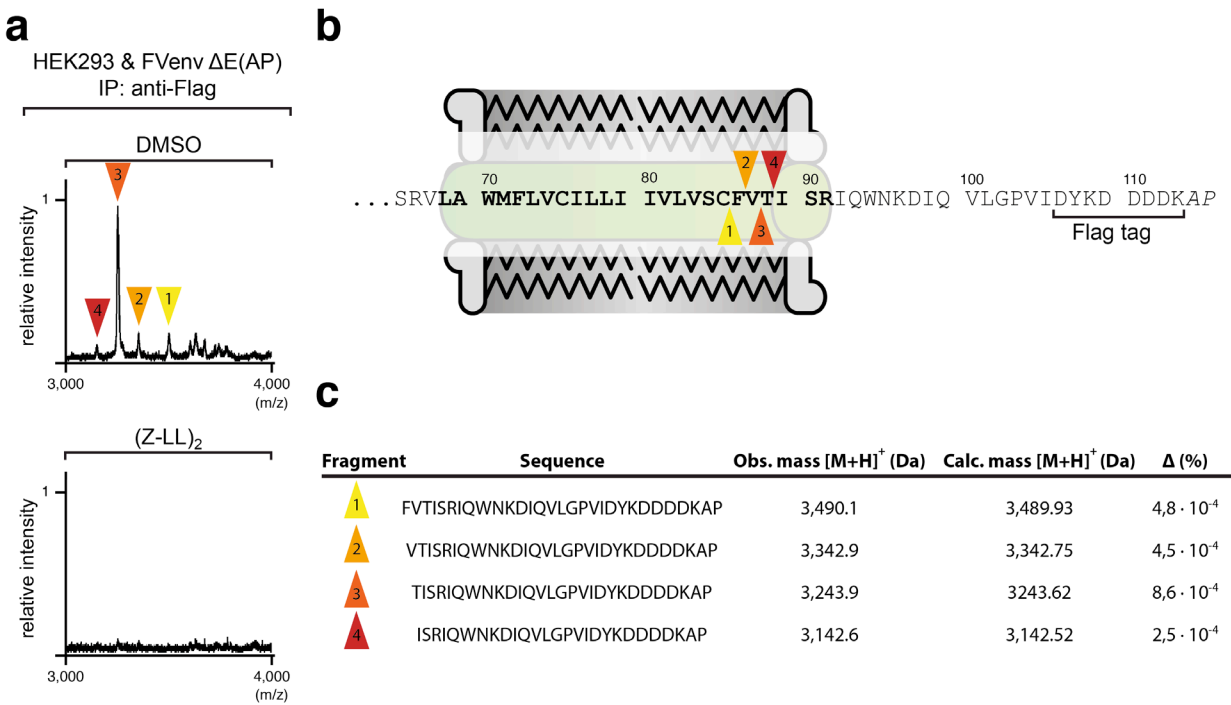


Fig. 4.13: Mass spectrometric analysis of C-peptides generated by SPPL-mediated intramembrane proteolysis. To allow for detection of FVenv-derived C-peptide species, a modified variant of FVenv ΔE (see Fig. 4.12), FVenv $\Delta E_{inv}(AP)$, was used. Unlike FVenv ΔE , this construct's terminal tags were inverted, i.e. C-terminal to the Flag tag two residues (alanine and proline, given in italics in (b)) were added in order to prevent degradation by carboxypeptidases. Identification of $(Z-LL)_2$ ketone-sensitive C-peptides (a). HEK293 cells stably transfected with FVenv $\Delta E_{inv}(AP)$ were treated with DMSO or 50 μ M $(Z-LL)_2$ ketone for 48 h. Conditioned supernatants were subjected to anti-Flag immunoprecipitation (IP) and immunoprecipitates were analysed by MALDI-TOF mass spectrometry together with angiotensin 1 peptide as a reference. Note that four $(Z-LL)_2$ ketone-sensitive peptides were detected within a m/z range of 3,000 and 4,000 (numbered coloured arrowheads). Mapping of the observed peptides to the FVenv $\Delta E_{inv}(AP)$ sequence (b, c). FVenv TMD in (b) is highlighted in bold according to TMHMM 2.0 predictions, numbering is according to the untagged FVenv sequence. $(Z-LL)_2$ ketone treatment of FVenv $\Delta E_{inv}(AP)$ -transfected cells was accompanied by accumulation of higher molecular weight peptides (green bracket) that could not be mapped to the FVenv sequence. (Mass spectrometric measurements were performed by Dr Akio Fukumori, DZNE Munich.)

comprising the intact C-terminus (Fig. 4.13a & b). Interestingly, all four peptides disappeared when cells were treated with $(Z-LL)_2$ ketone (Fig. 4.13a), suggesting that they were generated by endogenous SPPL2a/SPPL2b activity. Collectively, these data point to SPPL2a/SPPL2b-mediated cleavage of FVenv occurring close to the luminal border of its TMD. SPPL3-specific C-peptide species, however, could not be detected using FVenv $\Delta E_{inv}(AP)$. Moreover, mass spectrometric analysis of ICD species generated by SPPL2a/SPPL2b or SPPL3 activity was not successful, in spite of various experimental approaches (data not shown).

4.2.5 SPPL3 isoform 1 exhibits no proteolytic activity towards FVenv

Databases list two isoforms of human SPPL3: isoform 1⁵, which encodes a putative 385 aa protein (GenBank entry CAD13135.1), and isoform 2, encoding a 384 aa protein (GenBank RefSeq entry NP_620584.2). In all the prior experiments (and in the one described in sections 4.3 and 4.4) over-expressed HA-tagged SPPL3 was exclusively isoform 2. Both

⁵ Isoform numbering is adopted from the human SPPL3 Uniprot entry (Q8TCT6), retrieved on March 12th 2014.

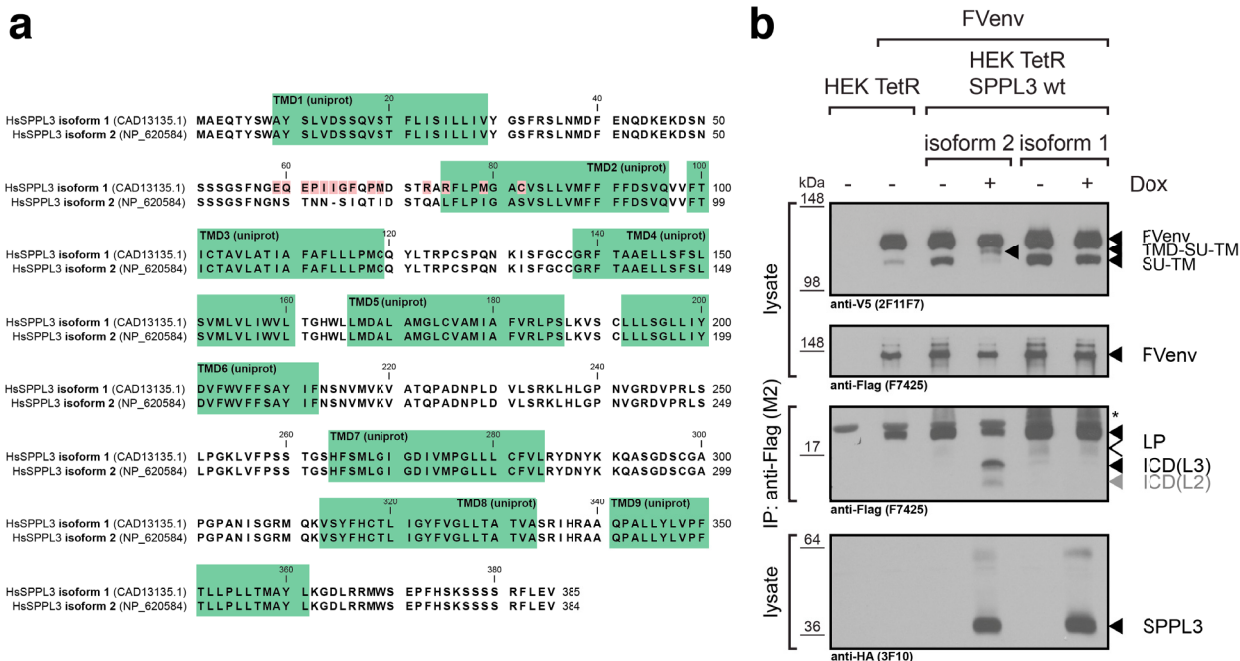


Fig. 4.14: Comparison of human SPPL3 isoforms. (a) ClustalW protein sequence alignment of human SPPL3 isoform 1 and isoform 2. Sequences were obtained from GenBank with the given entry ID. Putative TMDs are highlighted in green according to Uniprot annotations. Note that isoform 1 and isoform 2 solely differ in region comprising the luminal juxtamembrane region close to TMD1 and the first half of TMD2. Residues in isoform 1 differing from the respective ones in isoform 2 are depicted with a red background. (b) Co-expression of FVenv and SPPL3 wild-type isoform 1 and isoform 2. Stably transfected HEK TetR cells inducibly over-expressing the respective SPPL3 isoform were transiently transfected with FVenv. FVenv cleavage was monitored by Western blot detection of TMD-SU-TM and ICD(L3)/ICD(L2). Note that both SPPL3 isoforms are expressed at comparable levels, yet only SPPL3 isoform 2 induction led to changes in ICD production and detection of TMD-SU-TM.

isoforms are highly homologous and differ only in a small stretch comprising the luminal juxtamembrane region preceding TMD1 up to the middle of TMD1 (Fig. 4.14a). To examine whether SPPL3 isoform 1 is also capable of endoproteolysing FVenv in a manner similar to SPPL3 isoform 2, both isoforms were co-expressed with FVenv in HEK293 cells (Fig. 4.14b). As expected, expression of SPPL3 isoform 2 led to generation of TMD-SU-TM as well of ICD(L3) and the down-stream cleavage product ICD(L2). Upon expression of SPPL3 isoform 1, however, neither ICD(L3) and ICD(L2) nor TMD-SU-TM could be detected. Taken together, these observations suggest that SPPL3 isoform 1 is not proteolytically active on FVenv.

4.3 SPPL3 affects cellular N-glycosylation under physiological conditions

SPPL3 appears to be one of the most ancient SPP homologues and is highly conserved in metazoa (Fig. 1.9) (Golde *et al*, 2009; Voss *et al*, 2013). Such high degree of conservation could point to a crucial physiological function in multicellular organisms. Presently, however, this has remained enigmatic, mostly for the lack of (a) known physiological substrate(s). Hence, in order to investigate its physiological function(s) in mammals, SPPL3-deficient mice were examined for a phenotype.

4.3.1 Characterisation of *Sppl3*-deficient mice

To examine the physiological function of SPPL3 a previously established mouse line deficient in *Sppl3*, B6;129S5-Sppl3^{Gt(OST279815)Lex}/Mmucd, was used (Tang *et al*, 2010). This mouse line harbours a genetrap insertion between exons 6 and 7 of the *Sppl3* open reading frame leading to an absence of *Sppl3* transcripts in homozygous mutant animals (Tang *et al*, 2010). Phenotypic analyses by Tang *et al*. revealed that homozygous B6;129S5-Sppl3^{Gt(OST279815)Lex}/Mmucd mice were viable but both *Sppl3*-deficient males and females exhibited signs of growth retardation such as decreased body weight and size (Tang *et al*, 2010). Behavioural abnormalities such as decreased exploratory activity and depression-like responses were also noted in homozygous *Sppl3* mutants and, importantly, mutant males were found to be compromised in fertility. Moreover, *Sppl3* knock-out animals had markedly reduced levels of NK cells in spleen, lymph node, and peripheral blood (by up to 75% compared to homozygous wild-type litter-mates).

As expected from these published observations, breeding performance of homozygous knock-out animals appeared to be very poor. Similar to observations made by Tang *et al*. male knock-outs were observed to be not fertile (Tang *et al*, 2010) and female knock-out mice produced very small litters (data not shown). Hence, to nevertheless obtain homozygous knock-out animals, heterozygous litter-mates were mated (Tab. 4.1). Genotyping of the F1 offspring obtained from such heterozygous breeding pairs revealed that viable *Sppl3*^{-/-} could be obtained, yet at a lower percentage than expected (8% vs. 25%). Macroscopically, animals deficient in *Sppl3* were phenotypically inapparent. To reproduce the previously observed NK cell deficiency (Tang *et al*, 2010), lymph nodes and spleen were removed from sacrificed B6;129S5 *Sppl3* knock-out animals and wild-type litter-mate controls and analysed by flow cytometry. To detect mature NK cells, surface expression of two NK cell markers, the integrin CD49b (Arase *et al*,

Tab. 4.1: F1 genotypes of *Sppl3*^{+/+} x *Sppl3*^{+/+} matings. After separation from the parents the F1 offspring of *Sppl3*^{+/+} x *Sppl3*^{+/+} matings from both *Sppl3*-deficient mouse lines was genotyped by PCR. Note that following back-crossing to the C57BL/6 background no *Sppl3*^{-/-} animals could be obtained. $n_{x/x}$, absolute number of animals of a given genotype, n_{total} , total number of F1 animals genotyped.

mouse line	<i>Sppl3</i> ^{+/+}		<i>Sppl3</i> ^{+/−}		<i>Sppl3</i> ^{−/−}		n_{total}
	$n_{+/+}$	%	$n_{+/-}$	%	$n_{-/-}$	%	
B6;129S5-Sppl3 ^{Gt(OST279815)Lex} /Mmucd	43	28.67	95	63.33	12	8.00	150
B6.129S5-Sppl3 ^{Gt(OST279815)Lex} /Mmucd (N5)	30	37.04	51	62.94	0	0.00	81

2001) and the NK cell activating receptor NKp46 (Walzer *et al*, 2007), was analysed (Fig. 4.15). While *Spp13^{+/+}* spleen and lymph nodes contained a minor population of CD49b⁺ NKp46⁺ double-positive cells (0.38 and 0.78% in spleen and roughly 0.2% in lymph node), the relative abundance of this population in *Spp13* knock-out animals was substantially reduced (< 0.06%), clearly supporting the previous observations (Tang *et al*, 2010) and demonstrating that reduced NK cell counts are a distinctive feature of B6;129S5 mice lacking *Spp13*.

A mixed genetic background could in principle affect the degree of severity of such a phenotype and could lead to variance within the population of animals studied. Therefore, *Spp13*-deficient animals were back-crossed to the C57BL/6 inbred mouse strain. Heterozygous B6.129S5-*Spp13*^{Gt(OST279815)Lex/Mmucd (N5) mutants were then similarly inter-crossed to obtain *Spp13*-}

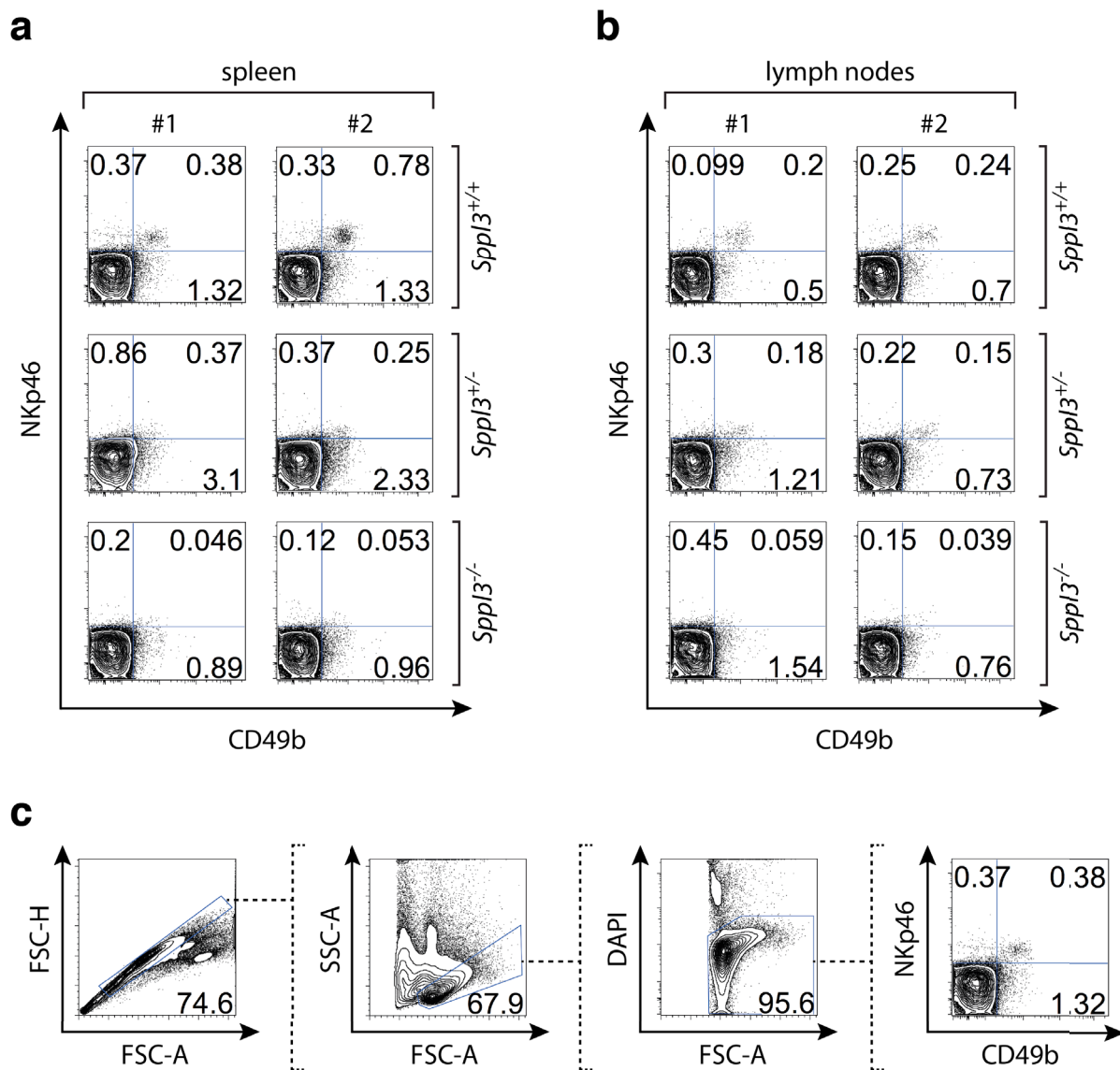


Fig. 4.15: Flow cytometric analysis of NK cells in *Spp13*^{-/-} mice. Splenic lymphocytes (a) and pooled lymphocytes from axillary, brachial, and inguinal lymph nodes (b) from two individual animals (#1 and #2) of each genotype (*Spp13*^{+/+}, *Spp13*^{+/-}, and *Spp13*^{-/-}) were examined for NKp46 and CD49b surface expression. Percentages are indicated for each quadrant. Both NKp46 (Walzer *et al*, 2007) as well as CD49b (Arase *et al*, 2001) are well established NK cell markers, yet they may also be found on other minor lymphocyte subpopulations such as $\gamma\delta$ T cells (Walzer *et al*, 2007) and NKT cells (Ortaldo *et al*, 1998), respectively. To exclude these populations, NKp46⁺ CD49b⁺ cells were analysed. (c) depicts the gating strategy for *Spp13*^{+/+} #1 spleen. Duplets were excluded and viable, i.e. DAPI-negative, lymphocytic cells were analysed. Percentages of cells in gate are given. (Flow cytometric analyses were performed together with Anne Behrendt, Institute of Immunology, LMU Munich.)

deficient animals. However, no homozygous *Spp3* mutants were observed in numerous litters produced by heterozygous parents (Tab. 4.1), suggesting that, on the C57BL/6 background, SPPL3 deficiency is associated with embryonic or early post-natal lethality. At the pre-natal developmental stage E13.5, however, homozygous knock-out embryos and wild-type controls exhibited no gross macroscopic phenotypic differences and were indistinguishable (not shown).

4.3.2 SPPL3 affects the electrophoretic mobility of cellular glycoproteins

Primary MEFs were prepared from E13.5 embryos of B6.129S5-*Spp3*^{Gt(OST279815)Lex}/ Mmucd (N5) mice. Genotyping by PCR revealed that two MEF preparations were in fact obtained from *Spp3*^{-/-} embryos (Fig. 4.16a). In line with this, no SPPL3 protein expression was detected in lysates of these MEF preparations by Western blot, while SPPL3 protein expression was observed in MEFs obtained from a litter-mate *Spp3*^{+/+} embryo (Fig. 4.16b, top panels). Striking differences between knock-out MEFs and wild-type MEFs became apparent when the running behaviour of endogenous glycoproteins, for instance of mature Nicastin (NCT_{mat}), was analysed (Fig. 4.16b, lower panels) in these cells. NCT_{mat} displayed a slightly lower electrophoretic mobility in SDS-PAGE gels in cells devoid of *Spp3* than in wild-type MEFs, suggesting it has a higher molecular weight in cells lacking *Spp3*. Interestingly, endogenous SPPL2a and the neuronal cell adhesion molecule N-cadherin behaved similarly and exhibited a slightly higher molecular weight in *Spp3*^{-/-} MEFs than in *Spp3*^{+/+} cells. Similar observations

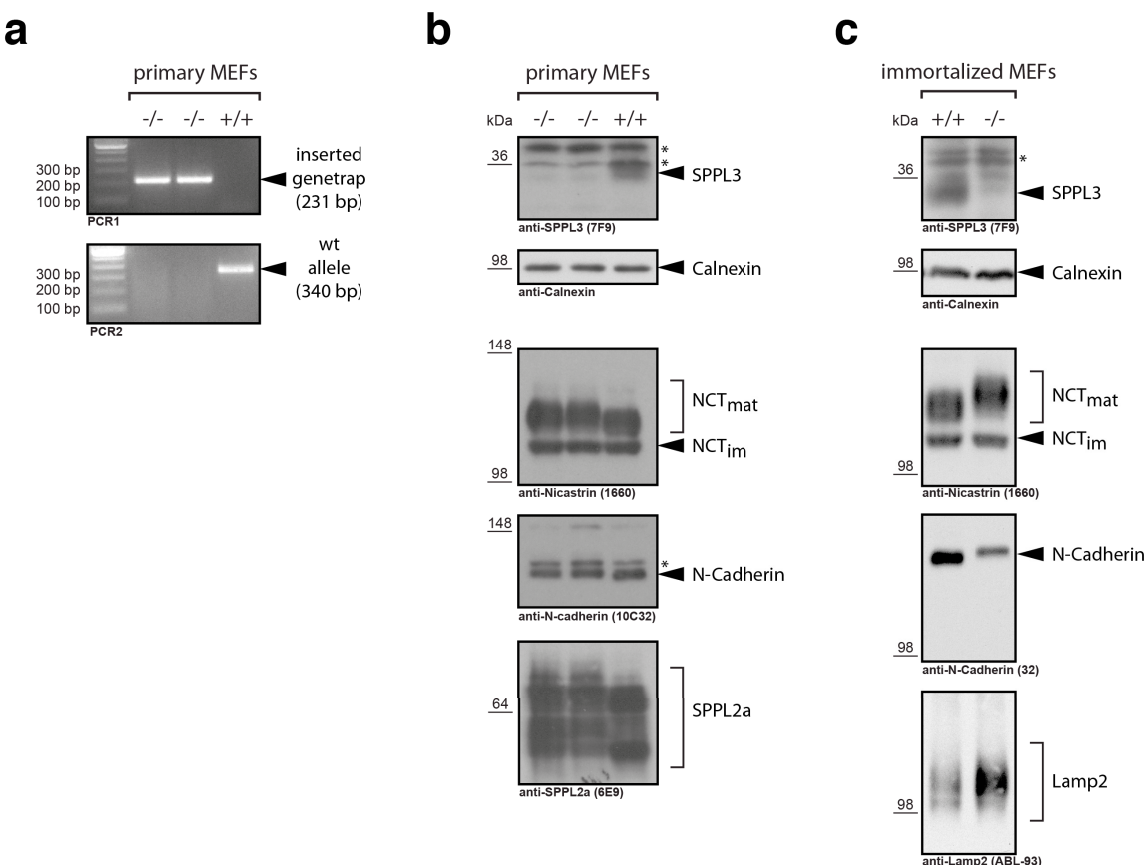


Fig. 4.16: Analysis of *Spp3*-deficient MEFs. Genotyping of primary MEFs (a). Genomic DNA was isolated from primary MEFs and analysed by PCR for the genetrap insertion in the *Spp3* locus (top panel) or for the wild-type locus (bottom panel). Analysis of primary (b) and immortalised (c) MEFs by SDS-PAGE and Western blot to monitor the absence of detectable SPPL3 expression in *Spp3*^{-/-} MEFs (-/-) compared to wild-type control MEFs (+/+) (top two panels). In addition, selected glycoproteins were analysed (lower panels). *, unspecific bands.

were made in MEFs following immortalisation (Fig. 4.16c). In immortalised *Spp3*^{-/-} MEFs, NCT_{mat} as well as the neuronal cell adhesion molecule N-cadherin and the lysosomal membrane protein Lamp2 displayed a slightly increased molecular weight compared to their respective molecular weight observed in lysates obtained from *Spp3*^{+/+} MEFs.

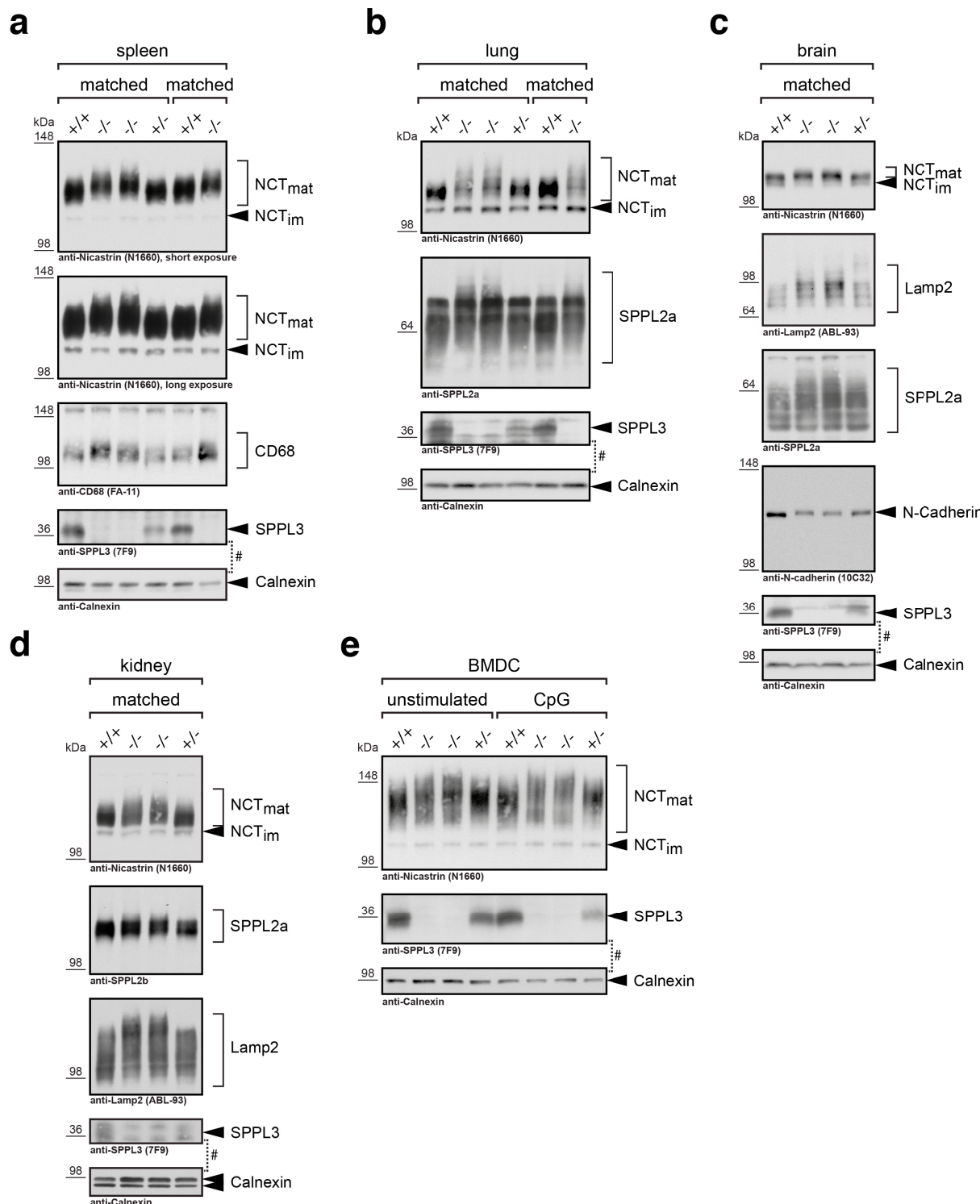


Fig. 4.17: Analysis of endogenous glycoproteins in *Spp3*^{-/-} mice and litter-mate controls. Homogenates of spleen (a), lung (b), brain (c), and kidney (d) obtained from age- and sex-matched B6;129S5 mice were examined for expression of SPPL3 (lower panels) and for the running behaviour of endogenous glycoproteins by SDS-PAGE and Western blot (top panels). Bone marrow-derived dendritic cells (BMDC, e) were generated by ex vivo differentiation of bone marrow-resident haematopoietic stem cells obtained from age- and sex-matched *Spp3*^{-/-} mice and litter-mate controls and left unstimulated or were stimulated with CpG overnight. #, upper blot was redecorated with anti-Calnexin antibody (lower blot) as loading control.

To address whether this phenotype also prevails in living, adult *Sppl3*-deficient mice, tissue homogenates obtained from B6;129S5-*Sppl3*^{Gt(OST279815)LeX/Mmucd mice were examined by SDS-PAGE and Western blotting to assess for electrophoretic mobility of endogenous glycoproteins (Fig. 4.17). As expected, *Sppl3*^{-/-} mice lacked any detectable SPPL3 expression and SPPL3 levels were also reduced in *Sppl3*^{+/+} compared to wild-type litter-mate controls. NCT_{mat} was found to have a slightly higher molecular weight in spleen homogenates of *Sppl3*^{-/-} mice compared to homogenates of *Sppl3*^{+/+} animals, while immature Nicastin (NCT_{im}) of all animals analysed had a highly similar running behaviour (Fig. 4.17a). While the extent of complex glycosylation of NCT_{mat} clearly differs in a tissue-specific manner, the increased molecular weight of NCT_{mat} associated with loss of *Sppl3* was consistently observed also in other tissues such as lung (Fig. 4.17b), brain (Fig. 4.17c), and kidney (Fig. 4.17d). Dendritic cells generated by ex vivo differentiation from *Sppl3*^{-/-} bone marrow exhibited a similar alteration in NCT_{mat} molecular weight (Fig. 4.17e). In addition to NCT_{mat}, other endogenous and ubiquitously expressed glycoproteins such as Lamp2 and SPPL2a also displayed a higher molecular weight in tissues of *Sppl3*^{-/-} than in samples obtained from wild-type litter-mates (Fig. 4.17). Finally, the running behaviour of glycoproteins that are expressed in a tissue-specific manner was also examined. Like NCT_{mat}, these proteins, for instance the monocytic marker CD68 expressed in spleen (Fig. 4.17a) or the neuronal cell adhesion factor N-cadherin expressed in the brain (Fig. 4.17c), displayed a lower electrophoretic mobility in animals that lacked SPPL3 expression.}

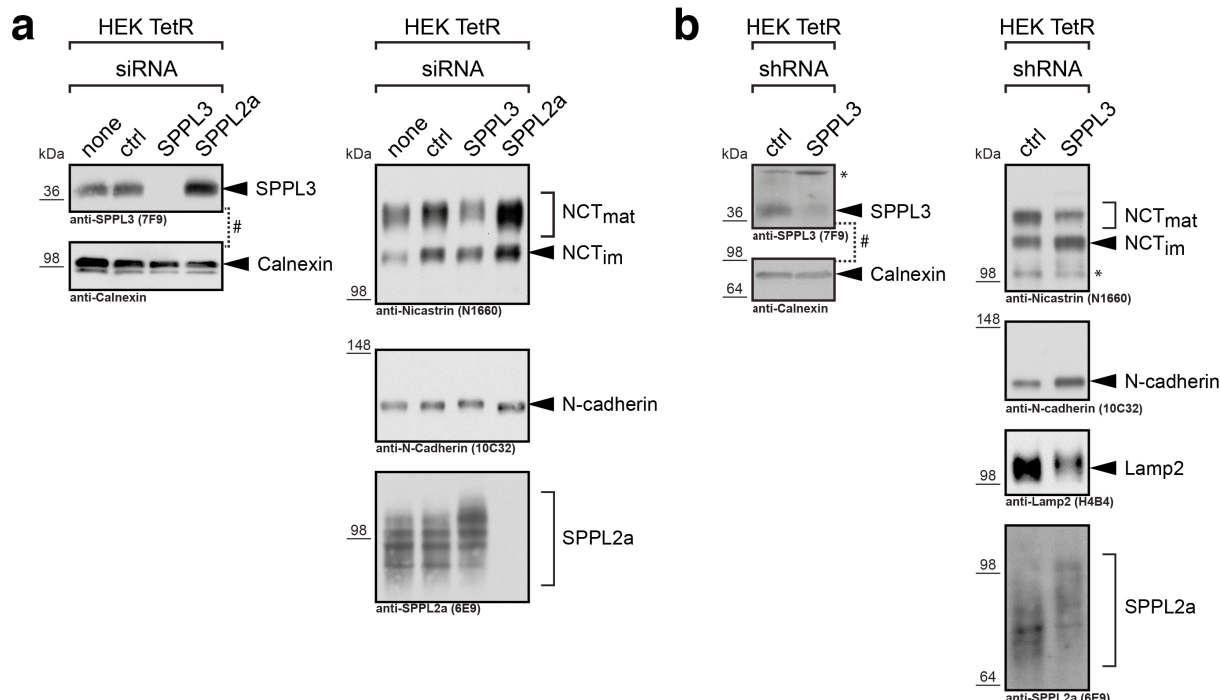


Fig. 4.18: Glycoprotein analysis following RNAi-mediated SPPL3 knock-down in HEK293 cells. Endogenous SPPL3 expression in HEK293 TetR cells was reduced by transient transfection with SPPL3-specific siRNAs (a) or by stable expression of a SPPL3-specific shRNA (b). For siRNA transfections (a), cells were reversely transfected with 20 nM of a non-targeting siRNA pool (ctrl), with SPPL3- or SPPL2a-specific siRNA pools or were left untransfected (none). Cells were harvested four days after transfection. Membranes were isolated from cells (a & b) and membrane lysates were examined by SDS-PAGE and Western blotting for SPPL3 expression levels (left panels) and glycoprotein electrophoretic mobility (right panels). #, upper blot was redecorated with anti-Calnexin antibody (lower blot) as loading control.

Taken together, *Spp3* deficiency in mice *in vivo* and *ex vivo* is accompanied by an increase in molecular weight of selected glycoproteins. To investigate whether such effects are also associated with the human orthologue, SPPL3 expression levels were modified in human HEK293 TetR cells. First, to mimic the murine knock-out setting (Fig. 4.16 & 4.17), endogenous SPPL3 expression was reduced by RNAi. Transient transfection with SPPL3-specific siRNA pools resulted in a marked reduction in SPPL3 protein levels compared to cells transfected with non-targeting control oligonucleotides (Fig. 4.18a). This, in turn, was accompanied by an increase in molecular weight of NCT_{mat}, SPPL2a and N-cadherin. A similar change was observed in cells that express substantially less endogenous SPPL3 due to a stable expression of a SPPL3-specific shRNA (Fig. 4.18b). Hence, reduction of endogenous human SPPL3 in HEK293 TetR cells mirrors the effects observed following genomic ablation of *Spp3* in murine cells.

Next, exogenous SPPL3 over-expression was induced in stably transfected HEK293 TetR cells to check whether this has the opposite effect on endogenous cellular glycoproteins (Fig. 4.19a). Indeed, SPPL3 wild-type over-expression had a profound impact on NCT_{mat}, N-cadherin, Lamp2 and SPPL2a. It led to a reduction in molecular weight of these glycoproteins and, interestingly, the extent of the molecular weight shift was even more pronounced than the increase in molecular weight associated with loss of SPPL3 expression. Moreover, no changes in

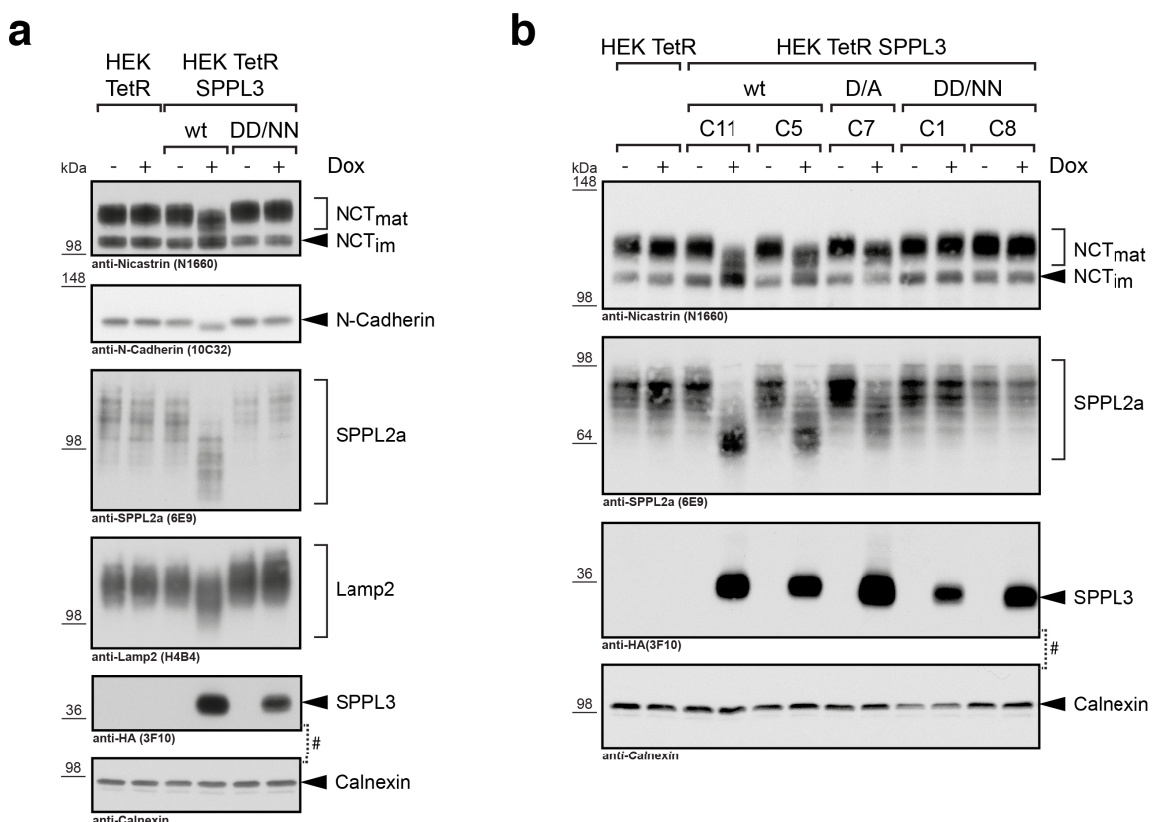


Fig. 4.19: Glycoprotein analysis following SPPL3 over-expression in HEK293 cells. Cell lysates of HEK TetR cells stably over-expressing SPPL3 wild-type (wt) or the active site D200N/D271N mutant (DD/NN) were analysed by SDS-PAGE and Western blot to monitor changes in the molecular weight of endogenous glycoproteins such as Nicastrin (NCT), N-cadherin, SPPL2a, and Lamp2 (a). To exclude clone-specific effects, the experiment depicted in (a) was repeated with individual single cell-derived clones (C#) of cells expressing SPPL3 wt and SPPL3 D200N/D271N (DD/NN). In addition, cells expressing the D271A mutant (D/A) were analysed. #, upper blot was redecorated with anti-Calnexin antibody (lower blot) as loading control.

glycoprotein molecular weight were associated with exogenous expression of the SPPL3 active site mutant D200N/D271N, suggesting that proteolytic activity of SPPL3 is crucially required to affect cellular glycoproteins. To exclude that these observations are simply due to an unspecific phenotype solely observed in one single cell-derived clone, two additional cell clones over-expressing SPPL3 wild-type and SPPL3 D200N/D271N, respectively, were examined (Fig. 4.19b). In both SPPL3 wild-type-expressing clones the glycoprotein molecular weight shift became apparent, while in clones expressing SPPL3 D200N/D271N glycoprotein molecular weights were unchanged. In addition, glycoprotein running behaviour in cell lysates obtained from cells expressing the SPPL3 D271A active site mutant was also examined and was found to be slightly changed upon expression of the mutant, yet the differences in molecular weight following doxycycline treatment in these cells were not as substantial as in SPPL3 wild-type-expressing cells (Fig. 4.19b).

4.3.3 SPPL3 alters cellular glycosylation of post-ER-localised glycoproteins

Interestingly, while changes in SPPL3 expression clearly affected NCT_{mat}, SPPL2a, N-Cadherin, and Lamp2, the ER chaperone calnexin was not affected (Fig. 4.16 to 4.19). Unlike Calnexin, which is not glycosylated, NCT_{mat}, SPPL2a, N-Cadherin, and Lamp2 are all membrane proteins that harbour several Nx(S/T) N-glycosylation sequons within their luminal ectodomains. In fact, there is abundant experimental evidence that these proteins are post-translationally modified by N-glycosylation (Yu *et al*, 2000; Leem *et al*, 2002; Friedmann *et al*, 2004; Guo *et al*, 2009; Carlsson *et al*, 1988). Accordingly, the assumption emerged that SPPL3 does not affect the glycoproteins themselves but instead alters cellular N-glycosylation globally which then leads to the molecular weight changes observed. To test this, lysates from cells over-expressing active or inactive SPPL3 were subjected to glycosidase treatment to remove N-glycans attached. PNGase F removes most N-glycan structures, including complex ones, by hydrolysing the β -N-glycosidic amide bond connecting the Asn side chain and the first GlcNAc residue of the N-glycan (Maley *et al*, 1989). Accordingly, PNGase F treatment reduced the molecular weight of N-cadherin, SPPL2a, and Lamp2 due to the removal of attached N-glycans (Fig. 4.20a). Strikingly, however, whereas in untreated cell lysates SPPL3 over-expression affected the glycoproteins' molecular weight as observed earlier, in lysates treated with PNGase F the SPPL3-mediated change in molecular weight was lost. Likewise, the molecular weight difference of NCT_{mat} and N-cadherin observed earlier in tissues from *Spp3*^{-/-} animals compared to wild-type litter-mates (Fig. 4.17b), was not apparent anymore in PNGase F-treated brain homogenates (Fig. 4.20b). Also, in PNGase F-treated lysates of *Spp3*^{+/+} and *Spp3*^{-/-} MEFs neither N-cadherin nor SPPL2a exhibited any differences in molecular weight, while in untreated lysates both glycoproteins had a slightly higher molecular weight in *Spp3*-deficient cells than in *Spp3*^{+/+} MEFs (Fig. 4.20c). Taken together, this clearly shows that changes in SPPL3 expression levels lead to alterations in the pattern and/or extent of glycosylation on the proteins analysed. In addition, to dissect at which step(s) SPPL3 interferes with the cellular synthesis of N-glycans, HEK cell lysates were digested with Endo H (Fig. 4.20a & b). Endo H hydrolyses the β 1,4-glycosidic bond within the chitobiose core of N-glycans. N-glycans that were acted upon by α -mannosidase II, however, become resistant to Endo H hydrolysis and, therefore, Endo H fails

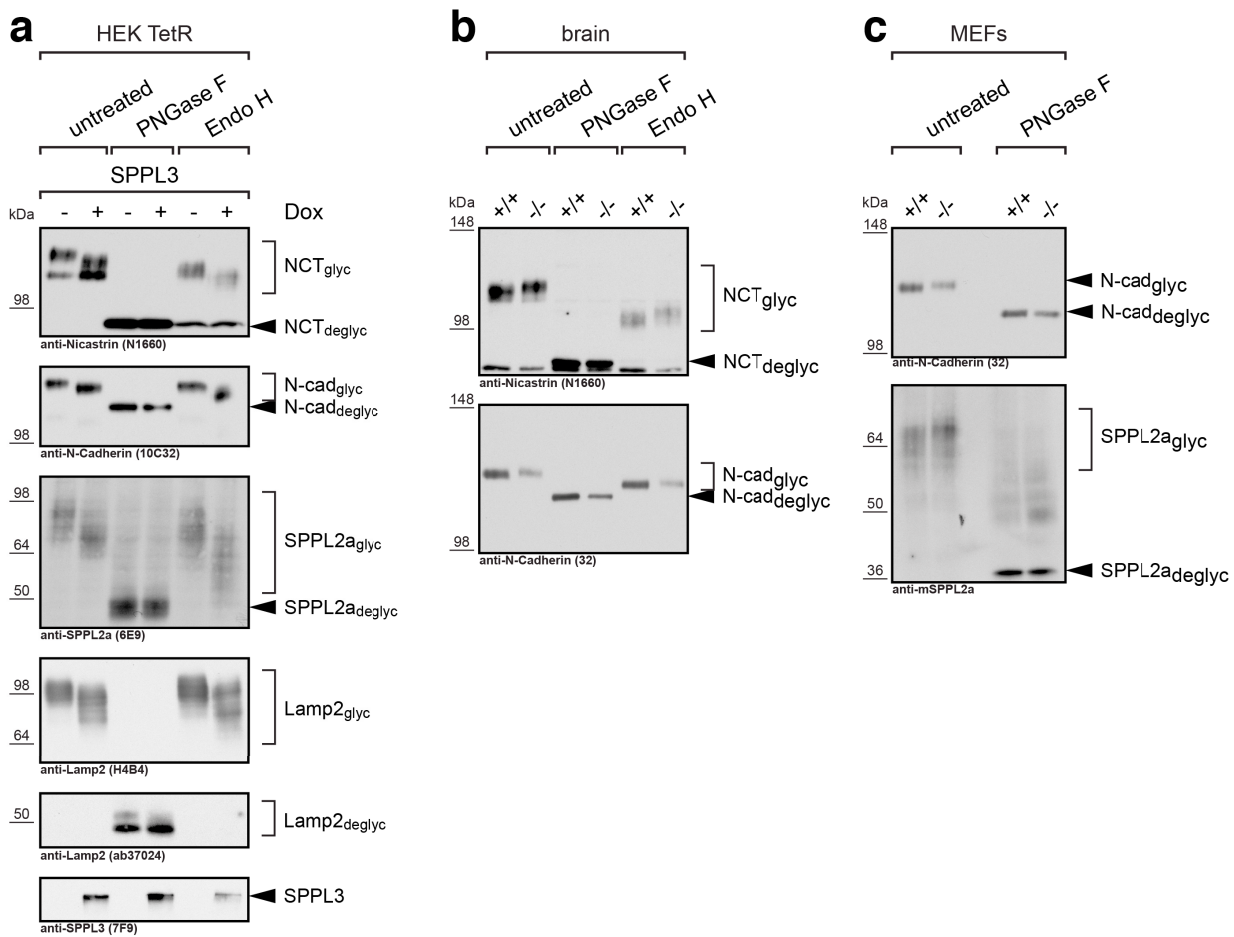


Fig. 4.20: Enzymatic N-deglycosylation. Lysates of HEK TetR cells stably over-expressing SPPL3 wild-type (wt) upon doxycycline (+ Dox) treatment (a), of wild-type (+/+) or *Sppl3*-deficient (-/-) mouse brain (b) and of immortalised MEFs (c) were subjected to endoglycosidase digestion by PNGase F (a, b, c) or Endo H (a, b) as indicated. Electrophoretic mobility of endogenous glycoproteins was analysed as depicted earlier. Note that PNGase F-digested N-Cadherin and SPPL2a were not affected by changes in SPPL3 expression anymore, while glycoproteins resistant to Endo H treatment were. PNGase F-treated human Lamp2 could not be detected using the anti-H4B4 antibody anymore, but instead was detected using another anti-Lamp2 antibody that in turn only recognised N-deglycosylation human Lamp2. glyc, glycosylated species, deglyc, N-deglycosylated species.

to remove complex glycan structures from glycopeptides (Maley *et al*, 1989). Endogenous NCT_{mat}, N-cadherin, SPPL2a, and Lamp2 in HEK293 cells (Fig. 4.20a) and NCT_{mat} and N-cadherin in brain homogenates (Fig. 4.20b) appear to be extensively modified by such complex glycans, as they were largely resistant to Endo H activity. Interestingly, though, these Endo H-digested glycoproteins were affected by alterations in SPPL3 expression as this led to changes in their electrophoretic mobility. In contrast to this, in cells treated with the alkaloid kifunensine, exogenously expressed active SPPL3 lost its ability to alter the electrophoretic mobility of NCT_{mat}, N-cadherin, SPPL2a, and Lamp2 (Fig. 4.21a). Kifunensine very potently inhibits α -mannosidase I activity and, as a result, cells fail to produce complex- as well as hybrid-type glycans and, consequently, high-mannose glycans prevail (Elbein *et al*, 1990). Hence, following kifunensine treatment, glycoproteins such as N-cadherin and SPPL2a become sensitive to Endo H hydrolysis (Fig. 4.21b). Moreover, it was also examined whether the ER-resident, glycosylated FVenv is affected by SPPL3 over-expression. In line with the earlier observations, FVenv wild-type was found to be Endo H-sensitive and its molecular weight was unchanged in cells expressing exogenous SPPL3 (Fig. 4.22). In cells expressing the ER retention signal

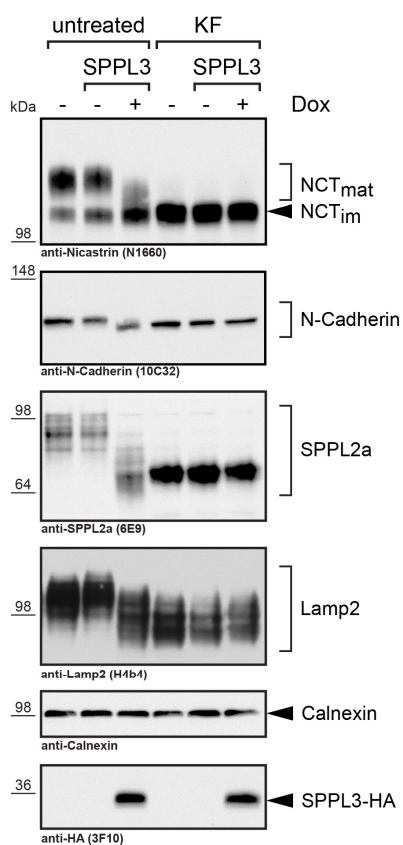
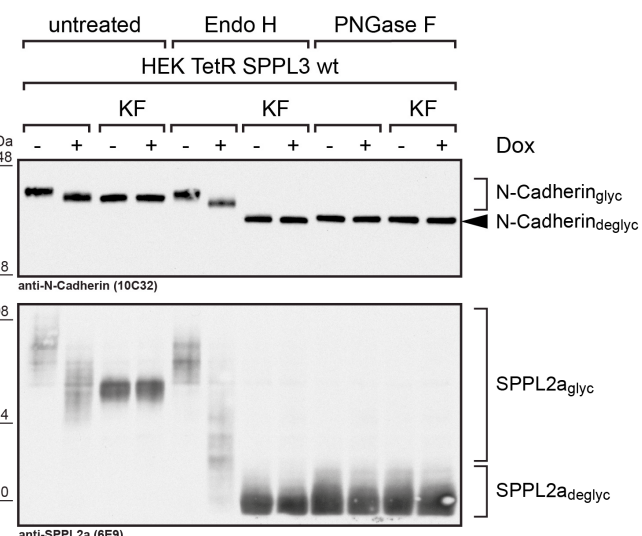
a**b**

Fig. 4.21: Kifunensine treatment of HEK293 cells over-expressing SPPL3. Lysates of HEK TetR cells as well as uninduced (-) and doxycycline-induced (+) HEK TetR SPPL3 wild-type cells (SPPL3) were examined for changes in glycoprotein molecular weight by SDS-PAGE and Western blot (**a**). SPPL3 expression was induced for 48 h and cells were in parallel treated with 4 µg/ml kifunensine (KF) or were left untreated. Note that kifunensine treatment globally changed the extent of glycosylation as Nicastrin maturation is impaired and N-Cadherin, SPPL2a, and Lamp2 feature a lower molecular weight following treatment. Enzymatic de-glycosylation of cell lysates following kifunensine treatment (**b**). Samples from (**a**) were treated with Endo H or PNGase F prior to electrophoresis to assess for effective kifunensine treatment. Note that following kifunensine treatment N-cadherin and SPPL2a were Endo H-sensitive. glyc, glycosylated glycoprotein species, deglyc, N-de-glycosylated species.

mutant of FVenv, FVenv mut Δ KKXX, however, LP-SU and TM were generated due to cleavage at the PC^* site of the FVenv holoprotein. LP-SU was found to be complexly glycosylated as it was Endo H-resistant and glycosylated LP-SU exhibited a lower molecular weight in cells over-expressing SPPL3 than in control cells. In sum, SPPL3 was shown to profoundly change the degree of N-glycosylation of complexly glycosylated, post-ER localised glycoproteins. This is also in line with the very initial observation that SPPL3 only affected NCT_{mat} and not NCT_{imat}, as only the former species is complexly glycosylated (Leem *et al*, 2002; Yang *et al*, 2002; Edbauer *et al*, 2002).

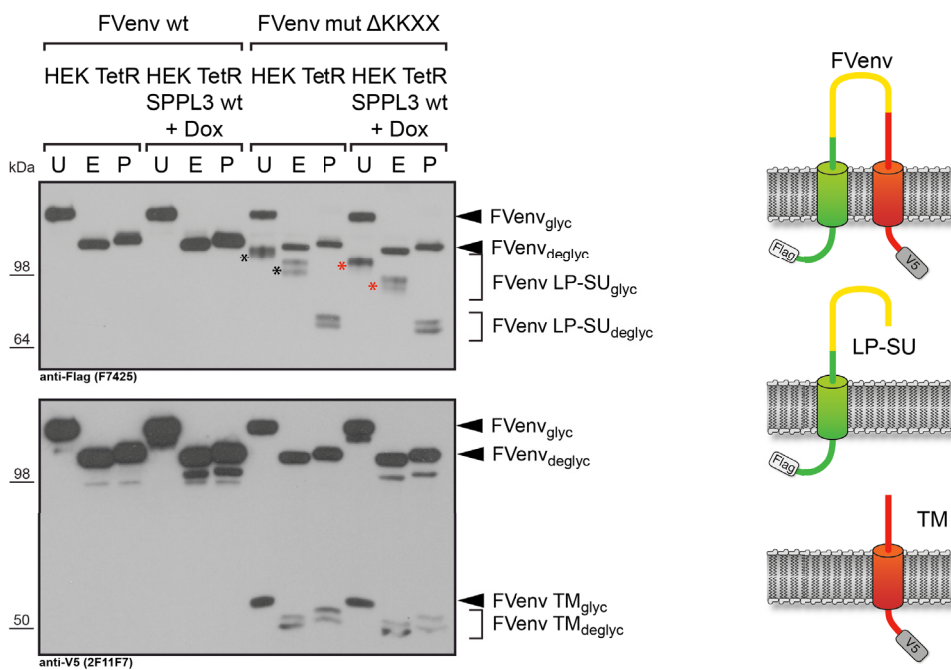


Fig. 4.22: Analysis of FVenv and FVenv mut Δ KKXX in cells over-expressing SPPL3. FVenv wild-type or FVenv mut Δ KKXX were transiently transfected in control HEK293 TetR cells or in cells over-expressing SPPL3. Cell lysates were left untreated (U) or were treated with either Endo H (E) or PNGase F (P) and were subsequently separated by SDS-PAGE and analysed by Western blot. FVenv mut Δ KKXX was endoproteolysed by PC* generating LP-SU (upper panel) and TM (lower panel). ER-resident, Endo H-sensitive full-length FVenv was not affected by SPPL3 over-expression. LP-SU, however, was exported from the ER, thus became Endo H-resistant and was affected by SPPL3 over-expression (compare bands with black asterisks with those with red ones). TM was observed to be Endo H-sensitive, suggesting that it is either not successfully exported from the ER or is not complexly glycosylated. Note that it is not affected by SPPL3 over-expression. glyc, glycosylated glycoprotein species, deglyc, N-deglycosylated species. Schematic illustrations of the respective epitope-tagged FVenv species analysed in this experiment are given on the right.

4.3.4 SPPL3 facilitates secretion of GnT-V

The experiments presented suggest that SPPL3 modulates the extent and nature of cellular Golgi N-glycosylation. Importantly, glycoproteins modified by high-mannose type glycans, such as NCT_{immat}, glycoproteins in cells treated with kifunensine (Fig. 4.21) or ER-resident glycoproteins (Fig. 4.22), are not affected by SPPL3, suggesting that SPPL3 does not interfere with early steps of the N-glycan synthesis. In contrast, glycosylation of Endo H-resistant glycoproteins clearly is altered by SPPL3 over-expression (Fig. 4.20). In sum, these observations suggest that SPPL3 intervenes in the N-glycosylation pathway downstream of α -mannosidase II. Following α -mannosidase II cleavage, N-glycans are subject to extensive branching of the glycan core mediated by GnTs and to elongations and terminal modifications of such branches by various other GTs (see 1.6.2). As most of these enzymes are type II membrane proteins, they represent candidate SPPL3 substrates and, therefore, it was investigated experimentally whether SPPL3 may affect cellular glycosylation by catalysing endoproteolysis of GTs and other GMEs.

β 1,6-N-acetylglucosaminyltransferase V (GnT-V) emerged as very promising substrate candidate. GnT-V is encoded by *MGAT5*. It is involved in GlcNAc branching of complex N-glycans and is crucially required for the formation of tetra-antennary complex glycans (reviewed

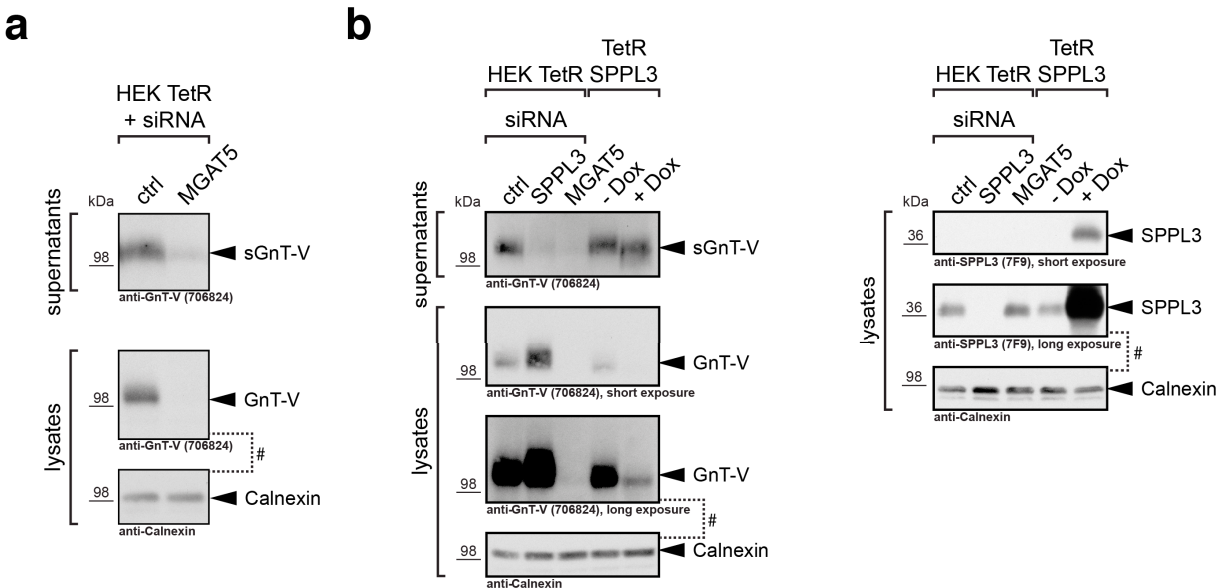


Fig. 4.23: Effects of SPPL3 on secretion and intracellular levels of endogenous GnT-V in HEK293.

(a) HEK293 cells endogenously express and secrete GnT-V which is specifically detected by the anti-GnT-V mAb. GnT-V expression in lysates (bottom panels) and conditioned supernatants (top panel) was examined using a commercial anti-GnT-V antibody. To check for specificity of the mAb, cells were transiently transfected with MGAT5-specific siRNA pools or a non-MGAT5-targeting control (20 nM each). sGnT-V, secreted GnT-V. (b) GnT-V secretion is affected by SPPL3. HEK TetR cells were transiently transfected with indicated siRNA pools or a non-targeting control pool (ctrl) (20 nM each). In parallel, SPPL3 expression was induced in HEK TetR SPPL3 wild-type (wt) cells by supplementing the media with doxycycline (+ Dox). Cell culture supernatants were conditioned for 48 h and GnT-V secretion was monitored by SDS-PAGE and Western blotting. At the same time cellular GnT-V as well as SPPL3 levels were analysed in cell lysates. #, upper blot was redecorated with anti-Calnexin antibody (lower blot) as loading control.

in (Dennis *et al*, 2002)). An anti-GnT-V mAb detected a prominent protein band with a molecular weight of roughly 100 kDa in both cell lysates and in conditioned media of HEK293 cells (Fig. 4.23a). In cells transfected with MGAT5-specific siRNAs, however, levels of this protein were reduced substantiating that the mAb is in fact specific for human GnT-V and that GnT-V is endogenously expressed and secreted in HEK293 cells. Next, it was tested whether reduction of endogenous SPPL3 levels by RNAi or SPPL3 over-expression affected endogenous GnT-V in HEK293 cells (Fig. 4.23b). Similar to cells transfected with MGAT5 siRNA, levels of secreted GnT-V (sGnT-V) in the cell culture supernatant were profoundly reduced by transfection with SPPL3-specific siRNA compared to cells transfected with a non-targeting control. In the cell lysate, however, two alterations were observed upon SPPL3 knock-down: First, GnT-V exhibited a slightly higher molecular weight than in the control sample. This is likely due to the glycosylation changes that accompany a SPPL3 knock-down (see 4.3.2) as GnT-V itself is complexly glycosylated (Kamar *et al*, 2004). Second, GnT-V markedly accumulated in SPPL3 knock-down cells. These observations are in favour of the notion that SPPL3 facilitates shedding and thus secretion of GnT-V. Moreover, over-expression of biologically active SPPL3 resulted in a pronounced reduction in intracellular levels of endogenous GnT-V. sGnT-V appeared to exhibit a slightly lower molecular weight in induced HEK293 TetR SPPL3 wild-type cells than in non-induced cells, yet its level in the conditioned supernatant did not change markedly.

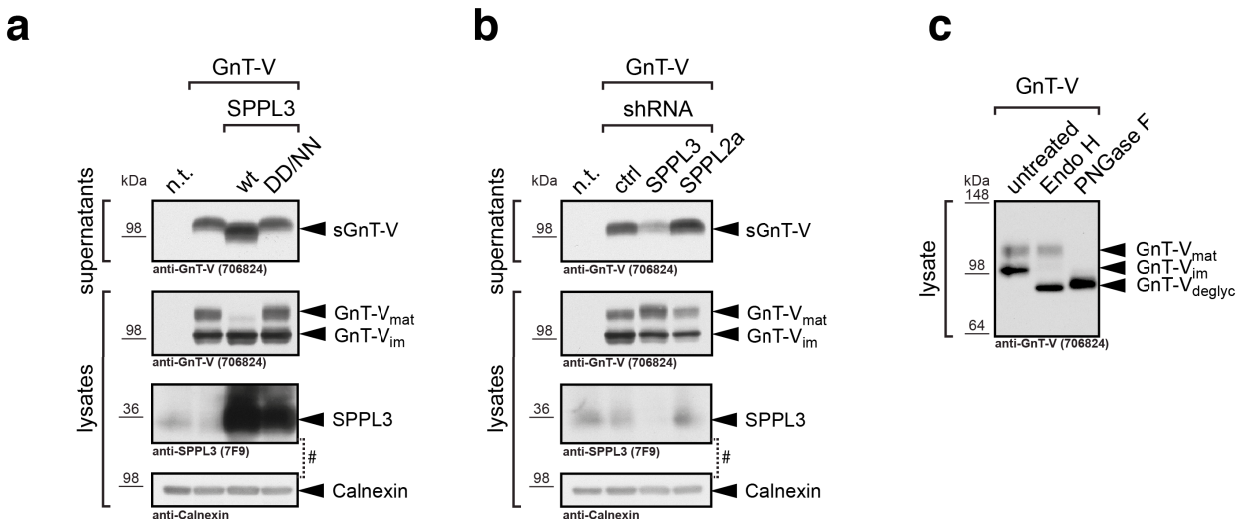


Fig. 4.24: Co-expression of human GnT-V and SPPL3 in HEK293 cells. HEK293 TetR cells were transiently transfected with human GnT-V-encoding expression constructs as indicated and conditioned cell culture supernatants and cell lysates were analysed for GnT-V secretion and expression, respectively, by Western blotting. To examine GnT-V processing by exogenously expressed SPPL3 HEK293 TetR cells were employed that over-express active SPPL3 wild-type (wt) or the active site mutant SPPL3 D200N/D271N (DD/NN) (a). In parallel, GnT-V was analysed in cells stably expressing non-targeting (ctrl), SPPL3- or SPPL2a-specific shRNA pools (b). To differentiate between mature GnT-V ($GnT-V_{mat}$) and immature ($GnT-V_{im}$) lysates of transfected cells were subjected to enzymatic deglycosylation (c). GnT-V_{deglyc}, deglycosylated GnT-V. #, upper blot was redecorated with anti-Calnexin antibody (lower blot) as loading control. (Experimental work presented herein was performed by Ullrike Künzel.)

Similar observations were made when GnT-V was over-expressed in HEK293 cells (Fig. 4.24a & b). Interestingly, unlike endogenous GnT-V, exogenously expressed GnT-V was detected as a double band in lysates of transfected cells. Enzymatic deglycosylation revealed that, whereas the upper GnT-V band was resistant to Endo H treatment, the lower molecular weight GnT-V band was Endo H sensitive (Fig. 4.24c). Hence, this band likely corresponds to immature, ER-resident GnT-V that accumulates following its over-expression. In line with this, alterations in cellular complex N-glycosylation upon co-expression of active SPPL3 or SPPL3 knock-down by RNAi did not affect immature GnT-V, while mature, Endo H-resistant GnT-V was subject to such changes (Fig. 4.24a & b). Moreover, co-expression of GnT-V and active SPPL3 reduced levels of mature GnT-V in cell lysates and at the same time led to a profound accumulation of sGnT-V in conditioned supernatants (Fig. 4.24a). Over-expression of the SPPL3 D200N/D271N mutant, however, was rather associated with slight accumulation of GnT-V in cell lysates. At the same time, sGnT-V was still detectable in amounts comparable to those secreted by untransfected cells and the SPPL3 D200N/D271N mutant did not alter the molecular weight of GnT-V. In cells that have markedly reduced endogenous SPPL3 due to stable expression of a SPPL3-specific shRNA exogenously expressed GnT-V displayed a slightly higher molecular weight (Fig. 4.24b). At the same time, sGnT-V levels in the supernatant of these cells were reduced, while mature GnT-V accumulated inside the cells compared to cells expressing non-targeting or SPPL2a-specific shRNAs. In sum, these observations demonstrate that, in HEK293 cells, SPPL3 selectively facilitates shedding of GnT-V and that this depends on its proteolytic activity.

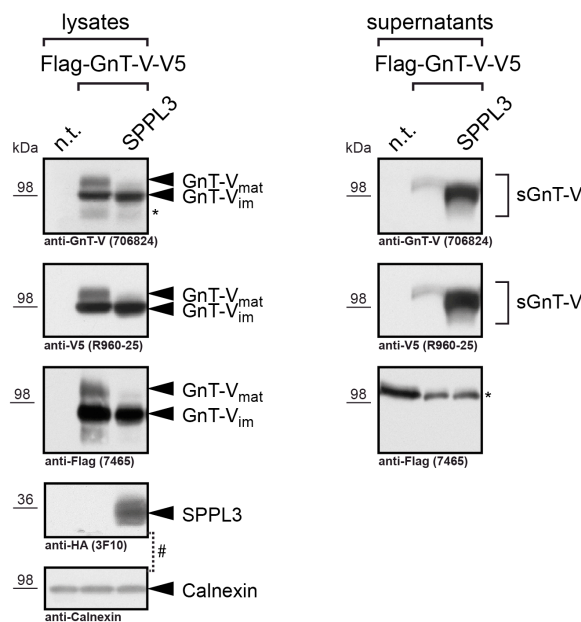


Fig. 4.25: Over-expression of epitope-tagged GnT-V in HEK293 cells. HEK293 TetR cells and HEK293 TetR cells over-expressing SPPL3 (SPPL3) were stably transfected with human N-terminally Flag- and C-terminally V5-tagged GnT-V (Flag-GnT-V-V5)-encoding expression constructs as indicated and conditioned cell culture supernatants (right panel) and cell lysates (left panel) were analysed for GnT-V secretion and expression, respectively. n.t., not transfected, *, unspecific band. #, upper blot was redecorated with anti-Calnexin antibody (lower blot) as loading control. (Experimental work presented in panel a was performed by Ulrike Künzel.)

In order to determine whether GnT-V secretion is - as suggested earlier (Nakahara *et al*, 2006) - a proteolytic process, N-terminally Flag- and C-terminally V5-tagged GnT-V (Flag-GnT-V-V5) was cloned and expressed in HEK293 cells (Fig. 4.25). In lysates of transfected cells immature and mature GnT-V (compare with Fig. 4.24c) were detected using an anti-V5 and an anti-Flag antibody as well as an antibody directed against the GnT-V ectodomain (Fig. 4.25), indicating that these cellular Flag-GnT-V-V5 species correspond to the full-length protein that had not been subject to limited proteolysis. Co-expression of Flag-GnT-V-V5 with SPPL3 led to a reduction of the intracellular mature species as observed earlier with untagged GnT-V. At the same time, over-expressed GnT-V was also detected with anti-V5 and anti-GnT-V antibodies in conditioned cell culture supernatants. This secreted GnT-V species was much more abundant (and had a slightly lower molecular weight) in cells over-expressing active SPPL3. Notably, however, sGnT-V generated from Flag-GnT-V-V5 in these cells lacked anti-Flag-reactivity, demonstrating that it had been N-terminally truncated.

Finally, to examine whether SPPL3 similarly impacts GnT-V under physiological conditions, GnT-V levels in immortalised *Spp3*-deficient MEFs were analysed and compared to *Spp3*^{+/+} control cells (Fig. 4.26). In the former intracellular GnT-V levels were strongly increased compared to wild-type MEFs. Moreover, sGnT-V levels in the conditioned supernatants of *Spp3*^{-/-} MEFs were substantially reduced, yet sGnT-V was not completely absent from these samples. These observations support the notion that SPPL3 facilitates GnT-V secretion under physiological conditions.

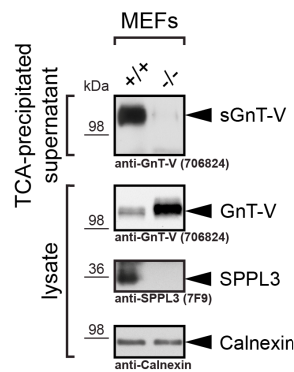


Fig. 4.26: Secretion of endogenous GnT-V in *Spp3*-deficient MEFs. Levels of endogenous GnT-V in TCA-precipitated conditioned supernatants (sGnT-V) and in whole-cell lysates (GnT-V) of *Spp3*-deficient (-/-) and wild-type (+/+) MEFs were analysed by Western blotting.

4.3.5 SPPL3-mediated GnT-V endoproteolysis occurs close to the lipid bilayer boundary

Recent structural studies demonstrated that the active centres of GxGD proteases are positioned within the lipid bilayer plane (Hu *et al*, 2011; Li *et al*, 2013) and in line with this these proteases are expected to cleave their substrates within or close to their respective membrane-spanning regions. To support that secretion of GnT-V is mediated by the intramembrane-cleaving activity of SPPL3, the site(s) at that GnT-V endoproteolysis occurs were determined by MALDI-TOF mass spectrometry (Fig. 4.27). To obtain GnT-V-derived peptidic cleavage products that can be reliably analysed and identified using this method, a strategy similar to the one described in section 4.2.4 was used. A GnT-V-based expression construct, GnT-V NTF, was cloned as depicted in Fig. 4.27a. It encodes the V5-tagged N-terminus of GnT-V (comprising aa 2 to 61 of human GnT-V) including the predicted TMD (residues 14 to 30 (Shoreibah *et al*, 1993)) but lacks most of GnT-V's ectodomain. At the C-terminus, the protein comprises a Flag epitope tag and terminates with an alanine-proline motif (described earlier, see 4.2.4). Hence, it allowed for immunoprecipitation of secreted cleavage products from conditioned supernatants of cells expressing GnT-V NTF. These immunoprecipitates were then analysed by mass spectrometry.

In immunoprecipitates from conditioned supernatants of GnT-V NTF-transfected HEK293 TetR cells and of non-induced control cells five unique peaks were observed (Fig. 4.27b). Their molecular weight corresponded well with the molecular weight of peptides generated by endoproteolysis of GnT-V between residues Met 28 and Thr 33 (Fig. 4.27a & c). The most prominent peaks corresponded to peptides commencing with Leu 29 and His 31, respectively, whereas only minor amounts of the three additional peptides (commencing with Leu 30, Phe 32 and Thr 33, respectively) were observed. These peaks were not detected in immunoprecipitates from supernatant of non-transfected cells proving that they are genuine cleavage products of GnT-V NTF. While co-expression of the inactive SPPL3 mutant did not affect the peak intensities, all five cleavage products appeared to be more abundant in supernatants collected from cells over-expressing SPPL3 wild-type (Fig. 4.27b). The peptide-to-peptide ratios, however, remained largely unaltered. Notably, the detected peptides originate in a stretch of GnT-V that is predicted to lie at the interface of the lipid bilayer and the luminal or extracellular space (Fig. 27a). These cleavage sites are likely not accessible to conventional proteases and it

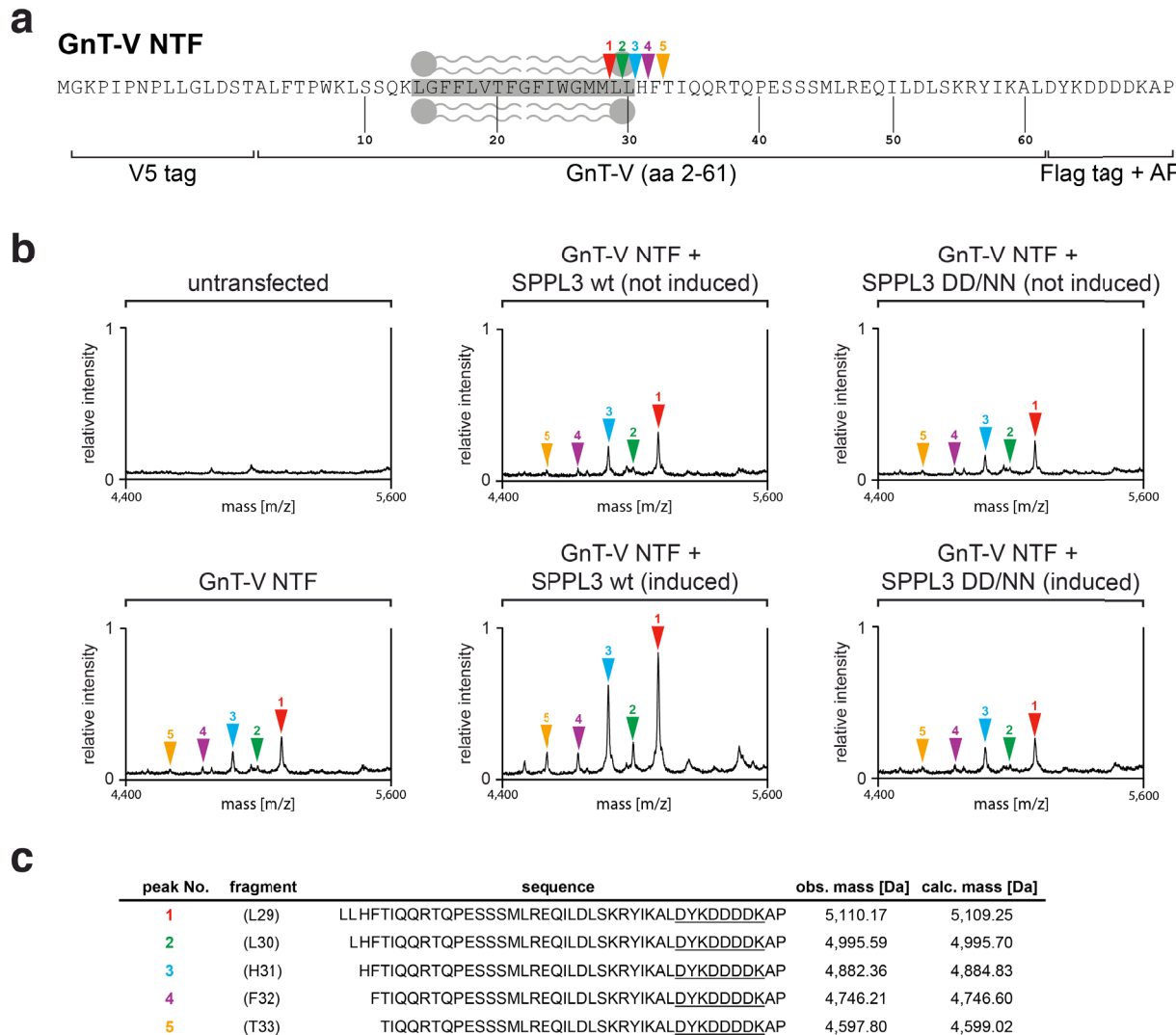


Fig. 4.27: Identification of GnT-V cleavage sites. (a) Schematic overview of GnT-V NTF. The encoded protein is tagged with a V5 epitope tag following its initiator methionine. It comprises amino acids 2 to 61 of the human GnT-V protein including its predicted TMD (grey background sketch). TMD prediction is based on the Uniprot annotation of human GnT-V (entry Q09328, version 119, May 14, 2014). A C-terminal Ala-Pro motif suppresses degradation by carboxypeptidases and the Flag tag allows for affinity purification of cleavage products from cell culture supernatants. Peptides detected experimentally are labelled with coloured arrowheads as in **b** and **c**. (b) Analysis of Flag immunoprecipitates by MALDI-TOF mass spectrometry. anti-Flag immunoprecipitates from conditioned supernatants of HEK293 cells (left) as well as cells over-expressing SPPL3 wild-type (wt, middle) or D200N/D271N (DD/NN, right) upon doxycycline induction (induced) were analysed by mass spectrometry using the ACTH 7 to 38 peptide as reference. Unique peaks are labelled with coloured arrowheads. (c) Peak assignment. Peaks observed and labelled in **b** are assigned to GnT-V NTF-derived peptides according to their observed mass (obs. mass). Peaks are colour-coded and correspond to arrowheads in **a** and **b**. calc. mass, calculated mass. (d) Expression control of transfected GnT-V NTF and doxycycline (Dox)-induced SPPL3 over-expression. Cells lysates were analysed by SDS-PAGE and Western blotting. Calnexin was used as loading control. (Mass spectrometry measurement of samples used here was performed by Dr. Akio Fukumori.)

is therefore well conceivable that cleavage is mediated by an I-CLIP. Hence, the identification of the GnT-V cleavage sites at the TMD boundary strongly corroborates that the five peptides observed constitute cleavage products generated by GnT-V endoproteolysis mediated directly by SPPL3.

4.3.6 GnT-V is not a γ -secretase substrate

An earlier study reported that secreted GnT-V is generated by γ -secretase-mediated intramembrane cleavage (Nakahara *et al*, 2006). This, however, is incompatible with the apparent selectivity of γ -secretase for type I transmembrane protein substrates (Haapasalo & Kovacs, 2011) and also contrasts with the findings presented here (see 4.3.4 & 4.3.5). To validate those previous observations, HEK293 TetR cells were treated with two structurally distinct GSIs and secretion of endogenous GnT-V was monitored (Fig. 4.28a). At the same time, proteolytic processing of endogenous APP by γ -secretase was analysed to ensure that inhibitor treatment was effective. At a final concentration of 10 μ M, DAPT potently inhibited APP intramembrane proteolysis resulting in a strong decrease in A β secretion and a concomitant accumulation of APP CTFs (Fig. 4.28a, lower panels), while APP full-length levels were unaffected. The effect of DAPT on APP intramembrane proteolysis was clearly concentration-dependent and at a concentration of 0.1 μ M DAPT treatment did not result in APP CTF

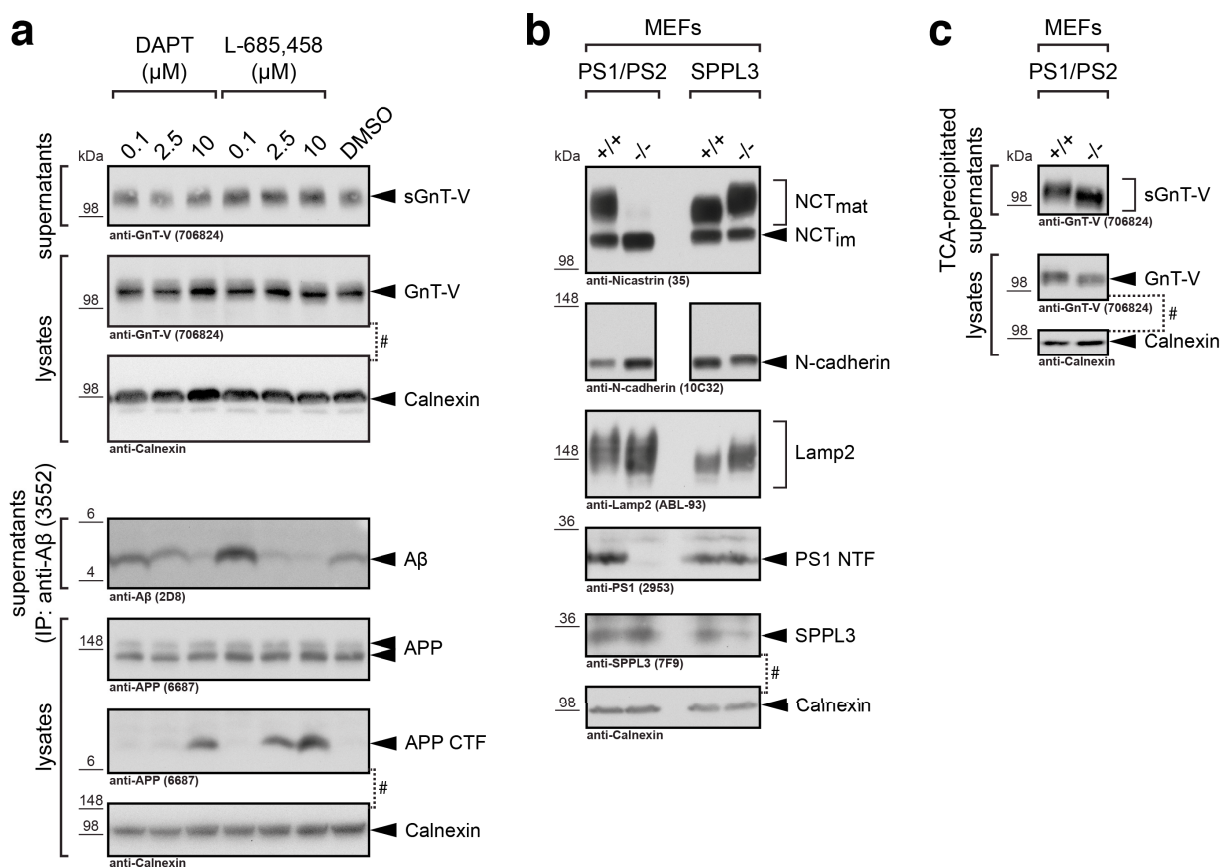


Fig. 4.28: Impact of loss of γ -secretase activity on GnT-V secretion and on cellular N-glycosylation. (a) Pharmacological inhibition of γ -secretase activity. HEK293 TetR cells were treated with indicated concentrations of DAPT, L-685,458 or with vehicle only (DMSO). Levels of secreted GnT-V (sGnT-V) in conditioned supernatants and cellular GnT-V in whole-cell lysates were analysed by Western blotting. To control for efficient inhibition of cellular γ -secretase activity, APP processing was analysed. To this end, A β was immunoprecipitated from conditioned supernatants. Levels of full-length APP and APP C-terminal fragments (CTF) were examined in cell lysates. (b) Electrophoretic mobility of endogenous glycoproteins was assessed by SDS-PAGE and Western blotting in lysates of PS1/PS2-deficient (-/-) and *Spp3*-deficient (-/-) MEFs and the respective wild-type controls (+/+). PS1/PS2-deficient MEFs lack PS1 N-terminal fragments (NTF) and mature Nicastrin. (c) GnT-V levels in TCA-precipitated conditioned supernatants and lysates of PS1/PS2-deficient cells. Samples used in (c) were the same used in (b), hence see (b) for presenilin expression controls. #, upper blot was redecorated with anti-Calnexin antibody (lower blot) as loading control.

accumulation and A β production was even stronger than in vehicle-treated cells, an effect that has already been previously observed for a number of GSIs (discussed in (Shen & Kelleher, 2007)). L-685,458 inhibited APP processing in a similar fashion, yet was not as potent an inhibitor as DAPT (Fig. 4.28a). Importantly, neither compound had a strong and concentration-dependent effect on secretion of endogenous GnT-V as both levels of cellular and sGnT-V were not markedly altered following inhibitor treatment (Fig. 4.28a, top panels). Assuming that γ -secretase endoproteolysed GnT-V, resulting in its premature secretion and, thus, interfering with its cellular function as postulated (Nakahara *et al*, 2006), it had to be expected that loss of γ -secretase activity leads to an intracellular accumulation of GnT-V and, hence, a hyperglycosylation in γ -secretase-deficient cells. To test this, electrophoretic mobility of endogenous glycoproteins in PS1/PS2-deficient MEFs that lack γ -secretase activity (Herreman *et al*, 2003) was analysed by SDS-PAGE and Western blotting and directly compared to *Sppl3*^{-/-} MEFs (Fig. 4.28b). As observed before (Fig. 4.16), *Sppl3*-deficient MEFs presented with an hypoglycosylation phenotype that became apparent when analysing the running behaviour of NCT_{mat}, N-cadherin and Lamp2 (Fig. 4.28b). In contrast, loss of γ -secretase activity was not associated with such an effect in PS1/PS2-deficient MEFs (Fig. 4.28b), arguing against GnT-V secretion being mediated by the γ -secretase complex. To finally exclude any direct effect of γ -secretase on GnT-V secretion, GnT-V levels in lysates and conditioned supernatants of PS1/PS2-deficient and wild-type control MEFs were analysed (Fig. 4.28c). Contrasting starkly with the results reported by Nakahara *et al*. (Nakahara *et al*, 2006), substantial amounts of GnT-V were secreted from PS1/PS2^{-/-} cells. *Sppl3*-deficiency in MEFs, however, was associated with almost complete loss of GnT-V secretion (Fig. 4.26). Collectively, these observations clearly disprove the assumption that γ -secretase facilitates GnT-V secretion.

4.3.7 SPPL3 modulates cellular GnT-V activity

The above presented experimental evidence substantiates that SPPL3 facilitates GnT-V secretion in a manner that relies on its proteolytic activity. Therefore, it was addressed whether SPPL3-induced alterations in cellular GnT-V levels ultimately lead to changes in cellular GnT-V activity and whether this could explain the phenotypic observations made *in vivo* and in cell culture (see 4.3.3). GnT-V is fundamentally required for the production of highly branched complex glycans (Sears & Wong, 1998; Schachter, 1991; Dennis *et al*, 2002; Stanley *et al*, 2009). More specifically, GnT-V catalyses the β 1,6-glycosidic addition of GlcNAc to the α 1,6-linked core mannose residue of N-glycans (Cummings *et al*, 1982). To directly assess whether glycoproteins synthesised in cells over-expressing active SPPL3 exhibit any alterations in the abundance of glycan structures formed by GnT-V activity, the leucoagglutinin PHA-L, a plant lectin from *Phaseolus vulgaris*, was used to analyse N-glycans. PHA-L preferentially binds the Gal β 1,4GlcNAc β 1,6[Gal β 1,4GlcNAc β 1,2]Man moiety in complex N-glycans (Cummings & Kornfeld, 1982). Thus, its binding motif contains the GlcNAc β 1,6Man product of GnT-V activity, and cell lines that lack normal GnT-V activity are resistant to PHA-L-mediated agglutination (Cummings *et al*, 1982; Stanley *et al*, 1975; Chaney *et al*, 1989). Nicastin N-glycosylation was analysed following its immunoprecipitation from HEK293 cell lysates by Western and lectin blotting (Fig. 4.29). As control, hybrid and complex N-glycosylation was blocked by kifunensine

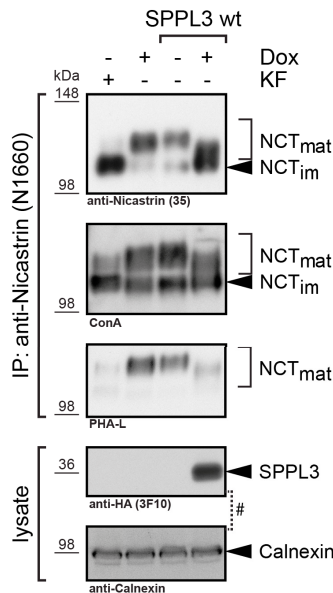


Fig. 4.29: Analysis of lectin binding to Nicastrin from cells over-expressing SPPL3. Endogenous Nicastrin was immunoprecipitated (IP) from lysates of either non-transfected HEK293 TetR cells or HEK293 TetR cells stably expressing SPPL3 wild-type upon doxycycline treatment (+ Dox). Immunoprecipitates were probed using an anti-Nicastrin mAb (first panel) or the lectins ConA (second panel) and PHA-L (third panel), respectively. To control for SPPL3 over-expression, lysates were directly analysed by Western blotting (bottommost panels). Kifunensine treatment (+ KF) was used to control for lectin binding specificity.

treatment. As expected, kifunensine treatment interfered with Nicastrin maturation and hardly any NCT_{mat} was observed in the anti-Nicastrin Western blot of these immunoprecipitates. Nicastrin maturation was likewise affected by SPPL3 over-expression which led to a reduction in the molecular weight of NCT_{mat}. Analysis of immunoprecipitated Nicastrin by lectin staining revealed that PHA-L preferentially bound complexly glycosylated NCT_{mat} and only exhibited weak reactivity towards NCT_{immat}. As expected, PHA-L reactivity was markedly reduced in cells treated with kifunensine. Interestingly, in cells expressing exogenous active SPPL3, PHA-L reactivity was also reduced supporting the notion that SPPL3 promotes GnT-V release and thus interferes with the generation of GlcNAc β 1,6[GlcNAc β 1,4]Man-modified glycans. To test whether alterations in lectin binding observed are specific for PHA-L, reactivity of Nicastrin glycans with Concanavalin A (Con A) was monitored in parallel. Con A has broad reactivity towards mannose-containing glycans and binds high mannose glycans with high affinity, while complex and hybrid glycans can also be bound yet with lower affinity (Cummings & Etzler, 2009). SPPL3 over-expression failed to interfere with Con A binding. Taken together, enhanced GnT-V secretion facilitated by SPPL3 over-expression results in decreased cellular GnT-V activity and, thus, alters the composition of cellular complex glycans.

4.3.8 Impact of SPPL3 on cellular N-glycosylation is not solely due to effects on GnT-V

As SPPL3 impacts cellular GnT-V activity (Fig. 4.29), it is conceivable that the alterations in cellular N-glycosylation observed upon exogenous expression of proteolytically active SPPL3 are due to SPPL3-mediated endoproteolysis of GnT-V (Fig. 4.19), since impaired intracellular GnT-V activity and consequently a less extensive GlcNAc branching associated with SPPL3 over-expression (Fig. 4.29) could explain the hypoglycosylation phenotype observed following

SPPL3 over-expression (Fig. 4.20). Assuming that SPPL3-induced alterations in N-glycosylation exclusively depend on proteolytic processing of GnT-V, SPPL3 over-expression should phenocopy the alterations in N-glycosylation associated with loss of cellular *MGAT5* expression. As expected, GnT-V expression levels were reduced in HEK293 cells transiently transfected with a siRNA pool targeting *MGAT5* (Fig. 4.30). This came along with alterations in glycoprotein running behaviour. More precisely, NCT_{mat}, N-cadherin, SPPL2a and Lamp2 had a slightly lower molecular weight in these cells compared to cells transfected with non-targeting siRNAs (Fig. 4.30), indicating a less pronounced N-glycosylation or hypoglycosylation that most likely is due to impaired GlcNAc branching. As observed earlier, SPPL3 over-expression similarly shifted endogenous glycoproteins to a lower molecular weight (Fig. 4.30). Importantly, however, the molecular weight alteration was much stronger in cells over-expressing SPPL3 than in cells transfected with *MGAT5*-specific siRNAs, even though low GnT-V expression levels were still apparent in the former. This clearly shows that SPPL3 over-expression does not phenocopy the *MGAT5* knock-down situation in HEK293 cells and that SPPL3 over-expression results in glycan structure alterations that are not restricted to mere GlcNAc branching. This suggests that SPPL3 may also affect other enzymes involved in cellular N-glycan biosynthesis, e.g. other GTs or GMEs apart from GnT-V.

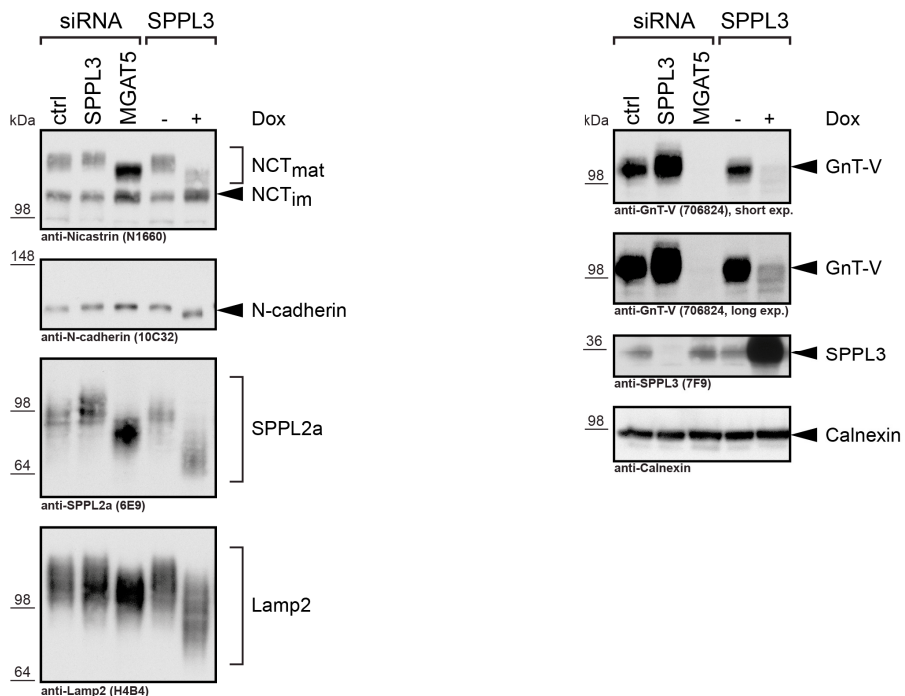
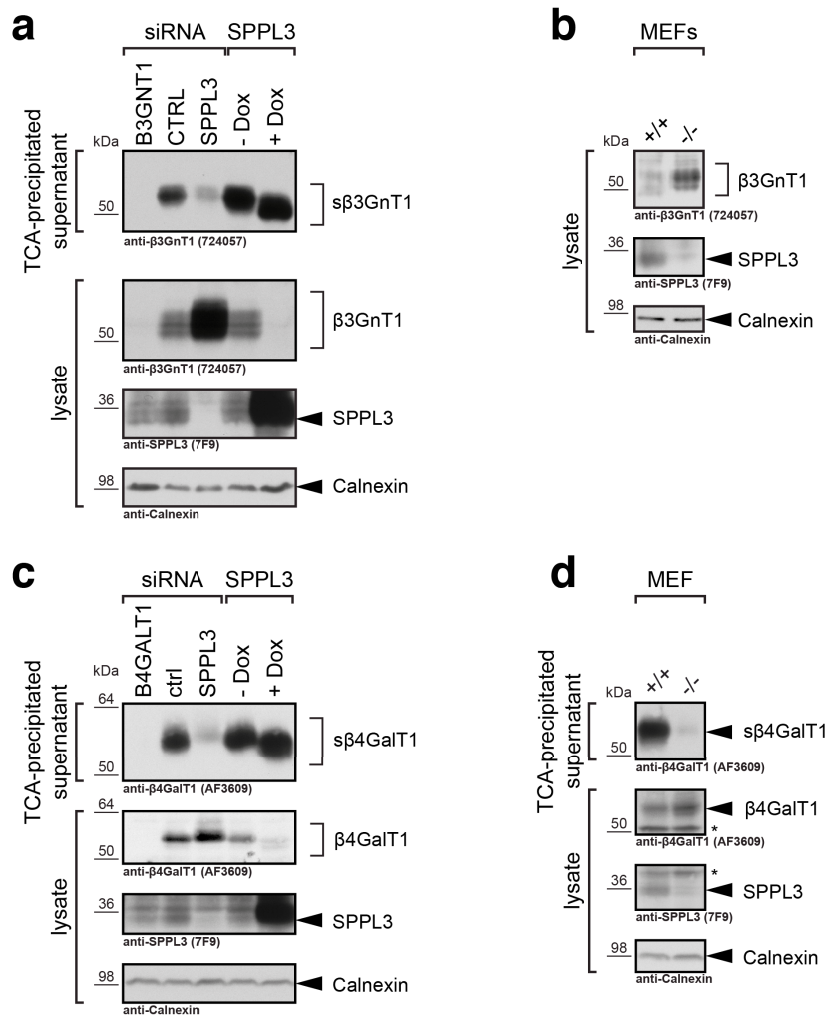


Fig. 4.30: Comparison of alterations in cellular N-glycosylation caused by SPPL3 over-expression and *MGAT5* siRNA transfection. Endogenous cellular glycoproteins (left panels) were analysed by SDS-PAGE and Western blotting in lysates of HEK293 TetR cells transiently transfected with siRNA pools (20 μ M each) directed against SPPL3 and *MGAT5*, respectively, and of cells that over-expressed SPPL3 following induction with doxycycline (+ Dox). In parallel, SPPL3 and GnT-V expression levels were monitored (right panels). Note that, even though residual GnT-V expression is higher following SPPL3 over-expression, the alteration in glycoprotein running behaviour is more pronounced in this condition than in cells transfected with *MGAT5* siRNAs.

4.3.9 SPPL3 facilitates β 3GnT1 and β 4GalT1 secretion

β 1,3 N-acetylglucosaminyltransferase 1 (β 3GnT1, gene name: *B3GNT1*) catalyses the formation of a β 1,3 bond between a GlcNAc and a galactose residue, the latter being within a Gal β 1,4GlcNAc motif, a motif frequently found on N-glycans (Sasaki *et al*, 1997). In HEK293 TetR cells, alterations in SPPL3 expression levels affected intracellular β 3GnT1 levels as well as the secretion of soluble β 3GnT1 (s β 3GnT1) in a manner that is reminiscent of SPPL3's effects on GnT-V levels and GnT-V secretion. Endogenous β 3GnT1 was detected as a roughly 55 kDa protein in cell lysates of HEK293 TetR cells (Fig. 4.31a). In addition, s β 3GnT1 was detected in TCA-precipitated conditioned cell culture supernatants. Signals for both protein species were diminished following transient transfection of a *B3GNT1*-targeting siRNA pool indicating that the mAb employed specifically detected β 3GnT1. Following SPPL3 knock-down, intracellular β 3GnT1 accumulated substantially and less s β 3GnT1 was secreted. Over-expression of catalytically active SPPL3 reduced intracellular β 3GnT1 levels but s β 3GnT1 was only slightly more abundant in the supernatant of SPPL3 over-expressing cells compared to non-induced control cells. β 3GnT1 bears two potential N-glycosylation sites (Sasaki *et al*, 1997) and, as a Golgi-resident enzyme (Buyssse *et al*, 2013), it is likely complexly glycosylated itself, and, accordingly, in addition to changes in β 3GnT1 levels, alterations in SPPL3 expression were accompanied with slight changes in β 3GnT1 running behaviour (Fig. 4.31a). SPPL3 knock-down, for instance, resulted in β 3GnT1 hyperglycosylation whereas SPPL3 over-expression was accompanied by a hypoglycosylation of s β 3GnT1. Next, β 3GnT1 levels in *Spp3*^{-/-} MEFs were analysed (Fig. 4.31b). β 3GnT1 was more abundant in MEFs deficient in *Spp3* than in control *Spp3*^{+/+} cells. This suggests that β 3GnT1 secretion is reduced in *Spp3*^{-/-} MEFs due to the lack of the protease facilitating its proteolysis and hence the intact holoprotein accumulates. s β 3GnT1 could however not be detected in TCA-precipitated supernatants of these cells and accordingly it could not be directly examined whether impaired β 3GnT1 in fact accounts for its intracellular accumulation.

In a manner similar to GnT-V and β 3GnT1, secretion of β 1,4 galactosyltransferase 1 (β 4GalT1, gene name: *B4GALT1*), another Golgi GT, in HEK293 TetR cells was also affected by SPPL3 (Fig. 4.31c). In immunoblots of TCA-precipitated conditioned cell culture supernatants of HEK293 cells, an antiserum specifically detected constitutively secreted β 4GalT1 (s β 4GalT1) which was absent from supernatants of cells transfected with *B4GALT1*-targeting siRNA. SPPL3 knockdown led to a marked reduction in β 4GalT1 secretion. In contrast, SPPL3 over-expression did not alter s β 4GalT1 levels but s β 4GalT1 was shifted to a slightly lower molecular weight, hence also s β 4GalT1 was hypoglycosylated under these conditions. SPPL3 also affected intracellular β 4GalT1 protein levels as assessed by immunoblotting of cell lysates (Fig. 4.31c). Transfection of SPPL3-targeting siRNAs resulted in an accumulation of intracellular β 4GalT1 and at the same time β 4GalT1 displayed signs of hyperglycosylation as it exhibited a slightly lower electrophoretic mobility than β 4GalT1 in control cells. Moreover, SPPL3 over-expression was accompanied by a pronounced reduction in intracellular β 4GalT1 levels. Finally, β 4GalT1 levels were examined in *Spp3*^{-/-} MEFs (Fig. 4.31c). Also in wild-type MEFs s β 4GalT1 was readily detectable in Western blots of TCA-precipitated supernatants. In cells lacking intact



Sppl3, however, generation of s β 4GalT1 was almost completely abolished and at the same time the β 4GalT1 holoprotein was found to be more abundant in lysates of these cells compared to wild-type control cells.

Collectively, the Golgi GTs β 3GnT1 and β 4GalT1 behaved essentially identically to GnT-V as their secretion was also impaired following SPPL3 knock-down or *Sppl3* knock-out and their intracellular levels were reduced following SPPL3 over-expression, suggesting that both GTs are likely additional novel SPPL3 substrates.

4.4 SPPL3 facilitates secretion of type II membrane protein ectodomains

FVenv was identified as the first SPPL3 substrate (see 4.1) and it was subsequently found that SPPL3-mediated intramembrane cleavage of FVenv is independent of prior membrane-proximal pre-cleavage or shedding (see 4.2.1). In light of these observations it is postulated that SPPL3 in fact could act on full-length protein substrates and, thus would facilitate proteolytic release or shedding of type II membrane protein ectodomains. This hypothesis receives strong support from the finding that SPPL3 facilitates proteolytic secretion of GnT-V and β 3GnT1 (see 4.3.4) under physiological conditions. To further corroborate these findings a proteome-wide analysis was performed to define the SPPL3 degradome in more detail.

4.4.1 SPECS analysis identifies new potential SPPL3 substrates

Numerous - though not all - secreted proteins are glycoproteins and are post-translationally modified by *de novo* assembled N- and O-glycans (see 1.6). The cellular secretome comprises proteins that are either directly synthesised as soluble luminal factors and are subsequently secreted by exocytosis or, alternatively, proteins that are derived from membrane-anchored pre-proteins subjected to proteolytic processing. One major challenge when analysing secretomes of cultured cells is to differentiate between *de novo* synthesised cell-derived factors and exogenously added, serum-derived protein factors and to enrich for the former. Kuhn *et al.* successfully achieved this by developing a technique termed secretome protein enrichment with click sugars (SPECS, Fig. 4.32) (Kuhn *et al.*, 2012). In brief, the authors supplemented media with tetraacetyl-N-azidoacetyl-mannosamine (ManAz). This compound is cell-permeable and is intracellularly converted into an azido-modified sialic acid derivative. This, in turn, is incorporated terminally into N- and O-glycans on *de novo* synthesised and secreted proteins and allows for selective biotin-labelling of such proteins by means of copper-free click chemistry. Biotin-conjugated *de novo* synthesised glycoproteins are then purified from cell culture supernatants and subsequently analysed by quantitative mass spectrometry (Fig. 4.32).

Here, this technique was employed to analyse and compare secretomes of HEK293 that express active human SPPL3 upon induction with doxycycline and of non-induced control cells

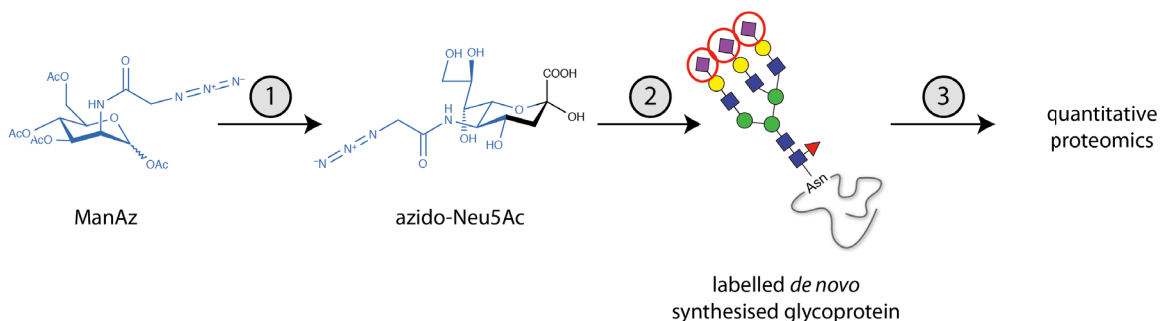


Fig. 4.32: SPECS workflow. Cell culture media are supplemented with peracetylated N-azidoacetyl mannosamine (ManAz). Due to its peracetylation, this compound is membrane permeable, is deacetylated by intracellular esterases and enzymatically converted into an N-azidoacetyl neuraminic acid (azido-Neu5Ac) (**step 1**). This, in turn, is incorporated terminally into glycans (red circles) on *de novo* synthesised secreted proteins by cellular sialyltransferases (**step 2**). Using click chemistry, azido-labelled secreted glycoproteins are conjugated to alkyne-linked biotin and can be purified using streptavidin beads. Proteins purified in this manner are subjected to quantitative mass spectrometry (**step 3**).

(Fig. 4.33). One important consideration has to be taken into account when applying this method to this setup, though. Experiments presented in sections 4.3.2 & 4.3.3 demonstrated that SPPL3 over-expression interferes with cellular N-glycosylation due to its effects on the cellular activity of certain Golgi GTs implicated in N-glycosylation. Therefore, SPPL3 over-expression indirectly leads to alterations, for example in the extent of N-glycan GlcNAc branching. This could theoretically result in reduction of terminal N-glycan sialylation. Therefore,

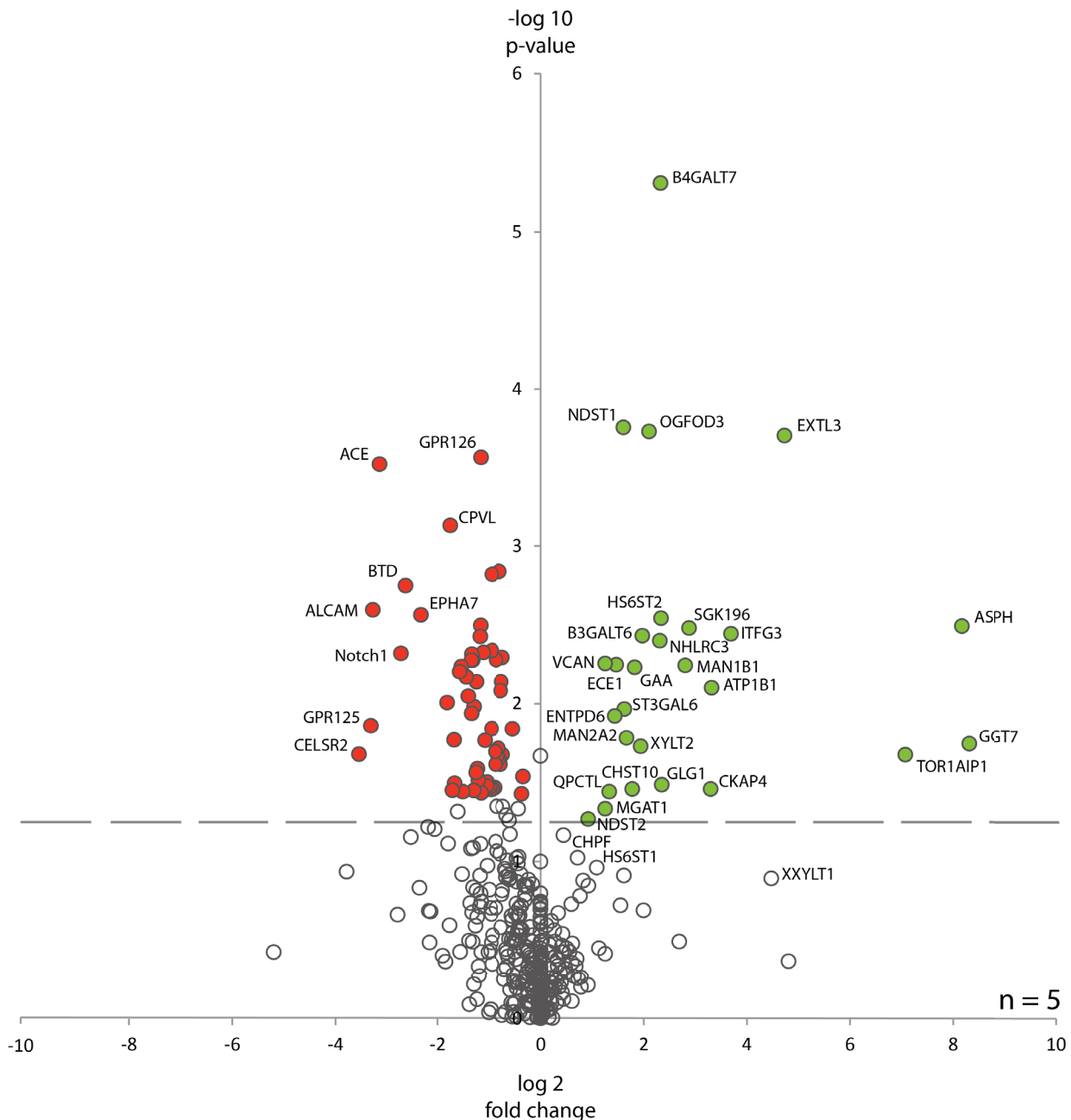


Fig. 4.33: SPECS analysis of HEK293 cells over-expressing active SPPL3. HEK293 TetR SPPL3 wild-type cells were either pre-treated with doxycycline to induce SPPL3 over-expression or left untreated. Labelling was performed by supplementing cell culture media with 50 μ M ManAz for 48 h and samples were subjected to the SPECS workflow. Data are represented in a volcano plot. The y-axis shows the negative decadic logarithm of the p-values for five biological replicates (two-tailed t-test, unequal variance). The relative abundance of respective secreted proteins in cells over-expressing SPPL3 compared to control cells is plotted on the x-axis (binary logarithm of fold change). Green dots represent proteins that are more abundantly secreted following SPPL3 over-expression whereas red dots highlight proteins that are secreted less following SPPL3 over-expression. Gene names are given for selected proteins. (Data depicted in this figure were obtained in close collaboration with Dr. Peer-Hendrik Kuhn, DZNE Munich.)

Tab. 4.2: Candidate SPPL3 substrates identified in HEK293 cells over-expressing active SPPL3 using SPECS. This table lists all proteins that were significantly more secreted in doxycycline-induced HEK293 TetR SPPL3 wt cells compared to non-induced control cells. Gene names and Uniprot IDs are given for the human orthologues. Topology entries are given based on Uniprot annotations or - indicated by an asterisks - by topology predictions, e.g. using Phobius (<http://phobius.sbc.su.se>). (Data summarised in this table were obtained in close collaboration with Dr. Peer-Hendrik Kuhn, DZNE Munich.)

gene name	Uniprot ID	protein name	topology	fold change	p-value
GGT7	Q9UJ14	γ-glutamyltransferase 7	II	317.43	1.799 x 10 ⁻²
ASPH	Q12797	Aspartyl/asparaginyl β-hydroxylase	II	287.58	3.226 x 10 ⁻³
TOR1AIP1	Q5JTV8	Torsin 1A-interacting protein 1	II*	134.34	2.112 x 10 ⁻²
EXTL3	O43909	Exostosin-like 3	II	26.56	1.971 x 10 ⁻⁴
ITFG3	Q9H0X4	Protein ITFG3	II	12.89	3.611 x 10 ⁻³
ATP1B1	P05026	Na ⁺ /K ⁺ -transporting ATPase subunit β-1	II	9.93	7.917 x 10 ⁻³
CKAP4	Q07065	Cytoskeleton-associated protein 4	II	9.82	3.487 x 10 ⁻²
SGK196	Q9H5K3	Probable inactive protein kinase-like protein SgK196	II	7.35	3.314 x 10 ⁻³
MAN1B1	Q9UKM7	ER mannosyl-oligosaccharide 1,2-α-mannosidase	II	6.99	5.714 x 10 ⁻³
GLG1	Q92896	Golgi apparatus protein 1	I	5.09	3.271 x 10 ⁻²
HS6ST2	Q96MM7	Heparan-sulfate 6-O-sulfotransferase 2	II	5.05	2.870 x 10 ⁻³
B4GALT7	Q9UBV7	β1,4-galactosyltransferase 7	II	5.00	4.909 x 10 ⁻⁶
NHLRC3	Q5JS37	NHL repeat-containing protein 3	secreted	4.96	3.996 x 10 ⁻³
OGFOD3	Q6PK18	2-oxoglutarate and iron-dependent oxygenase domain-containing protein 3		4.30	1.858 x 10 ⁻⁴
B3GALT6	Q96L58	β1,3-galactosyltransferase 6	II	3.92	3.708 x 10 ⁻³
XYLT2	Q9H1B5	Xylosyltransferase 2	II	3.84	1.866 x 10 ⁻²
GAA	P10253	Lysosomal α-glucosidase	II*	3.53	5.893 x 10 ⁻³
CHST10	O43529	Carbohydrate sulfotransferase 10	II	3.43	3.485 x 10 ⁻²
MAN2A2	P49641	α-mannosidase 2x	II	3.18	1.652 x 10 ⁻²
ST3GAL6	Q9Y274	Type 2 lactosamine α2,3-sialyltransferase	II	3.08	1.083 x 10 ⁻²
NDST1	P52848	Bifunctional heparan sulfate N-deacetylase/N-sulfotransferase 1	II	3.05	1.751 x 10 ⁻⁴
ECE1	P42892	Endothelin-converting enzyme 1	II	2.76	5.670 x 10 ⁻³
ENTPD6	O75354	Ectonucleoside triphosphate diphosphohydrolase 6	II	2.71	1.198 x 10 ⁻²
QPCTL	Q9NXS2	Glutaminyl-peptide cyclotransferase-like protein	II*	2.51	3.617 x 10 ⁻²
VCAN	P13611	Versican core protein	secreted	2.38	5.571 x 10 ⁻³
MGAT1	P26572	α1,3-mannosyl-glycoprotein 2-β-N-acetylglucosaminyltransferase		2.38	4.638 x 10 ⁻²
NDST2	P52849	Bifunctional heparan sulfate N-deacetylase/N-sulfotransferase 2	II	1.90	5.394 x 10 ⁻²

click sugar labelling could potentially suffer from poor efficiency in cells over-expressing SPPL3 compared to control cells, making absolute quantification of differences in secretomes impossible.

Results from five independent experiments are depicted in Fig. 4.33. The abundance of numerous proteins detected in conditioned supernatants from HEK293 cells was found to be altered significantly following over-expression of catalytically active SPPL3 (red and green dots in Fig. 4.33). Importantly, in most cases secretion of proteins was found to be reduced following SPPL3 over-expression. While it can presently be not completely ruled out that this is due to inhibitory effects of SPPL3 on secretion of these protein factors, this apparent reduction in secretion is most likely due to a reduced efficacy of azido-sialic acid labelling and not due to a genuine reduction in protein secretion (see above). In contrast, a selected number of other proteins were found to be more abundant in conditioned supernatants of HEK293 TetR cells over-expressing SPPL3 than in conditioned supernatants of control cells (Fig. 4.33). A total number of 27 proteins were reliably ($p < 5.4 \times 10^{-2}$) observed to be > 1.9 fold more abundant in supernatants of cells over-expressing SPPL3 (Tab. 4.2 and green dots in Fig. 4.33). The increase in secretion of these hits following SPPL3 over-expression, however, was rather variable. Some proteins, for instance γ -glutamyltransferase 7 and aspartyl-/asparaginyl β -hydroxylase, were > 250 -fold more abundant in conditioned supernatants in cells that over-express SPPL3 than in control cells, while most other hits were only mildly affected and altered two- to five-fold (Tab. 4.2). Interestingly, analysis of candidate substrate hits using the QARIP web server (Ivankov *et al*, 2013) revealed that unique peptides detected experimentally map exclusively to extracellular and/or luminal regions of the hits (Fig. 4.34), indicating that proteins detected in the conditioned supernatants had properly been secreted and did not derive from dead or damaged cells or other experimental flaws. In addition, these extracellular/luminal peptides are in most cases (25 of 27 hits) derived from annotated (or predicted) transmembrane proteins (Fig. 4.35a) and, with a single exception (Golgi apparatus protein 1), are known or predicted to display a type II topology (Tab. 4.2 & Fig. 4.35b). Therefore, a total number 24 novel potential candidate SPPL3 substrates could be identified.

Where available, additional GO information suggests that the majority of these type II transmembrane proteins localises to Golgi membranes, the ER, and/or the plasma membrane (Fig. 4.35c). From a functional perspective, hits include proteins implicated in quite diverse cellular processes, such as enzymes involved in glutathione metabolism like γ -glutamyltransferase 7, the bifunctional Ca^{2+} sensor aspartyl-/asparaginyl β -hydroxylase, the metalloprotease endothelin-converting enzyme 1 that generates the vasoconstrictive peptide hormone endothelin 1, the β -1 subunit of the cell surface Na^+/K^+ ATPase that regulates the number of active Na^+/K^+ ATPase at the cell surface, and several others. Strikingly, however, the majority of candidate SPPL3 substrates identified have GO annotations that link them to carbohydrate metabolism and protein glycosylation (Fig. 4.35d). Seven candidates appear to be involved in GAG biosynthesis (Fig. 4.35e).

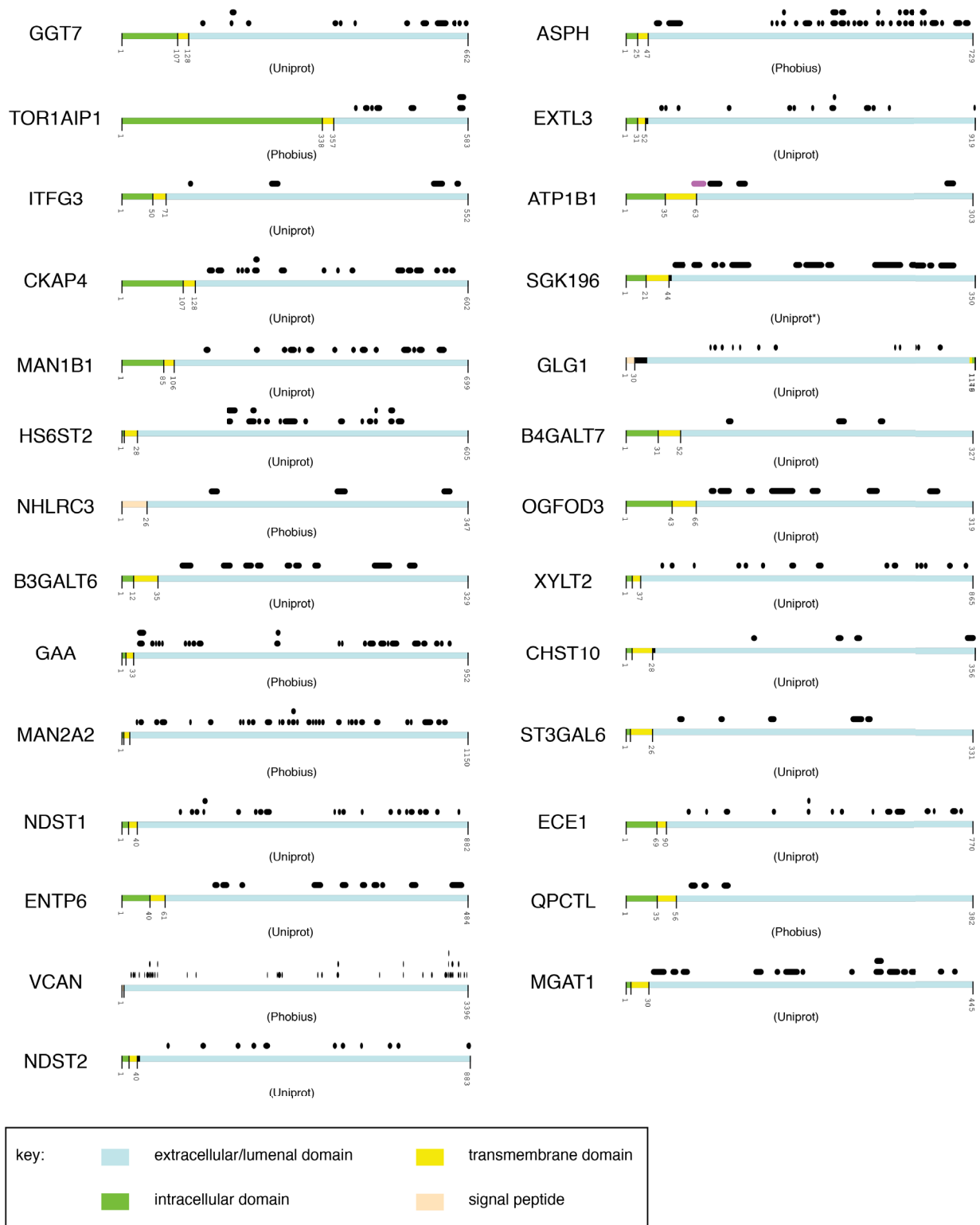


Fig. 4.34: QARIP analysis of tryptic peptides identified using SPECS. SPPL3 candidate substrates (Fig. 4.33 and Tab. 4.2) were analysed using the QARIP web server (Ivankov *et al*, 2013). Protein topology is depicted schematically according to Uniprot annotations or to Phobius predictions as indicated. Tryptic peptides detected experimentally are mapped to the respective candidate substrates (black bars). Note that exclusively peptides derived from the respective proteins extracellular domains were detected. (Data depicted in this figure were obtained in close collaboration with Dr. Peer-Hendrik Kuhn, DZNE Munich.)

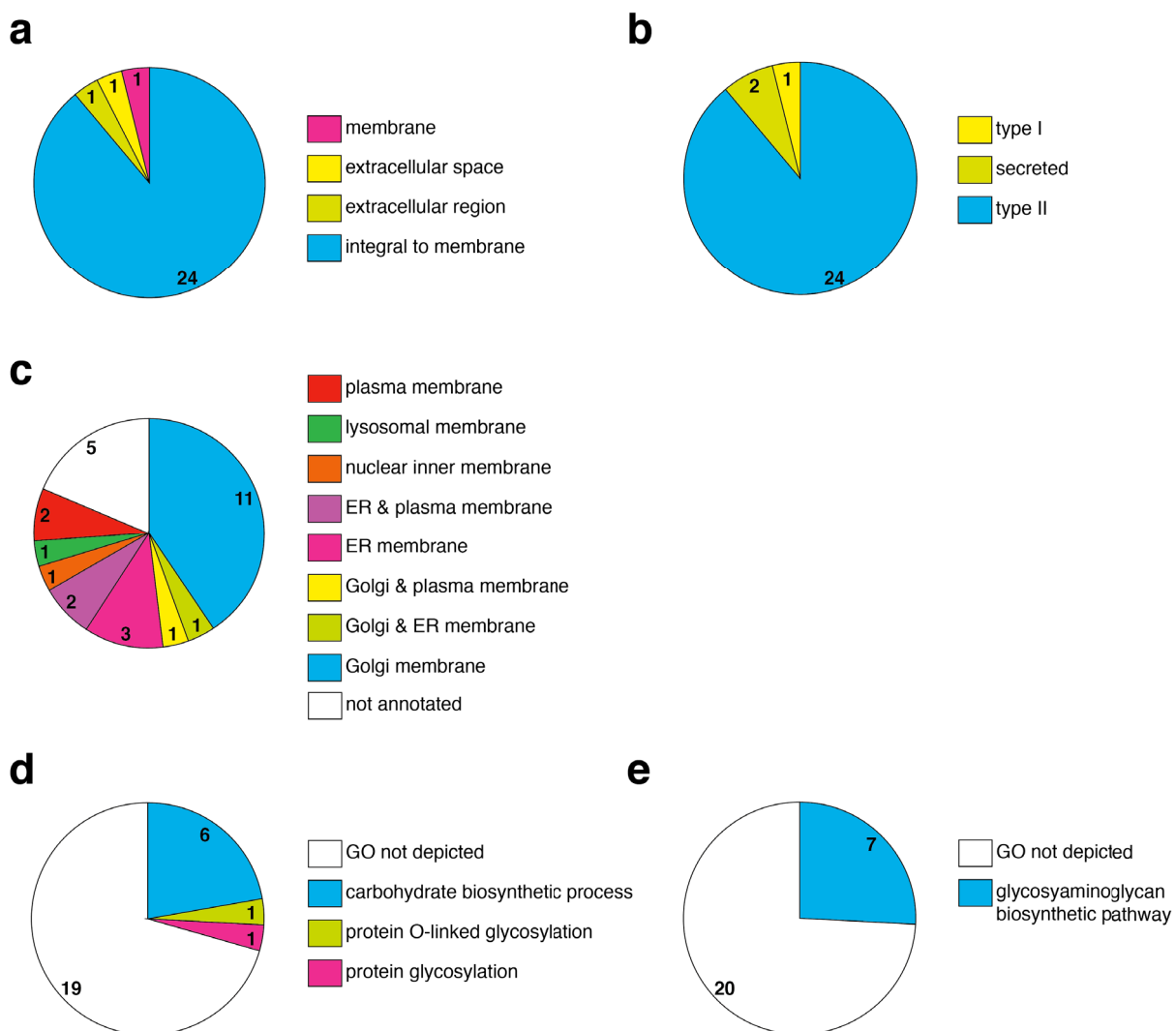


Fig. 4.35: Gene ontology (GO) analysis of candidate SPPL3 substrates. GO (a, c to e) and topology (b) information deposited in Uniprot for candidate SPPL3 substrates identified in HEK293 cells (see Fig. 4.33 and Tab. 4.2 for the hits and the respective entry IDs) are summarised. Subfigures **a** and **c** contain GO "cellular_component" terms concerning membrane integrity and localisation in sub-cellular membranous compartments, respectively. **(b)** depicts the distribution of membrane topology among candidate substrates. **(d)** and **(e)** highlight selected functional annotations regarding glycosylation and carbohydrate mechanism in general and glycosaminoglycan biosynthesis, respectively (GO "biological_process").

4.4.2 Validation of selected newly identified candidate SPPL3 substrates

A major caveat of the method employed to identify novel SPPL3 substrates is that only the abundance of secreted proteins and protein fragments in conditioned cell culture supernatants is assessed. Therefore, it needs to be excluded that alterations in the abundance of these simply relate back to an altered expression of the respective gene due to indirect effects of SPPL3 over-expression. Hence, all candidate SPPL3 substrates identified here (see 4.4.1) require further validation.

To this end, levels of seven candidate SPPL3 substrates in lysates and conditioned supernatants were analysed in conditions of altered SPPL3 expression by Western blotting (Fig. 4.36). These included GTs such as the N-acetylglucosaminyltransferase EXT3 (Fig. 4.36a), the xylosyltransferase XylT2 (Fig. 4.36b) and the galactosyltransferase β 3GalT6 (Fig. 4.36d) and in addition other GMEs like ER Man I (Fig. 4.36c) and the heparan sulphate

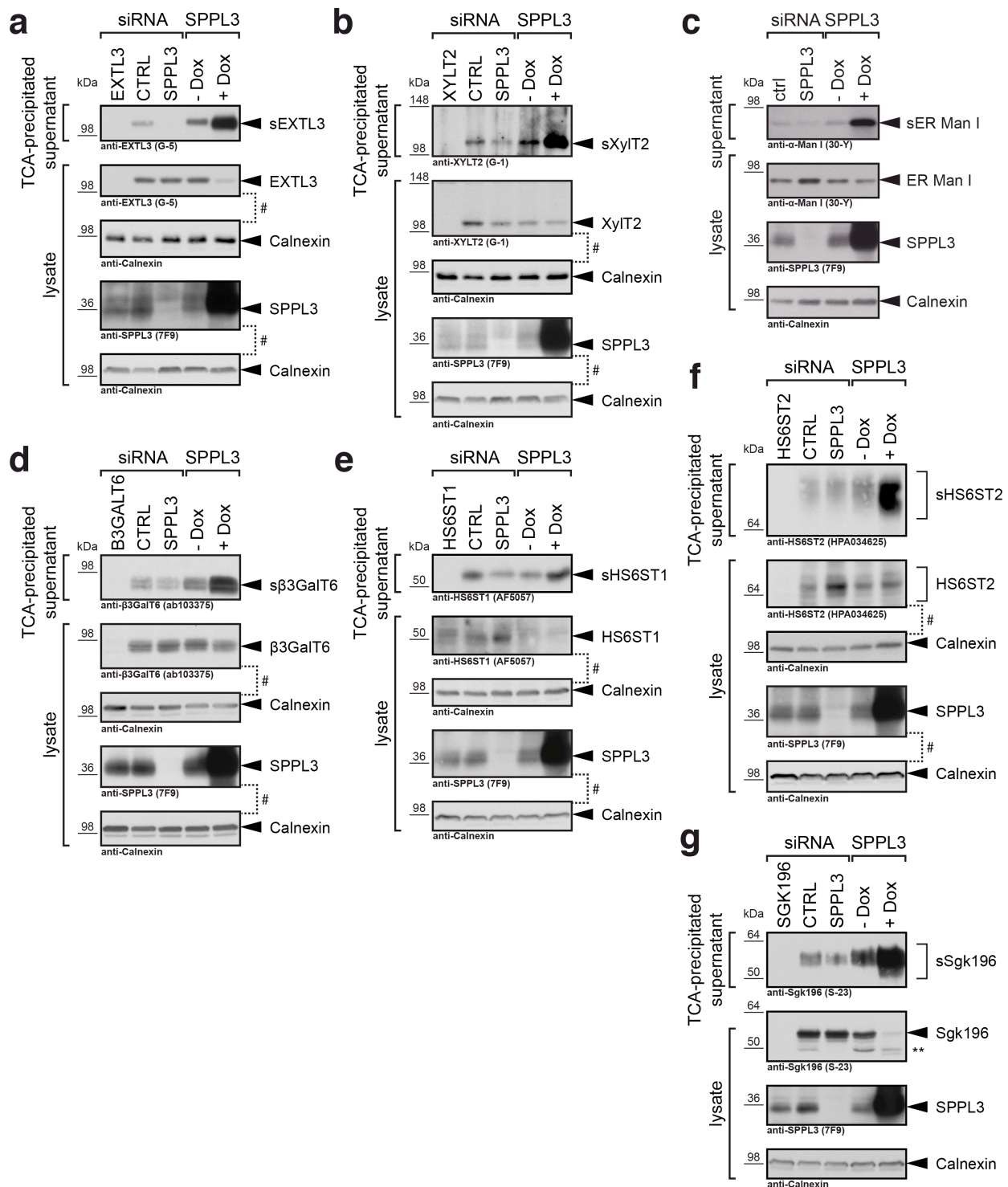


Fig. 4.36: Validation of candidate SPPL3 substrates uncovered by the proteome-wide approach.
 Effects of alterations in SPPL3 expression levels on secreted and intracellular levels of EXTL3 (a), XylT2 (b), ER α-mannosidase I (ER Man I, c), β3GalT6 (d), HS6ST1 (e), HS6ST2 (f) and Sgk196 (g) were monitored. HEK293 TetR cells were transfected with siRNA pools targeting SPPL3 or a non-targeting control siRNA pool (ctrl) (20 nM each). siRNA pools targeting the individual candidate substrates were used to test for specificity of the antibodies used for immunoblotting. In parallel, SPPL3 over-expression was induced by doxycycline treatment (+ Dox) in stably transfected cells. Levels of secreted protein species (sEXTL3, sXylT2, sER Man I, sβ3GalT6, sHS6ST1, sHS6ST2 and sSgk196 respectively) in the TCA-precipitated (a and b, d to g) or crude (c) conditioned supernatant and of the respective holoproteins in whole-cell lysates were analysed by SDS-PAGE and Western blotting. SPPL3 expression levels were similarly analysed. Loaded supernatant samples were normalised to total protein content of cell lysates. #, upper blot was redecorated with anti-Calnexin antibody (lower blot) as loading control. **, Sgk196 fragment(s) of unknown origin.

sulphotransferases HS6ST1 (Fig. 4.36e) and HS6ST2 (Fig. 4.36f) as well as Sgk196 (Fig. 4.36g). All candidate substrates were detected in lysates and conditioned supernatants of HEK293 TetR cells indicating that they are constitutively secreted. Importantly, proteins detected were absent when cells had been transfected with siRNA pools targeting the respective mRNA (Fig. 4.36a & b, d-g, not shown for ER α-Man I), demonstrating that the ectodomain-specific commercial mAbs used for immunoblot detection were specific. For all six candidate substrates secreted species were found to be more abundant in supernatants of cells over-expressing active SPPL3 (Fig. 4.36), confirming the previous observations by SPECS and mass spectrometry. In addition, siRNA-mediated knockdown of SPPL3 expression led to reduced secretion of EXTL3 (Fig. 4.36a), XylT2 (Fig. 4.36b) and HS6ST1 (Fig. 4.36e). Similar to other SPPL3 substrates identified here, intracellular levels of the candidate substrates were likewise affected by alterations in SPPL3 expression levels. EXTL3 (Fig. 4.36a), ER Man I (Fig. 4.36b), HS6ST1 (Fig. 4.36e) and Sgk196 (Fig. 4.36g) for instance were less abundant in cell lysates following SPPL3 over-expression, while ER Man I (Fig. 4.36c), HS6ST1 (Fig. 4.36e) and HS6ST2 (Fig. 4.36f) accumulated intracellularly in cells transfected with SPPL3-targeting siRNA. For Sgk196 (Fig. 4.36g), protein fragments were specifically detected with a Sgk196-specific mAb that displayed a slightly lower molecular weight than the holoprotein. Interestingly, this fragment was reduced in cells transfected with SPPL3-specific siRNA and remained present in SPPL3 over-expressing cells but its nature and its generation is currently unclear.

In sum, this preliminary validation of a selected number of candidate SPPL3 substrates recapitulates the earlier observation that SPPL3 over-expression promotes their secretion. At the same time, the reduction of their respective intracellular levels argues in favour of a SPPL3-dependent proteolytic secretion of these candidate substrates. Moreover, in most cases secretion and/or intracellular levels of these candidate substrates were also changed upon reduction of cellular SPPL3 activity indicating that their proteolytic secretion proceeds in a SPPL3-dependent fashion under physiological conditions. Strikingly, however, these observations made here for the candidate substrates identified using the proteomics approach contrast with the observations made for e.g. GnT-V (see 4.3.4) in a similar experimental setting. Over-expression of SPPL3 for instance reduced intracellular levels of GnT-V much stronger than it did of most of the candidate substrates validated. At the same time, however, secretion of endogenous GnT-V was hardly increased following SPPL3 over-expression whereas the validated candidate substrate were much more efficiently secreted in cells over-expressing proteolytically active SPPL3. This similarly applies to knockdown experiments: Reduced SPPL3 expression for instance impaired secretion of GnT-V and β3GnT1 and at the same time led to an intracellular accumulation of these GTs. Similar effects were observed for the candidate substrates yet they were not as pronounced. Taken together, these experiments support that the candidate SPPL3 substrates identified using the proteomics approach are genuine SPPL3 substrates like e.g. GnT-V, but also indicate that not all SPPL3 substrates in HEK293 cells are endoproteolysed in the very same manner.

5. Discussion

In 2002, the intramembrane protease SPP and its homologues, the SPPLs, were described for the first time (Weihofen *et al*, 2002; Ponting *et al*, 2002; Grigorenko *et al*, 2002). Since then, a number of substrates have been identified that are endoproteolysed by SPP, SPPL2a or SPPL2b *in vitro* or in cultured cells but also *in vivo*. SPPL3, on the other hand, has not been studied in detail. In particular, the physiological function of SPPL3 has remained unclear and to date no physiological substrates have been reported.

Herein, an initial in-depth characterisation of SPPL3 is provided and potential implications of these observations are discussed in the following. First, FVenv is identified as the first SPPL3 substrate (section 5.1) and subsequent detailed analyses of FVenv's intramembrane proteolytic processing by SPPL3 reveal unexpected properties of this protease (section 5.1.5). Second, SPPL3 emerges as a cellular type II membrane protein-selective sheddase as a number of type II membrane proteins are identified as novel SPPL3 substrates in this study and SPPL3 appears to facilitate proteolytic secretion of these substrates' ectodomain (section 5.2). Finally, this study reveals that SPPL3 fundamentally affects cellular N-glycosylation by facilitating proteolytic shedding of Golgi GTs and glycosidases (section 5.3.1). In light of these novel insights, SPPL3's potential physiological functions (section 5.3.2) as well as upcoming questions (section 5.4. & 5.5) will be discussed.

5.1 Identification of FVenv as the first SPPL3 substrate

Based on the meanwhile strongly challenged (Schrul *et al*, 2010; Casso *et al*, 2012) assumption of functional redundancy between SPP and SPPL3 (see 1.4.2.2.3), signal peptides were examined as potential SPPL3 substrates leading to the identification of FVenv, more specifically its N-terminal LP, as first SPPL3 substrate.

5.1.1 FVenv LP: signal peptide or type III membrane protein signal anchor?

N-terminal signal peptides that ensure proper targeting of nascent secretory and membrane proteins to the ER often exhibit no obvious primary sequence homology, but feature a highly conserved modular structure with (i) an N-terminal positively charged n-region, variable in length, (ii) a central hydrophobic h-region, 7 to 15 aa in length, and (iii) a C-terminal polar c-region harbouring the signal peptidase cleavage site (Paetzel *et al*, 2002). In most cases, signal peptides are cleaved off the pre-protein co-translationally by signal peptidase (Paetzel *et al*, 2002). Most liberated signal peptides are short-lived and will be quickly degraded, but some are discussed to be rather stable and to fulfil downstream, so-called post-targeting functions (reviewed in (Kapp *et al*, 2009)).

The N-terminus of the FVenv pre-protein was initially described as such a conventional - albeit rather long - signal peptide and, accordingly, FVenv as a type I membrane protein (Wang & Mulligan, 1999; Lindemann *et al*, 2001). Proteolytic removal of the N-terminus, however, occurs post-translationally as full-length FVenv was detected in Western blots with an antiserum

directed against the N-terminal LP (Lindemann *et al*, 2001). Moreover, it has meanwhile been established that FVenv LP is an integral component of mature virions and is essential for progeny virion egress (Lindemann *et al*, 2001; Wilk *et al*, 2001), likely because it physically interacts with the viral capsid (Wilk *et al*, 2001; Geiselhart *et al*, 2003). Importantly, release of LP from full-length FVenv is not - as initially suspected (Wang & Mulligan, 1999; Lindemann *et al*, 2001) - mediated by signal peptidase but instead by furin- or a furin-like PC (Duda *et al*, 2004; Geiselhart *et al*, 2004). In sum, these observations suggest that the term *signal peptide* is misleading and does not adequately apply to FVenv LP. Instead, FVenv should be considered a type III membrane protein (Lindemann & Rethwilm, 2011) and LP a genuine FVenv subunit that is liberated post-translationally from the holoprotein. The hydrophobic, membrane-spanning stretch in FVenv LP thus represents a conventional type II-oriented TMD that at the same time acts as a type III signal anchor sequence. Such sequences ensure insertion into the ER translocon and anchoring in the membrane (Goder & Spiess, 2001).

5.1.2 FVenv is endoproteolysed by SPPL3 and SPPL2a/SPPL2b

Upon co-expression of FVenv and active human SPPL3 a FVenv-derived ICD(L3) was detected which was absent from cells that co-expressed FVenv and the SPPL3 D271A mutant (Fig. 4.2). Moreover, the SPPL3 D271A mutant co-immunoprecipitated FVenv (Fig. 4.6), i.e. FVenv, and SPPL3 interact physically. Collectively, these data demonstrate that SPPL3 endoproteolyses FVenv and that FVenv is a novel SPPL3 substrate. To date, proteolytic activity of SPPL3 has only been observed using a synthetic peptide based on the bovine prolactin signal peptide (Narayanan *et al*, 2007) or an artificial signal peptide-based fusion protein (Nyborg *et al*, 2006) (discussed in 5.1.5.2). As no epitope tags were introduced into membrane-proximal regions of FVenv and epitope-tagging of FVenv did not interfere with its cellular processing and trafficking (Fig. 4.1), FVenv represents the first authentic SPPL3 substrate identified. It needs to be emphasised, though, that SPPL3-mediated FVenv endoproteolysis was primarily analysed in conditions of SPPL3 over-expression.

While proteolysis also occurs in cells that solely harbour endogenous SPPL3 activity (Fig. 4.10) and seems to follow the same basic principle (see 5.1.5), generation of ICD(L3) under such conditions is not as efficient as e.g. proteolysis of other newly identified SPPL3 substrates such as the GT GnT-V and others. This may well be explained with the differential sub-cellular localisation of these proteins. As a primarily ER-resident protein (Fig. 4.1), only a minor fraction of FVenv will co-localise with endogenous, likely Golgi-resident SPPL3 and consequently ICD(L3) generation is not very efficient. It is, however, conceivable that sub-cellular localisation of over-expressed SPPL3 is not as tightly restricted to the Golgi and, hence, under these conditions FVenv and SPPL3 may be more likely to meet, explaining the efficient ICD(L3) generation under these conditions.

Surprisingly, the data presented here demonstrate that FVenv is also a SPPL2a/SPPL2b substrate: Co-expression of FVenv with active SPPL2a or SPPL2b was similarly accompanied by endoproteolysis of FVenv and generation of ICD(L2). Physical interaction of FVenv LP with an inactive SPPL2b mutant was verified by co-immunoprecipitation (Fig. 4.6). ICD(L2) generated by either SPPL2a or SPPL2b is likely identical in nature (Fig. 4.4b), suggesting that SPPL2a

and SPPL2b endoproteolyse FVenv LP in a similar manner under over-expression conditions. In line with this, SPPL2a and SPPL2b both cleave NTFs of TNF α (Friedmann *et al*, 2006; Fluhrer *et al*, 2006), Bri2 (Martin *et al*, 2008) and CD74 (Schneppenheim *et al*, 2014) in a similar manner when over-expressed suggesting that under these conditions both protease can process the same substrates. In addition, FVenv LP accumulated in cells over-expressing catalytically inactive mutants of SPPL2a or SPPL2b (Fig. 4.3), a phenomenon that had also been observed in previous studies for TNF α (Fluhrer *et al*, 2006; Friedmann *et al*, 2006) and Bri2 (Martin *et al*, 2008) and, in these studies, has been attributed to a possible dominant-negative effect of such mutants on the endogenous SPPL2a or SPPL2b pool, respectively. Importantly, cleavage products (i.e. ICD and C-peptide species) observed following intramembrane proteolysis of FVenv mediated by either SPPL2a/SPPL2b or SPPL3 are not identical as they display a different molecular weight (Fig. 4.4b), suggesting that SPPL2a/SPPL2b and SPPL3 endoproteolyse FVenv at different sites.

The finding that the rather distinct SPP/SPPL family members SPPL2a/SPPL2b and SPPL3 proteolytically process FVenv within or in the vicinity of its first, type II-oriented TMD is in fact surprising. Presently, no SPPL2a/SPPL2b substrate has been reported that is at the same time cleaved by SPPL3. In fact, two studies addressed this experimentally but in cells co-expressing SPPL2a and/or SPPL2b substrates with active SPPL3 no ICD generation and/or substrate turnover was documented (Martin *et al*, 2008; Zahn *et al*, 2013). Furthermore, SPPL3 also fails to process another type III membrane protein, the type III splice variant of the EGF-like growth factor Neuregulin 1(III β Nrg1), that was recently identified as a new SPPL2a/SPPL2b substrate (Fleck *et al*, unpublished), demonstrating that the proteolytic processing by both SPPL2a/SPPL2b and SPPL3 is not generally applying for type III membrane proteins.

5.1.3 Implications of FVenv intramembrane proteolysis for the virus life cycle

Compared to other retroviral surface glycoproteins FVenv is unique due to its N-terminal leader peptide (Lindemann & Goepfert, 2003) which also plays a fundamental role during virus egress (Lindemann & Rethwilm, 2011). Accordingly, cells expressing N-terminally truncated FVenv mutants produce substantially less infectious virus particles (Lindemann *et al*, 2001). Unlike their orthoretroviral counterparts, foamy viral gag proteins lack a membrane-targeting signal and, hence, fail to induce budding of virus-like particles (Lindemann & Rethwilm, 2011). Instead, FVenv LP mediates physical interaction with gag via its N-terminal cytosolic portion and recruits viral capsids to the membrane to ensure proper virus assembly and budding (Lindemann *et al*, 2001; Wilk *et al*, 2001; Lindemann & Rethwilm, 2011). Taken together, these observations highlight the fundamental role of FVenv LP in the viral life cycle. At the same time, however, it is clear that in order to fulfil its function and to recruit viral capsids to the membrane FVenv LP must be firmly anchored in the membrane.

Intramembrane proteolysis of a given transmembrane protein substrate may result in the generation of soluble products (see 1.4.1.2.2). Therefore, intramembrane proteolysis of FVenv LP by SPPL2a/SPPL2b and/or SPPL3 could in principle release the cytosolic LP N-terminus from its membrane anchor. Hence, promotion of FVenv LP intramembrane proteolysis could impair gag recruitment (Fig. 5.1), interfere with FV particle egress and, ultimately, restrict FV

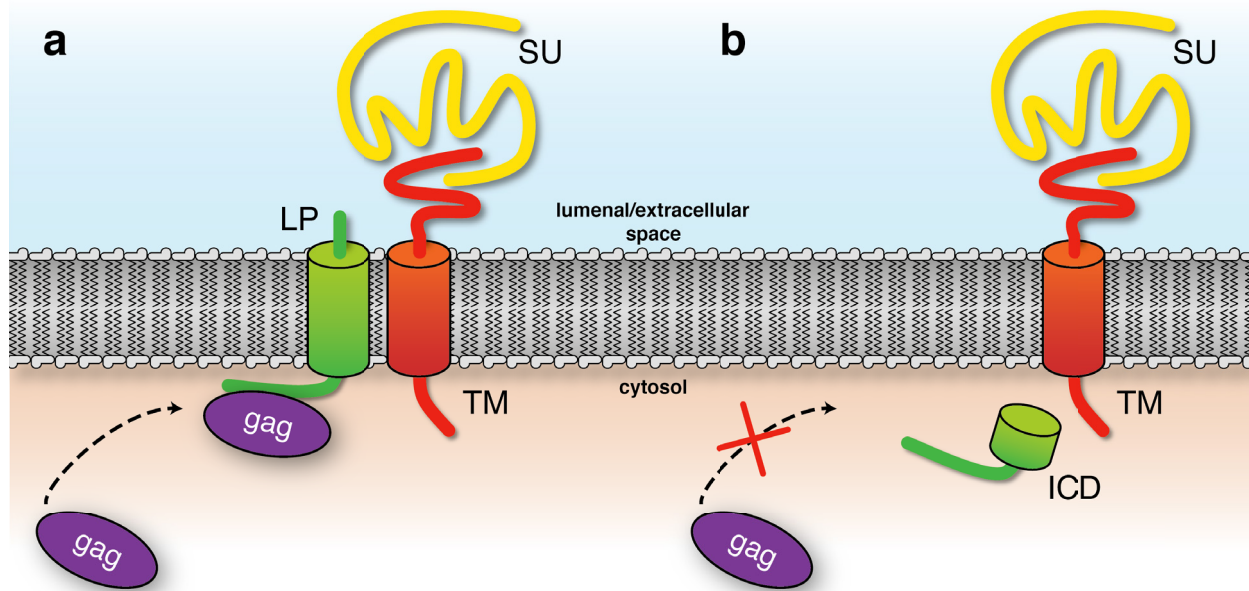


Fig. 5.1: FVenv LP intramembrane proteolysis could interfere with membrane recruitment of gag. Under normal conditions (a), cytosolic FV gag (purple) is recruited to the host cell plasma membrane (black dashed arrow) by interacting with the membrane-integral FVenv LP (green) and then initiates virion assembly and packaging. Assuming that FVenv LP is quantitatively endoproteolysed by either SPPL3 or SPPL2a/SPPL2b and that the cleavage product (ICD) is not tightly anchored in the membrane bilayer (b), this would impair proper membrane recruitment of gag. FVenv SU, yellow, FVenv TM, red.

propagation. Several aspects, however, have to be taken into account when considering such potential implications of SPPL-mediated intramembrane proteolysis for the FV life cycle: (i) Does FVenv LP intramembrane proteolysis occur under physiological conditions? In HEK293 cells, generation of ICD(L2) and ICD(L3) produced by SPPL2a/SPPL2b and SPPL3, respectively, was readily observed when the respective proteases were over-expressed (Fig. 4.2 & 4.3). ICD generation by endogenous protease activity, however, appeared to be much less efficient. Therefore, it needs to be investigated whether and to what extent FVenv LP is turned over by SPPLs under physiologically conditions. In naturally infected rhesus monkeys active virus replication is mainly restricted to superficial epithelial layers of the oral mucosa (Murray *et al*, 2008). Expression levels of SPPL2a/SPPL2b and SPPL3 in these tissues could be analysed and, using antisera directed against the simian FVenv N-terminus (Lindemann *et al*, 2001), FVenv ICD generation could be monitored directly in homogenates of these tissues in infected animals. Assuming that SPPL-mediated endoproteolysis of FVenv interferes with its propagation, such permissive host tissues should harbour low endogenous activity of SPPL2a/SPPL2b or SPPL3. Up-regulation of their expression may then be expected to suppress virus propagation. Similarly, FVs can be propagated in mice (Schmidt *et al*, 1997) and FV infections could be examined in detail in SPPL-deficient or transgenic mouse models. (ii) Are FVenv ICDs released from the membrane? It needs to be examined whether FVenv ICDs are released from membranes or whether they remain integral to the membrane and are incorporated into virus particles like LP in order to assess whether ICDs can still fulfil FVenv LP's function. (iii) Do SPPLs interfere with the generation of FV particles? Ultimately, this question has to be addressed experimentally. Using established vector systems (described e.g. in (Trobbridge *et al*, 2002)), release of recombinant FV particles could be monitored in HEK293 cells that over-

express catalytically active SPPL3 or that were transfected with SPPL3-targeting siRNA or shRNA.

5.1.4 Signal/leader peptides of other retroviral env proteins

As discussed in 5.1.1, FVenv LP cannot be considered a conventional signal peptide. Interestingly, env proteins of several other retroviruses also have N-terminal signal or leader peptides that display unusual characteristics. In contrast to conventional signal peptides, retroviruses have evolved signal peptides that appear to exert intricate post-targeting functions as they serve important purposes during the viral life cycle. Also, such retroviral signal peptides are often cleaved post-translationally. Therefore, it is tempting to speculate that SPP/SPPL intramembrane proteases could also be involved in proteolytic processing of these peptides. Exemplary retroviral env proteins will be discussed in the following.

The human immunodeficiency virus (HIV) surface glycoprotein precursor gp160 is predicted to have an N-terminal signal peptide of approximately 30 aa (Martoglio & Dobberstein, 1998), but its length may vary. In contrast to the commonly co-translational removal of N-terminal signal sequences from pre-proteins, HIV-1 env's leader peptide is removed post-translationally (Li *et al*, 1994; 2000a; Land *et al*, 2003) and this process is slow and inefficient (Martoglio *et al*, 1997; Li *et al*, 2000a). Moreover, the HIV-1 signal peptide serves purposes beyond protein targeting and modulates the association of gp160 with ER chaperones such as calnexin (Li *et al*, 1996) and the folding state of gp160 critically determines whether and when removal of the leader peptide occurs (Land *et al*, 2003). Importantly, while N-terminal HIV-1 gp160 leader peptide fragments were released enzymatically from microsomal membranes *in vitro* (Martoglio *et al*, 1997), the exact nature of the proteases involved in HIV-1 gp160 signal peptide removal and its liberation from ER membranes has not been unambiguously determined.

While the HIV-1 gp160 signal peptide is already exceptionally long for a conventional signal sequence, other lentiviral env glycoproteins such as those of ungulate lentiviruses or of the feline immunodeficiency virus (FIV) harbour much longer leader peptides. FIV env, for instance, comprises a roughly 20 kDa N-terminal leader peptide that includes two hydrophobic stretches (Verschoor *et al*, 1993). This leader peptide is post-translationally removed by an elusive proteolytic activity (Verschoor *et al*, 1993). Small N-terminal truncations of FIV env are well tolerated and do not affect the protein synthesis and maturation, but deletion of most of env's leader peptide led to profoundly impaired protein maturation (Stephens *et al*, 1992). In sum, FIV env proteolytic processing and the nature of its leader peptide resemble that of FVenv. However, the exact role of FIV env's leader peptide in the viral life cycle remains largely enigmatic. In addition, several studies report that β -retroviral signal/leader peptides, being initially targeted to the ER as part of the env holoprotein, subsequently translocate to the cytosol and/or the nucleus. Examples include the env signal peptides of the human endogenous retrovirus HERV-K(HML-2), which is associated with seminoma incidence in young adults (Ruggieri *et al*, 2009), and of the Jaagsiekte sheep retrovirus (JSRV), a β -retrovirus that causes transmissible lung adenocarcinomas in sheep (Caporale *et al*, 2009).

Taken together, it is obvious that retroviral signal or leader peptides often display rather unusual stability and at the same time possess important, yet also very diverse functions beyond the

mere targeting of nascent proteins to the secretory pathway. In light of the finding that the FVenv leader is subject to SPPL-mediated intramembrane proteolysis (see 5.1.2), other retroviral leader peptides could, in principle, also constitute interesting SPPL substrates. Whether this in fact is the case remains to be determined.

5.1.5 Analysis of SPPL3-mediated intramembrane proteolysis of FVenv

Having identified the a novel substrate that is endoproteolysed by SPPL3 in a cellular setting allowed to examine SPPL3-mediated intramembrane proteolysis in more detail. As FVenv is at the same time subject to intramembrane cleavage mediated by SPPL2b, the characteristics of these proteases could be directly compared. Key characteristics of SPPL2b such as its substrate requirements (Martin *et al*, 2009; Fluhrer *et al*, 2012) and its sensitivity towards various small molecule inhibitors (Fluhrer *et al*, 2006; Friedmann *et al*, 2006; Martin *et al*, 2008) had already been studied before and, taken together with similar studies on SPP as well as on γ -secretase, revealed conserved characteristic features of mammalian GxGD proteases (see 1.4.4). Therefore, comparison of SPPL3- and SPPL2b-mediated intramembrane proteolysis of FVenv directly allowed to examine whether the poorly characterised protease SPPL3 likewise shares these conserved characteristics.

5.1.5.1 SPPL3 is hardly sensitive to transition state analogue GxGD protease inhibitors

A common and apparently conserved characteristic of GxGD proteases analysed is their sensitivity towards active site-directed GSIs and the peptidomimetic (Z-LL)₂ ketone (see 1.4.4.4). SPPL2b-mediated intramembrane proteolysis of the TNF α NTF and the Bri2 NTF, for instance, is impaired following treatment with either (Z-LL)₂ ketone or L-685,458 (Fluhrer *et al*, 2006; Friedmann *et al*, 2004; Martin *et al*, 2008). In line with this, SPPL2b-mediated FVenv cleavage was also inhibited in a concentration-dependent manner by both inhibitors (Fig. 4.7a) and both compounds inhibited subsequent proteolytic processing of the SPPL3-specific cleavage product ICD(L3) by endogenous SPPL2a/SPPL2b activity (Fig. 4.7b, see 5.1.5.3). In contrast, the GSI DAPT failed to impair SPPL2b-mediated processing of FVenv LP as well as the SPPL2a-/SPPL2b-dependent processing of ICD(L3). Similarly, DAPT neither inhibits SPPL2b-mediated processing of the Bri2 NTF (Martin *et al*, 2008) nor SPP activity (Weihofen *et al*, 2003), suggesting that the DAPT binding site, which is not the active site in presenilin (Morohashi *et al*, 2006), is not conserved among GxGD proteases. Taken together the results obtained for SPPL2b-mediated processing of FVenv LP nicely conform with the inhibitor profile of SPP/SPPL-type GxGD proteases.

Unexpectedly, SPPL3-dependent production of ICD(L3) from FVenv was inhibited neither by the active site-directed inhibitors (Z-LL)₂ ketone or L-685,458 nor by DAPT (Fig. 4.7b). In fact, ICD(L3) was found to accumulate in a dose-dependent manner following (Z-LL)₂ ketone and L-685,458 treatment. This, however, appears to be due the inhibition of endogenous SPPL2a and SPPL2b activity resulting in a block of ICD(L3) processing by SPPL2a/SPPL2b (discussed in 5.1.5.3). Therefore, in sum, SPPL3 activity on FVenv is not affected by these active site-directed compounds.

While - in light of the conserved GxGD protease inhibitor profile - the inefficacy of DAPT treatment to inhibit SPPL3 activity was expected, the lack of SPPL3 inhibition following (Z-LL)₂ ketone or L-685,458 treatment was not and also contrasts with earlier observations. In the assumption that SPPL3 and SPP are to some degree functionally redundant, two studies claimed having observed proteolytic activity of SPPL3 towards artificially engineered signal peptide-based substrates (Nyborg *et al*, 2006; Narayanan *et al*, 2007). Narayanan *et al*. recombinantly expressed the *Drosophila* orthologue of human SPPL3 in *E. coli* and monitored activity of solubilised *E. coli* membranes towards an epitope-tagged reporter substrate based on a mutant of the prolactin signal peptide (Narayanan *et al*, 2007) that had been used before to monitor SPP activity (Sato *et al*, 2006b). They observed proteolytic turn-over of the substrate that was impaired following addition of 10 μ M (Z-LL)₂ ketone (Narayanan *et al*, 2007). Nyborg *et al*. transiently over-expressed SPPL3 in HEK293T cells and employed a cellular reporter assay to monitor intramembrane cleavage (Nyborg *et al*, 2006). This assay had been developed earlier and employs a fusion protein that comprises the membrane-spanning region of the cytomegaloviral gpUL40 signal sequence (Nyborg *et al*, 2004). This signal sequence, however, is resistant to SPP-mediated intramembrane proteolysis and only is turned into a SPP substrate following mutagenesis (Lemberg & Martoglio, 2002). In cells expressing the mutated reporter substrate, Nyborg *et al*. documented reporter activity that was boosted dose-dependently when co-expressing SPPL3 and that was impaired following (Z-LL)₂ ketone treatment (Nyborg *et al*, 2006). Taken together, both studies suggest that human SPPL3 is sensitive towards (Z-LL)₂ ketone treatment and, hence, contrast with observations presented herein. Notably, FVenv is the first "native" SPPL3 substrate identified and the terminal epitope tags introduced to allow for detection of cleavage products do not interfere with the protein's normal intracellular trafficking and proteolytic processing by pro-protein convertases (Fig. 4.1) and do presumably not interfere with intramembrane processing. In contrast, the assay substrate used in the study of Narayanan *et al*. and in particular the fusion protein used by Nyborg *et al*. are no natural SPPL3 substrates and are highly artificial in nature. Therefore, examination of SPPL3 activity by means of such substrates may be artefact-prone. Moreover, Narayanan *et al*. who reported proteolytic activity of recombinantly expressed human SPPL3 in *E. coli* membranes cannot rule out that the observed (Z-LL)₂ ketone-sensitive proteolytic activity towards the prolactin signal peptide substrate is due to an endogenous bacterial protease. Finally, however, it can presently not be excluded that the characteristics of SPPL3 are perhaps also dependent on the substrate employed to study its proteolytic activity. Therefore, examination of the secretion of the numerous new candidate SPPL3 substrates identified herein (see 5.2) will likely reveal on a proteome-wide scale whether SPPL3 is in general not sensitive towards treatment with active site GSIs or less sensitive than other GxGD proteases.

Importantly, this is a particularly pressing question considering that GSIs have been developed as drug candidates for prevention of AD development and progression (see 1.4.4.4). Cross-reactivity of these compounds with the SPP/SPPL family members and inhibition of their physiological function(s) may therefore pose a certain risk and may contribute to potential side-effects of GSI therapy. With that said, the observed lower sensitivity of SPPL3 towards transition

state analogue GSIs may in fact be promising and could suggest that GSI therapy does not interfere with SPPL3's physiological function.

Moreover, the lower sensitivity or possibly insensitivity of SPPL3 towards substrate-mimicking active site-targeting GSIs observed raises the question whether SPPL3's active site architecture is fundamentally distinct, e.g. regarding the spatial dimension of peptide side chain accommodating pockets, from that of most other mammalian GxGD proteases. L-685,458 and (Z-LL)₂ ketone are both peptidomimetics, i.e. the more they resembled a natural, physiological substrate, the better their binding into the target enzyme's active site would be. Therefore, a promising approach to identify inhibitors that would efficiently impair SPPL3 activity could be to screen peptidomimetics that display a greater variety in amino acid side chain-mimicking moieties or design such compounds according to the cleavage site features of the newly identified SPPL3 substrates (see 5.2).

5.1.5.2 SPPL3 cleaves a full-length membrane protein substrate

Another common characteristic of GxGD proteases is that they can only catalyse intramembrane proteolysis of membrane protein substrates with sufficiently shortened ectodomains and, in most instances, these particular substrates are cleaved by (an)other protease(s) prior to intramembrane cleavage (Struhl & Adachi, 2000; Lemberg & Martoglio, 2002; Hemming *et al.*, 2008; Martin *et al.*, 2009). FVenv is endoproteolysed in its TMD1-proximal region by a furin-like PC (Duda *et al.*, 2004; Geiselhart *et al.*, 2004), leaving behind LP with an approximately 40 amino acid luminal moiety. PC cleavage of FVenv therefore constitutes a shedding-like event, the difference from conventional shedding being that the FVenv ectodomain (SU-TM) is not released from the cell but remains cell-attached due to its C-terminal TMD. To reproduce earlier findings for the SPPL2b substrate Bri2 (Martin *et al.*, 2009), the PC cleavage site was mutagenised to abolish generation of LP and SU-TM. Notably, this mutant was not endoproteolysed by SPPL2b (Fig. 4.5), which is in good agreement with the data obtained by Martin *et al.* and suggests that the selectivity for substrates with a short ectodomain is a general requirement of SPPL2b and not a substrate-specific phenomenon.

Unexpectedly, however, SPPL3-mediated processing of FVenv was unimpaired when the same PC cleavage site mutant was analysed (Fig. 4.5) and, hence, contrasts with the observations made for substrates of SPP (Lemberg & Martoglio, 2002; Boname *et al.*, 2014) and of SPPL2b (Martin *et al.*, 2008). A possible explanation is that SPPL3 does not necessarily only accept substrates with short luminal domains but instead readily proteolyses full-length substrates. Subsequent experimental data strongly favour this explanation. First, co-immunoprecipitation studies revealed that a SPPL3 mutant preferentially associates with FVenv full-length and only to a minor extent with FVenv LP, the truncated substrate available in the cell (Fig. 4.6b). Second, an additional high molecular weight cleavage product, TMD-SU-TM, was identified that is generated together with ICD(L3) when SPPL3 cleaves full-length FVenv (Fig. 4.5). Moreover, in light of TMD-SU-TM also being generated in conditions where FVenv LP is available as a substrate and in light of the co-immunoprecipitation results it appears that SPPL3 exhibits indeed a preference for the full-length substrate. Finally, SPPL3 was found to facilitate secretion of a number of other full-length substrate proteins (discussed in section 5.2), implying that the

processing of a full-length substrate is not specific for FVenv but rather a general feature of SPPL3.

It is presently unclear why SPPL3 lacks the preference for substrates with short ectodomains that is typical of other mammalian GxGD proteases. In fact, even for the latter the exact molecular mechanism underlying the substrate selectivity is enigmatic. An initial study proposed that Nicastin with its large, highly glycosylated luminal ectodomains functions as a γ -secretase substrate receptor by associating with the N-terminus of substrate stubs (Shah *et al*, 2005). This study, however, has subsequently been challenged (Chávez-Gutiérrez *et al*, 2008). Hence, to date no protease-intrinsic domain has been identified to ensure selectivity for substrates with truncated ectodomains. It has to be emphasised, though, that SPPL3 is probably the most primitive mammalian GxGD protease as its luminal and cytosolic N- and C-termini, respectively, are extremely short as are the internal loops connecting the nine individual TMDs. It could therefore lack domains ensuring selectivity for substrates of a particular ectodomain size, but this in turn raises the question whether and how SPPL3 selectivity is regulated (see 5.4).

5.1.5.3 *SPPL2a/SPPL2b cleave the SPPL3 cleavage product*

In-depth analyses of ICD(L3) running behaviour on different gel systems revealed that generation of ICD(L3) in cells over-expressing active SPPL3 was accompanied by production of a smaller N-terminal fragment (Fig. 4.8). This fragment co-migrated with ICD(L2) generated in cells co-expressing SPPL2b and FVenv. Moreover, its generation was substantially impaired in cells treated with (Z-LL)₂ ketone or L-685,458 or in cells transfected with SPPL2a- and SPPL2b-specific siRNAs. At the same time ICD(L3) accumulated (Fig. 4.8). ICD(L2) was also observed in cells co-expressing SPPL3 and the furin/PC cleavage site mutant of FVenv (Fig. 4.11). Under these conditions, FVenv LP is hardly produced, but SPPL3-expression was still accompanied by production of both species. Therefore, this particular experiment provides evidence that ICD(L2) is in fact produced from ICD(L3). Collectively, these data unambiguously show that, following its generation by SPPL3, ICD(L3) can subsequently be processed by SPPL2a and/or SPPL2b.

In the present study a region within the first FVenv TMD in which intramembrane proteolysis occurs could be defined by analysis of the C-peptides released (Fig. 4.13). Their production was abolished following (Z-LL)₂ ketone treatment suggesting that they were generated in a SPPL2a/SPPL2b-dependent fashion. These C-peptides originate in a region close to the C-terminal, i.e. luminal border of the predicted TMD1 of FVenv. Since ICD(L3) has a slightly higher molecular weight than the ICD(L2) (Fig. 4.4b), it has to be anticipated that endoproteolysis mediated by SPPL3 occurs C-terminal to the putative SPPL2b cleavage site. Therefore, it presently cannot be excluded that SPPL3 cleaves FVenv C-terminal of its TMD, e.g. in the luminal juxtamembrane region. Importantly, this does not contradict the intramembrane proteolysis concept as other I-CLiPs, e.g. the rhomboids, may also cleave substrates outside of their membrane-spanning stretches, likely by folding into the membrane-buried active site (Strisovsky *et al*, 2009). Ultimately, however, this requires experimental verification and the exact SPPL3 cleavage site has to be determined in FVenv.

Tab. 5.1: Comparison of SPPL3 with other intramembrane proteases. Results obtained in this study are indicated including a reference to respective section. n.a., not applicable; * The strict topological selectivity of rhomboids for type I membrane proteins has recently been questioned.

	SPPL3	SPP	SPPL2b	γ -secretase	rhomboids
substrate topology	type II	type II	type II	type I	type I*
sensitivity towards GSIs	no (4.2.2)	yes	yes	yes	n.a.
substrate truncation required	no (4.2.1)	yes	yes	yes	no

The finding that ICD(L3) is subject to proteolytic processing by SPPL2a/SPPL2b is rather unexpected as processing of a GxGD protease cleavage product by another, distinct GxGD protease has not been previously reported. Moreover, it raises numerous mechanistic questions, in particular how a given TMD can be subject to endoproteolysis by two distinct proteolytic activities and how the product of the first intramembrane cleavage is efficiently recruited as a substrate for the protease(s) catalysing the second cleavage event, in particular as these distinct protease are differentially localised within the cell. Assuming SPPL3-mediated FVenv endoproteolysis occurs in the C-terminal (i.e. luminal) portion of the TMD (see above), ICD(L3) would retain a large degree of hydrophobicity and could therefore remain firmly embedded in the lipid bilayer. It may then display mobility due to lateral diffusion in the membrane which could in turn allow ICD(L3) to traffic from the active site of SPPL3 to the respective on in either SPPL2a or SPPL2b. Alternatively, SPPL3 could also interact physically with either SPPL2a or SPPL2b which would enable direct delivery from one enzyme to the other. The latter model, however, seems less likely in light of the reported differential sub-cellular localisation of the proteases involved (Krawitz *et al*, 2005; Friedmann *et al*, 2006).

5.1.5.4 Comparison of SPPL3 and other intramembrane proteases

Tab. 5.1 summarises the observations made for SPPL3-mediated intramembrane proteolysis of FVenv and compares those features to other proteases. As expected, SPPL3 appears to display selectivity towards type II transmembrane proteins (see also section 4.4) like other SPP/SPPL proteases. Unlike all other mammalian GxGD proteases characterised (i.e. SPP, SPPL2a, SPPL2b and the γ -secretase complex), SPPL3 activity seems not to be profoundly impaired by treatment with substrate analogous active site-targeting GSIs. In addition, SPPL3 clearly differs from other mammalian GxGD protease regarding its ability to endoproteolysis membrane protein substrates with intact (and bulky) ectodomains. In sum, significant differences between SPPL3 and other mammalian GxGD proteases regarding inhibitor sensitivity and substrate requirements become evident. Instead, the independence of substrate truncation is a key feature of the rhomboid I-CLiPs (see 1.3) and thus there seems to be striking similarity of rhomboids and SPPL3 in that regard.

5.2 SPPL3 facilitates secretion of selected type II membrane proteins

The identification of FVenv as SPPL3 substrate allowed for the first time to functionally characterise SPPL3 and this revealed properties not expected for a mammalian GxGD protease (discussed in 5.1.5), most importantly that SPPL3 does not require a shedding-like event that tailors its substrate FVenv for intramembrane proteolysis and instead endoproteolyses full-length FVenv directly (5.1.5.3). This finding led to the hypothesis that SPPL3 could act as membrane protein convertase that liberates protein ectodomains from their membrane anchor, i.e. acting functionally similar to classical sheddases (see 1.1) or rhomboid I-CLiPs (see 1.3).

5.2.1 SPPL3 acts as a type II membrane-selective protein convertase or sheddase

The viral protein FVenv is certainly not the only SPPL3 substrate. Instead, in light of SPPL3's high degree of evolutionary conservation (Fig. 1.9), it has to be anticipated that there are vital cell-intrinsic SPPL3 substrates. Since another type III protein is not endoproteolysed by SPPL3 (Fleck *et al.*, unpublished) and since multi-pass membrane proteins are generally less abundant than single-pass proteins (Almén *et al.*, 2009; Fagerberg *et al.*, 2010), it was hypothesised that SPPL3 could similarly endoproteolysis full-length single-pass type II membrane proteins (Fig. 5.2). SPPL3-mediated endoproteolysis of a given type II protein would then result in disengagement of the substrate's ectodomain from its membrane anchor and its liberation into the Golgi lumen (and possibly into the extracellular space). At the same time SPPL3 cleavage produces a membrane-embedded substrate stub which, in analogy to the FVenv ICD(L3), could

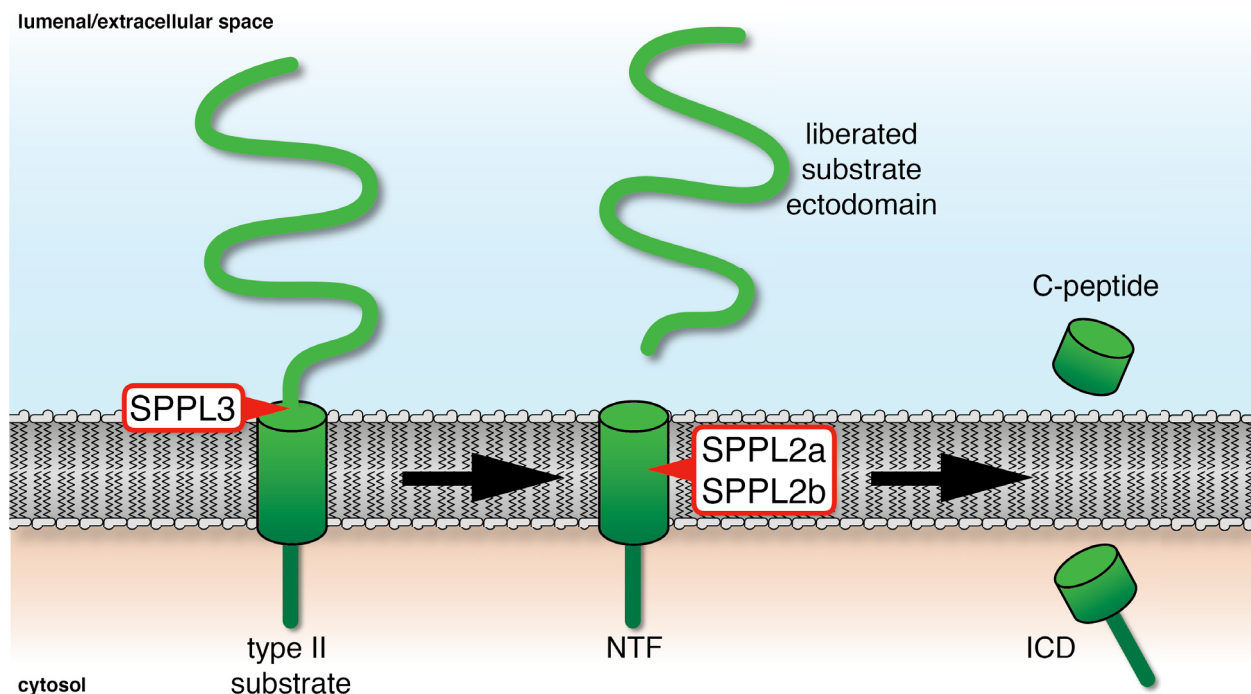


Fig. 5.2: Hypothetical model of SPPL3 acting as a type II membrane protein-selective sheddase. SPPL3-mediated cleavage of a given type II membrane protein substrate in a stretch close to the interface of the membrane and the Golgi lumen could liberate a substrate's ectodomain from its membrane anchor. It can subsequently be trafficked intracellularly, secreted or degraded (not depicted). The putative TMD cleavage product could remain within the membrane and may potentially be subject to downstream intramembrane cleavage by SPPL2a/SPPL2b resulting in the release of indicated cleavage products from the membrane.

be subsequently endoproteolysed by SPPL2a or SPPL2b. SPPL3 would then act in a manner reminiscent of a classical sheddase (compare with Fig. 1.1) as it facilitates release of a soluble ectodomain of a given substrate and allows for subsequent intramembrane proteolysis (Fig. 5.2).

This hypothesis receives strong support from the identification of several novel (candidate) SPPL3 substrates in this study using two distinct approaches, a candidate-based approach (see 4.3.4 & 4.3.9) and a less biased proteome-wide approach (see 4.4). Obviously, SPPL3 substrates are expected to (i) adopt a type II topology, (ii) co-localise sub-cellularly with SPPL3, and (iii) physically interact with the protease. Regarding the topology, it is well-documented that SPP/SPPL I-CLiPs exclusively endoproteolysate membrane protein substrates that adopt a type II orientation (Voss *et al*, 2013) and SPPL3 apparently shares this characteristic as the FVenv N-terminus also spans the membrane in a type II orientation. In addition, it is obvious that protease and substrate have (at least transiently) to co-localise sub-cellularly and to interact physically for proteolysis to occur. In view of this, the results obtained and the (candidate) substrates identified will be discussed in the following, while the physiological implications of their proteolytic processing by SPPL3 will be subject to in-depth discussion later (section 5.3). The finding that FVenv ICD(L3) generated by SPPL3 activity is subsequently also endoproteolysed by SPPL2a/SPPL2b (see 5.1.5.4) of course raises the question whether this likewise happens to the newly identified candidate SPPL3 substrates (Fig. 5.2). Presently, however, this can neither be disproven nor verified as no ICD species have yet been observed for these new substrates.

5.2.2 SPPL3 substrates identified by a candidate-based approach

In light of the observation that alterations in SPPL3 levels in cultured cells and *in vivo* translate into global changes in cellular N-glycosylation (discussed in 5.3.1), Golgi-localised GTs were examined as candidate SPPL3 substrates and the experimental data strongly support that SPPL3 proteolytically cleaves the GTs GnT-V, β 3GnT1 and β 4GnT1.

In accordance with an earlier study (Nakahara *et al*, 2006), secretion of GnT-V was observed to be a proteolytic process that leads to N-terminal truncation of the full-length protein (Fig. 4.25 & 4.27). In cells lacking endogenous SPPL3 activity, GnT-V secretion is almost completely abolished and the full-length protein accumulates intracellularly (Figs. 4.23 & 4.26) which could be attributed to impaired proteolytic liberation of GnT-V from its membrane anchor. In cells over-expressing active SPPL3, intracellular levels of endogenous GnT-V are drastically reduced (Fig. 4.23), but no marked increase in GnT-V secretion could be detected under these conditions suggesting that, following its cleavage by SPPL3, GnT-V could be also subject to degradation. SPPL3 over-expression did only lead to enhanced GnT-V secretion following co-expression of exogenous GnT-V (Figs. 4.24 & 4.25), indicating that excessive amounts of GnT-V saturate its degradation and under these conditions SPPL3 over-expression then results in increased GnT-V secretion. Taken together, these observations are in fact in line with SPPL3 catalysing GnT-V shedding. In addition, two other type II membrane proteins implicated in cellular N-glycosylation, β 3GnT1 and β 4GnT1, were found to be affected by SPPL3 in a manner similar to GnT-V (see 4.3.9). Importantly, knock-down of endogenous SPPL3 using

RNAi or genomic ablation of SPPL3 expression in MEFs nearly abolished secretion of GnT-V, β 3GnT1 and β 4GalT1, strengthening that these GTs are subject to SPPL3-mediated cleavage under physiological conditions.

GnT-V, β 3GnT1 and β 4GalT1 all lack N-terminal signal peptides and are predicted to adopt a type II topology (Shoreibah *et al*, 1993; Sasaki *et al*, 1997; Masri *et al*, 1988), being well compatible with the expected topological substrate preference of SPPL3. SPPL3 is considered a Golgi-resident protease as over-expressed, epitope-tagged SPPL3 co-localised with the Golgi marker Giantin (Friedmann *et al*, 2006). Based on their catalytic activity on N-glycans, GnT-V, β 3GnT1 and β 4GalT1 are considered *medial/trans* Golgi enzymes (Roth, 2002) and endogenous β 4GalT1 (Roth & Berger, 1982) as well as over-expressed GnT-V and β 3GnT1 (Chaney *et al*, 1989; Chen *et al*, 1995; Buisse *et al*, 2013) co-localise with Golgi markers. This suggests that SPPL3 co-localises with the substrates identified and that GT endoproteolysis occurs within the Golgi. This receives additional strong support from experiments with exogenously expressed GnT-V (Figs. 4.24 & 4.25): In HEK293 cells, two distinct species of over-expressed GnT-V were detected and enzymatic deglycosylation revealed that the higher molecular weight species localises to post-ER compartments whereas the other species is ER-resident. Exclusively the Endo H-resistant, Golgi-resident GnT-V species was affected by loss of SPPL3 expression or SPPL3 over-expression, indicating that SPPL3 endoproteolyses GnT-V in the Golgi network (or later).

Taken together, the experimental evidence points to GnT-V, β GnT1 and β 4GalT1 being genuine SPPL3 substrates. However, while the model outlined here (Fig. 5.2) suggests a direct proteolytic effect of SPPL3 on the GT substrates leading to their liberation, this direct effect of SPPL3 on the GT substrates still requires experimental support and it can presently not be completely ruled out that the effects on substrate secretion are indirect. SPPL3, for instance, could proteolytically activate another proteases that in turn mediates ectodomain shedding of such substrates, but alternative indirect mechanism can also be imagined (e.g. an effect of SPPL3 (intra-)Golgi trafficking etc.). To clarify this matter, it is essential to unambiguously demonstrate that SPPL3 directly acts on substrates, for instance by monitoring proteolytic activity of SPPL3 towards its substrate(s) in an *in vitro* assay. Given that SPPL3 is an I-CLiP, it is a rather challenging task to establish such an assay. First, both the polytopic protease SPPL3 and the membrane-spanning substrate protein must be expressed recombinantly and purified in an active conformation. Then, recombinant protease and substrate have to be reconstituted into an environment containing specific lipids and/or detergents that adequately support catalysis. For rhomboid I-CLiPs for example such assays have been developed (Urban & Wolfe, 2005; Lemberg *et al*, 2005; Maegawa *et al*, 2005) and have been valuable tools to study their catalytic properties and validate substrates identified. Alternatively, co-immunoprecipitation assays of an inactive mutant of SPPL3 and the respective substrate could be established. The latter approach, however, requires careful validation to ensure that the interaction is specific. Of note, such co-precipitation assays only allow to examine whether a physical interaction of substrate and protease is possible but they do not unequivocally exclude that other factors contribute to the proteolytic cleavage.

5.2.3 SPPL3 substrates identified by a proteome-wide approach

In addition, a proteomics approach was undertaken to identify novel SPPL3 substrates. This revealed that over-expression of catalytically active SPPL3 is accompanied by enhanced secretion of a number of protein factors (Fig. 4.33 & Tab. 4.2) which constitute candidate SPPL3 substrates. Importantly, as this method only assesses the abundance of secreted protein and as higher protein levels in the conditioned supernatant can in principle also be due to an overall increase in expression of a given substrate protein, candidate SPPL3 substrates require careful validation by Western blot analysis of both conditioned supernatants and cell lysates. Such experiments were performed for a selection of the candidate SPPL3 substrates in HEK293 cells (Fig. 4.36) and indeed revealed that SPPL3 over-expression promoted secretion of these candidate substrates while there was no indication of a higher expression of these proteins in cells that over-express SPPL3. Moreover, secretion of some of the candidate substrates (e.g. of EXTL3, Fig. 36a) was reduced in cells transfected with SPPL3-targeting siRNA pools, suggesting that their secretion under normal conditions is likewise dependent on SPPL3. Collectively, these experiments support the notion that secretion of these candidate SPPL3 substrates is facilitated by SPPL3.

Notably, most of the candidate SPPL3 substrates identified on a proteome-wide scale also conform with SPPL3's expected substrate selectivity. With only few exceptions, those factors are single-span membrane proteins with an annotated or predicted type II topology, i.e. adopt the topology expected for SPP/SPPL substrates (reviewed in (Voss *et al*, 2013)). However, it should still be assessed why and how SPPL3 over-expression affected secretion of the one type I protein, Golgi apparatus protein 1 (Fig. 4.33 & Tab. 4.2). For rhomboids, for instance, the suspected strict selectivity for type I membrane protein substrates (Urban, 2006; Freeman, 2008) has been questioned by recent studies identifying also type II and multi-pass rhomboid substrates (Tsruya *et al*, 2007; Erez & Bibi, 2009).

Regarding the sub-cellular localisation of the SPPL3 candidate substrates identified in this manner, in particular in view of a potential sub-cellular co-localisation of protease and substrate, the situation is much more complex than for the three GT substrates discussed earlier (see 5.2.2). Database annotations suggest predominantly a Golgi localisation of the majority of the candidate substrates identified, yet several of these proteins are considered to localise to other non-Golgi membranes such as the lysosomal membrane (e.g. lysosomal α -glucosidase) or the plasma membrane (e.g. the β -1 subunit of the Na^+/K^+ ATPase) (Fig. 4.35). However, in several cases the exact sub-cellular localisation is controversial. Xylosyltransferase activity, for example, has been observed in either the ER or the Golgi network (discussed in (Schön *et al*, 2006)), while XylT1 and XylT2 were observed to localise to the Golgi when analysed by immunocytochemistry (Schön *et al*, 2006). It is, however, important to scrutinise how the sub-cellular localisation of a given candidate substrate was determined because often such experiments are performed by immunocytochemistry following over-expression of epitope-tagged proteins or chimeric GFP fusion proteins; rarely such an annotation is based on the localisation of endogenous protein. Over-expression may cause artefacts e.g. due to an "over-spill" of cellular compartments (discussed in (Multhaupt & Couchman, 2012)) and, hence,

results from such experiments may not necessarily reflect the sub-cellular localisation of a given protein under physiological conditions. This not only applies to the candidate substrates, but at the same time also to SPPL3 itself as its Golgi localisation has so far also only been observed following over-expression of an epitope-tagged variant (Friedmann *et al*, 2006). Therefore, it remains to be carefully re-evaluated (e.g. by biochemical sub-cellular fractionation) whether and where SPPL3 and the newly identified candidate substrates co-localise. Moreover, candidate substrates identified by this approach require in-depth validation to unambiguously show that these proteins are endoproteolysed by SPPL3 under physiological conditions.

5.2.4 Two distinct classes of SPPL3 substrates

As delineated earlier (see 5.2.2 and 5.2.3), novel SPPL3 substrates and candidate substrates uncovered in this study conform with the expected selectivity of SPPL3 for type II proteins. However, a closer look at their SPPL3-mediated processing in cultured cells reveals that there are marked differences between the substrates uncovered by these two distinct approaches and the substrates can therefore be categorised accordingly.

Secretion of *class I substrates* - being those identified by the candidate-based approach, i.e. endogenous GnT-V, β 3GnT1 and β 4GalT1 - is strongly impaired in cells that lack or express substantially less SPPL3, yet SPPL3 over-expression does not strongly promote secretion of these proteins and, hence, they did not come up as candidate substrates when the secretomes of cells over-expressing catalytically active SPPL3 and of control cells were compared (see 4.4). At the same time, alterations in SPPL3 expression levels are accompanied by strong effects on the intracellular levels of these substrates as SPPL3 knockdown or knockout and over-expression results in robust intracellular accumulation and loss of the intracellular substrate species, respectively. Consequently, it follows that (i) following their disengagement from their membrane anchor, cleaved, luminal substrates may be subject to degradation, explaining why SPPL3 over-expression does not promote release of more secreted substrates, that (ii) cleavage of these substrates by endogenous SPPL3 occurs most likely also under physiological conditions, and that (iii) SPPL3-mediated cleavage of these substrates probably impacts cellular glycosylation as the intracellular levels, i.e. the active intracellular pool of these enzymes, are strongly affected (which then, in turn, explains the glycosylation phenotypes discussed in section 5.3.1). It is tempting to speculate that other endogenous cellular proteins also belong to this category of SPPL3 substrates and they could for instance be identified by applying the proteome-wide SPECS approach to a SPPL3 knockdown or knockout setting.

In contrast, secretion of *class II substrates* - i.e. candidate substrates identified by the proteome-wide approach - is strongly promoted by SPPL3 over-expression which is associated with rather mild (yet variable) reduction in their intracellular levels, depending on the individual candidate substrate. SPPL3 knockdown also had variable effects on secretion, ranging from a markedly reduced secretion observed for EXTL3 (Fig. 4.36b) to a rather unaffected secretion of HS6ST2 (Fig. 4.36f). Following liberation from their membrane anchors, these substrates are likely not subject to degradation and appear to be directly secreted. It is, however, questionable whether endoproteolysis of these substrates catalysed by SPPL3 affects their intracellular function as alterations in SPPL3 expression levels hardly affected intracellular levels of these

substrates. Moreover, as these substrates are primarily affected by SPPL3 over-expression it also remains to be examined to which extent these substrates are endoproteolysed by SPPL3 under physiological conditions and whether this is a direct effect of SPPL3 on the candidate substrate. In fact, it is well conceivable that these proteins are only processed by SPPL3 in substantial amounts following SPPL3 mis-localisation which could be a consequence of the protease's over-expression (discussed in 5.2.3).

In sum and in spite of these open questions, the newly identified candidate SPPL3 substrates underpin the initial hypothesis (Fig. 5.2) that SPPL3 acts as a type II membrane protein-selective sheddase that cleaves full-length type II membrane proteins leading, in turn, to the secretion of their ectodomains. Notably, the apparent selectivity of SPPL3-facilitated secretion for type II membrane proteins is already indicative that the observed effects are not due to global cellular effects that SPPL3 has on, for instance, the secretory pathway or intracellular trafficking.

5.3 Physiological function(s) of SPPL3

Single-celled organisms lack orthologues of mammalian *SPPL3* but such orthologues are present in multi-cellular organisms (Golde *et al*, 2009; Voss *et al*, 2013) and, astonishingly, there is hardly variation in SPPL3's primary structure in metazoa⁶ (Fig. 1.9). Such high degree of conservation implies a strong selective pressure on *SPPL3* which, in turn, points to an indispensable physiological function fulfilled by SPPL3 in metazoa. Primarily due to the lack of adequate *in vivo* models and of known substrates this physiological function has remained completely enigmatic. Here, the putative implications of this study regarding SPPL3's function *in cellulo* and *in vivo* will be discussed.

5.3.1 SPPL3 is a global cellular regulator of complex N-glycosylation

This study demonstrates that changes in cellular SPPL3 expression and/or activity result in alterations in the composition of N-glycan moieties attached to endogenous cellular glycoproteins in cultured cells and *in vivo*. To be more specific, a hypo-glycosylation phenotype was observed following over-expression of active SPPL3 (Fig. 4.19), whereas loss of endogenous SPPL3 activity in cultured murine (Fig. 4.16) or humans (Fig. 4.18) cells or in mouse tissues (Fig. 4.17) was accompanied by a hyper-glycosylation.

Several experiments were performed in order to dissect the cellular N-glycosylation pathway in more detail and to identify the steps in N-glycan metabolism SPPL3 is interfering with. Kifunensine treatment, for instance, prevented SPPL3 over-expression to cause any alterations in glycoprotein running behaviour (Fig. 4.21), indicating that the generation of high-mannose glycans in the ER is not affected. Additional data point to SPPL3 affecting primarily post-ER localised glycoproteins and interfering with complex N-glycosylation in the Golgi, the cellular compartment in which active SPPL3 is expected to be localised (Friedmann *et al*, 2006). Transition from ER N-glycan precursors to complex glycans is catalysed by a number cellular

⁶ Note that this high degree of conservation exclusively applies to isoform 2 of human SPPL3. Uniprot also lists another isoform, isoform 1 (Fig. 4.14a, www.uniprot.org, query: SPPL3_HUMAN, entry ID: Q8TCT6, information retrieved August 28, 2013). A discernible orthologue of isoform 1, however, is not conserved in other species species and also appears to be not catalytically active towards FVenv (Fig. 4.14b).

GTs and glycosidases (Fig. 1.15). These are almost exclusively type II transmembrane proteins and localise to the Golgi network (reviewed in (Paulson & Colley, 1989; Sears & Wong, 1998; Ohtsubo & Marth, 2006)), hence they fulfil two major requirements one would impose on a SPPL3 substrate (discussed in 5.2.1). Moreover, a hypothetical model postulating that SPPL3 is engaged in GT and/or glycosidase endoproteolysis and secretion could in fact well explain the alterations in N-glycosylation observed (Fig. 5.3): In conditions of SPPL3 over-expression,

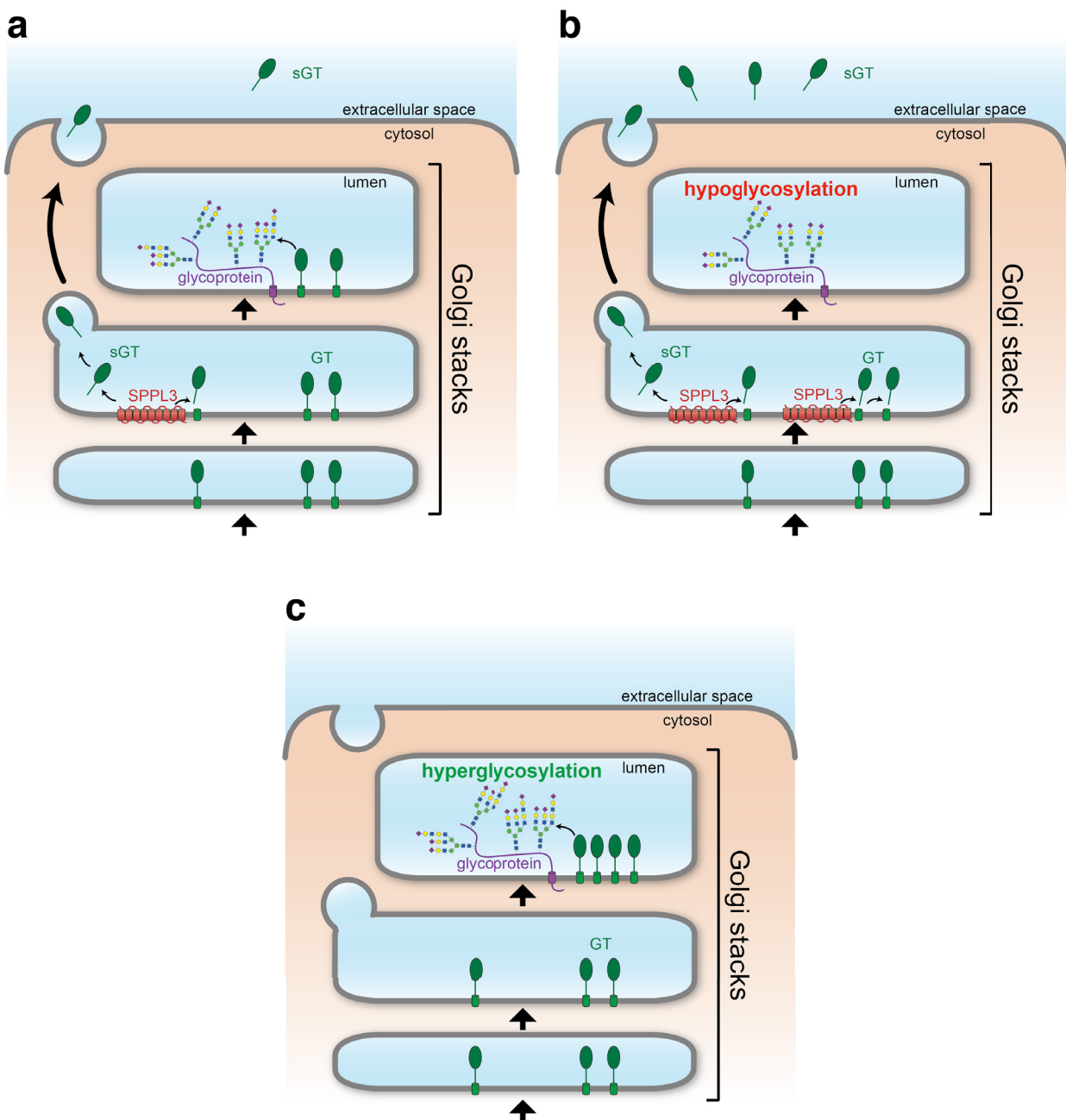


Fig. 5.3: Model explaining the observed glycosylation phenotypes by SPPL3-mediated proteolytic glycosyltransferase secretion. (a) Under physiological conditions, a certain fraction of the Golgi glycosyltransferase pool (GT) is proteolytically cleaved off its membrane anchor by SPPL3 and subsequently secreted (left bold black arrow) or intracellularly degraded (not depicted). Unaffected GT molecules reach their destination within the Golgi and catalyse glycan modifications (depicted here: Gnt-V-mediated β 1,6-GlcNAc branching). (b) In cells over-expressing active SPPL3, GT cleavage is nearly quantitative and no active GT is available for glycan elaboration leading to the hypoglycosylation phenotype observed. (c) In cells lacking SPPL3, no GT secretion is catalysed and hence active GT molecules accumulate in the Golgi leading to hyperglycosylation. This may similarly affect the activity of other Golgi glycan-modifying enzymes.

cleavage and thus secretion of a given GT is promoted and likely occurs prematurely, leading to a reduction in intracellular GT levels and precluding the transferase to fulfil its normal physiological function. This then results in less extensively modified glycans on glycoproteins, i.e. the hypoglycosylation phenotype associated with SPPL3 over-expression. In contrast, loss of SPPL3 expression leads to profoundly impaired GT cleavage. Consequently, cells accumulate active GT which then leads to a more extensive N-glycosylation and, hence, the hyperglycosylation phenotype observed. Under physiological conditions, however, SPPL3-mediated GT secretion is at equilibrium allowing for a normal extent of N-glycan elaboration. Altogether, this suggests that SPPL3 indirectly alters the extent of cellular glycosylation by endoproteolysing such GTs and/or other GMEs, thereby interfering with their cellular activity in glycan assembly.

5.3.1.1 Glycosyltransferase proteolysis

Secretion of cellular GTs that is ascribed to proteolytic liberation of these GTs from their membrane anchors is a well-known phenomenon, yet the physiological consequences and implications of this process are unclear (Paulson & Colley, 1989; Ohtsubo & Marth, 2006; Varki *et al*, 2009). Several studies have already reported enzymatic activities of distinct GTs in bodily fluids such as human (Kim *et al*, 1972a; 1972b; Hosomi *et al*, 1984) and porcine (Hudgin & Schachter, 1971a; 1971b; 1971c) serum as well as bovine colostrum (Elhammer & Kornfeld, 1986). Moreover, using antibodies generated against GT ectodomains, secreted variants of specific GTs were identified in and purified from such biological samples, respectively (Elhammer & Kornfeld, 1986; Kitazume *et al*, 2009). In addition, soluble GTs were found to be released from cultured cells (Borsig *et al*, 1998; Saito *et al*, 2002; El-Battari *et al*, 2003).

Most GTs (but also other GMEs) involved in the assembly of Golgi (N)-glycans have a type II topology and their C-terminal luminal catalytic domain is tethered to its membrane anchor, the TMD, via a so-called stem region (Paulson & Colley, 1989; Varki *et al*, 2009) (Fig. 5.4). The N-terminal cytosolic regions are usually rather short (< 30 aa). Soluble GTs are generally believed to be generated via proteolytic cleavage of their membrane-anchored precursor and subsequent secretion of the liberated ectodomain (Paulson & Colley, 1989; Ohtsubo & Marth, 2006; Varki *et al*, 2009) as sequence analyses of secreted individual GTs purified from tissue homogenates or cell culture media revealed N-terminal truncation (Weinstein *et al*, 1987; Kitazume *et al*, 2001; 2003; Nakahara *et al*, 2006). Whether a GT is subject to endoproteolysis appears to be defined by a region comprising its cytosolic stretch, the TMD and the stem region, often collectively referred to as CTS region (Grabenhorst & Conradt, 1999).

Interestingly, however, the protease(s) involved in this wide-spread shedding of GTs have less well been defined and the few studies investigating this matter have been somewhat contradictory. Importantly, to date no single protease has been defined that globally and exclusively mediates GT proteolysis. One study addressed the proteolytic liberation of GnT-V from its membrane anchor and claims that this is mediated by the γ -secretase complex (Nakahara *et al*, 2006) (discussed in 5.3.1.2). Several other studies have focussed on the proteolytic release of TGN sialyltransferases. Initially, α 2,6-sialyltransferase 1 (ST6Gal1)

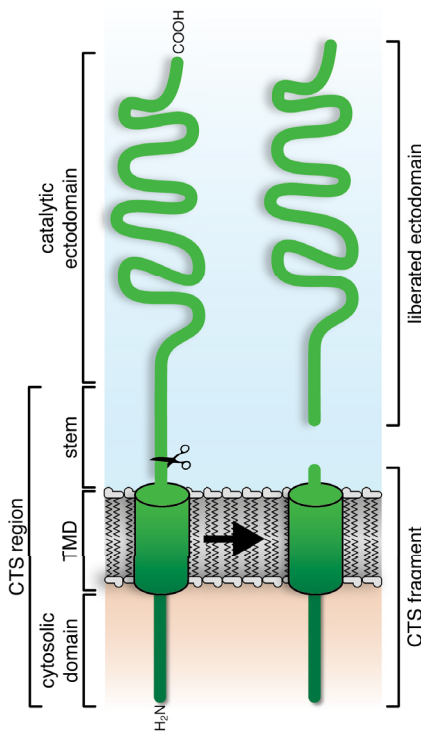


Fig. 5.4: Structure and proteolytic processing of Golgi GTs and GMEs. Golgi GTs and GMEs are type II transmembrane proteins that feature a characteristic domain structure. Their catalytic ectodomains are tethered to the luminal membrane via their CTS region. This comprises a short N-terminal cytosolic domain, a TMD and a luminal stem region. The CTS region also controls intracellularly trafficking and the sub-cellular localisation of GTs and GMEs. In addition, most Golgi GTs and GMEs undergo proteolytic cleavage within a membrane-proximal stretch in their stem regions (scissors). Cleavage liberates the GT/GME ectodomain into the luminal space and leaves behind a presently uncharacterised putative CTS fragment (black arrow). Liberated GT or GME ectodomains may subsequently be secreted or proteolytically degraded. Individual domain lengths are not drawn to scale.

liberation had been attributed to a cathepsin D-like protease (Lammers & Jamieson, 1988; McCaffrey & Jamieson, 1993), which had similarly been implicated in proteolytic release of another GT (Jaskiewicz *et al.*, 1996). Subsequent studies, however, suggest that ST6Gal1 is endoproteolysed by BACE1 *in vitro* and in cultured cell lines (Kitazume *et al.*, 2001) as well as, to a certain extent, *in vivo* (Kitazume *et al.*, 2005). BACE1 is also suspected of endoproteolysing other sialyltransferases (Kitazume *et al.*, 2006). Importantly, while BACE1-mediated ST6Gal1 release occurs *in vivo*, substantial amounts of secreted ST6Gal1 could still be detected in plasma of *Bace1*-deficient mice (Kitazume *et al.*, 2005). A proteome-wide secretome analysis also found that proteolytic secretion of another sialyltransferase, ST3Gal1, was reduced following inhibition of BACE1 activity, but its release was not blocked completely (Kuhn *et al.*, 2012), underscoring that BACE1 is not the only protease that liberates these sialyltransferase substrates. Importantly, apart from ST3Gal1, no other BACE1 substrates implicated in (N)-glycosylation were identified in two independent proteomic studies (Hemming *et al.*, 2009; Kuhn *et al.*, 2012).

As shedding is such a conserved feature among Golgi GTs, it is tempting to speculate that it is of particular physiological importance. Secreted variants of GTs comprise the enzymes' active sites and, accordingly, retain their catalytic activity *in vitro* when reactions are supplemented with nucleotide-conjugated monosaccharides (Elhammer & Kornfeld, 1986). To catalyse

glycosidic bond formation, GTs strictly require such nucleotide-conjugated monosaccharides as donors. *In vivo*, these are generally believed not to be present extracellularly in adequate concentrations for GT catalysis and, hence, GTs are expected not to be catalytically active following secretion in a physiological setting (Colley, 1997; Varki *et al*, 2009; Stanley, 2011). Proteolytic liberation of GTs from their membrane tethers is therefore considered a way to negatively regulate intracellular GT activity (Varki *et al*, 2009; Ohtsubo & Marth, 2006). Formal and conclusive prove for this concept is, however, still missing. Moreover, there is evidence that in certain micro-environments sufficient amounts of sugar donors can be provided to fuel extracellular GT activity. Interestingly, secretion of ST6Gal1 from liver, for instance, is known to be triggered by inflammatory hepatopathological conditions and during acute phase response (Lammers & Jamieson, 1988; McCaffrey & Jamieson, 1993; Kitazume *et al*, 2005; 2009), indicating that GT proteolysis is in fact a dynamic process under physiological conditions. Importantly, GTs may fulfil functions in the extracellular space that are independent of their catalytic activity (Saito *et al*, 2002).

5.3.1.2 *SPPL3 facilitates GnT-V secretion*

As delineated earlier (see 5.2.2), this study identifies GnT-V as a novel SPPL3 substrate. Importantly, its processing essentially follows the previously proposed model (Fig. 5.3) and, hence, could contribute to SPPL3's effect on cellular N-glycosylation. GnT-V activity generates tri- and tetraantennary N-glycans by transferring β 1,6-linked GlcNAc to the N-glycan core (Cummings *et al*, 1982; Dennis *et al*, 2002) and GnT-V products are specifically bound by the plant lectin PHA-L (Cummings & Kornfeld, 1982). In fact, SPPL3 over-expression was accompanied by an overt reduction in PHA-L reactivity towards NCT (Fig. 4.29), demonstrating that SPPL3 not only affects cellular GnT-V levels but also GnT-V activity. This supports the assumption that proteolytic GT secretion can negatively regulate intracellular GT activity (see 5.3.1.1).

GnT-V is a type II membrane protein (Shoreibah *et al*, 1993) and localises to the Golgi apparatus (Chaney *et al*, 1989; Chen *et al*, 1995). Given its action late during N-glycan biosynthesis, it most likely resides in the *medial* or *trans* Golgi (Roth, 2002) and could therefore, in principle, co-localise with SPPL3. Intriguingly, GnT-V had already been reported before to be secreted from cultured cells (Saito *et al*, 2002; Nakahara *et al*, 2006), likely due to a proteolytic activity since secreted GnT-V was found to lack its cytosolic N-terminus as well as the adjacent TMD (Nakahara *et al*, 2006). It can therefore be postulated that SPPL3 proteolytically cleaves membrane-anchored GnT-V upon encounter in the Golgi network, liberating the GnT-V ectodomain from its membrane anchor which then could be trafficking to the cell surface and be secreted. In addition, however, the data also point to (likely intracellular) degradation of cleaved GnT-V (discussed in 5.2.2).

The finding that SPPL3 endoproteolyses GnT-V contrasts starkly with a previous study which claims that GnT-V is liberated by γ -secretase (Nakahara *et al*, 2006). This is rather puzzling as, apart from GnT-V, all γ -secretase substrates identified are type I membrane proteins (Haapasalo & Kovacs (Haapasalo & Kovacs, 2011) provide a detailed list) and a proteomic screen for novel γ -secretase substrates also uncovered exclusively type I membrane proteins

as novel substrate candidates (Hemming *et al*, 2008) and, accordingly, γ -secretase is considered a type I membrane-protein selective protease (Steiner *et al*, 2008a). Moreover, experimental data presented by Nakahara *et al*. (Nakahara *et al*, 2006) in order to support their findings are not convincing. The authors observed that GnT-V secretion from cells was blocked by treatment with the GSI DFK167 (Nakahara *et al*, 2006). In contrast, in the present studies two other highly potent GSIs were found to neither affect GnT-V secretion nor intracellular GnT-V levels, while at the same time APP CTF β processing was clearly inhibited indicating that cellular γ -secretase activity was inhibited (Fig. 4.28a). Moreover, Nakahara *et al*. reported a loss of GnT-V secretion in MEFs lacking PS1 and PS2 (Nakahara *et al*, 2006). Using the very same cells, GnT-V secretion was found to be unaltered compared to the respective control cell line obtained from PS1/PS2 $^{+/+}$ embryos in this study (Fig. 4.28b). Experiments performed in the course of this study therefore disprove Nakahara *et al*.s assertion that γ -secretase mediates GnT-V secretion.

Irrespective of the conclusion that GnT-V cleavage is γ -secretase-dependent, Nakahara *et al*. also show that secreted GnT-V commences at residue His 31 (Nakahara *et al*, 2006). In this study, a different experimental strategy was adopted to determine the SPPL3 cleavage sites within GnT-V (Fig. 4.27). The data obtained suggest that SPPL3 cleaves GnT-V within stretch predicted to lie close to the membrane boundary, hence in a region that could well be accessible to an I-CLiP. Moreover, it suggests that SPPL3-mediated intramembrane proteolysis is not entirely precise explaining the five distinct cleavage products observed. It can, however, presently not be excluded that a single cleavage product generated by SPPL3 is subject to exopeptidase digestion giving rise to the successively trimmed cleavage products observed. Importantly, the cleavage product described earlier (Nakahara *et al*, 2006) was also observed, confirming the observations made here and indicating that the cleavage site(s) identified using the truncated GnT-V construct likely correspond to the respective cleavage(s) of physiological, full-length GnT-V. However, in this setting another cleavage product, commencing at Leu 29, was found to be most abundant. This discrepancy may originate in the different cell lines used or in the different approaches employed. In addition, it remains unclear whether SPPL3 cleaves GnT-V at the five sites identified here with variable efficiency or whether cleavage occurs at one site and the cleavage product is successively trimmed.

5.3.1.3 SPPL3 facilitates secretion of β 3GnT1 and β 4GalT1

While SPPL3 affects cellular N-glycan synthesis by modulating cellular GnT-V activity, SPPL3's effects were not entirely due to GnT-V (Fig. 4.30), indicating that SPPL3 might act similarly on other Golgi GTs or GMEs leading to more profound alterations in cellular N-glycosylation. Indeed, such other additional SPPL3 (candidate) substrates could be identified and will be discussed in the following.

Experiments in human and murine cells (Fig. 4.31a & b) demonstrate that secretion of β 3GnT1 is also affected by SPPL3. β 3GnT1 was predicted to adopt a type II topology (Sasaki *et al*, 1997) and over-expressed β 3GnT1 was reported to co-localise with Giantin and, therefore, likely resides in the Golgi network (Buysse *et al*, 2013). β 3GnT1 hence matches the expected SPPL3 substrate requirements. β 3GnT1 is critically involved in the generation poly-N-

acetyllactosamines (poly-LacNAc) moieties on N- and O-glycans (Sasaki *et al*, 1997; Ujita *et al*, 1999). Until now, secreted β 3GnT1 has not been observed using specific antibodies, but an N-acetyllactosamine (LacNAc)-modifying, β 1,3-N-acetylglucosaminyltransferase activity in human serum was already described in 1984 (Hosomi *et al*, 1984), which could be attributed to β 3GnT1. Indeed, β 3GnT1 was constitutively secreted from HEK293 cells (Fig. 4.31a).

Loss of SPPL3 led to an accumulation of intracellular β 3GnT1 and at the same time β 3GnT1 secretion was reduced (Fig. 4.31). Thus, β 3GnT1 secretion is affected by alterations in SPPL3 expression levels in a manner reminiscent of GnT-V and, hence, follows the model proposed for SPPL3's impact on GTs (Fig. 5.3). Importantly, also β 3GnT1 secretion is only slightly increased following SPPL3 over-expression, while the intracellular β 3GnT1 signal is strongly reduced, suggesting that, similar to GnT-V, β 3GnT1 may be subject to degradation following disengaged from its membrane anchor. Collectively, these observations support that β 3GnT1 is another newly identified SPPL3 substrate (even though the formal proof of this concept e.g. using an *in vitro* cleavage assay is currently missing).

Constitutive secretion of the galactosyltransferase β 4GalT1, like of GnT-V and β 3GnT1, was also found to be reduced in HEK293 cells following transfection with SPPL3-targeting siRNAs (Fig. 4.31c) and almost abolished in *Sppl3*-deficient MEFs (Fig. 4.31d). At the same time, the intracellular β 4GalT1 levels were elevated pointing to an intracellular accumulation of the holoprotein due to impaired proteolytic secretion. As for GnT-V and β 3GnT1, intracellular β 4GalT1 was reduced following SPPL3 over-expression in HEK 293. In sum, this points to β 4GalT1 being another endogenous Golgi GT that is a substrate of SPPL3. Cellular β GalT1 produces LacNAc and, in tandem with β 3GnT1, poly-LacNAc moieties (Ujita *et al*, 1999; 2000). Interestingly, there is also indication that β 3GnT1 and β 4GalT1 interact physically (Lee *et al*, 2009).

Taken together, SPPL3-mediated proteolysis of β 3GnT1 and β 4GalT1 could also hinder the physiological function of these GTs and thus likely contributes to the N-glycosylation phenotypes associated with SPPL3 over-expression or loss of SPPL3 expression. Furthermore, in light of β 3GnT1 and β 4GalT1 being involved in the formation of LacNAc and poly-LacNAc moieties that can also be found on mucin-type O-glycans and glycolipids, this may imply that SPPL3 could likewise interfere with the generation of these glycoconjugates.

5.3.1.4 Other glycan-modifying SPPL3 substrates and candidate substrates

The comparison of secretomes of SPPL3 over-expressing cells and control cells by quantitative proteomics revealed a number of candidate SPPL3 substrates (Tab. 4.2 and Fig. 4.33) that are also involved in cellular glycoconjugate anabolism and therefore could likewise contribute to the alterations in glycan composition associated with loss of SPPL3 expression or SPPL3 over-expression (see 5.3.1). Regarding cellular Golgi N-glycosylation these include β 1,2-N-acetylglucosaminyltransferase 1 (GnT-I, gene name: *MGAT1*) and α -mannosidase IIx (α -Man IIx, gene name: *MAN2A2*) that are both crucially involved in cellular N-glycosylation, the former being required for the generation of both hybrid and complex N-glycans, the latter being required for the generation of complex N-glycans (Schachter, 1991; Sears & Wong, 1998; Stanley *et al*, 2009). Secretion of ER Man I (gene name: *MAN1B1*) was likewise affected by

SPPL3 over-expression. Its name, however, is rather misleading as ER Man I is a type II membrane protein (Gonzalez *et al*, 1999) involved in targeting of ERAD substrates (Pan *et al*, 2011; Moremen *et al*, 2012) yet it localises to the Golgi network (Pan *et al*, 2011). In addition, the list of candidate substrates includes additional GTs such as the N-acetylglucosaminyltransferase exostosin-like 3 (EXTL3), β 1,4-galactosyltransferase 7 (β 4GALT7, gene name: *B4GALT7*), β 1,3-galactosyltransferase 6 (β 3GALT6, gene name: *B3GALT6*) and xylosyltransferase II (XT-II, gene name: *XYLT2*), which are all involved in GAG biosynthesis (Almeida *et al*, 1999; Götting *et al*, 2000; Bai *et al*, 2001), as well as the α 2,3-sialyltransferase VI (ST3GAL6, gene name: *ST3GAL6*). Finally, other GMEs, in particular several sulphotransferases were observed to be more abundantly secreted in SPPL3-over-expressing cells. Interestingly, all these candidate substrates brought up are (predicted) type II membrane proteins (Tab. 4.2) and localise to the Golgi compartment (Bai *et al*, 2001; Schön *et al*, 2006; Humphries *et al*, 1997; Pan *et al*, 2011). Collectively, the identification of these candidate SPPL3 substrates underscores the notion that SPPL3 facilitates proteolytic secretion of (primarily) Golgi-localised glycan-modifying type II membrane proteins.

5.3.1.5 *SPPL3 may serve as global cellular Golgi enzyme sheddase*

Taken together, SPPL3 emerges as novel sheddase of Golgi-localised GTs and GMEs. Indeed, there is strong evidence from *Sppl3* knockout MEFs that constitutive secretion of GnT-V is largely SPPL3-dependent (Fig. 4.26). Moreover, SPPL3 is capable of facilitating secretion of a variety of other Golgi-resident enzymes pointing to a fundamental function of SPPL3-mediated GME secretion in Golgi proteostasis (discussed in 6.2). It remains, however, to be worked out to what extent SPPL3 affects secretion of an individual GME and whether there is competition with other proteases, e.g. BACE1 (see 5.3.1.1).

Moreover, it has to be carefully tested, in principle for every individual substrate, that SPPL3 directly mediates endoproteolysis to exclude indirect effects of SPPL3, e.g. on intra-Golgi trafficking. In particular, future experiments should examine integrity of the conserved oligomeric Golgi (COG) complex as COG complex defects, e.g. in CDG patients, are well known to cause Golgi enzyme mis-localisation and alter cellular glycosylation (reviewed in (Reynders *et al*, 2011)).

5.3.2 Potential physiological implications of other newly identified SPPL3 substrates

This study unveiled several new (candidate) SPPL3 substrates implicated in very diverse cellular pathways (Tab. 4.2). Assuming that these proteins are genuine SPPL3 substrates and are endoproteolysed under physiological conditions, they could contribute to SPPL3's physiological functions. In the following, SPPL3's potential physiological role(s) in three distinct cellular pathways - the formation of (poly-)LacNAc-bearing N- and O-glycans (section 5.3.2.1), GAG biosynthesis (section 5.3.2.2) and O-mannosylation (section 5.3.2.3) - will be discussed. Furthermore, alterations in glycosylation may affect the individual function of the various cellular glycoproteins that are subject to such post-translational modifications (see section 5.3.2.4).

5.3.2.1 *SPPL3 may control integrity of the glycoprotein-galectin lattice*

Glycoprotein-linked mature N-glycans but also mucin-type O-glycans often harbour specific disaccharidic patterns, the LacNAc units (Gal β 1,4GlcNAc or Gal β 1,3GlcNAc) (Stanley & Cummings, 2009). On β 1,6GlcNAc N-glycan branches in particular, these units can be found as polymers, poly-LacNAc ([β -3Gal β 1,4GlcNAc β 1-]_n) (Dennis *et al*, 2009; Stanley & Cummings, 2009; Boscher *et al*, 2011). These structures are preferred binding sites for lectins, primarily for members of the galectin family, such as galectin-3 (Boscher *et al*, 2011). Galectins form a family of evolutionary conserved lectins. They are produced in the cytosol and are secreted via a non-conventional, ER-/Golgi-independent export pathway (Boscher *et al*, 2011). Interactions of multivalent galectins with their ligands, primarily branched, poly-LacNAc-bearing N-glycans on cell surface glycoproteins are considered to form a supramolecular lattice, the so-called glycoprotein-galectin lattice that fundamentally affects the motility and versatility of N-glycosylated cell surface membrane proteins, e.g. it restricts their oligomerisation, their recruitment into lipid raft membrane microdomains or their endocytosis (reviewed in (Dennis *et al*, 2002; Grigorian *et al*, 2009; Dennis *et al*, 2009; Boscher *et al*, 2011)). The glycoprotein-galectin lattice has received particular attention as it appears to be intricately linked to tumourigenesis (reviewed in (Lau & Dennis, 2008)) as well as T cell biology (reviewed in (Grigorian *et al*, 2009)) and is subject to nutritional regulation (Lau *et al*, 2007; Grigorian *et al*, 2007).

Interestingly, three GTs identified here as novel SPPL3 substrates are implicated in the generation of poly-LacNAc motifs. GnT-V catalyses the transfer of GlcNAc from the cellular UDP-GlcNAc donor to the C6 hydroxy group of the α 1,6-linked core mannose residue that is part of the cellular precursor of complex N-glycans (Cummings *et al*, 1982) and is thus crucial to the formation of tri- and tetraantennary N-glycans. N-glycans harbouring a GlcNAc β 1,2-(GlcNAc β 1,6)Man α 1,6 motif generated by enzymatic activities of both GnT-V and GnT-II, are preferentially extended by poly-LacNAcs (van den Eijnden *et al*, 1988; Ujita *et al*, 1999). LacNAc repeating units are added to GlcNAc β 1,2(GlcNAc β 1,6)Man α 1,6-carrying N-glycans (but also to mucin-type O-glycans) by the repetitive action of β 4GalT1 and β 3GnT1, leading to the formation of linear poly-LacNAc structures (Sasaki *et al*, 1997; Ujita *et al*, 1999; 2000). As SPPL3 can control the intracellular active pool of GnT-V, β 3GnT1 and β 4GalT1 and in this way affect the composition and structure of cellular glycans, it is conceivable that alterations in SPPL3 expression levels may also specifically alter a given cell surface glycoprotein's capacity to integrate into the glycoprotein-galectin lattice. Over-expression of the active protease interferes, for instance, with cellular GnT-V activity (Fig. 4.29) and can similarly be expected to reduce β 3GnT1 and β 4GalT1 activity, which would then result in a reduction of galectin binding to carbohydrates on the cellular glycoproteins. In contrast, loss or reduction of active cellular SPPL3 could lead to a higher abundance of galectin binding motifs, i.e. a higher affinity of the cellular N-glycan pool for the lattice. Presently, however, this is merely speculative and it remains to be examined whether alterations of SPPL3 expression levels really alter the cellular affinity for galectins. This could be tested by assessing for instance binding of labelled recombinant galectins to cells over-expressing or lacking SPPL3.

In particular, the newly identified SPPL3 substrate GnT-V has recently attracted strong attention as a crucial regulator of the glycoprotein-galectin lattice, in particular in the context of cellular malignancies and T cell biology (reviewed in (Lau & Dennis, 2008; Dennis *et al*, 2009; Grigorian *et al*, 2009)). Tumours, for instance, often display profoundly up-regulated *MGAT5* expression (Dennis *et al*, 2002; Lau & Dennis, 2008) and, in fact, expression levels may correlate with tumour metastatic potential and patient prognosis (Murata *et al*, 2000). In line with this, in an oncogene-driven mouse mammary tumour model, tumour growth and metastatic potential was reduced in *Mgat5*^{-/-} animals (Granovsky *et al*, 2000). GnT-V also negatively regulates T cell receptor (TCR) signalling by controlling the recruitment of the TCR and co-receptors into glycoprotein-galectin lattice (Demetriou *et al*, 2001; Lau *et al*, 2007) and loss of GnT-V was therefore associated with autoimmunity in mice (Demetriou *et al*, 2001; Lee *et al*, 2007). Therefore, it is particularly worthwhile to consider that due to its capacity to control GnT-V activity SPPL3 may functionally be tightly linked to such pathophysiological conditions.

5.3.2.2 *SPPL3 may affect glycosaminoglycan biosynthesis*

CAGs are linear, high-molecular weight polysaccharides with a disaccharidic repeating unit. As integral components of the extracellular matrix (ECM) they fulfil diverse physiological functions in multicellular organisms (Esko *et al*, 2009). Depending on the underlying disaccharide, a distinction is made between hyaluronan, dermatan sulphate (DS), keratan sulphate (KS), chondroitin sulphate (CS) (including several subtypes), and heparan sulphate (HS). Hyaluronan aside, which will not be considered here any further as it is synthesised via a completely distinct pathway (Hascall & Esko, 2009), CAGs are often highly sulphated and are found covalently attached to secreted or membrane-bound proteins, the so-called proteoglycans. KS is essentially a sulphated poly-LacNAc and, accordingly, is attached to proteoglycans via N-glycans or a mucin-type O-glycans (Esko *et al*, 2009). Its synthesis strictly relies on the formation of poly-LacNAc precursors (see 5.3.2.1) (Esko *et al*, 2009). In contrast, HS, CS, and DS are linked to proteoglycan serine residues via a tetrasaccharide linker (GAG-GlcA β 1,3Gal β 1,3Gal β 1,4Xyl β 1-Ser) (Sugahara & Kitagawa, 2002; Esko *et al*, 2009). Hence, biosynthesis of these types of GAGs occurs via a common cellular pathway (depicted in Fig. 5.5). Following completion of the tetrasaccharide linker synthesis of either HS or CS is initiated by distinct Golgi enzymes (Fig. 5.5).

Biosynthesis of sulphated GAGs is generally thought to occur predominantly within the *cis*/medial Golgi compartment as this is the cellular compartment in which most enzymes implicated in their biosynthesis reside (Sugahara & Kitagawa, 2002; Multhaupt & Couchman, 2012; Kreuger & Kjellén, 2012). It has, however, been somewhat controversial (see discussion in (Schön *et al*, 2006; Multhaupt & Couchman, 2012)) where exactly the first step - the xylosylation - occurs, but both exogenously expressed XylT1 and XylT2 appear to co-localise with α -Man II in the Golgi compartment (Schön *et al*, 2006). Similar findings were reported for β 3Galt6 (Bai *et al*, 2001), NDST1 (Humphries *et al*, 1997), the EXT1/EXT2 complex (McCormick *et al*, 2000), heparan sulphate 6-O sulphotransferases (Nagai *et al*, 2004), and others. Hence, like complex N-glycosylation, sulphated GAG biosynthesis is another crucial cellular process proceeding in the Golgi network that is executed by type II membrane proteins and could also be modulated

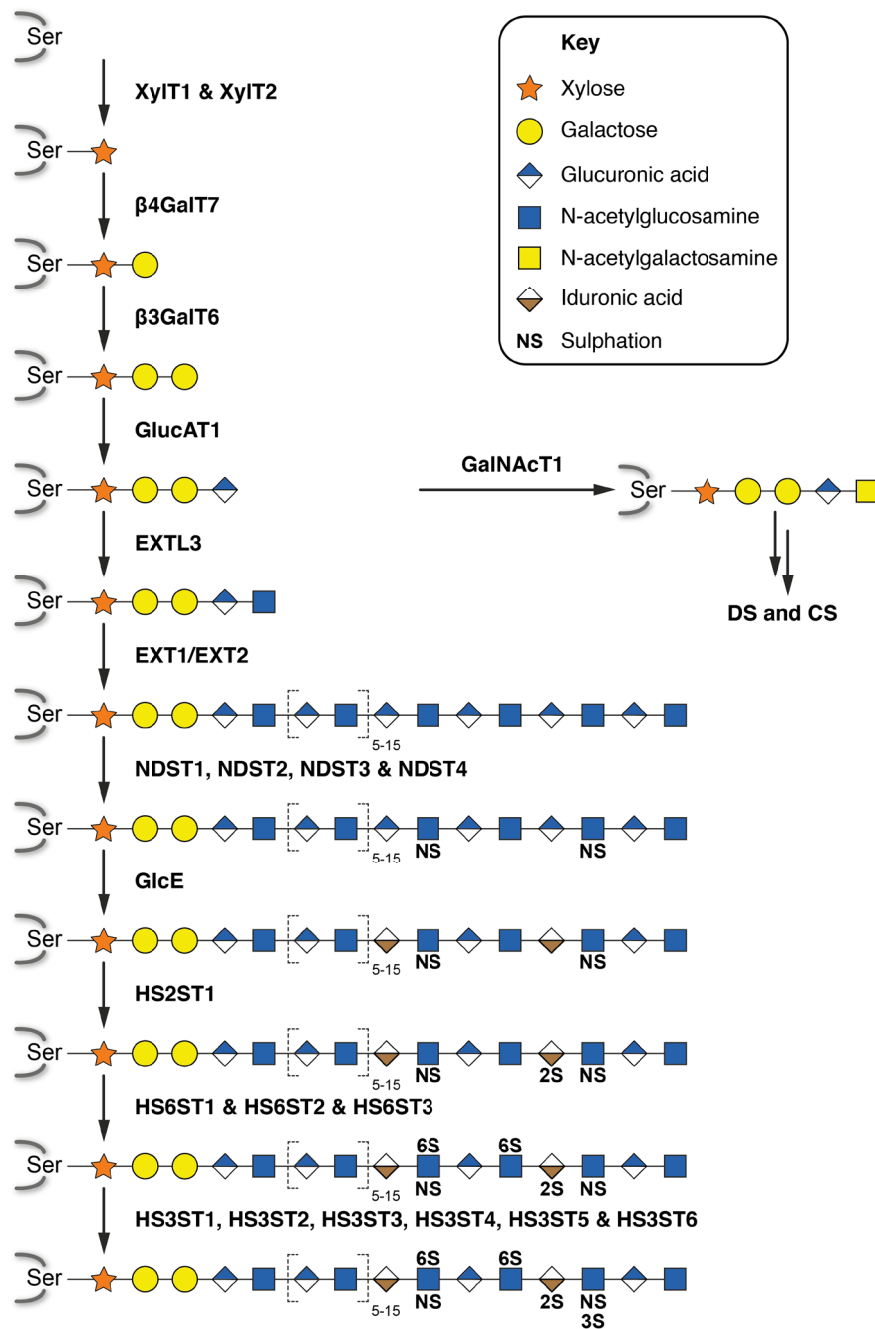


Fig. 5.5: Heparan sulphate biosynthesis. Biosynthesis of heparan sulphate (HS) as well as dermatan sulphate (DS) and chondroitin sulphate (CS) proceeds initially via a common pathway and diverges later. Initially, a tetra-saccharide linker is generated. A xylosyltransferase, of which there are two isoforms, XylT1 and XylT2, transfers a xylose to the proteoglycan's serine residue. Other sugar residues are then successively added by β 1,4-galactosyltransferase 7 (β 4GALT7, gene name: *B4GALT7*), β 1,3-galactosyltransferase 6 (β 6GALT6, gene name: *B6GALT6*) and finally by β 1,3-glucuronosyltransferase 3 (β 3GlcAT3, gene name: *B3GAT3*). The tetrasaccharide linker may then be subject to sub-stoichiometrical phosphorylation and/or sulphation by undefined kinases and sulphotransferases, respectively (not depicted). Depending on the enzyme acting next on the linker, biosynthesis of either CS/DS or HS is initiated. In case of the former, β 1,4-N-acetylgalatosaminyl transferase 1 attaches an N-acetylgalactosamine (GlcNAc) residue to the terminal glucuronic acid (GlcA). In contrast, the N-acetylglucosaminyltransferase exostosin-like 3 (EXT3, gene name: *EXTL3*) takes up HS biosynthesis by attaching α 1,4-linked GlcNAc. HS polymerisation is then performed by a co-polymerising heterodimeric enzyme complex of EXT1 and EXT2 that successively adds β 1,4-linked GlcA and α 1,4-linked GlcNAc to the nascent HS chain. In addition, the HS precursor is subject to GlcA epimerisation and extensive sulphation. Sulphation at C2 of GlcNAc residues is performed by the bifunctional heparan sulphate N-deacetylases/N-sulphotransferases (NDST) 1 (gene name: *NDST1*) or NDST1 isoforms, while distinct sulphotransferases catalyse sulphation at other sites. Adapted from (Sugahara & Kitagawa, 2002; Esko *et al.*, 2009).

by SPPL3 activity.

Indeed, the secretome analysis (see 4.4) supports this assumption. It revealed that, upon SPPL3 over-expression, a number of key enzymes implicated in the biosynthesis of CS (XylT2, β 4GalT7, β 3GalT6) and, even more strikingly, HS (XylT2, β 4GalT7, β 3GalT6, EXTL3, NDST1, NDST2 and HS6ST2) were more abundantly secreted, raising the possibility that SPPL3 facilitates their proteolytic secretion. While the identification of such a number of candidate substrates implicated in the very same cellular pathway is indeed surprising, it is unlikely that this is merely a coincidental finding. Rather, this underscores that HS biosynthesis might indeed be tightly controlled by SPPL3 activity. It should be directly assessed (e.g. with HS composition-specific antibodies (van Kuppevelt *et al*, 1998)) whether altered secretion of these enzymes associated with changes in SPPL3 expression translates into alterations in HS formation in cultured cells and *in vivo*.

There is conclusive evidence that HS biosynthesis is tightly regulated as there are, for instance, tissue-specific HS modification patterns (van Kuppevelt *et al*, 1998; Kreuger & Kjellén, 2012). It is unclear, however, by which mechanisms its regulation is ensured but several possibilities including regulation on a transcriptional level as well as sub-cellular localisation/targeting have been discussed (Kreuger & Kjellén, 2012; Multhaupt & Couchman, 2012). As for GTs (see 5.3.1.1), proteolytic liberation of membrane-anchored enzymes involved in HS biosynthesis is likewise a plausible mechanism by which this process could be concerted. Indeed, activity of enzymes involved in HS biosynthesis has already been reported in extracellular samples. For instance, xylosyltransferase activity was observed in conditioned supernatants of human dermal fibroblasts and in human and murine serum (Götting *et al*, 1999; Condac *et al*, 2009). It is attributed to secretion of XylT1 and XylT2 (Götting *et al*, 1999; Condac *et al*, 2009). As these proteins are expected to be membrane-anchored (Götting *et al*, 2000), their secretion is considered a proteolytic process. The protease(s) generating secreted variants thereof are unknown. Also, an enzyme with heparan sulphate 6-O sulphotransferase activity was purified from conditioned supernatants of CHO cells (Habuchi *et al*, 1995) and this arises from proteolytic cleavage in the luminal membrane proximal region of the type II membrane-anchored precursor (Nagai *et al*, 2007). One study reported a reduction in secretion of C-terminally GFP-tagged over-expressed HS6ST3 following treatment with a BACE1 inhibitor (Nagai *et al*, 2007). This finding is interesting as BACE1 has also been discussed to liberate sialyltransferases from their membrane anchors (see 5.3.1). Notably, however, the isoenzymes HS6ST2 (which was identified as a candidate SPPL3 substrate here) and HS6ST1 remained unaffected by inhibitor treatment and the authors failed to conclusively show that BACE1 directly acts on HS6ST3 (Nagai *et al*, 2007). Hence, their findings could likewise be explained by BACE1-independent effects of the inhibitor used. It is therefore crucial to verify the findings of the proteomic screen in order to firmly establish whether - and to what extent - SPPL3 mediates proteolytic release of enzymes implicated in the generation of sulphated GAGs under physiological conditions and what the consequences of altered GAG are.

5.3.2.3 *SPPL3* may affect O-mannosylation

Apart from N-glycosylation and mucin-type O-glycosylation, a variety other types of glycosylation are known, including the covalent attachment of mannose to Ser/Thr residues, the so-called O-mannosylation. Numerous studies have been conducted to unravel the cellular pathway leading to O-mannosylation of α -dystroglycan, since disruptions in this pathway are linked to congenital muscular dystrophies (CMDs) in humans (Barresi & Campbell, 2006; Dobson *et al*, 2013). Clinically, CMDs are rather heterogenous ranging from patients presenting with mild muscle wasting that does not lower life expectancy to patients suffering from Walker-Warburg syndrome (WWS), a condition diagnosed in new-borns that is characterised by severe developmental defects such as neurological and ophthalmological abnormalities and a life expectancy of usually only a few months after birth.

α -dystroglycan is part of a multi-protein complex, the dystrophin-glycoprotein complex, that links structural ECM components of the basal lamina to the cellular cytoskeleton (Barresi & Campbell, 2006; Dobson *et al*, 2013). α -dystroglycan associates non-covalently with the membrane-spanning β -dystroglycan which in turn is tethered to the actin network. Development of mice lacking α - and β -dystroglycan is severely compromised and ceases early *in utero* underscoring its physiological importance (Williamson *et al*, 1997). α -dystroglycan is heavily glycosylated, predominantly by O-mannosylation, and the interaction of ECM proteins such as laminin with α -dystroglycan is strictly dependent on this post-translational modification (Barresi & Campbell, 2006; Dobson *et al*, 2013). O-mannosylation is initiated by ER-resident mannosyltransferases which transfer a mannose residue from a dolichol-linked precursor to a Ser/Thr residue. O-linked mannose is then subject to further modifications in the Golgi apparatus.

In this study, two enzymes implicated in protein O-mannosylation were identified as candidate *SPPL3* substrates. On the one hand, Sgk196 secretion was found to be elevated > 7-fold following *SPPL3* over-expression in HEK293 cells (Tab. 4.2). This observation could be reproduced by Western blotting and *SPPL3* over-expression was also accompanied by a reduction in intracellular Sgk196 levels (Fig. 4.36g). Sgk196 presumably matches *SPPL3*'s substrate requirements as sequence analysis predicts a type II topology. It remains, however, to be tested whether Sgk196 is also secreted in an *SPPL3*-dependent fashion under physiological conditions. This is indeed needed as Sgk196 likely resides in the ER (Yoshida-Moriguchi *et al*, 2013). In contrast, it was also conclusively shown that secretion of β 3GnT1 is dependent on endogenous levels of *SPPL3* (see 5.3.1.3). Notably, both Sgk196 and β 3GnT1 have only recently been linked to α -dystroglycan O-mannosylation when mutations in *SGK196* (Jae *et al*, 2013) and *B3GNT1* (Buysse *et al*, 2013; Shaheen *et al*, 2013), respectively, were uncovered in families with WWS-afflicted patients. While it was meanwhile demonstrated that *SGK196* encodes a kinase that generates 6-O-phosphorylated mannose within the core laminin-binding glycan moiety of α -dystroglycan (Yoshida-Moriguchi *et al*, 2013), the role of β 3GnT1 in O-mannosylation remains elusive. Interestingly, also GnT-V was recently shown to contribute to some extent to β 1,6-GlcNAc branching of O-mannosyl glycans in brain (Lee *et al*, 2012). To establish that *SPPL3* controls cellular O-mannosylation via GT/GME shedding, it has to be examined whether alterations in *SPPL3* expression levels also lead to changes in O-

mannosylation patterns, for instance using α -dystroglycan glycoepitope-specific antibodies, and whether this also has functional consequences regarding in particular dystrophin-glycoprotein complex integrity and cell-basal membrane interactions.

5.3.2.4 Effects on the biological activity of cellular glycoproteins

It is important to bear in mind that glycosylation is a very common cellular post-translational modification. Numerous proteins are modified by glycans and, in many cases, their biological function is markedly affected by or dependent on the nature, i.e. the stereochemical composition, of these glycans (Ohtsubo & Marth, 2006; Marth & Grewal, 2008; Dennis *et al*, 2009; Moremen *et al*, 2012). Hence, in addition to the cellular pathways discussed in the previous section, alterations in SPPL3 expression levels and the concomitant changes in glycosylation could - in principle - affect the physiological function(s) of many cellular glycoproteins.

There is abundant body of evidence that altered glycosylation may interfere with or alter a given glycoproteins physiological function. The cell adhesion molecule N-cadherin, for instance, mediates cell-cell adhesion and is post-translationally modified by N-glycosylation at several NxS/T sites (Guo *et al*, 2009). Interestingly, N-cadherin-dependent cell-cell adhesion and outside-in signalling are strongly affected by N-alterations in N-glycan composition, e.g. by changes in the extent of GnT-V-mediated β 1,6GlcNAc branching (Guo *et al*, 2003; 2009). Elevated GnT-V levels, for instance, led to decreased cell adhesion in a cell culture model (Guo *et al*, 2003), an effect that may be in part responsible for GnT-V's role in tumour invasiveness. Here, it was demonstrated that SPPL3 clearly alters the extent of N-glycosylation of N-cadherin (Figs. 4.16 to 4.20), therefore SPPL3 could also regulate N-cadherin function. In addition, other glycosylated proteins may likewise be affected in their physiological functions by SPPL3.

5.3.3 *Sppl3* deficiency in mice

Animals models often are very useful to elucidate the physiological function of a gene product of interest. Only recently, for example, *Sppl2a* knockout mouse models revealed previously unknown roles of this I-CLIP in B lymphocyte development (Schneppenheim *et al*, 2013; Beisner *et al*, 2013; Bergmann *et al*, 2013). Accordingly, such models could similarly be helpful to study SPPL3's *in vivo* function and to examine the potential physiological implications of SPPL3-mediated processing of substrates identified here (section 5.2 & 5.3). As discussed earlier (section 5.3.1), this study revealed that loss of SPPL3 causes hyperglycosylation *in vivo*. Therefore, the key question is whether and to what extent the hyperglycosylation contributes to or accounts for the phenotypic abnormalities associated with loss of murine *Sppl3*, specifically NK cell deficiency (5.3.3.2), male infertility (5.3.3.3) and the apparently strain-dependent problems in embryonic or early post-natal development (5.3.3.4).

5.3.3.1 General considerations

Proteases exhibit proteolytic activity towards a number of distinct substrates *in vivo* - the entire substrate repertoire of a given protease being referred to as substrate degradome (López-Otín & Overall, 2002). A major challenge, therefore, is to attribute phenotypic abnormalities caused

by e.g. knockout of a protease of interest to impaired proteolytic processing of a certain substrate within the substrate degradome of that particular protease. The vast number of candidate SPPL3 substrates identified (see 5.2), however, might complicate analysis of the molecular mechanisms underlying phenotypic abnormalities in *Spp3*^{-/-} mice. While this study at the same time provides evidence that impaired proteolytic processing of GnT-V, β 3GnT1 and β 4GnT1 contributes to the hypoglycosylation phenotype associated with loss of *Spp3*, it can presently not be excluded that phenotypic abnormalities are entirely independent of SPPL3's effect on glycosylation and relate back to impaired processing of other, non-GT/GME substrates.

Another obstacle is that, considering substrate biological function(s), knowledge of such is often based on animal models or other model systems deficient in substrate expression and/or bioactivity. This similarly applies to the glycobiology field, in which on the one hand several mouse lines have been generated that lack enzymes implicated in glycan biosynthesis (reviewed in (Lowe & Marth, 2003; Sarrazin *et al.*, 2011; Dobson *et al.*, 2013)) and on the other hand clinical human CDG models are at hand (Hennet, 2012). While such models allow crucial insight into a given substrate's biological function, they cannot directly be phenotypically compared to the *Spp3*-deficient mouse line used here as lack of *Spp3* is expected to result in blocked substrate turnover and concomitant substrate accumulation. Hence, *Spp3* deficiency will likely rather mimic substrate over-expression. Therefore, mice lacking *Spp3* may potentially phenocopy transgenic over-expression models of certain GT substrates, yet only few such models are available for direct comparison and parallel analysis.

5.3.3.2 NK cell deficiency

Initial in-depth characterisation of a *Spp3* genetrap mouse line established that both male and female homozygous *Spp3* knockout mice display reduced NK cell numbers when kept on a mixed background (Tang *et al.*, 2010). Using the established NK cell markers CD49b and NKp46 (Arase *et al.*, 2001; Walzer *et al.*, 2007), substantially reduced numbers of CD49b⁺ NKp46⁺ mature NK cells were detected in spleen and lymph node homogenates of *Spp3*^{-/-} animals compared to controls (Fig. 4.15) and, hence, the observations of Tang *et al.* could be reproduced. When kept under specific pathogen-free housing conditions, NK cell deficiency appears to be relatively well tolerated *in vivo* as *Spp3*^{-/-} animals can survive into adulthood. As NK cells are effector cells of the innate immune system equipped to combat viral infections and malignancies (Vivier *et al.*, 2008), an open question is how animals lacking *Spp3* can cope with such challenges in an experimental setting.

Mature NK cells are of lymphoid origin, i.e. they ultimately derive from haematopoietic stem cells that eventually differentiate into committed NK cell precursors in the bone marrow (reviewed in (Di Santo, 2006; Huntington *et al.*, 2007; Yu *et al.*, 2013)). There, but also in extra-medullary tissues, NK cell precursors develop into mature, CD49b⁺ NKp46⁺ NK cells which then reach peripheral tissues and, upon proper stimulation, exert their effector functions (e.g. cytotoxicity and cytokine release) (Huntington *et al.*, 2007; Yu *et al.*, 2013).

Therefore, either differentiation of progenitors into mature NK cells is interrupted or homeostasis of mature NK cells is severely disturbed in *Spp3*-deficient mice. Of note, the severity of NK cell

deficiency observed in *Sppl3* knockouts is well comparable with for example mice lacking IL-15 (Kennedy *et al*, 2000), a key cytokine during NK differentiation (Yu *et al*, 2013). It is therefore of particular interest, to examine NK cell function and specifically NK cell development in more detail in the *Sppl3* genetrap mouse line. Additional cell surface markers (e.g. CD122, CD117, CD127 and NKG2D) that allow for detection of and discrimination between committed NK cell precursors and immature NK cells in the bone marrow by multi-colour flow cytometry could be employed to assess whether such developmental intermediates exist under *Sppl3*^{-/-} conditions. Also, parallel *in vitro* differentiation of *Sppl3*^{+/+} and *Sppl3*^{-/-} bone marrow progenitors into mature NK cells (Williams *et al*, 1999; Fathman *et al*, 2011) could allow to elucidate potential disturbances due to the loss of *Sppl3*.

Another pressing question is what the physiological role of SPPL3 in NK cells or NK cell precursors is and how its loss leads to the drastic reduction in NK cells numbers observed. Data showing an elevated expression of murine *Sppl3* in NK cells compared to other tissues and blood cell populations⁷ argue against an essential function of stromal cell SPPL3 expression during NK cell development but rather point to an important NK cell-intrinsic function of murine *Sppl3* during NK cell development or in homeostasis of mature NK cells. In that regard, it needs to be examined whether SPPL3's role in NK cell biology is linked to its function as regulator of glycosylation. Not unexpectedly, many NK cell-specific surface molecules are glycosylated and their glycosylation appears to be of functional relevance (McCoy & Chambers, 1991). In fact, human NK cells feature a glycosylation pattern distinct from that of other peripheral blood cells as assessed by binding of plant lectins: *Maackia amurensis* lectin that displays binding specificity for α 2,3-sialylated LacNAc moieties (Knibbs *et al*, 1991) strongly binds NK cells (McCoy & Chambers, 1991) whereas *Erythrina cristagalli* lectin that binds asialo-Gal β 1,4GlcNAc structures (Teneberg *et al*, 1994) neglects NK cells (Harris *et al*, 1987; McCoy & Chambers, 1991). Interestingly, the degree of sialylation of individual NK cell receptors has been subject to investigation recently and seems to be of functional importance (Margraf-Schönfeld *et al*, 2011; Bar-On *et al*, 2013). Taken together, this could imply that NK cells require fine-tuned sialylation of their cell surface receptors for proper development and function. It is possible that this can be achieved by regulating SPPL3 expression, assuming that SPPL3 could control the extent of sialylation (e.g. by endoproteolysing sialyltransferases such as ST3Gal6, a candidate substrate identified here, Tab. 4.2, or by affecting GnT-V-mediated GlcNAc branching and hence indirectly the abundance of sialylation sites). Alternatively, it is conceivable that SPPL3 exerts a pivotal function independent of its effect on glycosylation and GTs, i.e. by endoproteolysing other type II membrane proteins crucially required in NK cell progenitors or NK cells.

5.3.3.3 Male infertility

On a mixed background, no offspring is obtained from *Sppl3*^{-/-} males suggesting that loss of *Sppl3* leads to male infertility (Tang *et al*, 2010). Obviously, future experiments need to follow up on this phenotypic abnormality to elucidate why and how loss of *Sppl3* compromises male

⁷ available online via www.biogps.com and <http://www.immgen.org/databrowser/index.html>, queried by "SPPL3".

fertility. In principle, disturbances in spermatogenesis but also in downstream processes including epididymal maturation, capacitation and motility of spermatozoa but also their egg-binding and egg-fusion capacity are conceivable explanations for this phenotype.

Interestingly, however, a considerable body of evidence suggests that glycosylation plays a fundamental role during spermatogenesis in mammals (reviewed in (Benoff, 1997)), raising the possibility that alterations in glycosylation associated with *Spp3* inactivation can be considered responsible for the infertility phenotype. In male *Mgat2* knockout mice that lack complex N-glycans, for instance, no spermatozoa were found in testicular seminiferous tubules and spermatogenesis ceased at the spermatocyte stage pointing to a crucial role of either GnT-II or complex N-glycosylation in spermatogenesis (Wang *et al*, 2001). Following spermatogenesis, spermatozoa pass through and mature in the epididymis and this is accompanied by remodelling of surface N-glycans (Benoff, 1997; Tulsiani, 2006). Interestingly, the epididymal luminal fluid was reported to be rich in soluble GTs and sugars and it was hypothesised - contrasting with the general assumption that secreted GTs are inactive in bodily fluids (see 5.3.1.1) - that secreted GTs enriched in the epididymal luminal fluid have a fundamental physiological function and act catalytically on maturing spermatozoa to remodel their surface glycans (Tulsiani, 2006). This is particularly interesting in light of SPPL3's role in proteolytic GT secretion (see 5.3.1). Accordingly, loss of *Spp3* would preclude GT secretion into the epididymal lumen and, in line with the aforementioned hypothesis, this could lead to impaired spermatozoan maturation and infertility. Interestingly, catalytic activity attributed to secreted xylosyltransferase (*XylT2* being likely a SPPL3 substrate, Tab. 4.2 & Fig. 3.36) was also described in seminal plasma of healthy human donors, but was significantly reduced in infertile men (Götting *et al*, 2002).

In addition to spermatogenesis, another essential step during fertilisation, the binding of a spermatozoon to an oocyte, is similarly dependent on cell surface glycosylation (reviewed in (Benoff, 1997)). A factor implicated in mediating sperm-oocyte binding is the galactosyltransferase β 4GalT1: Spermatozoa exclusively express a unique long β 4GalT1 isoform that is, unlike the commonly expressed short isoform (Roth & Berger, 1982), present on the cell surface where it engages in a lectin-like fashion as cell adhesion molecule that mediates binding to the oocyte zona pelucida glycans. The exact significance of this interaction *in vivo* is, however, not entirely clear. Sperm from mice lacking β 4GalT1 displays a reduced acrosome reaction *in vitro* but *B4galT1*^{-/-} males are still fertile (reviewed in (Shur *et al*, 2006)). Interestingly, β 4GalT1 is also a novel candidate SPPL3 substrate (Fig. 31c) and can consequently be expected to accumulate in cells lacking SPPL3. Elevated β 4GalT1 levels in spermatozoa also restrain egg binding due to precocious acrosome reactions (Youakim *et al*, 1994). This could likewise explain the observed infertility in *Spp3*^{-/-} mice.

Taken together, the exact mechanism underlying the male infertility associated with loss of *Spp3* in mice remains to be elucidated. However, mammalian fertilisation seems to rely heavily on tightly controlled cell surface glycosylation, a process that may be subject to regulation by SPPL3.

5.3.3.4 Strain-dependency of the *Sppl3* knockout phenotype

On a mixed B6;129S5 background, homozygous animals of the previously described *Sppl3* genetrap mouse line display the phenotypic abnormalities described in sections 5.3.3.2 and 5.3.3.3 (Tang *et al*, 2010). Importantly, however, *Sppl3*^{-/-} offspring on this particular genetic background is not obtained at expected Mendelian ratios (see 4.3.1) pointing to potential difficulties during embryonal or early postnatal development linked to loss of *Sppl3* expression, a notion supported by the early of expression *sppl3* mRNA in zebrafish embryos (Krawitz *et al*, 2005). Moreover, when crossed back into the C57BL/6 background, no viable *Sppl3*^{-/-} mice were obtained from matings of heterozygous males with heterozygous females (see 4.3.1), clearly indicating that the phenotype associated with loss of *Sppl3* is strain-dependent - which is a general caveat of inbred mouse models (Ermann & Glimcher, 2012). Therefore, in order to entirely dissect the *Sppl3*^{-/-} phenotype, more elaborate animal studies are required. First, mice carrying the *Sppl3* genetrap insertion should be crossed into other inbred backgrounds. Previous observations for instance suggest that the 129S5 background harbours protective alleles (see 4.3.1), but the effects of loss of SPPL3 expression should similarly be assessed in other inbred mouse strains as this could uncover additional important physiological functions of SPPL3. Also, information on the nature of such protective alleles could provide crucial insight, in particular since the hypoglycosylation phenotype appears to be independent of the genetic background used as it was encountered both in living *Sppl3*^{-/-} mice on a B6;129S5 background but also in MEFs obtained from *Sppl3*^{-/-} embryos of a mouse line crossed back to the C57BL/6 background. Second, development of *Sppl3*-deficient embryos *in utero* should be carefully followed, in particular in B6.129S5 mice, to determine which developmental processes or pathways are defective due to lack of SPPL3 expression and how this leads to embryonic or early post-natal lethality.

Interestingly, similar to the observations made here for *Sppl3*, phenotypes of mouse lines deficient in genes implicated in complex N-glycosylation seem to be often critically dependent on the (inbred) mouse strain used. Strain-dependent severity and nature of phenotypic abnormalities was reported for instance for mice deficient in *Mgat5* (Dennis *et al*, 2002; Lee *et al*, 2007). Another particularly interesting example is a mouse model that lacks complex N-glycans due a deficiency in *Mgat2*, which codes for GnT-II (Wang *et al*, 2001). *Mgat2*-deficient embryos were found at lower frequencies than expected *in utero* and born mice died early postnatally due to severe gastrointestinal, haematological and osteogenic abnormalities (Wang *et al*, 2001). When crossed into an outbred mouse strain, however, *Mgat2*-deficient mice lived much longer, however, like *Sppl3*^{-/-} mice on a mixed background, male *Mgat2*^{-/-} mice failed to generate mature spermatids and were found to be infertile (Wang *et al*, 2001). Taken together, there appear to be interesting parallels between such glycosylation mouse models and *Sppl3*-deficient mice.

5.3.3.5 Other SPPL3 *in vivo* models

Orthologues of human SPPL3 are highly conserved in many multicellular eukaryotes (Fig. 1.9). Apart from murine *Sppl3* ((Tang *et al*, 2010) and this study), however, the physiological

functions of *SPPL3* orthologues have presently only been under investigation in zebrafish and in *Drosophila*.

In zebrafish, *sppl3* mRNA is ubiquitously expressed during early embryonal developmental stages, even before onset of zygotic transcription suggesting maternal inheritance (Krawitz *et al*, 2005). To elucidate *sppl3*'s role during embryonal development antisense technology was used to reduce endogenous *sppl3* expression levels (Krawitz *et al*, 2005). *sppl3* knockdown led to a phenotype characterised by neuronal cell death in brain and spinal cord (Krawitz *et al*, 2005). This supports the previously discussed notion of a pivotal role of *SPPL3* during embryonal development (see 5.3.3.4). It is presently unclear whether reduction of cellular *SPPL3* activity also alters N-glycosylation in zebrafish and whether this accounts for the phenotypic observation. Knowledge of glycosylation pathways in zebrafish is rather scarce, but, in principle, complex N-glycosylation occurs (Guérardel *et al*, 2006).

Insect genomes also harbour a conserved orthologue of human *SPPL3* referred to as *sppL* (Casso *et al*, 2005; 2012) but loss of this gene was phenotypically inapparent (Casso *et al*, 2012). This contrasts with the previously discussed studies in mice and zebrafish. Hence, either a phenotype has so far been overlooked or more rigorous phenotypic characterisation of *sppL*-deficient flies is required (e.g. looking into glycosylation patterns). Alternatively, *sppL*'s function in *Drosophila* may not be as fundamentally required as in vertebrates. In that regard it is important to note that, while *Drosophila* can in principle synthesise complex N-glycans, such structures can only be detected in trace amounts and the *Drosophila* glycome is dominated by high-mannose- and paucimannose-type N-glycans (North *et al*, 2006). Hence, unlike vertebrates in which complex N-glycans prevail, insects appear to lack substantial amounts of triantennary, (poly-)LacNAc-modified glycans that are affected by changes in *SPPL3* expression in vertebrates. This, in turn, could explain the discrepancy between arthropod and vertebrate models deficient in *SPPL3*.

5.4 How is *SPPL3* activity regulated?

This study provides an initial insight into the cellular and physiological function(s) of *SPPL3* and identifies first physiological substrates of this protease. This, however, inevitably raises the question of how *SPPL3* activity is regulated.

Unlike other post-translational modifications, proteolysis is an irreversible process and, hence, has to be tightly controlled in a physiological context. Nature has evolved a myriad of mechanisms to control protease activity, including regulation of protease gene expression, the production of protease zymogens, the expression of endogenous protease inhibitors and many others (reviewed in (Turk *et al*, 2012)). This study revealed that, unlike other mammalian GxGD proteases, *SPPL3* catalyses endoproteolysis of full-length substrates and, thus, this process appears not to be regulated in a cascade-like fashion by a preceding proteolytic cleavage as described earlier (see 1.1). The fundamental implication of this is that *SPPL3* may in principle be constitutively active towards its substrates. A pressing question therefore is how *SPPL3* activity is regulated.

In light of its capability to endoproteolyse full-length membrane proteins, *SPPL3* bears strong resemblance to rhomboids (see 5.1.5.5). These particular I-CLiPs are likewise constitutively

active and liberate membrane protein ectodomains from their TMD anchors. Nonetheless their activity is tightly regulated by compartmentalisation in *Drosophila* (Fig. 5.7). Active *Drosophila* rhomboid-1, for example, resides in the Golgi compartment. Its substrate, the EGFR ligand Spitz, is, however, actively retained in the ER, i.e. it is not accessible to the active rhomboid. Only upon expression of Star, another membrane protein, Spitz is trafficked to the Golgi. There, it is cleaved off its membrane anchor by rhomboid-1 and is subsequently secreted (reviewed in (Urban, 2006; Freeman, 2008)). A similar mechanism of regulation could likewise be employed to ensure controlled activity of SPPL3. Interestingly, the observation that distinct candidate SPPL3 substrates are differentially affected by either SPPL3 knockdown or over-expression points to a certain importance of SPPL3's sub-cellular localisation in determining whether and to what extent a given substrate is endoproteolysed by SPPL3.

While SPPL3 appears to be constitutively expressed, microarray datasets show that there is a certain degree of variation in the expression profile of *SPPL3* (Friedmann *et al*, 2004)⁸, which is exemplified by the higher abundance of *Spp3* mRNA in murine NK cells compared to other lymphocyte populations and tissues (see 5.3.3.2). This suggests that expression of *SPPL3* may indeed be subject to regulation on the transcriptional or post-transcriptional level. Future efforts should therefore be directed at identifying potential transcription factor binding sites conserved in *SPPL3* promoter regions or binding sites of regulatory factors within *SPPL3* mRNA untranslated regions.

Moreover, there is indication that SPPL3 could itself be subject to post-translational modification. In cultured human and murine cells, SPPL3-directed mAbs reliably detect a small molecular weight fragment of SPPL3 that accumulates following inhibition of lysosomal

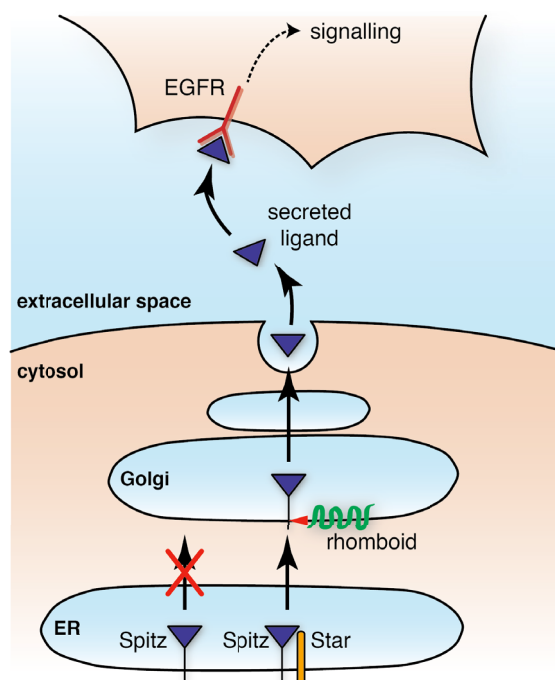


Fig. 5.7: Rhomboid activity is regulated by sub-cellular compartmentalisation. In the absence of Star, the *Drosophila* EGFR ligand Spitz is retained in the ER. Only upon encounter with Star, Spitz reaches the Golgi. There it is endoproteolysed by rhomboid-1, secreted and initiates EGFR signalling in a target cell (top). Adapted from (Freeman, 2008).

⁸ More detailed microarray data are available online via <http://www.biogps.com> and <http://www.immgen.org/databrowser/index.html>, queried by "SPPL3".

acidification (Fluhrer *et al.*, unpublished). The abundance of this fragment - in particular in relation to full-length SPPL3 detected with the very same mAbs in parallel - appears to be different in distinct murine tissue homogenates analysed. A possible explanation for these observations is that the cellular pool of active SPPL3 could be controlled by the holoprotein's lysosomal degradation. Given its nature as multi-pass membrane protein, this could proceed via an ubiquitin- and ESCRT-dependent recruitment into endocytic multivesicular bodies, the primary site of the cell's membrane protein degradative machinery (Hanson & Kashikar, 2012), but this requires experimentally verification.

5.5 Does SPPL3 have a role in Golgi proteostasis?

SPPL3 is highly conserved (Fig. 1.9) and, hence, likely fulfils a very pivotal cellular function. The identification of individual GTs and GMEs as novel SPPL3 substrates and the alterations in glycosylation following reduction or elevation of SPPL3 levels in an experimental setting obviously raise the possibility that the cell can control specific aspects of glycan biosynthesis, for example the extent of GlcNAc branching via SPPL3-mediated GnT-V endoproteolysis. Astonishingly, however, employing a proteomics approach, this study does not solely identify selected individual GTs as novel SPPL3 substrate. On the contrary, the list of newly identified (candidate) SPPL3 substrates includes a multitude of mostly Golgi-localised GTs and GMEs (but also other Golgi-localised proteins) and is certainly not yet complete. In fact, this study fails to identify any GT or GME of which secretion is not affected by SPPL3 (a possible candidate being fucosyltransferase VII that is not secreted (Grabenhorst & Conradt, 1999; de Vries *et al.*, 2001; El-Battari *et al.*, 2003)). Together with the wide-spread phenomenon of proteolytic secretion among most post-ER-localised glycan-modifying enzymes (Paulson & Colley, 1989; Varki *et al.*, 2009) and the lack of a known and generally accepted physiological function of their secreted ectodomains, this can also imply that SPPL3 may fulfil a rather general function within the Golgi cisternae.

In an eukaryotic cell, the Golgi network is integral part of the secretory pathway and serves as central hub that receives protein and lipid input cargo from the ER, post-translationally processes these macromolecules and orchestrates their ultimate intracellular targeting (Mellman & Simons, 1992). In spite of the Golgi's first description more than 100 years ago, key aspects of Golgi biology - in particular how protein cargo is trafficked from *cis* Golgi through the organelle to the TGN and at the same time organelle-resident enzymes are kept in place - are presently not completely understood (discussed in (Glick & Luini, 2011; Morriswood & Warren, 2013)) and new models such as the recently proposed *rim progression* model (Lavieu *et al.*, 2013) keep emerging. In fact, recent observations suggest that several Golgi trafficking modes exist in parallel and that it depends on the nature of the respective cargo which route of trafficking within the Golgi is used (Beznoussenko *et al.*, 2014).

GTs and other type II-oriented GMEs constitute the majority of Golgi-resident proteins that catalytically act on the transiting cargo. Interestingly, they are arranged in an orderly fashion within the polarised Golgi stack that corresponds well with the order in which these individual enzymes act on their glycan substrates, e.g. N-acetylglucosaminyltransferase involved in GlcNAc branching reside in the *medial* and/or *trans* Golgi whereas most sialyl- and

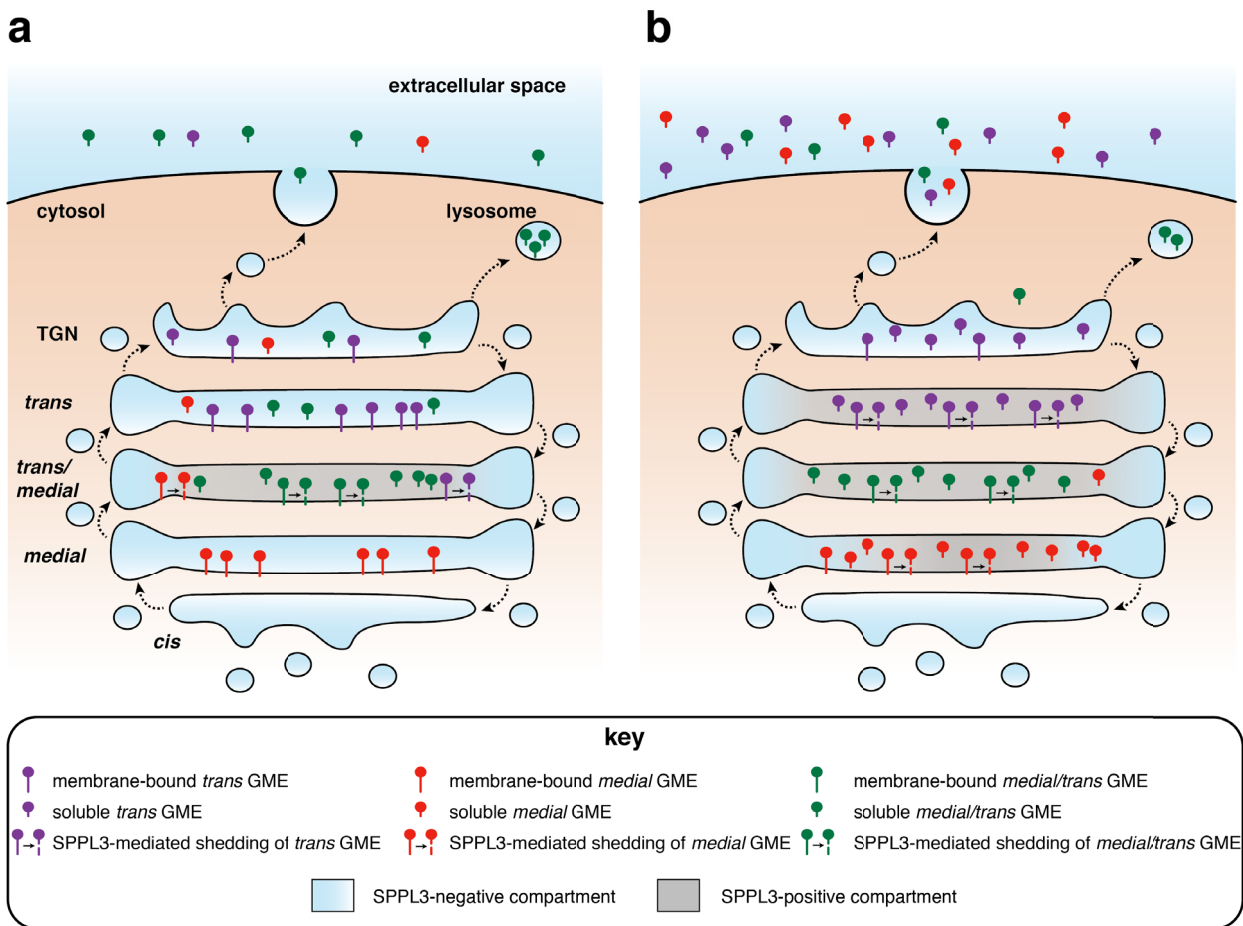


Fig. 5.8: Model of SPPL3's function within the Golgi complex. To explain the differential effects of endogenous and over-expressed SPPL3 on distinct Golgi-resident GMEs the existence of a SPPL3-enriched Golgi sub-compartment is proposed. Under physiological conditions (a), this could explain why only a certain fraction of GMEs (such as GnT-V or other *medial/trans* Golgi GTs) is affected by SPPL3-mediated endoproteolysis. This would for instance restrict intra-Golgi trafficking (e.g. of *cis* GMEs). Whether and how such an SPPL3-enriched sub-compartment can be reconciled with current Golgi models remains to be established. On condition of SPPL3 over-expression (b), it can be assumed that localisation of exogenous SPPL3 is less well restricted and, hence, SPPL3 may encounter other Golgi GMEs (such as *trans* or *cis* GMEs) more readily leading to much more pronounced secretion of such factors. Intra-Golgi and post-Golgi vesicular trafficking is indicated by dashed arrows.

fucosyltransferases that catalyse terminal glycan modifications are found in the TGN (Colley, 1997; Tu & Banfield, 2010). In fact, it is well established that these enzymes harbour intrinsic determinants mapping to their CTS region that govern their steady-state localisation within the respective Golgi sub-compartment, the exact underlying mechanisms that ensure sub-compartment-specific protein targeting and retention, however, are still under debate and none of the in-depth characterised targeting motifs can explain global GT and GME localisation⁹ (Colley, 1997; Tu & Banfield, 2010). Of note, the length of a membrane protein's TMD appears to be a strong determinant of its sub-cellular localisation and TMDs of Golgi-resident factors are generally shorter than those of for instance plasma membrane proteins (Sharpe *et al*, 2010). In addition, proper Golgi localisation can also be ensured by protein-protein interactions via the GTs' N-terminal cytosolic domain. In yeast, for instance, the majority of Golgi-localised GTs

⁹ Also, Golgi retention is not an absolutely insurmountable barrier as cell surface expression of Golgi enzymes is also observed (reviewed in (Berger, 2002).)

interact with Vps74p via their N-termini and Vps74p mediates retention of such enzymes in the Golgi (Tu *et al.*, 2008).

Another feature of GTs and GMEs that is defined by determinants residing in their CTS regions is whether they are subject to endoproteolysis (Grabenhorst & Conradt, 1999). Disengagement of GTs and other GMEs from their membrane anchors essentially excludes the ectodomain cleavage products from the reach of the machinery that ensures proper Golgi protein targeting and retention (see above). Accordingly, they can be secreted or intracellularly degraded. Hence, SPPL3 activity may in fact control Golgi proteostasis by mediating GT and GME shedding, i.e. catalysing the first (and possible rate-limiting) step of their disposal. In theory, a Golgi sub-compartment enriched in SPPL3 (Fig. 5.8a), for instance, may serve such a purpose by initiating disposal of mal-sorted or corrupt proteins. This would limit intra-Golgi trafficking of such enzymes and control functional Golgi sub-compartmentalisation. This assumption, however, requires proper validation and it has to be assessed how this can be reconciled with the current understanding of Golgi trafficking.

The vast number and diversity of candidate SPPL3 substrates identified here demonstrates that many Golgi-resident factors harbour in principle an intrinsic susceptibility to SPPL3-mediated processing. At the same time, however, these substrates are differentially affected by SPPL3 knock-down or over-expression (see 5.2.4) and this could be due to the exact sub-cellular co-localisation of both substrate and protease. In particular an irregular Golgi sub-compartmental localisation of SPPL3 on conditions of its over-expression (see 5.2.3) could very well explain why the protease encounters and cleaves substrates that are hardly affected by endogenous SPPL3 (Fig. 5.8b). To test this hypothesis, subsequent studies should exactly define the sub-cellular compartment harbouring endogenous and over-expressed SPPL3, ideally by immunocytochemistry and biochemical cell fractionation. In parallel, sub-cellular localisation of the numerous newly identified Golgi substrates of SPPL3 should be examined and in particular it needs to be tested whether and to what extent their localisation is altered upon SPPL3 knock-down as well as upon over-expression of catalytically active but also mutant SPPL3.

References

Achong BG, Mansell PW, Epstein MA & Clifford P (1971) An unusual virus in cultures from a human nasopharyngeal carcinoma. *J. Natl. Cancer Inst.* **46**: 299–307

Adrain C & Freeman M (2012) New lives for old: evolution of pseudoenzyme function illustrated by iRhom. *Nat. Rev. Mol. Cell Biol.* **13**: 489–498

Adrain C, Zettl M, Christova Y, Taylor N & Freeman M (2012) Tumor necrosis factor signaling requires iRhom2 to promote trafficking and activation of TACE. *Science* **335**: 225–228

Ali M, Taylor GP, Pitman RJ, Parker D, Rethwilm A, Cheingsong-Popov R, Weber JN, Bieniasz PD, Bradley J & McClure MO (1996) No evidence of antibody to human foamy virus in widespread human populations. *AIDS Res. Hum. Retroviruses* **12**: 1473–1483

Almeida R, Levery SB, Mandel U, Kresse H, Schwientek T, Bennett EP & Clausen H (1999) Cloning and expression of a proteoglycan UDP-galactose:beta-xylose beta1,4-galactosyltransferase I. A seventh member of the human beta4-galactosyltransferase gene family. *J. Biol. Chem.* **274**: 26165–26171

Almén MS, Nordström KJV, Fredriksson R & Schiöth HB (2009) Mapping the human membrane proteome: a majority of the human membrane proteins can be classified according to function and evolutionary origin. *BMC Biol.* **7**: 50

Arase H, Saito T, Phillips JH & Lanier LL (2001) Cutting edge: the mouse NK cell-associated antigen recognized by DX5 monoclonal antibody is CD49b (alpha 2 integrin, very late antigen-2). *J. Immunol.* **167**: 1141–1144

Artavanis-Tsakonas S, Rand MD & Lake RJ (1999) Notch signaling: cell fate control and signal integration in development. *Science* **284**: 770–776

Bai X, Zhou D, Brown JR, Crawford BE, Hennet T & Esko JD (2001) Biosynthesis of the linkage region of glycosaminoglycans: cloning and activity of galactosyltransferase II, the sixth member of the beta 1,3-galactosyltransferase family (beta 3GalT6). *J. Biol. Chem.* **276**: 48189–48195

Ballard C, Gauthier S, Corbett A, Brayne C, Aarsland D & Jones E (2011) Alzheimer's disease. *Lancet* **377**: 1019–1031

Bammens L, Chávez-Gutiérrez L, Tolia A, Zwijsen A & De Strooper B (2011) Functional and topological analysis of Pen-2, the fourth subunit of the gamma-secretase complex. *J. Biol. Chem.* **286**: 12271–12282

Bansal A, Shaw KL, Edwards BH, Goepfert PA & Mulligan MJ (2000) Characterization of the R572T point mutant of a putative cleavage site in human foamy virus Env. *J. Virol.* **74**: 2949–2954

Bar-On Y, Glasner A, Meningher T, Achdout H, Gur C, Lankry D, Vitenshtein A, Meyers AFA, Mandelboim M & Mandelboim O (2013) Neuraminidase-mediated, NKp46-dependent immune-evasion mechanism of influenza viruses. *Cell Rep.* **3**: 1044–1050

Bardy SL & Jarrell KF (2003) Cleavage of preflagellins by an aspartic acid signal peptidase is essential for flagellation in the archaeon *Methanococcus voltae*. *Mol. Microbiol.* **50**: 1339–1347

Barresi R & Campbell KP (2006) Dystroglycan: from biosynthesis to pathogenesis of human disease. *J. Cell. Sci.* **119**: 199–207

Bauer TR, Allen JM, Hai M, Tuschong LM, Khan IF, Olson EM, Adler RL, Burkholder TH, Gu Y-C, Russell DW & Hickstein DD (2008) Successful treatment of canine leukocyte adhesion deficiency by foamy virus vectors. *Nat. Med.* **14**: 93–97

Bauer TR, Tuschong LM, Calvo KR, Shive HR, Burkholder TH, Karlsson EK, West RR, Russell DW & Hickstein DD (2013) Long-Term Follow-up of Foamy Viral Vector-Mediated Gene Therapy for Canine Leukocyte Adhesion Deficiency. *Mol. Ther.* **21**: 964–972

Beel AJ & Sanders CR (2008) Substrate specificity of gamma-secretase and other intramembrane proteases. *Cell. Mol. Life Sci.* **65**: 1311–1334

Behnke J, Schneppenheim J, Koch-Nolte F, Haag F, Saftig P & Schröder B (2011) Signal-peptidase-like 2a (SPPL2a) is targeted to lysosomes/late endosomes by a tyrosine motif in its C-terminal tail. *FEBS Lett.* **585**: 2951–2957

Beisner DR, Langerak P, Parker AE, Dahlberg C, Otero FJ, Sutton SE, Poirot L, Barnes W, Young MA, Niessen S, Wiltshire T, Bodendorf U, Martoglio B, Cravatt B & Cooke MP (2013) The intramembrane protease Sppl2a is required for B cell and DC development and survival via cleavage of the invariant chain. *J. Exp. Med.* **210**: 23–30

Benoff S (1997) Carbohydrates and fertilization: an overview. *Mol. Hum. Reprod.* **3**: 599–637

Berger EG (2002) Ectopic localizations of Golgi glycosyltransferases. *Glycobiology* **12**: 29R–36R

Bergmann H, Yabas M, Short A, Miosge L, Barthel N, Teh CE, Roots CM, Bull KR, Jeelall Y, Horikawa K, Whittle B, Balakishnan B, Sjollema G, Bertram EM, Mackay F, Rimmer AJ, Cornall RJ, Field MA, Andrews TD, Goodnow CC, et al (2013) B cell survival, surface BCR and BAFFR expression, CD74 metabolism, and CD8- dendritic cells require the intramembrane endopeptidase SPPL2A. *J. Exp. Med.* **210**: 31–40

Berka U, Hamann MV & Lindemann D (2013) Early events in foamy virus-host interaction and intracellular trafficking. *Viruses* **5**: 1055–1074

Betsem E, Rua R, Tortevoye P, Froment A & Gessain A (2011) Frequent and Recent Human Acquisition of Simian Foamy Viruses Through Apes' Bites in Central Africa. *PLoS Pathog.* **7**: e1002306

Beznoussenko GV, Parashuraman S, Rizzo R, Polishchuk R, Martella O, Di Giandomenico D, Fusella A, Spaar A, Sallese M, Capestrano MG, Pavelka M, Vos MR, Rikers YG, Helms V, Mironov AA & Luini A (2014) Transport of soluble proteins through the Golgi occurs by diffusion via continuities across cisternae. *Elife*: e02009

Bihel F, Das C, Bowman MJ & Wolfe MS (2004) Discovery of a Subnanomolar helical D-tridecapeptide inhibitor of gamma-secretase. *J. Med. Chem.* **47**: 3931–3933

Bland FA, Lemberg MK, McMichael AJ, Martoglio B & Braud VM (2003) Requirement of the proteasome for the trimming of signal peptide-derived epitopes presented by the nonclassical major histocompatibility complex class I molecule HLA-E. *J. Biol. Chem.* **278**: 33747–33752

Blumenthal R, Durell S & Viard M (2012) HIV Entry and Envelope Glycoprotein-mediated Fusion. *J. Biol. Chem.* **287**: 40841–40849

Boname JM, Bloor S, Wandel MP, Nathan JA, Antrobus R, Dingwell KS, Thurston TL, Smith DL, Smith JC, Rando F & Lehner PJ (2014) Cleavage by signal peptide peptidase is required for the degradation of selected tail-anchored proteins. *J. Cell. Biol.* **205**: 847–862

Borsig L, Katopodis AG, Bowen BR & Berger EG (1998) Trafficking and localization studies of recombinant alpha1, 3-fucosyltransferase VI stably expressed in CHO cells. *Glycobiology* **8**: 259–268

Boscher C, Dennis JW & Nabi IR (2011) Glycosylation, galectins and cellular signaling. *Curr. Opin. Cell Biol.* **23**: 383–392

Brady OA, Zhou X & Hu F (2014) Regulated intramembrane proteolysis of the frontotemporal lobar degeneration (FTLD) risk factor, TMEM106B, by Signal Peptide Peptidase-like 2a (SPPL2a). *J. Biol. Chem.* **289**: 19670–19680.

Brockhausen I, Schachter H & Stanley P (2009) O-GalNAc Glycans. In *Essentials of Glycobiology*, Varki A, Cummings RD, Esko JD, Freeze HH, Stanley P, Bertozzi CR, Hart GW & Etzler ME (eds) pp 115–127. Cold Spring Harbor: Cold Spring Harbor Laboratory Press

Bronckers AL, Güneli N, Lüllmann-Rauch R, Schneppenheim J, Moraru AP, Himmerkus N, Bervoets TJ, Fluhrer R, Everts V, Saftig P & Schröder B (2013) The intramembrane protease SPPL2A is critical for tooth enamel formation. *J. Bone Miner. Res.* **28**: 1622–1630

Brown MS & Goldstein JL (1997) The SREBP pathway: regulation of cholesterol metabolism by proteolysis of a membrane-bound transcription factor. *Cell* **89**: 331–340

Brown MS, Ye J, Rawson RB & Goldstein JL (2000) Regulated intramembrane proteolysis: a control mechanism conserved from bacteria to humans. *Cell* **100**: 391–398

Buyssse K, Riemersma M, Powell G, van Reeuwijk J, Chitayat D, Roscioli T, Kamsteeg E-J, van den Elzen C, van Beusekom E, Blaser S, Babul-Hirji R, Halliday W, Wright GJ, Stemple DL, Lin Y-Y, Lefeber DJ & van Bokhoven H (2013) Missense mutations in β -1,3-N-acetylglucosaminyltransferase 1 (B3GNT1) cause Walker-Warburg syndrome. *Hum. Mol. Genet.* **22**: 1746–1754

Capell A, Beher D, Prokop S, Steiner H, Kaether C, Shearman MS & Haass C (2005) Gamma-secretase complex assembly within the early secretory pathway. *J. Biol. Chem.* **280**: 6471–6478

Capell A, Grünberg J, Pesold B, Diehlmann A, Citron M, Nixon R, Beyreuther K, Selkoe DJ & Haass C (1998) The proteolytic fragments of the Alzheimer's disease-associated presenilin-1 form heterodimers and occur as a 100–150-kDa molecular mass complex. *J. Biol. Chem.* **273**: 3205–3211

Caporale M, Arnaud F, Mura M, Golder M, Murgia C & Palmarini M (2009) The signal peptide of a simple retrovirus envelope functions as a posttranscriptional regulator of viral gene expression. *J. Virol.* **83**: 4591–4604

Carlsson SR, Roth J, Piller F & Fukuda M (1988) Isolation and characterization of human lysosomal membrane glycoproteins, h-lamp-1 and h-lamp-2. Major sialoglycoproteins carrying polygalactosaminoglycan. *J. Biol. Chem.* **263**: 18911–18919

Cassio DJ, Liu S, Biehs B & Kornberg TB (2012) Expression and characterization of *Drosophila* signal peptide peptidase-like (sppL), a gene that encodes an intramembrane protease. *PLoS ONE* **7**: e33827

Cassio DJ, Tanda S, Biehs B, Martoglio B & Kornberg TB (2005) *Drosophila* signal peptide peptidase is an essential protease for larval development. *Genetics* **170**: 139–148

Chaney W, Sundaram S, Friedman N & Stanley P (1989) The Lec4A CHO glycosylation mutant arises from miscompartmentalization of a Golgi glycosyltransferase. *J. Cell. Biol.* **109**: 2089–2096

Chávez-Gutiérrez L, Tolia A, Maes E, Li T, Wong PC & De Strooper B (2008) Glu(332) in the Nicastin ectodomain is essential for gamma-secretase complex maturation but not for its activity. *J. Biol. Chem.* **283**: 20096–20105

Chen G & Zhang X (2010) New insights into S2P signaling cascades: regulation, variation, and conservation. *Protein Sci.* **19**: 2015–2030

Chen L, Zhang N, Adler B, Browne J, Freigen N & Pierce M (1995) Preparation of antisera to recombinant, soluble N-acetylglucosaminyltransferase V and its visualization in situ. *Glycoconj. J.* **12**: 813–823

Christianson JC, Olzmann JA, Shaler TA, Sowa ME, Bennett EJ, Richter CM, Tyler RE, Greenblatt EJ, Harper JW & Kopito RR (2012) Defining human ERAD networks through an integrative mapping strategy. *Nat. Cell Biol.* **14**: 93–105

Citron M, Oltersdorf T, Haass C, McConlogue L, Hung AY, Seubert P, Vigo-Pelfrey C, Lieberburg I & Selkoe DJ (1992) Mutation of the beta-amyloid precursor protein in familial Alzheimer's disease increases beta-protein production. *Nature* **360**: 672–674

Colley KJ (1997) Golgi localization of glycosyltransferases: more questions than answers. *Glycobiology* **7**: 1–13

Condac E, Dale GL, Bender-Neal D, Ferencz B, Towner R & Hinsdale ME (2009) Xylosyltransferase II is a significant contributor of circulating xylosyltransferase levels and platelets constitute an important source of xylosyltransferase in serum. *Glycobiology* **19**: 829–833

Cummings RD & Etzler ME (2009) Antibodies and Lectins in Glycan analysis. In *Essentials of Glycobiology*, Varki A Cummings RD Esko JD Freeze HH Stanley P Bertozzi CR Hart GW & Etzler ME (eds) pp 633–647. Cold Spring Harbor: Cold Spring Harbor Laboratory Press

Cummings RD & Kornfeld S (1982) Characterization of the structural determinants required for the high affinity interaction of asparagine-linked oligosaccharides with immobilized *Phaseolus vulgaris* leukoagglutinating and erythroagglutinating lectins. *J. Biol. Chem.* **257**: 11230–11234

Cummings RD, Trowbridge IS & Kornfeld S (1982) A mouse lymphoma cell line resistant to the leukoagglutinating lectin from *Phaseolus vulgaris* is deficient in UDP-GlcNAc: alpha-D-mannoside beta 1,6 N-acetylglucosaminyltransferase. *J. Biol. Chem.* **257**: 13421–13427

Cupers P, Bentahir M, Craessaerts K, Orlans I, Vanderstichele H, Saftig P, De Strooper B & Annaert W (2001) The discrepancy between presenilin subcellular localization and gamma-secretase processing of amyloid precursor protein. *J. Cell. Biol.* **154**: 731–740

De Strooper B, Annaert W, Cupers P, Saftig P, Craessaerts K, Mumm JS, Schroeter EH, Schrijvers V, Wolfe MS, Ray WJ, Goate A & Kopan R (1999) A presenilin-1-dependent gamma-secretase-like protease mediates release of Notch intracellular domain. *Nature* **398**: 518–522

de Vries T, Storm J, Rotteveel F, Verdonk G, van Duin M, van den Eijnden DH, Joziasse DH & Bunschoten H (2001) Production of soluble human alpha3-fucosyltransferase (FucT VII) by membrane targeting and in vivo proteolysis. *Glycobiology* **11**: 711–717

Demetriou M, Granovsky M, Quaggin S & Dennis JW (2001) Negative regulation of T-cell activation and autoimmunity by Mgat5 N-glycosylation. *Nature* **409**: 733–739

Dennis JW, Nabi IR & Demetriou M (2009) Metabolism, cell surface organization, and disease. *Cell* **139**: 1229–1241

Dennis JW, Pawling J, Cheung P, Partridge E & Demetriou M (2002) UDP-N-acetylglucosamine:alpha-6-D-mannoside beta1,6 N-acetylglucosaminyltransferase V (Mgat5) deficient mice. *Biochim. Biophys. Acta* **1573**: 414–422

Di Santo JP (2006) Natural killer cell developmental pathways: a question of balance. *Annu. Rev. Immunol.* **24**: 257–286

Dobson CM, Hempel SJ, Stalnaker SH, Stuart R & Wells L (2013) O-Mannosylation and human disease. *Cell. Mol. Life Sci.* **70**: 2849–2857

Doody RS, Raman R, Farlow M, Iwatsubo T, Vellas B, Joffe S, Kieburtz K, He F, Sun X, Thomas RG, Aisen PS, Alzheimer's Disease Cooperative Study Steering Committee, Siemers E, Sethuraman G, Mohs RS, Semagacestat Study Group (2013) A phase 3 trial of semagacestat for treatment of Alzheimer's disease. *N. Engl. J. Med.* **369**: 341–350

Dovey HF, John V, Anderson JP, Chen LZ, de Saint Andrieu P, Fang LY, Freedman SB, Folmer B, Goldbach E, Holsztynska EJ, Hu KL, Johnson-Wood KL, Kennedy SL, Kholodenko D, Knops JE, Latimer LH, Lee M, Liao Z, Lieberburg IM, Motter RN, et al (2001) Functional gamma-secretase inhibitors reduce beta-amyloid peptide levels in brain. *J. Neurochem.* **76**: 173–181

Duda A, Lüftenerger D, Pietschmann T & Lindemann D (2006) Characterization of the prototype foamy virus envelope glycoprotein receptor-binding domain. *J. Virol.* **80**: 8158–8167

Duda A, Stange A, Lüftenerger D, Stanke N, Westphal D, Pietschmann T, Eastman SW, Linial ML, Rethwilm A & Lindemann D (2004) Prototype foamy virus envelope glycoprotein leader peptide processing is mediated by a furin-like cellular protease, but cleavage is not essential for viral infectivity. *J. Virol.* **78**: 13865–13870

Dulin F, Léveillé F, Ortega JB, Mornon J-P, Buisson A, Callebaut I & Colloc'h N (2008) P3 peptide, a truncated form of A beta devoid of synaptotoxic effect, does not assemble into soluble oligomers. *FEBS Lett.* **582**: 1865–1870

Edbauer D, Winkler E, Haass C & Steiner H (2002) Presenilin and nicastrin regulate each other and determine amyloid beta-peptide production via complex formation. *Proc. Natl. Acad. Sci. U.S.A.* **99**: 8666–8671

Edbauer D, Winkler E, Regula JT, Pesold B, Steiner H & Haass C (2003) Reconstitution of gamma-secretase activity. *Nat. Cell Biol.* **5**: 486–488

Edwards DR, Handsley MM & Pennington CJ (2008) The ADAM metalloproteinases. *Mol. Aspects Med.* **29**: 258–289

El-Battari A, Prorok M, Angata K, Mathieu S, Zerfaoui M, Ong E, Suzuki M, Lombardo D & Fukuda M (2003) Different glycosyltransferases are differentially processed for secretion, dimerization, and autoglycosylation. *Glycobiology* **13**: 941–953

Elbein AD, Tropea JE, Mitchell M & Kaushal GP (1990) Kifunensine, a potent inhibitor of the glycoprotein processing mannosidase I. *J. Biol. Chem.* **265**: 15599–15605

Elhammer A & Kornfeld S (1986) Purification and characterization of UDP-N-acetylgalactosamine: polypeptide N-acetylgalactosaminyltransferase from bovine colostrum and murine lymphoma BW5147 cells. *J. Biol. Chem.* **261**: 5249–5255

Erez E & Bibi E (2009) Cleavage of a Multispanning Membrane Protein by an Intramembrane Serine Protease. *Biochemistry* **48**: 12314–12322

Ermann J & Glimcher LH (2012) After GWAS: mice to the rescue? *Curr. Opin. Immunol.* **24**: 564–570

Esch FS, Keim PS, Beattie EC, Blacher RW, Culwell AR, Oltersdorf T, McClure D & Ward PJ (1990) Cleavage of amyloid beta peptide during constitutive processing of its precursor. *Science* **248**: 1122–1124

Esko JD, Kimata K & Lindahl U (2009) Proteoglycans and Sulfated Glycosaminoglycans. In *Essentials of Glycobiology*, Varki A Cummings RD Esko JD Freeze HH Stanley P Bertozzi CR Hart GW & Etzler ME (eds) pp 229–248. Cold Spring Harbor: Cold Spring Harbor Laboratory Press

Esler WP, Kimberly WT, Ostaszewski BL, Diehl TS, Moore CL, Tsai JY, Rahmati T, Xia W, Selkoe DJ & Wolfe MS (2000) Transition-state analogue inhibitors of gamma-secretase bind directly to presenilin-1. *Nat. Cell Biol.* **2**: 428–434

Fagerberg L, Jonasson K, Heijne von G, Uhlén M & Berglund L (2010) Prediction of the human membrane proteome. *Proteomics* **10**: 1141–1149

Fathman JW, Bhattacharya D, Inlay MA, Seita J, Karsunky H & Weissman IL (2011) Identification of the earliest natural killer cell-committed progenitor in murine bone marrow. *Blood* **118**: 5439–5447

Feng L, Yan H, Wu Z, Yan N, Wang Z, Jeffrey PD & Shi Y (2007) Structure of a Site-2 Protease Family Intramembrane Metalloprotease. *Science* **318**: 1608–1612

Fleig L, Bergbold N, Sahasrabudhe P, Geiger B, Kaltak L & Lemberg MK (2012) Ubiquitin-Dependent Intramembrane Rhomboid Protease Promotes ERAD of Membrane Proteins. *Mol. Cell* **47**: 558–569

Fluhrer R, Fukumori A, Martin L, Grammer G, Haug-Kröper M, Klier B, Winkler E, Kremmer E, Condron MM, Teplow DB, Steiner H & Haass C (2008) Intramembrane proteolysis of GXGD-type aspartyl proteases is slowed by a familial Alzheimer disease-like mutation. *J. Biol. Chem.* **283**: 30121–30128

Fluhrer R, Grammer G, Israel L, Condron MM, Haffner C, Friedmann E, Böhland C, Imhof A, Martoglio B, Teplow DB & Haass C (2006) A gamma-secretase-like intramembrane cleavage of TNF α by the GxGD aspartyl protease SPPL2b. *Nat. Cell Biol.* **8**: 894–896

Fluhrer R, Martin L, Klier B, Haug-Kröper M, Grammer G, Nuscher B & Haass C (2012) The α -helical content of the transmembrane domain of the British dementia protein-2 (Bri2) determines its processing by signal peptide peptidase-like 2b (SPPL2b). *J. Biol. Chem.* **287**: 5156–5163

Fortini ME (2002) Gamma-secretase-mediated proteolysis in cell-surface-receptor signalling. *Nat. Rev. Mol. Cell Biol.* **3**: 673–684

Fortna RR, Crystal AS, Morais VA, Pijak DS, Lee VMY & Doms RW (2004) Membrane topology and nicastrin-enhanced endoproteolysis of APH-1, a component of the gamma-secretase complex. *J. Biol. Chem.* **279**: 3685–3693

Freeman M (2008) Rhomboid Proteases and their Biological Functions. *Annu. Rev. Genet.* **42**: 191–210

Freeze HH & Elbein AD (2009) Glycosylation Precursors. In *Essentials of Glycobiology*, Varki A Cummings RD Esko JD Freeze HH Stanley P Bertozzi CR Hart GW & Etzler ME (eds) pp 47–61. Cold Spring Harbor: Cold Spring Harbor Laboratory Press

Friedmann E, Hauben E, Maylandt K, Schleeger S, Vreugde S, Lichtenthaler SF, Kuhn P-H, Stauffer D, Rovelli G & Martoglio B (2006) SPPL2a and SPPL2b promote intramembrane proteolysis of TNF α in activated dendritic cells to trigger IL-12 production. *Nat. Cell Biol.* **8**: 843–848

Friedmann E, Lemberg MK, Weihofen A, Dev KK, Dengler U, Rovelli G & Martoglio B (2004) Consensus analysis of signal peptide peptidase and homologous human aspartic proteases reveals opposite topology of catalytic domains compared with presenilins. *J. Biol. Chem.* **279**: 50790–50798

Fukumori A, Fluhrer R, Steiner H & Haass C (2010) Three-amino acid spacing of presenilin endoproteolysis suggests a general stepwise cleavage of gamma-secretase-mediated intramembrane proteolysis. *J. Neurosci.* **30**: 7853–7862

Geiselhart V, Bastone P, Kempf T, Schnölzer M & Löchelt M (2004) Furin-mediated cleavage of the feline foamy virus Env leader protein. *J. Virol.* **78**: 13573–13581

Geiselhart V, Schwantes A, Bastone P, Frech M & Löchelt M (2003) Features of the Env leader protein and the N-terminal Gag domain of feline foamy virus important for virus morphogenesis. *Virology* **310**: 235–244

Glick BS & Luini A (2011) Models for Golgi traffic: a critical assessment. *Cold Spring Harb Perspect Biol* **3**: a005215

Goate A, Chartier-Harlin MC, Mullan M, Brown J, Crawford F, Fidani L, Giuffra L, Haynes A, Irving N & James L (1991) Segregation of a missense mutation in the amyloid precursor protein gene with familial Alzheimer's disease. *Nature* **349**: 704–706

Goder V & Spiess M (2001) Topogenesis of membrane proteins: determinants and dynamics. *FEBS Lett.* **504**: 87–93

Goepfert PA, Shaw K, Wang G, Bansal A, Edwards BH & Mulligan MJ (1999) An endoplasmic reticulum retrieval signal partitions human foamy virus maturation to intracytoplasmic membranes. *J. Virol.* **73**: 7210–7217

Goepfert PA, Shaw KL, Ritter GD & Mulligan MJ (1997) A sorting motif localizes the foamy virus glycoprotein to the endoplasmic reticulum. *J. Virol.* **71**: 778–784

Goepfert PA, Wang G & Mulligan MJ (1995) Identification of an ER retrieval signal in a retroviral glycoprotein. *Cell* **82**: 543–544

Golde TE, Wolfe MS & Greenbaum DC (2009) Signal peptide peptidases: A family of intramembrane-cleaving proteases that cleave type 2 transmembrane proteins. *Semin. Cell Dev. Biol.* **20**: 225–230

Gonzalez DS, Karaveg K, Vandersall-Nairn AS, Lal A & Moremen KW (1999) Identification, expression, and characterization of a cDNA encoding human endoplasmic reticulum mannosidase I, the enzyme that catalyzes the first mannose trimming step in mammalian Asn-linked oligosaccharide biosynthesis. *J. Biol. Chem.* **274**: 21375–21386

Götting C, Kuhn J, Brinkmann T & Kleesiek K (2002) Xylosyltransferase activity in seminal plasma of infertile men. *Clin. Chim. Acta* **317**: 199–202

Götting C, Kuhn J, Zahn R, Brinkmann T & Kleesiek K (2000) Molecular cloning and expression of human UDP-d-Xylose:proteoglycan core protein beta-d-xylosyltransferase and its first isoform XT-II. *J. Mol. Biol.* **304**: 517–528

Götting C, Sollberg S, Kuhn J, Weilke C, Huerkamp C, Brinkmann T, Krieg T & Kleesiek K (1999) Serum xylosyltransferase: a new biochemical marker of the sclerotic process in systemic sclerosis. *J. Invest. Dermatol.* **112**: 919–924

Grabenhorst E & Conradt HS (1999) The cytoplasmic, transmembrane, and stem regions of glycosyltransferases specify their in vivo functional sublocalization and stability in the Golgi. *J. Biol. Chem.* **274**: 36107–36116

Granovsky M, Fata J, Pawling J, Muller WJ, Khokha R & Dennis JW (2000) Suppression of tumor growth and metastasis in Mgat5-deficient mice. *Nat. Med.* **6**: 306–312

Grigorenko AP, Moliaka YK, Korovaitseva GI & Rogaev EI (2002) Novel class of polytopic proteins with domains associated with putative protease activity. *Biochemistry Mosc.* **67**: 826–835

Grigorenko AP, Moliaka YK, Soto MC, Mello CC & Rogaev EI (2004) The *Caenorhabditis elegans* IMPAS gene, *imp-2*, is essential for development and is functionally distinct from related presenilins. *Proc. Natl. Acad. Sci. U.S.A.* **101**: 14955–14960

Grigorian A, Lee S-U, Tian W, Chen I-J, Gao G, Mendelsohn R, Dennis JW & Demetriou M (2007) Control of T Cell-mediated autoimmunity by metabolite flux to N-glycan biosynthesis. *J. Biol. Chem.* **282**: 20027–20035

Grigorian A, Torossian S & Demetriou M (2009) T-cell growth, cell surface organization, and the galectin-glycoprotein lattice. *Immunol. Rev.* **230**: 232–246

Guérardel Y, Chang L-Y, Maes E, Huang C-J & Khoo K-H (2006) Glycomic survey mapping of zebrafish identifies unique sialylation pattern. *Glycobiology* **16**: 244–257

Guo H-B, Johnson H, Randolph M & Pierce M (2009) Regulation of homotypic cell-cell adhesion by branched N-glycosylation of N-cadherin extracellular EC2 and EC3 domains. *J. Biol. Chem.* **284**: 34986–34997

Guo H-B, Lee I, Kamar M & Pierce M (2003) N-acetylglucosaminyltransferase V expression levels regulate cadherin-associated homotypic cell-cell adhesion and intracellular signaling pathways. *J. Biol. Chem.* **278**: 52412–52424

Haapasalo A & Kovacs DM (2011) The many substrates of presenilin/γ-secretase. *J. Alzheimers Dis.* **25**: 3–28

Haass C (2004) Take five—BACE and the gamma-secretase quartet conduct Alzheimer's amyloid beta-peptide generation. *EMBO J.* **23**: 483–488

Haass C & Selkoe DJ (2007) Soluble protein oligomers in neurodegeneration: lessons from the Alzheimer's amyloid β-peptide. *Nat. Rev. Mol. Cell Biol.* **8**: 101–112

Habuchi H, Habuchi O & Kimata K (1995) Purification and characterization of heparan sulfate 6-sulfotransferase from the culture medium of Chinese hamster ovary cells. *J. Biol. Chem.* **270**: 4172–4179

Hage El F, Stroobant V, Vergnon I, Baurain J-F, Echchakir H, Lazar V, Chouaib S, Coulie PG & Mami-Chouaib F (2008) Preprocalcitonin signal peptide generates a cytotoxic T lymphocyte-defined tumor epitope processed by a proteasome-independent pathway. *Proc. Natl. Acad. Sci. U.S.A.* **105**: 10119–10124

Hanson PI & Cashikar A (2012) Multivesicular body morphogenesis. *Annu. Rev. Cell Dev. Biol.* **28**: 337–362

Harbut MB, Patel BA, Yeung BKS, McNamara CW, Bright AT, Ballard J, Supek F, Golde TE, Winzeler EA, Diagana TT & Greenbaum DC (2012) Targeting the ERAD pathway via inhibition of signal peptide peptidase for antiparasitic therapeutic design. *Proc. Natl. Acad. Sci. U.S.A.* **109**: 21486–21491

Hardy JA & Higgins GA (1992) Alzheimer's disease: the amyloid cascade hypothesis. *Science* **256**: 184–185

Harris DT, Iglesias JL, Argov S, Toomey J & Koren HS (1987) Heterogeneity of human natural killer (NK) cells: enrichment of NK by negative-selection with the lectin from *Erythrina cristagalli*. *J. Leukoc. Biol.* **42**: 163–170

Hartley BS (1960) Proteolytic enzymes. *Annu. Rev. Biochem.* **29**: 45–72

Hascall V & Esko JD (2009) Hyaluronan. In *Essentials of Glycobiology*, Varki A Cummings RD Esko JD Freeze HH Stanley P Bertozzi CR Hart GW & Etzler ME (eds) pp 219–227. Cold Spring Harbor: Cold Spring Harbor Laboratory Press

Heijne von G (2006) Membrane-protein topology. *Nat. Rev. Mol. Cell Biol.* **7**: 909–918

Heimann M, Roman-Sosa G, Martoglio B, Thiel H-J & Rümenapf T (2006) Core protein of pestiviruses is processed at the C terminus by signal peptide peptidase. *J. Virol.* **80**: 1915–1921

Hemming ML, Elias JE, Gygi SP & Selkoe DJ (2008) Proteomic profiling of gamma-secretase substrates and mapping of substrate requirements. *PLoS Biol.* **6**: e257

Hemming ML, Elias JE, Gygi SP & Selkoe DJ (2009) Identification of β-Secretase (BACE1) Substrates Using Quantitative Proteomics. *PLoS ONE* **4**: e8477

Heneine W, Switzer WM, Sandstrom P, Brown J, Vedapuri S, Schable CA, Khan AS, Lerche NW, Schweizer M, Neumann-Haefelin D, Chapman LE & Folks TM (1998) Identification of a human population infected with simian foamy viruses. *Nat. Med.* **4**: 403–407

Hennet T (2012) Diseases of glycosylation beyond classical congenital disorders of glycosylation. *Biochim. Biophys. Acta* **1820**: 1306–1317

Henricson A, Käll L & Sonnhammer ELL (2005) A novel transmembrane topology of presenilin based on reconciling experimental and computational evidence. *FEBS J.* **272**: 2727–2733

Herchenröder O, Renne R, Loncar D, Cobb EK, Murthy KK, Schneider J, Mergia A & Luciw PA (1994) Isolation, cloning, and sequencing of simian foamy viruses from chimpanzees (SFVcpz): high homology to human foamy virus (HFV). *Virology* **201**: 187–199

Herremans A, Van Gassen G, Bentahir M, Nyabi O, Craessaerts K, Mueller U, Annaert W & De Strooper B (2003) gamma-Secretase activity requires the presenilin-dependent trafficking of nicastrin through the Golgi apparatus but not its complex glycosylation. *J. Cell. Sci.* **116**: 1127–1136

Hill CL, Bieniasz PD & McClure MO (1999) Properties of human foamy virus relevant to its development as a vector for gene therapy. *J. Gen. Virol.* **80**: 2003–2009

Holtzman DM, Morris JC & Goate AM (2011) Alzheimer's disease: the challenge of the second century. *Sci. Transl. Med.* **3**: 77sr1

Hooper JD, Clements JA, Quigley JP & Antalis TM (2001) Type II transmembrane serine proteases. Insights into an emerging class of cell surface proteolytic enzymes. *J. Biol. Chem.* **276**: 857–860

Hosomi O, Takeya A & Kogure T (1984) Human serum contains N-acetyllactosamine: beta 1-3 N-acetylglucosaminyltransferase activity. *J. Biochem.* **95**: 1655–1659

Hsu F-F, Yeh C-T, Sun Y-J, Chiang M-T, Lan W-M, Li F-A, Lee W-H & Chau L-Y (2014) Signal peptide peptidase-mediated nuclear localization of heme oxygenase-1 promotes cancer cell proliferation and invasion independent of its enzymatic activity. *Oncogene (in press)*

Hu J, Xue Y, Lee S & Ha Y (2011) The crystal structure of GXGD membrane protease FlaK. *Nature* **475**: 528–531

Hua X, Sakai J, Ho YK, Goldstein JL & Brown MS (1995) Hairpin orientation of sterol regulatory element-binding protein-2 in cell membranes as determined by protease protection. *J. Biol. Chem.* **270**: 29422–29427

Hudgin RL & Schachter H (1971a) Porcine sugar nucleotide: glycoprotein glycosyltransferases. 3. Blood serum and liver N-acetylglucosaminyltransferase. *Can. J. Biochem.* **49**: 847–852

Hudgin RL & Schachter H (1971b) Porcine sugar nucleotide: glycoprotein glycosyltransferases. I. Blood serum and liver sialyltransferase. *Can. J. Biochem.* **49**: 829–837

Hudgin RL & Schachter H (1971c) Porcine sugar nucleotide: glycoprotein glycosyltransferases. II. Blood serum and liver galactosyltransferase. *Can. J. Biochem.* **49**: 838–846

Humphries DE, Sullivan BM, Aleixo MD & Stow JL (1997) Localization of human heparan glucosaminyl N-deacetylase/N-sulphotransferase to the trans-Golgi network. *Biochem. J.* **325**: 351–357

Huntington ND, Vosshenrich CAJ & Di Santo JP (2007) Developmental pathways that generate natural-killer-cell diversity in mice and humans. *Nat. Rev. Immunol.* **7**: 703–714

Iben LG, Olson RE, Balandia LA, Jayachandra S, Robertson BJ, Hay V, Corradi J, Prasad CVC, Zaczek R, Albright CF & Toyn JH (2007) Signal peptide peptidase and gamma-secretase share equivalent inhibitor binding pharmacology. *J. Biol. Chem.* **282**: 36829–36836

Ivankov DN, Bogatyreva NS, Höninghschmid P, Dislich B, Hogl S, Kuhn P-H, Frishman D & Lichtenthaler SF (2013) QARIP: a web server for quantitative proteomic analysis of regulated intramembrane proteolysis. *Nucleic Acids Res.* **41**: W459–64

Jae LT, Raaben M, Riemersma M, van Beusekom E, Blomen VA, Velds A, Kerkhoven RM, Carette JE, Topaloglu H, Meinecke P, Wessels MW, Lefebvre DJ, Whelan SP, van Bokhoven H & Brummelkamp TR (2013) Deciphering the glycosylome of dystroglycanopathies using haploid screens for lassa virus entry. *Science* **340**: 479–483

Jakob-Roetne R & Jacobsen H (2009) Alzheimer's disease: from pathology to therapeutic approaches. *Angew. Chem. Int. Ed. Engl.* **48**: 3030–3059

Jaskiewicz E, Zhu G, Bassi R, Darling DS & Young WW (1996) Beta 1,4-N-acetylgalactosaminyltransferase (GM2 synthase) is released from Golgi membranes as a neuraminidase-sensitive, disulfide-bonded dimer by a cathepsin D-like protease. *J. Biol. Chem.* **271**: 26395–26403

Kaether C, Schmitt S, Willem M & Haass C (2006) Amyloid precursor protein and Notch intracellular domains are generated after transport of their precursors to the cell surface. *Traffic* **7**: 408–415

Kamar M, Alvarez-Manilla G, Abney T, Azadi P, Kumar Kolli VS, Orlando R & Pierce M (2004) Analysis of the site-specific N-glycosylation of beta1,6 N-acetylglucosaminyltransferase V. *Glycobiology* **14**: 583–592

Kapp K, Schrempf S, Lemberg MK & Dobberstein B (2009) Post-targeting functions of signal peptides. In *Protein Transport Into the Endoplasmic Reticulum*, Zimmermann R (ed) pp 1–16. Landes Bioscience

Karran E, Mercken M & Strooper BD (2011) The amyloid cascade hypothesis for Alzheimer's disease: an appraisal for the development of therapeutics. *Nat. Rev. Drug. Discov.* **10**: 698–712

Kaufman RJ, Scheuner D, Schröder M, Shen X, Lee K, Liu CY & Arnold SM (2002) The unfolded protein response in nutrient sensing and differentiation. *Nat. Rev. Mol. Cell Biol.* **3**: 411–421

Kennedy MK, Giaccum M, Brown SN, Butz EA, Viney JL, Embers M, Matsuki N, Charrier K, Sedger L, Willis CR, Brasel K, Morrissey PJ, Stocking K, Schuh JC, Joyce S & Peschon JJ (2000) Reversible defects in natural killer and memory CD8 T cell lineages in interleukin 15-deficient mice. *J. Exp. Med.* **191**: 771–780

Kim YS, Perdomo J & Whitehead JS (1972a) Glycosyltransferases in human blood. I. Galactosyltransferase in human serum and erythrocyte membranes. *J. Clin. Invest.* **51**: 2024–2032

Kim YS, Perdomo J, Whitehead JS & Curtis KJ (1972b) Glycosyltransferases in human blood. II. Study of serum galactosyltransferase and N-acetylgalactosaminyltransferase in patients with liver diseases. *J. Clin. Invest.* **51**: 2033–2039

Kimberly WT, LaVoie MJ, Ostaszewski BL, Ye W, Wolfe MS & Selkoe DJ (2003) Gamma-secretase is a membrane protein complex comprised of presenilin, nicastrin, Aph-1, and Pen-2. *Proc. Natl. Acad. Sci. U.S.A.* **100**: 6382–6387

Kirkin V, Cahuzac N, Guardiola-Serrano F, Huault S, Lückerath K, Friedmann E, Novac N, Wels WS, Martoglio B, Hueber A-O & Zörnig M (2007) The Fas ligand intracellular domain is released by ADAM10 and SPPL2a cleavage in T-cells. *Cell. Death Differ.* **14**: 1678–1687

Kitazume S, Nakagawa K, Oka R, Tachida Y, Ogawa K, Luo Y, Citron M, Shitara H, Taya C, Yonekawa H, Paulson JC, Miyoshi E, Taniguchi N & Hashimoto Y (2005) In vivo cleavage of alpha2,6-sialyltransferase by Alzheimer beta-secretase. *J. Biol. Chem.* **280**: 8589–8595

Kitazume S, Oka R, Ogawa K, Futakawa S, Hagiwara Y, Takikawa H, Kato M, Kasahara A, Miyoshi E, Taniguchi N & Hashimoto Y (2009) Molecular insights into beta-galactoside alpha2,6-sialyltransferase secretion in vivo. *Glycobiology* **19**: 479–487

Kitazume S, Tachida Y, Oka R, Kotani N, Ogawa K, Suzuki M, Dohmae N, Takio K, Saido TC & Hashimoto Y (2003) Characterization of alpha 2,6-sialyltransferase cleavage by Alzheimer's beta-secretase (BACE1). *J. Biol. Chem.* **278**: 14865–14871

Kitazume S, Tachida Y, Oka R, Nakagawa K, Takashima S, Lee Y-C & Hashimoto Y (2006) Screening a series of sialyltransferases for possible BACE1 substrates. *Glycoconj. J.* **23**: 437–441

Kitazume S, Tachida Y, Oka R, Shirotani K, Saido TC & Hashimoto Y (2001) Alzheimer's beta-secretase, beta-site amyloid precursor protein-cleaving enzyme, is responsible for cleavage secretion of a Golgi-resident sialyltransferase. *Proc. Natl. Acad. Sci. U.S.A.* **98**: 13554–13559

Knibbs RN, Goldstein IJ, Ratcliffe RM & Shibuya N (1991) Characterization of the carbohydrate binding specificity of the leukoagglutinating lectin from Maackia amurensis. Comparison with other sialic acid-specific lectins. *J. Biol. Chem.* **266**: 83–88

Kopan R & Ilagan MXG (2004) Gamma-secretase: proteasome of the membrane? *Nat. Rev. Mol. Cell Biol.* **5**: 499–504

Kopan R, Schroeter EH, Weintraub H & Nye JS (1996) Signal transduction by activated mNotch: importance of proteolytic processing and its regulation by the extracellular domain. *Proc. Natl. Acad. Sci. U.S.A.* **93**: 1683–1688

Kornilova AY, Bihel F, Das C & Wolfe MS (2005) The initial substrate-binding site of gamma-secretase is located on presenilin near the active site. *Proc. Natl. Acad. Sci. U.S.A.* **102**: 3230–3235

Krawitz P, Haffner C, Fluhrer R, Steiner H, Schmid B & Haass C (2005) Differential localization and identification of a critical aspartate suggest non-redundant proteolytic functions of the presenilin homologues SPPL2b and SPPL3. *J. Biol. Chem.* **280**: 39515–39523

Kreuger J & Kjellén L (2012) Heparan sulfate biosynthesis: regulation and variability. *J. Histochem. Cytochem.* **60**: 898–907

Kuhn P-H, Koroniak K, Hogl S, Colombo A, Zeitschel U, Willem M, Volbracht C, Schepers U, Imhof A, Hoffmeister A, Haass C, Roßner S, Bräse S & Lichtenhaller SF (2012) Secretome protein enrichment identifies physiological BACE1 protease substrates in neurons. *EMBO J.* **31**: 3157–3168

Kuhn P-H, Wang H, Dislich B, Colombo A, Zeitschel U, Ellwart JW, Kremmer E, Roßner S & Lichtenhaller SF (2010) ADAM10 is the physiologically relevant, constitutive alpha-secretase of the amyloid precursor protein in primary neurons. *EMBO J.* **29**: 3020–3032

Lammers G & Jamieson JC (1988) The role of a cathepsin D-like activity in the release of Gal beta 1-4GlcNAc alpha 2-6-sialyltransferase from rat liver Golgi membranes during the acute-phase response. *Biochem. J.* **256**: 623–631

Land A, Zonneveld D & Braakman I (2003) Folding of HIV-1 envelope glycoprotein involves extensive isomerization of disulfide bonds and conformation-dependent leader peptide cleavage. *FASEB J.* **17**: 1058–1067

LaPointe CF & Taylor RK (2000) The type 4 prephilin peptidases comprise a novel family of aspartic acid proteases. *J. Biol. Chem.* **275**: 1502–1510

Lau KS & Dennis JW (2008) N-Glycans in cancer progression. *Glycobiology* **18**: 750–760

Lau KS, Partridge EA, Grigorian A, Silvescu CI, Reinhold VN, Demetriou M & Dennis JW (2007) Complex N-glycan number and degree of branching cooperate to regulate cell proliferation and differentiation. *Cell* **129**: 123–134

Laudon H, Hansson EM, Melén K, Bergman A, Farmery MR, Winblad B, Lendahl U, Heijne von G & Näslund J (2005) A nine-transmembrane domain topology for presenilin 1. *J. Biol. Chem.* **280**: 35352–35360

Laudon H, Mathews PM, Karlström H, Bergman A, Farmery MR, Nixon RA, Winblad B, Gandy SE, Lendahl U, Lundkvist J & Näslund J (2004) Co-expressed presenilin 1 NTF and CTF form functional gamma-secretase complexes in cells devoid of full-length protein. *J. Neurochem.* **89**: 44–53

Lavieu G, Zheng H & Rothman JE (2013) Stapled Golgi cisternae remain in place as cargo passes through the stack. *Elife* **2**: e00558

LaVoie MJ, Fraering PC, Ostaszewski BL, Ye W, Kimberly WT, Wolfe MS & Selkoe DJ (2003) Assembly of the gamma-secretase complex involves early formation of an intermediate subcomplex of Aph-1 and nicastrin. *J. Biol. Chem.* **278**: 37213–37222

Lecellier CH & Saïb A (2000) Foamy viruses: between retroviruses and pararetroviruses. *Virology* **271**: 1–8

Lee J-K, Matthews RT, Lim J-M, Swanier K, Wells L & Pierce JM (2012) Developmental expression of the neuron-specific N-acetylglucosaminyltransferase Vb (GnT-Vb/IX) and identification of its in vivo glycan products in comparison with those of its paralog, GnT-V. *J. Biol. Chem.* **287**: 28526–28536

Lee PL, Kohler JJ & Pfeffer SR (2009) Association of beta-1,3-N-acetylglucosaminyltransferase 1 and beta-1,4-galactosyltransferase 1, trans-Golgi enzymes involved in coupled poly-N-acetyllactosamine synthesis. *Glycobiology* **19**: 655–664

Lee S-U, Grigorian A, Pawling J, Chen I-J, Gao G, Mozaffar T, McKerlie C & Demetriou M (2007) N-glycan processing deficiency promotes spontaneous inflammatory demyelination and neurodegeneration. *J. Biol. Chem.* **282**: 33725–33734

Leem JY, Vijayan S, Han P, Cai D, Machura M, Lopes KO, Veselits ML, Xu H & Thinakaran G (2002) Presenilin 1 is required for maturation and cell surface accumulation of nicastrin. *J. Biol. Chem.* **277**: 19236–19240

Lemberg MK & Freeman M (2007a) Functional and evolutionary implications of enhanced genomic analysis of rhomboid intramembrane proteases. *Genome Res.* **17**: 1634–1646

Lemberg MK & Freeman M (2007b) Cutting proteins within lipid bilayers: rhomboid structure and mechanism. *Mol. Cell* **28**: 930–940

Lemberg MK & Martoglio B (2002) Requirements for signal peptide peptidase-catalyzed intramembrane proteolysis. *Mol. Cell* **10**: 735–744

Lemberg MK & Martoglio B (2004) On the mechanism of SPP-catalysed intramembrane proteolysis; conformational control of peptide bond hydrolysis in the plane of the membrane. *FEBS Lett.* **564**: 213–218

Lemberg MK, Bland FA, Weihofen A, Braud VM & Martoglio B (2001) Intramembrane proteolysis of signal peptides: an essential step in the generation of HLA-E epitopes. *J. Immunol.* **167**: 6441–6446

Lemberg MK, Menendez J, Misik A, Garcia M, Koth CM & Freeman M (2005) Mechanism of intramembrane proteolysis investigated with purified rhomboid proteases. *EMBO J.* **24**: 464–472

Levy-Lahad E, Wasco W, Poorkaj P, Romano DM, Oshima J, Pettingell WH, Yu CE, Jondro PD, Schmidt SD & Wang K (1995a) Candidate gene for the chromosome 1 familial Alzheimer's disease locus. *Science* **269**: 973–977

Levy-Lahad E, Wijsman EM, Nemens E, Anderson L, Goddard KA, Weber JL, Bird TD & Schellenberg GD (1995b) A familial Alzheimer's disease locus on chromosome 1. *Science* **269**: 970–973

Li T, Ma G, Cai H, Price DL & Wong PC (2003) Nicastin is required for assembly of presenilin/gamma-secretase complexes to mediate Notch signaling and for processing and trafficking of beta-amyloid precursor protein in mammals. *J. Neurosci.* **23**: 3272–3277

Li X, Dang S, Yan C, Gong X, Wang J & Shi Y (2013) Structure of a presenilin family intramembrane aspartate protease. *Nature* **493**: 56–61

Li Y, Bergeron JJ, Luo L, Ou WJ, Thomas DY & Kang CY (1996) Effects of inefficient cleavage of the signal sequence of HIV-1 gp 120 on its association with calnexin, folding, and intracellular transport. *Proc. Natl. Acad. Sci. U.S.A.* **93**: 9606–9611

Li Y, Luo L, Thomas DY & Kang CY (1994) Control of expression, glycosylation, and secretion of HIV-1 gp120 by homologous and heterologous signal sequences. *Virology* **204**: 266–278

Li Y, Luo L, Thomas DY & Kang CY (2000a) The HIV-1 Env protein signal sequence retards its cleavage and down-regulates the glycoprotein folding. *Virology* **272**: 417–428

Li YM, Xu M, Lai MT, Huang Q, Castro JL, DiMuzio-Mower J, Harrison T, Lellis C, Nadin A, Neduvelli JG, Register RB, Sardana MK, Shearman MS, Smith AL, Shi XP, Yin KC, Shafer JA & Gardell SJ (2000b) Photoactivated gamma-secretase inhibitors directed to the active site covalently label presenilin 1. *Nature* **405**: 689–694

Lichtenthaler SF, Haass C & Steiner H (2011) Regulated intramembrane proteolysis--lessons from amyloid precursor protein processing. *J. Neurochem.* **117**: 779–796

Lindemann D & Goepfert PA (2003) The foamy virus envelope glycoproteins. *Curr. Top. Microbiol. Immunol.* **277**: 111–129

Lindemann D & Rethwilm A (2011) Foamy virus biology and its application for vector development. *Viruses* **3**: 561–585

Lindemann D, Pietschmann T, Picard-Maureau M, Berg A, Heinkelein M, Thurow J, Knaus P, Zentgraf H & Rethwilm A (2001) A particle-associated glycoprotein signal peptide essential for virus maturation and infectivity. *J. Virol.* **75**: 5762–5771

Loureiro J, Lilley BN, Spooner E, Noriega V, Tortorella D & Ploegh HL (2006) Signal peptide peptidase is required for dislocation from the endoplasmic reticulum. *Nature* **441**: 894–897

Lowe JB & Marth JD (2003) A genetic approach to Mammalian glycan function. *Annu. Rev. Biochem.* **72**: 643–691

López-Otín C & Overall CM (2002) Protease degradomics: A new challenge for proteomics. *Nat. Rev. Mol. Cell Biol.* **3**: 509–519

Lu P, Bai X-C, Ma D, Xie T, Yan C, Sun L, Yang G, Zhao Y, Zhou R, Scheres SHW & Shi Y (2014) Three-dimensional structure of human gamma-secretase. *Nature (in press)*

Lückerath K, Kirkin V, Melzer IM, Thalheimer FB, Siele D, Milani W, Adler T, Aguilar-Pimentel A, Horsch M, Michel G, Beckers J, Busch DH, Ollert M, Gailus-Durner V, Fuchs H, Hrabe de Angelis M, Staal FJT, Rajalingam K, Hueber A-O, Strobl LJ, et al (2011) Immune modulation by Fas ligand reverse signaling: lymphocyte proliferation is attenuated by the intracellular Fas ligand domain. *Blood* **117**: 519–529

Lüftenegger D, Picard-Maureau M, Stanke N, Rethwilm A & Lindemann D (2005) Analysis and function of prototype foamy virus envelope N glycosylation. *J. Virol.* **79**: 7664–7672

Maegawa S, Ito K & Akiyama Y (2005) Proteolytic action of GlpG, a rhomboid protease in the *Escherichia coli* cytoplasmic membrane. *Biochemistry* **44**: 13543–13552

Maley F, Trimble RB, Tarentino AL & Plummer TH (1989) Characterization of glycoproteins and their associated oligosaccharides through the use of endoglycosidases. *Anal. Biochem.* **180**: 195–204

Manolaridis I, Kulkarni K, Dodd RB, Ogasawara S, Zhang Z, Bineva G, O'Reilly N, Hanrahan SJ, Thompson AJ, Cronin N, Iwata S & Barford D (2013) Mechanism of farnesylated CAAX protein processing by the intramembrane protease Rce1. *Nature* **504**: 301–305

Margraf-Schönfeld S, Böhm C & Watzl C (2011) Glycosylation affects ligand binding and function of the activating natural killer cell receptor 2B4 (CD244) protein. *J. Biol. Chem.* **286**: 24142–24149

Marth JD & Grewal PK (2008) Mammalian glycosylation in immunity. *Nat. Rev. Immunol.* **8**: 874–887

Martin L, Fluhrer R & Haass C (2009) Substrate requirements for SPPL2b-dependent regulated intramembrane proteolysis. *J. Biol. Chem.* **284**: 5662–5670

Martin L, Fluhrer R, Reiss K, Kremmer E, Saftig P & Haass C (2008) Regulated intramembrane proteolysis of Bri2 (Itm2b) by ADAM10 and SPPL2a/SPPL2b. *J. Biol. Chem.* **283**: 1644–1652

Martoglio B & Dobberstein B (1998) Signal sequences: more than just greasy peptides. *Trends Cell. Biol.* **8**: 410–415

Martoglio B, Graf R & Dobberstein B (1997) Signal peptide fragments of preprolactin and HIV-1 p-gp160 interact with calmodulin. *EMBO J.* **16**: 6636–6645

Masri KA, Appert HE & Fukuda MN (1988) Identification of the full-length coding sequence for human galactosyltransferase (beta-N-acetylglucosaminide: beta 1,4-galactosyltransferase). *Biochem. Biophys. Res. Commun.* **157**: 657–663

Matsumura N, Takami M, Okochi M, Wada-Kakuda S, Fujiwara H, Tagami S, Funamoto S, Ihara Y & Morishima-Kawashima M (2013) γ -Secretase associated with lipid rafts: multiple interactive pathways in the stepwise processing of β -carboxyl terminal fragment. *J. Biol. Chem.* **289**: 5109–5121

McCaffrey G & Jamieson JC (1993) Evidence for the role of a cathepsin D-like activity in the release of Gal beta 1-4GlcNAc alpha 2-6sialyltransferase from rat and mouse liver in whole-cell systems. *Comp. Biochem. Physiol., B* **104**: 91–94

McCormick C, Duncan G, Goutsos KT & Tufaro F (2000) The putative tumor suppressors EXT1 and EXT2 form a stable complex that accumulates in the Golgi apparatus and catalyzes the synthesis of heparan sulfate. *Proc. Natl. Acad. Sci. U.S.A.* **97**: 668–673

McCoy JP & Chambers WH (1991) Carbohydrates in the functions of natural killer cells. *Glycobiology* **1**: 321–328

McIlwain DR, Lang PA, Maretzky T, Hamada K, Ohishi K, Maney SK, Berger T, Murthy A, Duncan G, Xu HC, Lang KS, Häussinger D, Wakeham A, Itie-Youten A, Khokha R, Ohashi PS, Blobel CP & Mak TW (2012) iRhom2 regulation of TACE controls TNF-mediated protection against Listeria and responses to LPS. *Science* **335**: 229–232

McLauchlan J, Lemberg MK, Hope G & Martoglio B (2002) Intramembrane proteolysis promotes trafficking of hepatitis C virus core protein to lipid droplets. *EMBO J.* **21**: 3980–3988

Meiering CD & Linial ML (2001) Historical perspective of foamy virus epidemiology and infection. *Clin. Microbiol. Rev.* **14**: 165–176

Mellman I & Simons K (1992) The Golgi complex: in vitro veritas? *Cell* **68**: 829–840

Miyashita H, Maruyama Y, Isshiki H, Osawa S, Ogura T, Mio K, Sato C, Tomita T & Iwatubo T (2011) Three-dimensional structure of the signal peptide peptidase. *J. Biol. Chem.* **286**: 26188–26197

Moremen KW, Tiemeyer M & Nairn AV (2012) Vertebrate protein glycosylation: diversity, synthesis and function. *Nat. Rev. Mol. Cell Biol.* **13**: 448–462

Morohashi Y, Kan T, Tominari Y, Fuwa H, Okamura Y, Watanabe N, Sato C, Natsugari H, Fukuyama T, Iwatsubo T & Tomita T (2006) C-terminal fragment of presenilin is the molecular target of a dipeptidic gamma-secretase-specific inhibitor DAPT (N-[N-(3,5-difluorophenacetyl)-L-alanyl]-S-phenylglycine t-butyl ester). *J. Biol. Chem.* **281**: 14670–14676

Morriswood B & Warren G (2013) Cell biology. Stalemate in the Golgi battle. *Science* **341**: 1465–1466

Multhaupt HAB & Couchman JR (2012) Heparan sulfate biosynthesis: methods for investigation of the heparanosome. *J. Histochem. Cytochem.* **60**: 908–915

Murata K, Miyoshi E, Kameyama M, Ishikawa O, Kabuto T, Sasaki Y, Hiratsuka M, Ohigashi H, Ishiguro S, Ito S, Honda H, Takemura F, Taniguchi N & Imaoka S (2000) Expression of N-acetylglucosaminyltransferase V in colorectal cancer correlates with metastasis and poor prognosis. *Clin. Cancer Res.* **6**: 1772–1777

Murray SM, Picker LJ, Axthelm MK, Hudkins K, Alpers CE & Linial ML (2008) Replication in a Superficial Epithelial Cell Niche Explains the Lack of Pathogenicity of Primate Foamy Virus Infections. *J. Virol.* **82**: 5981–5985

Nagai N, Habuchi H, Esko JD & Kimata K (2004) Stem domains of heparan sulfate 6-O-sulfotransferase are required for Golgi localization, oligomer formation and enzyme activity. *J. Cell. Sci.* **117**: 3331–3341

Nagai N, Habuchi H, Kitazume S, Toyoda H, Hashimoto Y & Kimata K (2007) Regulation of heparan sulfate 6-O-sulfation by beta-secretase activity. *J. Biol. Chem.* **282**: 14942–14951

Nakahara S, Saito T, Kondo N, Moriwaki K, Noda K, Ihara S, Takahashi M, Ide Y, Gu J, Inohara H, Katayama T, Tohyama M, Kubo T, Taniguchi N & Miyoshi E (2006) A secreted type of beta1,6 N-acetylglucosaminyltransferase V (GnT-V), a novel angiogenesis inducer, is regulated by gamma-secretase. *FASEB J.* **20**: 2451–2459

Narayanan S, Sato T & Wolfe MS (2007) A C-terminal region of signal peptide peptidase defines a functional domain for intramembrane aspartic protease catalysis. *J. Biol. Chem.* **282**: 20172–20179

Nasimuzzaman M & Persons DA (2012) Cell Membrane-associated Heparan Sulfate Is a Receptor for Prototype Foamy Virus in Human, Monkey, and Rodent Cells. *Mol. Ther.* **20**: 1158–1166

Nilsberth C, Westlind-Danielsson A, Eckman CB, Condron MM, Axelman K, Forsell C, Stenb C, Luthman J, Teplow DB, Younkin SG, Näslund J & Lannfelt L (2001) The 'Arctic' APP mutation (E693G) causes Alzheimer's disease by enhanced Abeta protofibril formation. *Nat. Neurosci.* **4**: 887–893

North SJ, Koles K, Hembd C, Morris HR, Dell A, Panin VM & Haslam SM (2006) Glycomic studies of *Drosophila melanogaster* embryos. *Glycoconj. J.* **23**: 345–354

Nyborg AC, Jansen K, Ladd TB, Fauq A & Golde TE (2004) A signal peptide peptidase (SPP) reporter activity assay based on the cleavage of type II membrane protein substrates provides further evidence for an inverted orientation of the SPP active site relative to presenilin. *J. Biol. Chem.* **279**: 43148–43156

Nyborg AC, Ladd TB, Jansen K, Kukar T & Golde TE (2006) Intramembrane proteolytic cleavage by human signal peptide peptidase like 3 and malaria signal peptide peptidase. *FASEB J.* **20**: 1671–1679

Ohtsubo K & Marth JD (2006) Glycosylation in cellular mechanisms of health and disease. *Cell* **126**: 855–867

Okamoto K, Mori Y, Komoda Y, Okamoto T, Okochi M, Takeda M, Suzuki T, Moriishi K & Matsuura Y (2008) Intramembrane processing by signal peptide peptidase regulates the membrane localization of hepatitis C virus core protein and viral propagation. *J. Virol.* **82**: 8349–8361

Okochi M, Fukumori A, Jiang J, Itoh N, Kimura R, Steiner H, Haass C, Tagami S & Takeda M (2006) Secretion of the Notch-1 Abeta-like peptide during Notch signaling. *J. Biol. Chem.* **281**: 7890–7898

Okochi M, Tagami S, Yanagida K, Takami M, Kodama TS, Mori K, Nakayama T, Ihara Y & Takeda M (2013) γ -secretase modulators and presenilin 1 mutants act differently on presenilin/ γ -secretase function to cleave A β 42 and A β 43. *Cell Rep.* **3**: 42–51

Ortaldo JR, Winkler-Pickett R, Mason AT & Mason LH (1998) The Ly-49 family: regulation of cytotoxicity and cytokine production in murine CD3+ cells. *J. Immunol.* **160**: 1158–1165

Paetzel M, Karla A, Strynadka NCJ & Dalbey RE (2002) Signal Peptidases. *Chem. Rev.* **102**: 4549–4580

Pan S, Wang S, Utama B, Huang L, Blok N, Estes MK, Moremen KW & Sifers RN (2011) Golgi localization of ERManI defines spatial separation of the mammalian glycoprotein quality control system. *Mol. Biol. Cell* **22**: 2810–2822

Paulson JC & Colley KJ (1989) Glycosyltransferases. Structure, localization, and control of cell type-specific glycosylation. *J. Biol. Chem.* **264**: 17615–17618

Plochmann K, Horn A, Gschmack E, Armbruster N, Krieg J, Wiktorowicz T, Weber C, Stirnnagel K, Lindemann D, Rethwilm A & Scheller C (2012) Heparan sulfate is an attachment factor for foamy virus entry. *J. Virol.* **86**: 10028–10035

Ponting CP, Hutton M, Nyborg A, Baker M, Jansen K & Golde TE (2002) Identification of a novel family of presenilin homologues. *Hum. Mol. Genet.* **11**: 1037–1044

Popot JL & Engelman DM (2000) Helical membrane protein folding, stability, and evolution. *Annu. Rev. Biochem.* **69**: 881–922

Prokop S, Shirotani K, Edbauer D, Haass C & Steiner H (2004) Requirement of PEN-2 for stabilization of the presenilin N/C-terminal fragment heterodimer within the gamma-secretase complex. *J. Biol. Chem.* **279**: 23255–23261

Qi-Takahara Y, Morishima-Kawashima M, Tanimura Y, Dolios G, Hirotani N, Horikoshi Y, Kametani F, Maeda M, Saido TC, Wang R & Ihara Y (2005) Longer forms of amyloid beta protein: implications for the mechanism of intramembrane cleavage by gamma-secretase. *J. Neurosci.* **25**: 436–445

Randall G, Panis M, Cooper JD, Tellinghuisen TL, Sukhodolets KE, Pfeffer S, Landthaler M, Landgraf P, Kan S, Lindenbach BD, Chien M, Weir DB, Russo JJ, Ju J, Brownstein MJ, Sheridan R, Sander C, Zavolan M, Tuschl T & Rice CM (2007) Cellular cofactors affecting hepatitis C virus infection and replication. *Proc. Natl. Acad. Sci. U.S.A.* **104**: 12884–12889

Rath A & Deber CM (2012) Protein structure in membrane domains. *Annu. Rev. Biophys.* **41**: 135–155

Rawson RB, Zelenski NG, Nijhawan D, Ye J, Sakai J, Hasan MT, Chang TY, Brown MS & Goldstein JL (1997) Complementation cloning of S2P, a gene encoding a putative metalloprotease required for intramembrane cleavage of SREBPs. *Mol. Cell* **1**: 47–57

Real PJ, Tosello V, Palomero T, Castillo M, Hernando E, de Stanchina E, Sulis ML, Barnes K, Sawai C, Homminga I, Meijerink J, Aifantis I, Basso G, Cordon-Cardo C, Ai W & Ferrando A (2009) Gamma-secretase inhibitors reverse glucocorticoid resistance in T cell acute lymphoblastic leukemia. *Nat. Med.* **15**: 50–58

Ren Z, Schenk D, Basi GS & Shapiro IP (2007) Amyloid beta-protein precursor juxtamembrane domain regulates specificity of gamma-secretase-dependent cleavages. *J. Biol. Chem.* **282**: 35350–35360

Rethwilm A (2010) Molecular biology of foamy viruses. *Med. Microbiol. Immunol.* **199**: 197–207

Reynders E, Foulquier F, Annaert W & Matthijs G (2011) How Golgi glycosylation meets and needs trafficking: the case of the COG complex. *Glycobiology* **21**: 853–863

Robakis T, Bak B, Lin S-H, Bernard DJ & Scheiffele P (2008) An internal signal sequence directs intramembrane proteolysis of a cellular immunoglobulin domain protein. *J. Biol. Chem.* **283**: 36369–36376

Rogaev EI, Sherrington R, Rogaeva EA, Levesque G, Ikeda M, Liang Y, Chi H, Lin C, Holman K & Tsuda T (1995) Familial Alzheimer's disease in kindreds with missense mutations in a gene on chromosome 1 related to the Alzheimer's disease type 3 gene. *Nature* **376**: 775–778

Rossner M & Yamada KM (2004) What's in a picture? The temptation of image manipulation. *J. Cell. Biol.* **166**: 11–15

Roth J (2002) Protein N-glycosylation along the secretory pathway: relationship to organelle topography and function, protein quality control, and cell interactions. *Chem. Rev.* **102**: 285–303

Roth J & Berger EG (1982) Immunocytochemical localization of galactosyltransferase in HeLa cells: codistribution with thiamine pyrophosphatase in trans-Golgi cisternae. *J. Cell. Biol.* **93**: 223–229

Ruggieri A, Maldener E, Sauter M, Mueller-Lantzsch N, Meese E, Fackler OT & Mayer J (2009) Human endogenous retrovirus HERV-K(HML-2) encodes a stable signal peptide with biological properties distinct from Rec. *Retrovirology* **6**: 17

Saito T, Miyoshi E, Sasai K, Nakano N, Eguchi H, Honke K & Taniguchi N (2002) A secreted type of beta 1,6-N-acetylglucosaminyltransferase V (GnT-V) induces tumor angiogenesis without mediation of glycosylation: a novel function of GnT-V distinct from the original glycosyltransferase activity. *J. Biol. Chem.* **277**: 17002–17008

Saito T, Suemoto T, Brouwers N, Sleegers K, Funamoto S, Mihira N, Matsuba Y, Yamada K, Nilsson P, Takano J, Nishimura M, Iwata N, Van Broeckhoven C, Ihara Y & Saido TC (2011) Potent amyloidogenicity and pathogenicity of A β 43. *Nat. Neurosci.* **14**: 1023–1032

Sarrazin S, Lamanna WC & Esko JD (2011) Heparan sulfate proteoglycans. *Cold Spring Harb Perspect Biol* **3**: a004952

Sasaki K, Kurata-Miura K, Ujita M, Angata K, Nakagawa S, Sekine S, Nishi T & Fukuda M (1997) Expression cloning of cDNA encoding a human beta-1,3-N-acetylglucosaminyltransferase that is essential for poly-N-acetyllactosamine synthesis. *Proc. Natl. Acad. Sci. U.S.A.* **94**: 14294–14299

Sato C, Morohashi Y, Tomita T & Iwatsubo T (2006a) Structure of the catalytic pore of gamma-secretase probed by the accessibility of substituted cysteines. *J. Neurosci.* **26**: 12081–12088

Sato C, Takagi S, Tomita T & Iwatsubo T (2008) The C-terminal PAL motif and transmembrane domain 9 of presenilin 1 are involved in the formation of the catalytic pore of the gamma-secretase. *J. Neurosci.* **28**: 6264–6271

Sato T, Diehl TS, Narayanan S, Funamoto S, Ihara Y, De Strooper B, Steiner H, Haass C & Wolfe MS (2007) Active gamma-secretase complexes contain only one of each component. *J. Biol. Chem.* **282**: 33985–33993

Sato T, Nyborg AC, Iwata N, Diehl TS, Saido TC, Golde TE & Wolfe MS (2006b) Signal peptide peptidase: biochemical properties and modulation by nonsteroidal antiinflammatory drugs. *Biochemistry* **45**: 8649–8656

Schachter H (1991) The 'yellow brick road' to branched complex N-glycans. *Glycobiology* **1**: 453–461

Schachter H (2000) The joys of HexNAc. The synthesis and function of N- and O-glycan branches. *Glycoconj. J.* **17**: 465–483

Scheuner D, Eckman C, Jensen M, Song X, Citron M, Suzuki N, Bird TD, Hardy J, Hutton M, Kukull W, Larson E, Levy-Lahad E, Viitanen M, Peskind E, Poorkaj P, Schellenberg G, Tanzi R, Wasco W, Lannfelt L, Selkoe D, et al (1996) Secreted amyloid beta-protein similar to that in the senile plaques of Alzheimer's disease is increased in vivo by the presenilin 1 and 2 and APP mutations linked to familial Alzheimer's disease. *Nat. Med.* **2**: 864–870

Schmidt M, Niewiesk S, Heeney J, Aguzzi A & Rethwilm A (1997) Mouse model to study the replication of primate foamy viruses. *J. Gen. Virol.* **78**: 1929–1933

Schneppenheim J, Dressel R, Hüttl S, Lüllmann-Rauch R, Engelke M, Dittmann K, Wienands J, Eskelinen E-L, Hermans-Borgmeyer I, Flührer R, Saftig P & Schröder B (2013) The intramembrane protease SPPL2a promotes B cell development and controls endosomal traffic by cleavage of the invariant chain. *J. Exp. Med.* **210**: 41–58

Schneppenheim J, Hüttl S, Mentrup T, Lüllmann-Rauch R, Rothaug M, Engelke M, Dittmann K, Dressel R, Araki M, Araki K, Wienands J, Flührer R, Saftig P & Schröder B (2014) The intramembrane proteases signal Peptidase-like 2a and 2b have distinct functions in vivo. *Mol. Cell. Biol.* **34**: 1398–1411

Schön S, Prante C, Bahr C, Kuhn J, Kleesiek K & Götting C (2006) Cloning and recombinant expression of active full-length xylosyltransferase I (XT-I) and characterization of subcellular localization of XT-I and XT-II. *J. Biol. Chem.* **281**: 14224–14231

Schroeter EH, Kisslinger JA & Kopan R (1998) Notch-1 signalling requires ligand-induced proteolytic release of intracellular domain. *Nature* **393**: 382–386

Schrul B, Kapp K, Sinning I & Dobberstein B (2010) Signal peptide peptidase (SPP) assembles with substrates and misfolded membrane proteins into distinct oligomeric complexes. *Biochem. J.* **427**: 523–534

Schweizer M, Falcone V, Gänge J, Turek R & Neumann-Haefelin D (1997) Simian foamy virus isolated from an accidentally infected human individual. *J. Virol.* **71**: 4821–4824

Schweizer M, Turek R, Hahn H, Schliephake A, Netzer KO, Eder G, Reinhardt M, Rethwilm A & Neumann-Haefelin D (1995) Markers of foamy virus infections in monkeys, apes, and accidentally infected humans: appropriate testing fails to confirm suspected foamy virus prevalence in humans. *AIDS Res. Hum. Retroviruses* **11**: 161–170

Sears P & Wong CH (1998) Enzyme action in glycoprotein synthesis. *Cell. Mol. Life Sci.* **54**: 223–252

Selkoe DJ (1991) The molecular pathology of Alzheimer's disease. *Neuron* **6**: 487–498

Serneels L, Dejaegere T, Craessaerts K, Horré K, Jorissen E, Tousseyn T, Hébert S, Coolen M, Martens G, Zwijnen A, Annaert W, Hartmann D & De Strooper B (2005) Differential contribution of the three Aph1 genes to gamma-secretase activity in vivo. *Proc. Natl. Acad. Sci. U.S.A.* **102**: 1719–1724

Seubert P, Vigo-Pelfrey C, Esch F, Lee M, Dovey H, Davis D, Sinha S, Schlossmacher M, Whaley J & Swindlehurst C (1992) Isolation and quantification of soluble Alzheimer's beta-peptide from biological fluids. *Nature* **359**: 325–327

Shah S, Lee S-F, Tabuchi K, Hao Y-H, Yu C, LaPlant Q, Ball H, Dann CE, Südhof T & Yu G (2005) Nicastin functions as a gamma-secretase-substrate receptor. *Cell* **122**: 435–447

Shaheen R, Faqeih E, Ansari S & Alkuraya FS (2013) A truncating mutation in B3GNT1 causes severe Walker-Warburg syndrome. *Neurogenetics* **14**: 243–245

Shao S & Hegde RS (2011) Membrane protein insertion at the endoplasmic reticulum. *Annu. Rev. Cell Dev. Biol.* **27**: 25–56

Sharpe HJ, Stevens TJ & Munro S (2010) A Comprehensive Comparison of Transmembrane Domains Reveals Organelle-Specific Properties. *Cell* **142**: 158–169

Shearman MS, Behar D, Clarke EE, Lewis HD, Harrison T, Hunt P, Nadin A, Smith AL, Stevenson G & Castro JL (2000) L-685,458, an Aspartyl Protease Transition State Mimic, Is a Potent Inhibitor of Amyloid β -Protein Precursor γ -Secretase Activity. *Biochemistry* **39**: 8698–8704

Shen J & Kelleher RJ (2007) The presenilin hypothesis of Alzheimer's disease: evidence for a loss-of-function pathogenic mechanism. *Proc. Natl. Acad. Sci. U.S.A.* **104**: 403–409

Shen J & Prywes R (2004) Dependence of site-2 protease cleavage of ATF6 on prior site-1 protease digestion is determined by the size of the luminal domain of ATF6. *J. Biol. Chem.* **279**: 43046–43051

Sherrington R, Rogaei EI, Liang Y, Rogaeva EA, Levesque G, Ikeda M, Chi H, Lin C, Li G, Holman K, Tsuda T, Mar L, Foncin JF, Bruni AC, Montesi MP, Sorbi S, Rainero I, Pinessi L, Nee L, Chumakov I, et al (1995) Cloning of a gene bearing missense mutations in early-onset familial Alzheimer's disease. *Nature* **375**: 754–760

Shoji M, Golde TE, Ghiso J, Cheung TT, Estus S, Shaffer LM, Cai XD, McKay DM, Tintner R & Frangione B (1992) Production of the Alzheimer amyloid beta protein by normal proteolytic processing. *Science* **258**: 126–129

Shoreibah M, Perng GS, Adler B, Weinstein J, Basu R, Cupples R, Wen D, Browne JK, Buckhaults P, Fregien N & Pierce M (1993) Isolation, characterization, and expression of a cDNA encoding N-acetylglucosaminyltransferase V. *J. Biol. Chem.* **268**: 15381–15385

Shur BD, Rodeheffer C, Ensslin MA, Lyng R & Raymond A (2006) Identification of novel gamete receptors that mediate sperm adhesion to the egg coat. *Mol. Cell. Endocrinol.* **250**: 137–148

Spasic D, Tolia A, Dillen K, Baert V, De Strooper B, Vrijens S & Annaert W (2006) Presenilin-1 maintains a nine-transmembrane topology throughout the secretory pathway. *J. Biol. Chem.* **281**: 26569–26577

Stanley P (2011) Golgi glycosylation. *Cold Spring Harb Perspect Biol* **3**: a005199

Stanley P & Cummings RD (2009) Structures Common to Different Glycans. In *Essentials of Glycobiology*, Varki A Cummings RG Esko JD Freeze HH Stanley P Bertozzi CR Hart GW & Etzler ME (eds) pp 175–198. Cold Spring Harbor: Cold Spring Harbor Laboratory Press

Stanley P, Caillibot V & Siminovitch L (1975) Selection and characterization of eight phenotypically distinct lines of lectin-resistant Chinese hamster ovary cell. *Cell* **6**: 121–128

Stanley P, Schachter H & Taniguchi N (2009) N-Glycans. In *Essentials of Glycobiology*, Varki A Cummings RG Esko JD Freeze HH Stanley P Bertozzi CR Hart GW & Etzler ME (eds) pp 101–114. Cold Spring Harbor: Cold Spring Harbor Laboratory Press

Steiner H, Duff K, Capell A, Romig H, Grim MG, Lincoln S, Hardy J, Yu X, Picciano M, Fechteler K, Citron M, Kopan R, Pesold B, Keck S, Baader M, Tomita T, Iwatsubo T, Baumeister R & Haass C (1999) A loss of function mutation of presenilin-2 interferes with amyloid beta-peptide production and notch signaling. *J. Biol. Chem.* **274**: 28669–28673

Steiner H, Fluhrer R & Haass C (2008a) Intramembrane proteolysis by gamma-secretase. *J. Biol. Chem.* **283**: 29627–29631

Steiner H, Kostka M, Romig H, Bassett G, Pesold B, Hardy J, Capell A, Meyn L, Grim ML, Baumeister R, Fechteler K & Haass C (2000) Glycine 384 is required for presenilin-1 function and is conserved in bacterial polytopic aspartyl proteases. *Nat. Cell Biol.* **2**: 848–851

Steiner H, Winkler E & Haass C (2008b) Chemical cross-linking provides a model of the gamma-secretase complex subunit architecture and evidence for close proximity of the C-terminal fragment of presenilin with APH-1. *J. Biol. Chem.* **283**: 34677–34686

Stephens EB, Buttiloski EJ & Monck E (1992) Analysis of the amino terminal presequence of the feline immunodeficiency virus glycoprotein: effect of deletions on the intracellular transport of gp95. *Virology* **190**: 569–578

Strisovsky K, Sharpe HJ & Freeman M (2009) Sequence-Specific Intramembrane Proteolysis: Identification of a Recognition Motif in Rhomboid Substrates. *Mol. Cell* **36**: 1048–1059

Struhl G & Adachi A (2000) Requirements for presenilin-dependent cleavage of notch and other transmembrane proteins. *Mol. Cell* **6**: 625–636

Sugahara K & Kitagawa H (2002) Heparin and heparan sulfate biosynthesis. *IUBMB Life* **54**: 163–175

Suguna K, Padlan EA, Smith CW, Carlson WD & Davies DR (1987) Binding of a reduced peptide inhibitor to the aspartic proteinase from Rhizopus chinensis: implications for a mechanism of action. *Proc. Natl. Acad. Sci. U.S.A.* **84**: 7009–7013

Suzuki N, Cheung TT, Cai XD, Odaka A, Otvos L, Eckman C, Golde TE & Younkin SG (1994) An increased percentage of long amyloid beta protein secreted by familial amyloid beta protein precursor (beta APP717) mutants. *Science* **264**: 1336–1340

Takami M & Funamoto S (2012) γ -Secretase-Dependent Proteolysis of Transmembrane Domain of Amyloid Precursor Protein: Successive Tri- and Tetrapeptide Release in Amyloid β -Protein Production. *Int J Alzheimers Dis* **2012**: 591392

Takami M, Nagashima Y, Sano Y, Ishihara S, Morishima-Kawashima M, Funamoto S & Ihara Y (2009) gamma-Secretase: successive tripeptide and tetrapeptide release from the transmembrane domain of beta-carboxyl terminal fragment. *J. Neurosci.* **29**: 13042–13052

Takasugi N, Tomita T, Hayashi I, Tsuruoka M, Niimura M, Takahashi Y, Thinakaran G & Iwatsubo T (2003) The role of presenilin cofactors in the gamma-secretase complex. *Nature* **422**: 438–441

Tang T, Li L, Tang J, Li Y, Lin WY, Martin F, Grant D, Solloway M, Parker L, Ye W, Forrest W, Ghilardi N, Oravecz T, Platt KA, Rice DS, Hansen GM, Abuin A, Eberhart DE, Godowski P, Holt KH, et al (2010) A mouse knockout library for secreted and transmembrane proteins. *Nat. Biotechnol.* **28**: 749–755

Targett-Adams P, Hope G, Boulant S & McLauchlan J (2008) Maturation of hepatitis C virus core protein by signal peptide peptidase is required for virus production. *J. Biol. Chem.* **283**: 16850–16859

Targett-Adams P, Schaller T, Hope G, Lanford RE, Lemon SM, Martin A & McLauchlan J (2006) Signal peptide peptidase cleavage of GB virus B core protein is required for productive infection in vivo. *J. Biol. Chem.* **281**: 29221–29227

Teneberg S, Angström J, Jovall PA & Karlsson KA (1994) Characterization of binding of Gal beta 4GlcNAc-specific lectins from *Erythrina cristagalli* and *Erythrina corallodendron* to glycosphinogolipids. Detection, isolation, and characterization of a novel glycosphingolipid of bovine buttermilk. *J. Biol. Chem.* **269**: 8554–8563

Thinakaran G, Borchelt DR, Lee MK, Slunt HH, Spitzer L, Kim G, Ratovitsky T, Davenport F, Nordstedt C, Seeger M, Hardy J, Levey AI, Gandy SE, Jenkins NA, Copeland NG, Price DL & Sisodia SS (1996) Endoproteolysis of presenilin 1 and accumulation of processed derivatives in vivo. *Neuron* **17**: 181–190

Tolia A, Chávez-Gutiérrez L & De Strooper B (2006) Contribution of presenilin transmembrane domains 6 and 7 to a water-containing cavity in the gamma-secretase complex. *J. Biol. Chem.* **281**: 27633–27642

Tolia A, Horré K & De Strooper B (2008) Transmembrane domain 9 of presenilin determines the dynamic conformation of the catalytic site of gamma-secretase. *J. Biol. Chem.* **283**: 19793–19803

Tomita T, Watabiki T, Takikawa R, Morohashi Y, Takasugi N, Kopan R, De Strooper B & Iwatsubo T (2001) The first proline of PALP motif at the C terminus of presenilins is obligatory for stabilization, complex formation, and gamma-secretase activities of presenilins. *J. Biol. Chem.* **276**: 33273–33281

Torres-Arancibia C, Ross CM, Chavez J, Assur Z, Dolios G, Mancia F & Ubarretxena-Belandia I (2010) Identification of an archaeal presenilin-like intramembrane protease. *PLoS ONE* **5**: e13072

Trobridge G, Josephson N, Vassilopoulos G, Mac J & Russell DW (2002) Improved foamy virus vectors with minimal viral sequences. *Mol. Ther.* **6**: 321–328

Tsruya R, Wojtalla A, Carmon S, Yoge S, Reich A, Bibi E, Merdes G, Schejter E & Shilo B-Z (2007) Rhomboid cleaves Star to regulate the levels of secreted Spitz. *EMBO J.* **26**: 1211–1220

Tu L & Banfield DK (2010) Localization of Golgi-resident glycosyltransferases. *Cell. Mol. Life Sci.* **67**: 29–41

Tu L, Tai WCS, Chen L & Banfield DK (2008) Signal-mediated dynamic retention of glycosyltransferases in the Golgi. *Science* **321**: 404–407

Tulsiani DRP (2006) Glycan-modifying enzymes in luminal fluid of the mammalian epididymis: an overview of their potential role in sperm maturation. *Mol. Cell. Endocrinol.* **250**: 58–65

Turk B, Turk DSA & Turk V (2012) Protease signalling: the cutting edge. *EMBO J.* **31**: 1630–1643

Uchiyama T, Adriani M, Jagadeesh GJ, Paine A & Candotti F (2012) Foamy Virus Vector-mediated Gene Correction of a Mouse Model of Wiskott-Aldrich Syndrome. *Mol. Ther.* **20**: 1270–1279

Ujita M, McAuliffe J, Hindsgaul O, Sasaki K, Fukuda MN & Fukuda M (1999) Poly-N-acetyllactosamine synthesis in branched N-glycans is controlled by complementary branch specificity of I-extension enzyme and beta1,4-galactosyltransferase I. *J. Biol. Chem.* **274**: 16717–16726

Ujita M, Misra AK, McAuliffe J, Hindsgaul O & Fukuda M (2000) Poly-N-acetyllactosamine extension in N-glycans and core 2- and core 4-branched O-glycans is differentially controlled by I-extension enzyme and different members of the beta 1,4-galactosyltransferase gene family. *J. Biol. Chem.* **275**: 15868–15875

Urban S (2006) Rhomboid proteins: conserved membrane proteases with divergent biological functions. *Genes Dev.* **20**: 3054–3068

Urban S (2010) Taking the plunge: integrating structural, enzymatic and computational insights into a unified model for membrane-immersed rhomboid proteolysis. *Biochem. J.* **425**: 501–512

Urban S & Dickey SW (2011) The rhomboid protease family: a decade of progress on function and mechanism. *Genome Biol.* **12**: 231

Urban S & Freeman M (2003) Substrate specificity of rhomboid intramembrane proteases is governed by helix-breaking residues in the substrate transmembrane domain. *Mol. Cell* **11**: 1425–1434

Urban S & Shi Y (2008) Core principles of intramembrane proteolysis: comparison of rhomboid and site-2 family proteases. *Curr. Opin. Struct. Biol.* **18**: 432–441

Urban S & Wolfe MS (2005) Reconstitution of intramembrane proteolysis in vitro reveals that pure rhomboid is sufficient for catalysis and specificity. *Proc. Natl. Acad. Sci. U.S.A.* **102**: 1883–1888

Urný J, Hermans-Borgmeyer I, Gercken G & Chica Schaller H (2003) Expression of the presenilin-like signal peptide peptidase (SPP) in mouse adult brain and during development. *Gene Expr. Patterns* **3**: 685–691

van den Eijnden DH, Koenderman AH & Schiphorst WE (1988) Biosynthesis of blood group i-active polylactosaminoglycans. Partial purification and properties of an UDP-GlcNAc:N-acetyllactosaminide beta 1---3-N-acetylglucosaminyltransferase from Novikoff tumor cell ascites fluid. *J. Biol. Chem.* **263**: 12461–12471

van Kuppevelt TH, Dennissen MA, van Venrooij WJ, Hoet RM & Veerkamp JH (1998) Generation and application of type-specific anti-heparan sulfate antibodies using phage display technology. Further evidence for heparan sulfate heterogeneity in the kidney. *J. Biol. Chem.* **273**: 12960–12966

Varki A, Esko JD & Colley KJ (2009) Cellular Organization of Glycosylation. In *Essentials of Glycobiology*, Varki A Cummings RG Esko JD Freeze HH Stanley P Bertozzi CR Hart GW & Etzler ME (eds) pp 37–46. Cold Spring Harbor: Cold Spring Harbor Laboratory Press

Verschoor EJ, Hulskotte EG, Ederveen J, Koolen MJ, Horzinek MC & Rottier PJ (1993) Post-translational processing of the feline immunodeficiency virus envelope precursor protein. *Virology* **193**: 433–438

Vivier E, Tomasello E, Baratin M, Walzer T & Ugolini S (2008) Functions of natural killer cells. *Nat. Immunol.* **9**: 503–510

Voss M, Schröder B & Fluhrer R (2013) Mechanism, specificity, and physiology of signal peptide peptidase (SPP) and SPP-like proteases. *Biochim. Biophys. Acta* **1828**: 2828–2839

Walzer T, Bléry M, Chaix J, Fuseri N, Chasson L, Robbins SH, Jaeger S, André P, Gauthier L, Daniel L, Chemin K, Morel Y, Dalod M, Imbert J, Pierres M, Moretta A, Romagné F & Vivier E (2007) Identification, activation, and selective in vivo ablation of mouse NK cells via NKp46. *Proc. Natl. Acad. Sci. U.S.A.* **104**: 3384–3389

Wang G & Mulligan MJ (1999) Comparative sequence analysis and predictions for the envelope glycoproteins of foamy viruses. *J. Gen. Virol.* **80**: 245–254

Wang J, Beher D, Nyborg AC, Shearman MS, Golde TE & Goate A (2006) C-terminal PAL motif of presenilin and presenilin homologues required for normal active site conformation. *J. Neurochem.* **96**: 218–227

Wang J, Brunkan AL, Hecimovic S, Walker E & Goate A (2004) Conserved 'PAL' sequence in presenilins is essential for gamma-secretase activity, but not required for formation or stabilization of gamma-secretase complexes. *Neurobiol. Dis.* **15**: 654–666

Wang Y, Tan J, Sutton-Smith M, Ditto D, Panico M, Campbell RM, Varki NM, Long JM, Jaeken J, Levinson SR, Wynshaw-Boris A, Morris HR, Le D, Dell A, Schachter H & Marth JD (2001) Modeling human congenital disorder of glycosylation type IIa in the mouse: conservation of asparagine-linked glycan-dependent functions in mammalian physiology and insights into disease pathogenesis. *Glycobiology* **11**: 1051–1070

Weihofen A, Binns K, Lemberg MK, Ashman K & Martoglio B (2002) Identification of signal peptide peptidase, a presenilin-type aspartic protease. *Science* **296**: 2215–2218

Weihofen A, Lemberg MK, Friedmann E, Rueege H, Schmitz A, Paganetti P, Rovelli G & Martoglio B (2003) Targeting presenilin-type aspartic protease signal peptide peptidase with gamma-secretase inhibitors. *J. Biol. Chem.* **278**: 16528–16533

Weihofen A, Lemberg MK, Ploegh HL, Bogoy M & Martoglio B (2000) Release of signal peptide fragments into the cytosol requires cleavage in the transmembrane region by a protease activity that is specifically blocked by a novel cysteine protease inhibitor. *J. Biol. Chem.* **275**: 30951–30956

Weinstein J, Lee EU, McEntee K, Lai PH & Paulson JC (1987) Primary structure of beta-galactoside alpha 2,6-sialyltransferase. Conversion of membrane-bound enzyme to soluble forms by cleavage of the NH₂-terminal signal anchor. *J. Biol. Chem.* **262**: 17735–17743

Weng AP, Ferrando AA, Lee W, Morris JP, Silverman LB, Sanchez-Irizarry C, Blacklow SC, Look AT & Aster JC (2004) Activating mutations of NOTCH1 in human T cell acute lymphoblastic leukemia. *Science* **306**: 269–271

Wilk T, Geiselhart V, Frech M, Fuller SD, Flügel RM & Löchelt M (2001) Specific interaction of a novel foamy virus Env leader protein with the N-terminal Gag domain. *J. Virol.* **75**: 7995–8007

Williams NS, Klem J, Puzanov IJ, Sivakumar PV, Bennett M & Kumar V (1999) Differentiation of NK1.1+, Ly49+ NK cells from flt3+ multipotent marrow progenitor cells. *J. Immunol.* **163**: 2648–2656

Williamson RA, Henry MD, Daniels KJ, Hrstka RF, Lee JC, Sunada Y, Ibraghimov-Beskrovnaya O & Campbell KP (1997) Dystroglycan is essential for early embryonic development: disruption of Reichert's membrane in Dag1-null mice. *Hum. Mol. Genet.* **6**: 831–841

Wiltfang J, Smirnov A, Schnierstein B, Kelemen G, Matthies U, Klafki HW, Staufenbiel M, Hüther G, Rüther E & Kornhuber J (1997) Improved electrophoretic separation and immunoblotting of beta-amyloid (A beta) peptides 1-40, 1-42, and 1-43. *Electrophoresis* **18**: 527–532

Winkler E, Hobson S, Fukumori A, Dämpfelfeld B, Luebbers T, Baumann K, Haass C, Hopf C & Steiner H (2009) Purification, Pharmacological Modulation, and Biochemical Characterization of Interactors of Endogenous Human γ -Secretase. *Biochemistry* **48**: 1183–1197

Wolfe MS (2009) Intramembrane proteolysis. *Chem. Rev.* **109**: 1599–1612

Wolfe MS (2012) γ -Secretase inhibitors and modulators for Alzheimer's disease. *J. Neurochem.* **120 Suppl 1**: 89–98

Wolfe MS & Kopan R (2004) Intramembrane proteolysis: theme and variations. *Science* **305**: 1119–1123

Wolfe MS, Xia W, Ostaszewski BL, Diehl TS, Kimberly WT & Selkoe DJ (1999) Two transmembrane aspartates in presenilin-1 required for presenilin endoproteolysis and gamma-secretase activity. *Nature* **398**: 513–517

Wong PC, Zheng H, Chen H, Becher MW, Sirinathsingji DJ, Trumbauer ME, Chen HY, Price DL, Van der Ploeg LH & Sisodia SS (1997) Presenilin 1 is required for Notch1 and Dll1 expression in the paraxial mesoderm. *Nature* **387**: 288–292

Xia W, Ray WJ, Ostaszewski BL, Rahmati T, Kimberly WT, Wolfe MS, Zhang J, Goate AM & Selkoe DJ (2000) Presenilin complexes with the C-terminal fragments of amyloid precursor protein at the sites of amyloid beta-protein generation. *Proc. Natl. Acad. Sci. U.S.A.* **97**: 9299–9304

Xu J (2005) Preparation, culture, and immortalization of mouse embryonic fibroblasts. *Curr. Protoc. Mol. Biol. Chapter 28*: Unit 28.1

Yang D-S, Tandon A, Chen F, Yu G, Yu H, Arawaka S, Hasegawa H, Duthie M, Schmidt SD, Ramabhadran TV, Nixon RA, Mathews PM, Gandy SE, Mount HTJ, St George-Hyslop P & Fraser PE (2002) Mature glycosylation and trafficking of nicastrin modulate its binding to presenilins. *J. Biol. Chem.* **277**: 28135–28142

Yoshida-Moriguchi T, Willer T, Anderson ME, Venzke D, Whyte T, Muntoni F, Lee H, Nelson SF, Yu L & Campbell KP (2013) SGK196 is a glycosylation-specific O-mannose kinase required for dystroglycan function. *Science* **341**: 896–899

Youakim A, Hathaway HJ, Miller DJ, Gong X & Shur BD (1994) Overexpressing sperm surface beta 1,4-galactosyltransferase in transgenic mice affects multiple aspects of sperm-egg interactions. *J. Cell. Biol.* **126**: 1573–1583

Yu G, Nishimura M, Arawaka S, Levitan D, Zhang L, Tandon A, Song YQ, Rogaeva E, Chen F, Kawarai T, Supala A, Levesque L, Yu H, Yang DS, Holmes E, Milman P, Liang Y, Zhang DM, Xu DH, Sato C, et al (2000) Nicastrin modulates presenilin-mediated notch/glp-1 signal transduction and betaAPP processing. *Nature* **407**: 48–54

Yu J, Freud AG & Caligiuri MA (2013) Location and cellular stages of natural killer cell development. *Trends Immunol.* **34**: 573–582

Yu SF, Eastman SW & Linial ML (2006) Foamy Virus Capsid Assembly Occurs at a Pericentriolar Region Through a Cytoplasmic Targeting/Retention Signal in Gag. *Traffic* **7**: 966–977

Zahn C, Kaup M, Flührer R & Fuchs H (2013) The transferrin receptor-1 membrane stub undergoes intramembrane proteolysis by signal peptide peptidase-like 2b. *FEBS J.* **280**: 1653–1663

Zelenski NG, Rawson RB, Brown MS & Goldstein JL (1999) Membrane topology of S2P, a protein required for intramembranous cleavage of sterol regulatory element-binding proteins. *J. Biol. Chem.* **274**: 21973–21980

Zettl M, Adrain C, Strisovsky K, Lastun V & Freeman M (2011) Rhomboid Family Pseudoproteases Use the ER Quality Control Machinery to Regulate Intercellular Signaling. *Cell* **145**: 79–91

Zhang H, Ma Q, Zhang Y-W & Xu H (2012) Proteolytic processing of Alzheimer's β -amyloid precursor protein. *J. Neurochem.* **120 Suppl 1**: 9–21

Zhou S, Zhou H, Walian PJ & Jap BK (2005) CD147 is a regulatory subunit of the gamma-secretase complex in Alzheimer's disease amyloid beta-peptide production. *Proc. Natl. Acad. Sci. U.S.A.* **102**: 7499–7504

Abbreviations

For description of protein and nucleic acid sequences abbreviations were used according to international recommendations described in *Eur J Biochem* (1984), 138, 9-37, and *Eur J Biochem* (1985), 150, 1-5, respectively. Other abbreviations used in this study are listed in the following.

A β	amyloid β
ACTH	adrenocorticotropic hormone
AD	Alzheimer's disease
ADAM	a disintegrin and metalloprotease
AICD	APP ICD
APH-1	anterior pharynx defective 1
APP	amyloid precursor protein
ATF6	activating transcription factor 6
β 3GnT1	β 1,3 N-acetylglucosaminyltransferase 1
β 3GalT6	β 1,3 galactosyltransferase 6
β 4GalT1	β 1,4 galactosyltransferase 1
BACE1	β -site of APP cleaving enzyme 1
BLAST	basic local alignment search tool
BSA	bovine serum albumin
BMDC	bone marrow-derived DC
CD	cluster of differentiation
CDG	congenital disorder of glycosylation
CHAPS	3-[(3-Cholamidopropyl)dimethylammonio]-1-propanesulphonate
CHAPSO	3-[(3-cholamidopropyl)dimethylammonio]-2-hydroxy-1-propanesulfonate
CHO (cells)	chinese hamster ovary (cells)
CMD	congenital muscular dystrophy
COG	conserved oligomeric Golgi
Con A	Concanavalin A
CS	chondroitin sulphate
CTF	C-terminal fragment
DAPT	N-[N-(3,5-Difluorophenacetyl)-L-alanyl]-S-phenylglycine t-butyl ester
DC	dendritic cell
DMSO	dimethylsulphoxide
DNA	deoxyribonucleic acid
DS	dermatan sulphate
DTT	dithiothreitol
ECL	enhanced chemiluminescence
ECM	extracellular matrix
EGF	epidermal growth factor
EM	electron microscopy
Endo H	endo- β -N-acetylglucosaminidase H
ER	endoplasmic reticulum
ERAD	ER-associated degradation
FACS	fluorescence-activated cell sorting
FAD	familial AD
FCS	fetal calf serum
FasL	Fas ligand

FIV	feline immunodeficiency virus
FV	foamy virus
FVenv	FV envelope glycoprotein
GAG	glycosaminoglycan
GME	glycan-modifying enzyme
GnT	N-acetylglucosaminyltransferase
GO	gene ontology
gp160	HIV env glycoprotein
GSI	γ -secretase inhibitor
GT	glycosyltransferase
HEK (cells)	human embryonic kidney (cells)
HIV	human immunodeficiency virus
HO-1	heme oxygenase-1
HS	heparan sulphate
HS6ST	heparan sulphate 6-O sulphotransferase
I-CLiP	intramembrane-cleaving protease
ICD	intracellular domain
IRHD	iRhom homology domain
IL-15	interleukin-15
KS	keratan sulphate
LP	leader peptide
LacNAc	N-acetyllactosamine
LB	lysogeny broth
mAb	monoclonal antibody
MALDI-TOF	matrix-assisted laser desorption/ionisation time-of-flight
Man I	α -mannosidase I
MEF	murine embryonic fibroblast
MHC	major histocompatibility complex
mRNA	messenger RNA
mut	mutant
NC	Nitrocellulose
NCT	Nicastrin
NCT _{im}	immature NCT
NCT _{mat}	mature NCT
NDST	bifunctional heparan sulphate N-deacetylase/N-sulphotransferase
NICD	Notch ICD
NK (cell)	natural killer (cell)
NP-40	Nonidet P-40
NTF	N-terminal fragment
pAb	polyclonal antibody
PAGE	polyacrylamide gel electrophoresis
PARL	presenilin-associated, rhomboid-like
PBS	phosphate-buffered saline
PC	pro-protein convertase
PCR	polymerase chain reaction
PEN-2	presenilin enhancer 2
PFA	paraformaldehyde
PFP	pre-flagellin peptidase
PHA-L	phytohaemagglutinin L
PNGase F	peptide:N-glycosidase F

PS1/2	presenilin 1/2
PSI-BLAST	position-specific iterated BLAST
PSH	presenilin/SPP homologue
PVDF	polyvinylidene fluoride
RIP	regulated intramembrane proteolysis
RNA	ribonucleic acid
S1P	site-1 protease
S2P	site-2 protease
SAGE	submerged agarose gel electrophoresis
sAPP	secreted/soluble APP
SCAP	SREBP cleavage-activating protein
SDM	site-directed mutagenesis
SDS	sodium dodecyl sulphate
shRNA	short hairpin RNA
siRNA	small interfering RNA
SPECS	secretome protein enrichment with click sugars
SPP	signal peptide peptidase
SPPL	signal peptide peptidase-like
SREBP	sterol regulatory element binding protein
ST3Gal1	β -galactoside α 2,3 sialyltransferase 1
ST6Gal1	β -galactoside α 2,6 sialyltransferase 1
SU	surface subunit
TAE	Tris acetate
TBS	Tris-buffered saline
TCA	trichloroacetic acid
TCR	T cell receptor
TFPP	type IV pre-pilin peptidases
TfR1	transferrin receptor 1
TGN	<i>trans</i> Golgi network
TM	transmembrane subunit
TMD	transmembrane domain
TMEM106B	transmembrane protein 106B
TNF α	tumour necrosis factor α
wt	wild-type
WWS	Walker-Warburg syndrome
XylT	xylosyltransferase
(Z-LL) ₂ ketone	1,3-di-(N-carboxybenzoyl-L-leucyl-L-leucyl)-amino acetone

Acknowledgements

Numerous people have in very diverse ways contributed to the successful completion of this study and deserve to be mentioned here.

First and foremost, I have to express my gratitude to Prof. Dr. Dr. Christian Haass and Dr. Regina Fluhrer for granting me the opportunity to work on this exciting project in their laboratory as well as for supervision, for creative scientific input, for granting me freedom to pursue also my own ideas and, finally, for proofreading this thesis. In addition to that, I particularly appreciate Prof. Haass' constant support, advice and mentorship beyond the mere laboratory business, e.g. for giving me the opportunity to be part of the graduate programme *Protein Dynamics in Health and Disease*. Also, I am indebted to Dr. Fluhrer for guidance, dedicated day-to-day supervision and for being a source of enthusiasm and motivation. Moreover, I thank the examiners, in particular Prof. Dr. Michael Mederos y Schnitzler, for their willingness to invest their precious time and efforts in reading and grading this study.

Importantly, this work would have not been possible without generous funding from a number of sources. In particular, I am deeply indebted to the Hans und Ilse Breuer-Stiftung for granting me a PhD fellowship and providing generous financial support. In addition, I thank the *Elitenetzwerk Bayern* for covering my expenses for conference visits. Finally, this study received financial support from the *Deutsche Forschungsgemeinschaft*.

In addition, I am grateful to the members of the SPP/SPPL laboratory - Martina Haug-Kröper, Bärbel Klier and Gudula Grammer - whose technical expertise was a valuable contribution to this study. Experimental contribution of Ulrike Künzel who was a laboratory intern and later a Master's student under my supervision is also acknowledged. Sabine Odoy's dedicated work ensured that I was never running dry on reagents or materials and that important items were delivered in time.

Of course, this work has greatly profited from numerous scientific collaboration partners. Above all, I have to express my gratitude to a good friend and colleague, Dr. Peer-Hendrik Kuhn, PhD, for being a fruitful source of helpful input and creative ideas and for conducting the proteomics experiments described in the last part of this study. In addition, I thank my other collaborators which include Dr. Alessio Colombo, Dr. Akio Fukumori, Dr. Fabian Higel and Anne Behrendt. Dr. Reinhard Obst's profound mouse expertise was particularly valuable and I am grateful to him and to Anna Kollar for taking care of the *Spp13* genetrap mouse line. Prof. Dr. Harald Steiner's and Prof. Dr. Stefan Lichtenthaler's knowledge and their always helpful comments are also gratefully acknowledged. Moreover, I thank the fellow members of the Haass laboratory, in particular my good friend and fellow in misery Daniel Fleck, but also Dr. Richard Page, Dr. Sebastian Hogl, Dr. Jasmin Sydow and many, many others for helpful discussions and for making it really enjoyable working together.

This study also heavily relied on essential reagents and I am very grateful to those that have so generously provided these. The *Spp1/3* genetrap mouse line, for instance, was established and made available to the research community by Genentech Inc. and Lexicon Pharmaceuticals Inc. Moreover, Prof. Dr. David W. Russell, Dr. Bernd Schröder, Dr. Elisabeth Kremmer, Dr. Anja Capell and Dr. Sabina Tahirovic kindly provided me with essential reagents.

I also thank all other members of the Haass lab - past and present - for providing a lovely work environment. Members of the *Mittagsrunde* and the *Coffee Connection* - Dr. Kathrin Müller-Rischart, Dr. Maria Sadic, Dr. Eva Bentmann, Carolin Schweimer, Benjamin Schwenk and, again, Daniel Fleck - deserve to be mentioned separately and our daily get-togethers will be - and are - sadly missed. I was also very lucky to be part of the graduate programme *Protein Dynamics in Health and Disease* which was funded by the *Elitenetzwerk Bayern*. I thank all my fellow students - again past and present - but also our academic organisers Prof. Dr. Walter Neupert and in particular Dr. Kai Hell for making this such a enjoyable and memorable experience.

Finally, I would like to take this opportunity to thank those not professionally involved in this study - namely my family - for being constantly supportive in so many ways. Above all, I am unbelievably grateful to my fiancé Kristin for her support, motivation, comfort and understanding.

Curriculum vitae

For privacy reasons, these pages are blanked in the publicly available version of this thesis.

For privacy reasons, these pages are blanked in the publicly available version of this thesis.

For privacy reasons, these pages are blanked in the publicly available version of this thesis.

Appendix

This appendix includes copies of manuscripts that either arose from work described in this thesis and/or that were published in the course of this study.

Voss, M., Fukumori, A., Kuhn, P.-H., Künzel, U., Klier, B., Grammer, G., Haug-Kröper, M., Kremmer E., Lichtenthaler, S.F., Steiner, H., Schröder, B., Haass, C., Fluhrer, R. (2012). Foamy virus envelope protein is a substrate for signal peptide peptidase-like 3 (SPPL3). *J. Biol. Chem.* **287**, 43401-43409.

(Page 175)

Voss, M., Schröder, B., Fluhrer R. (2013). Mechanism, specificity, and physiology of signal peptide peptidase (SPP) and SPP-like proteases. *Biochim. Biophys. Acta* **1828**, 282-2839.

(Page 185)

Voss, M., Künzel, U., Higel, F., Kuhn, P.-H., Colombo, A., Fukumori, A., Haug-Kröper, M., Klier, B., Grammer, G., Seidl, A., Schröder, B., Obst, R., Steiner, H., Lichtenthaler, S.F., Haass, C., Fluhrer, R. Shedding of glycan-modifying enzymes by signal peptide peptidase-like 3 (SPPL) affects cellular N-glycosylation. *EMBO J.*, *in revision*.

(Page 197)

Supplemental Material can be found at:
<http://www.jbc.org/content/suppl/2012/11/06/M112.371369.DC1.html>

THE JOURNAL OF BIOLOGICAL CHEMISTRY VOL. 287, NO. 52, pp. 43401–43409, December 21, 2012
 © 2012 by The American Society for Biochemistry and Molecular Biology, Inc. Published in the U.S.A.

Foamy Virus Envelope Protein Is a Substrate for Signal Peptide Peptidase-like 3 (SPPL3)^{*§}

Received for publication, April 11, 2012, and in revised form, October 26, 2012. Published, JBC Papers in Press, November 6, 2012, DOI 10.1074/jbc.M112.371369

Matthias Voss[†], Akio Fukumori[‡], Peer-Hendrik Kuhn[§], Ulrike Künzel[‡], Bärbel Klier[‡], Gudula Grammer[‡], Martina Haug-Kröper[‡], Elisabeth Kremmer^{§¶}, Stefan F. Lichtenthaler^{§||**}, Harald Steiner^{†§}, Bernd Schröder^{‡‡}, Christian Haass^{‡§||‡}, and Regina Fluhrer^{‡§}

From the [†]Adolf Butenandt Institute for Biochemistry, Ludwig-Maximilians University Munich, the [§]German Center for Neurodegenerative Diseases (DZNE), and the [‡]Munich Cluster for Systems Neurology (SyNergy), 80336 Munich, Germany, the [¶]Institute of Molecular Immunology, Helmholtz Zentrum München, German Research Center for Environmental Health and ^{||}Technische Universität München, 81377 Munich, Germany, and the ^{‡‡}Biochemical Institute, Christian-Albrechts University Kiel, 24118 Kiel, Germany

Background: SPPL proteases are intramembrane-cleaving aspartyl proteases of the GxGD type.

Results: Under certain circumstances, SPPL3 cleaves FVenv independent of prior shedding, generating substrates for subsequent intramembrane proteolysis.

Conclusion: Unlike other known GxGD proteases, SPPL3 can act as a sheddase and an intramembrane protease within the regulated intramembrane proteolysis cascade.

Significance: This initial biochemical characterization of SPPL3 will help to address its physiological role in later studies.

Signal peptide peptidase (SPP), its homologs, the SPP-like proteases SPPL2a/b/c and SPPL3, as well as presenilin, the catalytic subunit of the γ -secretase complex, are intramembrane-cleaving aspartyl proteases of the GxGD type. In this study, we identified the 18-kDa leader peptide (LP18) of the foamy virus envelope protein (FVenv) as a new substrate for intramembrane proteolysis by human SPPL3 and SPPL2a/b. In contrast to SPPL2a/b and γ -secretase, which require substrates with an ectodomain shorter than 60 amino acids for efficient intramembrane proteolysis, SPPL3 cleaves mutant FVenv lacking the protein convertase cleavage site necessary for the prior shedding. Moreover, the cleavage product of FVenv generated by SPPL3 serves as a new substrate for consecutive intramembrane cleavage by SPPL2a/b. Thus, human SPPL3 is the first GxGD-type aspartyl protease shown to be capable of acting like a sheddase, similar to members of the rhomboid family, which belong to the class of intramembrane-cleaving serine proteases.

Regulated intramembrane proteolysis describes a two-step proteolytic processing pathway required for protein degradation and cellular signaling of many membrane proteins (1).

Typically, regulated intramembrane proteolysis substrates are first cleaved within their luminal domain to release a large part of their ectodomain or to clip a hairpin loop between two transmembrane domains (TMDs).⁴ This cleavage is termed “shedding” and generates a membrane-retained fragment, which is subsequently processed by an intramembrane-cleaving protease (2–4). Intramembrane proteases are defined as proteolytic enzymes “which reside within cellular membranes and their active sites are buried within the TMD, where they cleave in, or immediately adjacent to, transmembrane domains of their substrates, thereby releasing soluble domains from membrane proteins” (5). So far, intramembrane aspartyl, serine, and metalloproteases have been described (4). Intramembrane-cleaving proteases of the aspartyl protease class are GxGD proteases (2, 3). GxGD describes the amino acid motif in TMD7 of the unconventional but highly conserved protease active site (6). In humans, two subfamilies of GxGD proteases are known: presenilin-1 and presenilin-2, which constitute the catalytic subunit of the γ -secretase complex, and signal peptide peptidase (SPP) and its homologs, the SPP-like (SPPL) proteases SPPL2a/b/c and SPPL3 (3). All known γ -secretase substrates are type I transmembrane proteins (2), whereas SPP/SPPLs selectively cleave type II transmembrane proteins (3). This is consistent with the opposite orientation of the catalytic sites of presenilin and SPP/SPPLs (7). One common requirement for substrate recognition by γ -secretase, SPP, and SPPL2a/b is truncation of the corresponding substrate by shedding, which always precedes intramembrane proteolysis and generates integral membrane proteins short enough to be recognized by these proteases (8–10).

* This work was supported in part by Deutsche Forschungsgemeinschaft Grant HA 1737-11 (to R. F. and C. H.) and the Competence Network for Neurodegenerative Diseases (KNDD) of the Bundesministerium für Bildung und Forschung.

§ This article contains supplemental Figs. S1 and S2.

[†] Supported by a Ph.D. fellowship from the Hans und Ilse Breuer Stiftung and by the Elitenetwork of Bavaria within the Graduate Program “Protein Dynamics in Health and Disease.”

[‡] Member of the Center for Integrated Protein Science Munich (CIPS^M). Supported by a “Forschungsprofessor” from the Ludwig-Maximilians University.

[¶] To whom correspondence should be addressed: Adolf Butenandt Institute for Biochemistry, Ludwig-Maximilians University Munich and DZNE, Schillerstr. 44, D-80336 Munich, Germany. Tel: 49-89-2180-75487; Fax: 49-89-2180-75415; E-mail: regina.fluhrer@dzne.lmu.de.

⁴ The abbreviations used are: TMD, transmembrane domain; SPP, signal peptide peptidase; SPPL, SPP-like; FVenv, foamy virus envelope protein; (Z-LL)₂ ketone, 1,3-di-(N-benzylloxycarbonyl-L-leucyl-L-leucyl)aminoacetone; DAPT, N-(N-(3,5-difluorophenacetyl)-L-alanyl-5-phenylglycine t-butyl ester; ER, endoplasmic reticulum; PC, protein convertase; Tricine, N-[2-hydroxy-1,1-bis(hydroxymethyl)ethyl]glycine.

Downloaded from www.jbc.org at UBW Bibliothek Grosshadern, on January 1, 2013

Endoproteolysis of FVenv by SPPL3

Because only artificial model substrates optimized for SPP cleavage have been used so far to study the proteolytic activity of human SPPL3 (11), very little is known about its biochemical properties. We noticed that, compared with other retroviral signal or leader peptides, the foamy virus envelope (FVenv) protein harbors an unusually long leader peptide (LP18, gp18^{LP}) that is stably integrated into mature virus particles as a type II-oriented transmembrane protein (12). Interestingly, budding of foamy virus particles is observed at intracellular membranes (12). On the basis of this knowledge and our previous observation that individual members of the SPP/SPPL family reside within early secretory compartments (3), we speculated that LP18 of FVenv might be a substrate for SPP/SPPL proteases.

Indeed, we found that the FVenv protein undergoes intramembrane proteolysis mediated by SPPL3 and, in addition, by SPPL2a/b. In contrast to intramembrane proteolysis by SPPL2a/b, cleavage of FVenv by SPPL3 is not dependent on the size of the substrate's ectodomain and is, surprisingly, not sensitive to treatment with known GxGD protease inhibitors. In addition, the cleavage product of LP18 generated by SPPL3 cleavage constitutes a substrate for consecutive intramembrane cleavage by SPPL2a/b.

EXPERIMENTAL PROCEDURES

Antibodies and Reagents—Monoclonal antibodies against SPPL2a and SPPL3 were produced by immunization with synthetic peptides. 2a01 6E9 (mouse IgG1) was generated against peptides comprising amino acids 199–217 of human SPPL2a, and L302 7F9 (mouse IgG1) against amino acids 247–261 of human SPPL3. Anti-FLAG monoclonal (M2) and polyclonal antibodies and anti-FLAG M2-agarose conjugates were obtained from Sigma-Aldrich. Other antibodies used were anti-V5 polyclonal antibody (Millipore), anti-KDEL and anti-calnexin polyclonal antibodies (Enzo Life Sciences), anti-V5 monoclonal antibody (Invitrogen), anti-HA antibody 3F10 (Roche Diagnostics), and anti-HA polyclonal and anti-actin monoclonal antibodies (Sigma-Aldrich). The SPPL2b-specific monoclonal antibody CADG-3F9 has been described previously (13). (Z-LL)₂ ketone and L-685,458 were obtained from Calbiochem, and N-[N-(3,5-difluorophenacetyl)-L-alanyl]-S-phenylglycine *t*-butyl ester (DAPT) was from Enzo Life Sciences. Inhibitor treatment was carried out for 16 h.

Expression Constructs, Cell Lines, and Transfections—SFVcpz(hu) coding sequences were amplified by PCR from pCiES (14), kindly provided by David W. Russell. To generate FVenv, an N-terminal FLAG tag (DYKDDDK) and a V5 tag (GKPIPNNPLGLDST) upstream of the C-terminal endoplasmic reticulum (ER) retention signal (KKKNQ) were introduced. The R123A/R126A mutation was introduced by site-directed mutagenesis according to the instructions of Stratagene.⁵ All FVenv constructs were cloned into pcDNA3.1/Hygro⁺ (Invitrogen) and sequenced for verification. Cell lines stably expressing the FVenv variants were generated, selecting for hygromycin resistance as described previously (13). HEK293 cell lines stably overexpressing WT and mutant SPPL proteases have been described (13). The cDNA

that encodes SPPL3 is based on GenBankTM RefSeq NM_139015.4. All experiments were performed on poly-L-lysine-coated cell culture dishes. Protease expression was induced for at least 48 h by supplementing the media with 1 μ g/ml doxycycline (BD Biosciences). Transient plasmid DNA transfections were carried out using Lipofectamine 2000 (Invitrogen) according to the manufacturer's instructions. Cells were analyzed for protein expression 48 h post-transfection.

siRNA-mediated Knockdown Experiments and TaqMan RT-PCR—siGENOME SMARTpool siRNAs targeting human SPPL3 and SPPL2a and controls were obtained from Dharmacon. Human SPPL2b-specific single oligonucleotides and controls were purchased from Qiagen. siRNAs were transfected using Lipofectamine RNAiMAX (Invitrogen). Cells were analyzed on day 4 or 5 post-transfection. Quantitative TaqMan RT-PCR was used to control knockdown efficiency. Total cellular RNA was isolated using the RNeasy kit and QIAshredder homogenizers (Qiagen). Up to 2 μ g of total RNA was reverse-transcribed using a high capacity reverse transcription kit (Applied Biosystems) according to the manufacturer's instructions. Quantitative PCR was performed using predesigned TaqMan probes for human SPPL2a, human SPPL2b, and human β -actin (Applied Biosystems). Signals obtained were normalized to β -actin, and relative mRNA levels were determined by the $\Delta\Delta C_T$ method.

Cell Lysates (Co)Immunoprecipitation, and Immunoblotting—Cells were harvested on ice and lysed in 150 mM NaCl, 50 mM Tris (pH 7.6), and 2 mM EDTA supplemented with 1% Nonidet P-40, 1% Triton X-100, and protease inhibitor mixture (Sigma-Aldrich). Lysates were either directly analyzed or subjected to immunoprecipitation as indicated in the figures. For co-immunoprecipitation of substrates and proteases, cellular membranes were prepared as described previously (15). Membranes were lysed in 25 mM HEPES-KOH (pH 7.6), 100 mM potassium acetate, 2 mM magnesium acetate, and 1 mM DTT supplemented with 1% CHAPSO (Sigma-Aldrich) on ice. Membrane lysates were subjected to immunoprecipitation as described (16). Electrophoresis and immunoblotting were carried out as described previously (17). Quantification of proteins from Western blots was carried out as described (18).

RESULTS

FVenv Is Proteolytically Processed by SPPL Proteases—FVenv glycoproteins are initially synthesized as type III transmembrane protein precursors and harbor unusually long membrane-tethered signal or leader peptides (Fig. 1A) (12). We studied proteolytic Env processing of the human isolate of the chimpanzee foamy virus (SFVcpz(hu)) (19). Post-translationally, the 130-kDa FVenv protein is proteolytically processed at two sites by furin or furin-like proprotein convertases (PCs) (Fig. 1A) (20–23). This generates the N-terminal 18-kDa leader peptide (LP18, gp18^{LP}), the 80-kDa surface subunit (SU, gp80^{SU}), and the C-terminal 48-kDa membrane-anchored subunit (TM, gp48TM) (Fig. 1A) (12). ER localization of FVenv is mediated by a C-terminal KKKNQ motif (24) and was not affected by the epitope tags that we attached to the FVenv protein (supplemental Fig. S1A).

⁵ Primer sequences are available upon request.

Endoproteolysis of FVenv by SPPL3

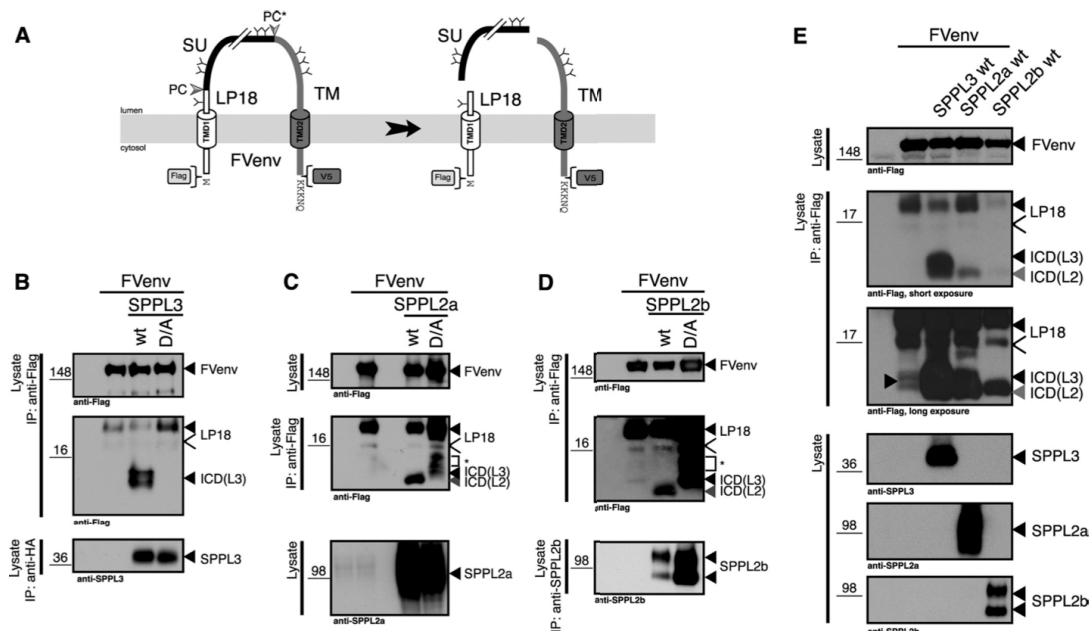


FIGURE 1. SPPL-mediated proteolysis of FVenv. *A*, schematic overview of FVenv processing by PCs. The FVenv glycoprotein consists of a leader peptide (LP18), a surface subunit (SU), and C-terminal membrane-spanning domain (TM). PC and PC* cleavage site (arrowheads), the C-terminal ER retrieval signal (KKKQQ), and the epitope tags (FLAG and VS) are indicated. Glycosylation sites are also indicated (Y). *B–E*, FVenv proteolytic fragments were isolated from HEK293 cells coexpressing FVenv and the indicated SPPL proteases either as catalytically active (WT) or inactive (Asp-to-Ala (D/A)) variants. The open arrowheads indicate unglycosylated LP18. Coexpression of WT SPPL3 resulted predominantly in generation of ICD(L3) (black arrowheads), whereas catalytically active SPPL2a/b produced predominantly ICD(L2) (gray arrowheads). Upon coexpression of FVenv and SPPL2a/b Asp-to-Ala mutants, ICD(L3) and protein fragments (marked with asterisks) accumulated. Depending on the resolution of the gel system, ICD(L3) was sometimes detected as a doublet. *IP*, immunoprecipitation.

Downloaded from www.jbc.org at UBM Bibliothek Grosshadern, on January 1, 2013

To test whether members of the SPP/SPPL family are capable of processing the type II-oriented LP18, FVenv was coexpressed with either biologically active SPPL (WT) or the corresponding catalytically inactive aspartate-to-alanine mutant. Upon coexpression of WT SPPL3, a low molecular mass intracellular fragment, termed ICD(L3), was detected that was almost completely absent in cells expressing SPPL3(D272A) (Fig. 1B). Coexpression of FVenv with SPPL2a also resulted in the generation a low molecular mass intracellular fragment, termed ICD(L2), which was suppressed upon coexpression of the catalytically inactive mutant SPPL2a(D412A) (Fig. 1C). Under the latter condition, additional low molecular mass protein fragments, slightly larger than ICD(L2), accumulated (Fig. 1C). As demonstrated by siRNA-mediated knockdown of SPPL3, the smallest of these fragments corresponds to ICD(L3) (supplemental Fig. S2), which is generated by endogenous SPPL3 activity. The other protein fragments (labeled with an asterisk in Fig. 1, C and D, and supplemental Fig. S2) remained unchanged upon SPPL3 siRNA treatment and most likely result from degradation of the accumulating LP18 (supplemental Fig. S2). Processing of FVenv by SPPL2b was highly similar to that by SPPL2a (Fig. 1D). Expression of SPP induced toxicity in our system; therefore, we were not able to study processing of FVenv by SPP (data not shown). Direct comparison of the ICD species generated by the different SPPL proteases confirmed

that ICD(L3) has a slightly different running behavior compared with ICD(L2) (Fig. 1E). Processing of FVenv by SPPL2a or SPPL2b predominantly resulted in the generation of ICD(L2), whereas only minor amounts of ICD(L3), probably resulting from endogenous SPPL3 activity, were detected (Fig. 1E). Coexpression of SPPL3 and FVenv resulted in massive production of ICD(L3) (Fig. 1E) and ICD(L2) (compare with Fig. 4A). However, because of the limited resolution of the gel system, we could not fully separate ICD(L3) and ICD(L2) under these conditions. Taken together, these data suggest that FVenv is a substrate for intramembrane proteolysis mediated by SPPL3 and its homologs SPPL2a and SPPL2b, which generate two distinct intracellular fragments of FVenv.

*Cleavage of FVenv by SPPL3 Is Independent of Shedding—*N-terminal PC cleavage of FVenv separates LP18 and SU/TM (Fig. 2A), whereas the more C-terminal PC* cleavage is hardly observed upon cellular expression of FVenv containing the ER retrieval signal (25). Thus, processing of FVenv at the N-terminal PC cleavage site is comparable with a classical shedding event of single-span transmembrane proteins required for subsequent intramembrane proteolysis. To inhibit processing of FVenv by PC, the R123A/R126A mutation (FVenv mut) was introduced (Fig. 2A). Subcellular localization of FVenv was not affected by the mutation (supplemental Fig. S1B). As expected, processing of FVenv mut by PC was strongly diminished, and

Endoproteolysis of FVenv by SPPL3

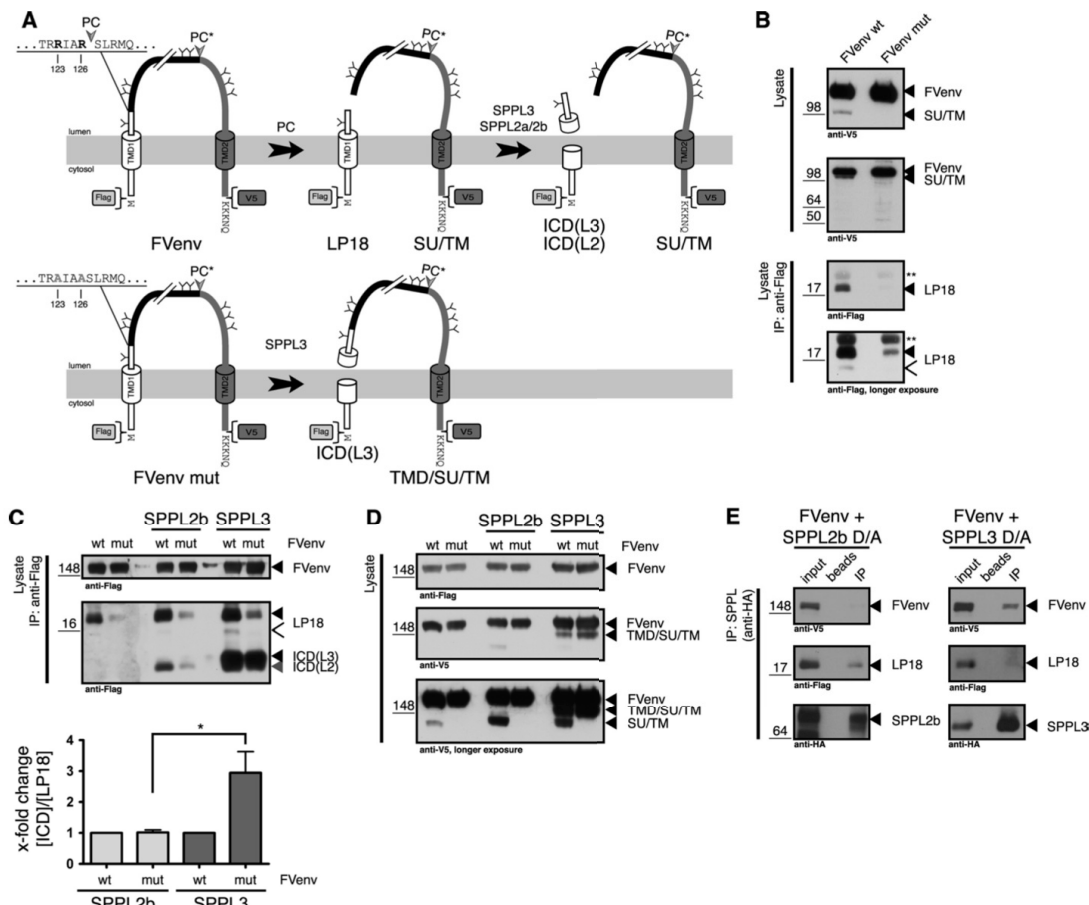


FIGURE 2. SPPL3 cleavage of FVenv is independent of shedding. *A*, model depicting the proteolytic processing of FVenv and FVenv mut disregarding the C-terminal PC* cleavage site, which is hardly observed upon cellular expression of FVenv containing the ER retrieval signal. FVenv mut carries a R123A/R126A mutation to abolish cleavage at the N-terminal PC cleavage site. The respective cleavage products are denoted. Amino acids are depicted using the single-letter code. *B*, WT FVenv and FVenv mut were transiently transfected into HEK293 cells, and cleavage products were monitored. Note that processing of FVenv mut by endogenous PC was strongly reduced at the N-terminal PC cleavage site due to the mutation introduced and that, as expected, the C-terminal PC* cleavage site was hardly used at all. The IgG background signal is indicated (**). All other species are labeled as described in the legend to Fig. 1. *C*, WT FVenv or FVenv mut was transiently coexpressed in HEK293 cells stably expressing catalytically active SPPL2b or SPPL3. LP18 and ICD species generated by SPPL are indicated. The quantification depicts ICD levels relative to LP18. Ratios in cells expressing the indicated protease and WT FVenv were set to 1. Data represent means \pm S.E. of three independent experiments. *, $p < 0.049$ (Student's unpaired *t* test). *D*, the samples shown in *C* were analyzed for high molecular mass fragments of FVenv. SPPL3-mediated cleavage of FVenv generated ICD(L3) and TMD/SU/TM. Note that TMD/SU/TM was detected exclusively in cells expressing SPPL3. The respective cleavage products in *B* and *C* are indicated according to *A*. *E*, CHAPSO lysates of cellular membranes from HEK293 cells coexpressing the catalytically inactive mutants of the indicated proteases and FVenv were subjected to immunoprecipitation (IP) against HA-tagged SPPL2b and SPPL3. Co-isolated FVenv fragments were detected as indicated. To determine the total amount of FVenv present in the lysate, 5% of the total lysate was applied (input). To trace unspecific binding, the respective CHAPSO lysates were incubated with protein A-Sepharose beads only (beads). Note that SPPL2b(D421A) preferentially co-immunoprecipitated LP18 and only minor amounts of FVenv, whereas SPPL3 selectively co-immunoprecipitated full-length FVenv.

Downloaded from www.jbc.org at IBM Bibliothek Grosshadern, on January 1, 2013

the levels of LP18 and SU/TM were significantly reduced (Fig. 2*B*). Thus, FVenv mut represents a valid model substrate that does not undergo shedding.

Initial shedding is known to be required for SPPL2b-mediated intramembrane proteolysis (10). In line with this, ICD(L2) production correlated with the reduction of LP18 upon coexpression of SPPL2b and FVenv mut (Fig. 2*C*). In contrast, coexpression of SPPL3 with FVenv mut hardly affected ICD(L3) generation, although LP18 was significantly reduced (Fig. 2*C*).

Moreover, an additional high molecular mass protein fragment (TMD/SU/TM) that was anti-V5 but not anti-FLAG immunoreactive was detected upon coexpression of FVenv and SPPL3 but not SPPL2b (Fig. 2*D*). Hence, TMD/SU/TM likely originated from intramembrane cleavage by SPPL3. Interestingly, TMD/SU/TM was observed upon SPPL3 overexpression even when FVenv was processed by PC. We therefore conclude that SPPL3 may preferentially cleave full-length FVenv to generate ICD(L3) and TMD/SU/TM, whereas SPPL2b preferentially cleaves LP18.

Endoproteolysis of FVenv by SPPL3

To address whether generation of ICD(L3) and TMD/SU/TM is a result of direct proteolytic cleavage of FVenv by SPPL3 or is catalyzed by an unknown protease that is activated by SPPL3, we performed co-immunoprecipitation assays using the catalytically inactive variants of SPPL2b and SPPL3. SPPL2b(D421A) predominantly co-isolated with LP18, whereas full-length FVenv was co-isolated only to a minor extent. In contrast, SPPL3(D272A) predominantly co-isolated with full-length FVenv and only to a minor extent with LP18 (Fig. 2E), indicating that both enzymes directly interact with the substrate, suggesting that proteolysis of LP18 and FVenv is mediated directly by SPPL2b and SPPL3, respectively. Furthermore, these data strengthen the previous observation that SPPL3 is capable of cleaving FVenv independent of prior processing by PC, whereas SPPL2b requires the short ectodomain of LP18 for efficient cleavage.

Cleavage of FVenv by SPPL3 Is Insensitive to GxGD Protease Inhibitors—To investigate whether GxGD protease inhibitors block SPPL-mediated intramembrane proteolysis of FVenv cells coexpressing either WT SPPL2b (Fig. 3A) or WT SPPL3 (Fig. 3B), FVenv was treated with increasing concentrations of (Z-LL)₂ ketone, L-685,458, or DAPT. Whereas (Z-LL)₂ ketone was shown to target the active site of SPP and SPPL2a/b but not γ -secretase (7, 13, 16, 26), L-685,458 targets γ -secretase, SPP, and SPPL2a/b (13, 16, 27, 28). In contrast, DAPT blocks only γ -secretase activity and fails to block SPP and SPPL2b activity (16, 27, 28). In line with this, treatment of cells expressing WT SPPL2b with (Z-LL)₂ ketone or L-685,458 resulted in a concentration-dependent reduction of ICD(L2) and a simultaneous accumulation of LP18 (Fig. 3A). In addition, a concomitant accumulation of ICD(L3) and higher molecular mass protein fragments (Fig. 3A), similar to those detected upon coexpression of SPPL2b(D421A) (compare with Fig. 1D), was observed. As expected, DAPT had no effect on the processing of LP18 by WT SPPL2b (Fig. 3A). Strikingly, none of the inhibitors was capable of reducing the generation of ICD(L3) from cells coexpressing WT SPPL3 and FVenv (Fig. 3B). (Z-LL)₂ ketone and L-685,458 even increased the amount of ICD(L3), whereas LP18 levels were hardly affected (Fig. 3B). These data demonstrate that cleavage of FVenv by SPPL3 is not inhibited by any of the GxGD protease inhibitors tested.

Consecutive Cleavage of FVenv by SPPL3 and SPPL2a/b—To address whether the increased generation of ICD(L3) observed upon treatment with (Z-LL)₂ ketone or L-685,458 (Fig. 3B) results from an increased availability of LP18 for SPPL3 cleavage due to inhibition of endogenous SPPL2a/b or from blockage of a subsequent cleavage of ICD(L3) by SPPL2a/b, we optimized our gel system to clearly separate the ICD species generated in cells coexpressing SPPL3 and FVenv (compare with Fig. 1E). Separation of the respective samples on a Tris/glycine gel system revealed that generation of ICD(L3) in cells coexpressing SPPL3 and FVenv was accompanied by the generation of a substantial amount of ICD(L2) (Fig. 4A). As observed before (Fig. 3B), treatment of these cells with L-685,458 or (Z-LL)₂ ketone induced an accumulation of ICD(L3) (Fig. 4B) and strongly reduced ICD(L2) generation (Fig. 4B). In contrast to L-685,458 and (Z-LL)₂ ketone, treatment with DAPT did not affect the generation of ICD(L3) or ICD(L2) (Fig. 4B). TMD/SU/TM, the

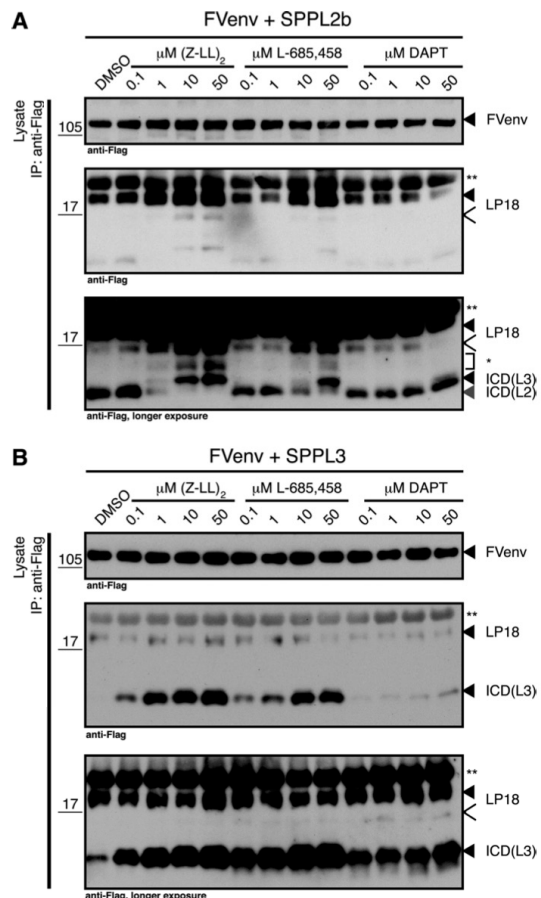
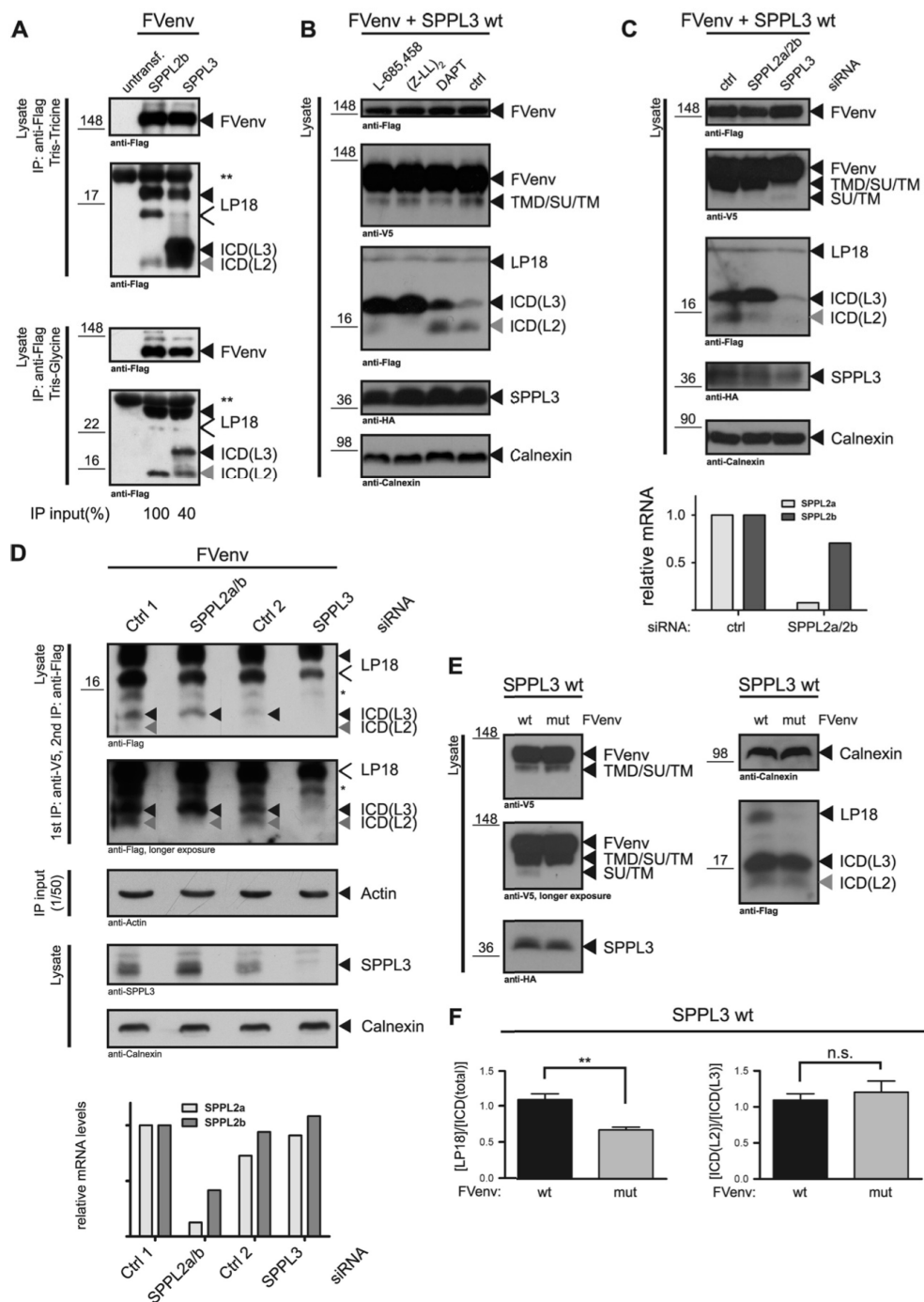


FIGURE 3. SPPL3 cleavage of FVenv is insensitive to GxGD protease inhibitors. HEK293 cells stably coexpressing FVenv and catalytically active SPPL2b (A) or SPPL3 (B) were treated with increasing concentrations of (Z-LL)₂ ketone, L-685,458, or DAPT. FVenv, LP18, and ICD levels were analyzed. Whereas L-685,458 affected ICD production in a similar manner to (Z-LL)₂ ketone, DAPT had no effect on intramembrane proteolysis of FVenv. Note that ICD(L3) generation was not decreased by any of the inhibitors. Upon treatment of cells coexpressing SPPL2b and FVenv, ICD(L3) and protein fragments (*) similar to those detected upon coexpression of SPPL2b(D421A) accumulated (compare with Fig. 1D). All species are labeled as described in the legend to Fig. 1. The IgG background signal is indicated (**). IP, immunoprecipitation.

Downloaded from www.jbc.org at UBM Bibliothek Grosshadern, on January 1, 2013

corresponding SPPL3 cleavage product of FVenv and LP18, was hardly affected by any of the inhibitor treatments (Fig. 4B). This again confirms that FVenv cleavage by SPPL3 is insensitive to common GxGD protease inhibitors, whereas SPPL2a/b activity is blocked by known SPP/SPPL inhibitors. To confirm that ICD(L2) in this context is generated by endogenous SPPL2a/b, SPPL2a/b levels were reduced using specific siRNA. Combined knockdown of SPPL2a and SPPL2b caused a selective reduction of ICD(L2), whereas ICD(L3) accumulated (Fig. 4C), indicating that ICD(L3) is turned over by SPPL2a/b to a certain extent. LP18 and TMD/SU/TM remained unchanged under these conditions (Fig. 4C). In contrast, siRNA-mediated knock-

Endoproteolysis of FVenv by SPPL3



Downloaded from www.jbc.org at UBM Bibliothek Grosshadern, on January 1, 2013

Endoproteolysis of FVenv by SPPL3

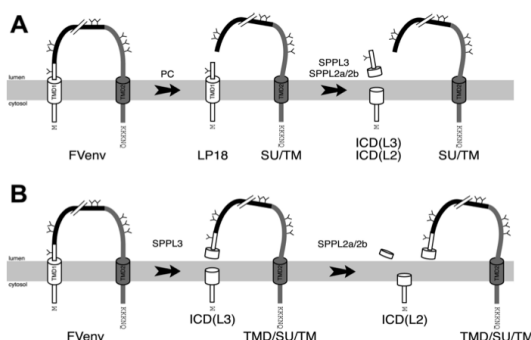


FIGURE 5. Intramembrane proteolysis of FVenv. Shown is a schematic overview of proteolytic FVenv processing. Glycosylation sites in FVenv are indicated (Y). Proteases and the respective FVenv fragments generated are indicated. FVenv is either processed by SPPL2a/b or SPPL3 following PC cleavage (A) or alternatively directly cleaved by SPPL3 and subsequently by SPPL2a/b (B).

down of SPPL3, targeting endogenous and overexpressed SPPL3, reduced TMD/SU/TM and both ICD species, whereas LP18 remained unchanged (Fig. 4C). A similar observation was made when FVenv processing by endogenous SPPL activity was analyzed (Fig. 4D). These data demonstrate that ICD(L2) is generated by endogenous SPPL2a/b. Surprisingly, ICD(L2) generation from cells coexpressing SPPL3 and FVenv was much more efficient than that from cells with reduced SPPL3 activity, although the levels of LP18 were similar, suggesting that ICD(L3) is either turned over more efficiently by SPPL2a/b than LP18 or is more readily available for SPPL2a/b-mediated cleavage. To ensure that ICD(L2) is directly generated from SPPL2a/b cleavage of ICD(L3) and not by enhanced turnover of LP18, ICD levels in cells coexpressing SPPL3 and either FVenv or FVenv mut (compare with Fig. 2) were compared (Fig. 4, E and F). Although LP18 levels in cells coexpressing SPPL3 and FVenv mut were significantly reduced by $42 \pm 9.0\%$ ($p < 0.004$) compared with FVenv-expressing cells (Fig. 4, E and F; compare with Fig. 2), the ICD(L2)/ICD(L3) ratio was not significantly affected (Fig. 4, E and F), excluding that ICD(L2) generation corresponds to the availability of LP18. Taken together, these data suggest that SPPL2a/b is capable of cleaving not only LP18, the PC cleavage product of FVenv, but also ICD(L3), the SPPL3 cleavage product of FVenv. Thus, SPPL3 cleavage of FVenv can serve as an alternative shedding process, generating ICD(L3), which, in addition to furin-generated LP18, serves as a substrate for intramembrane cleavage by SPPL2a/b (Fig. 5).

DISCUSSION

In this study, we have described FVenv as a novel substrate for intramembrane proteolysis by SPPL proteases. In contrast to all SPPL substrates described so far (3), FVenv is cleaved not only by SPPL2a/b but also by SPPL3. In line with previous studies (10), cleavage of FVenv by overexpressed SPPL2a/b is dependent on PC-mediated cleavage, which precedes the intramembrane cleavage and generates LP18, a single-span transmembrane protein with a short ectodomain (Fig. 5A). Contrary to our expectations, under the same conditions, SPPL3 is capable of cleaving FVenv also without prior PC-mediated shedding (Fig. 5B). Thus, SPPL3 differs from other mammalian intramembrane GxGD aspartyl proteases, as it has the ability to cleave substrates without prior shedding under conditions in which SPPL2a/b and presenilin-1/2 strictly depend on shedding. Interestingly, however, rhomboid intramembrane-cleaving serine proteases do not require truncation of their substrate prior to intramembrane proteolysis but cleave intact single-span transmembrane proteins, leading to release of large, soluble, and bioactive factors (29). Hence, in this regard, SPPL3 acts like the members of the rhomboid family and unlike its homologs among the GxGD aspartyl proteases. In addition, SPPL3 cleavage of FVenv is the first example of an intact type III transmembrane protein processed by an intramembrane protease because, so far, only single-span transmembrane proteins or polytopic transmembrane proteins, which are converted into single-span transmembrane proteins by an independent proteolytic cleavage, have been shown to undergo intramembrane cleavage by GxGD proteases (2, 3, 30, 31).

Because FVenv cleavage by SPPL3 is not reduced by GxGD protease inhibitors such as (Z-LL)₂ ketone, L-685,458, and DAPT, our results suggest that SPPL3 displays characteristics distinct from other human GxGD proteases. In contrast to our findings, *in vitro* experiments with recombinant *Drosophila melanogaster* SPPL3 and synthetic peptides based on the bovine preprolactin signal sequence (a putative SPP substrate) (32) and cellular assays combining overexpressed human SPPL3 and a model substrate optimized for SPP cleavage (11) demonstrated that SPPL3 may be inhibited by (Z-LL)₂ ketone and L-685,458. However, the findings by Narayanan *et al.* (32) were recently challenged (33), suggesting that such artificial substrates may not be suitable to study the properties of an intramembrane-cleaving protease. The discrepancies regarding the effects of GxGD protease inhibitors on SPPL3 may also be explained by substrate- and species-specific effects, as well as

Downloaded from www.jbc.org at UBM Bibliothek Grosshadern, on January 1, 2013

FIGURE 4. SPPL3 generates a substrate for consecutive SPPL2a/b cleavage. *A*, HEK293 cells stably coexpressing WT SPPL2b or WT SPPL3 and FVenv were immunoprecipitated (*IP*) using anti-FLAG antibody and separated on a Tris/Tricine gel, as in the previous figures (*upper panels*), or on a Tris/glycine gel (*lower panels*). Note that despite less starting material for the immunoprecipitation (*IP input*), a significant amount of ICD(L2) was generated from cells coexpressing SPPL3 and FVenv. The IgG background signal is indicated (**). *untransf.*, untransfected. *B*, HEK293 cells stably coexpressing WT SPPL3 and FVenv were treated with the indicated inhibitors ($10 \mu\text{M}$) or the respective carrier (control (*ctrl.*)) for 16 h, and generation of ICD(L3) and ICD(L2) was analyzed in cell lysates. Knockdown efficiency was verified by Western blotting (SPPL3) or TaqMan RT-PCR (SPPL2a/b, normalized to actin mRNA levels). *D*, HEK293 cells stably transfected with FVenv were transiently transfected with siRNAs targeting SPPL2a and SPPL2b or SPPL3 (10 nM) or the respective controls (*Ctrl 1* and *Ctrl 2*). Knockdown efficiency was assessed by immunoblotting (SPPL2a and SPPL2b) or TaqMan RT-PCR (SPPL2a/b). ICD levels were determined by anti-FLAG immunoprecipitation following clearance of FVenv by anti-V5 immunoprecipitation. The asterisk indicated the degradation product of LP18 (see supplemental Fig. S2). *E*, cell lysates of HEK293 cells coexpressing SPPL3 and either FVenv or FVenv mut (compare with Fig. 2) were analyzed with regard to the indicated FVenv species. Note that ICD(L2) levels remained unchanged, although LP18 was strongly reduced. *n.s.*, not significant. All species are labeled as described in the legend to Fig. 1.

Endoproteolysis of FVenv by SPPL3

the different context applied in the individual studies. This hypothesis is supported by the observation that a reporter construct based on a signal sequence that is not cleaved by SPP *in vitro* (9) is cleaved by SPP in a cellular context (34). Therefore, additional studies of various enzyme-substrate combinations will be needed to address the issue of whether SPPL3 activity in general is insensitive to common GxGD protease inhibitors or only in context with the substrate FVenv.

In accordance with previous studies (10, 35), SPPL2a and SPPL2b only accept FVenv species with a type II membrane orientation and a truncated luminal domain as their substrates. Both LP18 generated by PC cleavage of FVenv and ICD(L3) generated by SPPL3 cleavage of FVenv fulfill this criteria and are cleaved by SPPL2a/b to generate ICD(L2) (Fig. 5). Because ICD(L2) generation by endogenous SPPL2a/b is greatly facilitated when substantial amounts of ICD(L3) are present, our results suggest that ICD(L3) is much more efficiently subjected to subsequent intramembrane cleavage by endogenous SPPL2a/b than LP18. Given its molecular mass, it is very likely that the luminal domain of ICD(L3) is significantly shorter than that of LP18. Therefore, our results are in line with the previous observation that SPPL2b most efficiently cleaves Bri2 substrates with an ectodomain shorter than 23 amino acids (10). We cannot, however, completely rule out that, for example, different subcellular localizations of LP18 and ICD(L3) favor a more efficient turnover of the latter by SPPL2a/b.

In contrast to other human GxGD proteases, SPPL3 accepts not only LP18 but also the full-length FVenv protein as substrate and, at the same time, generates a product that is an excellent substrate for subsequent intramembrane proteolysis by SPPL2a/b. We therefore conclude that SPPL3 has the ability to serve as an additional sheddase in regulated intramembrane proteolysis of FVenv (Fig. 5B). However, whether cleavage of full-length FVenv by SPPL3 also occurs under physiological conditions remains to be elucidated. In addition, future work should address whether SPPL3-mediated proteolysis of FVenv also impacts on virus particle maturation and/or infectivity.

Because it has been shown that cleavage of TNF α by SPPL2a/b occurs within the hydrophobic core of the TMD (16), SPPL2a/b cleavage of FVenv most likely also takes place within the TMD of LP18. Taking into account that the molecular mass of ICD(L3) is larger than that of ICD(L2) but smaller than that of LP18, which contains only 35 amino acids of the luminal part of FVenv, SPPL3 cleavage of FVenv will most likely take place at the very C-terminal part of the FVenv TMD or in the luminal part of FVenv in close vicinity to its TMD. To exactly determine the cleavage sites of SPPLs in FVenv, analysis of the respective cleavage products will be required. However, although extensively tried, we have been unable so far to detect FVenv-derived ICD and C-peptide species using MALDI-TOF-MS (data not shown).

Our study on the intramembrane proteolysis of FVenv indicates that SPPL3 has certain biochemical properties that, based on the current knowledge, were not expected for intramembrane aspartyl proteases of the GxGD type but rather for members of the rhomboid family. Future studies will need to address whether this alternative, SPPL3-initiated regulated intramembrane proteolysis pathway is also observed for other physiolog-

ical substrates of SPPL3 and whether SPPL3 activity itself is regulated.

REFERENCES

1. Lichtenhaler, S. F., Haass, C., and Steiner, H. (2011) Regulated intramembrane proteolysis—lessons from amyloid precursor protein processing. *J. Neurochem.* **117**, 779–796
2. Steiner, H., Fluhrer, R., and Haass, C. (2008) Intramembrane proteolysis by γ -secretase. *J. Biol. Chem.* **283**, 29627–29631
3. Fluhrer, R., Steiner, H., and Haass, C. (2009) Intramembrane proteolysis by signal peptide peptidases: a comparative discussion of GXGD-type aspartyl proteases. *J. Biol. Chem.* **284**, 13975–13979
4. Wolfe, M. S. (2009) Intramembrane-cleaving proteases. *J. Biol. Chem.* **284**, 13969–13973
5. Freeman, M. (2008) Rhomboid proteases and their biological functions. *Annu. Rev. Genet.* **42**, 191–210
6. Steiner, H., Kostka, M., Romig, H., Basset, G., Pesold, B., Hardy, J., Capell, A., Meyn, L., Grim, M. L., Baumeister, R., Fechete, K., and Haass, C. (2000) Glycine 384 is required for presenilin-1 function and is conserved in bacterial polytopic aspartyl proteases. *Nat. Cell Biol.* **2**, 848–851
7. Weihofen, A., Binns, K., Lemberg, M. K., Ashman, K., and Martoglio, B. (2002) Identification of signal peptide peptidase, a presenilin-type aspartic protease. *Science* **296**, 2215–2218
8. Struhl, G., and Adachi, A. (2000) Requirements for presenilin-dependent cleavage of Notch and other transmembrane proteins. *Mol. Cell* **6**, 625–636
9. Lemberg, M. K., and Martoglio, B. (2002) Requirements for signal peptide peptidase-catalyzed intramembrane proteolysis. *Mol. Cell* **10**, 735–744
10. Martin, L., Fluhrer, R., and Haass, C. (2009) Substrate requirements for SPPL2b-dependent regulated intramembrane proteolysis. *J. Biol. Chem.* **284**, 5662–5670
11. Nyborg, A. C., Ladd, T. B., Jansen, K., Kukar, T., and Golde, T. E. (2006) Intramembrane proteolytic cleavage by human signal peptide peptidase-like 3 and malaria signal peptide peptidase. *FASEB J.* **20**, 1671–1679
12. Lindemann, D., and Rethwilm, A. (2011) Foamy virus biology and its application for vector development. *Viruses* **3**, 561–585
13. Martin, L., Fluhrer, R., Reiss, K., Kremmer, E., Saftig, P., and Haass, C. (2008) Regulated intramembrane proteolysis of Bri2 (Itm2b) by ADAM10 and SPPL2a/SPPL2b. *J. Biol. Chem.* **283**, 1644–1652
14. Trobridge, G., Josephson, N., Vassilopoulos, G., Mac, J., and Russell, D. W. (2002) Improved foamy virus vectors with minimal viral sequences. *Mol. Ther.* **6**, 321–328
15. Edbauer, D., Winkler, E., Regula, J. T., Pesold, B., Steiner, H., and Haass, C. (2003) Reconstitution of γ -secretase activity. *Nat. Cell Biol.* **5**, 486–488
16. Fluhrer, R., Grammer, G., Israel, L., Condron, M. M., Haffner, C., Friedmann, E., Böhlund, C., Imhof, A., Martoglio, B., Teplow, D. B., and Haass, C. (2006) A γ -secretase-like intramembrane cleavage of TNF α by the GxGD aspartyl protease SPPL2b. *Nat. Cell Biol.* **8**, 894–896
17. Fluhrer, R., Capell, A., Westmeyer, G., Willem, M., Hartung, B., Condron, M. M., Teplow, D. B., Haass, C., and Walter, J. (2002) A non-amyloidogenic function of BACE-2 in the secretory pathway. *J. Neurochem.* **81**, 1011–1020
18. Fluhrer, R., Martin, L., Klier, B., Haug-Kröper, M., Grammer, G., Nuscher, B., and Haass, C. (2012) The α -helical content of the transmembrane domain of the British dementia protein-2 (Bri2) determines its processing by signal peptide peptidase-like 2b (SPPL2b). *J. Biol. Chem.* **287**, 5156–5163
19. Meiering, C. D., and Linial, M. L. (2001) Historical perspective of foamy virus epidemiology and infection. *Clin. Microbiol. Rev.* **14**, 165–176
20. Lindemann, D., Pietschmann, T., Picard-Maureau, M., Berg, A., Heinkelein, M., Thurow, J., Knaus, P., Zentgraf, H., and Rethwilm, A. (2001) A particle-associated glycoprotein signal peptide essential for virus maturation and infectivity. *J. Virol.* **75**, 5762–5771
21. Geiselhart, V., Schwantes, A., Bastone, P., Frech, M., and Löchelt, M. (2003) Features of the Env leader protein and the N-terminal Gag domain of feline foamy virus important for virus morphogenesis. *Virology* **310**, 235–244

Endoproteolysis of FVen by SPPL3

22. Duda, A., Stange, A., Lüftenegger, D., Stanke, N., Westphal, D., Pieschmann, T., Eastman, S. W., Linial, M. L., Rethwilm, A., and Lindemann, D. (2004) Prototype foamy virus envelope glycoprotein leader peptide processing is mediated by a furin-like cellular protease, but cleavage is not essential for viral infectivity. *J. Virol.* **78**, 13865–13870

23. Geiselhart, V., Bastone, P., Kempf, T., Schnölzer, M., and Löchelt, M. (2004) Furin-mediated cleavage of the feline foamy virus Env leader protein. *J. Virol.* **78**, 13573–13581

24. Goepfert, P. A., Wang, G., and Mulligan, M. J. (1995) Identification of an ER retrieval signal in a retroviral glycoprotein. *Cell* **82**, 543–544

25. Bansal, A., Shaw, K. L., Edwards, B. H., Goepfert, P. A., and Mulligan, M. J. (2000) Characterization of the R572T point mutant of a putative cleavage site in human foamy virus Env. *J. Virol.* **74**, 2949–2954

26. Friedmann, E., Hauben, E., Maylandt, K., Schleeger, S., Vreugde, S., Lichtenhaller, S. F., Kuhn, P. H., Stauffer, D., Rovelli, G., and Martoglio, B. (2006) SPPL2a and SPPL2b promote intramembrane proteolysis of TNF α in activated dendritic cells to trigger IL-12 production. *Nat. Cell Biol.* **8**, 843–848

27. Shearman, M. S., Beher, D., Clarke, E. E., Lewis, H. D., Harrison, T., Hunt, P., Nadin, A., Smith, A. L., Stevenson, G., and Castro, J. L. (2000) L-685,458, an aspartyl protease transition state mimic, is a potent inhibitor of amyloid β -protein precursor γ -secretase activity. *Biochemistry* **39**, 8698–8704

28. Weihofen, A., Lemberg, M. K., Friedmann, E., Rueeger, H., Schmitz, A., Paganetti, P., Rovelli, G., and Martoglio, B. (2003) Targeting presenilin-type aspartic protease signal peptide peptidase with γ -secretase inhibitors. *J. Biol. Chem.* **278**, 16528–16533

29. Lemberg, M. K., and Freeman, M. (2007) Cutting proteins within lipid bilayers: rhomboid structure and mechanism. *Mol. Cell* **28**, 930–940

30. Chen, G., and Zhang, X. (2010) New insights into S2P signaling cascades: regulation, variation, and conservation. *Protein Sci.* **19**, 2015–2030

31. Freeman, M. (2009) Rhomboids: 7 years of a new protease family. *Semin. Cell Dev. Biol.* **20**, 231–239

32. Narayanan, S., Sato, T., and Wolfe, M. S. (2007) A C-terminal region of signal peptide peptidase defines a functional domain for intramembrane aspartic protease catalysis. *J. Biol. Chem.* **282**, 20172–20179

33. Schrul, B., Kapp, K., Sinning, I., and Dobberstein, B. (2010) Signal peptide peptidase (SPP) assembles with substrates and misfolded membrane proteins into distinct oligomeric complexes. *Biochem. J.* **427**, 523–534

34. Nyborg, A. C., Jansen, K., Ladd, T. B., Faug, A., and Golde, T. E. (2004) A signal peptide peptidase (SPP) reporter activity assay based on the cleavage of type II membrane protein substrates provides further evidence for an inverted orientation of the SPP active site relative to presenilin. *J. Biol. Chem.* **279**, 43148–43156

35. Friedmann, E., Lemberg, M. K., Weihofen, A., Dev, K. K., Dengler, U., Rovelli, G., and Martoglio, B. (2004) Consensus analysis of signal peptide peptidase and homologous human aspartic proteases reveals opposite topology of catalytic domains compared with presenilins. *J. Biol. Chem.* **279**, 50790–50798

For copyright reasons, these pages are blanked in the publicly available version of this thesis.

For copyright reasons, these pages are blanked in the publicly available version of this thesis.

For copyright reasons, these pages are blanked in the publicly available version of this thesis.

For copyright reasons, these pages are blanked in the publicly available version of this thesis.

For copyright reasons, these pages are blanked in the publicly available version of this thesis.

For copyright reasons, these pages are blanked in the publicly available version of this thesis.

For copyright reasons, these pages are blanked in the publicly available version of this thesis.

For copyright reasons, these pages are blanked in the publicly available version of this thesis.

For copyright reasons, these pages are blanked in the publicly available version of this thesis.

For copyright reasons, these pages are blanked in the publicly available version of this thesis.

For copyright reasons, these pages are blanked in the publicly available version of this thesis.

For copyright reasons, these pages are blanked in the publicly available version of this thesis.

Shedding of glycan-modifying enzymes by signal peptide peptidase-like 3 (SPPL3) regulates cellular N- glycosylation¹⁰

**Matthias Voss¹, Ulrike Künzel^{1,9}, Fabian Higel², Peer-Hendrik Kuhn^{3,8}, Alessio Colombo³,
Akio Fukumori³, Martina Haug-Kröper¹, Bärbel Klier³, Gudula Grammer¹, Andreas Seidl²,
Bernd Schröder⁵, Reinhard Obst⁶, Harald Steiner^{1,3}, Stefan F. Lichtenthaler^{3,4,7}, Christian
Haass^{1,3,4} and Regina Fluhrer^{1,3,*}**

¹ Adolf Butenandt Institute for Biochemistry, Ludwig-Maximilians University Munich, Schillerstr. 44, D-80336 Munich, Germany

² Sandoz Biopharmaceuticals/HEXAL AG, Keltenring 1 + 3, 82041 Oberhaching, Germany

³ DZNE – German Center for Neurodegenerative Diseases, Munich, Schillerstr. 44, D-80336 Munich, Germany

⁴ Munich Cluster for Systems Neurology (SyNergy), Munich, Germany

⁵ Biochemical Institute, Christian-Albrechts-University Kiel, Olshausenstrasse 40, D-24118 Kiel, Germany

⁶ Institute for Immunology, Ludwig-Maximilians University Munich, Goethestr. 29-31, D-80336 Munich, Germany

⁷ Neuroproteomics, Klinikum rechts der Isar, Technische Universität München, 81675 Munich, Germany

⁸ Institute for Advanced Study, Technische Universität München, 85748 Garching, Germany

⁹ Present address: Sir William Dunn School of Pathology, University of Oxford, South Parks Road, Oxford OX1 3RE, United Kingdom

* Corresponding author. Adolf-Butenandt-Institute, Biochemistry, Ludwig-Maximilians-University and German Center for Neurodegenerative Diseases (DZNE) - Munich; Schillerstr. 44, 80336 Munich, Germany. Phone: +49 89 218075487; Fax: +49 89 218075415; Email: rfluhrer@med.uni-muenchen.de

Running title:

SPPL3 regulates cellular N-glycosylation

Character count: 60,606

Abstract

Protein N-glycosylation is involved in a variety of physiological and pathophysiological processes such as autoimmunity, tumour progression and metastasis. Signal peptide peptidase-like 3 (SPPL3) is an intramembrane-cleaving aspartyl protease of the GxGD-type. Its physiological function, however, has remained enigmatic, since presently no physiological substrates have been identified. We demonstrate that SPPL3 alters the pattern of cellular N-glycosylation by triggering the proteolytic release of active site-containing ectodomains of glycosidases and glycosyltransferases such as N-acetylglucosaminyltransferase V, α -mannosidase I, β 1,3 N-acetylglucosaminyltransferase 1 and β 1,4 galactosyltransferase 1. Cleavage of these enzymes leads to a reduction in their cellular activity. In line with that, reduced expression of SPPL3 results in a hyperglycosylation phenotype whereas elevated SPPL3 expression causes hypoglycosylation. Thus, SPPL3 plays a central role in an evolutionary highly conserved posttranslational process in eukaryotes.

Keywords

Glycosyltransferases/GxGD aspartyl proteases/protein glycosylation/signal peptide peptidase like-3 (SPPL3)/protein glycosylation

Introduction

Signal peptide peptidase-like 3 (SPPL3) is a multi-pass transmembrane protein that is highly conserved among multi-cellular eukaryotes and belongs to the family of intramembrane-cleaving GxGD proteases (Voss *et al*, 2013). Together with its mammalian paralogues, signal peptide peptidase (SPP) and the signal peptide peptidase-like (SPPL) proteases SPPL2a, SPPL2b and SPPL2c, it was first identified by database queries in 2002 (Weihofen *et al*, 2002; Ponting *et al*, 2002; Grigorenko *et al*, 2002). Notably, all members of the SPP/SPPL family share characteristic structural features and catalytic motifs with the presenilins, the catalytically active subunits of the γ -secretase complex (Voss *et al*, 2013). The two catalytic aspartate residues required for the proteolytic activity of SPP/SPPL proteases are embedded in conserved YD and GxGD amino acid motifs in transmembrane domain (TMD) 6 and TMD7, respectively (Voss *et al*, 2013). Mutagenesis of either aspartate residue inactivates the respective SPP/SPPL (Weihofen *et al*, 2002; Fluhrer *et al*, 2006; Friedmann *et al*, 2006; Kirkin *et al*, 2007; Voss *et al*, 2012). In contrast to presenilins, which exclusively accept type I transmembrane substrates (Kopan & Ilagan, 2004), SPP/SPPLs seem to be selective towards transmembrane substrates in type II orientation (Weihofen *et al*, 2002; Friedmann *et al*, 2004; Nyborg *et al*, 2004). While recent studies on SPP, SPPL2a and SPPL2b identified substrates of these proteases *in vitro* and *in vivo* and consequently gave a first impression of the physiological function of these family members (reviewed in (Voss *et al*, 2013)), the physiological function of SPPL3 has remained completely enigmatic. Highly conserved orthologues of mammalian SPPL3, however, are found in most multi-cellular eukaryotes pointing to a fundamental cellular function of SPPL3 (Voss *et al*, 2013). SPPL3 most likely adopts the nine TMD topology conserved among GxGD proteases (Friedmann *et al*, 2004), localises to the Golgi network (Friedmann *et al*, 2006) and is not glycosylated (Friedmann *et al*, 2004). Recently, we described the first SPPL3 substrate in a cell

culture model system, confirming the assumption that SPPL3 indeed is proteolytically active (Voss *et al*, 2012).

In eukaryotic organisms, N-glycan synthesis is initiated in the ER resulting in high-mannose type glycans attached to the luminal domain of secretory and membrane proteins (Kornfeld & Kornfeld, 1985). Within the *medial*- and *trans*-Golgi network numerous glycosyltransferase and glycosidases compete for these high-mannose type precursor glycans converting them into higher-order, complex N-glycans (Sears & Wong, 1998; Moremen *et al*, 2012). Most glycosyltransferases are single-span type II transmembrane proteins with a short N-terminal cytoplasmic tail. Their large C-terminal ectodomain that harbours the glycosyltransferase activity faces the lumen of the Golgi (Paulson & Colley, 1989; Sears & Wong, 1998; Varki *et al*, 2009).

Secreted glycosyltransferases were observed in conditioned media of cultured cells (Elhammer & Kornfeld, 1986; Saito *et al*, 2002; El-Battari *et al*, 2003), but also in bodily fluids (Kim *et al*, 1972a; 1972b; Elhammer & Kornfeld, 1986; Kitazume *et al*, 2009) and tissues (Weinstein *et al*, 1987). Secretion of the catalytically active glycosyltransferase domain has been discussed to negatively regulate cellular protein glycosylation, since the crucially required nucleotide- or lipid-linked sugar donor substrates that exclusively occur intracellularly are not available for secreted glycosyltransferases (Paulson & Colley, 1989; Ohtsubo & Marth, 2006; Varki *et al*, 2009). Secretion is generally believed to be due to proteolytic cleavage within the so called stem region that tethers the catalytic glycosyltransferase ectodomain to its membrane anchor (Paulson & Colley, 1989; Ohtsubo & Marth, 2006; Varki *et al*, 2009). However, the exact nature of the protease(s) involved in this process remains controversial. The sialyltransferase ST6Gal1, for instance, was initially described to be released by a cathepsin D-like protease (Lammers & Jamieson, 1988; McCaffrey & Jamieson, 1993). Others identified the β -site amyloid precursor protein-cleaving enzyme 1 (BACE1) as protease responsible for ST6Gal1 cleavage in cultured cells (Kitazume *et al*, 2001) and, to a certain extent, *in vivo* (Kitazume *et al*, 2005). Secretion of the N-acetylglucosaminyltransferase V (GnT-V) was suggested to be mediated by the γ -secretase complex (Nakahara *et al*, 2006).

Using *Spp13* knockout mice as well as human and murine cell lines, we identify SPPL3 as a new fundamental mediator of glycosyltransferase secretion. SPPL3 controls the proteolytic release of the ectodomain of various glycosyltransferases and glycosidases, most likely by direct cleavage, and consequently alters cellular N-glycosylation. Therefore, we define the protease responsible for proteolytic cleavage of glycan-modifying enzymes and provide the first insight into the physiological function of SPPL3.

Results

SPPL3 expression affects glycosylation pattern of endogenous cellular glycoproteins

Analysis of cell lysates obtained from T-RexTM-293 (HEK293) cells stably expressing SPPL3 under a doxycycline-inducible promoter revealed a markedly reduced molecular weight of mature Nicastin, a complexly N-glycosylated γ -secretase component (Haass, 2004) (Fig. 1A). In addition, the molecular weight of other endogenous glycoproteins, for instance N-cadherin, SPPL2a and Lamp2, was similarly affected in cells expressing proteolytically active SPPL3 compared to non-induced cells (Fig. 1A). Notably, expression of the catalytically inactive SPPL3 D200N/D271N mutant (SPPL3 DD/NN) had no effect on the molecular weight of these glycoproteins (Fig. 1A), indicating that proteolytic activity of

SPPL3 is crucially required for the observed molecular weight changes. Doxycycline treatment of non-transfected HEK293 cells had no effect on the molecular weight of the respective glycoproteins analysed (Fig. E1). In contrast to SPPL3 overexpression, siRNA-mediated SPPL3 knockdown induced a slight increase in the molecular weight of various glycoproteins compared to cells transfected with non-targeting control siRNAs or untransfected cells (Fig. 1B). Importantly, solely the molecular weight of the mature, complexly glycosylated variant of Nicastrin was changed by alterations in SPPL3 expression levels, while the immature variant remained unaffected (Fig. 1A & B). Moreover, non-glycosylated proteins such as the ER chaperone calnexin were not affected by alterations in SPPL3 expression levels (Fig. 1A & B). We consequently hypothesised that SPPL3 interferes with cellular N-glycosylation, resulting in a reduced extent of N-glycan modifications, i.e. hypoglycosylation, upon SPPL3 overexpression and a more extensive N-glycan modification, i.e. hyperglycosylation, upon reduction of SPPL3 expression. To support this hypothesis, lysates from HEK293 cells expressing SPPL3 were subjected to enzymatic deglycosylation by peptide:N-glycosidase F (PNGase F) or endoglycosidase H (Endo H) (Fig. 1C). As expected, the hypoglycosylation phenotype induced by SPPL3 overexpression was completely abolished by treatment with PNGase F, but was still detectable after treatment with Endo H (Fig. 1C). Moreover, glycoproteins in SPPL3 overexpressing cells remained Endo H-resistant, indicating that SPPL3 selectively interferes with complex N-glycosylation. To verify this, we treated cells with the plant alkaloid kifunensine (Fig. 1D) which is a potent inhibitor of cellular α -mannosidase I activity and, accordingly, blocks generation of both hybrid- and complex-type N-glycans (Elbein *et al.*, 1990). As expected, kifunensine treatment completely eliminated generation of mature glycoproteins and SPPL3 failed to decrease the molecular weight of glycoproteins in kifunensine-treated cells (Fig. 1D), demonstrating that SPPL3 interferes with complex N-glycosylation occurring in the *medial*- and *trans*-Golgi network following modification by α -Man I but not with early steps of ER-based N-glycan assembly.

Sppl3-deficient mice exhibit a hyperglycosylation phenotype

To address whether a similar function of SPPL3 is apparent under physiological conditions, we analysed glycoproteins in tissue homogenates of *Sppl3*-deficient mice and littermate controls. On a mixed C57BL/6;129S5 background *Sppl3*-deficient mice are viable and present with a rather mild phenotype that is characterised by growth retardation and hematologic abnormalities as well as sterility in male homozygous mice (Tang *et al.*, 2010). Similar to our observations upon SPPL3 knockdown (Fig. 1B), the molecular weight of mature Nicastrin and SPPL2a slightly increased in brain (Fig. 2A), lung (Fig. 2B), spleen (Fig. 2C) and immortalized mouse embryonic fibroblasts (MEFs) (Fig. 2D) obtained from *Sppl3*^{-/-} mice compared to *Sppl3*^{+/+} littermate controls. In addition to these rather ubiquitously expressed glycoproteins, glycoproteins expressed in a tissue-specific manner, for instance N-cadherin in brain (Fig. 2A) or CD68 in spleen (Fig. 2C), similarly displayed a hyperglycosylation phenotype in *Sppl3*^{-/-} mice, suggesting that SPPL3 has a rather global effect on cellular N-glycosylation. Similar to hypoglycosylation in SPPL3 overexpressing cells, hyperglycosylation in brain homogenates of *Sppl3*^{-/-} mice and in *Sppl3*^{-/-} MEFs was absent after treatment with PNGase F (Fig. E2A & B). Taken together, these data demonstrate that SPPL3 expression influences complex cellular N-glycosylation not only in a cellular model system but also *in vivo*.

SPPL3 mediates secretion of GnT-V

In light of the results obtained upon kifunensine treatment (Fig. 1D), we reasoned that SPPL3 affects N-glycosylation either by interfering with α -mannosidase I activity or another glycan-modifying enzyme downstream of α -mannosidase I. In addition, the molecular weight changes observed upon SPPL3 expression in HEK293 cells (Fig. 1a) were rather substantial. Thus, it is likely that SPPL3 does not exclusively affect terminal glycan modifications as a deregulation of these would not lead to such pronounced differences in molecular weight of glycoproteins. We rather assumed that SPPL3 interferes with N-acetylglucosaminyl (GlcNAc) branching and/or the generation of N-acetyllactosamine moieties (Fig. 3A).

Accordingly, we investigated whether SPPL3 directly or indirectly affects cellular levels of glycosyltransferases implicated in these processes. We found that SPPL3 profoundly affects GnT-V (gene name: *MGAT5*), which is involved in GlcNAc branching (Fig. 3A). GnT-V levels in both supernatant and lysate were strongly reduced following transfection with a *MGAT5*-specific siRNA pool (Fig. 3B), demonstrating that the GnT-V signal obtained in Western Blot was specific and that endogenous GnT-V is secreted in HEK293 cells. Upon siRNA-mediated knockdown of SPPL3, secretion of endogenous GnT-V was markedly reduced and the protein strongly accumulated intracellularly (Fig. 3B). Moreover, cellular GnT-V, which itself is known to be complexly glycosylated (Kamar *et al*, 2004), was found to shift to a slightly higher molecular weight, indicating that SPPL3 knockdown also induces GnT-V hyperglycosylation (Fig. 3B). In contrast, doxycycline-induced SPPL3 overexpression, yet not doxycycline treatment *per se*, caused GnT-V hypoglycosylation accompanied by a strong reduction of cellular GnT-V levels (Fig. 3B & Fig. E3). Similar results were obtained from HEK293 cells co-expressing exogenous GnT-V and either SPPL3 wt (Fig. 3C) or a *SPPL3*-specific shRNA (Fig. 3D). In HEK293 cells over-expressing GnT-V we observed two distinct GnT-V species, immature, EndoH-sensitive GnT-V and complex glycosylated, mature GnT-V (Fig. 3C, D & Fig. E4). Exogenous co-expression of active SPPL3 and GnT-V resulted in slightly increased GnT-V secretion and reduction of intracellular mature GnT-V, while immature GnT-V remained unaffected (Fig. 3C). Moreover, SPPL3 overexpression induced hyperglycosylation of secreted GnT-V but did not affect the molecular weight of immature GnT-V (Fig. 3C). Catalytically inactive SPPL3 did not affect levels of secreted and intracellular GnT-V (Fig. 3C). In contrast, shRNA mediated knock-down of SPPL3 slightly reduced secretion of exogenous GnT-V and induced hyperglycosylation exclusively of the mature intracellular GnT-V species (Fig. 3D). This received additional support from pulse-chase experiments performed in cells expressing epitope-tagged GnT-V that were either co-expressing catalytically active SPPL3 (Fig. E5A) or were transfected with SPPL3-specific siRNA (Fig. E5B). Taken together, this suggests that SPPL3 acts on GnT-V most likely in the Golgi, where both GnT-V (Chen *et al*, 1995) and SPPL3 (Friedmann *et al*, 2006) may co-localise. Next, we examined cellular GnT-V levels and GnT-V secretion in *SPPL3*^{-/-} MEFs (Fig. 3E). As expected, GnT-V was more abundant in lysates from *Sppl3*^{-/-} MEF than in wild-type control cells and its secretion was almost completely abolished in *Sppl3*-deficient cells (Fig. 3E).

To finally investigate whether SPPL3 also modulates cellular GnT-V activity, we performed lectin blots (Fig. 3F). Both mature and immature Nicastin immunoprecipitated from HEK293 cells expressing active SPPL3 were detected by Concanavalin A, which has a broad reactivity towards mannose-containing glycans (Cummings & Etzler, 2009). Strikingly, reactivity towards PHA-L, a leucoagglutinin that predominantly binds N-glycans that harbour the GlcNAc β 1,6Man motif generated by GnT-V activity

(Cummings & Kornfeld, 1982), was strongly reduced in cells over-expressing SPPL3 (Fig. 3F, lane 4) compared to cell with endogenous SPPL3 levels (Fig. 3F, lane 2). To control for specificity of lectin binding, cells were treated with kifunensine, which resulted in impaired complex glycosylation of mature Nicastrin. As expected, immature Nicastrin was only detected by ConA but not by PHA-L. In contrast, mature Nicastrin from non-treated cells was readily detected by both lectins (Fig. 3F). This indicates that, upon SPPL3 expression, glycans on mature Nicastrin are less extensively modified by GnT-V. To investigate whether this generally applies, we isolated secreted glycoproteins from cells overexpressing SPPL3 and control cells, isolated attached N-glycans and analysed the latter by liquid chromatography-mass spectrometry (LCMS, Fig. 3G, E6 and Suppl. Tab. 1). Differences between both samples became already apparent in LC chromatograms (Fig. E6A). Subsequent analysis of N-glycan species by mass spectrometry revealed that, as expected from previous experiments (Fig. 1D), SPPL3 overexpression was not associated with marked changes in high mannose or hybrid N-glycans (Fig. 3G & Suppl. Tab. 1). It did, however, affect the relative abundance of complex N-glycan species. Cells overexpressing SPPL3 were found to secrete glycoproteins more extensively modified with complex bi-antennary as well as bisected complex bi-antennary N-glycans. These N-glycan species are expected to accumulate when GnT-V activity is impaired (Fig. 3A) (Lee *et al*, 2012). Moreover, under these conditions, tri-antennary and tetra-antennary N-glycans were less abundant on secreted glycoproteins. Since GnT-V activity contributes to the generation of tri-antennary and tetra-antennary N-glycans (Fig. 3A), this further demonstrates that reduction in intracellular GnT-V levels observed following SPPL3 over-expression (Fig. 3A & B) is also associated with impaired cellular GnT-V activity.

GnT-V secretion results from proteolytic cleavage

In order to confirm that GnT-V secretion is due to proteolytic cleavage (Fig. 4A), we co-expressed N-terminally Flag- and C-terminally V5-tagged GnT-V and SPPL3 wt (Fig. 4B). The secreted variant of the epitope-tagged GnT-V retained its anti-V5 immunoreactivity, yet was not anti-Flag reactive, demonstrating that it had been N-terminally truncated (Fig. 4B). In addition, we determined the cleavage site within GnT-V using a GnT-V expression construct that lacks the bulk of the GnT-V ectodomain and allows for purification and mass spectrometric analysis of secreted, GnT-V-derived peptides (Fig. E7). In conditioned supernatants from cells expressing this construct we detected five individual peptides with N-termini between residues L29 and T33 at the luminal membrane interface. As demonstrated before (Nakahara *et al*, 2006), one of the most abundant peptides originates from proteolytic cleavage between L30 and H31. Since it was previously suggested that γ -secretase is responsible for the release of GnT-V in a pancreas carcinoma cell line (Nakahara *et al*, 2006), we treated HEK293 cells with the potent γ -secretase inhibitors (GSIs) L-685,458 (Shearman *et al*, 2000) or *N*-[*N*-(3,5-difluorophenacetyl)-L-alanyl]-S-phenylglycine *t*-butyl ester (DAPT) (Dovey *et al*, 2001). Both GSIs efficiently interfered with γ -secretase activity, as demonstrated by the drastically impaired secretion of endogenous A β , a well-established γ -secretase cleavage product (Haass, 2004), and the intracellular accumulation of APP C-terminal fragments, the corresponding γ -secretase substrates (Haass, 2004), in a concentration-dependent fashion (Fig. 4C). We failed, however, to detect an inhibitor concentration-dependent reduction of GnT-V secretion and a concomitant intracellular GnT-V accumulation (Fig. 4C). Moreover, endogenous glycoproteins were not hyperglycosylated in PS1/PS2 double-deficient MEFs that lack the catalytically active γ -secretase subunits (Fig. 4D) as observed in *Sppl3*^{-/-} cells (Fig. 2D & Fig. 4D). Instead, we

observed a mild hypoglycosylation on endogenous glycoproteins in these MEFs compared to control cells that could be due to a slightly higher SPPL3 expression in the PS1/PS2 double-deficient MEFs (Fig. 4D). Finally, we did not observe a reduction of GnT-V secretion in PS1/2 double-deficient MEFs (Fig. 4E), while GnT-V secretion was clearly impaired in *Sppl3*^{-/-} cells (Fig. 3E). In sum, this clearly demonstrates that alterations in cellular N-glycosylation observed before (Figs. 1-4) are not linked to γ -secretase activity. Instead, our data suggest that the secretion of GnT-V is due to proteolytic cleavage of GnT-V by SPPL3.

SPPL3 mediates secretion of other glycan-modifying enzymes

Assuming that SPPL3 over-expression in HEK293 cells results in hypoglycosylation solely due to the loss of intracellular GnT-V activity, we expected that SPPL3 over-expression would phenocopy a siRNA-mediated knockdown of GnT-V. As expected, both SPPL3 over-expression and GnT-V knockdown resulted in hypoglycosylation of endogenous glycoproteins, but the extent of glycoprotein molecular weight changes were more drastic upon SPPL3 over-expression (Fig. 5A). This observation suggested that GnT-V is not the only glycan-modifying enzyme affected by SPPL3. Indeed, we found that β 1,3 N-acetylglucosaminyltransferase 1 (β 3GnT1, gene name: B3GNT1) and β 1,4 galactosyltransferase 1 (β 4GalT1, gene name: B4GALT1) were affected by SPPL3 in a manner resembling its effect on GnT-V. SPPL3 over-expression caused hypoglycosylation of secreted β 3GnT1 (Fig. 5B & E8A) and β 4GalT1 (Fig. 5D) accompanied by a reduction of cellular β 3GnT1 (Fig. 5B & E8A) or β 4GalT1 (Fig. 5D) levels, respectively. Upon SPPL3 knockdown (Fig. 5B, 5D & E8A) as well as in lysates from *Sppl3*^{-/-} MEF (Fig. 5C & 5E) intracellular β 3GnT1 and β 4GalT1 accumulated and secretion of β 4GalT1 was strongly reduced (Fig. 5B, 5D, 5E & E8A). In addition, SPPL3 over-expression resulted in a statistically significant increase in secretion of α -Man I (gene name: MAN1B1) (Fig. 5F & Fig. E8B).

Taken together, our results demonstrate that SPPL3 alters cellular N-glycosylation, most likely by directly cleaving several glycosyltransferases and glycosidases to release their active site-containing ectodomain and thus reducing their respective intracellular activity.

Discussion

Proteolytic secretion of a number of distinct glycosyltransferases is a well-established concept (Paulson & Colley, 1989; Ohtsubo & Marth, 2006; Varki *et al*, 2009) and has been previously observed in cell culture as well as *in vivo* (Kim *et al*, 1972a; 1972b; Elhammer & Kornfeld, 1986; Weinstein *et al*, 1987; Saito *et al*, 2002; El-Battari *et al*, 2003). However, the protease(s) involved in this process have not been unambiguously identified and the physiological implications of proteolytic glycosyltransferase secretion are unclear.

In the present study, we identify ER-/Golgi-resident type II-oriented glycan-modifying enzymes as a novel substrate class for SPPL3. Recently, we reported that SPPL3, unlike γ -secretase (Struhl & Adachi, 2000), SPP (Lemberg & Martoglio, 2002), and SPPL2b (Martin *et al*, 2009), can cleave a viral full-length membrane protein substrate without previous shortening of its ectodomain (i.e. shedding) and thus is, in contrast to all other members of the GxGD protease family, capable of acting like a sheddase. Since most glycosyltransferases and glycosidases are type II transmembrane proteins, which are the preferred substrates for proteolytic cleavage by SPP/SPPL proteases (reviewed in (Voss *et al*, 2013)), it is very likely that SPPL3 may directly mediate, shedding of glycosyltransferases and glycosidases. This notion,

however, requires further experimental validation, ideally in an *in vitro* setting that is devoid of any other cellular factors than SPPL3 and the respective substrate.

Another unresolved question is to what extent proteolytic cleavage affects glycosyltransferase activity *in vivo*. Isolated soluble glycosyltransferases retain their catalytic activity *in vitro* when reactions are supplemented with nucleotide-conjugated monosaccharides (Elhammer & Kornfeld, 1986), but *in vivo* nucleotide-conjugated monosaccharides are only present intracellularly. Accordingly, secretion of the active site-containing glycosyltransferase domain is discussed as a potential mechanism to regulate the extent of cellular glycan modifications (Paulson & Colley, 1989; Ohtsubo & Marth, 2006; Varki *et al*, 2009). Here, we demonstrate that SPPL3 alters N-glycosylation in a cell culture model but also in living animals by mediating the proteolytic release of glycosyltransferases and glycosidases. While, under physiological conditions, glycosyltransferase secretion is in equilibrium with membrane-bound glycosyltransferase, ensuring a particular pattern of glycan modifications (Fig. 6a), over-expression of SPPL3 reduces the amount of catalytically active glycosyltransferases within the Golgi compartment causing hypoglycosylation of cellular glycoproteins (Fig. 6b). In case of α -Man I and overexpressed GnT-V this reduction of active enzyme in cell lysates and the concomitant effect of hypoglycosylation is accompanied by a strong increase of glycosidase secretion. Secretion of endogenous GnT-V, β 4GalT1 and β 3GnT1, however, was only marginally increased under these conditions, indicating that a certain amount of glycosyltransferases released from Golgi compartments may rather be subjected to intracellular degradation than being secreted. In contrast, reduced levels of endogenous SPPL3 strongly diminish glycosyltransferase secretion and catalytically active glycosyltransferases accumulate within the Golgi compartment resulting in more extensive modification of cellular N-glycans, i.e. hyperglycosylation (Fig. 6c). In line with this, we were able to show using LCMS that SPPL3 over-expression was accompanied by reduction in tri-antennary and tetra-antennary N-glycans. Consequently, SPPL3 functions as a mediator of cellular N-glycosylation, providing the first insight into one possible physiological function of this GxGD intramembrane protease.

Using a truncated GnT-V model substrate, we mapped the cleavage site of SPPL3 within a peptide stretch predicted to localise to the membrane border of GnT-V. One of the major cleavage sites (L30-H31) had previously been identified by N-terminal sequence analysis of purified secreted GnT-V, but was attributed to a cleavage by the γ -secretase complex (Nakahara *et al*, 2006). γ -secretase is generally considered to selectively cleave type I transmembrane protein substrates with a rather short ectodomain (Steiner *et al*, 2008; Hemming *et al*, 2008; Haapasalo & Kovacs, 2011). Nonetheless, we tested whether inhibition of γ -secretase affects secretion of endogenous GnT-V. Two potent GSIs, which are not cross-reactive with SPPL3 (Voss *et al*, 2012), however, did not impact on GnT-V secretion. Moreover, while we observed neither impaired GnT-V secretion nor alterations in N-glycosylation in γ -secretase-deficient MEFs, both phenotypic abnormalities were apparent in *Sppl3*^{-/-} MEF cells. Since secretion of GnT-V was not completely abolished in SPPL3^{-/-} MEFs, it is, however, possible that other proteases also marginally contribute to the secretion of GnT-V.

SPPL3 is found in multicellular organisms, including plants, arthropods, and mammals (Voss *et al*, 2013). In addition, its degree of conservation is extraordinarily high (e.g. human and murine SPPL3 proteins are > 99.7% identical), suggesting it was evolved to fulfil a fundamentally important physiological function in multicellular organisms. N-glycosylation is such a fundamental physiological process. Complex N-glycans are critically involved in various physiological processes including, for instance the regulation of cell-to-

cell interactions and cell signalling - processes that are essentially required for multi-cellularity (Ohtsubo & Marth, 2006). While defects in Golgi N-glycosylation, are well tolerated and often phenotypically unapparent in cultured cells, they have often been associated with overt phenotypic abnormalities in murine genetic models but also in inherited human diseases (Lowe & Marth, 2003). On a mixed C57BL/6;129S5 background, *Sppl3*-deficient animals feature a rather mild phenotype (Tang *et al*, 2010), though they are not obtained at expected Mendelian ratios (data not shown). Interestingly, when backcrossed to the C57BL/6 background, we failed to obtain viable homozygous knockout animals suggesting that *Sppl3* deficiency leads to embryonic or early post-natal lethality (data not shown). Hence, we assume that SPPL3 orchestrates cellular N-glycosylation in multicellular organisms, but the respective phenotype of SPPL3 deficiency strongly depends on strain-dependent modifier alleles, a phenomenon also observed in animals lacking GnT-II or GnT-V (Wang *et al*, 2001; Dennis *et al*, 2002). Presently, however, we cannot exclude that SPPL3 fulfils additional biological functions that could likewise lead to the observed phenotypic abnormalities.

Moreover, glycosylation plays a fundamental role in the pathophysiology of human diseases (Ohtsubo & Marth, 2006; Dennis *et al*, 2009), for instance in cancer progression and metastasis (Dennis *et al*, 1999). GlcNAc branching and cellular hexoseamine metabolism in particular have emerged as important cellular processes recently and deregulation has been linked to human developmental defects or other disorders (Lau & Dennis, 2008; Dennis *et al*, 2009; Grigorian *et al*, 2009). GnT-V expression, for instance, is up-regulated in tumours and, consequently, PHA-L reactivity is higher in such tumours (reviewed in (Dennis *et al*, 1999)). Moreover, high GnT-V expression levels correlate with the metastatic potential and poor prognosis in colorectal carcinoma (Murata *et al*, 2000). On the other hand, loss of β 1,6GlcNAc branching results in hyperreactive T cells and autoimmune disorders in mice (Demetriou *et al*, 2001). Importantly, all these observations are thought to be intricately linked to the generation of poly-N-acetyllactosamine binding motifs that allow recruitment of a given glycoprotein into the glycoprotein-galectin lattice (Dennis *et al*, 2009). Therefore, it is particularly interesting that we identified GnT-V, β 3GnT1 and β 4GnT1, which are all implicated in the generation of poly-N-acetyllactosamine-carrying N-glycans, as SPPL3 substrates. GnT-V generates N-glycans preferably modified by poly-N-acetyllactosamines (van den Eijnden *et al*, 1988; Ujita *et al*, 1999) and β 3GnT1 (Sasaki *et al*, 1997), together with β 4GnT1 (Ujita *et al*, 2000), elongates these sugar chains.

In summary, we identify a family of biological substrates of SPPL3, providing a first insight into the physiological function of this GxGD intramembrane protease. SPPL3 emerges as mediator of cellular N-glycosylation in mammals, as it appears to control the cellular availability of glycosyltransferases and glycosidases for N-glycan elaboration by facilitating their proteolytic liberation. Therefore, it is tempting to speculate that other Golgi glycosyltransferases may similarly be subject to endoproteolysis mediated by SPPL3 and that SPPL3 may interfere with disease processes in which cellular glycosylation is dysregulated.

Materials and methods:

Antibodies, lectins, and other reagents

Monoclonal antibodies directed against human SPPL3 (clone 7F9) and SPPL2a (clone 6E9) as well as a polyclonal antibody directed against murine SPPL2a were described previously (Behnke *et al*, 2011; Voss

et al, 2012; Schneppenheim *et al*, 2013). The monoclonal (2D8) and polyclonal (3552 & 6687) anti-A β antibodies have been described elsewhere (Shirotani *et al*, 2007; Yamasaki *et al*, 2006; Steiner *et al*, 2000) as well as the polyclonal anti-PS1 antibody (rabbit pAb, 2953) (Walter *et al*, 1997). Other antibodies used in this study were obtained from commercial sources as follows: Anti-Nicastrin (rabbit pAb, N1660, Sigma-Aldrich, St. Louis, USA), anti-Nicastrin (mouse mAb, clone 35, BD Biosciences, Franklin Lanes, USA), anti-human Lamp2 (mouse mAb, clone H4B4, Developmental Studies Hybridoma Bank, University of Iowa, USA), anti-human Lamp2 (rabbit pAb, ab37024, Abcam, Cambridge, UK), anti-mouse Lamp2 (mouse mAb, clone ABL-93, Developmental Studies Hybridoma Bank), anti-N-cadherin (mouse mAb, clone 10C32, BD Biosciences), anti-GnT-V (mouse mAb, clone 706824, R&D Systems, McKinley Place, USA), anti-CD68 (rat mAb, FA-11, AbD serotec, Düsseldorf, Germany), anti-V5 (mouse mAb, R960-25, Life Technologies, Carlsbad, USA), anti-Flag (rabbit mAb, F7425, Sigma), anti-Calnexin (rabbit pAb, Enzo Life Sciences, Farmingdale, USA), anti-B3GNT1 (mouse mAb, clone 724057, R&D Systems), anti-MAN1B1 (mouse mAb, clone 30-Y, Santa Cruz Biotechnology (Dallas, USA), anti-B4GALT1 (goat pAb, AF3609, R&D Systems). Horseradish peroxidase (HRP)-conjugated secondary antibodies were purchased from Promega (Madison, USA) and Dianova (Hamburg, Germany). For immunoblotting, all antibodies were diluted in phosphate buffered saline (PBS) containing 0.5% (v/v) Tween-20 (PBS-T) and supplemented with 2% (w/v) Tropix® I-BLOCK™ blocking reagent (Applied Biosystems, Life Technologies, Carlsbad, USA). The HRP-conjugated anti-HA antibody 3F10 was from Roche Diagnostics (Rotkreuz, Switzerland). Biotinylated lectins and HRP-conjugated streptavidin were obtained from Vector Laboratories (Burlingame, USA). Kifunensine was purchased from Santa Cruz Biotechnology and was dissolved in double-distilled water. The γ -secretase inhibitors DAPT and L-685,458, were from Enzo Life Sciences and Calbiochem (Darmstadt, Germany), respectively. All protease inhibitors were dissolved in DMSO.

Molecular cloning and cDNA constructs

The cDNA that encodes SPPL3 is based on Genbank RefSeq NM_139015.4. Mutations to generate SPPL3 D200N/D271N were introduced by site-directed mutagenesis (primer sequences are available upon request) as described earlier (Voss *et al*, 2012). SPPL3 D200N/D271N containing a C-terminal HA-tag (YPYDVPDYA) was subcloned into the EcoRI and Xhol sites of pcDNA 4/TO A (Invitrogen). Human MGAT5 coding sequences were purchased from Source BioScience (Nottingham, UK), PCR-amplified and sub-cloned using Xhol and KpnI restriction enzymes into pcDNA3.1hygro+ (Life Technologies). To obtain tagged full-length GnT-V, an N-terminal Flag (DYKDDDDK) epitope tag after the initiating methionine residue and a C-terminal in-frame V5 (GKPIPPLLGLDST) epitope tag, respectively, were introduced using PCR amplification. Tagged GnT-V was subcloned into pcDNA3.1hygro+ using Xhol and KpnI. All primer sequences are available upon request and all cloned expression constructs were sequenced verified prior to experimental use.

Cell lines and cell culture experiments

All cells were cultured in DMEM GlutaMAX™ media (Life Technologies) supplemented with L-glutamine (Life Technologies), 10% (v/v) fetal calf serum (Sigma-Aldrich) and 1% (v/v) penicillin/streptomycin (Life Technologies). Stably transfected HEK293 cells expressing SPPL3 under the control of a doxycycline-inducible promoter have been described before (Martin *et al*, 2008). To obtain stable cell lines expressing

SPPL3 D200N/D271N T-Rex™-293 (Invitrogen) were transfected with the respective plasmid DNA as described above. Transfection of cells was carried out using Lipofectamine 2000 (Invitrogen) according to the manufacturer's instructions, and single cell clones were generated by selection in 200 µg/ml zeocine (Invitrogen). To induce expression of SPPL3, cells were incubated with 1 µg/ml doxycycline (BD Biosciences) added to the cell culture medium for at least 48 h. T-Rex™-293-derived clonal cell lines that express plasmids encoding SPPL3-, SPPL2a- and non-targeting shRNAs (Sigma-Aldrich), respectively, or epitope-tagged Flag-GnT-V-V5 were generated as described before (Martin *et al*, 2008). PS1/PS2 double-deficient MEFs that lack active γ -secretase were described elsewhere (Herreman *et al*, 2003) and were kindly provided by Dr Bart de Strooper. Transient transfections with plasmid DNA were carried out using Lipofectamin 2000 (Life Technologies) according to the manufacturer's instructions. To achieve transient knock-downs, T-Rex™-293 cells were reversely transfected with siGENOME SMARTpools (Thermo Scientific, Waltham, USA) targeting human SPPL3 (#M-006042-02), B3GNT1 (#M-012307-01), B4GALT1 (#M-012965-00) or MGAT5 (#M-011334-01) (all dissolved in RNase-free water (Qiagen, Hilden, Germany)) at a final concentration of 20 nM using Lipofectamin RNAiMax™ (Life Technologies) according to the manufacturer's instructions. To collect conditioned supernatants, the respective culture media were removed from cells after 24 h or 48 h and cleared from detached cells by centrifugation or 0.2 µm filtration. Protease inhibitor treatment was performed for 16 h at the concentrations indicated. To inhibit complex- and hybrid-type N-glycosylation, cultured cells were treated with kifunensine at a final concentration of 4 µg/ml for 48 h. To detect secretion of endogenous A β , cells were incubated in serum-free Optimem™ + GlutaMAX™ (Life Technologies) over night. To enrich for secreted factors by trichloroacetic acid (TCA) precipitation, cells were washed twice and then incubated in pre-warmed Optimem™ + GlutaMAX™. Following harvest, 1/5 volume 100% (w/v) TCA was added, samples were mixed and incubated on ice for 1 h. Following centrifugation (13,000 rpm, 4°C, 30 min), supernatants were discarded and pellets washed twice with cold acetone. Dried pellets were re-suspended in non-reducing sample buffer and normalised to lysate protein content prior to loading.

Mice, tissue homogenates, and MEFs

The genetrap mouse line C57BL/6;129S5-Sppl3^{Gt(OST279815)Lex}/Mmucd was obtained from the Mutant Mouse Regional Resource Center (MMRRC) at the University of California at Davis, CA, USA. These mice were described earlier (Tang *et al*, 2010) and have generously been made available to the research community by Genentech, Inc., and Lexicon Pharmaceuticals, Inc. These mice were inter-crossed to maintain the C57BL/6;129S5 hybrid background. Age- and sex-matched animals were sacrificed and indicated organs were removed and snap-frozen on dry ice. Thawed organs were cut into pieces and homogenised in ice-cold buffer (5 mM Tris x HCl, pH 7.4, 250 mM sucrose, 5 mM EGTA, supplemented with protease inhibitor mix (1:500, Sigma)), first using a Wheaton tissue grinder (Thermo Scientific), then 23G needles. Homogenates were centrifuged for 5 min at 5,000 rpm in a tabletop centrifuge. The supernatants were again subjected to centrifugation (13,000 rpm, 1 h, 4°C). Pellets were re-suspended in homogenisation buffer containing 2% (v/v) Triton X-100 and incubated on ice for 30 min. Lysates were cleared from cell debris by centrifugation (13,000 rpm, 1 h, 4°C) and subjected to SDS-PAGE and Western blotting. MEFs were obtained from mice that had been backcrossed to the C57BL/6 background for five generations. Heterozygous mice were mated and embryos were removed at E13.5. Cells were

taken into culture and immortalised as described earlier (Xu, 2005). All animals and derived cells were genotyped by PCR (primer sequences are available upon request).

Immunoblotting, lectin blotting, enzymatic deglycosylation and immunoprecipitation

Cells were harvested on ice and lysed in ice-cold STE buffer (150 mM NaCl, 50 mM Tris (pH 7.6), 2 mM EDTA) supplemented with 1% (v/v) NP-40 and 1% (v/v) Triton X-100 and protease inhibitor mix (1:500). Protein concentrations in lysates were determined using the BCA assay (Interchim, Montluçon, France) and, prior to loading on gels, samples were normalised accordingly. For lectin blotting, membranes were first incubated in 5% (w/v) BSA in PBS-T over-night. Biotin and streptavidin blocking was performed using a commercial kit (Vector Laboratories) according to the manufacturer's instructions. Membranes were incubated with the respective biotinylated lectin (2 µg/ml in lectin buffer (10 mM HEPES, pH 7.5, 150 mM NaCl, 0.1 mM Ca²⁺, 0.08% (w/v) NaN₃) for one hour at room temperature. Following three washing steps (10 min each with PBS-T), blots were incubated with a streptavidin-HRP conjugate (2 µg/ml, diluted in PBS-T) at room temperature for 30 min. After three additional washing steps, blots were developed using conventional ECL chemistry (GE Healthcare, Chalfont St Giles, UK). For enzymatic deglycosylation, proteins in cell lysates were denatured in glycoprotein denaturation buffer (New England Biolabs, Ipswich, USA) supplemented with 1% (w/v) SDS by incubation at 95°C for 10 min. Samples were diluted tenfold with deglycosylation buffer (50 mM Na₂HPO₄, pH 7.2, 12 mM EDTA, 0.4% (v/v) NP-40) and digested with endoglycosidase H (Endo H) (Roche) or peptide:N-glycosidase F (PNGase F) (Roche) overnight. PNGase F removes all N-glycans irrespective of their exact structure and composition (Maley *et al*, 1989), while Endo H only removes high-mannose and hybrid but not complex glycan structures from glycoproteins (Maley *et al*, 1989). Immunoprecipitations, gel electrophoresis, and immunoblotting were carried out as described previously (Krawitz *et al*, 2005; Fluhrer *et al*, 2006). Immunoblots and lectin blots were developed using ECL™ or ECL™ Prime chemistry (GE Healthcare, Chalfont StGiles, UK) and X-ray films.

N-glycan analysis by nanoLCMS

One day after plating of cells, SPPL3 over-expression was induced by supplementing culture medium with doxycycline as described earlier. 48 h later cells were washed twice with pre-warmed, serum-free DMEM and incubated in serum-free DMEM supplemented with doxycycline for another 72 h to collect secreted glycoproteins. Conditioned supernatants were harvested and detached cells were removed by centrifugation. Supernatants were concentrated roughly 40-fold by centrifugation (4,200 rpm at 4°C) in an ultrafiltration unit with a molecular weight cut-off of 5,000 (Vivaspin, Sartorius, Göttingen, Germany). Concentrated proteins were collected by TCA precipitation as detailed earlier. Dried pellets were resuspended in PBS and transferred into ultrafiltration vials with a molecular weight cut-off of 10,000 (Vivaspin, Sartorius, Göttingen, Germany). Samples were washed and buffer was exchanged to denaturation solution (6 M Guanidine hydrochloride, 50 mM Tris HCl and 5 mM EDTA) by centrifugation. Samples were reduced (16 mM dithiothreitol, DTT) for 15 min at 37°C followed by alkylation (30 mM iodoacetamide) for 1 hour at 37°C in the ultrafiltration units. Denaturation solution was subsequently removed by centrifugation and samples were diluted in PBS. N-glycans were released by digestion with PNGaseF which was conducted for 17 h at 37°C. Released N-glycans were eluted by centrifugation and desalting using 96-well PGC (porous graphitized carbon) plates (Thermo Scientific, Waltham, USA). PGC

resin was conditioned with 70% (v/v) acetonitrile (ACN); 0.1% (v/v) trifluoroacetic acid (TFA) and equilibrated with 0.1% (v/v) TFA in water. After sample application resin was washed with 0.1% (v/v) TFA in water. N-glycans were eluted with 40% (v/v) ACN; 0.1% (v/v) TFA and dried using vacuum centrifugation. Dried N-glycans were resuspended in water (10 μ l) and 2-aminobenzoic acid (2-AA) labelling solution (15 μ l; 50 mg/ml 2-AA; 80 mg/ml picoline borane in 70:30 DMSO: acetic acid (v/v)). Reductive amination was performed at 37°C for 17 h. Excess label was removed by gelfiltration using Sephadex G-10 columns (GE Healthcare). NanoLCMS analysis of 2-AA N-glycans was performed as described earlier (Higel *et al*, 2014).

Acknowledgments:

The *Spp1/3* knockout mouse line was kindly provided by Genentech, Inc., and Lexicon Pharmaceuticals, Inc., and was obtained through the MMRRC at the University of California at Davis. Dr. T. Tang (Genentech, Inc.) kindly provided us with a genotyping protocol and primer sequences. We thank Dr. Bart De Strooper for PS-/- MEF cells. This work was supported by the Deutsche Forschungsgemeinschaft (HA 1737-11) and by start-up funding for female researchers provided by the Center for Integrated Protein Science Munich (CIPSM) (to RF). This work was supported by the European Research Council under the European Union's Seventh Framework Program (FP7/2007–2013)/ERC Grant Agreement No. 321366-Amyloid (advanced grant to CH) and by BMBF-KNDD (to SFL and CH). MV was generously supported by a PhD fellowship of the Hans und Ilse Breuer Stiftung and by the Elitenetwork of Bavaria within the Graduate Program "Protein Dynamics in Health and Disease".

Author contribution:

MV and RF conceived the experiments. UK performed GnT-V overexpression experiments. FH and AS conducted mass spectrometric analysis of the N-glycome. PHK, SFL, AF and HS performed mass spectrometric analysis of the GnT-V cleavage site. AC, SFL and BS assisted with the generation of MEF cells. MHK, BK and GG provided technical assistance. RO supervised the backcrosses of the *Spp1/3*-/- mice. MV performed all other experiments. RF and CH supervised the project. MV and RF wrote the manuscript with input from all authors.

Conflict of interest:

The authors declare that they have no conflict of interest.

Expanded View information is available at The EMBO Journal online.

References:

Behnke J, Schneppenheim J, Koch-Nolte F, Haag F, Saftig P & Schröder B (2011) Signal-peptidase-like 2a (SPPL2a) is targeted to lysosomes/late endosomes by a tyrosine motif in its C-terminal tail. *FEBS Lett.* **585**: 2951–2957

Chen L, Zhang N, Adler B, Browne J, Freigen N & Pierce M (1995) Preparation of antisera to recombinant, soluble N-acetylglucosaminyltransferase V and its visualization in situ. *Glycoconj. J.* **12**: 813–823

Cummings RD & Etzler ME (2009) Antibodies and Lectins in Glycan analysis. In *Essentials of Glycobiology*, Varki A Cummings RD Esko JD Freeze HH Stanley P Bertozzi CR Hart GW & Etzler

ME (eds) pp 633–647. Cold Spring Harbor: Cold Spring Harbor Laboratory Press

Cummings RD & Kornfeld S (1982) Characterization of the structural determinants required for the high affinity interaction of asparagine-linked oligosaccharides with immobilized *Phaseolus vulgaris* leukoagglutinating and erythroagglutinating lectins. *J. Biol. Chem.* **257**: 11230–11234

Demetriou M, Granovsky M, Quaggin S & Dennis JW (2001) Negative regulation of T-cell activation and autoimmunity by Mgat5 N-glycosylation. *Nature* **409**: 733–739

Dennis JW, Granovsky M & Warren CE (1999) Glycoprotein glycosylation and cancer progression. *Biochim. Biophys. Acta* **1473**: 21–34

Dennis JW, Nabi IR & Demetriou M (2009) Metabolism, cell surface organization, and disease. *Cell* **139**: 1229–1241

Dennis JW, Pawling J, Cheung P, Partridge E & Demetriou M (2002) UDP-N-acetylglucosamine:alpha-6-D-mannoside beta1,6 N-acetylglucosaminyltransferase V (Mgat5) deficient mice. *Biochim. Biophys. Acta* **1573**: 414–422

Dovey HF, John V, Anderson JP, Chen LZ, de Saint Andrieu P, Fang LY, Freedman SB, Folmer B, Goldbach E, Holsztynska EJ, Hu KL, Johnson-Wood KL, Kennedy SL, Kholodenko D, Knops JE, Latimer LH, Lee M, Liao Z, Lieberburg IM, Motter RN, et al (2001) Functional gamma-secretase inhibitors reduce beta-amyloid peptide levels in brain. *J. Neurochem.* **76**: 173–181

El-Battari A, Prorok M, Angata K, Mathieu S, Zerfaoui M, Ong E, Suzuki M, Lombardo D & Fukuda M (2003) Different glycosyltransferases are differentially processed for secretion, dimerization, and autoglycosylation. *Glycobiology* **13**: 941–953

Elbein AD, Tropea JE, Mitchell M & Kaushal GP (1990) Kifunensine, a potent inhibitor of the glycoprotein processing mannosidase I. *J. Biol. Chem.* **265**: 15599–15605

Elhammer A & Kornfeld S (1986) Purification and characterization of UDP-N-acetylgalactosamine: polypeptide N-acetylgalactosaminyltransferase from bovine colostrum and murine lymphoma BW5147 cells. *J. Biol. Chem.* **261**: 5249–5255

Fluhrer R, Grammer G, Israel L, Condon MM, Haffner C, Friedmann E, Böhland C, Imhof A, Martoglio B, Teplow DB & Haass C (2006) A gamma-secretase-like intramembrane cleavage of TNF α by the GxGD aspartyl protease SPPL2b. *Nat. Cell Biol.* **8**: 894–896

Friedmann E, Hauben E, Maylandt K, Schleeger S, Vreugde S, Lichtenthaler SF, Kuhn P-H, Stauffer D, Rovelli G & Martoglio B (2006) SPPL2a and SPPL2b promote intramembrane proteolysis of TNF α in activated dendritic cells to trigger IL-12 production. *Nat. Cell Biol.* **8**: 843–848

Friedmann E, Lemberg MK, Weihofen A, Dev KK, Dengler U, Rovelli G & Martoglio B (2004) Consensus analysis of signal peptide peptidase and homologous human aspartic proteases reveals opposite topology of catalytic domains compared with presenilins. *J. Biol. Chem.* **279**: 50790–50798

Fukumori A, Fluhrer R, Steiner H & Haass C (2010) Three-amino acid spacing of presenilin endoproteolysis suggests a general stepwise cleavage of gamma-secretase-mediated intramembrane proteolysis. *J. Neurosci.* **30**: 7853–7862

Grigorenko AP, Moliaka YK, Korovaitseva GI & Rogaev EI (2002) Novel class of polytopic proteins with domains associated with putative protease activity. *Biochemistry Mosc.* **67**: 826–835

Grigorian A, Torossian S & Demetriou M (2009) T-cell growth, cell surface organization, and the galectin-glycoprotein lattice. *Immunol. Rev.* **230**: 232–246

Haapasalo A & Kovacs DM (2011) The many substrates of presenilin/ γ -secretase. *J. Alzheimers Dis.* **25**: 3–28

Haass C (2004) Take five--BACE and the gamma-secretase quartet conduct Alzheimer's amyloid beta-peptide generation. *EMBO J.* **23**: 483–488

Hemming ML, Elias JE, Gygi SP & Selkoe DJ (2008) Proteomic profiling of gamma-secretase substrates and mapping of substrate requirements. *PLoS Biol.* **6**: e257

Herreman A, Van Gassen G, Bentahir M, Nyabi O, Craessaerts K, Mueller U, Annaert W & De Strooper B (2003) gamma-Secretase activity requires the presenilin-dependent trafficking of nicastrin through the Golgi apparatus but not its complex glycosylation. *J. Cell. Sci.* **116**: 1127–1136

Higel F, Seidl A, Demelbauer U, Sörgel F & Frieß W (2014) Small scale affinity purification and high sensitivity reversed phase nanoLC-MS N-glycan characterization of mAbs and fusion proteins. *MAbs* **6**: 894–903

Kamar M, Alvarez-Manilla G, Abney T, Azadi P, Kumar Kolli VS, Orlando R & Pierce M (2004) Analysis of the site-specific N-glycosylation of beta1,6 N-acetylglucosaminyltransferase V. *Glycobiology* **14**: 583–592

Kim YS, Perdomo J & Whitehead JS (1972a) Glycosyltransferases in human blood. I. Galactosyltransferase in human serum and erythrocyte membranes. *J. Clin. Invest.* **51**: 2024–2032

Kim YS, Perdomo J, Whitehead JS & Curtis KJ (1972b) Glycosyltransferases in human blood. II. Study of serum galactosyltransferase and N-acetylgalactosaminyltransferase in patients with liver diseases. *J. Clin. Invest.* **51**: 2033–2039

Kirkin V, Cahuzac N, Guardiola-Serrano F, Huault S, Lückerath K, Friedmann E, Novac N, Wels WS, Martoglio B, Hueber A-O & Zörnig M (2007) The Fas ligand intracellular domain is released by ADAM10 and SPPL2a cleavage in T-cells. *Cell. Death Differ.* **14**: 1678–1687

Kitazume S, Nakagawa K, Oka R, Tachida Y, Ogawa K, Luo Y, Citron M, Shitara H, Taya C, Yonekawa H, Paulson JC, Miyoshi E, Taniguchi N & Hashimoto Y (2005) In vivo cleavage of alpha2,6-sialyltransferase by Alzheimer beta-secretase. *J. Biol. Chem.* **280**: 8589–8595

Kitazume S, Oka R, Ogawa K, Futakawa S, Hagiwara Y, Takikawa H, Kato M, Kasahara A, Miyoshi E, Taniguchi N & Hashimoto Y (2009) Molecular insights into beta-galactoside alpha2,6-sialyltransferase secretion in vivo. *Glycobiology* **19**: 479–487

Kitazume S, Tachida Y, Oka R, Shirotani K, Saido TC & Hashimoto Y (2001) Alzheimer's beta-secretase, beta-site amyloid precursor protein-cleaving enzyme, is responsible for cleavage secretion of a Golgi-resident sialyltransferase. *Proc. Natl. Acad. Sci. U.S.A.* **98**: 13554–13559

Kopan R & Ilagan MXG (2004) Gamma-secretase: proteasome of the membrane? *Nat. Rev. Mol. Cell Biol.* **5**: 499–504

Kornfeld R & Kornfeld S (1985) Assembly of asparagine-linked oligosaccharides. *Annu. Rev. Biochem.* **54**: 631–664

Krawitz P, Haffner C, Fluhrer R, Steiner H, Schmid B & Haass C (2005) Differential localization and identification of a critical aspartate suggest non-redundant proteolytic functions of the presenilin homologues SPPL2b and SPPL3. *J. Biol. Chem.* **280**: 39515–39523

Lammers G & Jamieson JC (1988) The role of a cathepsin D-like activity in the release of Gal beta 1-4GlcNAc alpha 2-6-sialyltransferase from rat liver Golgi membranes during the acute-phase response. *Biochem. J.* **256**: 623–631

Lau KS & Dennis JW (2008) N-Glycans in cancer progression. *Glycobiology* **18**: 750–760

Lee J-K, Matthews RT, Lim J-M, Swanier K, Wells L & Pierce JM (2012) Developmental expression of the neuron-specific N-acetylglucosaminyltransferase Vb (GnT-Vb/IX) and identification of its in vivo glycan products in comparison with those of its paralog, GnT-V. *J. Biol. Chem.* **287**: 28526–28536

Lemberg MK & Martoglio B (2002) Requirements for signal peptide peptidase-catalyzed intramembrane proteolysis. *Mol. Cell* **10**: 735–744

Lowe JB & Marth JD (2003) A genetic approach to Mammalian glycan function. *Annu. Rev. Biochem.* **72**:

Maley F, Trimble RB, Tarentino AL & Plummer TH (1989) Characterization of glycoproteins and their associated oligosaccharides through the use of endoglycosidases. *Anal. Biochem.* **180**: 195–204

Martin L, Fluhrer R & Haass C (2009) Substrate requirements for SPPL2b-dependent regulated intramembrane proteolysis. *J. Biol. Chem.* **284**: 5662–5670

Martin L, Fluhrer R, Reiss K, Kremmer E, Saftig P & Haass C (2008) Regulated intramembrane proteolysis of Bri2 (Itm2b) by ADAM10 and SPPL2a/SPPL2b. *J. Biol. Chem.* **283**: 1644–1652

McCaffrey G & Jamieson JC (1993) Evidence for the role of a cathepsin D-like activity in the release of Gal beta 1-4GlcNAc alpha 2-6sialyltransferase from rat and mouse liver in whole-cell systems. *Comp. Biochem. Physiol., B* **104**: 91–94

Moremen KW, Tiemeyer M & Nairn AV (2012) Vertebrate protein glycosylation: diversity, synthesis and function. *Nat. Rev. Mol. Cell Biol.* **13**: 448–462

Murata K, Miyoshi E, Kameyama M, Ishikawa O, Kabuto T, Sasaki Y, Hiratsuka M, Ohigashi H, Ishiguro S, Ito S, Honda H, Takemura F, Taniguchi N & Imaoka S (2000) Expression of N-acetylglucosaminyltransferase V in colorectal cancer correlates with metastasis and poor prognosis. *Clin. Cancer Res.* **6**: 1772–1777

Nakahara S, Saito T, Kondo N, Moriwaki K, Noda K, Ihara S, Takahashi M, Ide Y, Gu J, Inohara H, Katayama T, Tohyama M, Kubo T, Taniguchi N & Miyoshi E (2006) A secreted type of beta1,6 N-acetylglucosaminyltransferase V (GnT-V), a novel angiogenesis inducer, is regulated by gamma-secretase. *FASEB J.* **20**: 2451–2459

Nyborg AC, Jansen K, Ladd TB, Fauq A & Golde TE (2004) A signal peptide peptidase (SPP) reporter activity assay based on the cleavage of type II membrane protein substrates provides further evidence for an inverted orientation of the SPP active site relative to presenilin. *J. Biol. Chem.* **279**: 43148–43156

Ohtsubo K & Marth JD (2006) Glycosylation in cellular mechanisms of health and disease. *Cell* **126**: 855–867

Paulson JC & Colley KJ (1989) Glycosyltransferases. Structure, localization, and control of cell type-specific glycosylation. *J. Biol. Chem.* **264**: 17615–17618

Ponting CP, Hutton M, Nyborg A, Baker M, Jansen K & Golde TE (2002) Identification of a novel family of presenilin homologues. *Hum. Mol. Genet.* **11**: 1037–1044

Saito T, Miyoshi E, Sasai K, Nakano N, Eguchi H, Honke K & Taniguchi N (2002) A secreted type of beta 1,6-N-acetylglucosaminyltransferase V (GnT-V) induces tumor angiogenesis without mediation of glycosylation: a novel function of GnT-V distinct from the original glycosyltransferase activity. *J. Biol. Chem.* **277**: 17002–17008

Sasaki K, Kurata-Miura K, Ujita M, Angata K, Nakagawa S, Sekine S, Nishi T & Fukuda M (1997) Expression cloning of cDNA encoding a human beta-1,3-N-acetylglucosaminyltransferase that is essential for poly-N-acetyllactosamine synthesis. *Proc. Natl. Acad. Sci. U.S.A.* **94**: 14294–14299

Schneppenheim J, Dressel R, Hüttl S, Lüllmann-Rauch R, Engelke M, Dittmann K, Wienands J, Eskelinen E-L, Hermans-Borgmeyer I, Fluhrer R, Saftig P & Schröder B (2013) The intramembrane protease SPPL2a promotes B cell development and controls endosomal traffic by cleavage of the invariant chain. *J. Exp. Med.* **210**: 41–58

Sears P & Wong CH (1998) Enzyme action in glycoprotein synthesis. *Cell. Mol. Life Sci.* **54**: 223–252

Shearman MS, Beher D, Clarke EE, Lewis HD, Harrison T, Hunt P, Nadin A, Smith AL, Stevenson G & Castro JL (2000) L-685,458, an Aspartyl Protease Transition State Mimic, Is a Potent Inhibitor of Amyloid β -Protein Precursor γ -Secretase Activity. *Biochemistry* **39**: 8698–8704

Shen J & Kelleher RJ (2007) The presenilin hypothesis of Alzheimer's disease: evidence for a loss-of-function pathogenic mechanism. *Proc. Natl. Acad. Sci. U.S.A.* **104**: 403–409

Shirotani K, Tomioka M, Kremmer E, Haass C & Steiner H (2007) Pathological activity of familial Alzheimer's disease-associated mutant presenilin can be executed by six different gamma-secretase complexes. *Neurobiol. Dis.* **27**: 102–107

Shoreibah M, Perng GS, Adler B, Weinstein J, Basu R, Cupples R, Wen D, Browne JK, Buckhaults P, Fregien N & Pierce M (1993) Isolation, characterization, and expression of a cDNA encoding N-acetylglucosaminyltransferase V. *J. Biol. Chem.* **268**: 15381–15385

Stanley P, Schachter H & Taniguchi N (2009) N-Glycans. In *Essentials of Glycobiology*, Varki A, Cummings RG, Esko JD, Freeze HH, Stanley P, Bertozzi CR, Hart GW & Etzler ME (eds) pp 101–114. Cold Spring Harbor: Cold Spring Harbor Laboratory Press

Steiner H, Fluhrer R & Haass C (2008) Intramembrane proteolysis by gamma-secretase. *J. Biol. Chem.* **283**: 29627–29631

Steiner H, Kostka M, Romig H, Basset G, Pesold B, Hardy J, Capell A, Meyn L, Grim ML, Baumeister R, Fechteler K & Haass C (2000) Glycine 384 is required for presenilin-1 function and is conserved in bacterial polytopic aspartyl proteases. *Nat. Cell Biol.* **2**: 848–851

Struhl G & Adachi A (2000) Requirements for presenilin-dependent cleavage of notch and other transmembrane proteins. *Mol. Cell* **6**: 625–636

Tang T, Li L, Tang J, Li Y, Lin WY, Martin F, Grant D, Solloway M, Parker L, Ye W, Forrest W, Ghilardi N, Oravecz T, Platt KA, Rice DS, Hansen GM, Abuin A, Eberhart DE, Godowski P, Holt KH, et al (2010) A mouse knockout library for secreted and transmembrane proteins. *Nat. Biotechnol.* **28**: 749–755

Ujita M, McAuliffe J, Hindsgaul O, Sasaki K, Fukuda MN & Fukuda M (1999) Poly-N-acetyllactosamine synthesis in branched N-glycans is controlled by complementary branch specificity of I-extension enzyme and beta1,4-galactosyltransferase I. *J. Biol. Chem.* **274**: 16717–16726

Ujita M, Misra AK, McAuliffe J, Hindsgaul O & Fukuda M (2000) Poly-N-acetyllactosamine extension in N-glycans and core 2- and core 4-branched O-glycans is differentially controlled by I-extension enzyme and different members of the beta 1,4-galactosyltransferase gene family. *J. Biol. Chem.* **275**: 15868–15875

van den Eijnden DH, Koenderman AH & Schiphorst WE (1988) Biosynthesis of blood group i-active polylactosaminoglycans. Partial purification and properties of an UDP-GlcNAc:N-acetyllactosaminide beta 1---3-N-acetylglucosaminyltransferase from Novikoff tumor cell ascites fluid. *J. Biol. Chem.* **263**: 12461–12471

Varki A, Esko JD & Colley KJ (2009) Cellular Organization of Glycosylation. In *Essentials of Glycobiology*, Varki A, Cummings RG, Esko JD, Freeze HH, Stanley P, Bertozzi CR, Hart GW & Etzler ME (eds) pp 37–46. Cold Spring Harbor: Cold Spring Harbor Laboratory Press

Voss M, Fukumori A, Kuhn P-H, Künzel U, Klier B, Grammer G, Haug-Kröper M, Kremmer E, Lichtenthaler SF, Steiner H, Schröder B, Haass C & Fluhrer R (2012) Foamy Virus Envelope Protein Is a Substrate for Signal Peptide Peptidase-like 3 (SPPL3). *J. Biol. Chem.* **287**: 43401–43409

Voss M, Schröder B & Fluhrer R (2013) Mechanism, specificity, and physiology of signal peptide peptidase (SPP) and SPP-like proteases. *Biochim. Biophys. Acta* **1828**: 2828–2839

Walter J, Grünberg J, Capell A, Pesold B, Schindzielorz A, Citron M, Mendla K, George-Hyslop PS, Multhaup G, Selkoe DJ & Haass C (1997) Proteolytic processing of the Alzheimer disease-associated presenilin-1 generates an in vivo substrate for protein kinase C. *Proc. Natl. Acad. Sci. U.S.A.* **94**: 5349–5354

Wang Y, Tan J, Sutton-Smith M, Ditto D, Panico M, Campbell RM, Varki NM, Long JM, Jaeken J, Levinson SR, Wynshaw-Boris A, Morris HR, Le D, Dell A, Schachter H & Marth JD (2001) Modeling human congenital disorder of glycosylation type Iia in the mouse: conservation of asparagine-linked

glycan-dependent functions in mammalian physiology and insights into disease pathogenesis.
Glycobiology **11**: 1051–1070

Weihofen A, Binns K, Lemberg MK, Ashman K & Martoglio B (2002) Identification of signal peptide peptidase, a presenilin-type aspartic protease. *Science* **296**: 2215–2218

Weinstein J, Lee EU, McEntee K, Lai PH & Paulson JC (1987) Primary structure of beta-galactoside alpha 2,6-sialyltransferase. Conversion of membrane-bound enzyme to soluble forms by cleavage of the NH₂-terminal signal anchor. *J. Biol. Chem.* **262**: 17735–17743

Xu J (2005) Preparation, culture, and immortalization of mouse embryonic fibroblasts. *Curr. Protoc. Mol. Biol. Chapter 28*: Unit 28.1

Yamasaki A, Eimer S, Okochi M, Smialowska A, Kaether C, Baumeister R, Haass C & Steiner H (2006) The GxGD motif of presenilin contributes to catalytic function and substrate identification of gamma-secretase. *J. Neurosci.* **26**: 3821–3828

Figure legends:

Figure 1 - SPPL3 expression affects cellular N-glycosylation.

A SPPL3 overexpression results in a reduced molecular weight of glycoproteins. Electrophoretic mobility of the endogenous glycoproteins Nicastrin (NCT), N-cadherin (N-cad), SPPL2a, and Lamp2 was studied in whole cell lysates of HEK293 cells by Western blotting following separation by SDS-PAGE. Expression of either HA-tagged catalytically active SPPL3 (wt) or an inactive SPPL3 mutant (DD/NN) was induced by doxycycline treatment (+ Dox) for 72 h. Cells not treated with doxycycline (- Dox) were used as controls. In cells expressing catalytically active SPPL3 the glycoproteins analysed displayed a reduced molecular weight. Note that only mature (NCT_{mat}) but not immature (NCT_{im}) Nicastrin is affected. Treatment of parental HEK293 cells with doxycycline had no effect on glycoprotein electrophoretic mobility (Fig. E1).

B SPPL3 knockdown results in a slightly higher molecular weight of endogenous glycoproteins. Lysates of non-transfected (none) HEK293 cells as well as of HEK293 cells transfected with non-targeting (ctrl) or SPPL3-targeting siRNA pools were analysed for electrophoretic mobility of endogenous glycoproteins as described in **A**. Reduction of SPPL3 protein levels was accompanied by a slight increase in glycoprotein molecular weight.

C Alterations in glycoprotein molecular weight induced by SPPL3 overexpression are due to altered N-glycosylation. Whole cell lysates from SPPL3-expressing HEK293 cells (+ Dox) and non-induced control cells (- Dox) were deglycosylated using peptide:N-glycosidase F (PNGase F) or endoglycosidase H (Endo H) prior to analysis by SDS-PAGE and immunoblotting. Non-treated cell lysates served as control (untreated). Arrows and/or brackets indicate the respective glycosylated (glyc) and deglycosylated (deglyc) protein species. SPPL3 overexpression had no impact on the molecular weight of deglycosylated proteins. Note that anti-Lamp2 (H4B4) immunoreactivity was lost following complete N-glycosylation. N-deglycosylated Lamp2 was detected using another anti-Lamp2 antibody (ab37024).

D Kifunensine treatment abolishes the effect of SPPL3 overexpression on cellular N-glycosylation. HEK293 cells overexpressing SPPL3 (+ Dox) were treated with solvent (control) or kifunensine for 16h to block complex N-glycosylation. Non-transfected as well as non-induced (- Dox) cells served as control. Electrophoretic mobility of the indicated endogenous glycoproteins was monitored as described in **A**. Upon kifunensine treatment, endogenous glycoproteins were less extensively glycosylated and migrated faster. SPPL3 failed to further reduce the glycoprotein molecular weight.

In all panels, Calnexin was used as a loading control. Antibodies used to visualize the respective proteins in Western blot are indicated.

Figure 2 - *Sppl3*-deficient mice exhibit a hyperglycosylation phenotype.

A, B, C Electrophoretic mobility of selected endogenous glycoproteins in brain **A**, lung **B** and spleen **C** homogenates obtained from *Sppl3*-deficient (-/-) mice was analysed by SDS-PAGE and subsequent immunoblotting. Age- and sex-matched wt (+/+) and heterozygous (+/-) littermates served as controls. As assessed by Western blotting (second panel from the bottom), SPPL3 protein expression was absent in homogenates of all tissues from *Sppl3*^{-/-} animals and was reduced in the heterozygous mouse. Note that, in all tissues analysed, glycoproteins such as mature Nicastin (NCT_{mat}), Lamp2 and SPPL2a but also tissue-specific glycoproteins such as N-cadherin (N-cad) in brain and CD68 in spleen exhibited a higher molecular weight in *Sppl3*-deficient animals compared to control animals. Note that, the molecular weight of immature Nicastin (NCT_{im}) was not altered in *Sppl3*^{-/-} tissues.

D Analysis of glycoprotein molecular weight in immortalised MEF derived from a *Sppl3*-deficient embryo (-/-). MEF derived from wt (+/+) and heterozygous (+/-) littermates served as controls. Total cell lysates were analysed as described in Fig. 1A. Similar to tissue homogenates, glycoproteins displayed a higher molecular weight in cultured *Sppl3*-deficient cells compared to control cells.

In all panels, Calnexin was used as a loading control. Antibodies used to visualize the respective proteins in Western blot are indicated.

Figure 3 - SPPL3 affects secretion of the N-acetylglucosaminyltransferase GnT-V.

A Schematic overview of Golgi asparagine (Asn)-linked N-glycan processing and GlcNAc branching resulting in the generation of high-mannose, hybrid and complex N-glycans (grey boxes). The latter types of glycans are subsequently subjected to terminal modification (not depicted). Kifunensine interferes with N-glycosylation by blocking α -mannosidase I (α -Man I) activity. After modification by α -mannosidase II (α -Man II) glycoproteins gain Endo H-resistance. Mannose (Man) residues are depicted as green circles. N-acetylglucosaminyltransferases (GnTs) attach N-acetylglucosamine (GlcNAc) residues (blue squares) to the core mannose residues in specific stereochemical configurations (red). Modified after (Sears & Wong, 1998) and (Stanley *et al*, 2009).

B SPPL3 affects secretion of endogenous GnT-V. HEK293 cells were transfected with non-targeting (ctrl), SPPL3-specific or MGAT5-specific siRNA pools (20 nM each). SPPL3 over-expression was induced by doxycycline (+ Dox). GnT-V levels were examined by SDS-PAGE and Western blotting in conditioned supernatants (sGnT-V) and whole cell lysates (GnT-V). Cellular SPPL3 levels were similarly analysed.

C & D SPPL3 affects secretion of over-expressed GnT-V. GnT-V was transiently transfected **C** into HEK293 cells stably over-expressing catalytically active SPPL3 (wt) or the inactive SPPL3 D200N/D271N mutant (DD/NN) or **D** into cells that stably expressed non-targeting (ctrl), SPPL2a- or SPPL3-specific shRNAs. GnT-V levels were analysed in conditioned supernatants (sGnT-V) and lysates (GnT-V) as described in **B**. Note that under over-expression conditions, two GnT-V species were detected, mature GnT-V (GnT-V_{mat}) and immature GnT-V (GnT-V_{im}) (see Fig. E4). n.t., not transfected.

E GnT-V secretion is impaired in *Sppl3*-deficient MEF cells. GnT-V levels were monitored in whole cell lysates and in TCA-precipitated conditioned supernatants of *Sppl3*-deficient (-/-) MEFs and wt (+/+) controls as described in **B**.

F SPPL3 over-expression reduces lectin binding. Nicastin (NCT) was immunoprecipitated from HEK293 cells over-expressing catalytically active SPPL3 following doxycycline induction (+ Dox) and from non-induced control cells (- Dox). Immunoprecipitates were visualized either with an anti-Nicastin monoclonal antibody or the biotinylated lectins, Concanavalin A (ConA) and PHA-L, respectively. Note that PHA-L only detected mature Nicastin (NCT_{mat}), and that PHA-L reactivity was reduced in cells over-expressing SPPL3. Kifunensine-treated (+ KF) cells were used as a control and lacked PHA-L-reactive N-glycans.

G SPPL3 over-expression reduces GnT-V-mediated glycan branching. N-glycans on secreted glycoproteins from HEK293 cells (empty bars) and cells over-expressing SPPL3 (hatched bars) following doxycycline induction were analysed by liquid chromatography-mass spectrometry. Bar graphs depict the relative abundance of the indicated N-glycan species. Bar graphs are colour-coded and the assigned individual N-glycan species are listed in Suppl. Tab. 1 accordingly.

In panels **B** to **F**, Calnexin was used as a loading control. Antibodies and lectins used to visualize the respective proteins in Western blots are indicated.

Figure 4 - GnT-V secretion in HEK293 cells occurs via a SPPL3-dependent proteolytic mechanism.

A Similar to most Golgi glycosyltransferases, GnT-V is a type II membrane protein. It comprises a short cytosolic N-terminus, a TMD, a luminal stem region and the luminal catalytic ectodomain. Its secretion is likely mediated by proteolytic cleavage (scissors) at the TMD/stem region boundary.

B GnT-V secretion occurs via a proteolytic mechanism. HEK293 cells were stably transfected with N-terminally Flag-tagged and C-terminally V5-tagged GnT-V (Flag-GnT-V-V5). In lysates, mature (GnT-V_{mat}) and immature (GnT-V_{im}) species of Flag-GnT-V-V5 were detected by Western blotting. Intracellular GnT-V_{mat} was reduced and soluble GnT-V (sGnT-V) enriched in conditioned supernatants of cells co-expressing SPPL3 (+ Dox). Note that sGnT-V was detected using the ectodomain-specific mAb and an anti-V5 antibody but was not reactive with antibodies directed against the N-terminal Flag tag, suggesting that sGnT-V lacks an intact Flag tag. n.t., not transfected, *, unspecific band.

C GnT-V secretion is not affected by GSI treatment. HEK293 cells were treated for 16 h with the GSIs DAPT and L-685,458 at the concentrations indicated. Vehicle-treated cells (DMSO) served as control. GnT-V levels were monitored by Western blotting in conditioned supernatants (sGnT-V) and in cell lysates (GnT-V). To control for γ -secretase inhibition, β -amyloid precursor protein (APP) processing by γ -secretase was monitored. To this end, total secreted amyloid- β peptide (A β) was immunoprecipitated (IP) from conditioned supernatants. Immunoprecipitates were analysed by Western blotting. Levels of full-length APP and APP C-terminal fragments (APP CTF) were likewise monitored in cell lysates. GSI treatment led to a concentration-dependent reduction in A β secretion and a concomitant intracellular accumulation of APP CTF indicating that APP processing by γ -secretase was blocked. Note, however, that GnT-V secretion was altered following GSI treatment. The increase in secreted A β at low GSI concentrations has been observed before (Shen & Kelleher, 2007).

D Loss of γ -secretase activity does not induce hyperglycosylation. Glycoproteins were analysed in PS1/PS2-deficient (-/-) and control (+/+) MEFs and compared to *Sppl3*-deficient (-/-) MEFs as described in Fig.

1A. Note that PS1/PS2^{-/-} MEFs display a mild hypoglycosylation phenotype which could be explained by the slightly higher SPPL3 expression compared to the respective control.

E GnT-V levels were analysed in lysates (GnT-V) and TCA-precipitated conditioned supernatants (sGnT-V) of PS1/PS2^{-/-} MEFs and of control cells as described in Fig. 3E. Note that GnT-V secretion was not

abrogated by loss of γ -secretase activity whereas loss of SPPL3 was associated with a marked reduction in secretion of GnT-V.

Figure 5 - SPPL3 similarly affects other glycosyltransferases and glycosidases.

A Loss of GnT-V expression does not phenocopy SPPL3 over-expression. HEK293 cells transiently transfected with non-targeting (ctrl), SPPL3-specific or MGAT5-specific siRNA pools (20 nM each) and HEK293 cells over-expressing SPPL3 (+ Dox) were analysed for electrophoretic mobility of endogenous mature Nicastin (NCT_{mat}), N-cadherin (N-cad), SPPL2a, and Lamp2 as described in Fig. 1A. Note, that hypoglycosylation induced by SPPL3 overexpression is more pronounced compared to transfection with MGAT5-specific siRNAs suggesting that GnT-V is not the only SPPL3 substrate contributing to SPPL3 effects on N-glycosylation.

B SPPL3 affects secretion of β 1,3 N-acetylglucosaminyltransferase 1 (β 3GnT1). HEK293 cells were transfected with B3GNT1-specific, non-targeting (ctrl) or SPPL3-specific siRNA pools as in **A**. β 3GnT1 levels were analysed by immunoblotting in conditioned supernatants (s β 3GnT1) and cell lysates (β 3GnT1). β 3GnT1 strongly accumulated intracellularly following siRNA-mediated SPPL3 knockdown in HEK293 cells and s β 3GnT1 secretion was significantly decreased (see also quantification in Fig. E7 A). Overexpression of SPPL3 in doxycycline-induced cells (+ Dox) resulted in a reduction of β 3GnT1 in cellular lysates. Antibody staining was specific as β 3GnT1 as well as s β 3GnT1 levels were reduced in cells transfected with a B3GNT1-specific siRNA pool.

C β 3GnT1 accumulates in *Sppl3*-deficient MEFs. β 3GnT1 levels were monitored by Western blotting in whole lysates (β 3GnT1) obtained from *Sppl3*-deficient (-/-) or wt control (+/+) MEFs. In *Sppl3*^{-/-} MEFs, β 3GnT1 strongly accumulated intracellularly.

D SPPL3 affects secretion of β 1,4 galactosyltransferase 1 (β 4GalT1). The experiment was conducted as in **B**, yet a siRNA pool targeting B4GALT1 was used to control for antibody specificity. Intracellular β 4GalT1 levels and levels of secreted β 4GALT1 (s β 4GalT1) were monitored by Western blotting using a specific antibody. Note that SPPL3 knockdown reduced β 4GalT1 secretion while intracellular β 4GalT1 accumulated intracellularly. SPPL3 overexpression reduced intracellular β 4GalT1 levels.

E β 4GalT1 secretion is impaired in *Sppl3*-deficient MEFs. β 4GalT1 and s β 4GalT1 levels were monitored in lysates and TCA-precipitated conditioned supernatants obtained from *Sppl3*-deficient (-/-) or wt control (+/+) MEFs by Western blotting.

F SPPL3 affects secretion of α -mannosidase I (α -Man I). In a setting similar to **B**, intracellular (α -Man I) and secreted (s α -Man I) levels of α -Man I were analysed in lysates and conditioned supernatants, respectively. Note that SPPL3 knockdown led to a mild intracellular accumulation of α -Man I and soluble α -Man I strongly accumulated in the supernatant of cells over-expressing SPPL3 (see also quantification in Fig. E7 B&C).

Antibodies used to visualise the respective proteins in Western blots are indicated.

Figure 6 - Model depicting the effect of SPPL3 on glycosyltransferase secretion and cellular N-glycosylation.

A Membrane-tethered glycosyltransferases (GT, green) mature in the Golgi stacks (bold arrows) and are destined to catalyse protein glycosylation in particular subcompartments (depicted here: generation of a tri-antennary N-glycan, e.g. by GnT-V activity) leading to a specific glycosylation profile on a particular

glycoprotein (purple). Under physiological conditions, the endogenous SPPL3 pool (red) facilitates proteolytic liberation of a certain fraction of the Golgi glycosyltransferases from their membrane anchor resulting in their subsequent secretion (soluble glycosyltransferases, sGT).

B More abundant SPPL3 protein in the Golgi, e.g. upon over-expression, results in a substantially larger fraction of glycosyltransferase turned over proteolytically, leading to enhanced glycosyltransferase secretion and loss of intracellular glycosyltransferase activity. Consequently and as proteolytic cleavage occurs prematurely, glycans are not modified by the given glycosyltransferase (depicted here: no triantennary N-glycans) resulting in a hypoglycosylation phenotype.

C In cells lacking SPPL3, glycosyltransferase secretion is impaired as glycosyltransferases are not endoproteolysed. Hence, active glycosyltransferases accumulate in their destined compartment, resulting in more extensively glycan modification (depicted here: only triantennary N-glycans) and a hyperglycosylation phenotype.

Expanded View legends:

Figure E1. Doxycycline treatment *per se* does not affect cellular glycoproteins. This figure depicts the very same experiment shown in Fig. 1A of the main text version. As a control, it includes non-transfected HEK293 cells (untransf.) that were treated with doxycycline (+ Dox) in the same manner as cells overexpressing SPPL3 to exclude that the effects observed following induction of SPPL3 overexpression in a clonal derivative of these cells are due to the doxycycline treatment *per se*.

Figure E2. Hyperglycosylation phenotype in *Sppl3*^{-/-} tissues and MEF is abolished by enzymatic deglycosylation. Brain homogenates **A** from a *Sppl3*-deficient mouse (-/-) and a wild-type (+/+) littermate control or whole cell lysates from immortalized MEFs obtained from a *Sppl3*-deficient (-/-) embryos and wild-type (+/+) control **B** were subjected to enzymatic deglycosylation with peptide:N-glycosidase F (PNGase F), endoglycosidase H (Endo H) prior to analysis by SDS-PAGE and Western blotting. Controls were left untreated. The indicated N-glycosylated (glyc) proteins were analysed. Complexly glycosylated mature Nicastrin (NCT_{glyc}), N-cadherin (N-cad_{glyc}) and SPPL2a (SPPL2a_{glyc}) are resistant to Endo H treatment and display a higher apparent molecular weight in brain tissue obtained from a *Sppl3*^{-/-} animal compared to the *Sppl3*^{+/+} control. Upon PNGase F digestion, no difference in the molecular weight of N-deglycosylated protein species (NCT_{deglyc}, N-cad_{deglyc} and SPPL2a_{deglyc}) between brain homogenates and MEF from *Sppl3*-deficient (-/-) and wt controls (+/+) was detectable. Antibodies used to visualize the respective proteins in Western blots are indicated.

Figure E3. Endogenous GnT-V, β 3GnT1 and α -Man I levels are not altered by doxycycline treatment *per se*. Intracellular levels of GnT-V, β 3GnT1 and α -Man I were monitored by Western blotting in total lysates of non-transfected control HEK293 cells and of cells overexpressing catalytically active SPPL3 following doxycycline treatment (+ Dox). Note that doxycycline treatment of non-transfected control cells does not affect intracellular levels of the indicated glycosyltransferases excluding that doxycycline treatment *per se* causes the alterations in glycosyltransferase levels.

Figure E4. Upon GnT-V overexpression immature GnT-V is detected in cellular lysates. Cell lysates of HEK293 cells transiently overexpressing GnT-V were subjected to enzymatic deglycosylation with

peptide:N-glycosidase F (PNGase F), endoglycosidase H (Endo H) or were left untreated prior to analysis by SDS-PAGE and Western blotting. Note that the higher molecular weight GnT-V species (GnT-V_{mat}) is resistant to Endo H treatment and was only deglycosylated by PNGase F, demonstrating that this species is complexly glycosylated and likely localises to post-ER compartments. In contrast, the lower molecular weight GnT-V species (GnT-V_{im}) is deglycosylated by Endo H as well as PNGase F treatment and, thus, harbours no complex N-glycans. Antibodies used to visualize the respective proteins in Western blots are indicated.

Figure E5. Effect of SPPL3 on GnT-V secretion and maturation. Intracellular and secreted levels of pulse-labelled Flag-GnT-V-V5 were analysed in cells overexpressing catalytically active SPPL3 and in control cells (**A**) or in cells transfected with SPPL3-specific or non-targeting siRNA pools (**B**). Three days after doxycycline-mediated induction of exogenous SPPL3 expression (**A**) and 4 days after transfection with siRNA pools (20 nM, **B**) cells were starved for 3 hours in serum-, methionine- and cysteine-free DMEM. For metabolic labelling, cells were incubated for 10 min in serum-, methionine- and cysteine-free DMEM supplemented with [³⁵ S] methione/[³⁵ S] cysteine (ca. 85 μ Ci/ 6 cm dish; Hartmann Analytics, Braunschweig, Germany). Subsequently, cells were incubated for the indicated time periods in DMEM supplemented with 10% (v/v) fetal calf serum, 2 mM methionine and 2 mM cysteine. Conditioned supernatants were collected and subjected to anti-V5 immunoprecipitation. Cells were washed once with ice-cold PBS and lysed. Lysates cleared by centrifugation were subjected to immunoprecipitations as indicated. Immunoprecipitates were separated by SDS-PAGE and transferred to PVDF membranes for documentation by autoradiography. Note that pulse-labelled immature intracellular GnT-V was not affected by SPPL3 over-expression, while under these conditions GnT-V secretion was strongly promoted and intracellular mature GnT-V was hardly detectable. siRNA mediated knockdown of SPPL3 reduced GnT-V secretion and caused hyperglycosylation of the mature intracellular GnT-V species.

Figure E6. N-glycan analysis by liquid chromatography-mass spectrometry. **A** Liquid chromatogram of N-glycans released by PNGase F digestion from secreted glycoproteins that were collected from HEK293 control cells (bottom) and cells overexpressing SPPL3 upon doxycycline induction (top). N-glycan species assigned are colour-coded as in Fig. 3G and Suppl. Tab. 1. **B** Expression controls. SPPL3 overexpression was tested in lysates from cells analysed in Fig. 3G, Suppl. Tab. 1 and **A**. In addition, Nicastrin running behaviour was analyzed and, as expected (Fig. 1A), SPPL3 overexpression was associated with an increased electrophoretic mobility of mature Nicastrin (NCT_{mat}), but not of immature Nicastrin (NCT_{im}).

Figure E7. Determination of SPPL3 cleavage sites within GnT-V. **A** Schematic presentation of the epitope-tagged GnT-V N-terminal fragment (NTF) model substrate comprising amino acids 2 to 61 of the GnT-V holoprotein and an N-terminal V5 as well as a C-terminal Flag epitope tag. Amino acids are depicted using the one letter code, the predicted TMD (amino acids 14 to 30 (Shoreibah *et al*, 1993)) is illustrated in grey. At the very C-terminus an alanine-proline motif was added to prevent degradation of liberated fragments by exopeptidases. To generate this expression construct, the GnT-V NTF coding sequence was amplified by PCR and tags were introduced via the respective primers (sequences available upon request). The PCR fragment was subcloned via Xhol and KpnI into pcDNA3.1hygro (+)

(Invitrogen). The expression construct was then transiently transfected into cells as indicated in **B**. **B** Mass spectrometric analysis of GnT-V NTF cleavage products secreted into conditioned supernatants of HEK293 cells (top panels) or HEK293 cells stably transfected with either SPPL3 wt (middle panels) or the SPPL3 D200N/D271N (DD/NN) mutant. Conditioned media of cells indicated were collected after 4 h and GnT-V NTF cleavage products were purified by immunoprecipitation using anti-Flag M2-conjugated agarose beads. Following agitation at 4°C overnight, beads were washed three times with IP/MS buffer (0.1% N-octylglucoside 10 mM Tris-HCl, pH 8.0, 5 mM EDTA, 140 mM NaCl) and three times with sterile water. Eluted peptides were analysed by MALDI-TOF MS as described earlier (Fukumori *et al*, 2010) with a ACTH (7 to 38) reference peptide to obtain relative peak intensities. SPPL3 wt or DD/NN expression was achieved by supplementing media with doxycycline (induced) and the respective uninduced cells were used as controls. Mass spectrometric analysis revealed five peptides (coloured and numbered (1 to 5) arrowheads) that mapped to the GnT-V NTF and were absent in immunoprecipitates of untransfected control cells. The very same peptides were more abundant in conditioned supernatants of SPPL3 wt-overexpressing cells but not of mutant SPPL3-expressing cells. **C** Overview of peptide fragments assigned to the peaks detected. obs. mass, observed mass. calc. mass, calculated mass.

Figure E8. Quantification of SPPL3 effects on β 3GnT1 and α -Man I secretion. Effects of SPPL3 expression levels on s β 3GnT1 (**A**), s α -Man I (**B**) and cellular α -Man I (**C**) described in Fig. 5 of the main text were quantified. Respective Western Blot panels depicting the particular protein quantified in lysates or in TCA-precipitated conditioned supernatants (sup) as well as the respective Calnexin controls are shown (upper panels). (**B**) and (**C**) were obtained from the same samples, therefore the Calnexin panel is identical. For quantification, Western blot signals from three independent experiments were acquired digitally using the LAS 4000 (Fujifilm, Japan). s β 3GnT1, s α -Man I and α -Man I signals, respectively, were quantified using the MultiGauge software (Fujifilm) and normalized to Calnexin Western blots signals obtained from cell lysates. Reference samples (non-targeting siRNA-transfected cells (ctrl) and cells not treated with doxycycline (- Dox), respectively) were set to 1. Statistical analysis using the two-tailed, unpaired t-test was conducted with the Graphpad Prism software. n.s., not significant, $p > 0.05$, *, $p \leq 0.05$, ***, $p \leq 0.001$. Error bars depict SEM ($n = 3$).

Suppl. Tab. 1. Overview of N-glycans identified by liquid chromatography-mass spectrometry in HEK293 cells and cells overexpressing SPPL3. The table summarises all N-glycan species identified, their calculated and observed masses as well as their relative abundance on secreted glycoproteins obtained from HEK293 control cells and cells over-expressing SPPL3. N-glycans are colour-coded as indicated and this code is also used in Fig. 3G and Fig. E6.

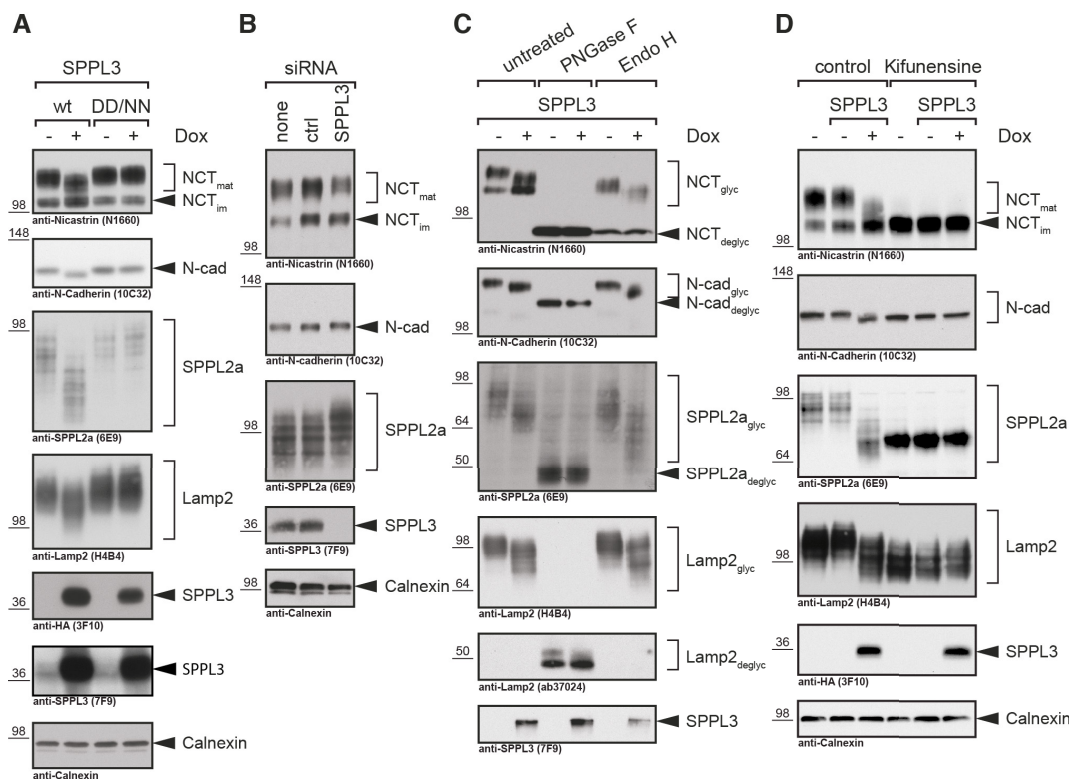


Figure 1

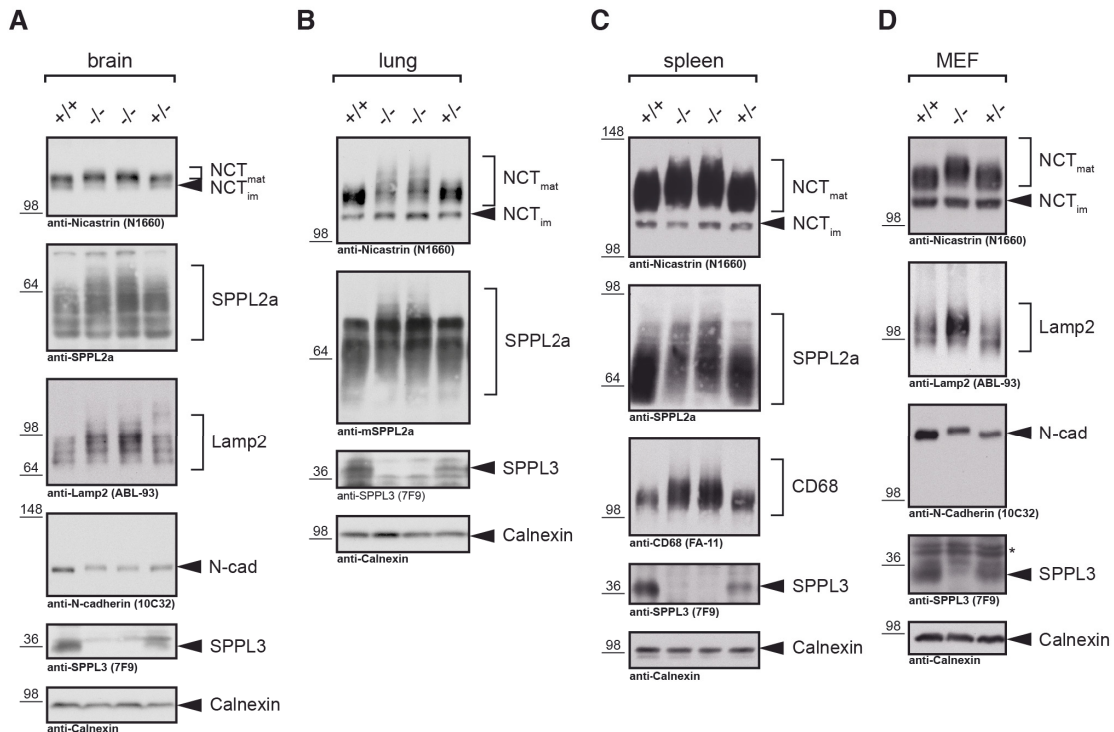


Figure 2

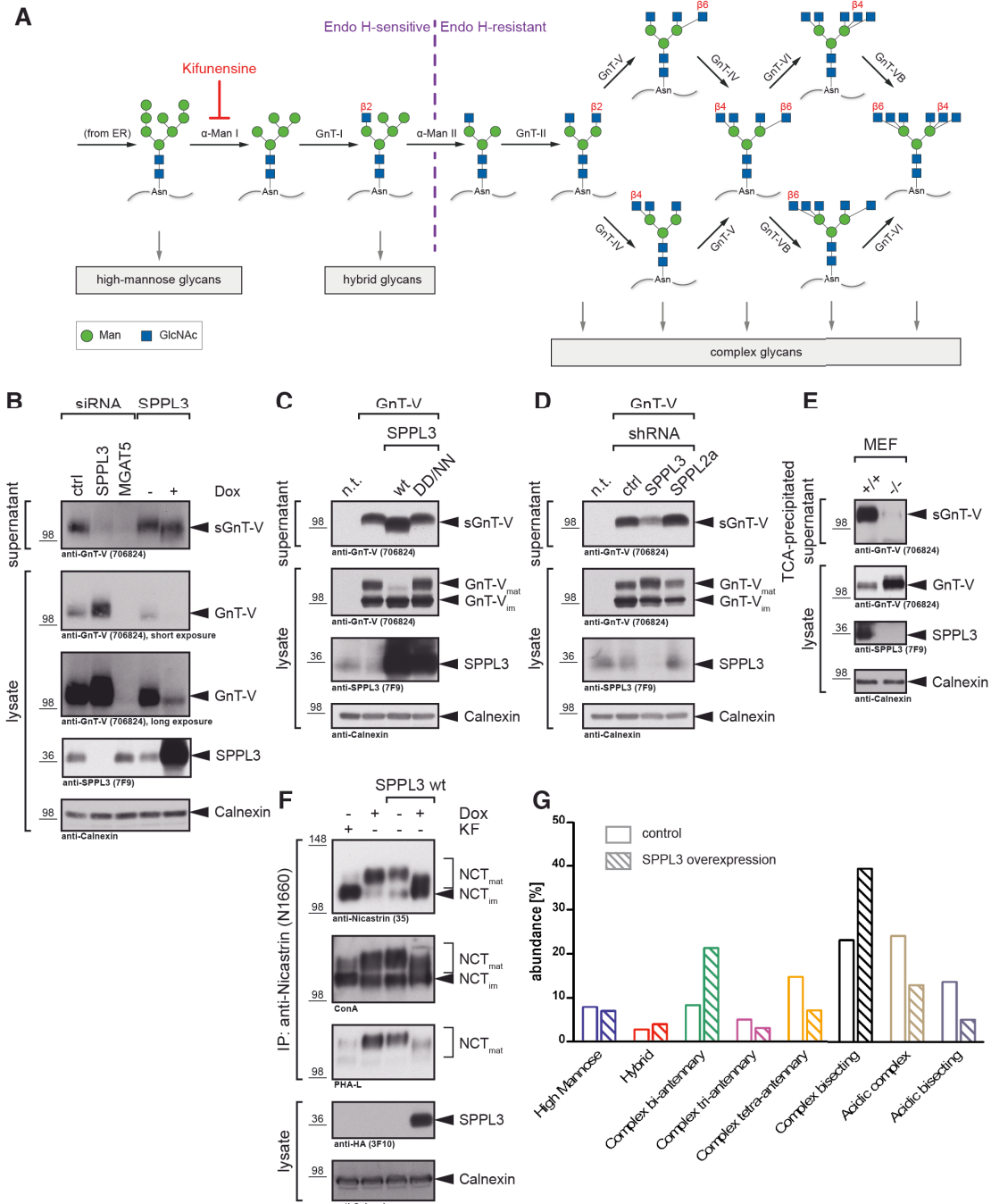


Figure 3

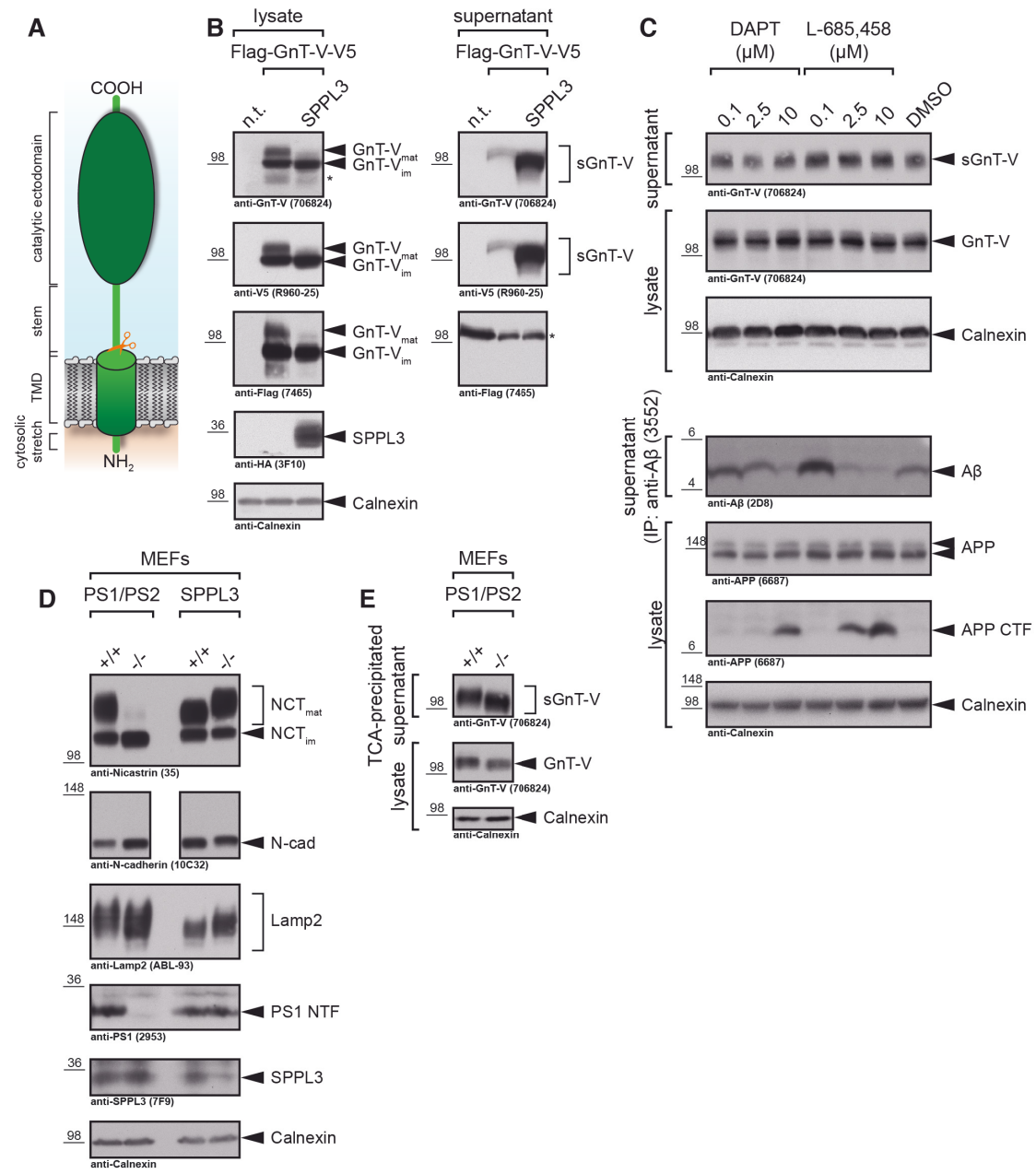


Figure 4

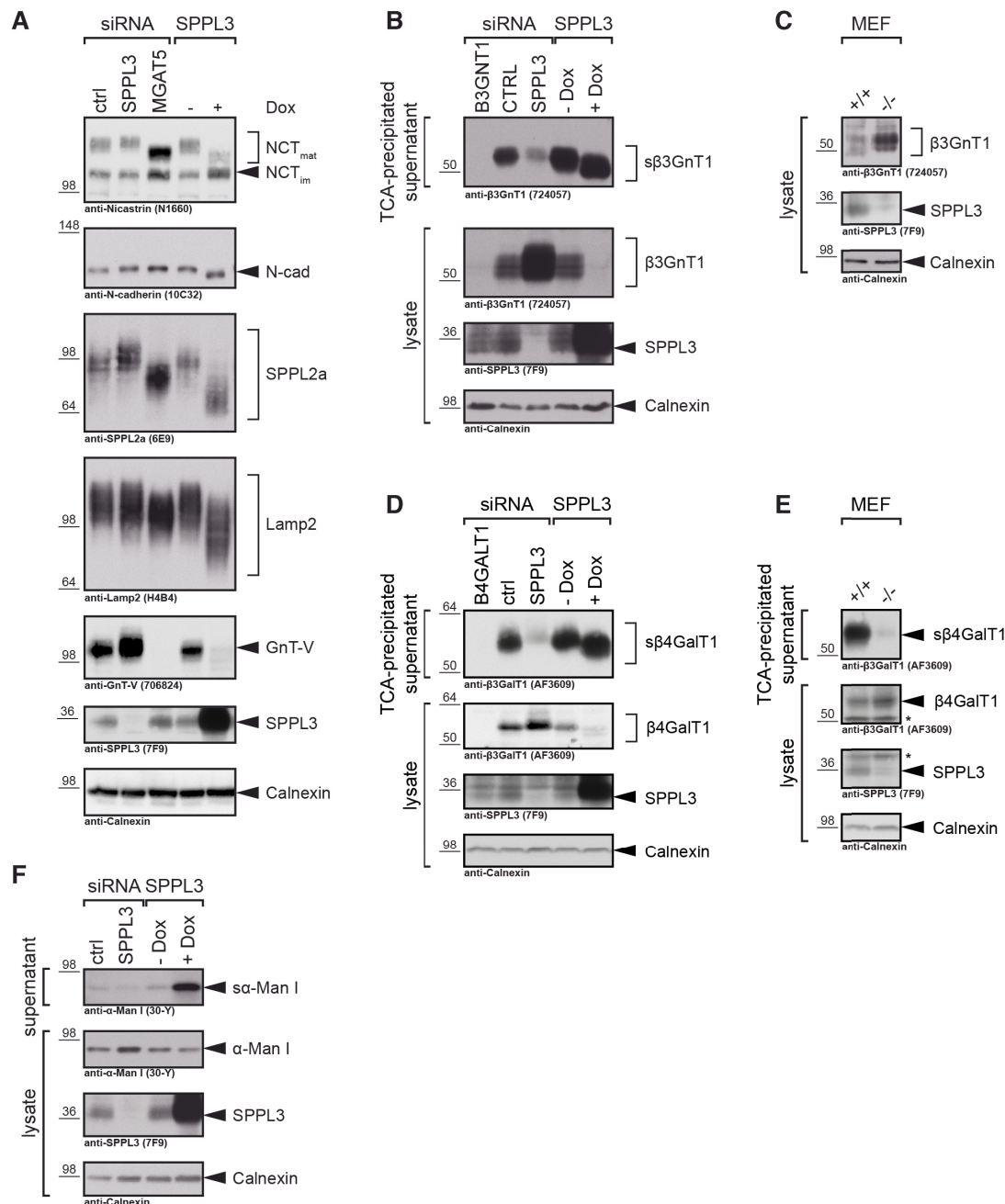


Figure 5

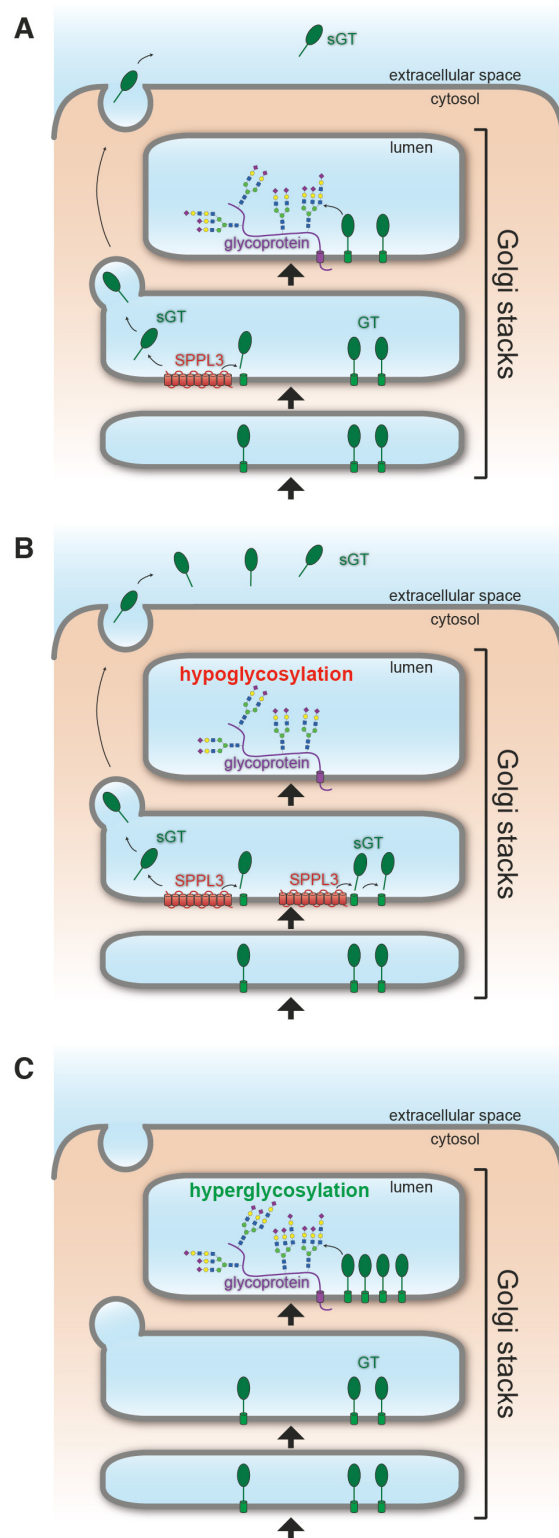


Figure 6

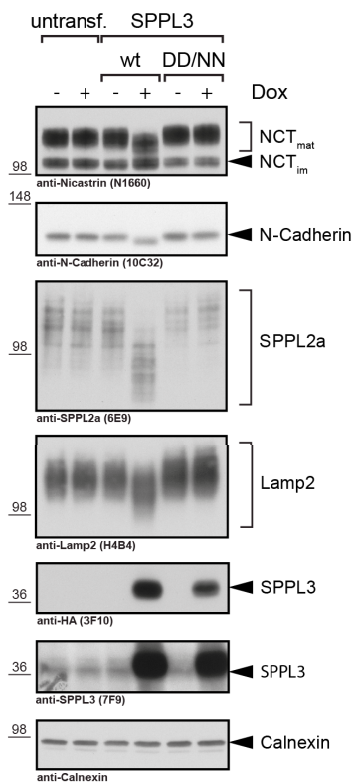


Figure E1

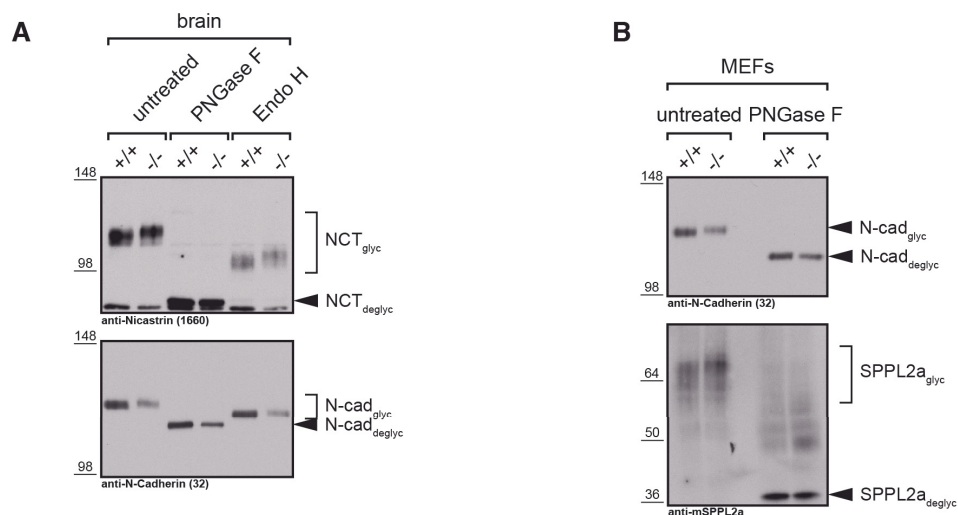


Figure E2

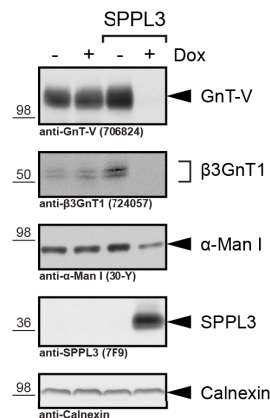


Figure E3

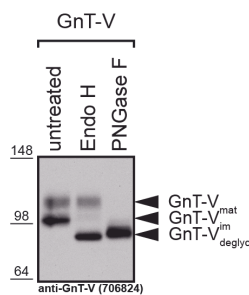


Figure E4

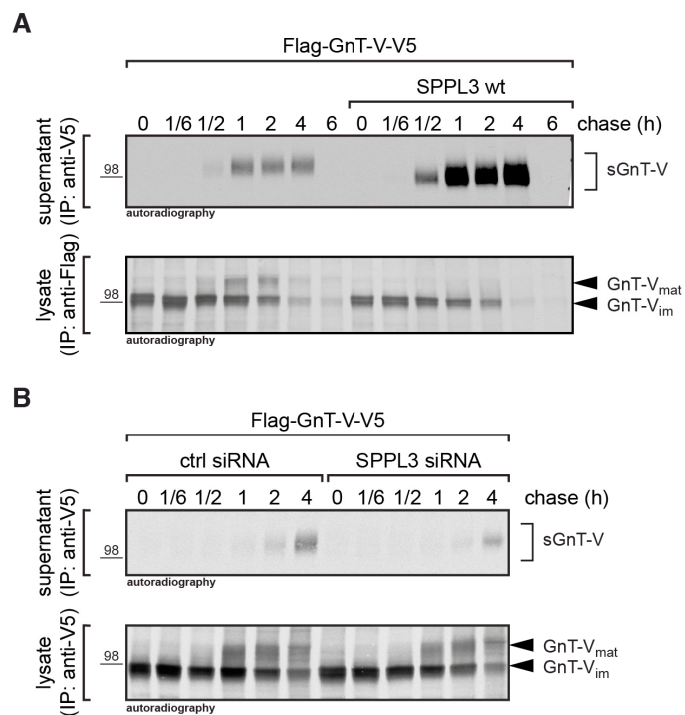


Figure E5

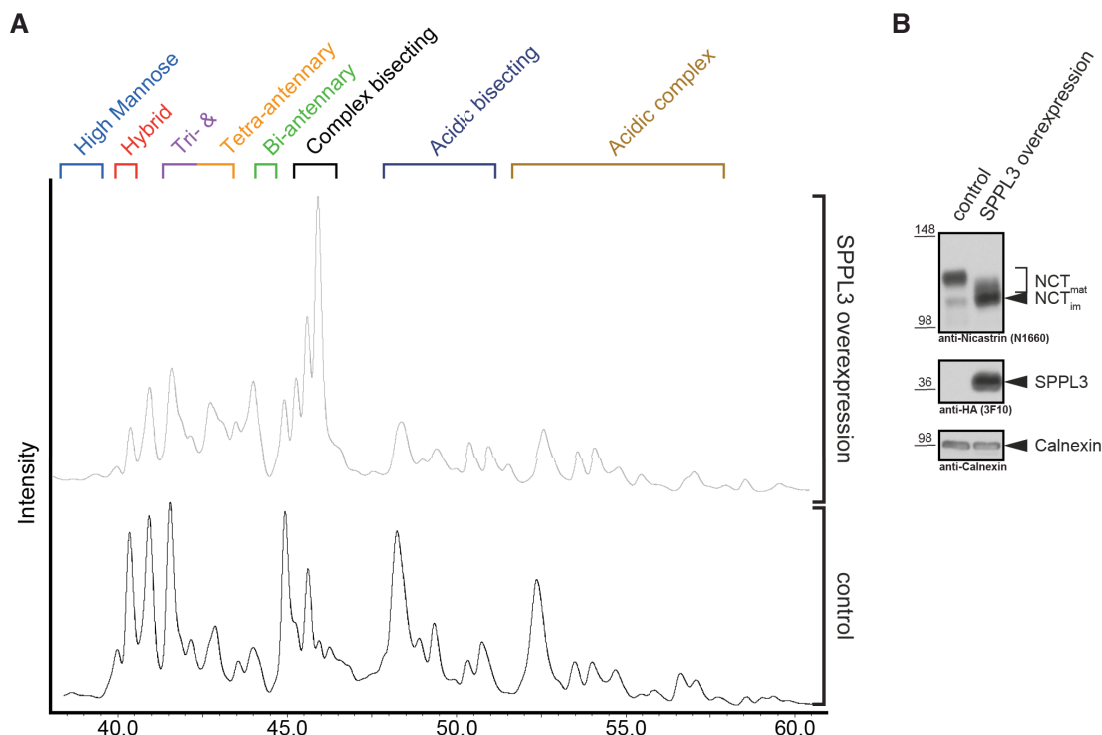
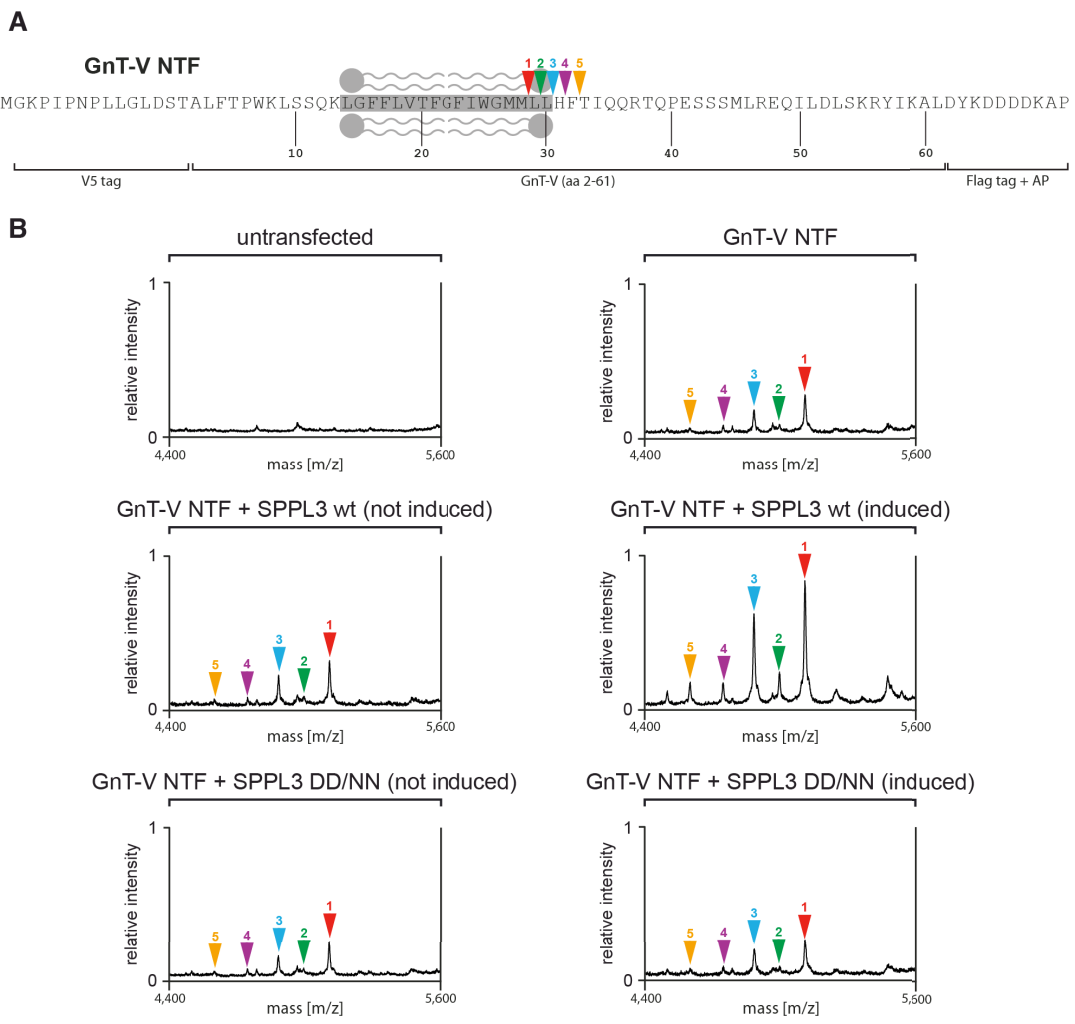


Figure E6



C

peak No.	fragment	sequence	obs. mass [Da]	calc. mass [Da]
1	(L29)	LLHFTIQRTQPESSSMLREQILDLSKRYIKALD Y KDDDDKAP	5,110.17	5,109.25
2	(L30)	LHFTIQRTQPESSSMLREQILDLSKRYIKALD Y KDDDDKAP	4,995.59	4,995.70
3	(H31)	HFTIQRTQPESSSMLREQILDLSKRYIKALD Y KDDDDKAP	4,882.36	4,884.83
4	(F32)	FTIQRTQPESSSMLREQILDLSKRYIKALD Y KDDDDKAP	4,746.21	4,746.60
5	(T33)	TIQRTQPESSSMLREQILDLSKRYIKALD Y KDDDDKAP	4,597.80	4,599.02

Figure E7

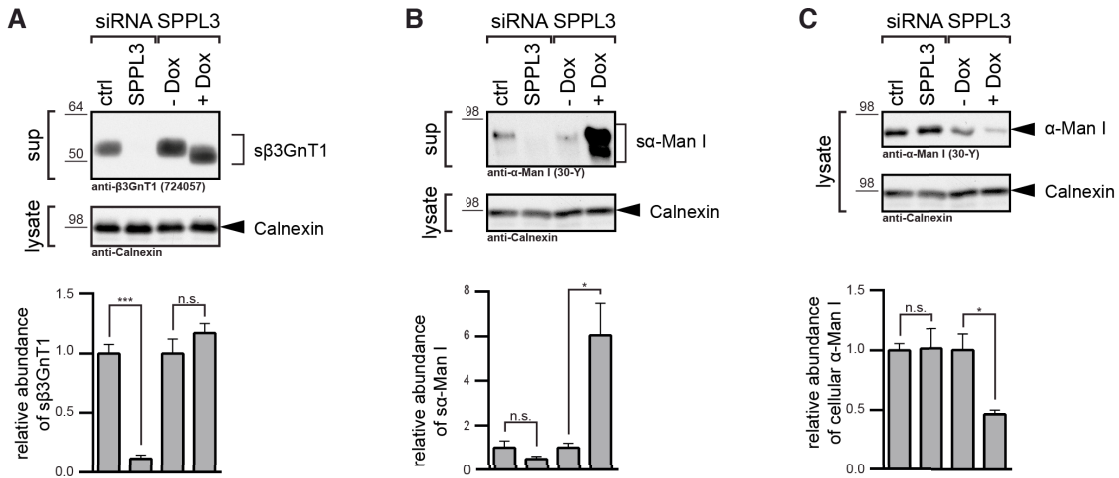


Figure E8

